CONF

~~AEC-660904~~

Volume 2

PROCEEDINGS
of the
NINTH AEC AIR CLEANING CONFERENCE

held in

Boston, Massachusetts

13-16 September 1966

Nuclear Consulting Services Inc.

Sponsors: The Harvard Air Cleaning Laboratory
Harvard University

and

Division of Reactor Development and Technology
U. S. Atomic Energy Commission

Editors

James M. Morgan, Jr.
Melvin W. First

January 1967

UNITED STATES ATOMIC ENERGY COMMISSION

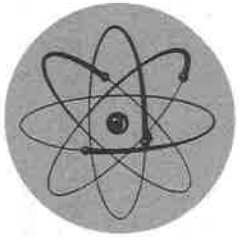

Certificate of Appreciation

awarded to

THE HARVARD AIR CLEANING LABORATORY
in the name of DR. LESLIE SILVERMAN

for Outstanding Services Rendered to the Atomic Energy Commission
in the Fields of Air Cleaning and Nuclear Safety

September 13, 1966
Date

Glenn T. Seaborg

EFFECT OF FIRE INTRUSION AND HEAT ON HEPA FILTER UNITS by Jack L. Murrow 96

Discussion 106

PROGRESS REPORT - FACTORS INFLUENCING HIGH-EFFICIENCY GASKET LEAKAGE by F. E. Adley 109

DEVELOPMENTS IN CONTAMINATED FILTER REMOVAL EQUIPMENT by C. A. Hahs 149

Discussion 158

Iodine and Iodide Removal
Session 2 - Wednesday, 14 September 1966
Chairman: George Parker, ORNL

DEVELOPMENT OF IMPREGNATED CHARCOALS FOR TRAPPING METHYL IODIDE AT HIGH HUMIDITY by D. A. Collins, L. R. Taylor and R. Taylor 159

RETENTION OF METHYL IODIDE BY IMPREGNATED CARBONS UNDER AMBIENT CONDITIONS by G. W. Parker, G. E. Cheek, and A. Ferreli . . 199

MECHANISMS THAT AFFECT THE ADSORPTION OF METHYL IODIDE ON CHARCOAL UNDER HUMID CONDITIONS by Frank J. Ackerman and John Z. Grens 230

Discussion 271

REMOVAL OF IODIDE AND METHYL IODIDE BY AEROSOL FORMATION WITH HYDRAZINES by F. J. Viles, Jr. and L. Silverman. 273

REMOVAL OF METHYL IODIDE FROM SIMULATED REACTOR CONTAINMENT ATMOSPHERES WITH HYDRAZINE by J. Mishima, L. C. Schwendiman, L. L. Burger and R. A. Hasty 298

Discussion 317

Luncheon - 14 September 1966

Introduction of Guest Speaker by Professor Theos Thompson, MIT 319

Address by Professor Manson Benedict, Head, Department of Nuclear Engineering, Massachusetts Institute of Technology 320

Volume II

Filtration and Filter Performance Evaluation
Session 4 - Thursday, 15 September 1966
Chairman: M. D. Thaxter, Lawrence Radioation Laboratory

SERIES DISTRIBUTION SAMPLING ERRORS INTRODUCED BY THE POINT - PLANE ELECTROSTATIC PRECIPITATOR SAMPLING DEVICE by Parker C. Reist 613

Discussion 625

EVALUATION OF THE EQUATION THAT GOVERNS THE COAGULATION OF AN AEROSOL by P. Spiegler, J. G. Morgan, M. A. Greenfield and R. L. Koontz 626

Discussion 646

MECHANICS OF COLLECTION OF PARTICLES BY INERTIA AND INTERCEPTION IN A FIBROUS AIR FILTER by Stanley V. Dawson 647

EFFECTS OF PARTICLE ACCUMULATION ON AEROSOL FILTER LIFE by Charles E. Billings 656

Discussion 676

CHARACTERIZATION OF RADIOACTIVE PARTICULATE AEROSOLS BY THE FIBROUS FILTER ANALYZER by M. D. Silverman, J. Truitt, W. E. Browning, Jr., L. F. Franzen and R. E. Adams 680

Discussion 700

PENETRATION OF SUBMICRON TI BACTERIOPHAGE AEROSOLS AND BACTERIAL AEROSOLS THROUGH COMMERCIAL AIR FILTERS by J. B. Harstad, Herbert M. Decker, Lee M. Buchanan and Melvin E. Filler 701

Discussion 714

PERFORMANCE OF FILTER SYSTEMS UNDER ACCIDENT CONDITIONS by R. E. Adams, J. S. Gill, W. D. Yuille, W. E. Browning, Jr., L. F. Parsley and C. E. Guthrie 715

Discussion 738

REMOVAL OF PLUTONIUM HEXAFLUORIDE FROM CELL EXHAUST AIR BY HYDROLYSIS AND FILTRATION by Robert W. Kessie 741

Discussion 762

Analysis and Monitoring of Contamination
Session 5C - Thursday, 15 September 1966
Chairman: J. Ege, Argonne National Laboratory

PORTABLE SMOKE PHOTOMETER by H. H. Hunter and R. I. Mitchell 928

Discussion 941

ZPPR ROOF SAND FILTRATION OF URANIUM, PLUTONIUM AND URANINE AEROSOLS by C. L. Cheever, D. R. McFee, J. Sedlet and T. L. Duffy 942

THE DESIGN, TEST AND USE OF THE BROOKHAVEN NATIONAL LABORATORY (BNL) REACTOR BYPASS FILTER FACILITY by R. O. McClintock 965

CONTINUOUS SAMPLER-MONITOR FOR FISSION PRODUCTS IN CONTAMINATED ATMOSPHERES by R. E. Schindler 974

Discussion 977

In-Place Testing
Session 6 - Friday, 16 September 1966
Chairman: J. Thomas, New York Operations

FILTER TESTING PROGRAM, ATOMIC ENERGY OF CANADA LIMITED by F. Panchuk and W. Rachuck 979

Discussion 1020

TESTING OF AIR CLEANING SYSTEMS - TESTING OF THE COMPONENTS - IN-PLACE TESTS by F. Billard and J. Brion 1021

Discussion 1031

ON-SITE TESTING OF FILTERS WITH SPECIAL REFERENCE TO SOLID AEROSOLS by Hans Flyger and H. C. Rosenbaum 1032

IN-PLACE TESTING OF CHARCOAL FILTER BANKS AT AMES LABORATORY RESEARCH REACTOR by G. A. Gukeisen and K. L. Malaby 1063

Discussion 1069

N-PLACE NONDESTRUCTIVE LEAK TEST FOR IODINE ADSORBERS by D. R. Muhlbaier 1071

SERIES DISTRIBUTION SAMPLING ERRORS INTRODUCED BY THE POINT-PLANE ELECTROSTATIC PRECIPITATOR SAMPLING DEVICE

by

Parker C. Reist, Sc.D.

Department of Industrial Hygiene
Harvard School of Public Health
665 Huntington Avenue
Boston, Massachusetts

ABSTRACT

In using the point plane electrostatic precipitator it is generally assumed that the size distribution of the sample collected represents reasonably well the actual particle size distribution of the test aerosol. This paper reports an investigation made to determine the accuracy of this assumption and concludes that for count size distributions the error introduced by this sampling device is insignificant.

This work was done in connection with contracts of Harvard University with the U. S. Atomic Energy Commission and the National Aeronautics and Space Administration.

TABLE 1

APPROXIMATE PARTICLE CONCENTRATIONS PRODUCED BY AEROSOL GENERATOR

Particle Diameter (Microns)	Particle Concentration, Particles Per Liter		
	Singlets	Doublets	Total
0.557	2.0×10^6	8.2×10^5	5.1×10^6
0.796	2.7×10^6	8.5×10^5	5.1×10^6
1.305	8.5×10^5	2.5×10^5	1.3×10^6
2.68	1.1×10^5	2.5×10^4	2.1×10^5

4.45×10^{-2} cm^2. Representative grid areas were photographed using a Phillips Model 75 electron microscope and the resulting negatives were printed on 8 x 10 photographic paper for counting. Photographs of a 28,800 line calibration grid were taken and printed in a similar way before and after each change of a magnification or film. Three grid areas were photographed per sample; one from the middle of the sample and the other two near the sample edge, at right angles to each other.

Similar to the counting procedure for the membrane filter samples, separate counts were made on the number of singlets and doublets collected by the electrostatic precipitator. Because of the relatively low concentration of aerosol used in these experiments, coagulation of the suspended particles was not considered to be significant and thus collection efficiencies for singlets and doublets could be considered to be independent of each other.

Collection efficiency was defined as 100 times the ratio of the total number of particles of a certain type collected by the electrostatic precipitator in a given period of time to the total number of particles of the same type which in the same time passed through the precipitator.

Runs were made to determine the collection efficiencies of the four homogeneous aerosols at flow through velocities of 5, 15, 30, and 70 centimeters per second. Flow at the highest velocity tested gave a Reynolds number of about 350, so that in all cases flow through the electrostatic precipitator was laminar.

IV. EXPERIMENTAL RESULTS AND DISCUSSION

The efficiencies measured, using the technique described above, are shown in Table 2. Because of difficulties during the experiment in getting proper loading of the aerosol, data for the 1.305 μ particles were collected for only one velocity.

From these efficiencies, there appears to be no indication that varying the collection velocity from 5 cm/sec to 70 cm/sec affects the collection efficiency of the point-plane electrostatic precipitator for any of the sizes studied. It was thus possible to average these values to compare collection efficiencies for the four sizes of particles. The averaged values are plotted as Figure 3.

Using various aerosols, Arnold, Morrow and Stöber[2], Morrow and Mercer[3], Ettinger and Posner[7], and Yoder[9], all found no sampling bias from the point-plane electrostatic precipitator with particles of mean diameters less than 0.5 μ. Thus it can be concluded that the curve shown in Figure 3 is essentially a straight line below 0.5 μ diameter.

A large increase in collection efficiency is observed for the 2.68 micron particles both singlets and doublets and it is reasonable to expect it to continue to increase for still larger particles. The greater efficiency found for the 2.68 μ particles agrees with observations of Arnold et al.[2], mentioned earlier, that particles greater than one micron in diameter were sampled in greater quantities by the electrostatic precipitator than by the thermal precipitator.

From Figure 3 particles of approximately 0.8 micron diameter appear to be collected with minimum efficiency. Comparison of the averaged results for the singlets and doublets (Table 3) also tends to indicate a minimum collection efficiency about this same size range. The efficiency goes down for doublets for the 0.577 μ particles, while in all other cases an increased collection efficiency for doublets is observed. J. Dyment, working at the U.K. Atomic Weapons Research Establish ent, found that point-plane electrostatic precipitator samples of a heterogeneous aerosol were deficient in particles in the range 0.5 to 1.0 μ when compared to the results obtained using an oscillating thermal precipitator[18]. This is similar to the results found by Ettinger and Posner[7], mentioned earlier. This decrease could be explained by the dip in efficiency shown in Figure 3.

TABLE 3

AVERAGED COLLECTION EFFICIENCIES, PERCENT

Particle Diameter (Microns)	Singlets	Doublets
0.557	1.98	1.93
0.796	1.38	1.83
1.305	1.65	1.96
2.68	3.38	6.35

V. CONCLUSIONS

1. The collection efficiency of the point-plane electrostatic precipitator is independent of the sample velocity through the unit when sampling in the laminar flow range.

2. From the information presented in previous sections of this report, it is concluded that there is no bias introduced by the electrostatic precipitator for particle sizes less than about 0.5 μ.

3. The point-plane electrostatic precipitator will tend to over-sample particles of sizes above about 1.5 microns, this effect increasing with increasing particle size.

4. There is a decrease in collection efficiency for particles whose sizes lie in the range 0.5 to 1.0 μ. For the determination of count size distributions this decrease should be negligible; for determining mass size distributions, however, the error introduced by this variation could be significant.

VI. ACKNOWLEDGEMENTS

The author would like to acknowledge the contributions of P. A. Schwartz who assisted him in the collection of the data for this report.

DISCUSSION

THOMAS: One of the conclusions you made was that the collection efficiency did not depend on sample velocity. I don't think you are able to support that conclusion because of the wide variation you are getting in efficiencies; for example, 1.6%, 1.1 at 15, etc. It seems to me there is a lot of variation. We ran into the same thing exactly, the same trouble, when we evaluated the Silverman precipitator. We didn't do a thorough job on it, but our results were so non-reproducible that we abandoned the device.

We finally went to the Mercer type of precipitator, which at least is a lot more reproducible, and on that precipitator we got efficiencies of 20 or 30% or more. I don't remember the data.

Another thing we observed was that the overall efficiency was fairly high, and that a lot of particles were coming out on parts of the precipitator other than the EM grid. I believe that some more study needs to be made of these precipitators, particularly on a reproducible model. The one Morrow and Mercer described, I believe, is your Reference 3.

ETTINGER: I also want to point out that there are at least two Mercer ESPs, the one described in the journal and a later one which developed at Lovess. On the later one, you cannot take random grid openings or microns from random grid openings because the collection is in a sort of ribbon affair and you must go at right angles to the ribbon since there is discrimination as you pass down the access of stream.

REIST: I am aware of that publication. As I understand it, the apparatus -- and correct me if I am wrong -- is not exactly a point-plane type of precipitator.

ETTINGER: It is a point-plane, but it is arranged so that there are channeling affairs there. Only part of the EM grid is exposed to airstream.

REIST: Right, but it is basically different from the other designs. This is why I didn't include it as one of my references.

LIU: Just as a point of information, there has been developed a two-stage electro static precipitator that avoids some of these problems at the point of planes, and this member has an efficiency on the order of about 80 per cent and works by electro miscroscope grids as well as optical microscope slides and cover slips, and the instrument will work in an oversize range of .01 microns to 5 microns with very little change in efficiency. If anyone is interested in this information, I would be happy to discuss it with them.

more complex expression for the time behavior of the density of particles. Also, the copious experimental data which they presented showed that the theory for homogeneous sols has wide application. The corrected integro-differential equation for heterogeneous aerosols first appeared in the Handbook of Aerosols[5] with authorship credited to D. E. Goldman, who, however, never published it in the open literature. Goldman also introduced a term to account for stirred settling. During the war, attempts at solving the Goldman equation were made by Friedman and Shiffman,[6] but these studies have not been published except as an NDRC memo. More recently, Zebel[7] and Friedlander,[8,9] rederived the integro-differential equations. Zebel programmed it on IBM 650 and observed the spectral changes of an initial specified aerosol. Friedlander looked for a generalized solution and showed that, as a result of agglomeration, aerosols tend to adopt in shape the distribution which he called self-preserving. Lately, Hidy[10,11,12] has used a digital computer to observe the behavior of a sol with a discrete spectrum. He solved a set of nonlinear differential equations, each equation governing one particle size. His work also represents an extensive review of the subject.

THE FUNDAMENTAL INTEGRO-DIFFERENTIAL EQUATION

Following the method of Smoluchowski, it can be shown that the basic equation[1,5] describing the change in time of the particle size distribution of a heterogeneous aerosol is as follows:

$$\frac{\partial n(r,t)}{\partial t} = \frac{K_0}{2}\left[\int_{\rho=0}^{\rho=r/3\sqrt{2}} \varphi(\rho,\rho')n(\rho,t)n(\rho',t)\frac{r^2}{(\rho')^2}\,d\rho - n(r,t)\int_0^{\infty}\varphi(r,\rho)n(\rho,t)\,d\rho\right] - \frac{v(r)}{h}n(r,t) + S(r) \quad . \qquad \ldots(1)$$

The quantity $K_0 = 4kT/3\eta$ is known as the coagulation constant; $\varphi(\rho,\rho')$ is the coagulation function and is given by:

$$\varphi(\rho,\rho') = \left\{\frac{1}{\rho}\left[1 + C(\rho)\right] + \frac{1}{\rho'}\left[1 + C(\rho')\right]\right\}(\rho + \rho') \quad . \qquad \ldots(2)$$

The expression $1 + C(x) = 1 + (1/x)(0.084 + 0.0264 \exp(-16.7x))$ is the so-called Cunningham correction factor.[13]

The first integral represents the formation rate of particles (r, r + dr) as a result of collisions between particles of radii ρ and ρ' such that

$$\rho^3 + \rho'^3 = r^3 \quad .$$

Similarly the second integral represents the disappearance rate of particles (r, r + dr) as a consequence of collisions with all other particles. The term with the settling velocity v(r) represents the loss due to stirred settling, with

If there is settling, the code also stores the spectra of the settled component and evaluates the integral

$$\int_o^\infty \frac{4}{3}\pi \frac{r^3}{h} n_s(r,t)\, dr \quad , \qquad \ldots(7)$$

with

$$n_s(r,t) = \int_o^t n(r,t) \frac{v(r)}{h}\, dt$$

and the sum of integral 5 and 7 must now remain constant or equal the integral 6 (note that the units of $n_s(r,t)$ are part/cm^2-μ). When there is no source, the time increments are evaluated from

$$\Delta t = f \frac{1}{K(r)N(t)} \quad , \qquad \ldots(8)$$

where N(t) is given by

$$N(t) = \int_o^\infty n(r,t)\, dr \quad , \qquad \ldots(9)$$

and K(r) is given by

$$K(r) = K_0 \left[1 + \frac{1}{r}(0.083 + 0.0264\, e^{-16.7r})\right] \quad . \qquad \ldots(10)$$

The code searches the r-value at which n(r,t) has a maximum and uses this value in Equation 10. The constant, f, a number considerably less than 1.0, is selected such that the integrals 5 or 5 plus 7 remain constant.

With a source term, the incremental time steps are calculated from

$$\Delta t = f\left[\frac{1}{SK(r)}\right]^{1/2} \quad , \qquad \ldots(11)$$

with

$$S = \int_o^\infty s(r)\, dr \quad , \qquad \ldots(12)$$

or Equation 8, whichever of the two is smaller.

CALCULATION RESULTS

A few test cases were performed to ensure that the code worked properly. One of the check cases, the problem discussed by Zebel, was duplicated by the

since the Cunningham correction still plays an important role in the coagulation function. Figure 1c shows the appearance and disappearance of particles of given sizes as a function of time. Figure 3 shows the total particle density versus time. The data can be fitted by an expression of the form

$$\frac{1}{N(t)} - \frac{1}{N(0)} = \text{constant } t^a \quad , \qquad \ldots(14)$$

where the exponent a is close to 1.0. As N(t) becomes much less than N(0), $N(t) \ll N(0)$, the curves also tend to overlap. Figure 4 illustrates more clearly that the data can be fitted by Equation 14. Figure 5 shows the mass median radius or 50% radius by volume versus time. This quantity is defined as

$$\int_o^{r_{mmr}} r^3 n(r, t)\, dr = \frac{1}{2} \int_o^{\infty} r^3 n(r, t)\, dr \quad . \qquad \ldots(15)$$

The data can be fitted by an equation of the form

$$r^3_{mmr}(t) - r^3_{mmr}(0) = \text{constant } t^m \quad , \qquad \ldots(16)$$

where the exponent m is close to 1/3, by interpolation, the data indicate that r_{mmr} reaches a value of 0.1μ at a time close to 100 sec. Thus, with concentrations of about 1μgm/cc, particles with near molecular sizes cannot survive and need not be considered in filter design problems.

With respect to the problem of agglomeration, it is noted that replacing n(r, t) in Equation 1 by $\alpha n(r, t)$, where α is a constant, is equivalent to changing the time scale from t to t/α; i.e., the effect of a change in density by a constant factor, α, just changes the time scale inversely by that factor.

Problem 2 – Agglomeration and Settling

In this problem, the code solved Equation 1 without the source term. Again two cases initially specified by log-normal distributions with the following parameters were examined:

	Case 1	Case 2
N(0) part/cm^3	5.26 x 10^6	1.275 x 10^6
r_g, μ	0.2	0.2
σ	1.5	2.0

The two distributions have initially the same particle volume, 0.371 x 10^6 μ^3/cm^3 (same as in Problem 1). For the constant $2\delta g/9\eta h$ in the settling term, a value of 1.31 x 10^{-4} was used when the dimensions of r and h are in μ and cm, respectively. When ρ = 2.27 gm/cm^3, h = 6.8 ft, a value close to the experimental setup at AI. These two cases were started with larger particles than in Problem 1, since settling became important only when the sizes reached magnitudes of 0.1μ or more. The problem was selected to observe the effects

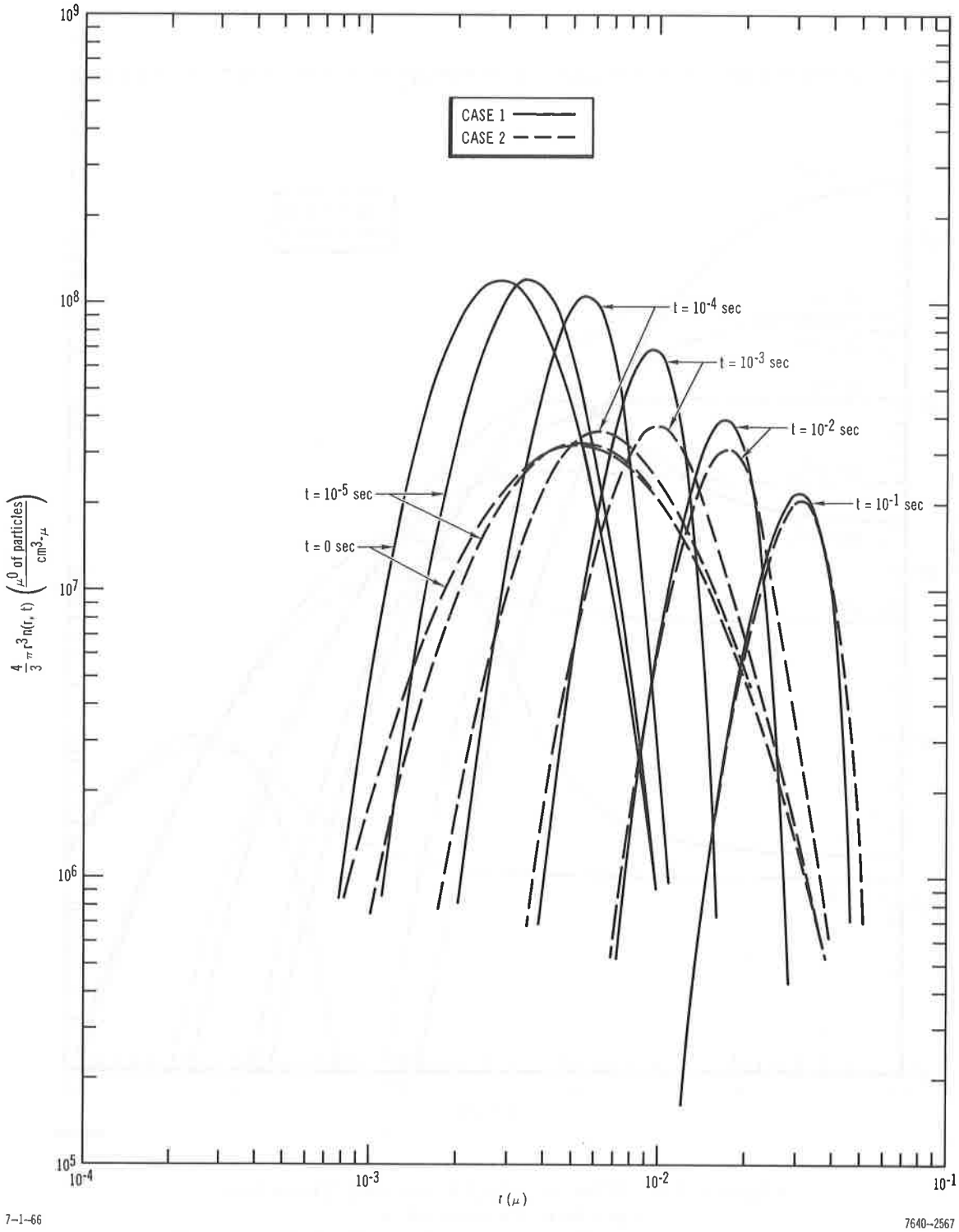

Figure 1b. Particle Distributions by Volume at Various Times for Cases 1 and 2 of Problem 1

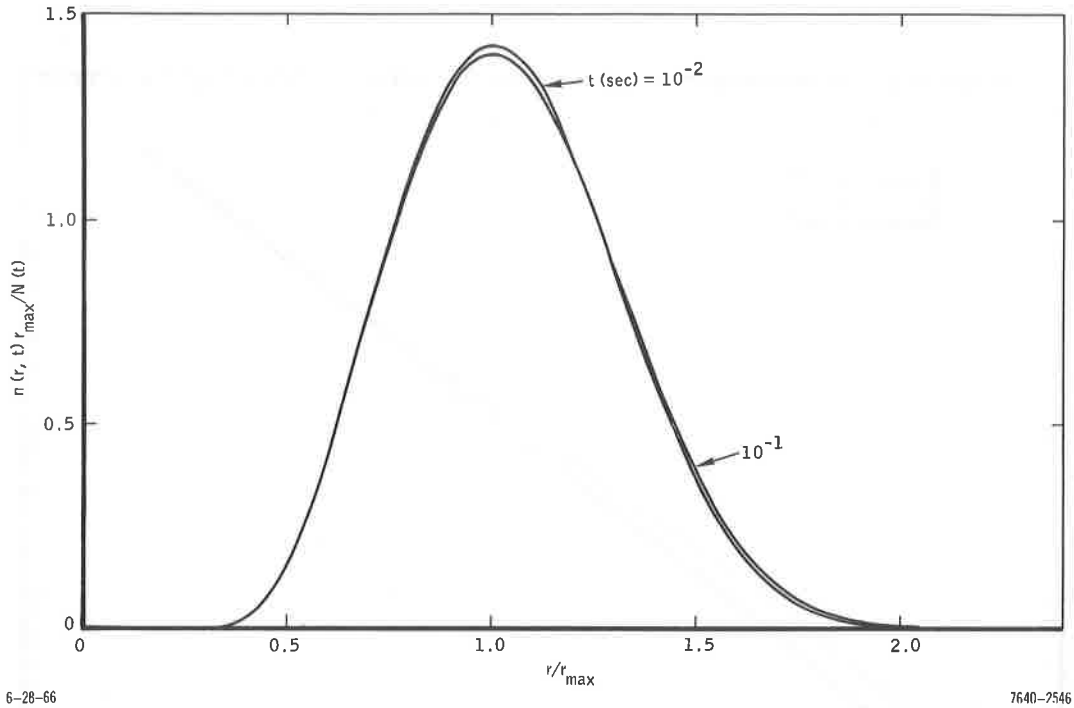

Figure 2. Plot of the Particle Size Spectrum at Two Different Times in a Dimensionless Form for Case 1 of Problem 1

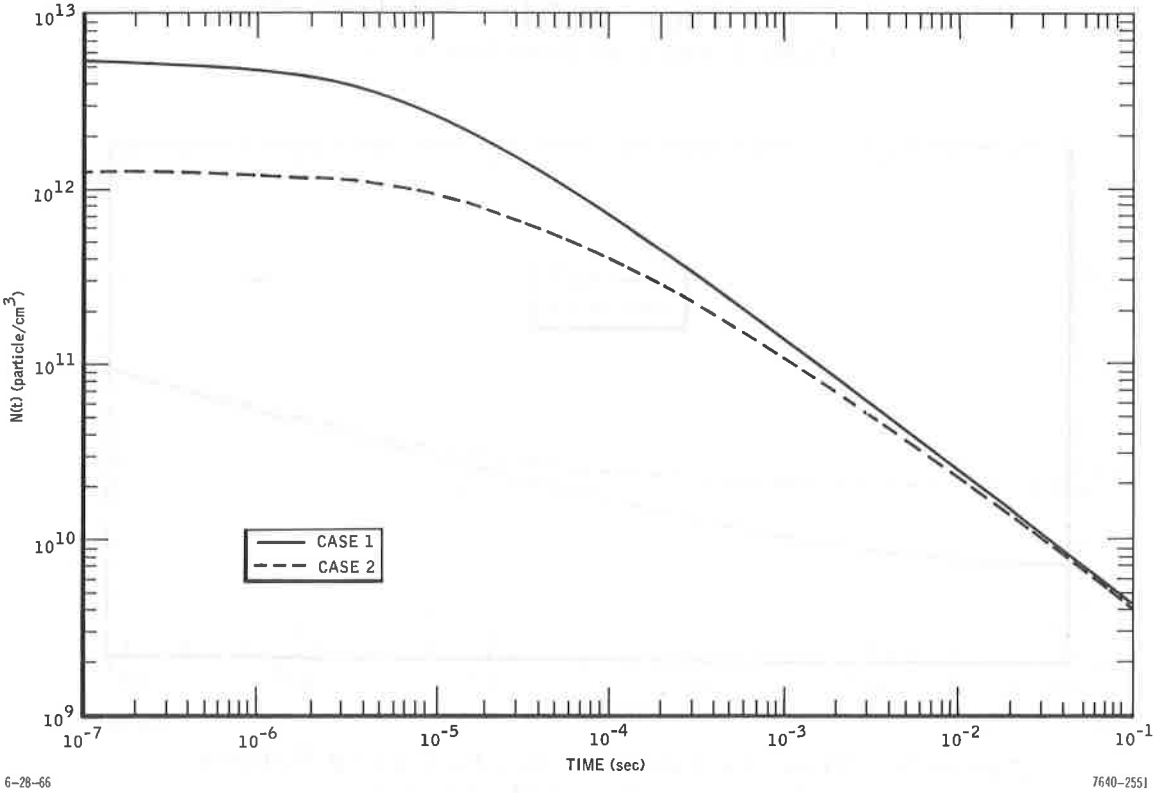

Figure 3. Particle Density as Computed by the Code for Problem 1

of stirred settling. Data obtained are illustrated in Figures 6 through 9. Figure 6 shows the particle size spectrum in suspension at various times. For Case 1, at first there is a disappearance of small particles and the appearance of larger ones. From 10^4 sec onward, observe the disappearance of all sizes of particles. Thus, agglomeration dominates initially, while settling comes into play later. For Case 2, all particle sizes decrease from the start, indicating that both mechanisms, agglomeration and settling, are important initially. Figure 7 shows the size spectrum of the settled component at various times. In both cases, as time increases, the most probable radius shifts to larger sizes, an effect caused by the mechanism of agglomeration. Figure 8 shows the particle density and the percentage-of-weight-settled versus time. Approximate ways of obtaining these data will be discussed later. Figure 9 shows the 50% radius by volume (of the suspended component) versus time. For Case 1, the magnitude of this parameter increases up to 1.5×10^4 sec, even though 67% of the weight settles over this time interval. For Case 2, where settling is important from the start, the magnitude of this parameter decreases steadily. In the following table, comparisons are made between the suspended and settled distributions:

	Case 1	Case 2
50% radius by volume of initial distribution in suspension (μ)	0.33	0.86
50% radius by volume of settled distribution* (μ)	0.80	1.05
Approximate σ of settled distribution†	1.28 to 1.35	1.52 to 1.71
Time necessary for 50% of weight to settle (sec)	1.05×10^4	5.1×10^3

Problem 3 – Source, Agglomeration, and Settling

In this problem, a case is studied in which three mechanisms occurred: Source, agglomeration, and settling. The input parameters were:

S_0 [part/(cm^3-sec)]	8.77×10^3
Shape of source	Log-normal
r_g of source distribution (μ)	0.2
σ of source distribution	1.5
Time interval over which particles are produced (sec)	0 to 600
Total particle volume generated (μ^3/cm^3)	0.371×10^6
Settling parameters	Same as problem 2

No particles were present in the volume element at time t = 0 sec. The data are illustrated in Figures 10 through 13 where the data of Case 1, Problem 2, were included for comparison. The size spectra of the suspended and

*90% of weight has settled.
†Settled distribution approximated by a log normal curve.

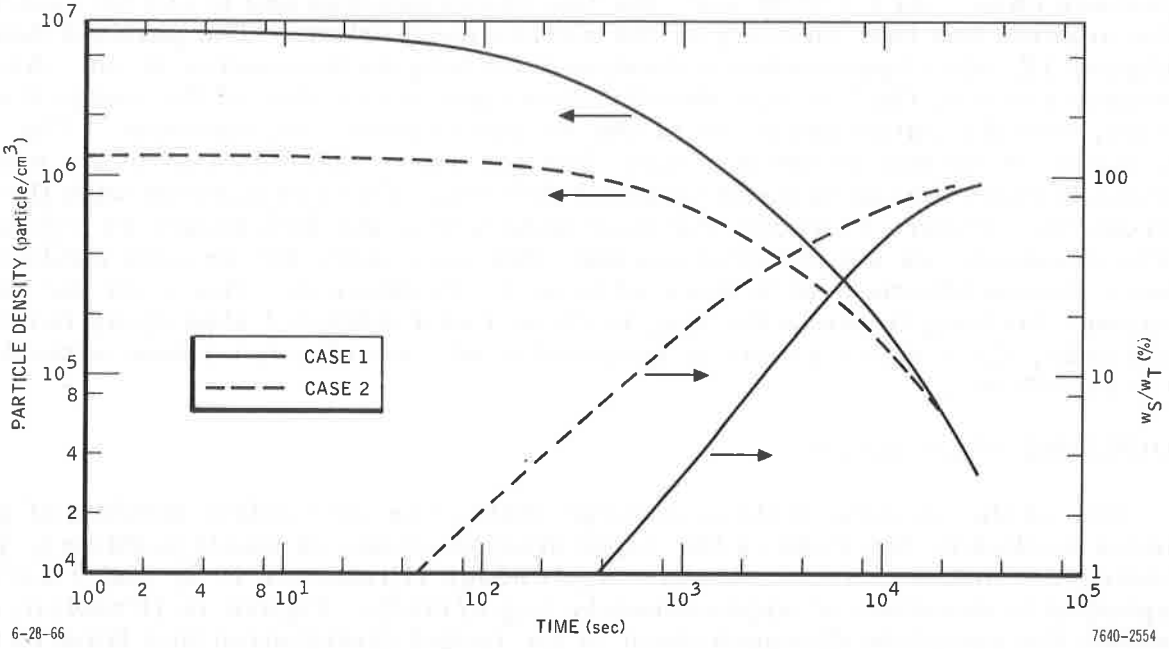

Figure 8. Time Behavior of Particle Density and Fraction of Settled Weight for Cases 1 and 2 of Problem 2

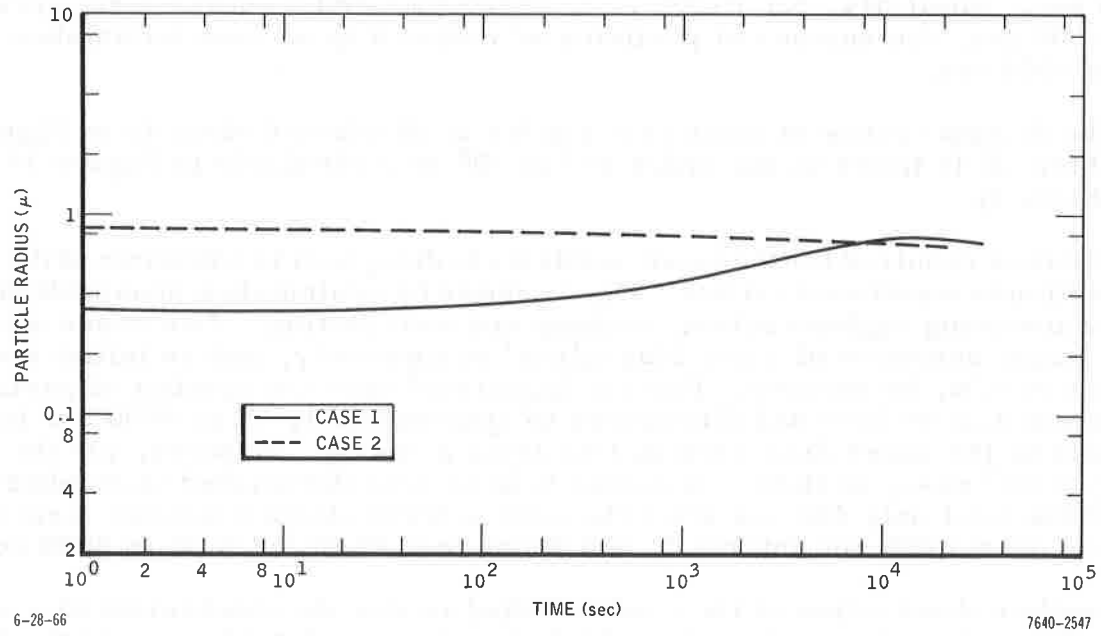

Figure 9. Time Behavior of 50% Radius by Volume of Suspended Component for Cases 1 and 2 of Problem 2

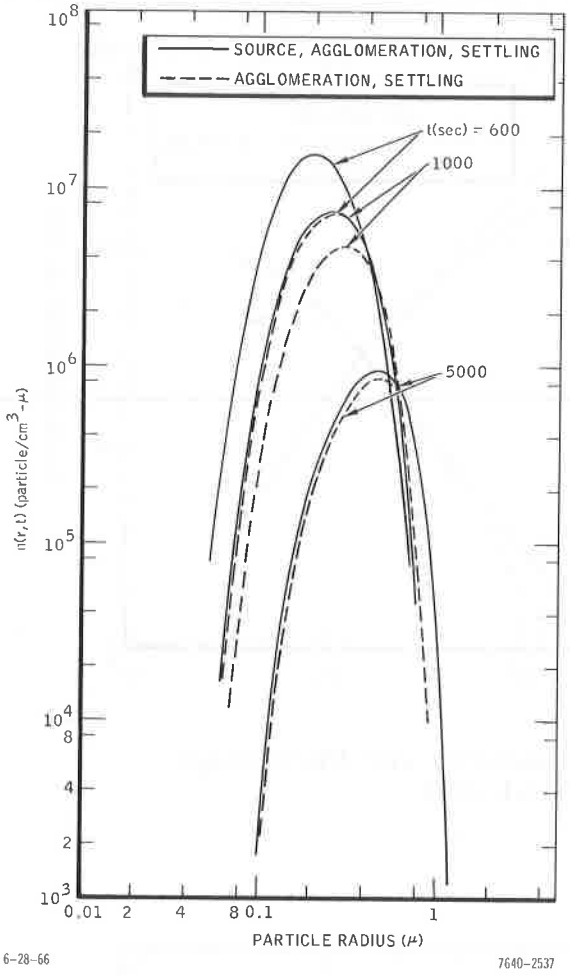

Figure 10. Particle Size Spectrum at Various Times for Suspended Component of Problem 3

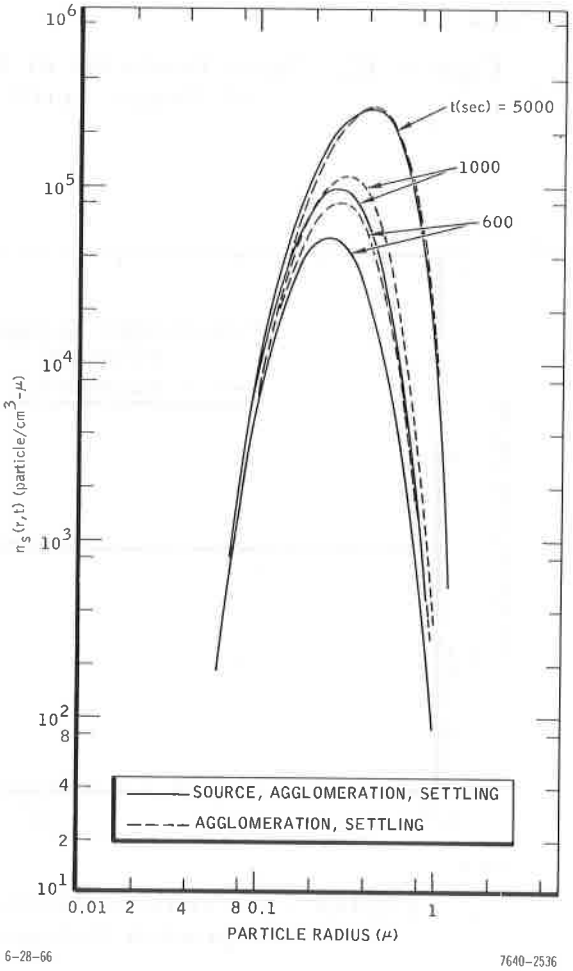

Figure 11. Particle Size Spectrum at Various Times of Settled Component for Problem 3

mass density present; this quantity will be proportional to the radioactivity present in the case when sodium is in the form of Na-24.

Code calculations are now being performed which include wall plating as well as settling and agglomeration. When obtained, these results will be compared to experimental findings for a relatively small closed chamber (volume $\sim 40\ ft^3$).

For some problems, Equation 1 may be approximated by simpler forms. For those cases in which a monosize distribution may be assumed, one may represent the rate of change of the total particle density, N(t), in terms of "monosize" agglomeration, settling, etc., as follows:

$$\frac{dN}{dt} = -K(r)N^2 - \frac{v(r)}{h} N - \beta(r)N \quad , \qquad \ldots(17)$$

where the first term represents agglomeration, the second, settling, and the last, wall plating. K, v, and β are all known functions of the radius, r. On account of the settling and plating, one may write for the volume of material in suspension, V:

$$\frac{dV}{dt} = -\frac{v(r)}{h} V - \beta(r)V \quad . \qquad \ldots(18)$$

V, N, and r are connected by the relation defining r:

$$r = \left[\frac{3V}{4\pi N}\right]^{1/3} \quad .$$

This set of equations may be solved with an analog computer, and comparisons made with code results for similar problems. Thus an evaluation will be made of the circumstances for which the simpler model may be adequate.

NOMENCLATURE

f	A constant
g	Gravitational constant
h	Height of settling chamber
K_0	Coagulation constant, $\frac{4kT}{3\eta}$
k	Boltzmann's constant
N(t)	Total number of particles in suspension at time, t
n(r, t) dr	Number of particles in suspension with radius between r and r + dr at time t
n_s(r, t) dr	Number of settled particles with radius between r and r + dr at time, t

11. G. M. Hidy and J. R. Brock, J. Colloid Sci. 20, 477 (1965)

12. G. M. Hidy and D. K. Lilly, J. Colloid Sci. 20, 867 (1965)

13. C. N. Davies, Supp. Trans. Inst. Chem. Eng. 25, 25 (1947)

14. H. L. Green and W. R. Lane, "Particulate Clouds: Dusts, Smokes and Mists," 2nd ed. (D. van Nostrand Co., Inc., Princeton, New Jersey, 1964)

MECHANICS OF COLLECTION OF PARTICLES BY INERTIA AND INTERCEPTION IN A FIBROUS AIR FILTER

By

Stanley V. Dawson

Department of Industrial Hygiene
School of Public Health, Harvard University
Boston, Massachusetts 02115

A B S T R A C T

An approximate expression is developed for the efficiency of collection of particles by small inertia force and by direct interception from an air stream around a circular cylinder. The field used to describe the fluid flow is in agreement with Darcy's Law for pressure drop through an array of cylinders. Efficiency is calculated by locating the grazing trajectory of a spherical particle. This location is determined by manipulating the equations of motion to facilitate an analytic approximation valid for small values of the impaction and interception parameters. Comparison of the predicted efficiency with values given in one experimental report proved inconclusive in assessing the validity of the prediction.

This study was performed in partial fulfillment of the requirements for the doctoral degree. The author was supported in part through a Training Grant from the Division of Air Pollution, U.S. Public Health Service, 5T1 AP 305.

b) $q = \frac{dy}{dt}$ (2)

x,y are the Cartesian coordinates of the particle,

u,v are the corresponding components of velocity of the fluid,

t = time,

$m = 4\pi h^3\gamma/3$ = mass of the particle

$B = 6\pi h\mu$ = Stoke's mobility of the particle

h = radius of the particle

γ = mass density of the particles,

μ = viscosity of the fluid medium.

According to equation (2a), the time derivative can be related to a space derivative by:

$$\frac{d}{dt} = p\frac{d}{dx} \qquad (3)$$

Using this expression in (1) and (2) removes explicit time dependence from the problem and makes it convenient to use dimensionless velocities which are referred to the upstream velocity, u_∞, of the fluid and to use dimensionless lengths which are referred to the radius L, of the cylindrical obstacle.

Let

$$p = u_\infty P, \qquad q = u_\infty Q,$$

$$u = u_\infty U, \qquad v = u_\infty V, \qquad (4)$$

$$x = LX, \qquad y = LY,$$

Three equations results from the substitutions (3) and (4) into (1) and (2):

a) $\varepsilon P \frac{dP}{dX} + P - U = 0$

b) $\varepsilon P \frac{dQ}{dX} + Q - V = 0$ (5)

c) $\frac{dY}{dX} = \frac{Q}{P}$

SPECIFICATION OF THE FLUID FIELD

The stream function that is used to characterize the field of velocity of the fluid in the present work was suggested as being appropriate at high porosity by Fuchs & Stechkina.[4]

$$\Psi = C \sin \theta . (1/2r^{-1} - 1/2\ r + r \ln r) \qquad (10)$$

where

$$C = (-\lambda - 1/2 \ln \alpha)^{-1} \qquad (11)$$

α = fraction of volume of fibers in the filter

$\alpha = \frac{\pi}{4} (\frac{L}{b})^2$ in the isotropic filter

b = average spacing of fibers transverse to the flow.

λ = 0.5 according to Happel[2]
0.75 according to Kuwabara.[3]

Expression (11) is in polar coordinates centered in the cylindrical obstacle of unit radius. Because a detailed analysis is to be given only for a stagnation region, that is the region $\theta \leq 0$, $r>1$, the origin of Cartesian coordinates is taken at the stagnation point $\theta = 0$, $r = 1$.

Thus

$$X + 1 = r \cos \theta, \quad Y = r \sin \theta. \qquad (12)$$

In the immediate vicinity of the stagnation point

$$\theta << 1, \quad X << 1.$$

So

$$\Psi = CX^2Y \qquad (13)$$

and

$$a) \quad U = -CX^2$$

$$b) \quad V = 2CXY \qquad (14)$$

The outer boundary of the approximation (13) is taken in this work to be at $X_1 = C^{-1/2}$, where $U = -1$. Then U and Ψ are made continuous by taking $U = -1$ for $X \geq X_1$.

which defines the trajectory together with (5a),

$$\varepsilon P \frac{dP}{dX} + P + CX^2 = 0 \qquad (20)$$

where U was given by (14a)

For $\varepsilon C^{1/2} < 0.2$ it can be shown that an accurate solution of (20) is simply

$$P = -CX^2, \qquad (21)$$

When this result is substituted into (19), then the significant part of the solution is

$$\Psi = \Psi_o (1 + 6\varepsilon CX) \qquad (22)$$

where Ψ_o is the limiting value of the stream function upon which the particle is riding after it has passed through the stagnation region. The use of the conditions (18) at X_1 gives

$$\eta_s = \Psi_o (1 + 6 \varepsilon C^{1/2}) \qquad (23)$$

Finally, under the above conditions it can usually be assumed that the particle continues on that same streamline around to the interception point on the top of the cylinder. So at $\theta = 1/2\pi$, set $r-1 = \frac{h}{L} << 1$, then

$$\Psi_o = C\left(\frac{h}{L}\right)^2 \qquad (24)$$

Thus for the assumed fluid velocity field the estimate of fiber efficiency is

$$\boxed{\eta_s = C\left(\frac{h}{L}\right)^2 (1 + 6\varepsilon C^{1/2})} \qquad (25)$$

where C is given by (11). It is emphasized that expression (25) is expected to be a good approximation for $\varepsilon C^{1/2} < 0.2$, and that it is certainly an upper bound on the efficiency in this range of $\varepsilon C^{1/2}$

REFERENCES

1. I. Langmuir, Report on Smokes and Filters, OSRD Report No. 865, 1942. Also in The Collected Works of Irving Langmuir, Vol. 10, 394-436.

2. J. Happel, Viscous flow relative to arrays of cylinders, A.I.Ch.E. J. 5, 174-7 (1959).

3. S. Kuwabara, The forces experienced by randomly distributed parallel cylinders or spheres in a viscous flow at small Reynold's numbers. J. Phys. Soc. Japan, 14, 527-32 (1959).

4. N.A. Fuchs and I.B. Stechkina, A note on the theory of fibrous aerosol filters. Ann. Occup. Hyg. 6, 27-30 (1963).

5. C.N. Davies and C. V. Peetz, Impingement of particles on a transverse cylinder. Proc. Roy. Soc. A 234, 269-95. (1956)

6. I. Gallili, On the filtration of aerosols by filter models of various porosities, J. Coll. Sci. 12, 161-72 (1957).

7. K. Tamada and H. Fujikawa, The steady two-dimensional flow of viscous fluid at low Reynold's numbers passing through an infinite row of equal parallel circular cylinders, Quart, J. Mech. & Appl. Math. 10, 425-32 (1957).

as larger drops if the velocity is high enough. Certain structural changes in the interstitial spaces have also been postulated. Efficiency and resistance appear to achieve equilibrium values during operation with liquid aerosols.

Aerosol filter performance for a particular application may be characterized by three factors: (a) the collection efficiency at the start of filtration, (b) the initial air-flow resistance caused by the clean filter, and (c) the changes in efficiency and resistance caused by accumulation of material during operation.

Several theoretical and experimental studies of initial collection efficiency of fibrous filters have been published. The components of a complete theory seem to be fairly well identified. It is possible to predict the initial collection efficiency of a clean fiber mat with limited success.

The air-flow resistance of clean fiber filters can be determined most simply by direct measurement. For flows at low Reynolds numbers, the resistance can be predicted by analysis in many cases. Extensions to higher Reynolds numbers and to the slip flow regime have been obtained.

The theoretical study of filter performance during operation has been largely neglected. The study described in this paper provides the basis for a quantitative explanation of fiber filter performance as a function of accumulation of solid particles.

Previous Experimental Studies of Filter Performance as a Result of Particle Accumulation

The effects of solid particle accumulation on aerosol filter performance have been studied experimentally by several investigators (3, 4, 5, 6, 7, 8, 9, 10, 11, 12, 13, 14, 15, 16). Most of these studies were performed with polydisperse particles in an attempt to simulate atmospheric dust aerosols for accelerated life tests. These data cannot be analyzed simply.

Some early studies of LaMer and coworkers (7, 9) were performed with monodisperse wax particles at constant velocities of $2.5 \leq U_o \leq 28$ cm/sec. Inlet aerosol particle concentrations (N_o) were varied somewhat during their tests $10^6 \leq N_o \leq 10^7$ p/cm^3. The recent study of Lindeken et al. (12) was performed with monodisperse polystyrene latex particles of radius $a_p = 0.182$ microns at inlet concentration of approximately 2×10^4 p/cm^3 and velocity of ~ 15 cm/sec.

Filter penetration data obtained by LaMer et al. (7) and by Lindeken et al. (12) are shown in Figure 1. The LaMer data were obtained on CC-5 filter paper composed of a rayon-cotton mixture with fiber radius $a = 6.5$ microns, filter fiber material density $\rho_m = 1.44$ gm/cm^3, depth of filter $L = 0.043$ cm and fiber fraction $\alpha = 0.128$. These measurements of filter media properties were apparently furnished by Walter J. Smith of Arthur D. Little, Inc., Cambridge, Mass. No specific information was furnished on the individual test filters. Properties of the analytical filter paper (Whatman 41) used in the Lindeken study were not reported.

Useful experiments on the increase of filter air-flow resistance during operation are limited to the work reported by LaMer and Drozin (9), and LaMer et al. (7). Their data are shown in Figure 2. Lindeken has stated that resistance measurements were not obtained during his test of filter efficiency.

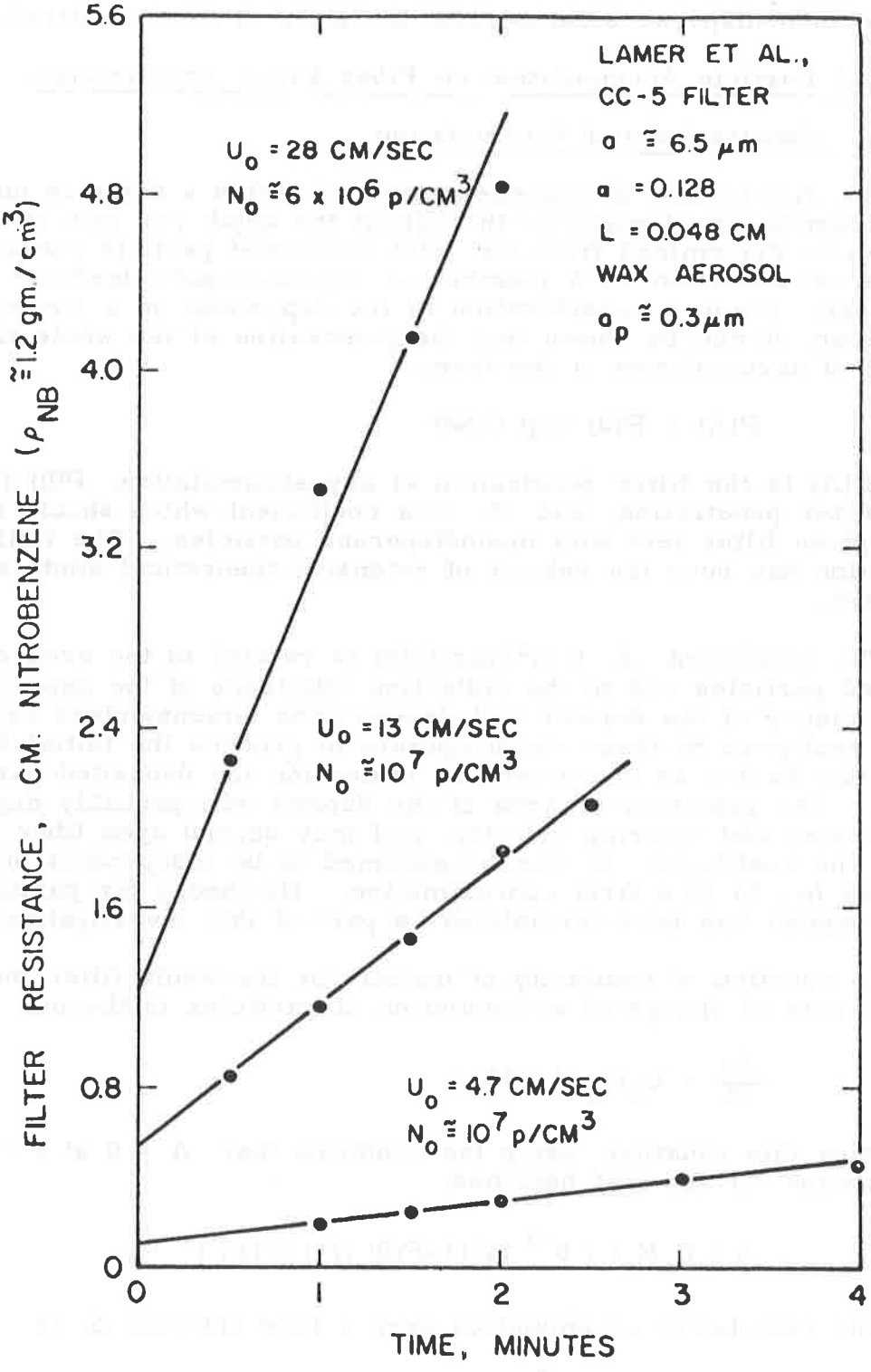

Figure 2. Filter Resistance During Operation

(b) Resistance and Accumulation

As particles accumulate on filter fibers and on previously deposited particles, the drag force on the combination will increase. Assume that the drag force consists of two independent terms: (1) the initial drag force on the fiber at the start of filtration, and (2) the drag per particle multiplied by the number of particles deposited locally. Upon setting the drag force per unit volume of filter mat equal to the pressure gradient, the filter resistance as a function of accumulation becomes:

$$\delta \Delta p = (S_p \mu U_o a_p) A \qquad (5)$$

where $\delta \Delta p$ is the change in filter resistance as a result of the accumulation of deposited solid particles, $(S_p \mu U_o a_p)$ is the assumed form for the drag per particle, S_p is the particle resistance coefficient, μ the gas viscosity, U_o the undisturbed fluid velocity, and a_p is the particle radius. The value of the particle resistance coefficient (S_p) has been determined from experiments described below.

As a first approximation, it has been assumed in equation (5) that the resulting drag of the deposited particles is independent of the characteristics of the filter material. It has been observed by others that, "Rapid clogging is more likely with materials of high packing density and fine fibers,...." (3, p. 103) and "Thick fluffy....materials....possess considerably greater dust holding capacity" (7, p. 213). These and similar observations (18, p. 332) indicate that there may be some effect on deposited particle resistance proportional to L, α, or a. Variation of the coefficient S_p with the filter depth (L) and fiber fraction (α) is discussed below. Effects of particle size (a_p) and fiber size (a) were not included in the present study.

EXPERIMENTAL APPARATUS AND PROCEDURES

To examine the functions developed in the previous section, several fiber filter mats were tested. Circles were cut (4.5 cm diam.) from laboratory glass wool lap. No binder, lubricant, or adhesive was present on the fibers (count median diameter 9.5 μm, σ_g = 1.07, > 10 cm long). Filters (0.11 cm thick) were formed from 1/3, 2/3 and 1 layer of the lap and were designed to provide essentially uniform particle deposition throughout the depth. The desired amount of filter media was weighed after dessication and then placed in the aerosol tunnel shown schematically in Figure 3. The filter was exposed to known concentrations of 1.305-micron diameter spheres* generated by spray-drying a suspension of monodisperse polystyrene latex particles.

Aerosol samples were taken up- and downstream of the test mat by means of probes containing membrane filters. Samples were analyzed by counting the number of individual particles in defined areas on the membrane filters. Inlet concentrations were maintained at about 10^3 p/cm^3. Filter efficiencies were generally 20 to 50%.

* 1.305-microns diameter polystyrene latex spheres, standard deviation 0.0158-microns, Run No. LS-464-E, kindly furnished for these studies by Bioproducts Dept., The Dow Chemical Co., Midland, Michigan (L. J. Lippie).

LEGEND FOR FIGURE 3

A. Liquid Sprayer for Particle Suspension

B. Silica Gel Drying Column

C. Aerosol-Ion Mixing Tee

D. Electrostatic Precipitator

E. Recording Millivoltmeter

F. Aerosol Tunnel Entrance

G. Aerosol Dilution and Mixing Section

H. Dilution Tube Bank

I. Extract Exhaust Line

J. Extraction Section

K. Upstream Sampling Probe

L. 16:1 Tunnel Contraction

M. Test Section

N. Test Section Static Pressure Taps

O. Downstream Sampling Probe

P. Main Exhauster

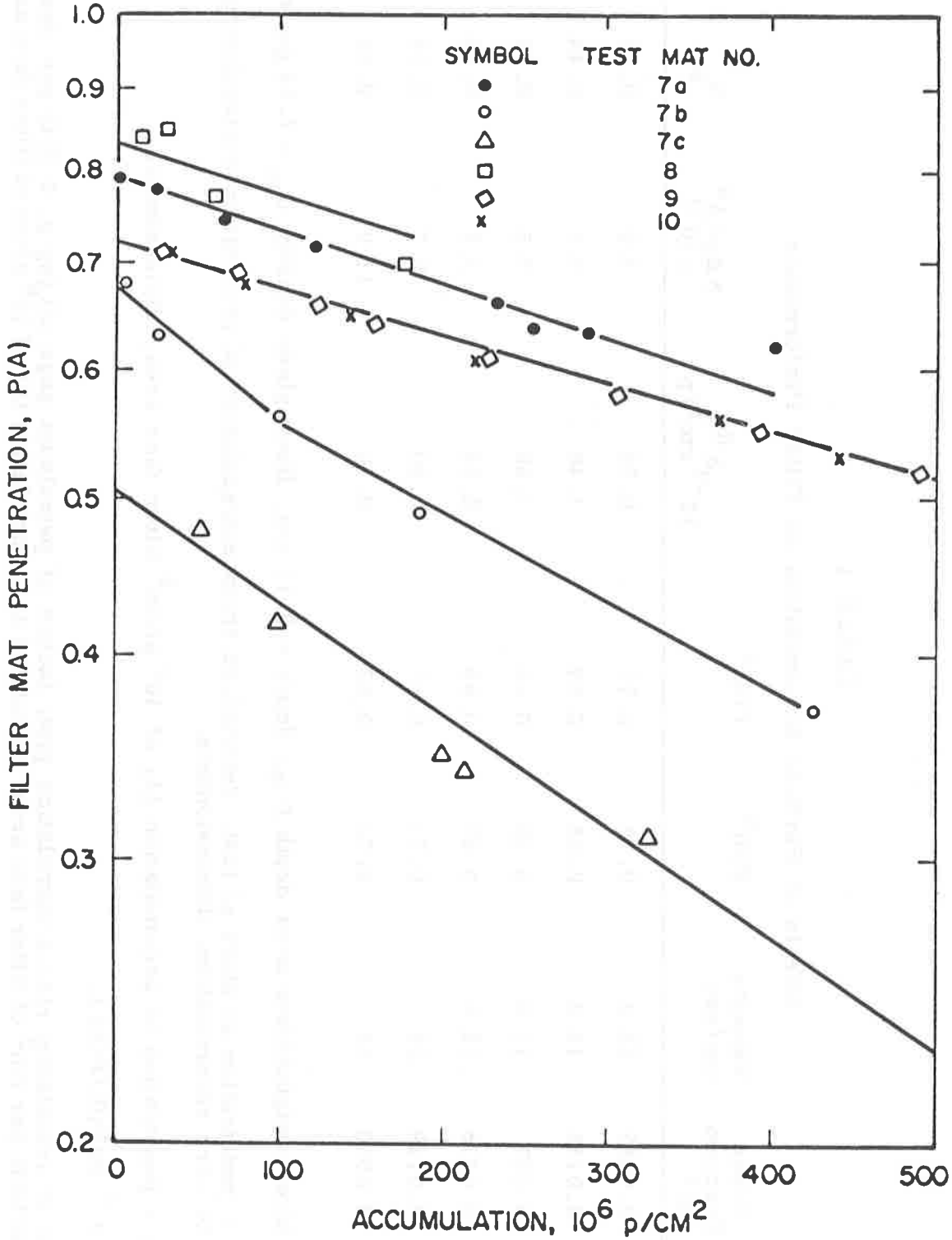

Figure 4. Penetration Decrease as a Result of Solid Particle Accumulation in Tests 7a-10.

velocities from the penetrations shown in Table 2. The average value of S estimated from the LaMer data was 0.51×10^{-9} cm^2/p, or slightly lower than the average found in the present experiments.

A similar calculation was made for the data of Lindeken et al. shown in Figure 1. The value of the particle accumulation coefficient was estimated to be about 5×10^{-9} cm^2/p, or slightly higher than calculated from the present study or from the work of LaMer et al.

Based on the results of these investigations of accumulation effects on penetration, a reasonable estimate of the order of magnitude of the accumulation coefficient is 10^{-9} cm^2/p ($0.18 \leq a_p \leq 0.65$). This implies that initial penetration will decrease by a factor of e^{-1} when the particle accumulation approaches 10^9 p/cm^2.

Effect of Particle Accumulation on Filter Resistance

Fiber filtration of an aerosol containing solid particles produces an increase in filter resistance as a function of the accumulation of particles. By assuming the drag force on each deposited particle contributes equally and independently to the total resistance, the increased filter resistance was estimated as:

$$\delta \Delta p = (S_p \mu U_o a_p) A. \qquad (5)$$

Experimental resistances were plotted at several values of accumulation for each test, as shown in Figure 5. The slopes of these lines ($\delta \Delta p/A$) and the calculated particle resistance coefficients (S_p) are presented in Table 1. The average value of S_p in these tests was 0.47 with a range from 0.33 to 0.95.

Particle resistance coefficients were plotted as a function of filter fiber fraction (α). A straight line was drawn among the 6 points, using as a basis the data for test nos. 7a, 7b, and 7c, and zero as the most reliable points. No attempt was made to apply statistical curve-fitting techniques. For these 6 tests the relationship between the particle resistance coefficient and the fiber fraction is reasonably represented by:

$$S_p = 33\alpha \qquad (6)$$

in the range $0.007 \leq \alpha \leq 0.027$. The resistance coefficient did not seem to be strongly influenced by filter depth or filtering velocity. Observations quoted previously indicated that the rate of resistance rise might be proportional to fiber fraction. This appears to be correct for this study. A more compact filter (higher α) produces a higher resistance per unit of accumulated material.

An analytical solution for the drag on one or more particles attached to a fiber in slow viscous flow has not been obtained. The velocity near the fiber is lower than the free stream velocity, and the coefficient S_p may be a function of the fiber and particle diameters. These effects were not investigated in the present study.

Resistance coefficients were computed from the data of LaMer (Figure 2). The resistance rise was estimated at one minute, as shown in Table 2. The average value of S_p was found to be 13.6. The estimated resistance coefficient based on an extrapolation of empirical equation (6) is 4.2 at the value of α reported in the LaMer study (0.128).

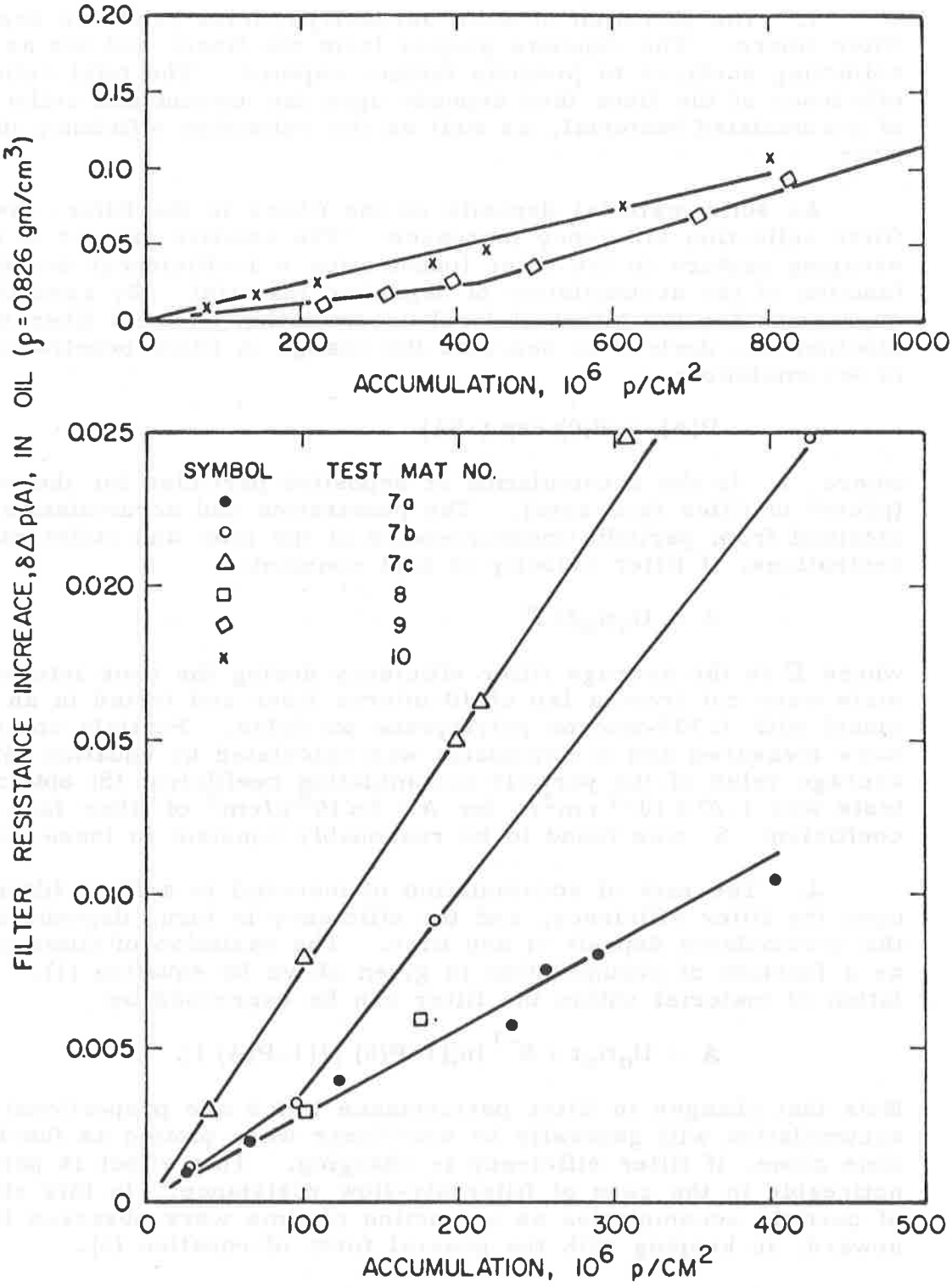

Figure 5. Resistance Increase as a Result of Solid Particle Accumulation in Tests 7a-10.

$$\delta\Delta p = (S_p \mu U_o a_p) A. \qquad (5)$$

The particle resistance coefficient (S_p) is unknown because the drag on multiple particle aggregates resting on fibers has not been solved. The resistance of experimental filters was observed as a function of accumulation. Values of the coefficient (S_p) were determined. It was found in the majority of tests that the coefficient was a function of fiber fraction, of the form:

$$S_p = 33\alpha \qquad (6)$$

for $0.007 < \alpha < 0.027$. The coefficient was not a function filtering velocity ($13 < U_o < 140$ cm/sec) or filter depth ($0.11 \leq L \leq 0.29$ cm) in the ranges studied. Effects of particle size and fiber size were not investigated.

4. Graphs of filter resistance-increase as a function of accumulation were generally linear. The general form of the resistance increase as a function of time should be concave upward, as long as the filter efficiency is changing with accumulation. When initial penetration is quite low, the second term on the right in Equation (3) is negligible. The change of resistance in high-efficiency media should be a linear function of time (at constant N_o, U_o, and a_p). Tests of Adley and Wisehart (11) for high-efficiency filter units seem to confirm this expectation (their figure nos. 5 and 6).

Applications of the Results

1. The results of this study can be applied to the design of filter systems to achieve an optimum balance between installation and capital costs, and operating and filter replacement costs. In practice, a filter system is designed and installed based on filter manufacturer's recommended air-flow. Filters are then operated until they "clog", that is, until filter resistance rises to some undesirable value. Filters then must be replaced or cleaned.

In general, filter efficiency is adequate for the designated task at the start of filtration, and an increase in filter efficiency as a result of accumulation is of no consequence. The governing economic consideration is filter "life" or the time required for the resistance to increase a certain amount. The results of the present research show that filter resistance resulting from accumulation is proportional to the accumulation and particle drag. Since accumulation is a function of U_o, the clogging resistance is approximately proportional to the square of the filtering velocity. For high-efficiency filters, a two-fold increase in the size of the initial installation of a filter system should produce approximately a four-fold increase in filter life. Effects of velocity on filter life (e.g. resistance rise) have been included in experimental studies of LaMer et al. (7, 9), Wisehart (10), Adley and Wisehart (11), and Dorman (3).

The relative cost of increasing the size of a filter system as opposed to more frequent filter changes depends upon capital charges and other considerations unique to a given system. It should be possible to optimize system design velocity with the information resulting from this study. The effect of velocity on filter efficiency has been well established.

$P(0)$ = filter penetration at start of filtration

S = a coefficient related to particle capture as a result of local particle deposition and geometry, cm^2/particle

S_p = a coefficient related to drag on deposited particles, dimensionless

U_o = undisturbed fluid velocity, cm/sec

a = radius of cylindrical fiber, cm

a_p = radius of spherical aerosol particle, cm

t = time, seconds

α = fraction solids, filter volume occupied by fiber

$\overline{\Delta N}$ = average difference in up- and downstream aerosol concentration during time interval Δt, p/cm^3

Δp = filter resistance to gas flow, $dynes/cm^2$

$\Delta p(0)$ = initial filter resistance, $dynes/cm^2$

$\Delta p(A)$ = filter resistance as a result of the accumulation of solid particles, $dynes/cm^2$

$\delta \Delta p(A)$ = change in filter resistance arising from the accumulation of deposited particles, $dynes/cm^2$, $= \Delta p(A) - \Delta p(0)$

Δt = a time interval, sec

μ = fluid viscosity, grams/cm-sec

μm = micron, 10^{-6} meter

ρ_b = fiber filter packing density, gm/cm^3

ρ_f = fluid density, gm/cm^3

ρ_m = filter fiber material density, gm/cm^3

ρ_p = aerosol particle density, gm/cm^3

σ_g = geometric standard deviation

BILLINGS: Well, I don't know; again, the model is uncoupled. If you put in one micron and then a five micron particle, the drag on the five micron particle is five times the drag on the one micron particle. I don't know how realistic this is; I really cannot answer it.

BURCHSTED: I think the theory is, if you have a uniform particle, it will coat the fibres more uniformly, whereas if you have a number of large particles, or perhaps lint in the dust, it will produce gaps between particles and give a tendency to longer filter life.

BILLINGS: Yes. We are going to get into a geometry problem in terms of what the deposit actually does in the filter, and I think it is a little too soon to try to analyze it. I think this kind of problem has certainly got to come up in theory, and later in stages of the development, as a deposit. I don't know how you handle it. Again, I really wouldn't care to predict what happens.

RIVERS: I think that the pressure drop data in the last slide indicated about a one per cent increase over initial pressure, or did I miss something?

BILLINGS: No, the pressurized data was plotted simply as the differential. I subtracted from that the initial pressure drop. The only thing you see is the drag of the particles there.

RIVERS: But weren't the data carried out only to the point of about one per cent increase over the initial resistance?

BILLINGS: No. For the filters I was using, I was doubling and tripling. I was using very, very thin filters.

RIVERS: I certainly agree with the conclusions of your paper. A couple of statements at the beginning from a practical case don't hold entirely. The statement that the efficiency goes up throughout the life of the filter is largely true.

However, in roughing filters, it is widely observed that the point comes where the filter will elute or pass collected dust. I believe Mitchell of Battelle, Columbus, did some studies which indicated this is also true for HEPA filters; that you can get to the state where a certain amount of migration results, and the efficiency then goes down. And when you look at the photograph #4, I think it is pretty obvious why. Little feathers break off and slowly pass through.

As to the other statement, that the resistance of filters has been resolved, I agree that this is largely true with regard to the media, but fortunately there is still room to develop better filter configurations, which includes flow geometry at the entrances and exits to the filters.

Discussion Contribution to Paper 4-4, by C. E. Billings,
Effects of Particle Accumulation on Aerosol Filter Life

by

H. C. Schwalbe

Dr. Billings, during the presentation of his paper, showed four electron microscope photographs of single glass fibers with polystyrene latex spheres extending normal to the fiber axis. Such chain like aggregation was found to increase air resistance of an aerosol filter.

A similar arrangement of pigment particles has been observed in studies of the mechanism of high opacity in printing or writing papers. Haslam[1] observed under the microscope the attachment of a single zinc sulfide particle to the cellulose fiber. This was followed by the rather strong bonding of the next zinc sulfide particles upon the first one in preference to an attachment to the bare cellulose fiber.

R. C. Johnson[2] described the deposit of 10 or more titanium dioxide particles in a column normal to the fiber axis.

Measuring light scattering and applying the Kubelka-Munk theory[3] establishes that such chain agglomeration reduces the opacifying efficiency of expensive Titanium Dioxide.

The writer[4] demonstrated that such agglomeration can be avoided. A new technique permitted to deposit individual titanium dioxide particles of 0.25 micron diameter upon the fiber. This increased the scattering coefficient of the pigment within the paper to far higher values than before. Novel ultra-thin cross sectioning of this paper by the Electron Microscopy Group of the Mead Corporation[5] confirmed the optical data. The pigment was present in the paper which had been produced on a high speed paper machine as individual particles of mainly 0.25 micron diameter, while some of these anatase titanium dioxide particles were as small as 0.07 micron.

An adaptation of this mechanism in aerosol filtration might well reduce the build up in air resistance and lengthen the filter life.

---

(1) Haslam, J. H. and Steele, F. A., Paper Trade Journal, 102 (2) 36-39, January 1936
(2) Johnson, R. C., TAPPI, 46 (5) 304-308, 1963
(3) Kubelka and Munk, Z. Techn. Physik, 12:539, 1931
(4) Schwalbe, H. C., "Consolidation of the Paper Web," Transactions of the Cambridge Symposium, September 1965 British Paper and Board Makers Association, London, England
(5) Electron Microscopy Group, Central Research, The Mead Corporation, Chillicothe, Ohio, Pictures published in Reference No. 4

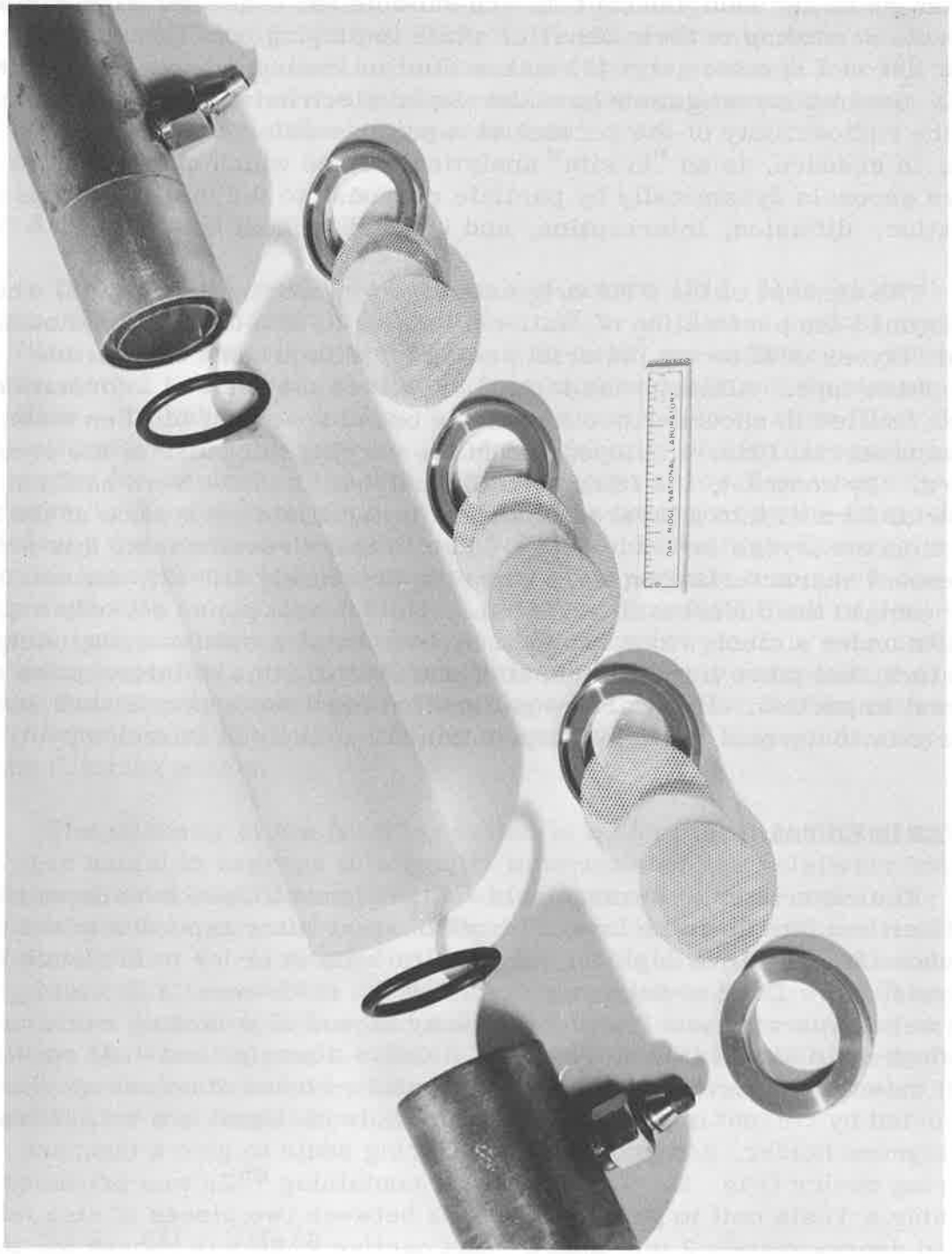

Fig. 1. Fibrous Filter Analyzer.

where N_o and N are the upstream and downstream particle concentrations, respectively, α is the volume fraction occupied by the fibers, L is the thickness of mat, and d_f the fiber diameter, all in consistent units.

The slopes of the linear portions of the distribution curves on a semilog plot such as Fig. 3 can be shown to be identical to the expression $(\ln N/N_o)/L$. The data plotted are the amounts of activity, A, deposited in the fiber bed per unit depth. When for an aerosol or for a single component of an aerosol the plot yields a straight line, then

$$\frac{d \ln (A)}{dL} = - a, \tag{2}$$

where - a is the slope of the plot. Integrating (2),

$$\ln (A) = - aL + I, \tag{3}$$

where I is the intercept at L = 0 on the plot.

$$A = e^{I} e^{-aL}. \tag{4}$$

But since the amount of activity deposited must equal the amount removed from the gas stream,

$$A = - dN/dL. \tag{5}$$

Substituting into (4) and integrating,

$$N = \frac{e^{I}}{a} e^{-aL} - c. \tag{6}$$

Since the data yields information about only those species which deposit in the filter, $N \to 0$ as $L \to \infty$, and c = 0. For L = 0,

$$N_o = \frac{e^{I}}{a}, \text{ and } (\ln N/N_o)/L = - a. \tag{7}$$

Table 1. The Effect of Packing Density on the Single Fiber Efficiency

v_o (cm/sec)	α Filter Volume Fraction Solids	η_T Experimental Single Fiber Efficiency
0.66	0.0408	0.0717
0.66	0.0804	0.0601
0.66	0.154	0.0303
1.8	0.0418	0.0283
1.8	0.0778	0.0280
1.8	0.131	0.0106
3.8	0.0373	0.0355
3.8	0.0779	0.0241
3.8	0.159	0.0172
4.9	0.0385	0.0345
4.9	0.0760	0.0346
4.9	0.155	0.0186
7.9	0.0384	0.0261
7.9	0.0769	0.0200
7.9	0.154	0.0141
7.9	0.154	0.0119
14.8	0.0368	0.0597
14.8	0.0703	0.0412
14.8	0.148	0.0198
29.6	0.0453	0.0571
29.6	0.0852	0.0102
29.6	0.158	0.0134
45.4	0.0472	0.0235
45.4	0.0897	0.0089
45.4	0.154	0.0076

Table 2. The Effect of Humidity on the Single Fiber Efficiency

v_o	Relative Humidity	η	Ratio W/D
0.66	2	0.0776	
0.66	100	0.121	1.56
2.0	2	0.0471	
2.0	100	0.0476	1.01
6.1	2	0.0395	
6.1	100	0.0476	1.20
10.8	2	0.0288	
10.8	100	0.0334	1.16
15.1	2	0.0248	
15.1	100	0.0332	1.34
21.0	2	0.0255	
21.0	100	0.0288	1.13
33.8	2	0.0421	
33.8	100	0.0379	0.90
35.7	2	0.0587	
35.7	100	0.124	2.11
43.3	2	0.0311	
43.3	100	0.0308	0.99
45.5	2	0.0785	
45.5	100	0.0654	0.83
322	2	0.0389	
322	100	0.0340	0.87
		Average	1.19

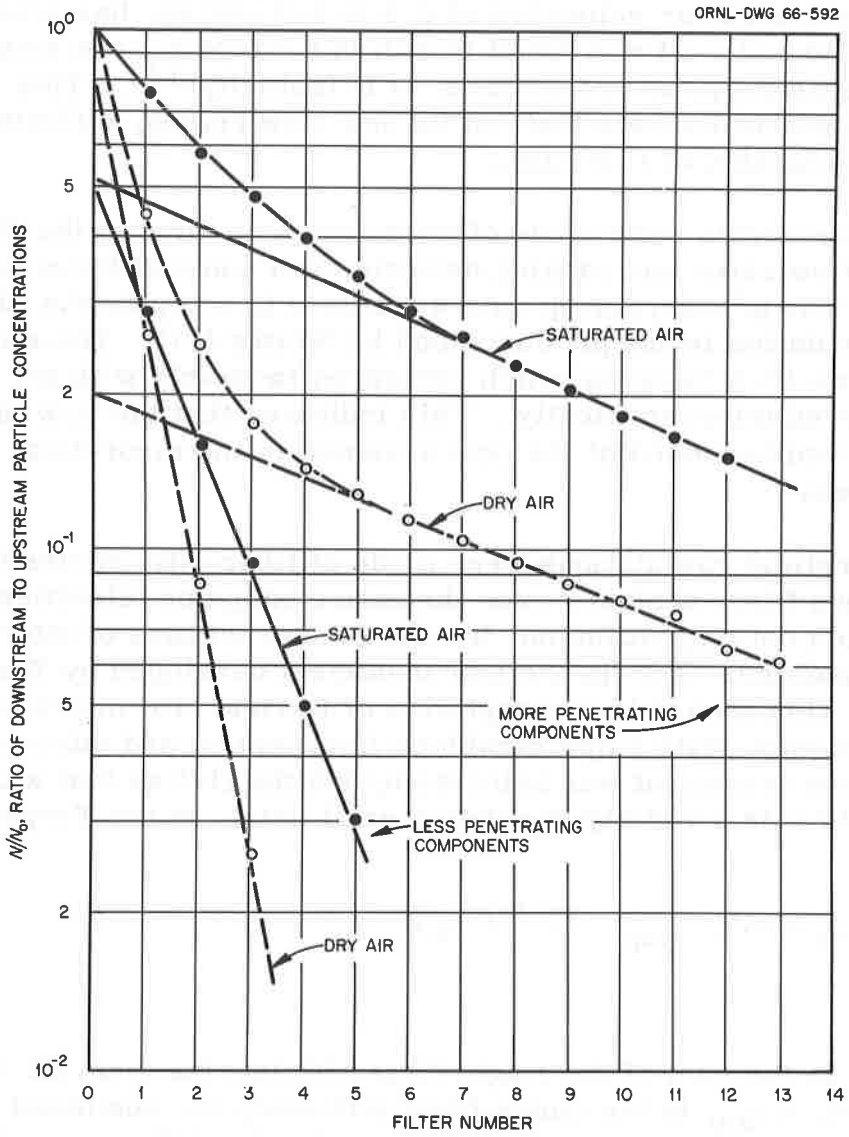

Fig. 5. Response of the Fibrous Filter Analyzer Under Wet and Dry Conditions at a Linear Velocity of 11.5 fpm.

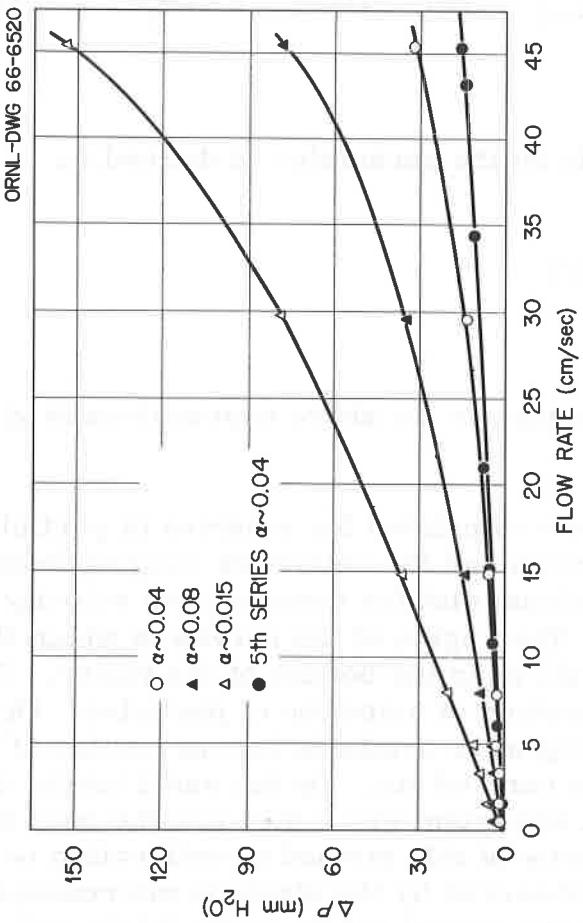

Fig. 6. The Effect of Packing Density on Pressure Drop for Varying Velocity.

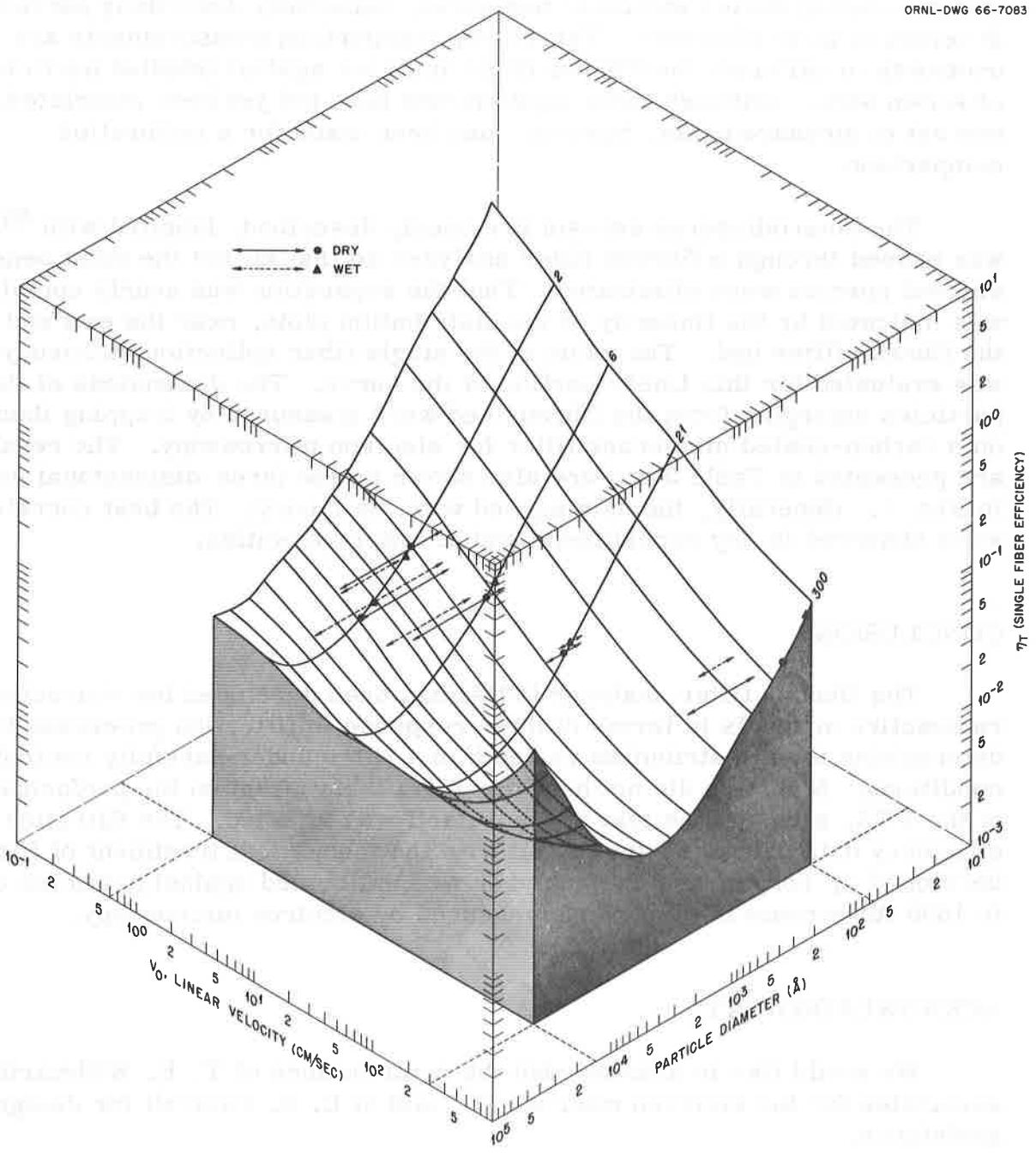

Fig. 7. Single Fiber Efficiency for Particle Filtration:

● ▲ Theoretical (Torgeson) and ⟶ ⟵ Experimental

Table 3. Comparison of Experimentally and Theoretically Determined Particle Diameters

v_o	Relative Humidity	η Experimental Single Fiber Efficiency	Particle Diameter Experimental EM Photo, A°	Particle Diameter Calculated A°
2.0	2	0.0413	2000	1700
2.0	100	0.0466	2895	1600
6.1	2	0.0395	1020	710
6.1	100	0.0476	2200	625
10.8	2	0.0288	300-600	750
10.8	100	0.0332	43 - 410	660
15.1	2	0.0249	150-1000	680
15.1	100	0.0332	3000-5000	600
21.0	2	0.0255	400-800	670
21.0	100	0.0284	400-600	600
35.7	2	0.103	70-500	130
35.7	100	0.0587	1450-3600	180
43.2	2	0.0311	500-2000	300
43.2	100	0.0308	500-5000	300
45.5	2	0.0785	300-3560	134
45.5	100	0.0654	740-3850	160
322	2	0.0389	200-700	100
322	100	0.0684	300-600	80

REFERENCES

1. K. R. May, J. Sci. Instrum 22, 187 (1945).

2. A. A. Andersen, "New Sampler for the Collection, Sizing, and Enumeration of Viable Airborne Particles," J. Bacteriology 76, 471-84 (1958).

3. A. Goetz and O. Preining, "Bestimmung der Grobenverteilung cines Aerosols Mittels des Goetz'schen Aerosolspektrometers," Acta Phys. Austriaca 14, 293-301 (1961).

4. M. H. Wilkening, "Natural Radioactivity as a Tracer in the Sorting of Aerosols According to Mobility," Rev. Sci. Instr. 23(1), 13 (1952).

5. V. Mohnen and K. Stierstadt, "Die Verteilung der Naturlichen Radioaktivitat auf das Grobenspektrum des Naturlichen Aerosols," Zeitschrift fur Physik 173, 273-293 (1963).

6. M. Gass, M. Saran and K. Stierstadt, "Das Grobenspektrum des Naturlichen Atmospharischen Aerosols," Zeitschrift fur Physik 185, 269-277 (1965).

7. R. S. Stuart, "The Analysis, Optimization, and Design of an Airborne Radiation Sampling Electrostatic Precipitator," Thesis, Master of Science, School of Engineering of the Institute of Technology Air University, May 1962.

8. K. T. Whitby and C. M. Peterson, "Electrical Neutralization and Particle Size Measurement of Dye Aerosols," I and EC Fundamentals 4, 66 (February 1965).

9. J. Sisefsky, "A Method for Determination of Particle Penetration Depths in a Filter," Nature 182, 1438 (1958).

10. M. D. Silverman and W. E. Browning, Jr., "Fibrous Filters as Particle Size Analyzers," Science 143, 572-3 (1964).

11. W. E. Browning, Jr., R. D. Ackley, and M. D. Silverman, "Characterization of Gas-borne Fission Products," pp. 155-162, Eighth AEC Air Cleaning Conference held at Oak Ridge National Laboratory, October 22-25, 1963, TID-7677.

12. M. D. Silverman and W. E. Browning, Jr., "Fibrous Filters as Particle Analyzers," Trans. Am. Nucl. Soc. 6(2) 401 (November 1963).

13. We thank the Cotton Spinning Laboratory of the University of Tennessee, Knoxville, Tennessee, for carding the Dacron fiber.

14. I. Langmuir, "Filtration of Aerosols and the Development of Filter Materials," OSRD Report No. 865 (1942).

PENETRATION OF SUBMICRON T1 BACTERIOPHAGE AEROSOLS AND BACTERIAL AEROSOLS THROUGH COMMERCIAL AIR FILTERS

J. Bruce Harstad, Herbert M. Decker, Lee M. Buchanan, and Melvin E. Filler
Department of the Army, Fort Detrick, Frederick, Maryland

ABSTRACT

A new method is described for evaluating air filters with submicron aerosols. The method is unique in that the aerosols were viable, highly concentrated, and composed entirely of submicron particles (0.1 micron NMD). Submicron aerosols were produced from concentrated aqueous suspensions of highly purified T1 bacteriophage. Tests were conducted to compare the effectiveness of several ultra-high-efficiency air filters in removing submicron T1 phage aerosols and bacterial aerosols of Bacillus subtilis var niger spores. The bacterial aerosols were composed mainly of single spores and had a NMD of 1 micron. Submicron aerosol penetration averaged $3 \times 10^{-3}\%$. Bacterial aerosol penetration averaged $7 \times 10^{-4}\%$. Architects, engineers, and research investigators concerned with the control of submicron particles might consider filtration rather than other methods of air cleaning.

I. INTRODUCTION

Filtration has been used extensively for removing microbial particles from air. Information on filter performance for microbial aerosols has been concerned mainly with bacterial aerosols in the 1-to-5-micron particle size range (Decker et al., 1962). There is a lack of critical information on filter performance for viral aerosols of a submicron particle size that can be attributed to the problems associated with the generation, sampling, and particle sizing of submicron viral aerosols. Initial studies by Decker et al. (1951) on the removal of bacteriophage from air by spun glass filter pads were conducted with an aerosol generator that produced aerosols in the 1- to 5-micron particle size range. The phage suspension used for aerosol production was not purified and the aerosol particles consisted mainly of the extraneous materials present in the suspension. The phage particles contributed little to the mass of the aerosols. Therefore, the filter efficiencies obtained were for virus particles with their associated menstrua rather than aerosols of a submicron particle size. However, with the advancement in aerosol technology, new techniques for virus purification and the development of improved aerosol generators such as the Dautrebande $D_{30}1$, it is now possible to evaluate air filters with submicron viral aerosols.

D. PHAGE AEROSOL TESTS

1. Phage Suspension

The virus used for the filter tests was T1 bacteriophage, one of the viruses parasitic to Escherichia coli, strain B. Aqueous suspensions of purified T1 phage were prepared by concentrating and purifying large volumes of broth cultures by differential centrifugation and washing with distilled water. This thorough cleansing of the phage suspensions was necessary to produce aerosols of minimal particle size. An electron micrograph of T1 phage particles from an aqueous purified suspension prepared by the phosphotungstic acid negative staining method of Brenner and Horne (1959) is shown in Figure 3. The purified phage suspension, used for evaluating the filters, titered 2×10^{11} phage/ml and contained 1×10^{-4} g/ml of Dextran 2000 (Pharmacia, Uppsala, Sweden) for enhancing the biological aerosol stability.

2. Phage Aerosol Sampling

The All-glass impinger (AGI-4) (Ace Glass Co., Vineland, N.J.) with a backup filter of ultra-high-efficiency filter paper was used to determine the phage aerosol concentrations before and after the test filter. The AGI-4 was filled with 22 ml of Bacto nutrient broth containing 0.06% Dow Corning Antifoam A (Dow Corning Corp., Midland, Michigan) and was operated at the maximum (approximately sonic) flow rate of 12.5 liters per minute. The backup filter, which collected the phage aerosol slipping through the impinger, was Type 6 and Type 5 Chemical Corps filter papers sealed in an in-line filter holder (Wolf et al. 1959). Chemical Corps Type 6 filter paper (Hollingsworth & Vose Co., East Walpole, Mass.) is an ultra-high-efficiency paper composed of Bolivian or African blue asbestos, esparto grass and kraft fibers. The Type 5 filter paper is a lower-efficiency paper of cellulose and asbestos fibers with a backing of cotton scrim. It was used only to support the more fragile Type 6 paper but was assayed with the Type 6 paper. Immediately after sampling, the filter papers were placed in 100 ml of Bacto nutrient broth containing 0.1% Tween 20 (Atlas Powder Co., Wilmington, Delaware) and then shaken for 15 minutes on a mechanical shaker to disintegrate the paper to pulp.

Flow rates of sampler air were calibrated with a wet test meter. The all-glass impingers were also calibrated for clearance of orifice to flask bottom and only those with a clearance of 4 mm were selected for these tests.

The phage aerosol particle size was determined by collecting a pre-filter aerosol sample on an electron microscope grid mounted in an electrostatic precipitator (Billings and Silverman, 1962; Morrow and Mercer, 1964). The grid was then examined in an electron microscope at a magnification of 7000 and the aerosol particles were photographed. Typical results are shown in Fig. 4 and 5. Figure 4 is a graph of a phage aerosol at 19% relative humidity showing the cumulative percentages by number and by mass plotted against particle diameter on log probability paper. The median diameters (50% intercepts) are 94 mμ NMD and 170 mμ MMD. Figure 5 is an electron micrograph of this aerosol.

ways: (a) electron microscopy of aerosol samples collected with the electrostatic precipitator and (b) phase microscopy of aerosol samples collected on membrane filters. Both of these methods revealed that B. subtilis aerosols were composed mainly of single spores and had a NMD of 1 micron.

III. RESULTS AND DISCUSSION

The penetration of phage aerosols and bacterial aerosols through air filters from four commercial manufacturers is compared in Table I. Dioctyl phthalate (DOP) penetration, obtained from the manufacturers, is also shown.

Overall mean phage aerosol penetration through ultra-high-efficiency filter units was $3 \times 10^{-3}\%$. The comparable value for the bacterial aerosols of B. subtilis var niger spores was $7 \times 10^{-4}\%$. Phage penetration through the ultra-high-efficiency filters is remarkably low and these filters will provide excellent protection against submicron virus aerosols. Design engineers concerned with the construction and remodeling of bio-medical research facilities in which infectious microorganisms are handled might consider ultra-high-efficiency filters instead of the more expensive air incinerators used in several laboratories. Only with a high concentration of pathogenic aerosols should serious consideration be given to some of the more complex and more efficient air purification systems.

The high-efficiency glass fiber filter material exhibited a mean penetration of 1.9% for the submicron T1 phage aerosols and 0.33% for the B. subtilis var niger aerosols. This is considered excellent for this category of filter and its application as a roughing filter or even as a final filter in certain laboratories might be practical.

Dioctyl phthalate (DOP) penetration shown in the table was stamped on each filter unit by the manufacturer and was verified by the DOP test apparatus at another government installation. The correlation among DOP phage, and bacterial penetration was not good. The DOP aerosol is a homogeneous fog of submicron particles that are uniform spheres of about 0.3 micron diameter. Phage and bacterial aerosols are heterogeneous in size and shape. The DOP method is useful for checking for possible major leaks resulting from damaged filters or inadequate sealing around the filters. Such leaks can be quickly detected by the DOP method and are usually in good agreement with bacterial leakage. However, with filters of ultra-high-efficiency such as those tested in this study, the DOP readings are near the bottom of the instrument scale, where background or noise level of the instrument precludes accurate measurement.

Table I. (Continued)

Description	Test Number	Relative Humidity %	Test Air Flow cfm	Filter Resistance in.water	Penetration T1 Phage %	Penetration Bacterial Spores d/ %	Penetration DOP e/ %
High-Efficiency Units							
0.5" thick fiber-glass pads containing 1.25μ diameter glass fibers	1	40 to 45	20 ft per min f/	0.50	1.8	0.23	
	2			0.50	2.0	0.26	
	3			0.51	1.9	0.50	
	Mean				1.9	0.33	

a/ T1 phage aerosol number median diameter (NMD) - 0.1 micron.

b/ B. subtilis var niger spore aerosol NMD - 1 micron.

c/ Pre-filter total sampler (impinger + backup filter) recovery - 10^6 phage/liter.

d/ Pre-filter cotton collector recovery - 10^5 spores/liter.

e/ DOP penetration as stamped on filter unit by manufacturer.

f/ Face velocity.

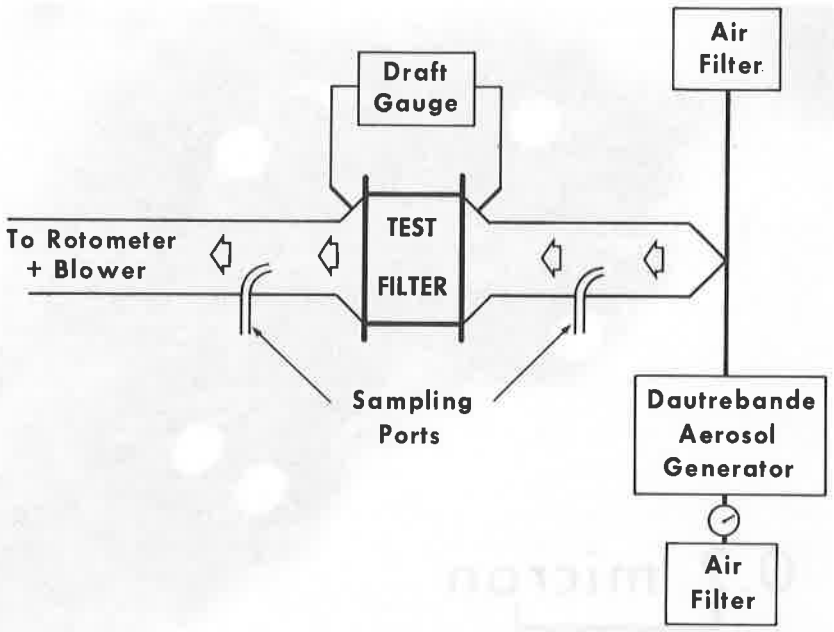

Fig. 2. Filter testing apparatus.

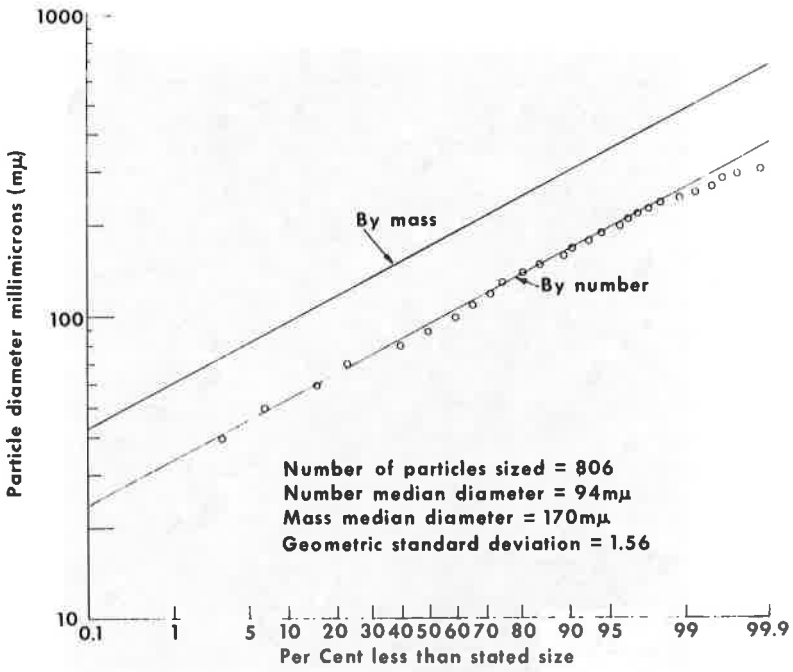

Fig. 4. Size distribution of T1 phage aerosol at 19% relative humidity dispersed with Dautrebande D_{30} aerosol generator.

LITERATURE CITED

Billings, C.E. and L. Silverman. 1962. Aerosol sampling for electron microscopy. J. Air Pollution Control Assoc. 12, 586-590.

Brenner, S., and R.W. Horne. 1959. A negative staining method for high resolution electron microscopy of viruses. Biochim. Biophys. Acta. 34, 103-110.

Decker, H.M., F.A. Geile, H.E. Moorman, and C.A. Glick. 1951. Removal of bacteria and bacteriophage from air by electrostatic precipitators and spun glass filter pads. ASHVE Journal Section, Heating, Piping and Air Conditioning. 23, 125-129.

Decker, H.M., J.B. Harstad, F.J. Piper, and M.E. Wilson. 1954. Filtration of microorganisms from air by glass fiber media. ASHVE Journal Section, Heating, Piping and Air Conditioning. 26, 155-158.

Decker, H.M., J.B. Harstad, and F.T. Lense. 1957. Removal of bacteria from air streams by glass fiber filters. J. Air Pollution Control Assoc. 7, 15-16.

Decker, H.M., L.M. Buchanan, L.B. Hall, and K.R. Goddard. 1962. Air filtration of microbial particles. U.S. Public Health Service Publication 953. U.S. Government Printing Office, Washington, D.C.

Fitzgerald, J.J., and C.G. Detweiler. 1957. Collection efficiency of filter media in the particle size range of 0.005 to 0.1 micron. Am. Indust. Hyg. Assoc. Quart. 18, 47-54.

Harstad, J.B. 1965. Sampling submicron T1 bacteriophage aerosols. Appl. Microbiol. 13, 899-908.

Morrow, P.E., and T.T. Mercer. 1964. A point-to-plane electrostatic precipitator for particle size sampling. Am. Ind. Hyg. Assoc. J. 25, 8-14.

Wolf, H.W., P. Skaliy, L.B. Hall, M.M. Harris, H.M. Decker, L.M. Buchanan, and C.M. Dahlgren. 1959. Sampling microbiological aerosols. Public Health Monograph No. 60. U.S. Government Printing Office, Washington, D.C.

PERFORMANCE OF FILTER SYSTEMS UNDER ACCIDENT CONDITIONS*

R. E. Adams, J. S. Gill, W. D. Yuille**, W. E. Browning, Jr., L. F. Parsly, and C. E. Guthrie

Reactor Chemistry Division, Oak Ridge National Laboratory, Oak Ridge, Tennessee

ABSTRACT

The effect of accident environments on the performance of filter systems is being studied on both a laboratory and a pilot-plant scale. In the laboratory the work has included the development of a simple method for generating a simulant aerosol, tests of these aerosols to determine their validity as simulants, and measurements, under various atmospheres, of the efficiency of high-efficiency filter media for removing these simulant aerosols. Moisture has been noted to have a significant effect on the behavior of the simulant aerosol. A limited number of large-scale filter tests have been conducted at the Nuclear Safety Pilot Plant.

Siting of nuclear power reactors is at the present time strongly influenced by the potential hazard of released fission products and only partial credit can be taken for gas cleaning systems. This is due, in part, to a lack of confidence in the performance of filter systems under reactor accident conditions and under subsequent accident environment. It is the purpose of this ORNL program to investigate under simulated accident conditions the effectiveness of various gas cleaning media and systems for removing particulate dispersions expected in accidents to reactors of various types. Because of the multiplicity of variables which must be investigated the major part of this study is being conducted on a laboratory scale using aerosols of proven validity as simulants. A limited number of larger-scale filter tests are being conducted in conjunction with experimental runs at the Nuclear Safety Pilot Plant (NSPP).

DEVELOPMENT OF A METHOD FOR SIMULATING REACTOR ACCIDENT AEROSOLS

Procedure - Arc Generator

A method was developed to generate in the laboratory an aerosol which is similar to aerosols generated in in-pile experiments as well as in the NSPP. A high-intensity arc, powered by a welding machine and struck between electrodes which simulate fuel materials, was investigated for this purpose. To date, tests have been conducted using arcs struck between carbon and stainless steel, carbon and stainless steel tubing packed with ZrO_2, two Zircaloy-2 rods, thoriated tungsten and a UO_2 rod, two UO_2

---

* Research sponsored by the U. S. Atomic Energy Commission under contract with the Union Carbide Corporation.

** Visiting scientist from United Kingdom Atomic Energy Authority.

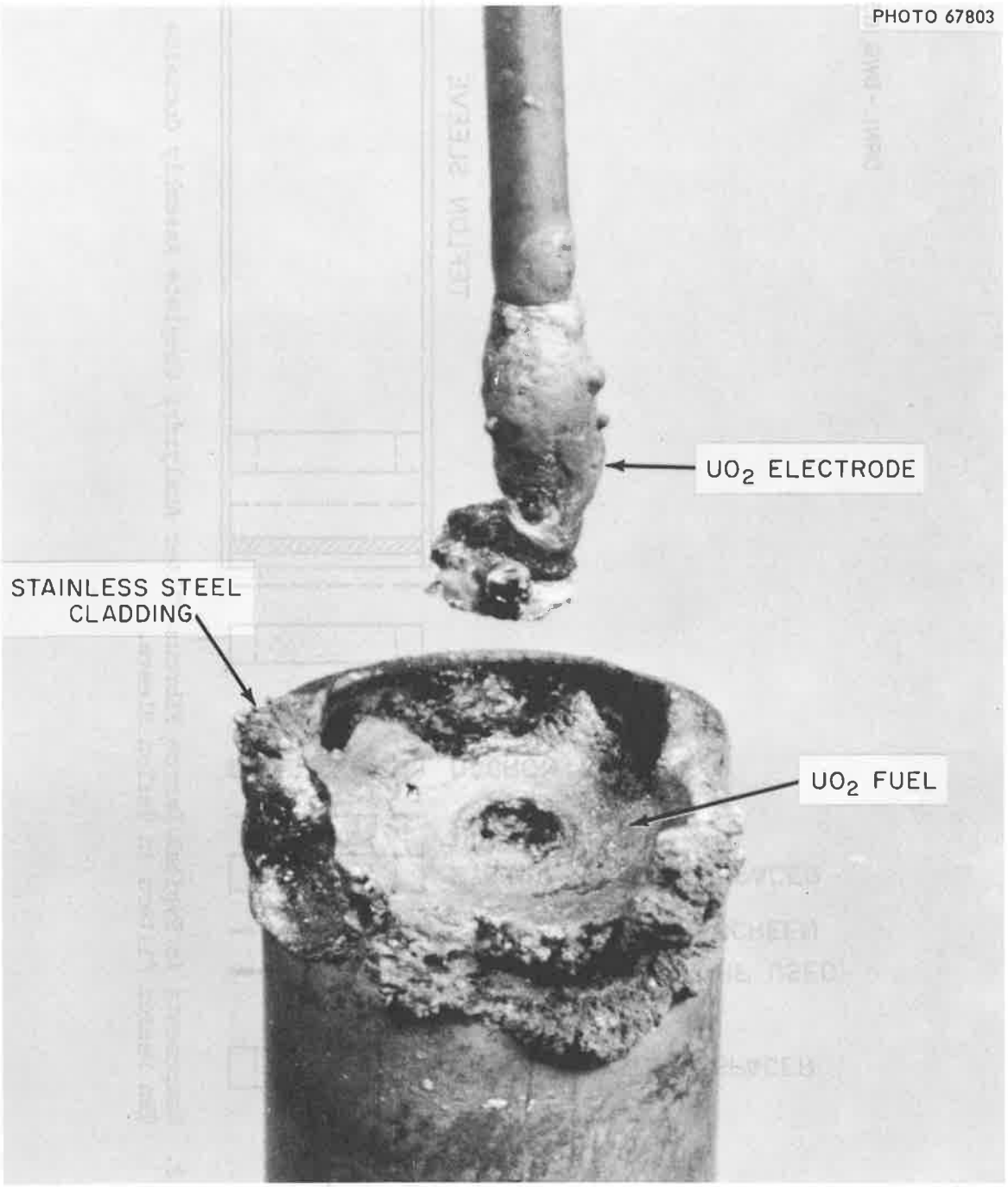

Fig. 1. Aerosol Generator which Simulates a Reactor Accident by Arc-Heating Electrodes of Uranium Oxide and Stainless Steel Packed with UO_2.

Early experiments indicated that when the aerosol from the UO_2 electrode system was processed through a fibrous-filter analyzer, two distinct particle size distributions were noted; this behavior was also noted in subsequent experiments. The distribution between size groups averages about 90% for the larger particles (Component A) and 10% for the smaller particles (Component B). As an example, Fig. 3 illustrates the distribution of particles in a helium atmosphere from an electrode pair consisting of a UO_2 bead on tungsten and UO_2 powder contained in an irradiated stainless steel tube. The compound nature of the distribution curves in Fig. 3, as evidenced by the lines having two distinct slopes, indicates the presence of two fairly distinct particle size groups in the aerosol. The similarity between curves indicates that the uranium and stainless steel are contained in or on the same particle or agglomerate. An electron micrograph from a similar experiment is presented as Fig. 4. The presence of single particles having a particle size ranging from 0.012 to 0.075 μ (median size, 0.018 μ) and of agglomerates should be noted. A particle size distribution (as determined from an electron microphotograph) of a similar aerosol is presented as Fig. 5. Particle size groups at the upper and lower limit of this size range could account for the distribution shown in Fig. 3.

The form of the uranium after volatilization in the arc was also studied. Under conditions where no oxygen is present (purified helium atmosphere), the uranium exists as UO_2; however, if oxygen is present, the predominant form is U_3O_8. The filtration behavior of each type was identical. In either form the simulant aerosol has been adequate for the needs of this study.

The similarity between aerosols produced by the arc technique and those produced by the in-pile melting of nuclear fuel is evidenced by their behavior in a fibrous-filter analyzer. For example, the distribution of cesium in Fig. 6 for the aerosol produced by in-pile fuel melting is quite similar to the distribution in Fig. 3, in that the presence of two particle size groups is indicated by the two distinct lines in the distribution pattern, and further that the relative quantities of the two size groups are similar. This, together with electron microscope data, indicates that these arc-produced aerosols are sufficiently similar to aerosols produced by fuel melting to quality as simulants for use in the laboratory.

EFFICIENCY OF HIGH EFFICIENCY FILTERS FOR AN ARC-GENERATED UO_2 AEROSOL

Dry Atmosphere

The effectiveness of samples of media from commercially-available high efficiency filters in removing simulated reactor accident aerosols is being tested under a filter evaluation program. In a typical test, an aerosol generated at two UO_2 electrodes was swept through a glass chamber (Fig. 7) by a stream of dry filtered air. Approximately 11 in. from the electrodes, the air stream (containing the aerosol) was split. One-half

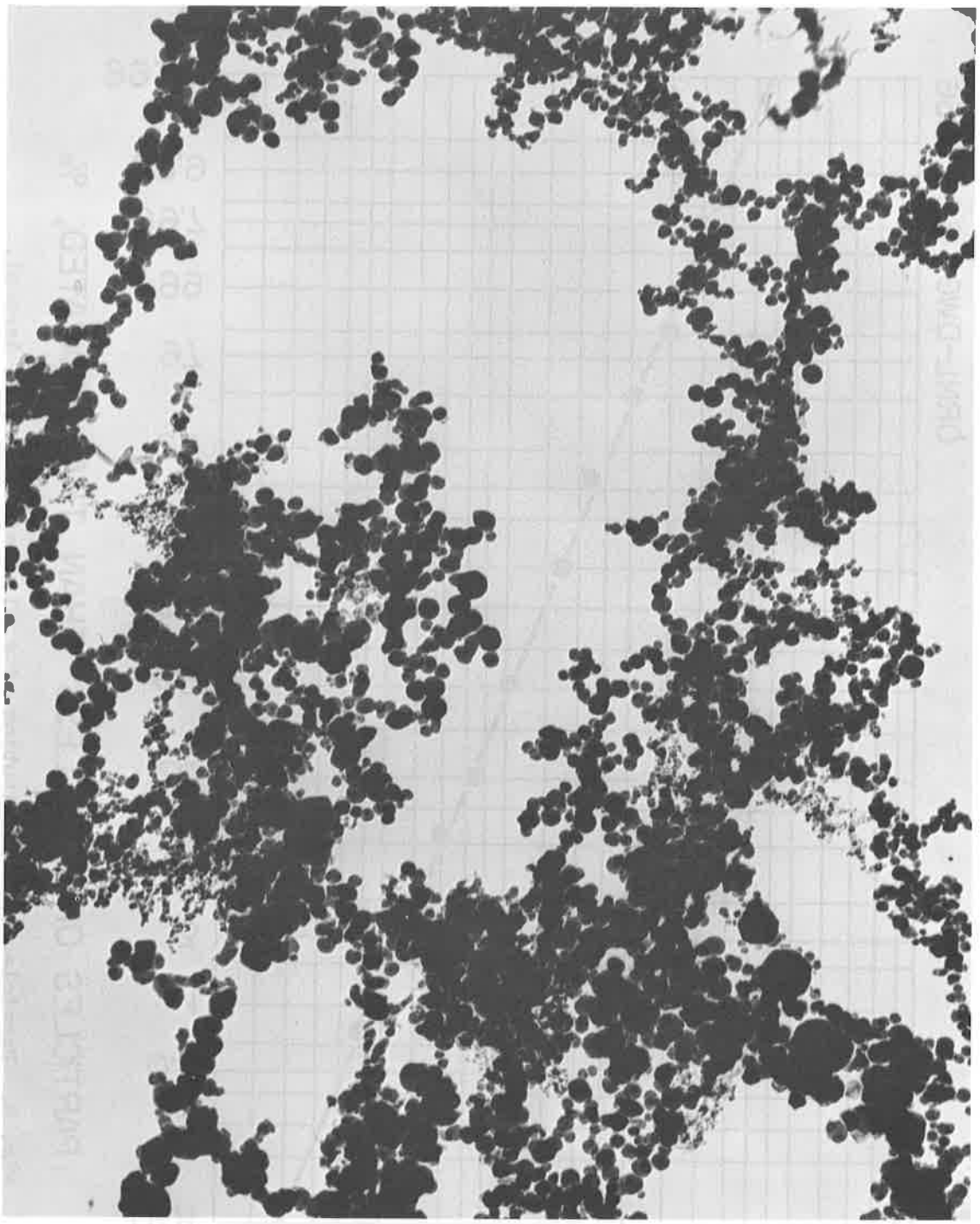

Fig. 4. Arc-Source Aerosol from Electrodes of UO_2 and Stainless Steel-Clad UO_2 in Helium Atmosphere; Particle Size, 0.012 to 0.075μ Median Size, 0.018μ (Magnification 132,000X).

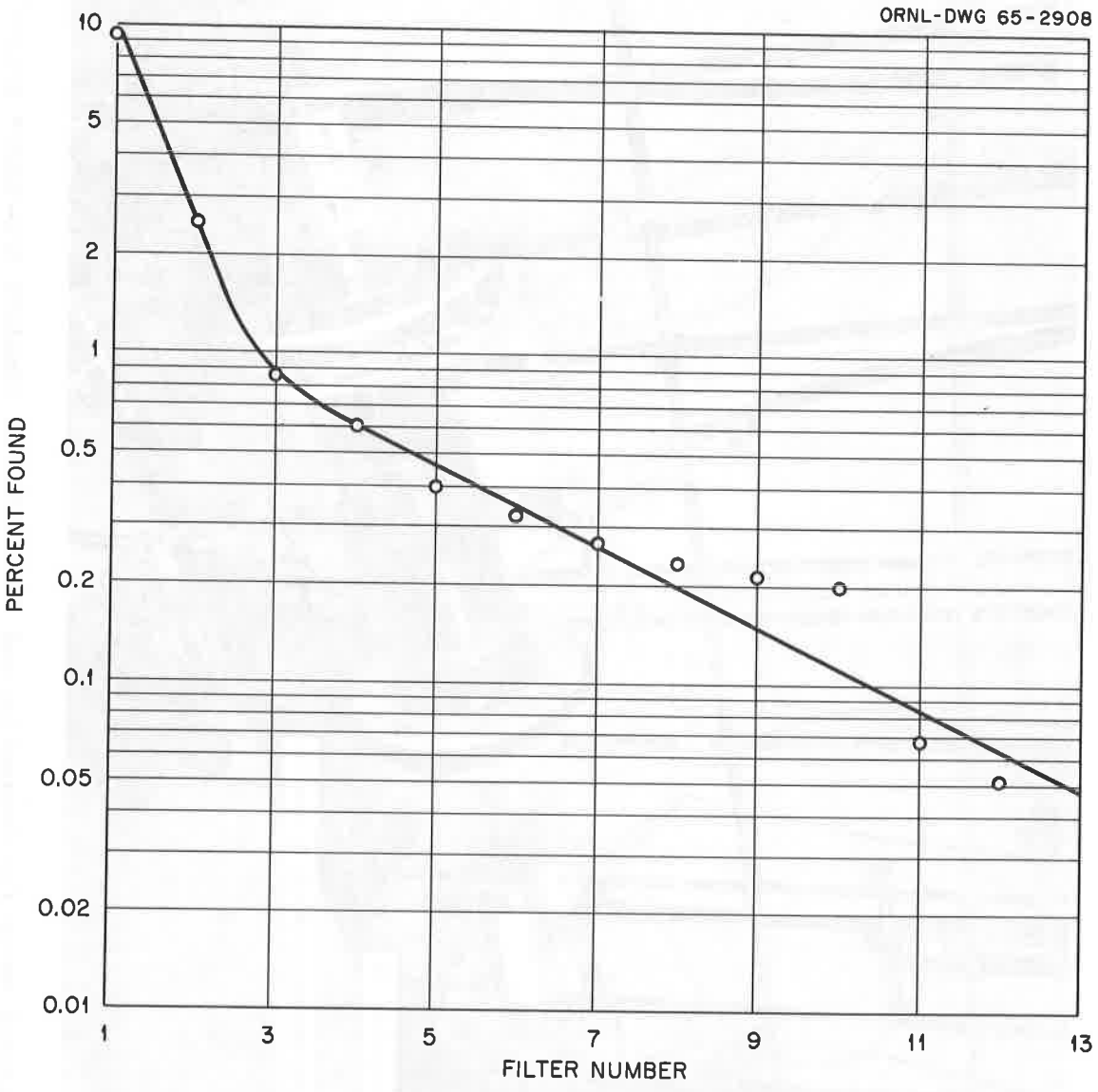

Fig. 6. Response of a Fibrous Filter Analyzer to ^{137}Cs in an Aerosol from In-Pile Melting of UO_2.

of the stream passed into a filter pack (white tubes, Fig.7) which contained a disc of high efficiency filter material, followed by ten Dacron filters of the FFA. The other half of the stream passed through ten Dacron filters of the FFA. This technique permits simultaneous filter evaluation and aerosol characterization. The material collected on the filters was analyzed for uranium by activation analysis using a delayed-neutron counting technique (2). The method is based on the fact that delayed neutrons are emitted from fission products produced by the interaction of neutrons with ^{235}U in the UO_2. In the present experiments, uranium containing 3% ^{235}U was used. With the proper choice of irradiation and counting times, a sensitivity of 1000 counts per 10^{-9}g of ^{235}U is obtained. The method can be used to analyze samples containing 10 to 10^{-3} μg of ^{235}U.

The distribution of the arc-generated particulate in the Dacron filters both preceded and not preceded by a high efficiency filter is shown in Fig. 8. As mentioned above, it appears that particles are distributed through the ten Dacron filters in at least two distinct size distributions, A and B. Mathematical analysis of the data from the experiment shows that the high efficiency filter has a filtration efficiency of > 99.99% for component A and > 99.91% for component B, under the experimental conditions described above.

Subsequent experiments were conducted on aerosols generated from UO_2 and stainless steel packed with UO_2 electrodes since that combination should most closely simulate melting of a reactor fuel rod. The analytical technique described above was altered in order to analyze for both uranium and stainless steel. Stainless steel was activated in a reactor and cooled to eliminate short-lived products. The major remaining activity was ^{51}Cr. When this stainless steel is used in combination with UO_2 to produce an aerosol, the resultant particulate on Dacron filters may be counted to determine stainless steel content, and then analyzed for uranium by activation analysis using delayed-neutron counting techniques. Thus, it was possible to determine filter efficiencies for the various sizes of particles containing the stainless steel and the UO_2.

The distribution of a smaller concentration of arc-generated particles in Dacron filters preceded and not preceded by a high efficiency absolute filter is shown in Fig. 9. In this experiment a U_3O_8 aerosol was used, and its concentration was made low by manipulation of the arc intensity. As mentioned above, it appears that particles are distributed through the ten Dacron filters in at least two distinct size distributions, A and B. Mathematical analysis of the data from the experiment showed that the Flanders absolute filter had a filtration efficiency of greater than 99.99% for component A and greater than 90% for component B under the conditions described. Because of the purposely low aerosol concentration, the filtration efficiency of the high efficiency filter for the B component could not be evaluated more precisely. Previous tests with higher aerosol concentrations indicated efficiencies of greater than 99.99% and greater than 99.91% for components A and B, respectively.

(Fig. 10) rather than clusters as observed under dry conditions (Fig. 4). Evidently the stability and filtration characteristics of these two types of aerosols differ in some respects.

To demonstrate moisture effect on the profile of a Dacron pack, an aerosol was generated in 1% relative humidity air; one stream continued under dry conditions, the other passed through a water bubbler before sampling. The deposition profiles are illustrated in Fig. 11. In another experiment the aerosol after passing the water bubbler was allowed to age before being sampled and, whereas in a dry environment this process would result in agglomeration, no agglomeration with aging had occurred in the wet aerosol. Next, an aerosol was generated in 80% relative humidity air, the steam divided, one-half being sampled in 80% relative humidity conditions, the other half passed through a water bubbler before sampling. Both fibrous filter analyzers gave similar flat profiles.

The conclusion from these experiments was that the presence of moisture is the governing factor and that it does not matter whether contact between the aerosol and moisture is established by bubbling through water or by mixing with water in the form of vapor in a high relative humidity atmosphere. The results also implied that the presence of moisture stabilized the aerosol and inhibited agglomeration. In experiments where an aerosol was produced in a dry atmosphere, subsequent passage through a water bubbler was presumably destroying agglomerates known by previous experience to have been found in the dry experiments. An alternative interpretation, of course, is that moisture was not affecting the physical size of the aerosol but was lowering the Dacron filtering efficiency. An attempt to resolve this question was made by generating in a wet atmosphere but sampling with a heated FFA to reduce the uptake of moisture by the Dacron fibers. In this experiment the aerosol formed in 80% relative humidity air was divided, one-half being sampled by the heated FFA, the other half, for comparison, was carried through a heated holdup vessel before sampling with a heated FFA. In this way the profile obtained by sampling a wet environment with a hot analyzer was compared with that of one sampled from a dry atmosphere with a hot analyzer. The flat distribution obtained from earlier experiments was not obtained and the conclusion drawn was that moisture must also reduce the efficiency of a Dacron filter; when the moisture content is reduced or eliminated by heating the analyzer, the Dacron filtering efficiency increases. However, a more complete comparison of the aerosol distribution through the two hot packs showed some differences. The FFA processing the wet aerosol showed a greater proportion of penetrating species on the final membrane filter of the analyzer and so tended towards a somewhat flatter profile than the FFA on the other leg. Although moisture was shown to affect the performance of Dacron packs, it must also operate on the aerosol to a certain extent. In the next experiment the aerosol concentration was reduced and again the difference between the two analyzers was apparent but not as pronounced. The results supported the conclusion of the previous experiment but also demonstrated that there is a concentration effect to be taken into account when considering the effect of moisture on the aerosol agglomeration mechanism.

Study of this moisture effect upon aerosols of uranium oxide and stainless steel and upon the filtration of these aerosols by high efficiency filter materials is continuing.

FILTER TESTS IN THE NUCLEAR SAFETY PILOT PLANT

A system has been designed and installed for the testing of high efficiency filter-charcoal bed combinations in the NSPP under accident conditions. Major components of the system include a demister, high efficiency filter, and a charcoal bed incorporated in a remotely removable canister (Figs. 11 and 12), a sealed compressor for gas circulation, and three May pack samplers. The system is designed for a flow of 20 cfm of steam and gas at 300°F and 50 psig pressure.

The demister design is based on the work of Peters (3). It contains a 2-in. thick style 321 SR York Demister (4) of Teflon (5) fibers (0.8 mil diam.) woven together with stainless steel wires (6 mil diam.). Velocities through the demister are up to 8 fps and the pressure drop is less than 1.0 in. H_2O. The high efficiency filter is a circular Flanders style 7C61R-q filter with aluminum separators and glass fiber filter media containing a binder to provide high wet strength. The pressure drop across a clean filter is about 1.8 in. H_2O. Two Flanders 11-in. square charcoal beds packed with Pittsburgh -12 + 30 mesh type PCB coconut-shell activated carbon are used for the final cleanup stage in the canister. To date, the loop has been operated in NSPP runs 10, 11, 12, and 14; runs 10 and 11 were primarily for deposition and transport studies in the containment vessel, with the filter loop operated as a secondary objective late in the runs to test the loop equipment and to obtain fission-product removal data from long-aged containment atmospheres. Run 12 was made primarily to test filter loop operation under conditions prevailing soon after an accident. Run 14 utilized actual irradiated fuel specimens for fission-product release and was operated under reducing conditions.

Briefly the runs have demonstrated that when fuel meltdown occurs under reducing conditions (steam and H_2 present), a large fraction of the iodine (~ 70%) is collected on the absolute filter. However, if fuel meltdown occurs under reducing conditions and moisture condensation is allowed to occur within the canister, then the iodine penetrates to the charcoal.

Run 10 - Furnace Atmosphere Reducing (He, H_2, H_2O), Steam-Air Mixture in Containment Vessel

Run 10 was the first run in which the filter loop was operated and was primarily a shakedown of the loop equipment and operation. The filter loop was therefore not used until very late in the run (12 hr) and was operated for 8 hr. The loop was operated without a demister since the demisters had to be returned to the manufacturer for repacking because of a deficiency in packing density. This did not compromise the performance of the loop, since at the end of 12 hr there was not appreciable moisture in the atmosphere. Because of the low initial level of activity and the rapid decrease after the start of the loop, the May pack samples taken around the

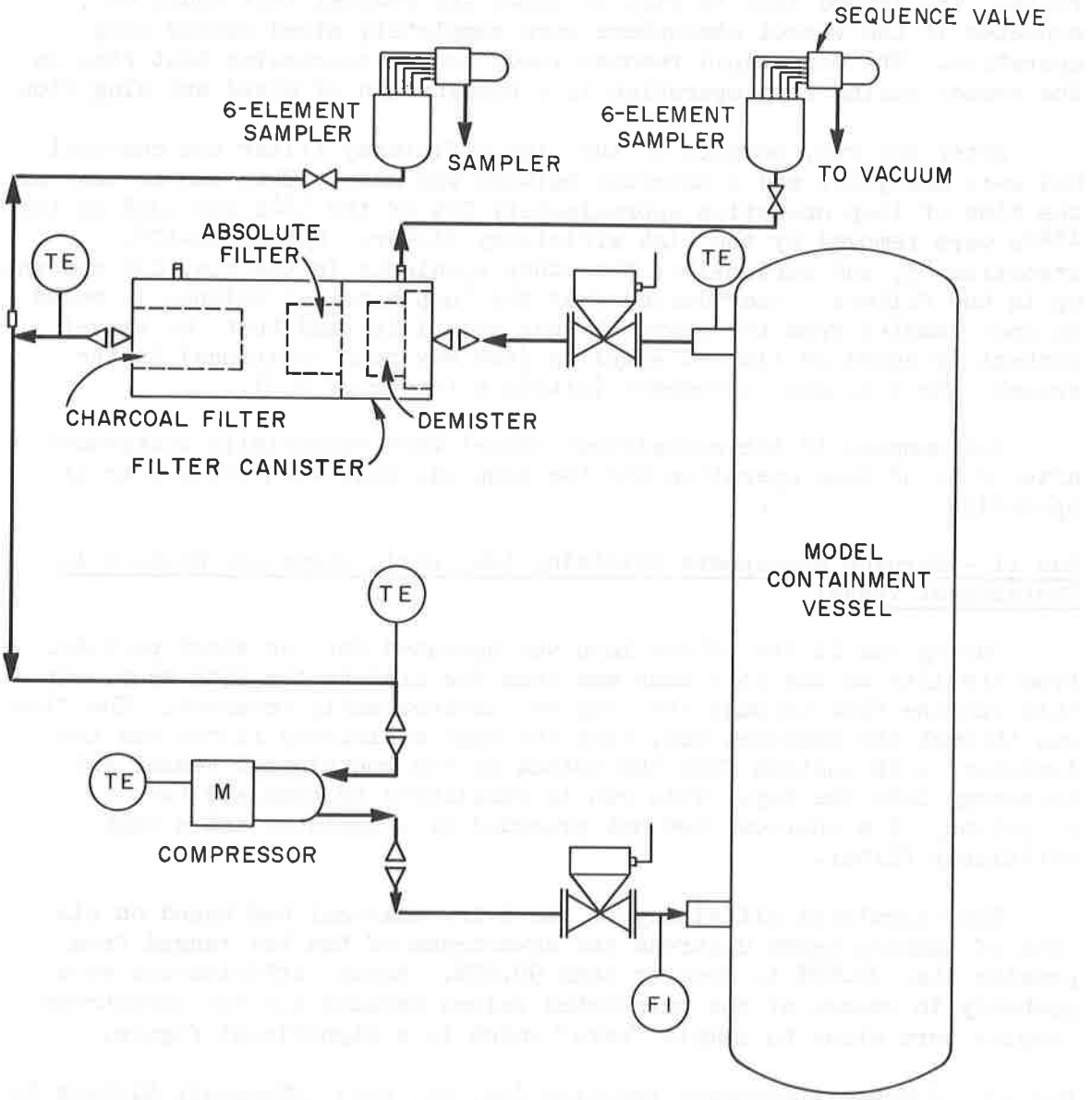

Fig. 12. Schematic Flow Diagram for NSPP Filter Tests.

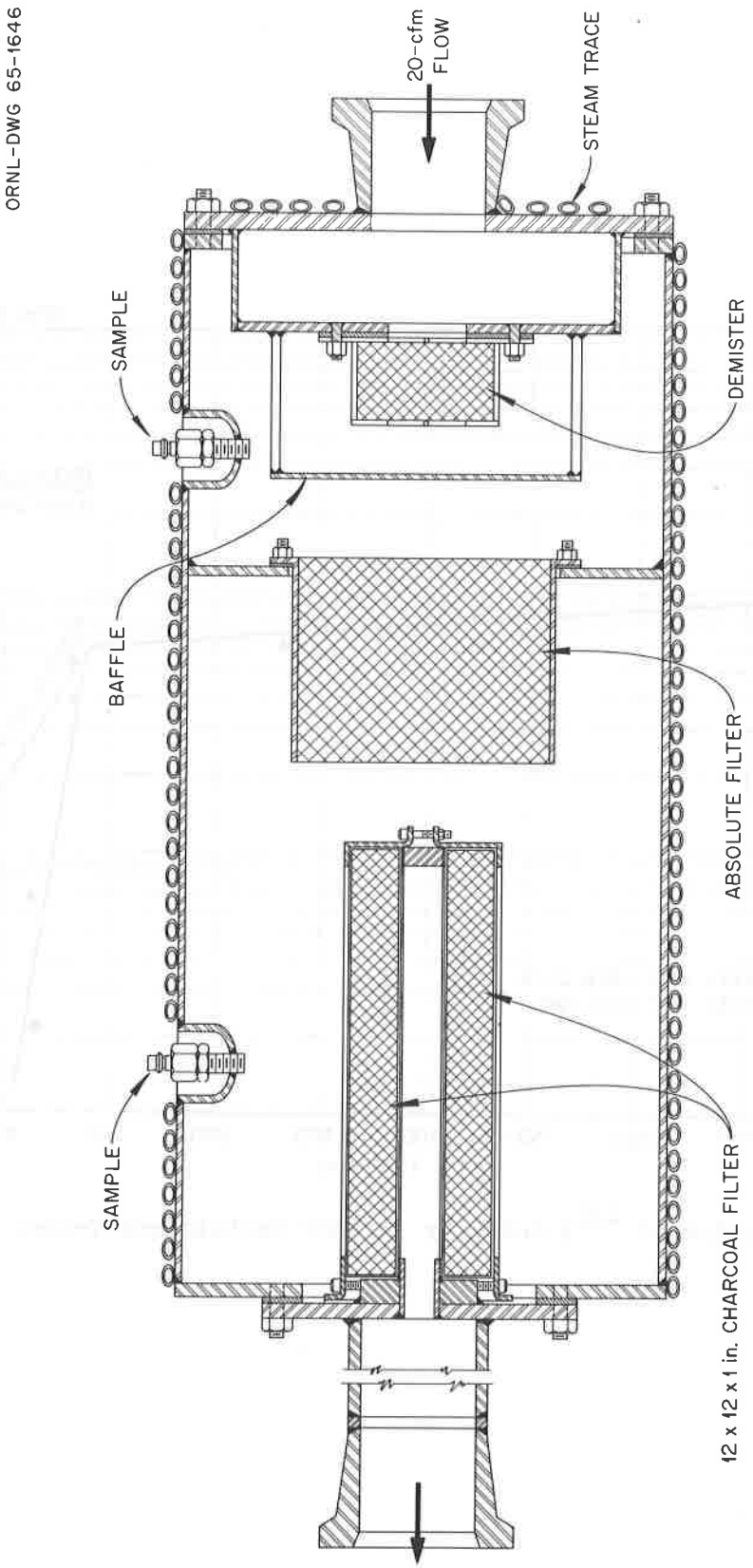

Fig. 13. Filter Canister for NSPP Filter Tests.

Very adverse conditions on the high efficiency and charcoal filters (maximum entrainment) were imposed by not heating the filter canister. The loop was operated continuously for 6 hr. There were 0.92 liters of dark-colored condensate found in the canister upstream of the high efficiency filter and 1.8 liters of clear condensate found downstream of the high efficiency filter. There appeared to be no damage to the high efficiency filter due to the condensing steam conditions.

The condensing steam conditions did interfere with the operation of the May pack samplers and no satisfactory sampling data were obtained. Therefore, the total amount of radioactivity in the filter, charcoal,and condensate was determined. Of the ^{134}Cs entering the loop canister, 0.7% was found on the demister, and 98.5% on the high efficiency filter, and 0.8% in the 0.92 liters of condensate between the demister and the filter; none was found in the charcoal. Of the ^{131}I entering the loop canister none was found on the demister or high efficiency filter; 7.3% was found in the 0.92 liters of condensate between the demister and the filter, 9.7% was found in the 1.8 liters of condensate between the filter and the charcoal filter, and 83.0% was found in the charcoal filter.

Run 14 - Furnace Atmosphere Reducing (He, H_2, H_2O), Steam-Air Mixture in Containment Vessel

This was the first of the NSPP runs with actual fission products from irradiated fuel specimens. Analytical results are not yet available from the samplers of the filter loop system.

COMMENTS

The effect of moisture on aerosol behavior and filtration efficiency has been demonstrated only in the laboratory. The low level of particulate radioactivity and the resultant loss of analytical sampling efficiency preclude such observations in the NSPP experiments. Primarily these NSPP experiments have been made to observe iodine behavior in a filter loop system. Other means will be sought to permit the study of the behavior of particulate aerosols in the presence of moisture to be performed on a somewhat larger scale.

REFERENCES

1. M. D. Silverman and W. E. Browning, Jr., "Fibrous Filters as Particle Size Analyzers," Science 143: 572-3 (1964).

2. F. Dyer, J. F. Emery, and G. W. Leddicotte, "A Comparative Study of the Neutron Activation Analysis of Uranium by Delayed-Neutron Counting," USAEC Report ORNL-3342, Oak Ridge National Laboratory, 1962.

3. A. H. Peters, "Application of Moisture Separators and Particulate Filters in Reactor Containment," USAEC Report DP-812, Savannah River Laboratory, December 1962.

isn't what we are primarily interested in. In the present paper, we are interested in the behavior of the particles in a filter system. The fibrous filter analyzer measures the particles in that respect. So, it doesn't really depend upon the calibration against zinc particles.

I have another item of information on the questions by Mr. Boyd a moment ago. The in-pile data that Adams presented was specifically from an experiment conducted with moist air at a dew point of 23° C.

GIESEKE: Another point along this line concerning the original question by Thomas. I think that the regime under primary consideration here is the diffusion regime and for this case the density of the particle has no effect on the deposition.

Have you any idea how reproducible your results are? Do you, say, split an aerosol into two parts and then analyze both parts under dry conditions so you get comparative measurements?

ADAMS: Yes. Early in our study we tested this and we did get reproducible depositions in fibrous filter analyzers on each part of the divided air stream.

THOMAS: I have a couple more comments. Some of them were quite large, of two or three microns. Certainly, you are going to have density effects; and I do think this test should be done on some other density aerosol.

THAXTER: If I recall Mr. Silverman's paper, they range from 30 or 40, up to about 15,000, a broad range.

BILLINGS: I would like to throw in a pitch for the product. What we see here may be an accumulation of effects. If you are considering a large experiment, a lot rides on it, and I mean a multi-million dollar one, you should look at the variation of filter efficiencies. As to a total number of particles, I have kind of a special feeling that kind of shape or curve is getting all the materials coming out on the first couple of filters, and then it is a gradual tapering off, maybe also due to the fact that efficiency of the first filter is getting better with accumulation. It's just a guess, though.

SILVERMAN: First of all, I would like to correct that statement that Thaxter made. Our theoretical calculations were made with that wide a range of particles, 60 to 13,000; actually, in the experiments, they ranged from about 30 angstrons up to 5,000. But the number at the upper end were usually quite small; furthermore, the statement by Gieseke regarding density, and to refer to Thomas' question previously, in our impaction calculations we used the value of a 10th for the density of zinc oxide aerosol because Kennedy and Nolan's data were heavy metals which indicated that the fine type of aerosol particles that are generated in this type of manner have a lot of entrapped air and, therefore, have low density.

Now, fortunately, in our experiments, the impaction effect was a minor effect because we had very few real large particles, but it does go up perceptibly if you get large parts of density. It then has a very important effect.

REIST: Just a very quick comment. The film around the particles which you noticed on your electron microscope photographs could possibly be due to wet particles being collected and then drying on the carbon film in the microscope. There is a reference on this, but I don't remember it.

REMOVAL OF PLUTONIUM HEXAFLUORIDE FROM CELL EXHAUST AIR BY HYDROLYSIS AND FILTRATION

by

Robert W. Kessie

Argonne National Laboratory

ABSTRACT

The fluoride volatility process for recovery of fissionable plutonium from spent reactor fuel as the volatile plutonium hexafluoride (PuF_6) requires a demonstrated ability to contain the highly toxic plutonium.

The experimental studies indicate that at low concentrations of PuF_6 and moisture, the hydrolysis reaction rate is directly proportional to both the partial pressure of the PuF_6 and moisture and to the area of the solid surfaces available for reaction. Adsorbed PuF_6 and HF reduce the reaction rate at partial pressures greater than 0.001 mm Hg.

At high concentrations of PuF_6 and moisture, the reaction proceeds rapidly in the gas phase to produce a finely dispersed product PuO_2F_2. Most of the particles are smaller than 0.1 micron. With air containing excess moisture, the fraction of released plutonium penetrating two high-efficiency filters in series amount to between 10^{-9} and 10^{-6} at a filter-media velocity of 1.0 cm/sec.

Filter efficiency is increased by the agglomeration of particles before filtration and by loading effects of the collected particles on the filters. When an excess of moisture is available, agglomeration effects tend to limit the maximum discharge rate of plutonium, and loading effects tend to limit the maximum total quantity of plutonium that can be discharged from a single filter.

INTRODUCTION

PuF_6 is the only known compound of plutonium having a significant vapor pressure at room temperature. Because of the extreme toxicity of plutonium-containing materials, highly effective means of containing of these materials are essential. The containment requirements for PuF_6 are magnified by its high volatility (b.p. 62°C). At present, 50-g batches of PuF_6 are being handled in process-development studies, and this quantity is expected to increase to kilogram amounts within a few years.

Engineering-scale facilities are in construction[1] for demonstrating the fluid-bed fluoride volatility process for reprocessing nuclear reactor fuels at Argonne National Laboratory, Oak Ridge National Laboratory, and the nuclear center at Mol, Belgium. In this reprocessing, the uranium and plutonium in the spent fuel are separated from the cladding materials and the fission products, and are recovered as their hexafluorides.

The maximum permissible concentration of plutonium in air is 3×10^{-8} mg of Pu^{239} per cubic meter.[2] This is the concentration of occupational exposure of 40 hr/week, 50 week/year, for 50 years that will result in a maximum permissible body burden of 0.6 μg.

The ventilation air from gloveboxes, shielded cells, or other enclosures containing experimental or process equipment in which PuF_6 is handled, will be discharged to the atmosphere after cleanup and not returned for a second pass through the cell. The main reason for the use of this once-through type ventilation system is the difficulty of removing trace quantities of fluorine and other fluorides, which, in a recirculating type system, would build up and corrode equipment, principally glass surfaces needed for viewing inside the enclosure. This effect would be significant even at concentrations of the fluorides that are safe for discharging to the atmosphere. Plutonium hexafluoride will not be intentially released, however accidental release to the enclosure is possible.

Plutonium hexafluoride, when released to the atmosphere reacts with the moisture in the air to form fine particles (diameter <0.1 μ) of PuO_2F_2. Up to 60% of the plutonium will remain airborn. With other plutonium compounds, this extent of dispersion can only be produced under special conditions.

The combination of high dispersibility and low permissible concentration usually requires a reduction in plutonium concentration by filtration or other processes by a factor of less than 10^{-6}. This high performance is beyond that normally reported in the literature for air-cleaning equipment, not because the equipment cannot be made to perform, but because their performance in this range cannot be readily measured. For example, the dioctyl phthalate (DOP) smoke test to evaluate the performance of AEC filters does not measure filter penetrations less than 10^{-5}. Because of the lack of experience in determining the effectiveness of filters in removing particulate material from gas streams in situations requiring very low penetrations, an intensive study was conducted to evaluate the performance of filters with PuF_6-air mixtures.

HYDROLYSIS REACTION OF PLUTONIUM HEXAFLUORIDE

When PuF_6 reacts slowly with moisture at room temperature, a solid product is formed, which was identified as PuO_2F_2 by x-ray diffraction isomorphism with UO_2F_2[3,4] and by weight change on conversion to dioxide.[4] Contact of PuF_6 with liquid water or moist air produces a violent reaction, accompanied by flashes of light, forming PuF_4 and PuO_2.[4] These products are likely to be formed because of the high temperatures generated. Above 300°C, PuF_6 is rapidly decomposed to PuF_4 and F_2.[5] No information is available on the thermal decomposition of PuO_2F_2, but UO_2F_2 decomposes to U_3O_8 above 300°C.[6]

In the current work, up to 20 mg of pure PuF_6 has been rapidly (<2 sec) injected into air containing up to 10 mm Hg of moisture without any evidence of the flashes of light from the reaction. The solid product from several of these releases was collected for obtaining the x-ray powder pattern. It was concluded that the reaction between PuF_6 and air of normal atmospheric moisture content yields PuO_2F_2 according to the equation.

$$PuF_6(g) + 2H_2O(g) \rightarrow PuO_2F_2(s) + 4HF(g).$$

THE BURST-TYPE RELEASE

The initial experimental program was designed to simulate the sudden release of pure PuF_6. This type of release has the potential for releasing more material in a shorter time than other types of releases. The majority of the PuF_6 in any operating system is normally in a condensed state in a cold trap or storage vessel; further, the only diluting component in the major source of PuF_6 in existing systems is UF_6. Consequently, the current investigation centered on a study of the behavior of these hexafluorides in their releases, either individually or in mixtures.

Experimental Equipment and Procedure

The equipment used for the release of PuF_6 (Figure 1) consists of a glass mixing chamber attached to a heated enclosure. Within the heated enclosure is a valved, release vessel, which contains the PuF_6 to be used for determining the filter efficiencies. The release vessel is so mounted that upon opening the valve the material contained in the vessel is discharged into the 385-ml, glass mixing chamber. Air enters the mixing chamber through the air prefilter containing AEC-type filter medium. The moisture content of the air that enters the mixing chamber is controlled by mixing dry air with air that has been humidified. The humidity of the air entering the mixing chamber is measured with an automatic dew-point recorder.

The filter series used for these experimental determinations consisted of two glass fiber filters (AEC type), mounted in positions 1 and 2, a water-filled bubbler, and two Millipore-type AA filters, mounted in positions 3 and 4. Small circular discs (37-mm diam) of the filter media, mounted in plastic aerosol sampler cartidges, were used for these tests. The bubbler was found to be effective in humidifying the air and completing the hydrolysis of the hexafluoride when the air input to the mixing chamber was dry and did not contain enough moisture to complete the hydrolysis before the material passed through the first two filters.

Alpha counting of the filter media and plates of the bubbler solution was done with an Eberline Instruments Corporation scintillation alpha counter, model SAC-1. This instrument has a combined geometry and counting efficiency of approximately 40% for the samples counted. The gamma counting of the samples was done with a single-channel pulse-height analyzer in the energy span of 11 to 22 keV.

When the PuF_6 was released, smoke from the hydrolysis reaction was immediately visible in the mixing chamber. An air flow of 0.54 liter/min removed the smoke from the mixing chamber within 3 min. A fraction of the smoke settled on the wall of the mixing chamber and was visible as a white deposit concentrated in the lower part of the mixing chamber. Very little deposit was observed in the lines or on the walls of the filter cartridges. The distribution of material deposited on the first filter appeared very uniform and the deposit was light brown. The color was not evident in the mixing-chamber deposit, apparently because of its low density.

The size distribution of particles resulting from the vapor-phase hydrolysis of PuF_6 was determined. The particulate matter was produced from the release of 6.0 mg of PuF_6 into a 385-ml volume, containing air at 1 atm and water vapor at 7.66 mm Hg. An electrostatic precipitator collected particles formed by the vapor-phase hydrolysis of PuF_6.

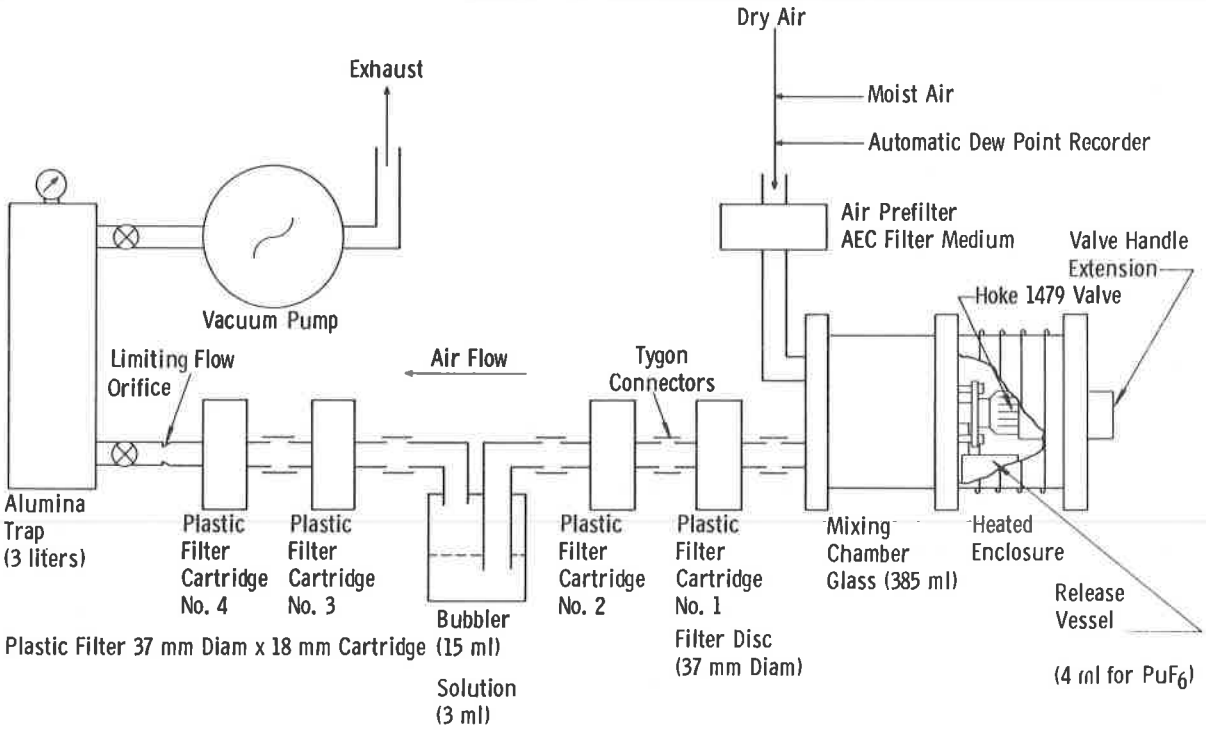

Fig. 1

Equipment for Studying Plutonium Particulate Filtration of AEC Filter-media Discs

Results and Discussion

The results from PuF_6 release experiments are given in Table 1 and are plotted in Figure 2. The data in Figure 2 show considerable scatter. One source of this variation is the different amounts of PuF_6 released into the moisture-containing atmosphere. The resulting differences in the particle concentration may affect the filtration by two mechanisms:

a. The particles of the hydrolysis product may agglomerate at different rates before reaching the filter.

b. Solid product may accumulate on the filter at different rates and may thereby affect the filter efficiency.

To obtain an improved correlation of filter efficiency by including the amount of PuF_6 released, mathematical models were developed for the processes of agglomeration and of filtration under loading (see Appendixes A and B). These models may also indicate the range of operating conditions in which the effects of agglomeration and filter loading are appreciable. These models may be used as a basis for estimating the experimental conditions under which agglomeration and filter loading have important effects on filtration efficiency. For this application of the model, information is required about the surface area and size of the fume particles and the filter medium.

Figure 3 is an electron-microscope picture of the material collected by using the electrostatic precipitator. The measured particle-size distribution of the unagglomerated particles is given in Figure 4. The particle-size distribution is accurately described by a logarithmic normal-frequency distribution with a geometric mean diameter of 0.0171 micron and a geometric standard deviation of 2.24. The mass mean particle size is 0.12 micron.

An electron micrograph of a very thin section cut from the surface of the filter media is shown in Figure 5. It indicates the wide range of fiber diameters and the regularity of the individual fiber diameters. The frequency distribution of fibers measured from several of these electron micrographs is given in Figure 4. The internal surface area of the filter media is 77 times the superficial area, as computed from the frequency distribution of fibers, and is in agreement within 10% of that measured by the BET nitrogen adsorption method on the same filter media used for the electron micrographs.

Substitutions of measured variables in the expression derived in Appendixes A and B for the agglomeration and loading numbers result in

$$a = 0.50 \frac{w_o}{\rho_p R d_p^3} \left(1 + \frac{0.18}{d_p}\right) \quad (1)$$

$$L = 0.68 \frac{w_o}{\rho_p A d_p} \ln (1/P_o), \quad (2)$$

where w_o = mass of PuF_6, mg; ρ_p = density of PuO_2F_2, g/cm^3; d_p = diameter of particle, microns; R = gas flow rate, cm^3/sec; and A = superficial area of filter media, cm^2. For $\rho_p = 6.5$ g/cm^3, $d_p = 0.1$ micron, and $P_o = 10^{-4}$,

Table 1

FILTRATION RESULTS FROM PLUTONIUM HEXAFLUORIDE RELEASE

Air Velocity at Filters: 0.97 cm/sec
Mixing Chamber Volume: 385 ml
Air Flow Rate: 0.54 liter/min
Area of Each Filter: 9.6 sq cm

Exp. No.	Partial Pressure of H_2O in Air Used (mm Hg)	Wt. PuF_6 Released (mg)	$\left(\frac{PuF_6}{H_2O}\right)$ mole	% Released Pu Incident on 1st AEC Filter	% Released Pu Beyond 1st AEC Filter	F % Released Pu Beyond 2nd AEC Filter
2	9.20	1.5	0.022	10	0.000051	0.000041
25	10.64	2.9	0.037	55	0.00035	0.000025
24	9.20	2.8	0.041	48	0.00044	0.000086
23	10.26	5.3	0.071	53	0.00086	0.000018
20	7.07	4.0	0.077	37	0.00012	0.0000050
26	9.88	8.3	0.115	55	0.000037	0.00000013
27	9.88	12.4	0.172	50	0.000022	0.00000077
30	9.20	12.4	0.184	57	0.000026	0.000017
2	7.62	10.4	0.186	13	0.000020	0.0000083
22	10.64	14.5	0.186	53	0.00082	0.00000012
31	9.88	15.3	0.212	45	0.0000085	0.0000014
32	9.88	15.9	0.220	61	0.000024	0.000016
29	9.88	18.7	0.258	52	0.000016	0.000012
13	1.44	2.9	0.275	6	0.00087	0.00015
33	9.88	20.4	0.282	46	0.000013	0.0000035
28	9.88	22.3	0.308	45	0.000026	0.000022
11	1.72	4.2	0.334	8	0.000038	0.000012
18	3.16	9.7	0.42	38	0.000064	0.000053
19	3.30	14.7	0.61	43	1.21	0.000017
14	1.37	9.5	0.95	19	0.032	0.000024
7	1.50	13.9	1.27	46	15.9	0.17
9	1.25	12.0	1.31	33	2.26	0.0039
10	1.37	14.7	1.47	31	3.01	0.000020
12	0.94	20.9	3.04	44	21.8	4.66
8	1.09	24.9	3.11	54	31.6	14.7
6	0.77	18.7	3.32	59	34.1	9.36

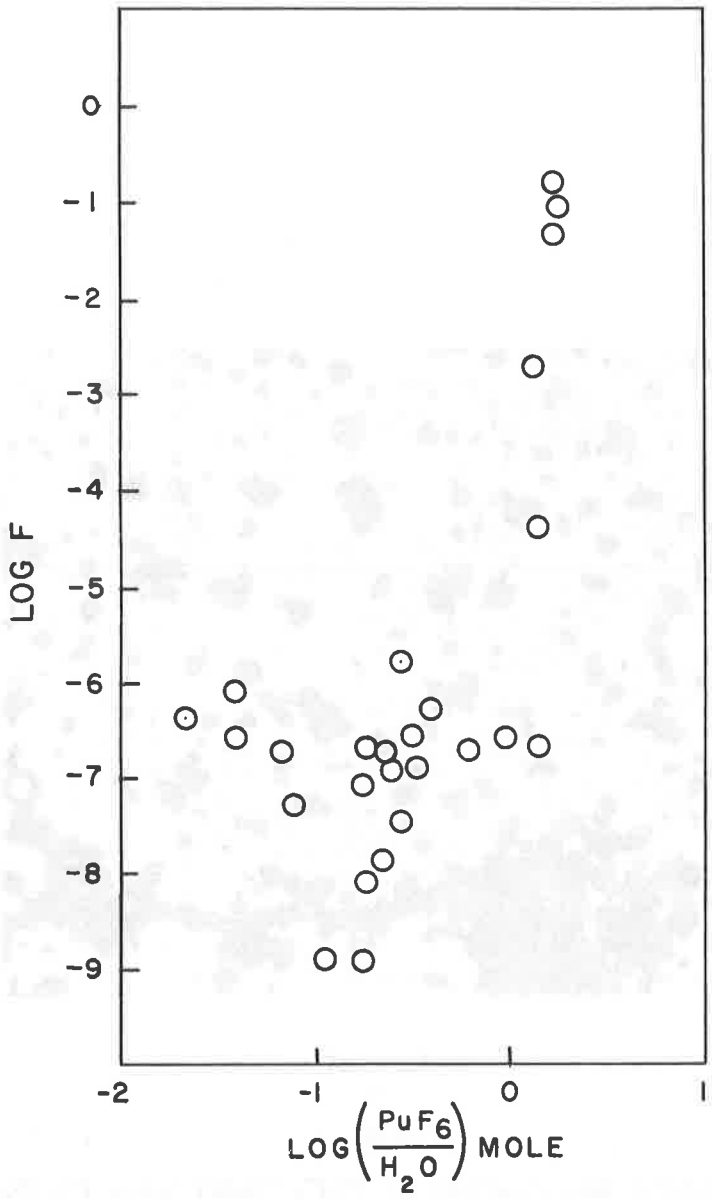

Fig. 2

Fraction of Released Plutonium Hexafluoride (F)
Passing through Two AEC Filter Discs

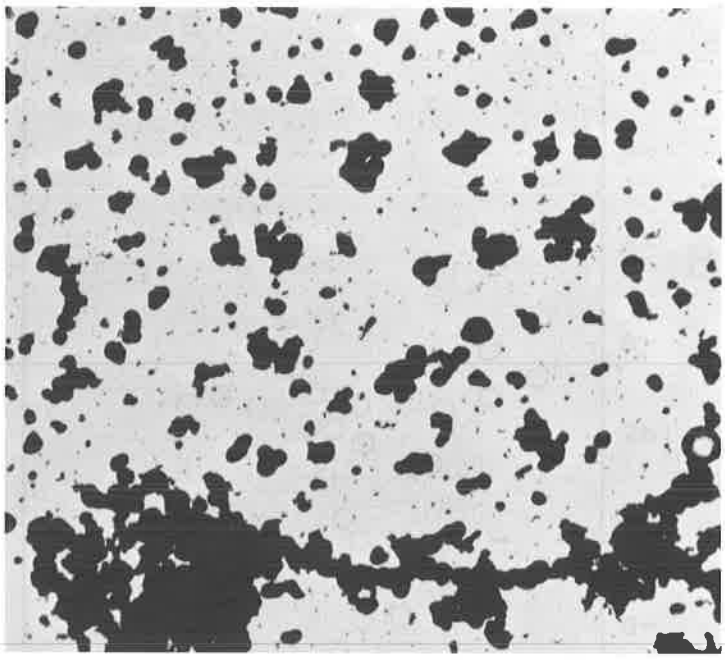

1 μ

Fig. 3

Electron Micrograph of PuF_6 Hydrolysis Product

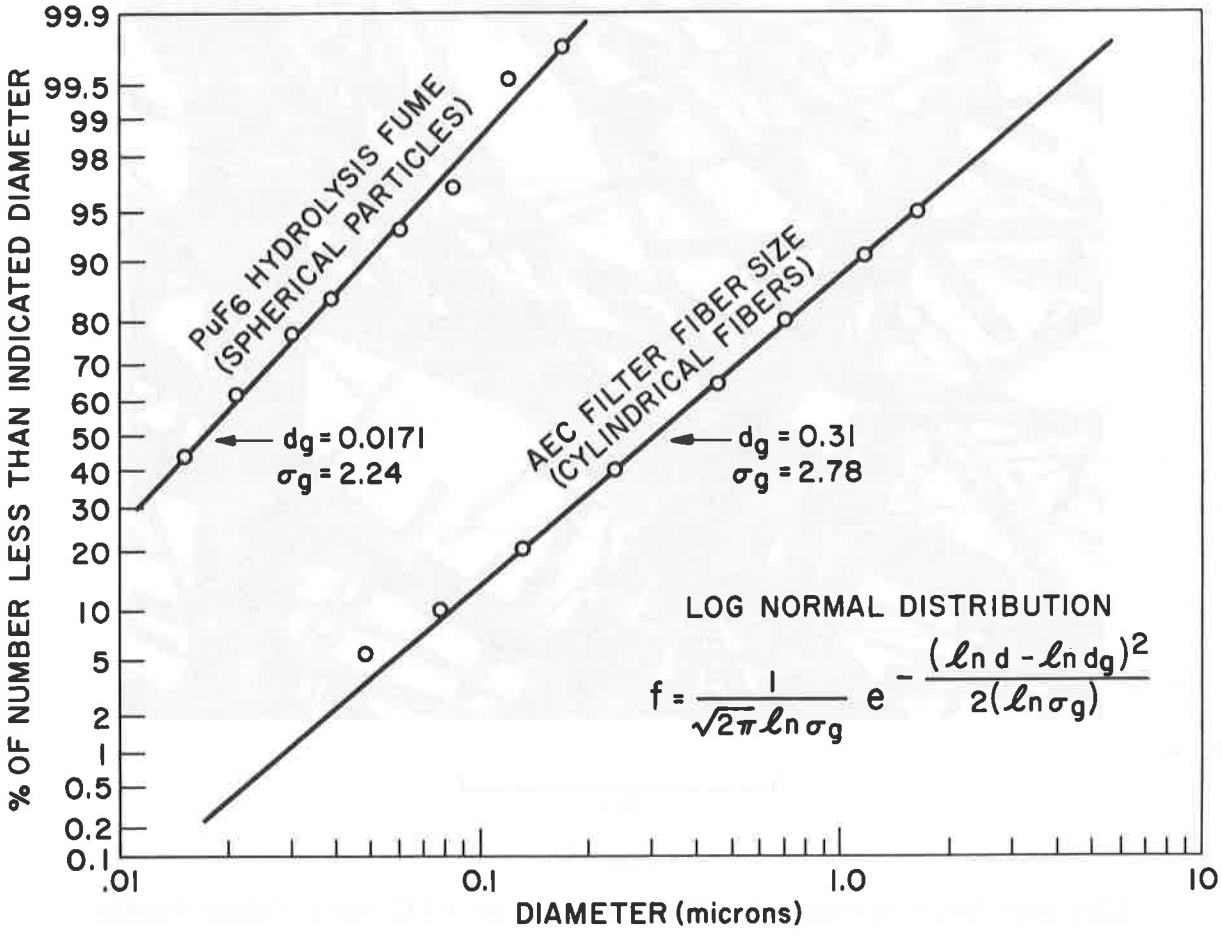

Fig. 4

Size Distribution of Hydrolyzed PuF_6 and AEC Filter Fibers

Fig. 5

Electron Micrograph of a Thin Section of AEC-type Filter Media

$$a = 200 \frac{w_o}{R} , \quad (3)$$

and

$$L = 10 \frac{w_o}{A} . \quad (4)$$

For the PuF_6 experiments, w_o varies from 1.5 to 25, R = 9 cm^3/sec, and A = 8.6 sq cm. Thus, a is between 30 and 600, and L is between 2 and 30. Values greater than one indicate that agglomeration and loading are strongly affecting the penetration of the first filter. An important result here is that the values of a and L can be estimated for any operating system.

According to the above analysis, an effect of the quantity of PuF_6 released would be expected to appear in the filter-penetration results shown in Figure 2. Consequently, a function including both the overall penetration factor F and the weight w_o of PuF_6 released may give a better correlation (against the PuF_6/H_2O mole ratio) than does F alone. Tests were made of Fw_o, Fw_o^2, and Fw_o^3; the best correlation was obtained with Fw_o^2, which is plotted in Figure 6. Although considerable scatter remains in Figure 6, a greater regularity of the data points is shown here than in Figure 2, and this correlation is believed to be superior to the original one. The dependence of the penetration on the square of w_o is what would be expected when the effects of agglomeration and loading take place simultaneously, since each factor (a or L) is proportional to w_o.

The value of d_p used in the agglomeration and loading equations is also likely to be a function of the filter penetration characteristics under some conditions. The penetration of filters by particles with the size if interest is unknown. Also, the scatter of the existing data does not allow a good experimental verification of the agglomeration and loading models presented. These models should only be considered as a first approximation to these effects and as an indication of the conditions under which these effects would be expected to be observable.

SURFACE REACTION

At low concentrations of reactants (H_2O and PuF_6) the reaction rate is dependent on the surface area contacted by the reactants. Although filters may provide large surface area for carrying out the reaction under these conditions, unreacted PuF_6 may nevertheless penetrate the filters.

A packed bed of glass spheres is better suited for measuring the surface reaction than are filters because (a) the surface area available for reaction can be accurately determined, (b) the packed bed can be removed and leached for the determination of deposited uranium and/or plutonium, and (c) a packed bed followed by filters will allow a separation of the effects of surface reaction and fume production. Since the diameter of the packed-bed particles is larger than that of the filter fibers, the packed beds will have a low interception efficiency for particulate.

Apparatus. The hydrolysis rate for PuF_6 was measured in an apparatus shown in Figure 7. Air dried to about 0.1 ppm of moisture was used as a carrier for PuF_6. Air with a controlled moisture content between 0.1 and 10 mm Hg was mixed with the PuF_6 carrier stream for studying the hydrolysis reaction rates. Another air stream saturated with moisture was combined with the mixed stream after passage through the packed bed of glass spheres and AEC filter discs. This final addition of moisture insured the complete hydrolysis of unreacted hexafluoride

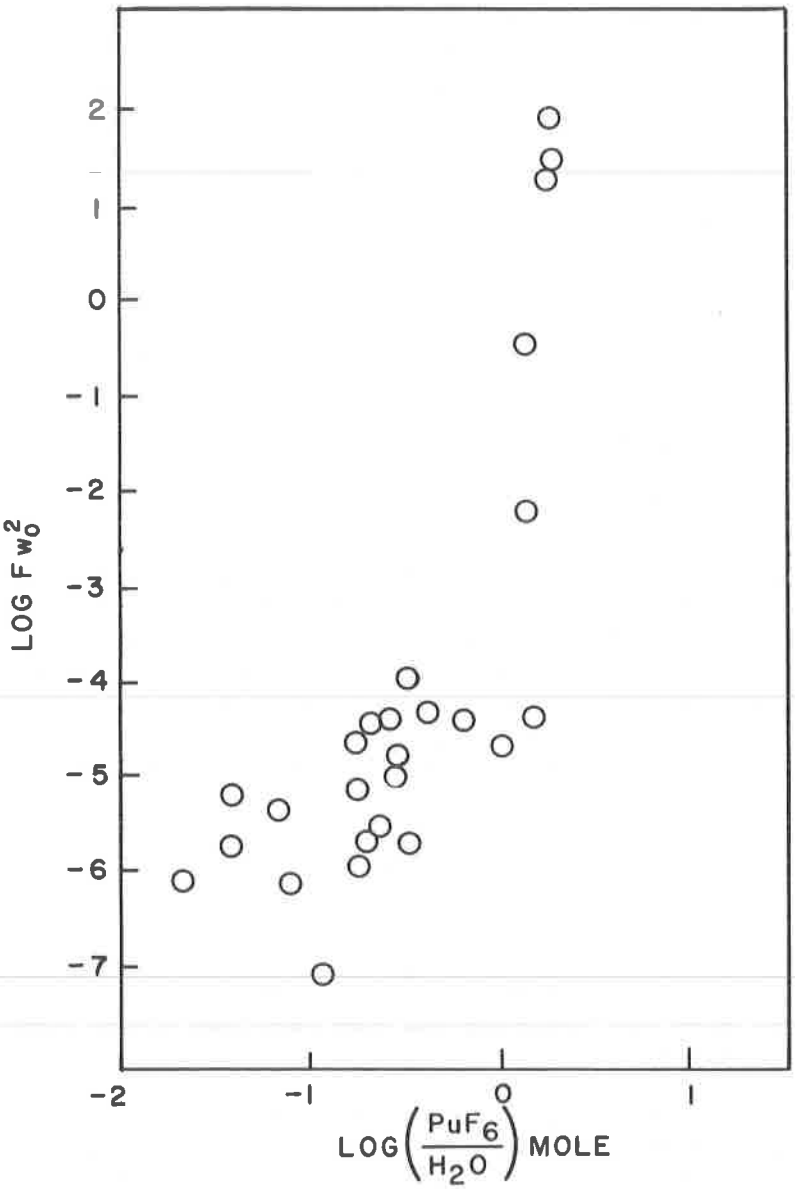

Fig. 6

Correlation of Data of Filter Penetration in PuF_6 Release Experiments

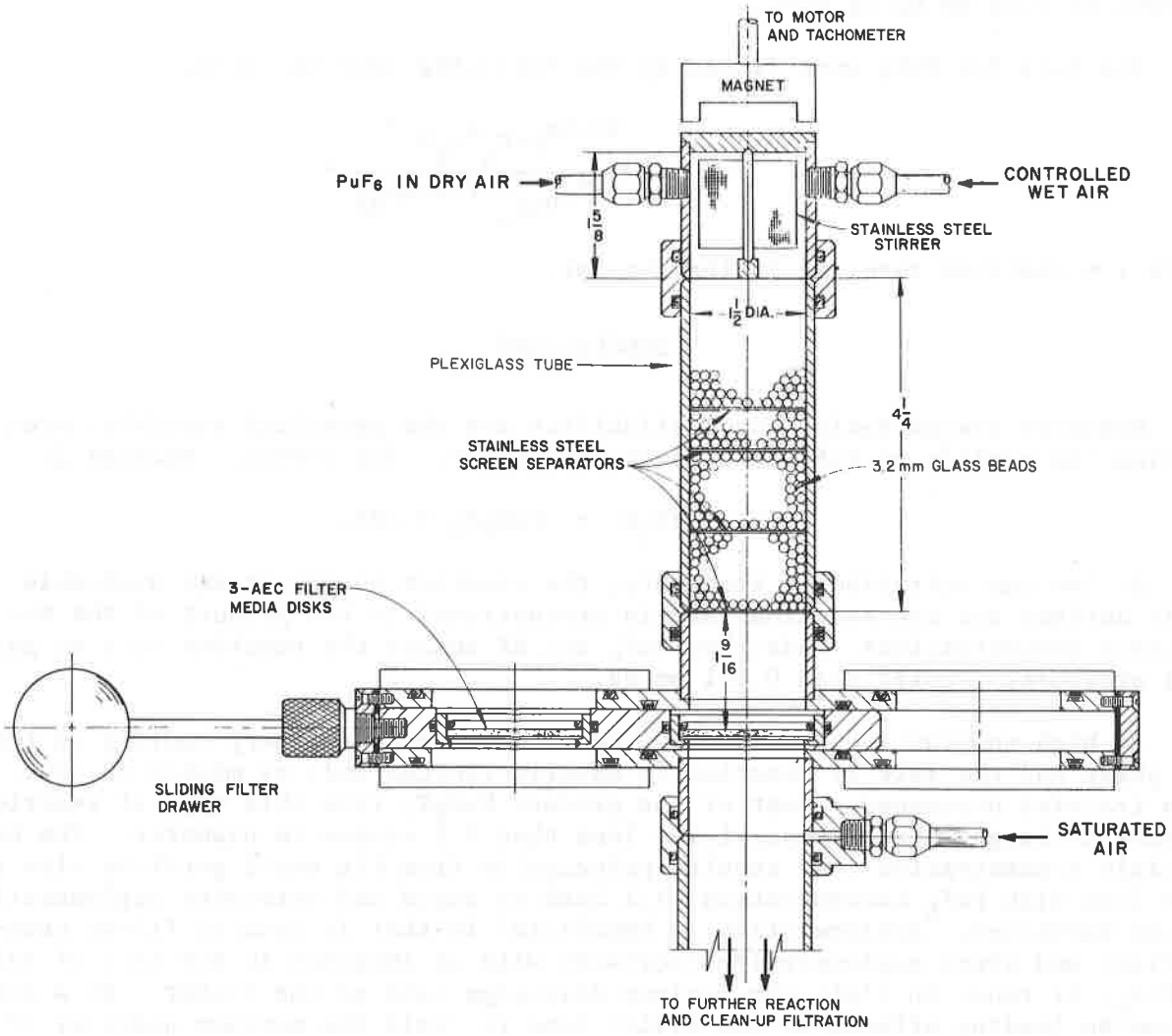

Fig. 7

Packed-bed Apparatus for Hydrolysis of PuF_6

and facilitated final cleanup of the gas before discharging to the glovebox atmosphere.

RESULTS AND DISCUSSION

The PuF_6 experimental results are reported in Table 2. The partial pressures in the initial mixed gas ranged from 0.06 to 5.6 mm Hg of water vapor and 0.00001 to 0.02 mm Hg of PuF_6.

The data for PuF_6 were fitted by the following rate equation,

$$r = \frac{53.5 p_{PuF_6} p_{H_2O}}{1 + 142 p_{PuF_6} + 1.9 p_{HF}} . \qquad (5)$$

where r = reaction rate, mg Pu/(hr)(sq cm).

CONCLUSIONS

Moisture concentration and availability are the principal variables preventing the passage of PuF_6 through an air filter. The overall reaction is

$$PuF_6 + 2H_2O \rightarrow PuO_2F_2 + 4HF.$$

At low concentration of reactants, the reaction occurs at any available solid surface and the reaction rate is proportional to the product of the two reactant concentrations. Adsorbed PuF_6 and HF reduce the reaction rate at partial pressures greater than 0.001 mm Hg.

At high reactant concentration, the reaction proceeds very rapidly in the gas phase and the rate of reaction is usually limited only by mixing or other mass transfer processes. Most of the product PuO_2F_2 from this type of reaction remains in the gas phase as particles less than 0.1 micron in diameter. The high particle concentration that results principally from the small particle size and also from high PuF_6 concentration will lead to rapid and extensive agglomeration of the particles. Agglomeration is beneficial in that it reduces filter penetration; and since agglomeration increases with an increase in the rate of release of PuF_6, it tends to limit the maximum discharge rate of the filter. By a similar mechanism loading effects in the filter tend to limit the maximum quantity of plutonium that could pass through the filter.

The use of high efficiency filters for collection of the fine particulate and for providing the large surface needed in the heterogeneous reaction appears to be the most practical technique. With an excess of moisture and normal filter velocities of 40% of rated flow, the fraction of released plutonium passing through two AEC filters in series ranged between 10^{-9} to 10^{-6}. The penetration of the second filter had even more variation than the combined result and was between 10^{-4} to 0.8. This high penetration and large variation cannot be explained at present but probably involves penetration of particulate in the size range of 0.01 to 0.1 micron diameter. More work is needed on this problem in order to more fully evaluate the use of multiple filters in series.

Table 2

SURFACE-REACTION DATA FOR HYDROLYSIS KINETICS OF PLUTONIUM HEXAFLUORIDE

Column diameter: 1.5 in.
Linear velocity: 9.8 cm/sec
Temperature: 22-25°C
Run time: 60.0 min

Run	$P^{o}_{H_2O}$, mm Hg	$P^{o}_{PuF_6}$ mm Hg	Feed, mg Pu/hr	mg of Pu per Bed Segment[a] 0-1/2 in.	1/2-1 in.	1-2 in.	2-3 in.	mg of Pu per Filter First	Second	Third	mg of Pu in Mixer	mg of Pu in Cylinder and Screens
PM-4	5.6	0.00098	5.06	1.067	0.0619	0.0863	0.0604	0.231	0.00123	0.00215	3.07	0.483
PM-1	0.54	0.00150	7.84	2.31	0.506	0.139	0.0438	0.0515	0.00152	0.00237	3.72	1.068
PM-6	0.060	0.00217	11.29	1.98	1.30	1.49	1.037	0.878	0.00088	0.00059	3.23	1.37
PM-5	0.49	0.0221	114.4	16.6	12.2	22.0	14.9	13.8	0.394	0.0364	20.7	13.8
PM-8	0.45	0.000303	1.56	0.316	0.0301	0.0317	0.0198	0.0531	--	--	0.963	0.148
PM-9	0.46	0.000181	0.938	0.192	0.0209	0.0129	0.0133	0.0186	0.000135	0.000246	0.587	0.0933
PM-7	0.45	0.0000115	0.059	0.00313	0.00102	0.0012	0.00212	0.00101	0.000073	0.000073	0.0471	0.00317

APPENDIX A

Model of the Agglomeration Process Affecting Filtration

In the model developed in this appendix, the change with time in the number of particles in the mixing chamber (upstream of the filter) is expressed in terms of simple mathematical relations for the processes of agglomeration and gas purging of the mixing chamber. The following assumptions were used in deriving the mathematical expressions:

1. The plutonium hexafluoride and water vapor are combined in a reaction chamber, where they are instantly reacted and the solid product is perfectly mixed, i.e., evenly distributed in the chamber. Subsequently, the product particles are swept out by air passing through the chamber and to the filters. The gas purge sweeps out particles regardless of size.

2. The hydrolysis product particles are initially of the same size (unagglomerated), and the range of sizes of the agglomerated particles may be described by a Poisson distribution.

3. All the penetration of the filter is due to unagglomerated particles; that is, the agglomerated particles make a negligible contribution to the amount of material penetrating the filter. A penetration factor for unagglomerated particles is taken as a property of the filter.

Other workers have found that, when agglomeration alone is considered, the particle concentration varies with time as follows:[7]

$$\frac{1}{n} = \frac{1}{n_o} + Kt, \tag{6}$$

where n is the number of particles per unit volume at time t, $n = n_o$ at $t = 0$, and

$$K = 4kTC/3\mu, \tag{7}$$

where k is the Boltzmann constant, T is the absolute temperature, C is Cunningham's correction factor to Stokes' law, and μ is the gas viscosity.

Differentiation of Equation (7) gives

$$-\frac{dn}{dt} = Kn^2. \tag{8}$$

This describes the change in particle concentration due to agglomeration alone.

The removal of particles from the mixing chamber by the gas purge is treated as follows: Perfect mixing without agglomeration would give

$$-\frac{dn}{dt} = \frac{Rn}{V}, \tag{9}$$

where R is the gas flow rate, and V is the volume of the mixing chamber. For both agglomeration and mixing, we have

$$-\frac{dn}{dt} = Kn^2 + (R/V)n. \tag{10}$$

Integration gives

$$-\int_{n_o}^{n} \frac{dn}{Kn^2 + (R/V)n} = \int_o^t dt, \tag{11}$$

or

$$n = \frac{n_o e^{-Rt/V}}{1 + (KVn_o/R)(1 - e^{-Rt/V})}. \tag{12}$$

The effect of gas purge in Equation (10) may be expressed also in mass terms, in which form it is independent of agglomeration. The weight w of plutonium in the mixing chamber is independent of agglomeration, and the rate of decrease of w is given by

$$-\frac{dw}{dt} = \frac{R}{V} w \tag{13}$$

or

$$w = w_o e^{-Rt/V}, \tag{14}$$

where w_o is the initial weight released at t = 0.

For the whole collection of particles in the mixing chamber, the initial (unagglomerated) particle weight m_o is given by

$$m_o = w_o/n_o V. \tag{15}$$

Similarly, the average particle weight m at any time is given by

$$m = w/nV. \tag{16}$$

The average number of particles per agglomerate, M, is the ratio of the average particle weight to the weight of the initial particle, and is given by

$$M = \frac{m}{m_o} = \frac{wn_o}{w_o n}. \tag{17}$$

Substitution of (12) and (14) in (17) gives

$$M = 1 + \frac{KVn_o}{R} (1 - e^{-Rt/V}). \tag{18}$$

The fraction p of unagglomerated particles is obtained by assuming that there is a Poisson distribution of the number x of (original) particles in an agglomerate. By the well-known statistical property of the mean, we may write this as

$$p(x - 1) = \frac{(M - 1)^{x-1} e^{-(M-1)}}{(x - 1)!} \tag{19}$$

Substituting (18) in (19) and setting x = 1 for unagglomerated particles gives

$$p = e^{-KVn_o/R} (1 - e^{-Rt/V}). \tag{20}$$

The total amount of plutonium passing through the filter is that fraction of unagglomerated material swept out of the mixing chamber that also is not trapped on the filter. Thus,

$$w_o P = \int_o^\infty np(w_o/n_o V) P_o R \, dt, \tag{21}$$

where P is the average weight-fraction penetration measured, and P_o is the weight fraction of unagglomerated material that passes through the filter. This P_o is a standard property of the filter (for a particular particle size) and is not the empirical, overall penetration P measured for agglomeration. The ratio P/P_o is less than one in all actual cases in which some agglomeration occurs. Substituting Equations (12) and (20) in (21) and letting

$$KVn_o/R = a \tag{22}$$

gives

$$\frac{P}{P_o} = \int_o^\infty \frac{e^{-Rt/V} + a(1 - e^{-Rt/V})dt}{1 + a(1 - e^{-Rt/V})} \tag{23}$$

The change of variables

$$Z = 1 + a(1 - e^{-Rt/V}) \tag{24}$$

gives

$$\frac{P}{P_o} = \frac{e}{a} \int_1^{1+a} \frac{e^{-Z}\, dZ}{Z} \tag{25}$$

This integral is known as the exponential integral and has been tabulated. The function is plotted in Figure 8.

The function P/P_o is the ratio of the following weight fraction:

$$\frac{\text{measured penetration}}{\text{penetration by unagglomerated particles}}$$

The abscissa, a, in Figure 8 is the dimensionless agglomeration number defined in Equations (22) and (7) in terms of physical constants, gas properties, flow rate, and the initial quantity of particles released.

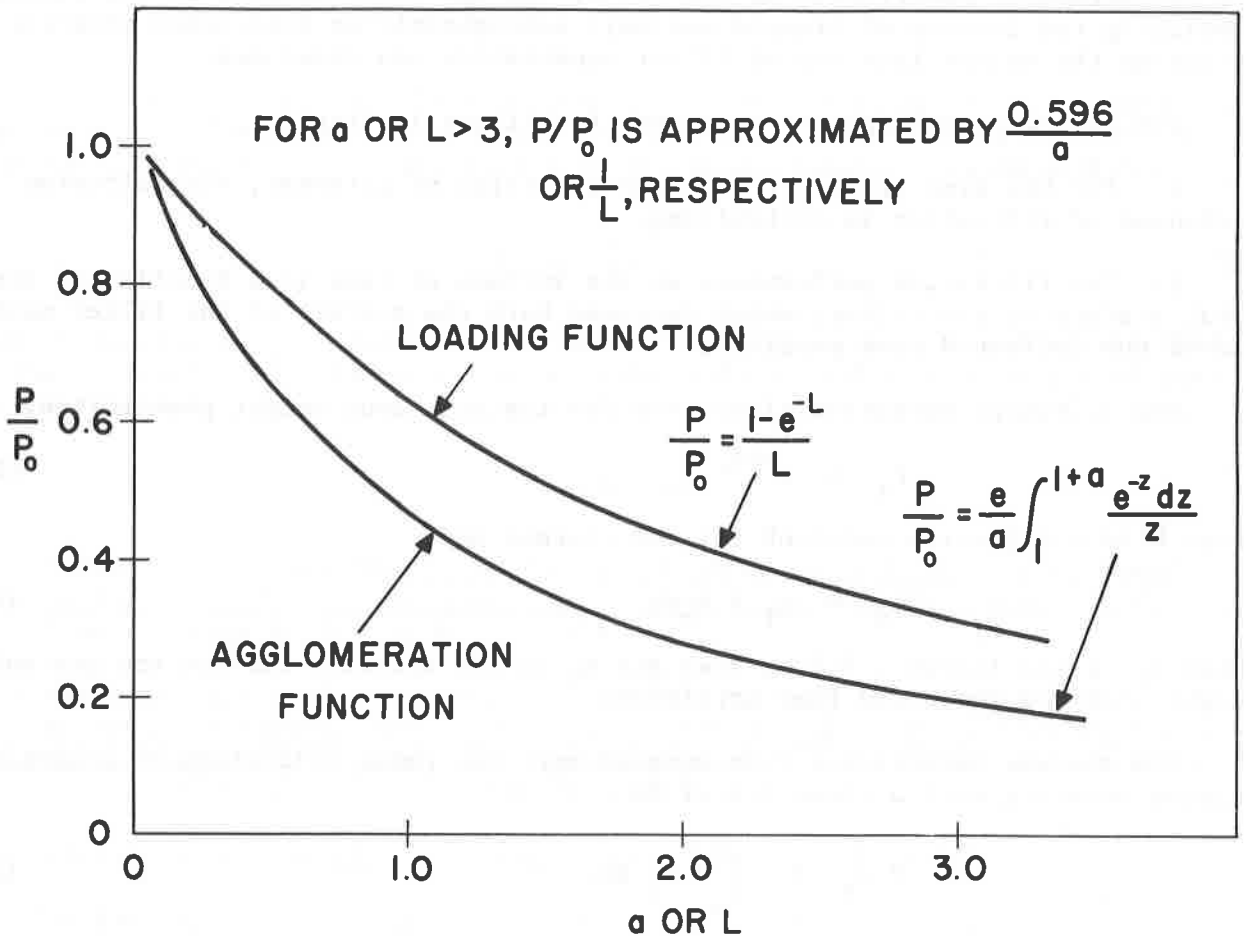

Fig. 8

Agglomeration and Loading Functions

DISCUSSION

BILLINGS: I don't think that when penetration or the first filter is very efficient the second one is not very efficient and the reverse is true. It is very surprising. Isn't that what you would expect? You have a distribution of particle sizes. If they are so large that the filter takes out, the first one takes out a lot, at least the spectrum rests in the larger component, it's going to give you a lower efficiency for the second one. Isn't this consistent with what you would expect, whatever the distribution?

KESSIE: Yes. Well, even the filtration theory doesn't indicate the possibility of getting the types of penetration that were seen here; say 50 per cent penetration of the high efficiency filter in particular seems to be a little bit out of line with the theory, but there are many effects that could contribute to this that have not been even considered in the theory today.

AN EVALUATION OF TWO PORTABLE THERMAL AEROSOL GENERATORS FOR IN-PLACE FILTER TESTING

R. H. Knuth

Health and Safety Laboratory
U. S. Atomic Energy Commission
New York, New York

ABSTRACT

Two commercial, portable thermal aerosol generators were evaluated to determine their practicability for in-place testing of high efficiency filters. Penetration values of various high-efficiency filters were determined with the two thermal generators and results were compared with values obtained using standard air-operated aerosol generators of the type developed by the Naval Research Laboratory. Very close agreement was found. It was also found that the aerosol produced by the thermal generators was quite stable, and that the particle size distribution was very close to that of the air-operated generators.

The thermal generators have the important advantage that compressed air is not required, and a small compact unit will service a large filter installation, for example 20,000 cfm. Although the thermal generators have minor design limitations, their use for in-place testing, particularly of high volume systems, is recommended.

INTRODUCTION

In installations using high-efficiency filters it is sometimes difficult to perform in-place tests with air-operated generators because compressed air may not be available at the location best suited for the introduction of an aerosol into the system. In large filter systems the available compressed air may not be of sufficient quantity to operate the number of generators required to produce the concentration of aerosol needed to evaluate the filter system. When the use of a number of generators is required, portability of in-place test equipment is greatly limited. Consequently, the evaluation of compact portable generators not requiring compressed air is of interest.

The two thermal type generators studied in this evaluation use 2 1/2 lb cylinders of CO_2, rather than compressed air, and operate on a 110 volt or 220 volt electrical supply. While 2 1/2 lb CO_2 cylinders are capable of operating the generators for a number of hours at maximum pressures, larger supplies of CO_2 can be used if portability of the generator is not required. Also the generators may be disconnected from the electrical supply and used for short periods of time after operating temperatures have been reached.

When di(2-ethylhexyl)phthlate (DOP) is the liquid medium, the thermal generators produce a polydisperse liquid aerosol having a light-scattering geometric mean diameter (LSGMD) of about 0.8 micron. Although the thermal generators were designed to operate with liquids other than DOP, DOP was used in this evaluation because of its desirable physical properties; low vapor pressure, viscosity, high flash point, nonhygroscopic and chemical inertness. Use of DOP also permitted direct comparisons of particle size distribution by the jet impactor-light scattering method[1,2].

With the obvious physical advantages of the thermal generators, the principal objective of this investigation was to determine if their use gave the same penetration values as the standard air-operated generators, making the thermal generators acceptable for in-place testing. Particle size distribution, light scattering power and stability were also investigated to provide additional comparisons of the aerosols.

DESCRIPTION OF THERMAL AEROSOL GENERATORS

The two thermal aerosol generators are similar in flow design. Figure 1 is a general schematic diagram of the major components of

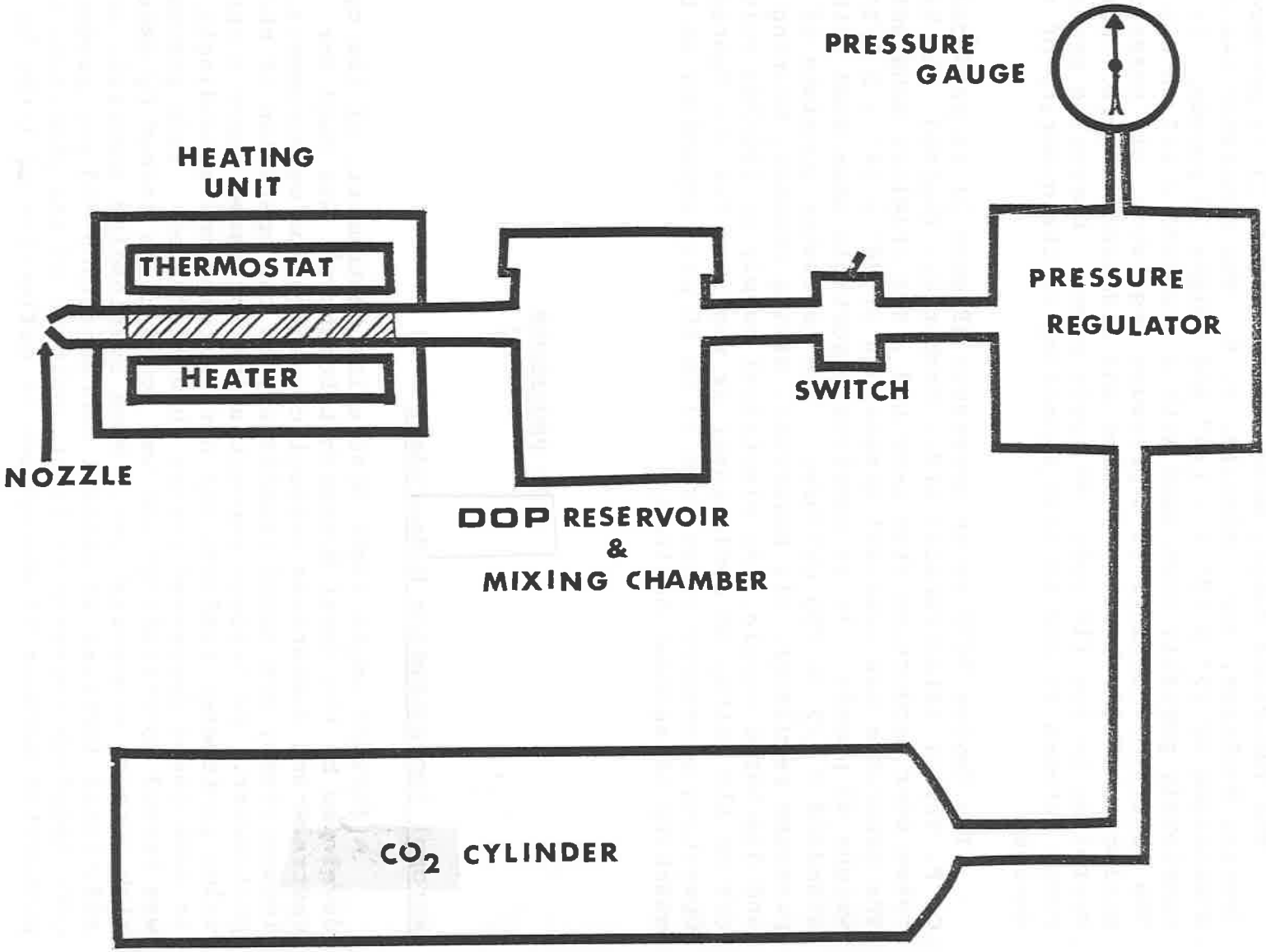

Figure 1. Major Components of Thermal Aerosol Generators

both generators. In the oil reservoir - mixing chamber which holds approximately 200 cc of liquid, a feeder nozzle with two small orifices, one below and one above the liquid level, provides a mixture of the CO_2 and liquid which is carried to the heating unit. Here it is raised to a high temperature before emerging from the generator nozzles as an aerosol.

The TMI-Cloud Maker, Model 11-48 (Figure 2) is produced by Testing Machines, Inc., Mineola, N. Y. The generator has over-all dimensions of 22" x 12" x 5 1/4" and weighs 25 pounds. It is completely portable when used with a standard 2 1/2 lb CO_2 cylinder. The generator consists of a pressure regulator, oil reservoir, mixing manifold, heating chamber and discharge nozzle. Normal operation is for 110 volt, 60 cycle power. Operating pressures range between 10 and 40 psig depending on the quantity of aerosol desired.

The Taylor 3020 smoke generator (Figure 3) is produced by C. F. Taylor (Electronics) Ltd., Camberley, England, who have taken over production from Lede Ltd., the original manufacturer. The generator has over-all dimensions of 24" x 14" x 5 1/2" and weighs 40 pounds. It is completely portable when used with a standard 2 1/2 lb CO_2 cylinder. The generator consists of a pressure regulator, oil reservoir, mixing chamber, heating unit, and discharge nozzle. An electrical supply of 220/240 volts, 50 c/s or 110 volts, 60 cycle power is required for the heater unit. Operating pressures range from 10 to 40 psig depending on the quantity of aerosol desired.

TEST PROCEDURE

Aerosol Concentration Measurement

A forward angle light scattering photometer, of the type developed by the Naval Research Laboratory[3], was used for upstream and downstream aerosol concentration measurements. An inconsistency was noted immediately in the operation of the photometer. As aerosol concentration increased above a certain value photometer readings did not increase correspondingly, and in some cases decreased rather than increased. This phenomenon was termed "overloading" and was found to be caused by excessively high aerosol concentrations. When overloading occurred, an additional increase in aerosol concentration did not produce a corresponding increase in light incident on the phototube of the photometer because of absorption or deflection of light by the

Figure 2. TMI - Thermal Aerosol Generator

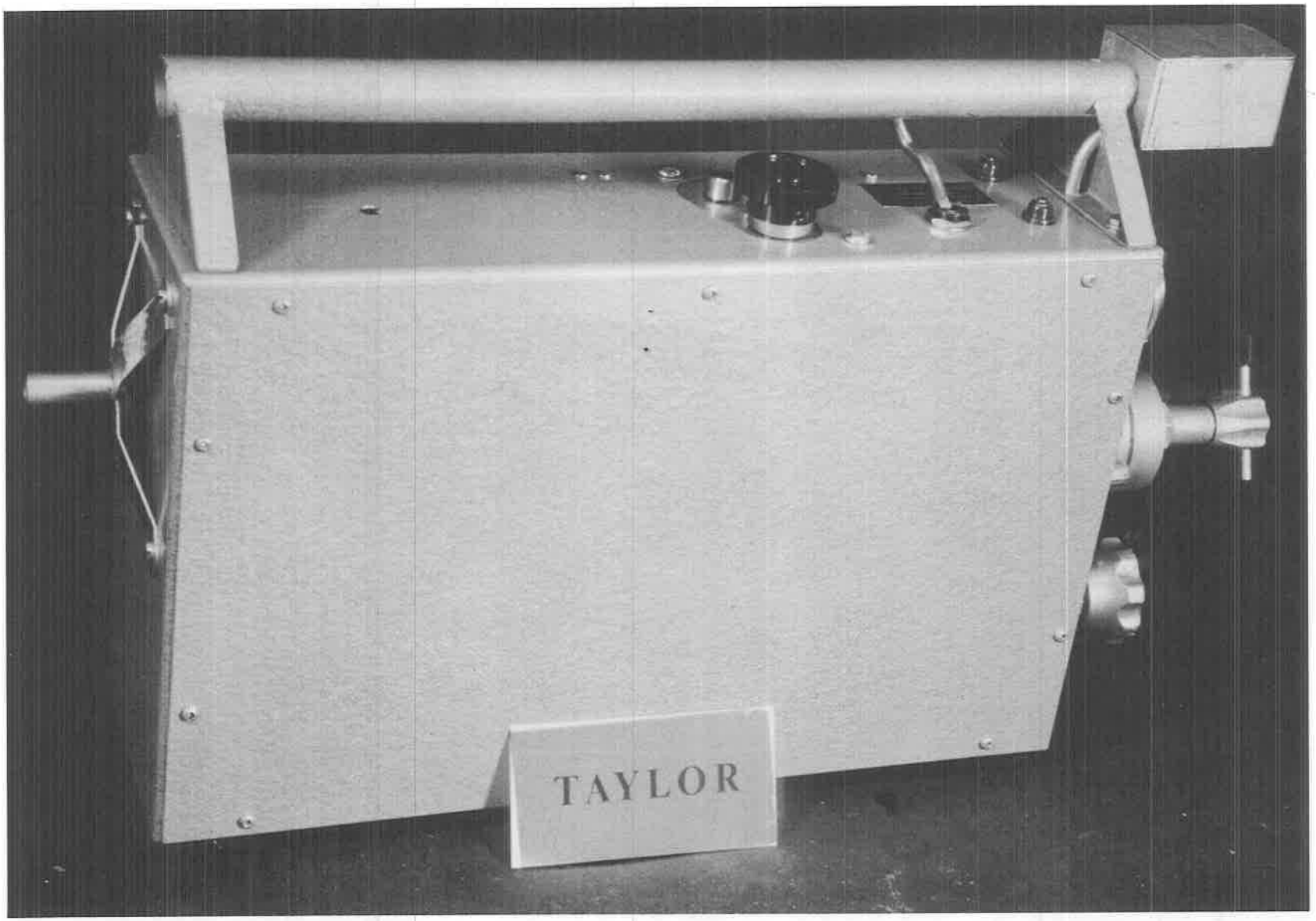

Figure 3. Taylor - Thermal Aerosol Generator

increased number of particles in the light path. Consequently, it was necessary to adjust input aerosol concentration so that the photometer was in a linear range.

To determine at what aerosol concentrations overloading occurs, data shown in Figure 4 were obtained. The open data points are photometer readings taken as the operating pressure of a thermal generator was increased, the air flow through the filter system being held constant. The lower curve, solid data points, is the same aerosol sample diluted 50% with clean air before entering the photometer. The dashed line curve was predicted from the lower curve and represents the photometer readings expected from the undiluted sample for a linear response (no overloading). The divergence from the predicted curve begins, in this instance, at a generator pressure of about 25 psig where the mass concentration was found to be about 200 μg/l.

A similar check on an air operated generator showed evidence of photometer overloading starting at about the same aerosol mass concentration. This value of 200 μg/l applies only to the aerosols used in this work. For aerosols of other size distributions, the value may be somewhat higher or lower.

Dispersion rates of the two thermal generators were quite similar. The TMI generator dispersed 5-18 gms/min of liquid DOP when operating at pressures between 10 and 40 psig, while the Taylor generator dispersed 3-15 gms/min over the same range of pressure.

Photometer overloading was found to exist when the aerosol from the thermal generators (operating at high pressures) was introduced directly into a 1000 cfm system. Since a 1000 cfm filter system was used for penetration measurements, it was necessary to dilute the thermal aerosols. Figure 5 is a diagram of the filter test system with provision for aerosol dilution.

Penetration Measurement

The air-operated aerosol generator used for comparison of penetration values was a TDA-4 DOP generator commercially produced by T. D. Associates, Baltimore, Maryland. This generator contains 12 atomizing nozzles of the type developed by the Naval Research Laboratory[4]. These nozzles using DOP as the dispersed liquid are now widely used for in-place testing of high efficiency filters.

The thermal generators were operated at pressures between 10 and 35 psig, and the air operated generator between 10 and 25 psig. Both the TMI and Taylor generator thermostats were adjusted to regulate at $300^{o} \pm 5^{o}C$. In the majority of tests the thermal

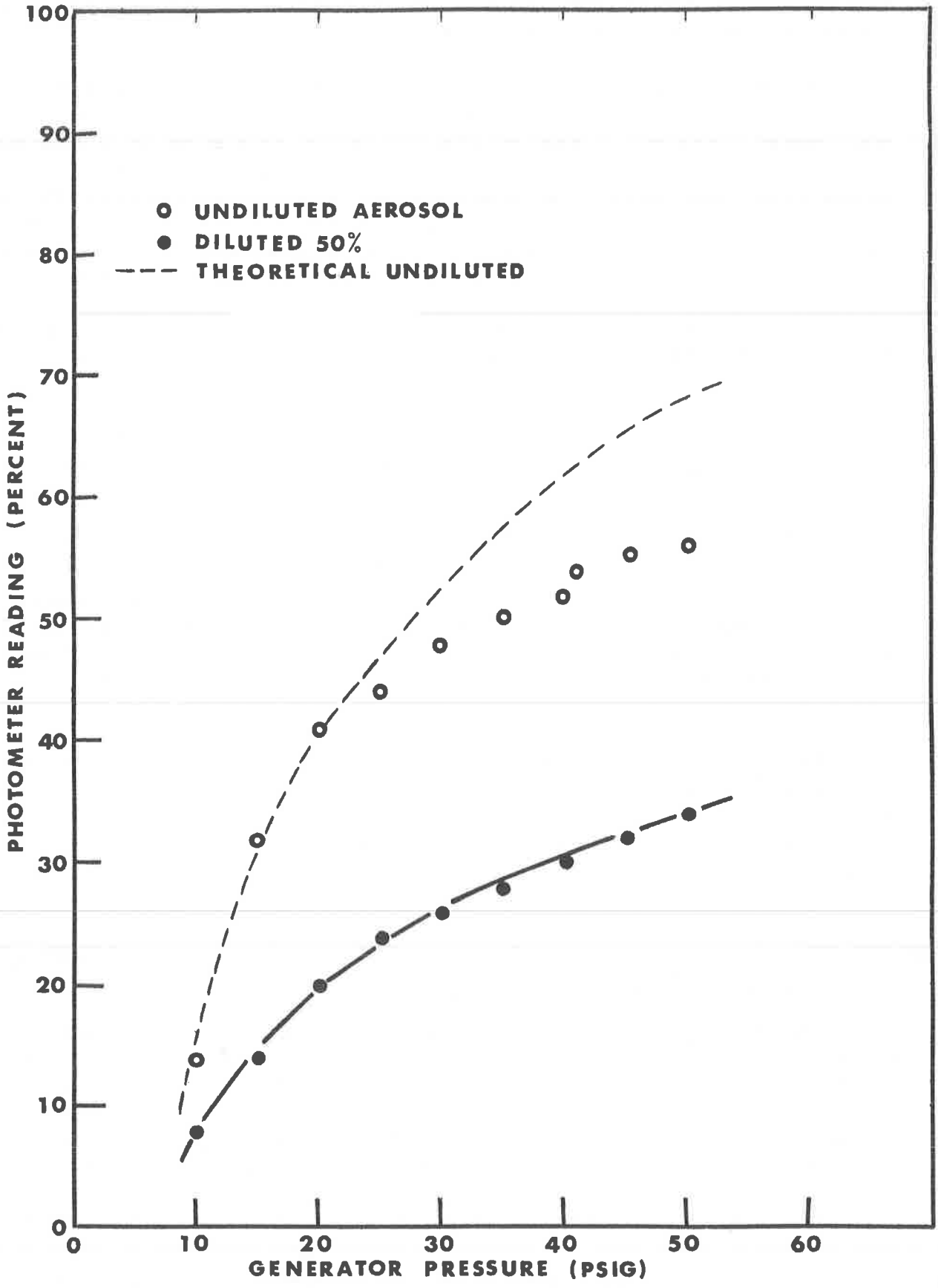

Figure 4. Photometer Overloading

generators were varied between 20-25 psig and the air operated generator between 15-25 psig. Below 10 psig both thermal generators had considerable amounts of condensate dripping from the discharge nozzle.

To avoid photometer overloading, the aerosol was first introduced into a 4000 cfm blower, and only a portion of the aerosol was allowed to enter the 1000 cfm blower system in which the test filter was installed (Figure 5).

The penetration of an intact filter was first determined with each of the three aerosol generators. Then a defect was made in the filter, and the test repeated. As subsequent defects were added a filter penetration value for each generator was obtained under identical test conditions. System air flow and sampling flows were held constant with the only variable being the change of the aerosol generator. This procedure was repeated for approximately 30 penetration values in the 0.02 to 5% penetration range.

Determination of Test Reproducibility - Since preliminary results of filter penetration tests using the three generators showed rather close agreement, it was desirable to determine the reproducibility of the test technique itself by making replicate runs with each generator.

Table 1 is a comparison of the standard deviation, σ, of penetration measurements for any one generator in four ranges of penetration.

TABLE 1

Penetration Measurements
Standard Deviation (%)

Penetration Range (%)	Generators: Air Operated TDA-4	Thermal TMI	Thermal Taylor	Avg.
.02 - .04	2.8	3.2	1.7	2.6
.05 - .09	2.1	1.0	2.1	1.7
.10 - .50	2.4	3.1	2.3	2.6
.60 - .90	1.2	1.7	1.3	1.4
Avg.	2.1	2.2	1.8	2.1

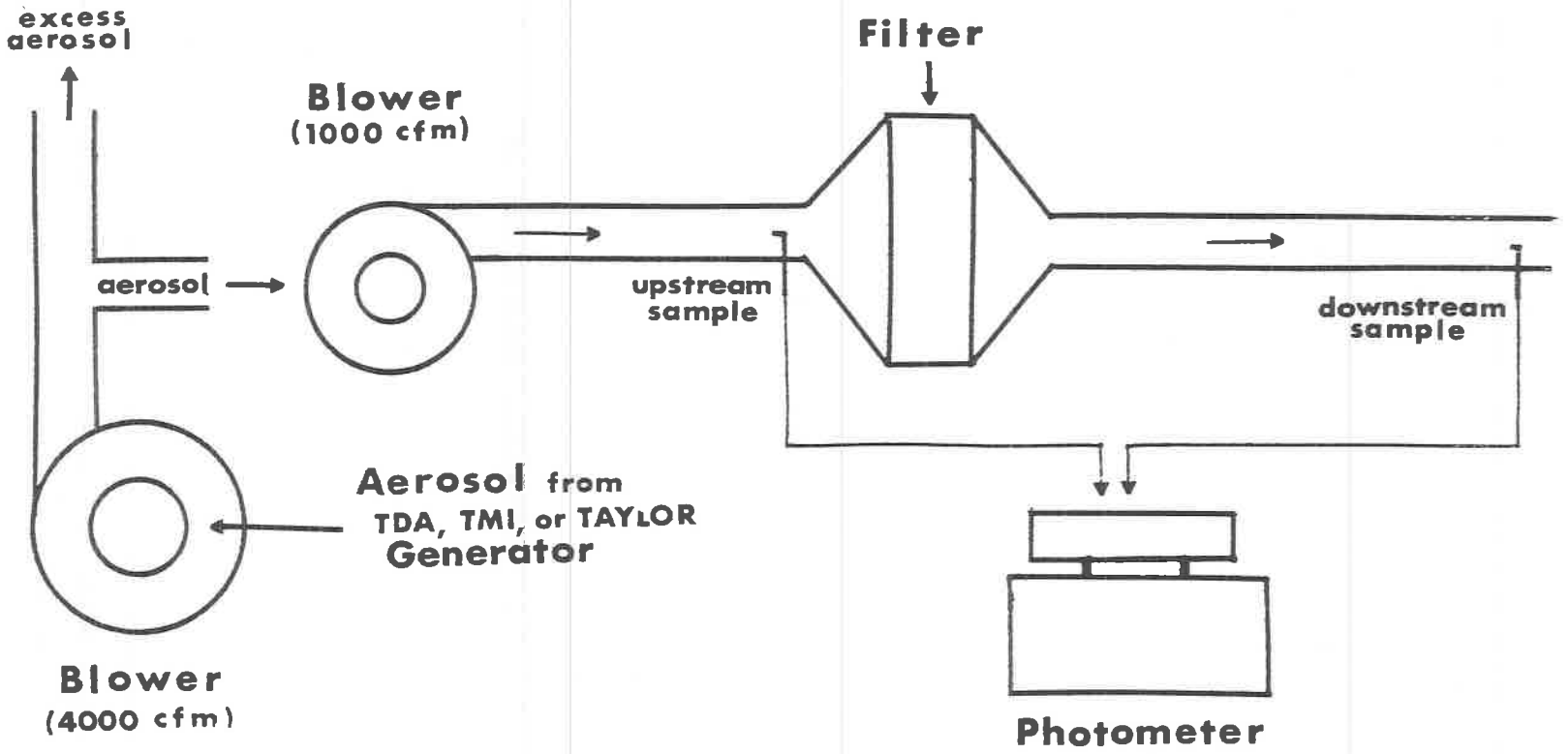

Figure 5. Filter Test System

Thus, the average test reproducibility of any one of the three generators is about ± 2% over the entire range of penetrations indicated. High deviations were found to usually correspond to experimental values read from the lower quarter of the photometer microammeter scale where less precision should be expected.

Particle Size Analysis

The jet impactor-light scattering technique[1,2] was used to compare the particle size distribution of the aerosols produced by the thermal and air operated generators.

At a given flow rate, the jet impactor removed 50 percent of all particles of a certain size. By using a series of these impactors having a range of characteristic diameters, size distribution data in terms of scattered light intensity was obtained. The light scattering intensity of the aerosol before and after it passed through each impactor was measured and plotted on logarithmic probability paper as particle size versus percent less than stated size. The average particle size in terms of light scattering geometric mean diameter (LSGMD) was read off the plot at the 50 percent size. The geometric mean standard deviation, σg, was calculated as the ratio of the 84.13 percent size to the 50.0 percent size[5].

COMPARISON OF THERMAL AND AIR-OPERATED GENERATORS

1000 cfm High Efficiency Filter System Penetration

A comparison of the penetration values obtained from the two thermal generators and the air-operated generator appears in Figures 6 and 7. It should be noted that deviations may reflect the descrepancies found in test reproducibility. These deviations were found to average ± 2%. In Figure 6, the Taylor values are plotted against the TDA-4 values, and in Figure 7 the TMI versus the TDA-4 values.

For each filter penetration the greatest deviation from the average of the sum of the penetration values for the three individual generators was determined. The average of these deviations for all of the tests was 2.8% with a maximum of 7.3% and a minimum of less than 1.0%. The deviation between the TDA-4 values and the TMI values averaged 3.5% with a maximum of 10.0%

RPD
3L-2.5L

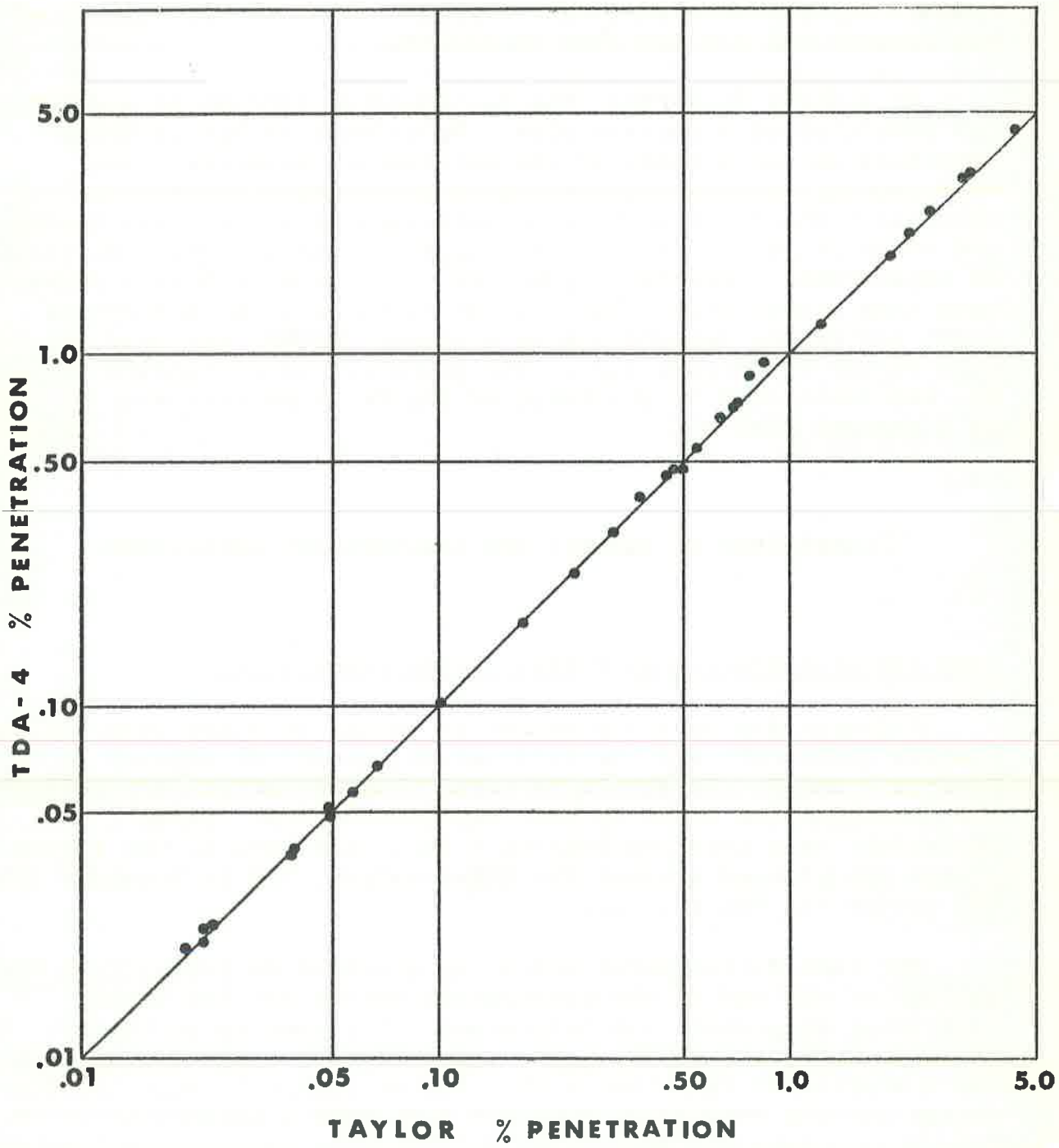

Figure 6. Filter Penetration TDA-4 vs. Taylor

RPD
3L-2.5L

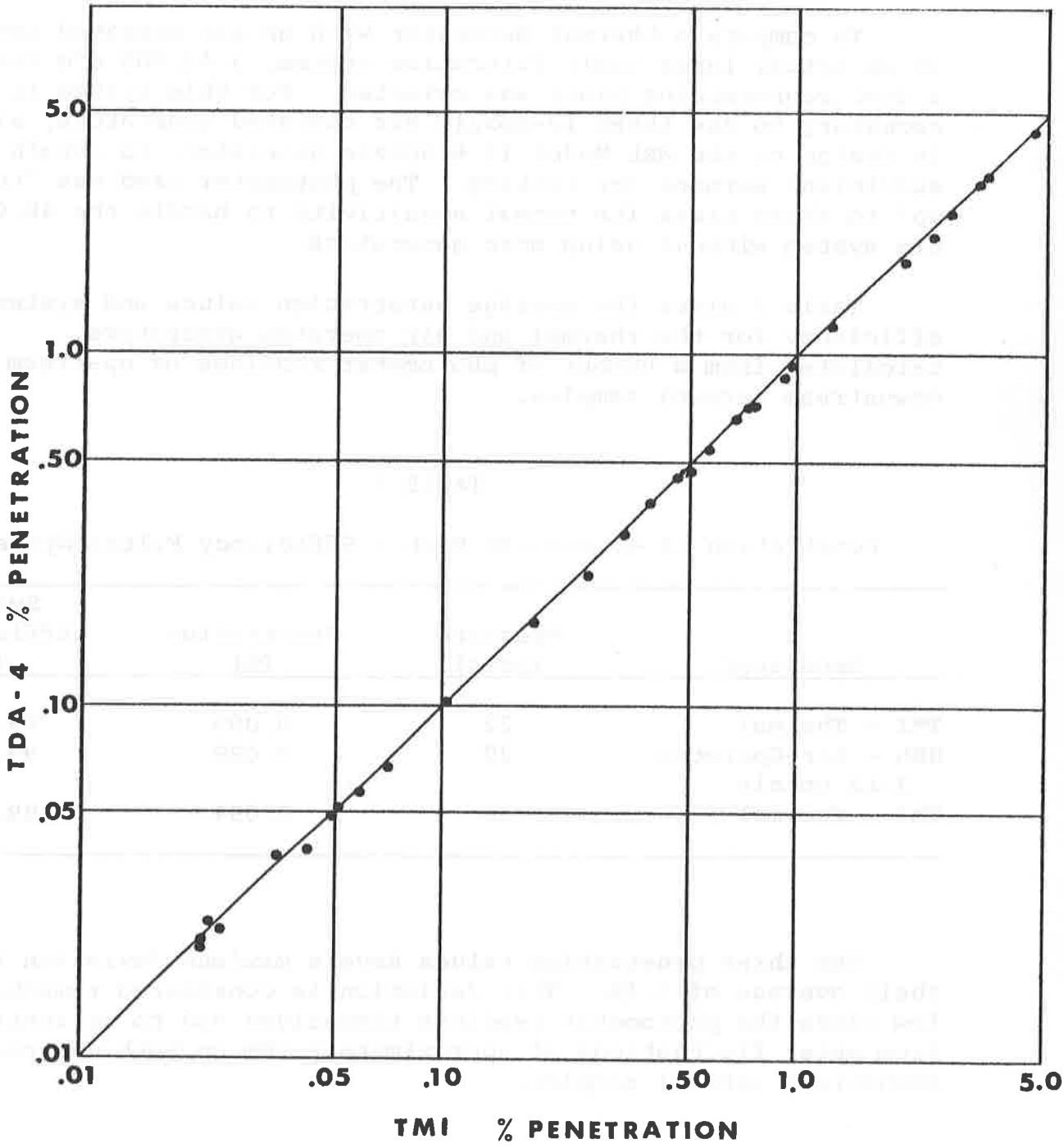

Figure 7. Filter Penetration TDA-4 vs. TMI

and a minimum of less than 1.0%, while the TDA-4 and Taylor comparisons gave an average deviation of 2.8% with a maximum of 8.0% and a minimum of less than 1.0%. The maximum deviations were found where penetration values were in the 0.02% - 0.05% range or when penetration readings were taken in the lower quarter of the photometer microammeter scale.

40,000 cfm High-Efficiency Filter System Penetration

To compare a thermal Generator with an air operated generator in an actual large scale filtration system, a 40,000 cfm system in a fuel reprocessing plant was selected. For this system it was necessary to use three 12-nozzle air operated generators, similar in design to the NRL Model II 6-nozzle generator, to obtain sufficient aerosol for testing. The photometer used was "tuned up" to three times its normal sensitivity to handle the 40,000 cfm system without using more generators.

Table 2 gives the average penetration values and system efficiency for the thermal and air operated generators, calculated from a number of photometer readings of upstream and downstream aerosol samples.

TABLE 2

Penetration of 40,000 cfm High - Efficiency Filter System

Generator	Pressure (psig)	Penetration (%)	System Efficiency (%)
TMI - Thermal	22	0.099	99.901
NRL - Air-Operated 3,12 nozzle	20	0.098	99.902
TMI - Thermal	30	0.094	99.906

The three penetration values have a maximum deviation from their average of 3.1%. This deviation is considered remarkably low since the photometer readings themselves had to be averaged from meter fluctuations of approximately 10% on both upstream and downstream aerosol samples.

Particle Size Distribution of Aerosols

Table 3 presents the geometric mean diameter, LSGMD (μ), and geometric mean standard deviation, σ_g (μ), in terms of light scattering for the three generators operating at various pressures.

TABLE 3

Aerosol Particle Size Analysis

Generator	Pressure (psig)	LSGMD (μ)	σ_g (μ)
Taylor	10	0.96	1.42
	15	0.89	1.37
	25	0.89	1.40
	35	0.77	1.36
TDA-4	10	0.77	1.42
	15	0.75	1.42
	25	0.75	1.46
TMI	15	0.75	1.33
	25	0.74	1.37
	35	0.72	1.37

From the table, at 25 lbs pressure the Taylor generator has a light scattering geometric mean diameter of about 0.9 μ. The TMI and TDA-4 generators at this pressure have LSGMDs of about 0.75 μ. While these values are not actual physical diameters, the close agreement of the data between the three generators shows that the particle size distribution for the three generators is very nearly the same. A typical log-probability plot[5] from which the tabulated data was obtained is shown in Figure 8.

Light-Scattering Power and Stability of Aerosols

The aerosols from the three generators were compared for light scattering power by determining the mass concentration required to produce a 100% reading on a photometer, set at standard sensitivity. (100% reading represents 100 μg/liter of 0.3 μ (DOP) monodisperse aerosol.) Mass concentrations were determined by sampling through a type AA Millipore filter, which had been shown to be 100% efficient in filtering the DOP aerosol.

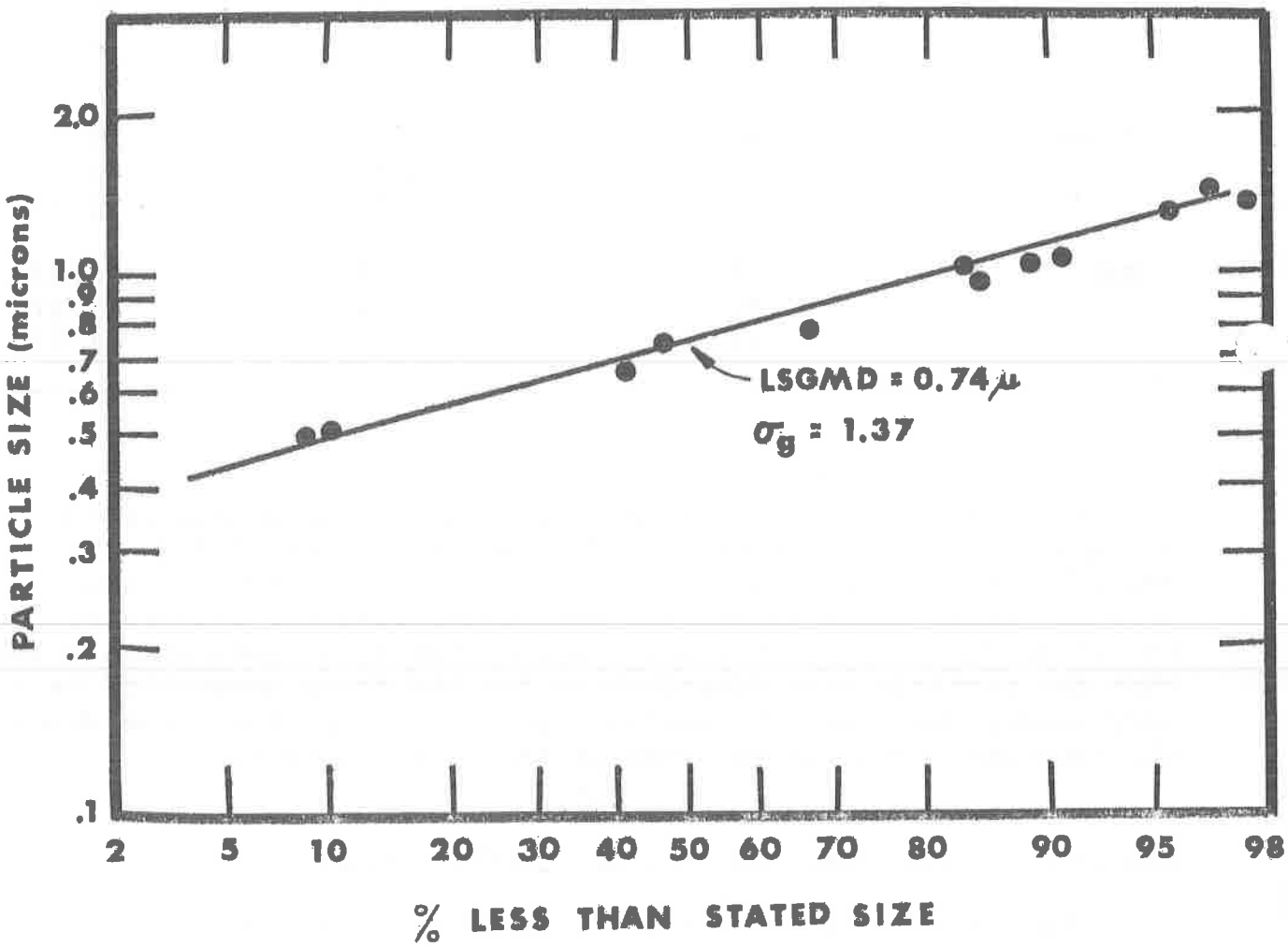

Figure 8. Particle Size Distribution - TMI Thermal Generator (25 psig).

It was found that 40.8 µg/liter produced a 100% reading for the TDA-4 air operated generator, and that the TMI and Taylor thermal generators required 39.8 and 39.6 µg/liter respectively. This close agreement showed that all three generators produce an aerosol having about the same light-scattering power, confirming the similarity of particle size distribution of the three aerosols.

To determine the stability of the three aerosols with respect to light scattering power, aerosol samples from each of the three generators were confined in the photometer (no flow) and the rate of change of photometer reading with time determined. At mass concentrations of either 40 or 80 µg/liter, it was found that the readings changed less than 5% in two minutes, indicating that all three aerosols were very stable.

Nuclear Consulting Services Inc.

CONCLUSIONS

The comparison of penetration values obtained with the three generators shows very close agreement. It establishes the fact that defective filters or filter systems tested with the three generators would result in values differing by less than 5% if a good in-place testing technique was observed.

The particle size analysis, although not a direct method of determining a physical particle diameter, indicates that all three aerosols have very nearly the same size distribution, since all had LSGMDs in the .75 µ - .95 µ range under normal generator operating conditions. Aerosol stability tests show the thermal aerosol to be as stable as the aerosol from air-operated generators.

The principal advantages of the thermal generators are compactness and elimination of need for compressed air when testing high volume air filtration systems. The thermal generators are capable of producing enough aerosol to test systems as high as 15,000 cfm with photometer readings in the 75-100% range at standard photometer sensitivity. Systems of higher volume could be tested by using lower aerosol input concentration, for example, a 25% aerosol reading rather than a 100% aerosol reading. Although testing at a 25% aerosol input reading reduces test sensitivity it is still possible to determine penetration to at least 0.01%. On most photometers it is possible to increase instrument sensitivity and in this manner also increase the size of flow systems the generator can test.

For systems of 1000 cfm or under, thermal generators cannot be used directly without taking precautions to avoid photometer overloading. The small volume of the liquid reservoir limits the length of tests, at maximum generator pressure, to approximately ten minutes. Also, at a set generator pressure, as the liquid level decreases in the reservoir the dispersed aerosol rate increases slowly. This increase was found to be faster at higher generator pressures but it is not of sufficient magnitude to seriously interfere with in-place testing, although it would disturb the inference of system flow rate from input aerosol concentration measurements. The thermal generators are considerably more complex than the air operated generators and more mechanical and electrical maintenance is necessary.

REFERENCES

1. J. K. Thompson, Determination of Aerosol Size Distribution by Jet-Impactor Light-Scattering Technique, Anal. Chem., 29: 1847 (1957).

2. W. E. Ranz, and J. B. Wong, Jet Impactors for Determining the Particle Size Distribution of Aerosols, U.S.A.E.C. Contract No. AT(30-3)-28, Tech. Report 4, Univ. of Ill., Engineering Experiment Station, July 31, 1951.

3. H. W. Knudson, and L. White, Development of Smoke Penetration Meters, NRL Report P2642, Naval Research Laboratory, Sept. 14, 1945.

4. W. H. Echols, and J. A. Young, Studies of Portable Air-Operated Generators, NRL Report 5929, Naval Research Laboratory, July 26, 1963.

5. P. Drinker, and T. Hatch, Industrial Dust, 2nd edition, pp. 190-200, McGraw-Hill Book Co. Inc., New York, 1954.

INCREASED DETECTION SENSITIVITY FOR KRYPTON-85

by

D. G. Smith, P. C. Reist, and L. Silverman*

Department of Industrial Hygiene
Harvard School of Public Health
665 Huntington Avenue
Boston, Massachusetts

ABSTRACT

A field method for increasing the sensitivity of the ionization chamber-vibrating reed electrometer system for detecting krypton-85 by use of an adsorption-desorption concentrating system was investigated. The krypton in the sample stream was concentrated by adsorbing it on an activated carbon bed at a low temperature (-78.5°C) and desorbing it into the ionization chamber at a higher temperature (20°C). A concentration factor was defined and observed to be independent of the inlet concentration of krypton-85.

This work was done under contract between Harvard University and the U. S. Atomic Energy Commission AT (30-1) 841.

* Deceased

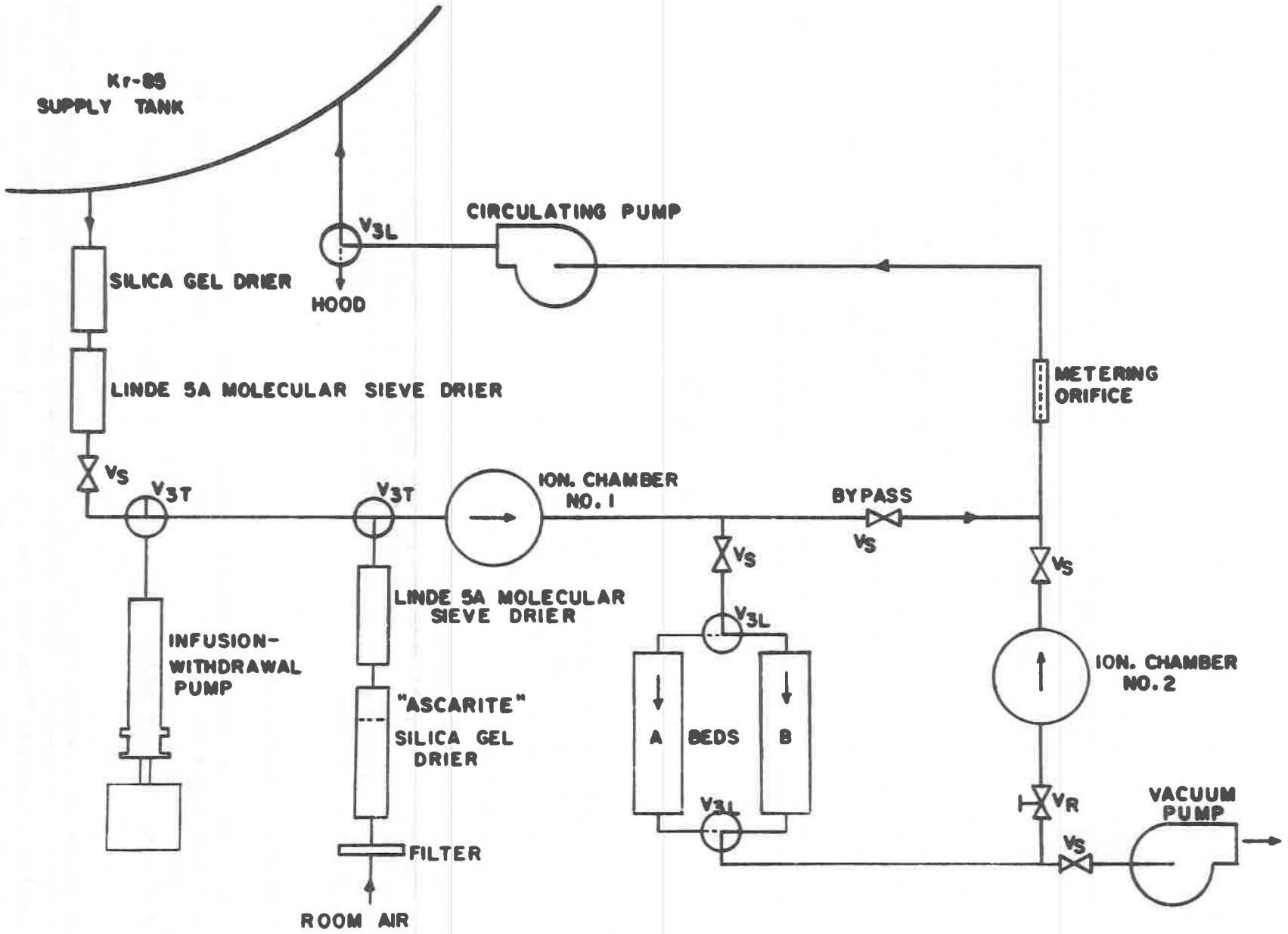

FIGURE 1. SCHEMATIC DIAGRAM OF ADSORPTION-DESORPTION SYSTEM.

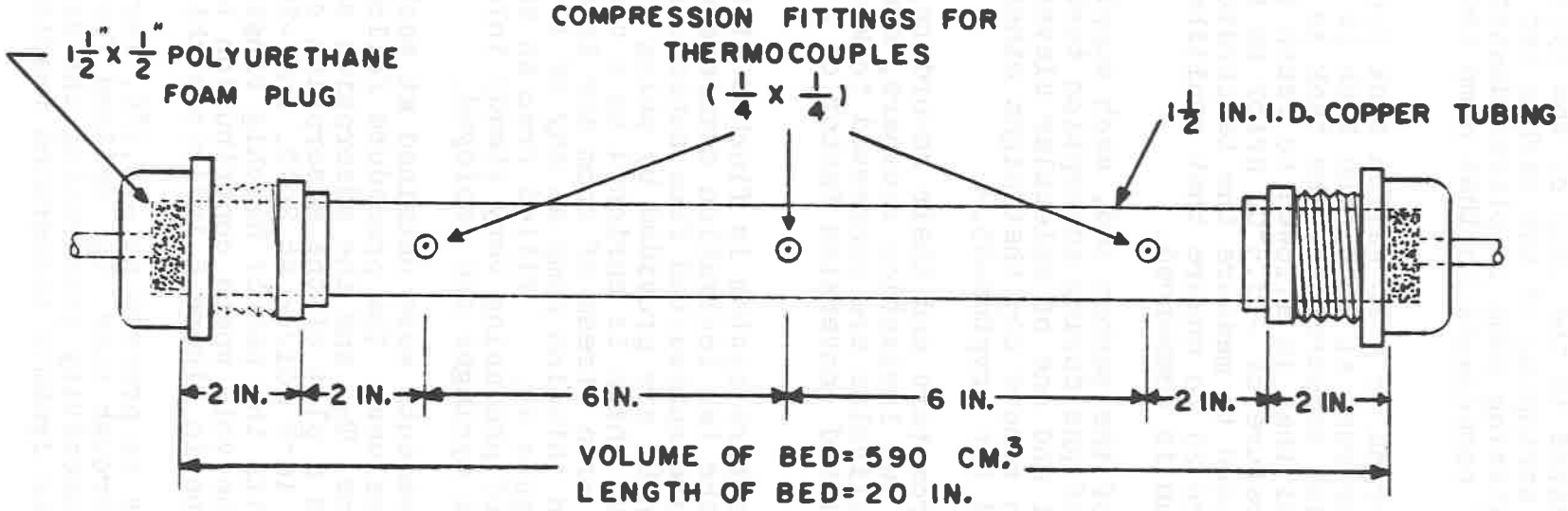

FIGURE 2. SCHEMATIC OF TEST BED DESIGN. SCALE: ⅓ ACTUAL SIZE

chamber. A vacuum pump is located in the loop of the system containing the beds to facilitate vacuum stripping of the carbon bed into the second ionization chamber. The circulating pump is placed downstream from the metering orifice and all other components so that pump leaks are insignificant.

The carbon beds are submerged in a 20 gallon tank containing a constant temperature bath. For runs at 20°C. the tank is filled with water. For the lower adsorption temperature, the tank is filled with a mixture of dry ice and ethanol that is allowed to reach the equilibrium CO_2 sublimination temperature of -78.5°C. prior to the start of each run. Thermocouples are used to measure the temperatures along the centerlines of the beds (Figure 2) to ensure that equilibrium temperatures are achieved before a run is commenced.

To prevent ice clogging of the carbon bed, each supply line that handles a significant amount of gas during adsorption tests has two drying beds, one of silica gel and one of molecular sieves. A bed of "Ascarite" is also provided to remove CO_2 that might otherwise reduce the capacity of the carbon bed for krypton-85.[3]

The vibrating reed electrometers and their recorders, which read the ionization current in the two ionization chambers, are shown in Figure 3. The readouts in millivolts are converted to krypton-85 concentrations with the calculated conversion factor of 2.85×10^7 mv./μCi.[4]

As an initial step, the entire system is flushed with clean dry room air. The readings from the two ionization chambers measure the radiation backgrounds, which are subtracted from subsequent readings. Test concentrations of krypton-85 are provided by using either the gas in the krypton supply tank, which is enriched to a concentration range of 3 to 7×10^{-5} μCi/cc, or a stream of room air into which the radionuclide is injected by an infusion pump at any of 12 different rates. The infusion pump (Figure 4), filled from an external krypton-85 supply, is capable of producing very steady inlet concentrations ($\pm$ 1%) when gas-tight syringes are employed.

Breakthrough curve measurements were obtained at each temperature to check the calculated values. The procedure followed in measuring the breakthrough time, T_B, and the adsorption curve is given in Appendix A. Figure 5 shows a plot of the adsorption curves for the tank concentration of 2×10^{-5} μCi/cc at 20°C. and -78.5°C. The entire process was repeated with the bed of Raschig rings in place of the carbon bed to determine the void space contribution to the breakthrough time. (The dotted line in Figure 5 indicates this contribution).

Originally adsorption was to proceed at -78.5°C. for a period slightly less than the breakthrough time, T_B, defined for our purposes as the time at which the radioactivity penetrating the carbon bed created a 50% increase over the dynamic background reading in the

Figure 3. Vibrating Reed Electrometer, 2.8 Liter Ionization Chamber, and Recorder

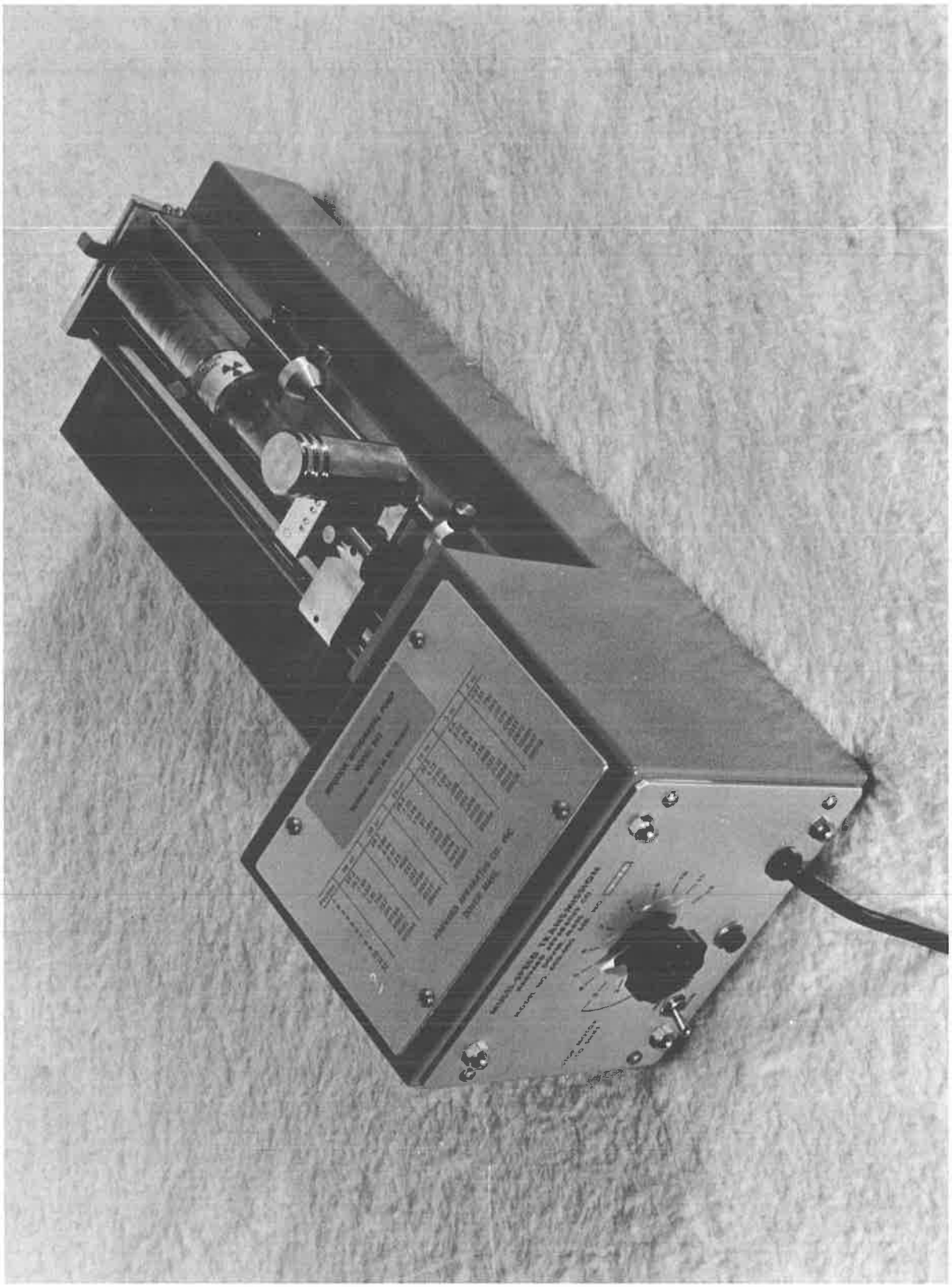

Figure 4. Variable Speed Infusion-Withdrawal Pump

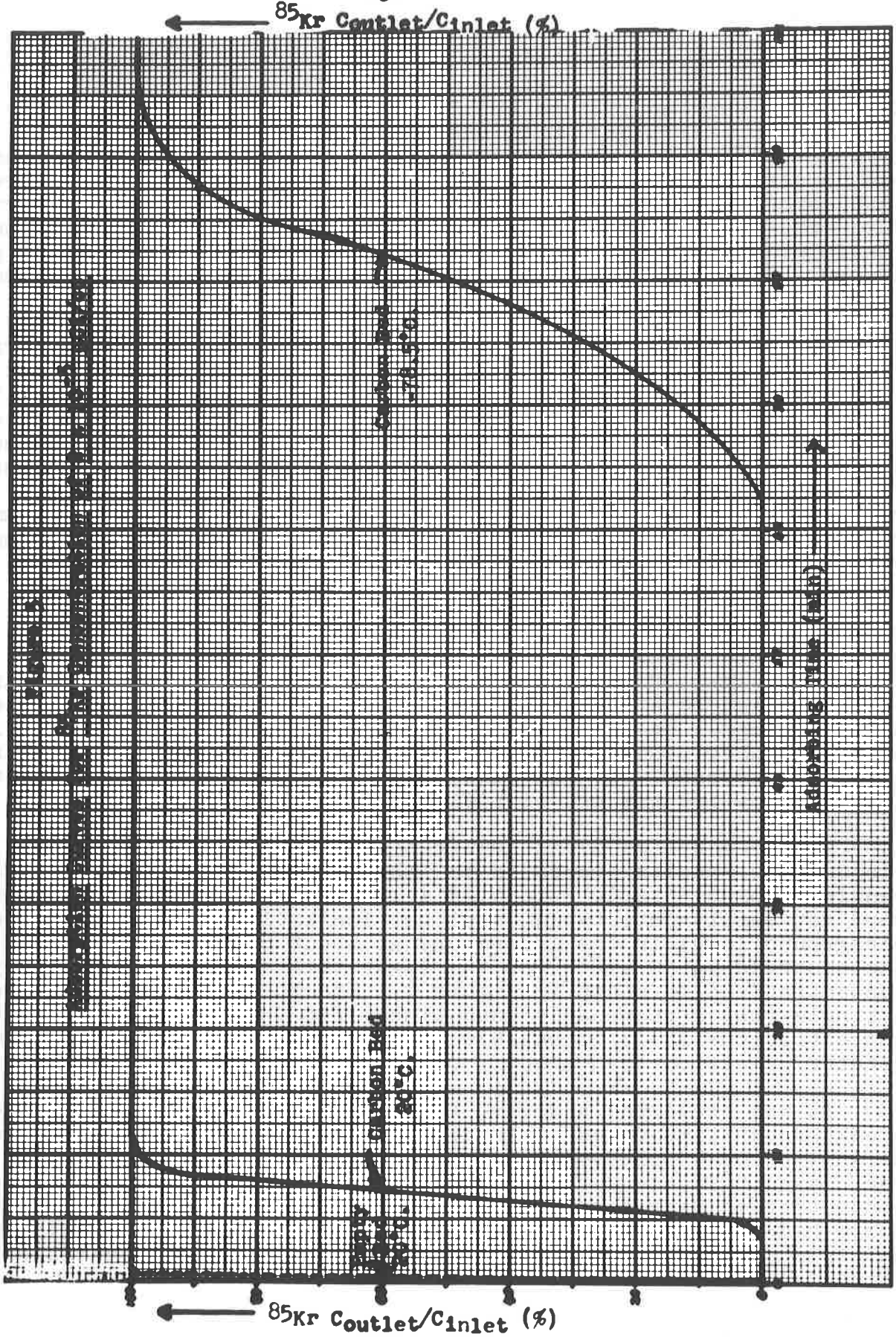
^{85}Kr Coutlet/Cinlet (%)
Adsorption Rate (arb.)
Desorption Rate (arb.)
^{85}Kr Coutlet/Cinlet (%)

downstream chamber. Since the bed was operating at essentially 100% holdup efficiency until breakthrough, the total amount of krypton-85 adsorbed could then be calculated. Desorption by successive vacuum strippings at 20°C. into the downstream chamber was to recover that same total amount minus the fraction that could not be stripped. Measurements of the breakthrough times for several concentrations in the inlet stream were made so that breakthrough times could be predicted for concentrations too low to monitor in the upstream chamber.

Because the results of the first krypton-85 recovery tests indicated that the desorbable fraction of the adsorbed activity was varying in an unpredictable manner, it was decided to allow the adsorption to continue until the bed was saturated at its equilibrium concentration at -78.5°C. At that temperature, the total krypton-85 adsorbed would equal the effective capacity of the bed. The amount desorbable should be a constant fraction of the equilibrium concentration adsorbed by the bed. The stripping procedure was then reduced to a single vacuum stripping at 20°C., since the maximum recoverable level of activity was yielded by the first stripping of a saturated bed.

RESULTS

The holdup of breakthrough due to the void space in the carbon bed was measured at both 20°C. and -78.5°C. by utilizing the bed of Raschig rings. At 20°C. the krypton-85 was observed at the outlet of the Raschig ring bed in 20 $\pm$ 2 seconds; at -78.5°C. it appeared in 22 $\pm$ 2 seconds. It was concluded that the effect of the void space in the bed was not significant at either temperature.

Measurements of breakthrough time, T_B, as defined previously, yielded the results presented in Table 1 for tracer concentrations ranging from 5.55×10^{-3} to 1.24×10^{-7} μCi/cc. Lower concentrations were not easily detectable in either ionization chamber with the background level in the laboratory at about 0.02 mR/hr. A plot of the observed T_B at -78°C for the logarithms of various inlet krypton-85 concentrations is shown in Figure 6. Though each point is based upon a single run, a reasonably good linear fit is observed. At low inlet concentrations it is impossible to identify the breakthrough time with greater precision than about 1 minute.

It was realized, however, that the reason for the dependence of breakthrough time on concentration was a consequence only of the definition of breakthrough time and not a time-concentration effect. The reason that the apparent breakthrough time increased as the concentration decreased was that a greater fraction of the adsorption curve had to pass through the detector to obtain the established multiple of the background reading. This effect is illustrated in in Figure 7.

TABLE 1

Krypton-85 Concentrations vs. Breakthrough Time, T_B, at -78°C. for Bed Illustrated in Figure 2 containing 267 gms. of Columbia 6GC, 10/24 Mesh, Carbon.

^{85}Kr Concentration (μCi/cc)	T_B (min.)
5.5×10^{-4}	54.5
3.7×10^{-5}	59.0
2.0×10^{-5}	63.5
7.3×10^{-6}	71.0
1.0×10^{-6}	74.0
7.4×10^{-7}	86.0
1.3×10^{-7}	96.0

Figure 6.

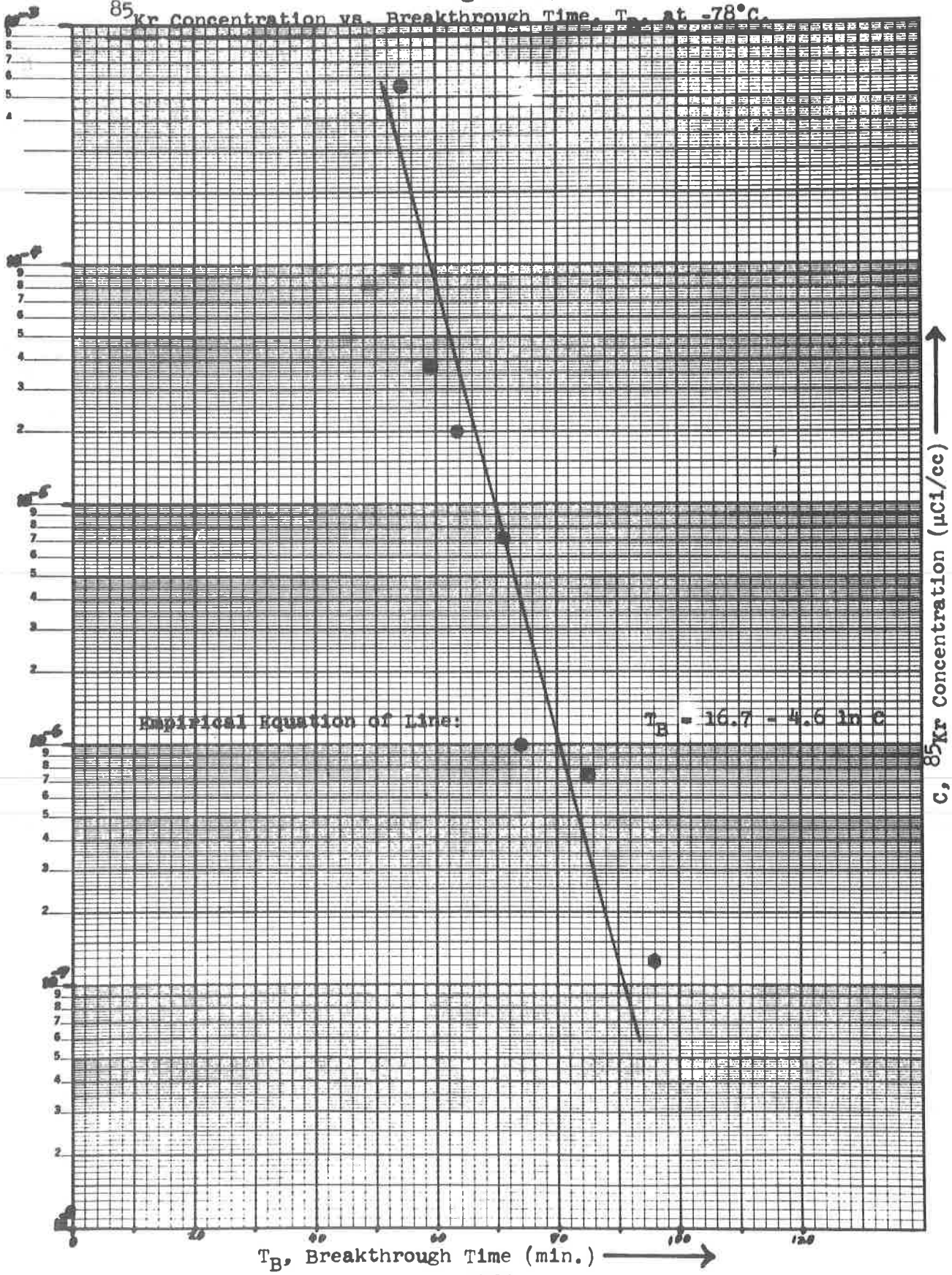
^{85}Kr Concentration vs. Breakthrough Time, T_B, at -78°C.
Empirical Equation of Line:
$T_B = 16.7 - 4.6 \ln C$
C, ^{85}Kr Concentration (μCi/cc)
T_B, Breakthrough Time (min.)

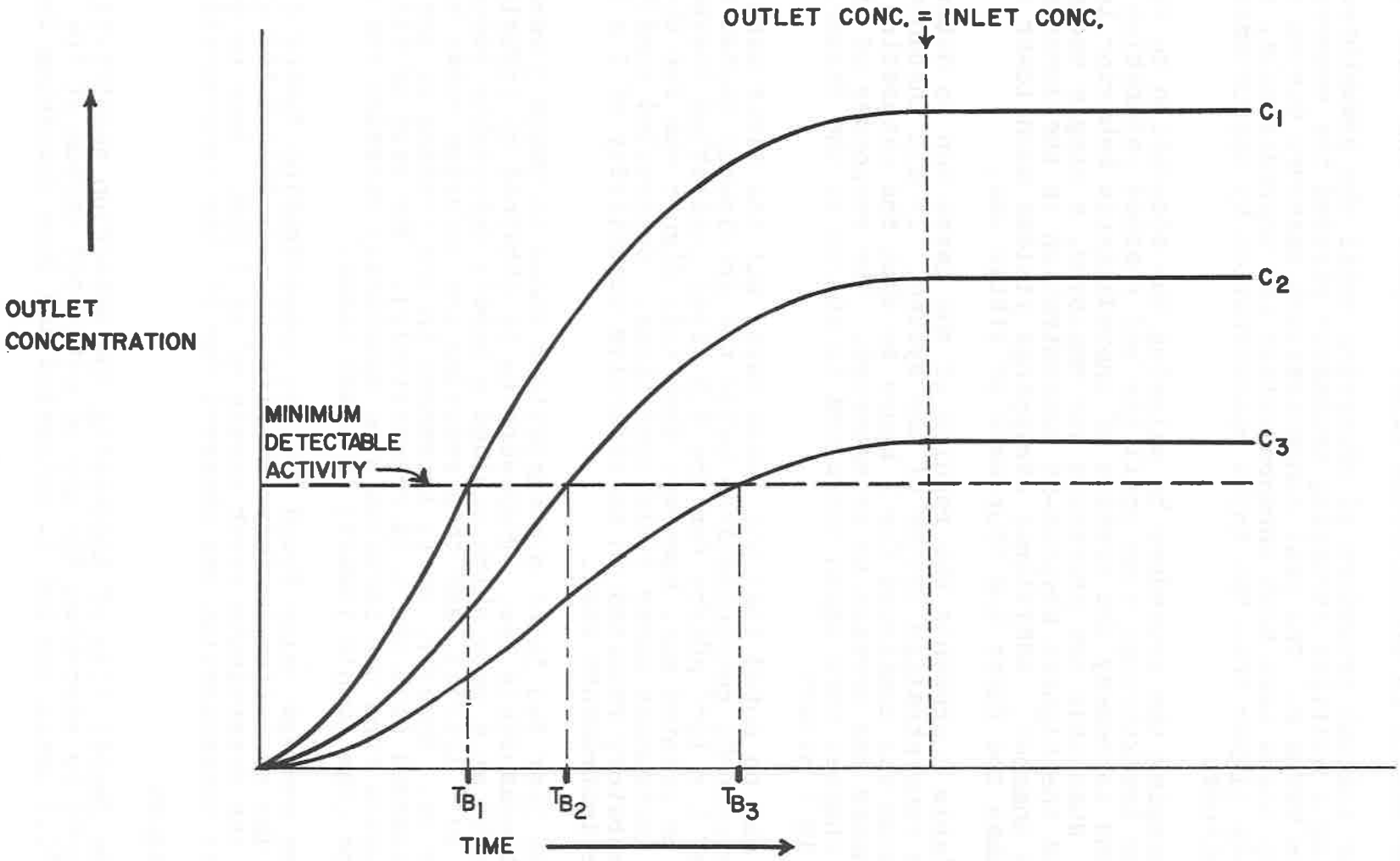

FIGURE 7. APPARENT DEPENDENCE OF BREAKTHROUGH TIME, T_B, UPON INLET CONCENTRATION

Carbon bed breakthrough time measurements at 20°C. were consistently 3.75 ± 0.25 min. independent of the inlet concentration, but the range of concentrations tested at this temperature was not wide enough to show the spread in breakthrough times evident at the lower temperature.

The initial procedure of adsorbing until the breakthrough time and using a multiple stripping technique yielded the recovery results shown in Table 2. The peak concentrations observed during these recovery tests were both unreproducible and unpredictable, even though they were higher than the inlet concentration by approximately an order of magnitude.

Changing the procedure by allowing the adsorption to continue past the breakthrough time until the bed reached saturation (>100 min.) was found to remedy the problem of unpredictable behavior in recovery tests. When this new procedure was employed, a single vacuum stripping produced the highest krypton-85 concentration in the downstream ionization chamber. Additional strippings yielded much lower concentrations than the first and thus were of little use.

Table 3 presents the results of the tests run to determine C', the concentration factor of the system. In all instances the adsorption was continued for 2 hours so that the saturation time of 100 minutes was certain to be exceeded. The responses of the downstream chamber were again converted to μCi/cc by the factor: 2.85×10^{7} mv/μCi.

It may be noted that all these tests but the first were run with krypton-85 concentrations below the previously quoted sensitivity limit of 1×10^{-7} μCi/cc for the 2.8 liter ionization chamber.[1] It should be pointed out, however, that this figure was for the sensitivity of the instrument under field conditions. Controlled conditions in the laboratory resulted in an effective sensitivity of 1×10^{-8} μCi/cc for the instruments used.

The last two inlet concentrations shown in Table 3 were intended to be immeasurably low. They were to be obtained by infusing the krypton-85 at a rate which yielded a barely detectable concentration ($\sim 3 \times 10^{-8}$ μCi/cc), and then reducing the infusion rates by factors of 5 or 10. However, small increases in the reading of the chamber were recorded (10% and ≃ 6% respectively). The rate of diffusion of the krypton from the infusion pump apparently exceeded the rate of infusion (the pump's lowest) in these cases.

The average value found for the concentration factor C' was 17.5. The variation in these results was less than ± 16% which is within the determinate error margin of of ± 20%. Thus no dependence on inlet concentration was observed for C', the concentration factor.

CONCLUSIONS

The feasibility of increasing the detection sensitivity for krypton-85 by adsorbing the gas on activated carbon at low temperatures (-78.5°C.) until the bed is saturated and then desorbing the

TABLE 2

Recovery vs. Krypton-85 Concentrations Adsorbed on C6GC-10/24 Carbon*

^{85}Kr Conc. (μCi/cc)	Adsorption Temp.	% Recovered
2×10^{-5}	-78°C.	70.0
2×10^{-6}	-78°C.	56.5
7.4×10^{-7}	-78°C.	80.8
1.3×10^{-7}	-78°C.	65.4
2×10^{-5}	+20°C.	100
2×10^{-6}	+20°C.	66

* Adsorption times were equal to the T_B values given for the various concentrations in Figure 6.

TABLE 3

Concentration Factor, C', Observed for Various Inlet Concentrations

^{85}Kr Concentration (μCi/cc)		
IN	OUT	C'
1.51×10^{-7}	2.94×10^{-6}	19.5
9.8×10^{-8}	1.58×10^{-6}	16.1
5.6×10^{-8}	1.12×10^{-6}	20.0
3.5×10^{-8}	6.43×10^{-7}	18.3
2.8×10^{-8}	5.17×10^{-7}	18.4
1.1×10^{-8}	1.61×10^{-7}	15.3
7×10^{-9}	1.02×10^{-7}	14.8
	Average	17.5

concentrated gas into a detection chamber at room temperature (20°C.) by a single vacuum stripping was confirmed. This method increased the concentration of krypton in the sample stream by a constant factor that appears to be independent of the inlet concentration to the system. This enabled the detection sensitivity for krypton-85 under field conditions to be increased to 2×10^{-8} µCi/cc.

It was found that the bed saturation time was the adsorption parameter of interest in a concentrating system. Adsorption until breakthrough time(defined as the time required to increase the response of the downstream detection chamber by 50% over background) yielded results which were not reproducible.

Several procedural details were found important in facilitating these experiments:

1. Adsorption data appeared to give a good basis for initial calculations of bed size and breakthrough times, even though the isotopic exchange rate was the controlling factor during these experiments.

2. A variable speed infusion pump proved valuable for establishing a wide range of steady and predictable radionuclide concentrations except at the slowest infusion rate where the krypton-85 diffusion rate appeared to be the controlling factor.

3. A mixture of dry ice and ethanol proved to be effective in providing a relatively safe constant temperature bath for establishing a lower adsorption temperature of -78.5°C.

Further tests will indicate whether the present detector can be replaced with the inherently more sensitive 1 liter GM/proportional chamber to attain a final detection sensitivity beyond the 2×10^{-8} µCi/cc now obtainable for a field monitor.

REFERENCES

1. D. G. Smith, P. C. Reist, and L. Silverman, A Review of Detection Sensitivity for Monitoring of Krypton-85. U.S.A.E.C. Report NYO-841-5, Harvard Air Cleaning Laboratory, Sept., 1966. (not yet published)

2. R. Dennis, and L. Silverman, Air Cleaning Studies Progress Report, U.S.A.E.C. Report HACL 103, pp. 1-5, Harvard Air Cleaning Laboratory, June 1964.

3. R. D. Ackley, R. E. Adams, and W. E. Browning, Jr. The Disposal of Radioactive Fission Gassed by Adsorption, Sixth AEC Air Cleaning Conference, July 7-9, 1959, USAEC Report TID-7593 pp. 199-216, 1959.

4. J. Shapiro, R. E. Yoder, and L. Silverman, Limits of Sensitivity in the Monitoring of Radioactive Gases with Particular Reference to Krypton-85, Eighth AEC Air Cleaning Conference, Oct. 22-25, 1963. USAEC Report TID-7677, pp. 317-329, 1963.

APPENDIX A

Procedure for Measuring the Breakthrough Time, T_B.

1. The entire system was flushed with dry air to measure radiation backgrounds.

2. The empty bed was switched into the system with room air being replaced by the krypton-85 from the supply tank. This permitted checking the agreement of the two ionization chamber readings at the same radioactive material concentration.

3. The system was flushed with room air to remove the krypton-85.

4. The beds were then bypassed.

5. Krypton-85 was again pumped through the first ionization chamber until the desired equilibrium inlet concentration was obtained.

6. Gas flow was switched from the bypass line to the carbon bed as "0" time was marked on the charts of both electrometer recorders.

7. Inlet concentration was monitored in ionization chamber #1 while the concentration penetrating the bed was monitored in ionization chamber #2.

8. The breakthrough point was identified on the chart when the electrometer reading increased by 50% over that of background.

9. The adsorption curve was plotted until the concentration in the second ionization chamber was equal to that in the first.

10. The bed was then bypassed so that the first ionization chamber could be flushed with room air until its activity returned to background.

11. By switching back to the carbon bed once again and admitting the room air to the bed, a desorption curve was similarly plotted.

DISCUSSION

RAY: In monitoring in the plant, quite often we find the practice of running the stack through the filter and then the charcoal bed and then the gas chamber, not looking for the concentration of the krypton on the charcoal. Are these charcoal chambers collecting iodine? How much would this perturb the krypton, seen in a less sensitive type of detecting ion chamber?

D. G. SMITH: Do you mean putting the detector down stream?

RAY: That is right.

D. G. SMITH: The carbon would delay the response to the iodine for a very long time depending on thickness. Actually, you would take the sample before it reached this filter.

I was thinking that you are not going to allow the krypton to escape at all. Is that the case?

RAY: We are monitoring a flowing stream and they are usually characterized in plants, by spikes. I would think a charcoal filter, preceding the krypton directly, would probably tend to iron out the spikes, bleed-out later, and absorb some, and knock off the peaks.

D. G. SMITH: That is true. The application of primary interest in designing the chamber was one of the monitoring, around a plant, rather than in the stack itself.

RAY: I was trying to find out how much the charcoal is going to perturb the common type of application.

D. G. SMITH: Levels in the stack are much, much higher. One gentleman from Oak Ridge, yesterday, described the system and the stack they were using, we estimated that they were at the extreme upper end.

RAY: Some of the commercial ones go to the gamma detection.

BROWNING: I would like to comment upon Mr. Ray's question as to whether the iodine adsorbers could interfere with the detection of krypton downstream. Usually, iodine adsorbers are much smaller than the adsorbers which would be required to trap krypton; therefore, at room temperature, the hold-up time for krypton could be measured in seconds and at most a fraction of a minute. A spike of krypton would be smeared out only slightly over such a brief period. The area under the curve, i.e., the total amount of krypton, would not be reduced after the same length of time passed.

I don't think the presence of iodine adsorber will perturb krypton measurements downstream appreciably under ordinary circumstances.

BRESLIN: In view of the fact that the MPC of krypton is based on whole body immersion, I wonder what the need is for such a sensitive method of measurement.

D. G. SMITH: Could you enlarge upon that a little bit?

BRESLIN: If you can't detect it on a survey, it can't be worth it.

D. G. SMITH: I think the idea was that we wanted to keep the ambient levels of krypton around reactor facilities below the ICRB guide all the time. It is true film badge will give you a reading over a long period of time. This unit was designed with the idea of trying to keep the level below the required level with a routine monitor.

BRESLIN: It is a half millirem per year.

VILES: Of course, as I understand it, this is, essentially, a monitored stack. Sometimes, there are discrepancies on the admission of the materials, too. But, as it was said before, it is essentially a monitor, and it is a question of application.

GREENFIELD: Could you give an estimate of the uncertainty in the procedure that you described in connection with the instrumentation bed?

D. G. SMITH: Well, the last slide showed the concentration factors, where the inlet concentration was down at 1×10^{-8} μ Ci/cc and there was one 7×10^{-9} μ Ci/cc. The latter one was an estimated figure.

Actually, the calculated inlet concentration in that particular test was supposed to be invisible. We found after we had been infusing the gas for about thirty minutes that it was visible on our recorder chart. We checked this discrepancy in two ways. When we got the result, the final outlet concentration, we calculated what the concentration factor would have been had the calculated amount of krypton infused and we found the value of the concentration factor around 60. In other words, there was something wrong with our infusion system. We were evidently infusing more krypton than we thought we were.

Then, the only thing we could blame this on was the fact that the krypton was probably diffusing from the infusion pump faster than it was being infused, because we were using the lowest infusion rate on the pump. The results came out beautifully if we used the inlet concentration that we were observing on the chart rather than the calculated inlet concentration.

As far as the errors are concerned, I would say we could hit any number within 20 per cent if the concentration tests were repeated.

PRELIMINARY RESULTS OF DIFFUSION MEMBRANE STUDIES FOR THE SEPARATION OF NOBLE GASES FROM REACTOR ACCIDENT ATMOSPHERES[1]

S. Blumkin[2] E. Von Halle[2]
H. Briggs[3] J. M. Holmes[4]
A. Dounoucos[3] R. H. Rainey[4]

[1]Research sponsored by the U. S. Atomic Energy Commission under contract with the Union Carbide Corporation.

[2]Oak Ridge Gaseous Diffusion Plant, Oak Ridge, Tennessee.
[3]General Electric Company, Research and Development Center, Schenectady, New York.
[4]Oak Ridge National Laboratory, Oak Ridge, Tennessee.

1. INTRODUCTION

The removal of krypton and xenon from off-gas streams during reactor emergencies and normal chemical reprocessing has long been the subject of research by the U. S. Atomic Energy Commission. Dr. Walter Belter, in his introductory remarks to the 8th Air Cleaning Conference,[1] mentioned this problem as one that "could be the controlling factor in the building of large power reactors in populated areas, as well as being the most restrictive factor in bringing some of our nuclear-powered ships into populated ports."

At least three low-temperature processes have been developed for the removal of both xenon and krypton from off-gas streams where air is the prime constituent and other contaminants, such as the oxides of nitrogen and water vapor, are present. One system used batch-adsorption of the rare gases on a coconut charcoal bed at liquid-nitrogen temperature after the oxides of nitrogen were removed in scrubbers and catalytic beds and the water vapor was removed in alumina adsorbers. Another system substituted a continuous liquid-nitrogen scrubber for the charcoal beds, followed by batch distillation to produce a mixture of rare gases dissolved in liquid oxygen. In this process, however, the presence of liquid oxygen in a gamma-radiation field introduces a potential hazard through the buildup of ozone. A more recent process developed by Steinberg[2] consists in absorbing the rare gases in a fluorocarbon solvent at temperatures near -70 to -100°C, thus eliminating the ozone hazard since a liquid-oxygen phase is not formed.

Recently, the General Electric Company's Research and Development Center developed a thin silicone-rubber membrane that has attractive selective permeability properties for the rare gases and can be operated at ambient temperature. Initial results of a study to develop a separation process using this membrane are reported.

A diffusion cascade has been designed to reduce the krypton level in a 3×10^6 ft^3 containment vessel by a factor of 100 in one week. It has been proposed[3] that such a system be made portable so that it could serve as an emergency standby for several reactors and thus save part of the cost of a permanent installation at each reactor site.

1.1 Consideration of Containment-Vessel Decontamination During a Reactor Accident

Efficient methods have been developed for the removal of iodine vapors and compounds during reactor accidents. Equipment has been installed to reduce the

iodine level in a secondary containment vessel either by circulating the contaminated gases through activated charcoal beds and then back to the vessel,[4] or by discharging the gases to a stack after filtration and decontamination in a similar charcoal unit. It can be shown that, if adequate circulation rates are provided for the recirculating system, reactor low-population-zone radii will no longer be fixed by the total thyroid dose caused by iodine leakage from the containment shell, but by the direct gamma dose caused by the leakage of rare gases. Figure 1 shows the effect of iodine and rare-gas decontamination on the low-population-zone radii required by the code of reactor site criteria.[5] The low-population-zone radii set by permissible thyroid dose rates with no decontamination have been given by DiNunno.[6] The thyroid-dose data after decontamination (of iodine) were calculated by using the equations proposed by Arnett,[4] assuming a circulation rate of 50,000 cfm for a 3×10^6 ft^3 containment vessel and a charcoal-bed efficiency of 99%. Figure 1 indicates that the gamma dose from a cloud containing primarily rare-gas leakage (assuming iodine decontamination) would necessitate moving the low-population zone to a distance about 30% beyond that set by the thyroid-dose zone. However, if decontamination of the rare gases is also assumed, the thyroid-dose limit again becomes the controlling factor. Containment-vessel decontamination for both the iodine and the rare gases would reduce the low-population-zone radius by a factor of about 22, which would probably result in a substantial reduction in reactor siting costs.

The calculations for the decontamination of the rare gases considered only those isotopes with half-lives greater than 5 hr since transport, installation, and startup of a rare-gas decontamination system probably could not be accomplished in less than 12 hr. Isotopes with half-lives less than 5 hr would have decayed significantly by the time the system was ready for operation.

Further justification for disregarding those rare-gas isotopes with half-lives less than 5 hr is provided by considering the relative magnitudes of the removal rate by the cascade and the radioactive decay rate. Actually, in the case of isotopes with half-lives less than 5 hr, decontamination achieved by the cascade in one week would be negligible when compared with the decay rate of these short-lived isotopes. As a result, the longer-lived radioactive isotopes that have to be removed from the reactor vessel by the gas separation cascade are:

Isotope	Half-life
^{131m}Xe	12.0 days
^{133m}Xe	2.3 days
^{133}Xe	5.3 days
^{135}Xe	9.1 hr
^{85}Kr	10.3 years

Selection of the one-week period for rare-gas decontamination of the containment vessel was the result of a compromise. Rapid cleanup is desirable to prevent excessive leakage to the atmosphere. However, since the size of the cascade is inversely proportional to the cleanup time, a period shorter than one week was considered to be an unreasonable requirement as an initial design criterion.

The design of the cascade was based on the separation of radioactive and stable krypton from air since this is the most difficult separation to be accomplished by the system. Separation of xenon, at the same time, is more efficient since the permeation rate of xenon through the membrane is much higher than that for krypton.

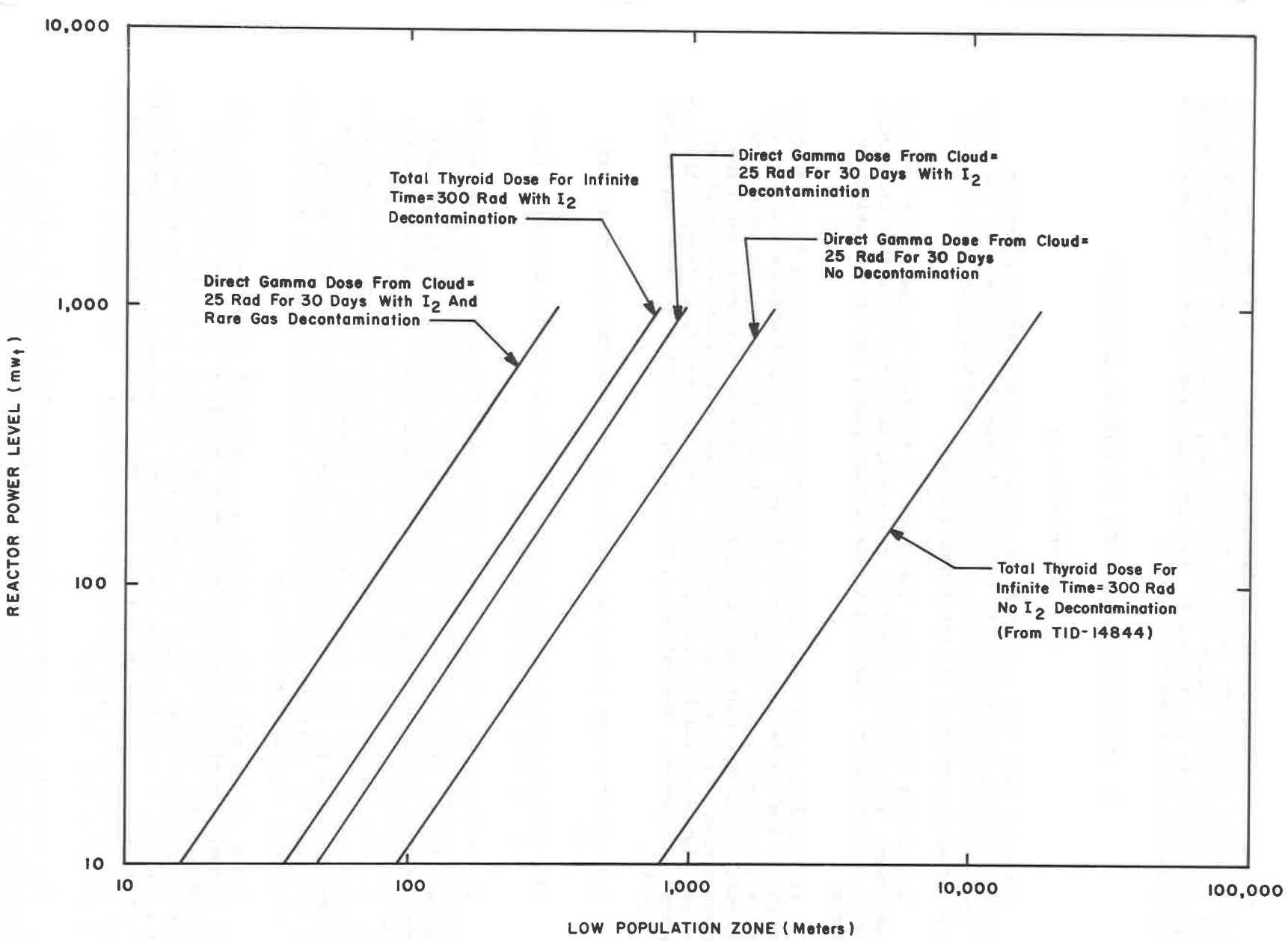

Low Population Zone Radius vs. Reactor Power Level for Decontamination of Iodine and Rare Gases.

Figure 1. Low Population Zone Radius vs Reactor Power Level for Decontamination of Iodine and Rare Gases

Two basic criteria for the design of the cascade are that the quantity of krypton in the containment vessel be reduced by a factor of 100 in one week, and that the maximum total volume of the air mixture, enriched in krypton and xenon, leaving the cascade be 50,000 scf. Estimates indicate that this volume could be transported in a shielded railroad car.

2. PERMSELECTIVE MEMBRANES FOR RARE-GAS SEPARATION

2.1 Membrane Theory

Since the late 19th century it has been known that certain materials exhibit selective permeability to the flow of gases. Under the same conditions of pressure difference across a thin membrane of such a material, one gas will flow through or permeate it faster than another.

This unique property led to the choice of the term "permselective" for such a membrane. This term distinguishes these materials from those that are merely porous, such as paper. Gases will pass through paper, but in a nonselective manner.

It should be noted that the term "selective" does not imply the passage of one gas to the complete exclusion of others. It merely indicates a difference in the flow rates of two molecular species through a permeable membrane. The net result is always that the concentration of the gas mixture on the high-pressure side of the membrane is depleted in the more permeable component as the gas mixture on the low-pressure side of the membrane is enriched in the more permeable component. Theoretically, then, a permselective membrane can be used either to:

(1) reject a more permeable contaminant from a multicomponent mixture, or

(2) produce a product from a multicomponent gas mixture that is enriched in the more permeable components.

The mechanism by which gas or vapor permeates the membrane is not a simple diffusion process as one might find in the case of a material that is porous. Instead, the gas dissolves in the membrane on the side having a high partial pressure, then diffuses through the membrane, and comes out of solution on the side having a low partial pressure. This mechanism is shown schematically in Fig. 2. When the idea of using permeable membranes to separate gases was first conceived, it was not practical because the permeation rates of the available materials were so low that prohibitively large membrane areas were required. In 1957, however, silicone rubber was found to have a uniquely high permeability to a variety of gases (see Table 1).

Table 1 shows that helium, which has the smallest molecular diameter, does not permeate the silicone-rubber membrane as readily as the gases with larger diameters, which is contrary to what might be expected if the gas transport were by diffusion alone. This is explained by the fact that the permeability is a function of both diffusion and solubility of the gases in the membrane.[7-10] If permeability is expressed in terms of diffusion and solubility, it is found that the permeability is proportional to the product of the diffusion coefficient and the solubility coefficient.

The variables that determine the magnitude of the driving force for the flow of a component through a membrane of given dimensions are the membrane's permeability to this component, and the partial pressure difference of this component across the membrane. Thus the membrane area required to effect a

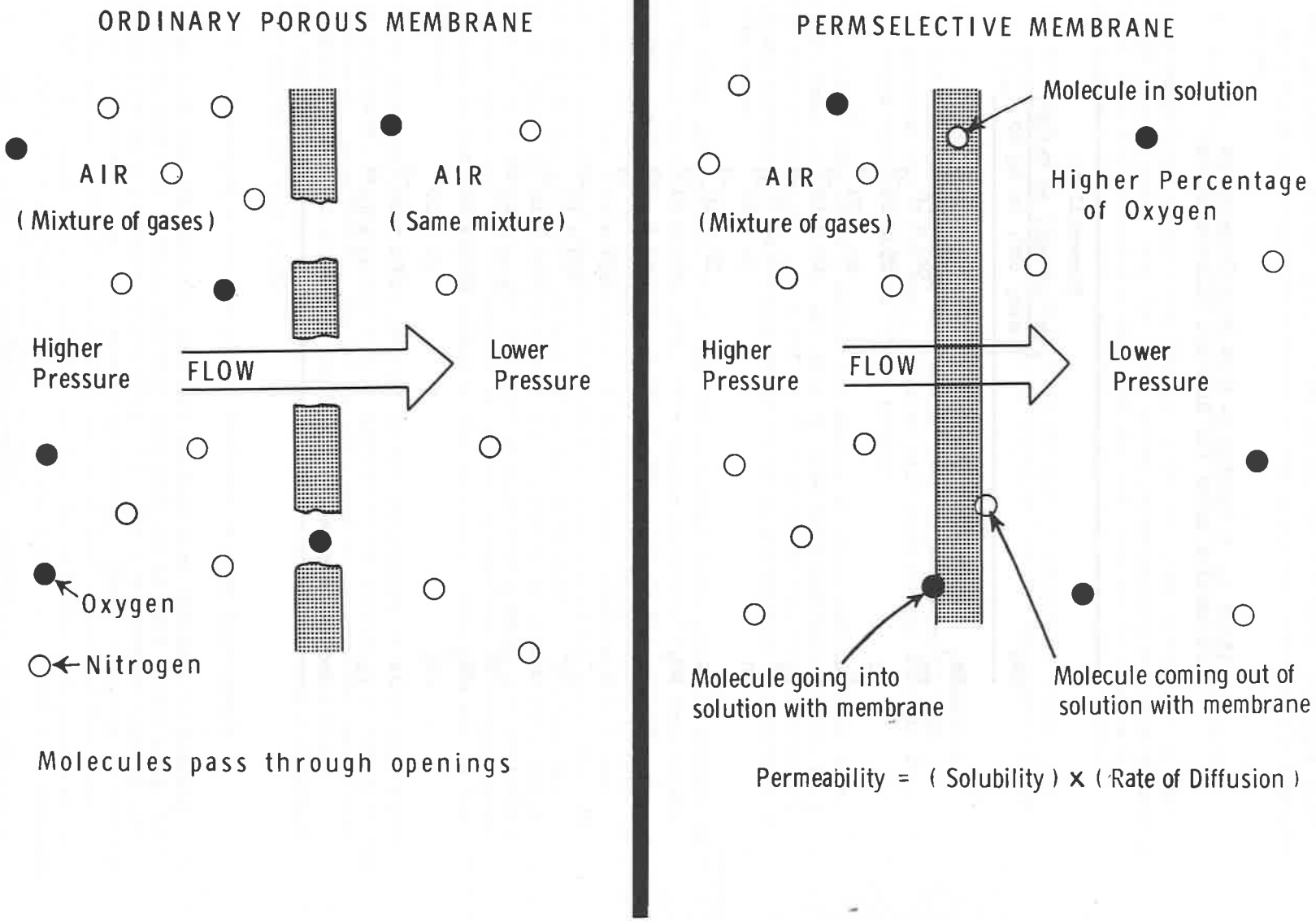

Figure 2. Comparison of Porous and Permselective Membranes

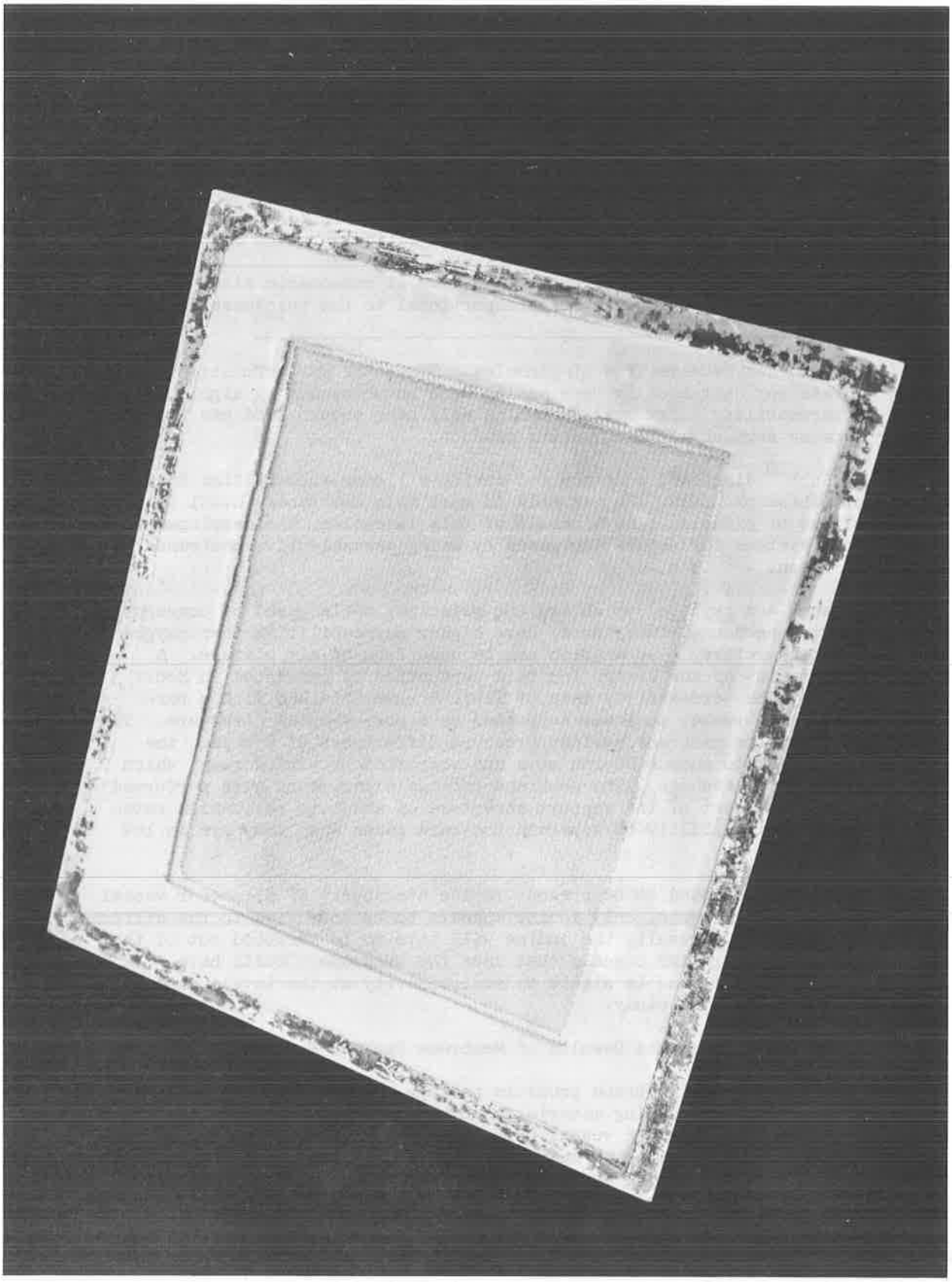

Figure 3. Membrane Pressure Test Block

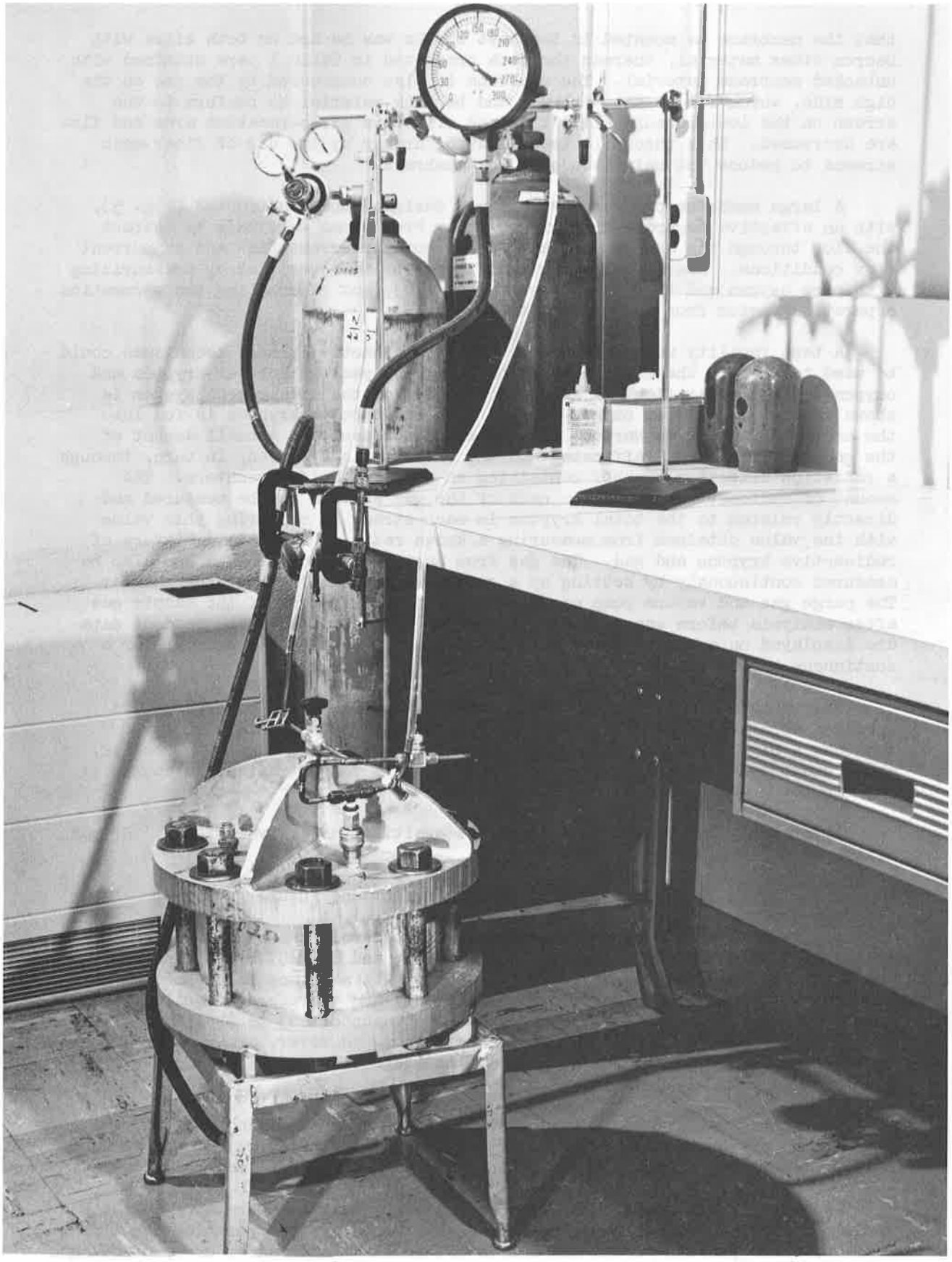

Figure 4. Pressure Test Vessel

that the membrane as mounted in the test blocks was backed on both sides with Dacron fiber material, whereas the data presented in Table 1 were obtained with unbacked membrane material. The membrane is also compressed by the gas on the high side, which forces the membrane and backing material to conform to the screen on the low-pressure side; thus the effective gas permeation area and flow are decreased. This theory is being tested further by the use of finer-mesh screens to reduce the unit stress on the membrane.

A large membrane pressure package was designed and constructed (Fig. 5), with an effective membrane area of 2.0 ft^2. Provisions were made to extract the flow through the membrane package under countercurrent flow and concurrent flow conditions. Design and structural integrity were verified by pressurizing with pure oxygen and then pure nitrogen (Fig. 6), and calculating the permeation separation factor from the extract flow rates.

A test facility was constructed whereby radioactive tracer techniques could be used to measure the efficiency of the membrane package for air-krypton and oxygen-krypton separation. A schematic diagram of the measurement system is shown in Fig. 7. Air or oxygen labeled with radioactive krypton is fed into the membrane package at various flow rates and pressures. A small amount of the gas from the feed, raffinate, and the extracts is bypassed, in turn, through a radiation detection chamber containing an array of Geiger counters. The amount of radioactive krypton in each of the gas streams can be measured and directly related to the total krypton in each stream by comparing this value with the value obtained from measuring a known ratio of a standard mixture of radioactive krypton and gas. The gas from any of the flow streams can also be measured continuously by setting up a constant flow rate through the chamber. The purge gas and vacuum pump are used to remove all traces of the sample gas after analysis before gas from another stream is introduced. The readout data are displayed on a scaler for a digital display or on a chart recorder for a continuous analog readout.

The radiation detection chamber contains two arrays of Geiger counters arranged parallel to the flow stream. The remaining electronic circuitry includes a high-voltage power supply, amplifiers, count-rate meter or scaler, and a chart recorder for continuously recording of concentrations in counts per minute.

At present, the radioactive tests are awaiting the arrival of the ^{85}Kr gas mixtures.

2.4 Cost of Membranes - Present and Future

At present, silicone rubber is being manufactured (though not yet commercially available) in nominally 0.0010-, 0.0015-, and 0.0020-in. thicknesses, supported and unsupported, in 2 x 5 ft sheets. The membrane is now being produced with hand-operated prototype equipment, and therefore is quite expensive. The manufacturing cost ranges from $25 (unsupported) to $45 (doubly backed with 0.005 in. Dacron mat) per square foot. However, order-of-magnitude estimates by the General Electric Company indicate an eventual mass-production cost of less than $1.50/$yd^2$.

Continuing assessment is being made of the potential demand for this membrane as the applications now under development approach realization so that the necessary production facilities will be available to meet this demand.

Packaging and support-structure costs are considerably more difficult to estimate since the choice of materials is determined by the operating conditions. However, where plastic screen and Dacron mat combinations can be used, a packaged cost of $10/$yd^2$ is a reasonable estimate.

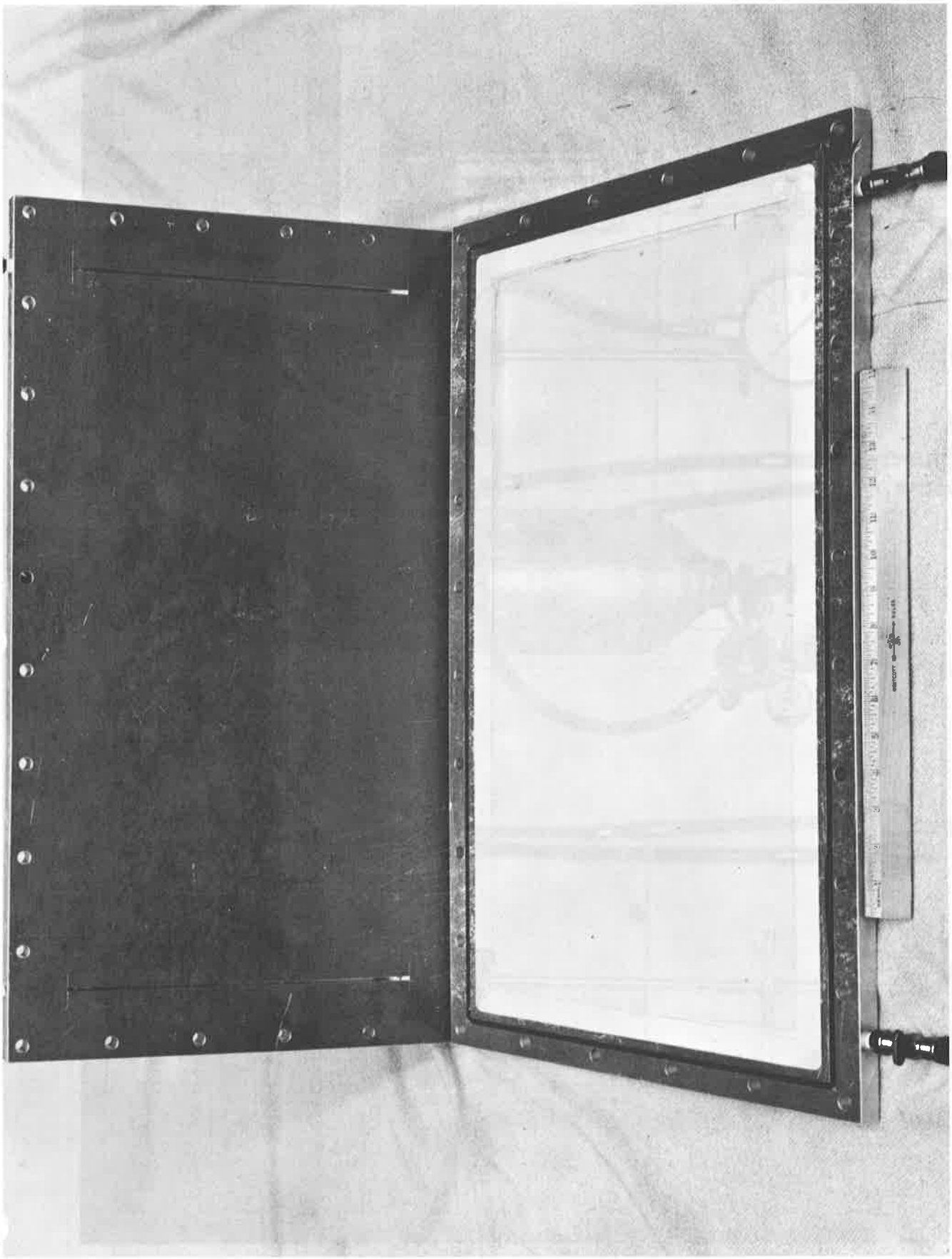

Figure 5. One by Two Foot Membrane Test Cell

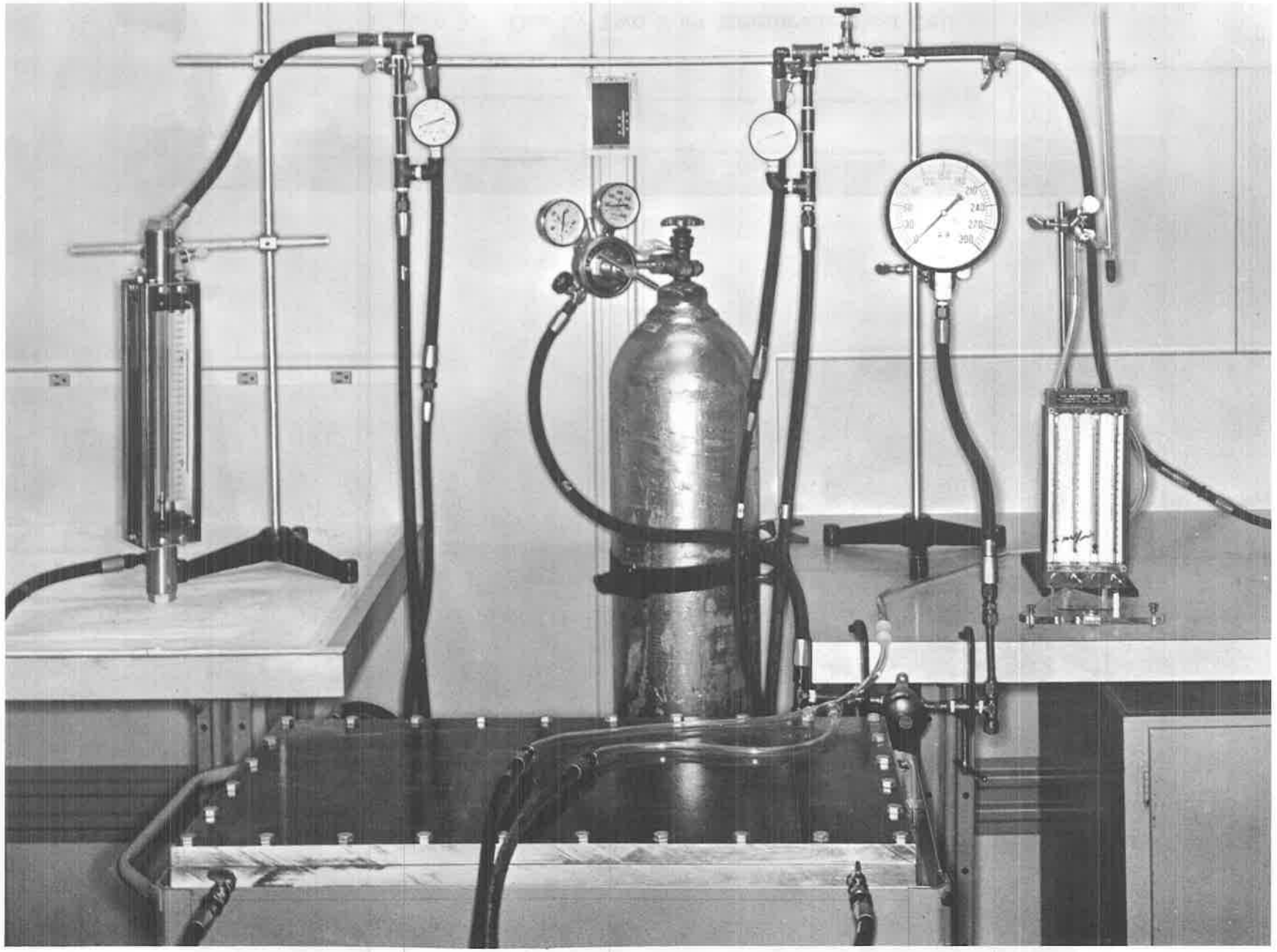

Figure 6. Test Apparatus for Pure Gases and Mixtures

3. DESIGN OF A GAS SEPARATION CASCADE

3.1 Magnitude of the Separation Job

A cascade having silicone-rubber membranes as the separating elements has been designed to clean up the atmosphere in a reactor containment vessel after an accidental release of fission-product gases. It was assumed that the reactor vessel has a capacity of 3×10^6 scf and that the air in it will be contaminated with 3 ppm of krypton and 12 ppm of xenon. The objective, as has already been indicated, is to reduce the krypton concentration in the vessel by a factor of 100 in one week and to collect for storage no more than 50,000 scf of air enriched in krypton and xenon.

The manner in which it is envisioned that the gas separation cascade will be utilized is shown schematically in Fig. 8. In this scheme the krypton is removed from the reactor vessel only through stream P. Thus, the rate of reduction of the krypton content in the containment vessel will depend only on the size of the cascade enricher; however, a minimal stripper will be necessary.

Now if it is assumed that the flow rates into and out of the cascade are time independent, that the ratio of x_p to x_t is a constant* for a given cascade with a specified F and P, and neglecting the decay of the radioactive isotopes it can be shown that

$$\ln\frac{x_0}{x_t} = \frac{\phi F}{V}t \ ,$$

where

t = time,

V = volume of reactor containment vessel,

x_0 = concentration of krypton in the reactor vessel prior to cascade startup, and is also the initial concentration of krypton in the cascade,

x_t = concentration of krypton in the reactor vessel, and also in the feed to the cascade,

F = the cascade feed rate (flow rate from vessel to cascade),

ϕ = krypton removal rate as a fraction of the krypton in the feed to the cascade; $\phi \equiv Px_p/Fx_t$.

Now, with given values for the vessel volume, the cleanup time, the desired reduction in concentration, and the limitation on the storage volume, one can compute the required initial x_p, which with P and x_0 specifies the magnitude of the separation job. Thus, to accomplish the specified objective, a cascade is required that is capable of enriching the krypton content in its feed by a factor of 276 at a product withdrawal rate of 5 scfm.

3.2 Cascade Design Bases

The cascade, of course, will consist of some number of membrane packages of various sizes. Each package will have associated with it a compressor, a

---

*The assumption is implicit here that the equilibrium time of the cascade is short with respect to the one-week processing time and that, though x_t decreases with time, x_p/x_t does not.

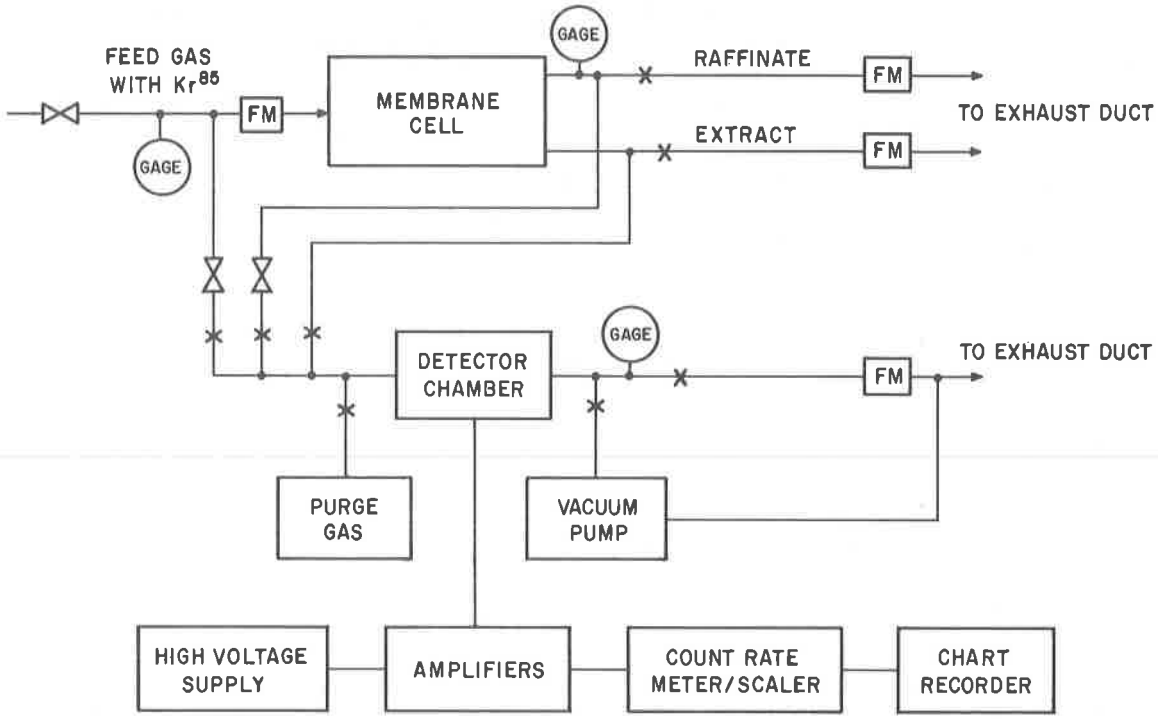

Fig. 7. Schematic - Radioactive Gas Tests

ORNL DWG 66-8343

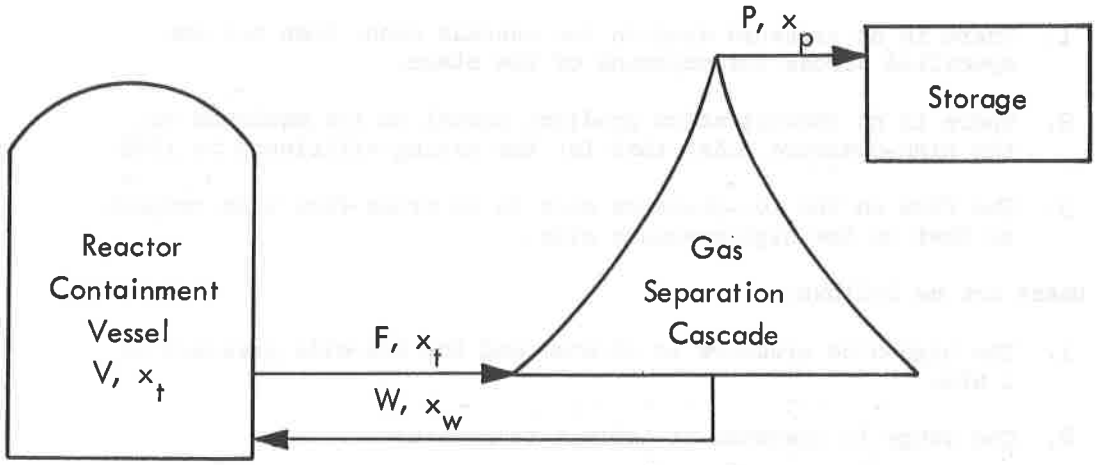

V is the volume of the reactor vessel.

F, P, and W are gas flow rates and are time independent.

x_t is the krypton concentration in the reactor vessel at any time and also the feed concentration to the separation cascade.

x_p and x_w are the product and reject krypton concentrations, respectively, and are time dependent. However x_p/x_t and x_w/x_t are time independent.

Fig. 8. Decontamination Scheme

gas cooler, interconnecting piping, and instrumentation, which together comprise a stage of the cascade. An arbitrary four-stage cascade is shown schematically in Fig. 9. Each stage, with the exception of the ones at the ends, has fed to it a mixture of the permeated stream from the preceding stage and the unpermeated one from the stage ahead.

The fundamental variables that determine the separation performance of the stage are: (1) the permeability of the membrane to each component, (2) the partial pressure difference across it for each component, and (3) the membrane area. The equations that govern the stage performance for a multicomponent system are given in Fig. 10. A description of the method used to solve these equations for the stage flows and concentration gradients across the stage, and of the iterative procedure used to match the cascade concentration gradients with the cascade material balances would increase the length of this presentation prohibitively and is therefore omitted from the discussion here. The assumptions and bases underlying the design calculations made for this study, then, will simply be enumerated. The major assumptions are:

1. There is no pressure drop in the cascade other than the one specified across the membrane of the stage.

2. There is no concentration gradient normal to the membrane on the high-pressure side; that is, the mixing efficiency is 100%.

3. The flow on the low-pressure side is in cross-flow with respect to that on the high-pressure side.

The bases are as follows:

1. The high-side pressure is 10 atm, and the low-side pressure is 1 atm.

2. The stage is operated at ambient temperature.

3. The membrane is 1 mil in thickness.

4. The system, as considered, has four components: Xe, Kr, O_2, and N_2. The concentration of these elements, respectively, in the initial feed is as follows: 12 ppm, 3 ppm, 21%, and 79%. The assumption is made that the iodine in the released gases has been removed by adsorption on a charcoal bed.

5. The permeability of the membrane to each of these components in the mixture is the value given in Table 1. This value was measured by the General Electric Company in tests performed with the pure gas with unbacked membrane at ambient temperature.

6. With the feed composition given above, the cascade must be capable of yielding 5 scfm of gas with a krypton content of 830 ppm.

3.3 Design Criteria

Generally, the optimum separating cascade is considered to be the one that yields the desired product at a minimum unit cost. For the case under consideration here, where mobility of the system is a requirement, minimum physical size of the cascade would be a better criterion. For a binary separation, the "ideal" cascade is the minimum-size cascade. Such a cascade is defined as one in which any two streams that mix are of identical composition. For a multicomponent mixture this is possible only with respect to one component. To

ORNL DWG 66-8342

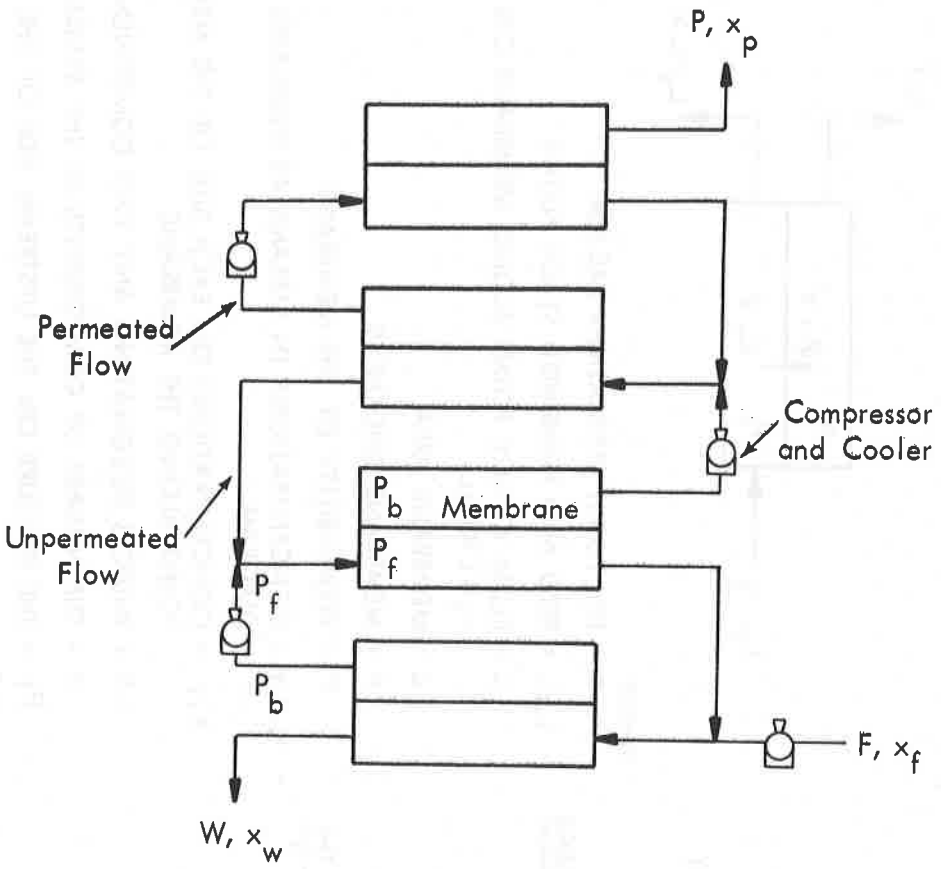

P_f = pressure on upstream side of the membrane.

P_b = pressure on the downstream side of the membrane.

P, W, F are product, reject, and feed streams, respectively.

x_p, x_w, x_f are concentrations in the product, reject, and feed streams, respectively.

Fig. 9. Schematic of a 4-Stage Cascade

ORNL DWG 66-8344

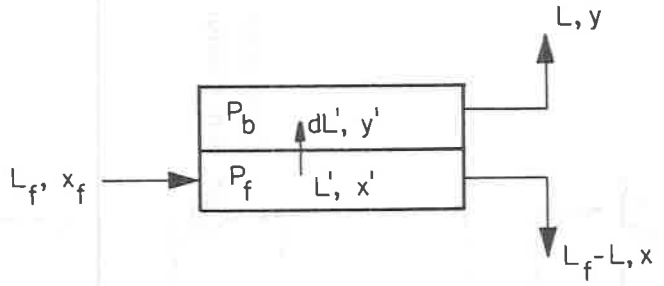

THE POINT EQUILIBRIUM EQUATION

$$\alpha_i \equiv \frac{y'_i/y'_k}{x'_i/x'_k} = \frac{\gamma_i}{\gamma_k} - \frac{P_b}{P_f} \cdot \frac{y'_i}{x'_i}\left(\frac{\gamma_i}{\gamma_k} - 1\right)$$

THE PERMEATION RATE THROUGH THE MEMBRANE

$$\frac{dL}{dA} = \sum_{i=1}^{n} \frac{\gamma_i}{s}\left(P_f x'_i - P_b y'_i\right)$$

TO OBTAIN THE CONCENTRATIONS ACROSS THE STAGE, THE FOLLOWING PERTAINS

$$\int_{L_f}^{L_f - L} \frac{dL'}{L'} = \int_{(x_f)_i}^{x_i} \frac{dx'_i}{y'_i - x'_i}$$

$$L_f(x_f)_i = L_{y_i} + (L_f - L)x_i$$

WHERE:

α_i = THE POINT SEPARATION FACTOR

L_f, L = FEED AND PERMEATED STAGE FLOWS

L' = FLOW AT ANY POINT ALONG MEMBRANE ON UPSTREAM SIDE; $L_f \geq L' \geq L_f - L$

A = MEMBRANE AREA

s = MEMBRANE THICKNESS

γ = PERMEABILITY OF THE MEMBRANE

x_f, x, y = CONCENTRATIONS IN STREAMS AS INDICATED IN THE STAGE DIAGRAM

x', y' = CONCENTRATIONS ON EACH SIDE OF THE MEMBRANE AT ANY POINT ALONG THE MEMBRANE

i, k = INDICES DESIGNATING ANY TWO COMPONENTS

n = THE NUMBER OF COMPONENTS IN THE SYSTEM

P_f = THE PRESSURE ON THE UPSTREAM SIDE OF THE MEMBRANE

P_b = THE PRESSURE ON THE DOWNSTREAM SIDE OF THE MEMBRANE

Fig. 10. The Performance Equations

design a no-mixing-loss cascade, the stage separation factor must be known. When the point separation factor is just slightly larger than 1, simplifying assumptions allow the stage separation factor to be computed directly for all stages. The theoretical point separation factors in this system are quite large (2 to 8), and the stage separation factors cannot be computed directly. As a consequence, a cascade for separating krypton from air using a dimethyl silicone-rubber membrane, designed for no-mixing of streams with unlike krypton concentrations, can be computed only by successive iterations.

Furthermore, the total size of such a cascade will, generally, vary inversely as the feed rate, since the lower the feed rate the larger the stripping section required. There is also a minimum feed rate (1382 scfm in this case) for a specified production goal, since, at less than this rate, it is impossible to satisfy the material balance for the system.

3.4 A Cascade Design

A cascade that will accomplish the cleanup job as specified has been designed. It is an approximation to a no-mixing loss cascade for krypton, and as such is also an approximation to the minimum size one. (However, continuing design calculations indicate that the optimum cascade will not be more than 10 to 15% smaller.) This cascade requires 31,300 yd^2 of membrane area, allocated into 17 stages of various sizes, with the largest stage at one end and each succeeding one smaller. Gas from the reactor vessel is fed to the largest stage. Thus the high-pressure side of the feed stage is the stripping section of the cascade, and the low-pressure side of this stage, plus all the other stages, comprises the enriching section. A minimum power supply of 2 Mw will be required to operate the cascade. The membrane area, the permeation rate, the krypton concentrations in the exit streams, and the power requirement for each stage are given in Table 2. For calculation of the power requirement, a single-stage compression with 75% efficiency was assumed. The computed concentrations of all four components in the feed and withdrawal streams of this cascade are given in Table 3. Since the separation factor for xenon (from air) is several times greater than that for krypton, the xenon in the containment vessel will be depleted by a factor of 3860 during the one week of cascade operation. To check the validity of the assumption that the ratio of x_p to x_t is independent of x_t, calculations were made with the krypton feed concentration at 0.03 ppm instead of 3 ppm. The x_p/x_t ratio obtained at the minimum feed concentration differed from the design value by less than 1%. An estimate of the time required for this cascade to attain steady-state conditions yielded a maximum value of 25 min, which is small relative to the planned cleanup time.

It should be noted here that the assumption of 100% mixing efficiency and no-pressure drop along the membrane and in the piping leads to a smaller cascade than that which would be obtained if these variables were taken into account.

3.5 Cascade Cost

A rough estimate (see Table 4) was made of the capital investment required for such a cascade, exclusive of the cost of the mobile equipment in which it would be installed. The construction cost is on the order of $1.1 million. The assumption was made that the cost of a membrane package is $10 per square yard of membrane*. The power consumption cost, at 4.5 mills/kwhr, will be $215/day.

---

*The current price of membrane sheet is several times this figure. However, this is a projected estimate by the manufacturer, the General Electric Company, of the eventual cost.

Table 2. Cascade Characteristics

Stage	Membrane Area (yd^2)	Permeation Rate (scfm)	Compressive Power (hp)	Krypton Concentration (ppm)* In Permeated Stream	Krypton Concentration (ppm)* In Unpermeated Stream
1	12,620	2134	595	5.7	1.6
2	5,820	1150	321	10.0	8.7
3	3,420	788	220	15.2	6.5
4	2,380	610	170	21.0	10.0
5	1,800	489	136	27.8	14.2
6	1,400	391	109	36.5	19.4
7	1,060	301	84	48.1	26.2
8	807	230	64	63.8	34.9
9	599	171	48	84.2	46.4
10	444	127	35	112	61.6
11	321	92	26	148	82.0
12	232	66	18	197	109
~~13~~	~~162~~	~~46~~	~~13~~	262	145
14	110	32	9	349	193
15	70	20	6	466	258
16	40	12	3	623	344
17	17	5	-	835	462
Total	31,300	6664	1856		
Feed stream		2900	808		
Total		9564	2664		

Note: The slant lines connect concentrations of streams that mix in the cascade.

*Steady-state values; based on initial feed concentrations.

Table 3. Cascade Streams

	To Storage (P)	Feed (F)	Return to Reactor Vessel (W)
Flow rate, scfm	5	2900	2895
Concentrations, mole fraction*			
Xenon	0.59×10^{-2}	0.12×10^{-4}	0.18×10^{-5}
Krypton	0.83×10^{-3}	0.3×10^{-5}	0.16×10^{-5}
O_2	0.993	0.210	0.2086
N_2	0.3×10^{-5}	0.789985	0.7913

*Steady-state values; based on initial feed concentrations.

Table 4. Estimate of Cascade Capital Cost

Item	Thousands of Dollars
Membrane packages	313
Compressors	141
Coolers	17
Auxiliaries	21
Piping and installation	349
Instrumentation	25
Electrical system	40
Engineering and inspection	91
Contingencies	149
	1146

3.6 Cascade Size

It is expected that the membrane packages and compressors would take up the greater part of the space required by this cascade. On the basis of 20 to 30 yd^2 of membrane per cubic foot of membrane package, the membrane packages would require about 1300 ft^3 of space. However, it is estimated that the compressors would occupy a larger volume. On the basis of a rough layout, the total volume of the system should be approximately 6000 ft^3. A cascade of this size would occupy three semitrailers of the type that can be air-lifted. Each of the semitrailers have inside dimensions of 40 x 7-1/2 x 7 ft.

3.7 Discussion and Conclusion

As already mentioned, additional design calculations that have been made indicate that a decrease in cost or size of the cascade by more than 10 to 15% is probably not realizable. To effect a significant decrease in the size of the separation cascade, one will have to resort to means other than optimization of the design. One way is to diminish the magnitude of the separation job by relaxing either the time specified for cleanup or the maximum storage volume. The cascade requirements would be cut approximately in half for a doubling in the time allowable for decontamination. Also, if the acceptable limit in storage volume for the hot gases is increased, the cascade size would be diminished, though probably not nearly in direct proportion. The quantitative relationship in this case is not obvious and would have to be developed from design calculations.

Another possibility is the removal of most of the oxygen by absorption or chemical reaction from the feed stream to the cascade. If this can be accomplished economically, the size of the membrane system would be reduced considerably.

Investigation of the possible use of permselective membranes for xenon, krypton, and air separation is continuing, not only for the particular application described here, but also for cleanup of off-gases from a reactor fuel element reprocessing plant. Membranes of different composition, which may exhibit larger separation factors for this mixture, thinner silicone-rubber membranes, and operation with larger pressure drops across the membrane, and the possibility that the separation factors may be larger at temperatures other than ambient are paths that are being examined for possible improvement of this separation method.

REFERENCES

1. W. G. Belter, U. S. Atomic Energy Commission, introductory remarks in Eighth AEC Air Cleaning Conference, Oak Ridge, Tennessee, October 22-25, 1963, USAEC Report TID-7677, pp. 3-6.

2. M. Steinberg, The Recovery of Fission Product Xenon and Krypton by Absorption Processes, USAEC R port BNL-542, Brookhaven National Laboratory, January 1959.

3. H. Bernard, U. S. Atomic Energy Commission, Washington, D. C., personal communication, 1966.

4. L. M. Arnett and B. C. Rusche, The Application of Iodine Absorber Units to the HWCTR Containment System, in Eighth AEC Air Cleaning Conference, Oak Ridge, October 22-25, 1963, USAEC Report TID-7677, pp. 248-257.

5. Reactor Site Criteria, Title 10, Code of Federal Regulations, Part 100 (10 CFR 100), Feb. 11, 1961.

6. J. J. DiNunno, Calculations of Distance Factors for Power and Test Reactor Sites, USAEC Report TID-14844, p. 30, Mar. 23, 1962.

7. R. M. Barrer, Diffusion in and Through Solids, p. 60, Cambridge University Press, London, 1941.

8. R. M. Barrer, Diffusion in and Through Solids, p. 403, Cambridge University Press, London, 1941.

9. R. M. Barrer and G. Skirrow, Transport and Equilibrium Phenomena in Gas-Elastomer Systems. I. Kinetic Phenomena, J. Polymer Sci. 3: 549 (1948).

10. W. L. Robb, Thin Silicone Membranes - Their Permeation Properties and Some Applications, Report 65-C-031, General Electric Corporation, October 1965.

MASS TRANSFER OF KRYPTON-85 IN CHARCOAL ADSORPTION BEDS

by

Dwight Underhill

Department of Industrial Hygiene
Harvard School of Public Health
665 Huntington Avenue
Boston, Massachusetts

- -

ABSTRACT

A fundamental factor in the design of charcoal adsorption beds for fission gases is the number of mass transfer units (theoretical plates) of the bed--the greater the number of transfer units the more efficient the bed. Using krypton-85 tracer in an air carrier, the number of mass transfer units in charcoal beds cooled with dry ice was determined over a wide range of flow velocities and charcoal particle diameters for both adsorption and desorption. The mechanisms of mass transfer as a function of reduced velocity were identified as gas phase diffusion, eddy diffusion and phase inequilibrium. The studies also confirmed the applicability of the Van Deemter equation.

INTRODUCTION

This report describes a study of the mass transfer of dilute fission gases in charcoal adsorption beds. Particular attention is given to the effect of carrier gas velocity on the shape of a front of dilute fission gas passing through the bed. The relationship between gas chromatography and fission gas adsorption is described, and equations commonly used in gas chromatography are applied to the results of fission gas adsorption experiments.

The model for the study is a charcoal adsorption bed into which a constant dilute concentration of a fission gas in an inert carrier gas is fed starting at a time, t = 0. With the assumptions of ideal mass transfer (no frontal broadening from local non-equilibrium and diffusional processes) and negligible radioactive decay, the concentration, C, of fission gas in the front remains constant. At the edge of the front the concentration abruptly drops to zero.

With non-ideal mass transfer, such a sharp concentration gradient is not possible and results in the broadening of the concentration profile. Broadening of the concentration profile reduces the ability of adsorption beds to concentrate or to hold up fission gases. In this paper the non-ideal effects observed when dilute krypton-85 in an air carrier is passed through a charcoal bed at 195°K, are reported and analyzed in terms of known mechanisms of mass transfer.

MECHANISMS OF MASS TRANSFER

Figure 1 shows the passage of a front of fission gases through an adsorption bed under ideal conditions and may be compared with Figure 2, which shows frontal broadening from non-ideal effects.

Frontal broadening is also apparent in a plot of C', the derivative of concentration with respect to the distance from the inlet (Figure 3). Initially C' is zero everywhere except at one sharp point where the concentration changes from zero to its final value. As the front spreads, C' assumes finite values on either side of the initial peak. Initially this spread is best described by Bessel functions, but with increasing bed length, C' approaches a Gaussian distribution. This leads to an important measure of mass transfer: H, the height equivalent of a transfer unit, is the rate with which the variance of C' increases with the distance x from the inlet.

$$H = \frac{d\sigma_c^2}{dx} \qquad \text{Equation 1.1}$$

Other factors remaining unchanged, decreasing values of H lead to increased adsorption bed efficiency.

The major contributions to frontal broadening in fission gas adsorption beds are expected to be from gas phase diffusion, eddy diffusion, gas phase resistance, and solid phase resistance. These mechanisms are discussed briefly below.

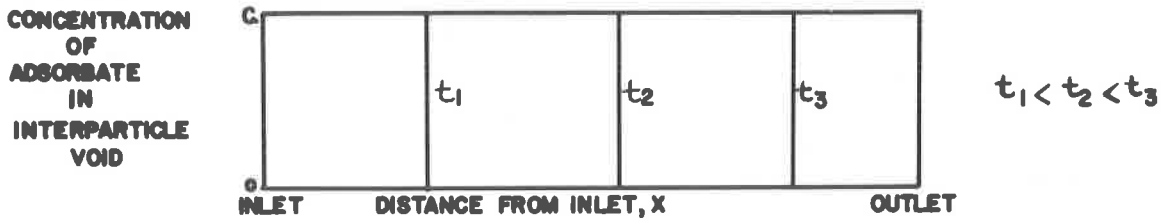

FIGURE 1 CONCENTRATION PROFILES ACROSS AN ADSORPTION BED ASSUMING IDEAL MASS TRANSFER

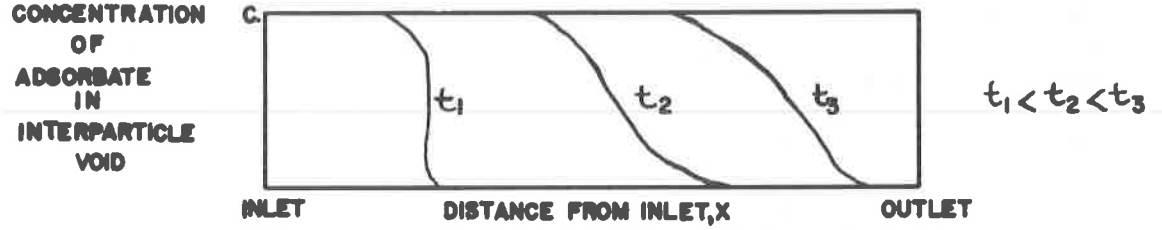

FIGURE 2 CONCENTRATION PROFILES ACROSS AN ADSORPTION BED ASSUMING NONIDEAL MASS TRANSFER

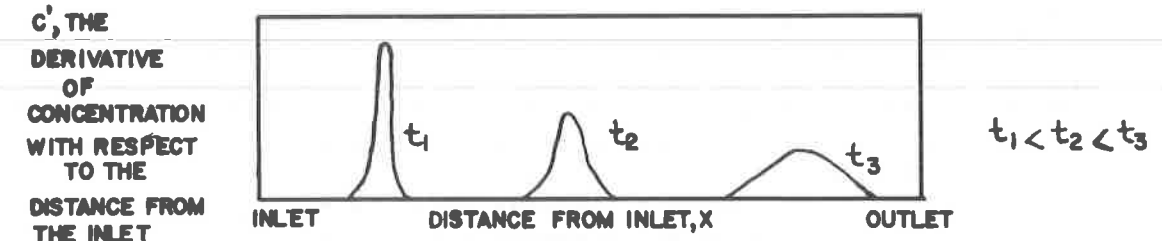

FIGURE 3 BROADENING OF C' AS A FRONT PASSES THROUGH AN ADSORPTION BED

Gas Phase Diffusion

If gas phase diffusion follows Fick's law

$$D_f \frac{d^2C}{dw^2} = \frac{dC}{dt} \qquad \text{Equation 1.2}$$

where C = Concentration of adsorbate

D_f = Coefficient for diffusion of the adsorbate through the carrier gas, $cm^2\ sec^{-1}$

$w = x - (k' + 1)V_i t$, (a convenient parameter whose dimensions are in cm)

t = Time following introduction of the adsorbate, sec

V_i = Interparticle velocity of the carrier gas, $cm\ sec^{-1}$

then for a sufficiently long column,

$$C'(w,t) = \frac{1}{2\sqrt{\pi D_f t}}\, e^{-\frac{w^2}{4D_f t}} \qquad \text{Equation 1.3}$$

and the variance in C' is $2D_f t$. When the factors γ and $1/(k' + 1)$ are included to account for the tortuosity of the diffusion path and for the fraction of adsorbate that is in the fixed phase, the variance in C' is given by Equation 1.4.

$$\sigma_{c'}^2 = \frac{2\gamma D_f t}{1 + k'} = \frac{2\gamma d_p L}{v_i} \qquad \text{Equation 1.4}$$

where k' = Ratio of adsorbate in adsorbent, at equilibrium, to adsorbate in the carrier gas

γ = Tortuosity factor for diffusion

d_p = Average diameter of adsorbent particle, cm

L = Length of adsorbent bed, cm

v_i = Interparticle reduced velocity (a Peclet number defined as $V_i d_p / D_f$)

t and D_f as defined above.

For gas-liquid chromatography, γ usually lies between 0.5 and 0.8. With glass beads Knox and McLaren[1] found the experimental value to be 0.6, which corresponds closely to the theoretical value of 0.63 for uniform spherical beads. Similar values of γ would be expected for the particles of charcoal in a fission gas adsorption bed.

The interparticle reduced velocity, v_i, which appears in Equation 1.4, is a modified Peclet number. Physically it represents a ratio of the interparticle transport of adsorbate by the movement of the carrier gas to the interparticle transport of adsorbate by diffusion through the carrier gas. In Equation 1.4, when v_i is large the contribution of gas phase diffusion to frontal broadening is small which, from the physical meaning of v_i is the expected result.

Eddy Diffusion

The manifold pathways followed by a front of adsorbate through a bed of adsorbent lead to a frontal spreading termed eddy diffusion. Even in laminar flow the mechanisms of eddy diffusion are extremely difficult to analyze mathematically, but their contribution to frontal broadening can be written in the simple form $2 \lambda d_p L$, where λ is a geometric mixing factor. If this mixing is completed within one to two particle diameters, λ has a mean value between one and two.

Gas Phase Resistance to Mass Transfer

The greater part of gas phase resistance is assumed to result from resistance across a laminar film surrounding each adsorbent particle. The magnitude of this resistance to mass transfer is known from experiments such as the evaporation of water from saturated adsorbents, the sublimination of naphthalene from solid naphthalene, etc., in which the mass transfer resistance of the solid phase is negligible. The contribution of gas phase resistance to frontal broadening is calculated from Equation 1.5, which has been derived from equations given by Wilke and Hougen.[2]

$$\sigma_{c'}^2 = \frac{L d_p}{14.8} v_i^{0.51} Sm^{-0.16} \qquad \text{Equation 1.5}$$

where Sm = Schmidt number for adsorbate fluid carrier

L, d_p, v_i as defined above.

The contribution of gas phase resistance to column variance increases with increasing carrier gas velocity and, when solid phase resistance to mass transfer is negligible, becomes the controlling factor in mass transfer at high carrier gas velocities.

Solid Phase Resistance to Mass Transfer

Van Deemter et al.[3] have calculated the variance due to diffusion in the solid phase as

$$\sigma_{c'}^2 = \frac{D_f k' v_i d_p L}{2\pi^2 D_s (1+k')^2} \qquad \text{Equation 1.6}$$

where D_s = Coefficient for diffusion of adsorbate through the adsorbent

d_p, D_f, k', L, v_i as defined above

Few measurments of solid phase resistance to mass transfer have been made for gas-solid chromatography.

Combined Variances

Van Deemter et al.[3] assumed that variances from the principal effects are additive and the resulting equations (which usually carry the name of Van Deemter) were the first capable of describing the performance of sorption beds over a wide range of conditions. The equations below differ from the usual Van Deemter equations because the variance is given for C' instead of C, and a term for gas phase resistance is included.

1. For Total Variance

$$\sigma_{C'}^2 = \frac{2\gamma d_p L}{v_i} + 2\lambda d_p L + \frac{D_g k' v_i d_p L}{2\pi^2 D_s (1+k')^2} + \frac{v_i^{0.51} S_m^{-0.16} d_p L}{14.8} \qquad \text{Equation 1.7}$$

2. For Height Equivalent of a Transfer Unit

$$H = \frac{d\sigma^2}{dx} = \frac{2\gamma d_p}{v_i} + 2\lambda d_p + \frac{D_g k' v_i d_p}{2\pi^2 D_s (1+k')^2} + \frac{v_i^{0.51} S_m^{-0.16} d_p}{14.8} \qquad \text{Equation 1.8}$$

3. For Reduced Height of a Transfer Unit

$$h = \frac{H}{d_p} = \frac{2\gamma}{v_i} + 2\lambda + \frac{D_g k' v_i}{2\pi^2 D_s (1+k')^2} + \frac{v_i^{0.51} S_m^{-0.16}}{14.8} \qquad \text{Equation 1.9}$$

With the assumptions

$\gamma = 0.6$

$\lambda = 1.2$

Sm = 0.86 (Schmidt number for krypton in air)

$D_s = \infty$ (i.e., no solid phase resistance)

a plot of h versus v_i (Figure 4) shows three distinct phases in passing from low to high v_i. These are areas of:

1. Decreasing h where h is controlled by gas phase diffusion.
2. Constant h where h is controlled by eddy diffusion.
3. Increasing h where h is controlled by gas phase resistance.

With finite values of D_s (representing a finite solid phase mass transfer resistance) a fourth factor is introduced which is first seen at the highest values of v_i, but as D_s decreases in value becomes important at lower v_i. This is illustrated by the two dashed curves in Figure 4, where the left and right hand dashed curves are given for lower and higher values of D_s, respectively. The value of h can not be known for higher reduced velocities until the solid phase resistance has been measured experimentally.

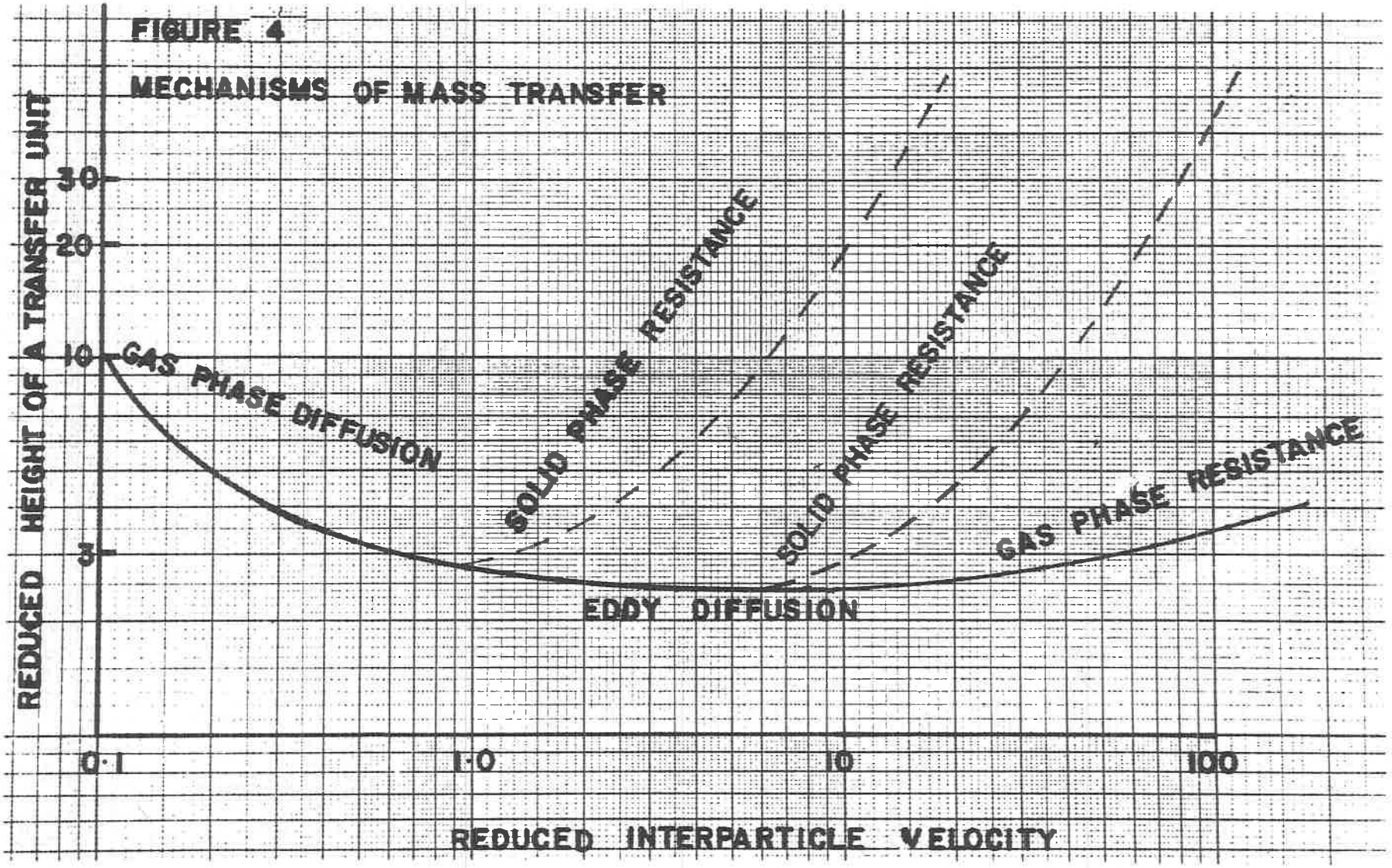
FIGURE 4
MECHANISMS OF MASS TRANSFER
REDUCED HEIGHT OF A TRANSFER UNIT
30
20
10
3
1
0·1
1·0
10
100
REDUCED INTERPARTICLE VELOCITY
GAS PHASE DIFFUSION
SOLID PHASE RESISTANCE
EDDY DIFFUSION
SOLID PHASE RESISTANCE
GAS PHASE RESISTANCE

The preceding discussion of chromatographic theory can be applied to fission gas adsorption beds. It is reasonable to assume that the physical mechanisms controlling mass transfer in gas chromatographic columns can also control mass transfer in fission gas adsorption beds. Still it is not clear how well the Van Deemter equation will describe fission gas adsorption on charcoal beds. Listed below are several reasons why it is difficult to extrapolate mass transfer data obtained from gas chromatography to fission gas adsorption.

1. The diameters of adsorbent particles used in fission gas recovery beds may be from ten to a thousand times greater than those normally used in gas-liquid chromatography and at least ten times greater than those normally used in gas-solid chromatography. Intraparticle mass transfer rates are strongly dependent on particle diameter.

2. Little data have been taken at the reduced temperatures at which fission gases best adsorb on charcoal. Extrapolations of mass transfer rates over a range of 100°C are subject to serious error.

3. Separation factors sufficient to convert reactor effluents into biologically safe materials are much greater than those needed for non-radiological separations. Breakthrough equations must be proven valid and reliable over a concentration range of a thousand or more.

4. Most of the work in gas chromatography has centered around gas-liquid chromatography. In the smaller body of gas-solid chromatography literature, unmodified charcoal has received little attention because its wide range of surface energies for most adsorbates leads to an undesirable broadening of adsorption peaks.

5. In gas-liquid chromatography, the constants obtained for the Van Deemter equation often disagree with those predicted from Van Deemter's original derivation, indicating that other, less understood, phenomena are controlling column operation.

For these reasons experimental tests of the applicability of the Van Deemter equation were required. An account of these tests and their subsequent analysis is given in the following sections.

THE EXPERIMENTAL SYSTEM

The experimental system described below was designed to measure the increase in width of a front of krypton-85 in an air carrier passing through a charcoal bed. The concentration of krypton (krypton-85 plus inert krypton carrier) added to the tank air gas < 0.03 ppm. This is small in comparison with the atmospheric concentration of 1.0 ppm of natural krypton. Therefore the exchange of krypton in the test system took place at essentially a constant concentration of krypton. The use of a constant concentration is advantageous as this eliminates the possibility of distortion of the breakthrough curves by a nonlinear isotherm.

The test system is illustrated in Figure 5. For the purpose of description, it is divided into three main sections: the supply and precleaning of the test gas, the charcoal beds, and the effluent gas analysis.

Supply and Precleaning of the Test Gas

Krypton-85 in air was withdrawn from a source tank containing 11,300 liters. Addition of 20 millicuries to this tank gave a concentration of $\sim 2 \times 10^{-3}$ μ Ci/cc, 200 times greater than the radiation protection guide level for occupational exposure. There was a potential hazard to local personnel, but constant monitoring of the atmosphere near the tank by a thin wall beta counter gave no evidence that the permissible level was exceeded during the course of any run.

Room air or tank air could be drawn through one of two parallel drying beds (see Figure 5). Two drying beds were necessary because the displacement of room air with tank air in a single large drying bed would have led to a large and undesirable broadening of the front of krypton-85 entering the charcoal beds. The drying beds contained layers of indicating silica gel, anhydrous magnesium perchlorate, ascarite, and 13X molecular sieves to remove carbon dioxide quantitatively and water vapor to concentrations below the vapor pressure of ice at 195°K. A Chemical Corps aerosol filter was placed on the room air line to remove entrained dust.

Air from either drying bed could be drawn through one of the solenoid valves V_1, V_2, by the pump P to the adsorption beds. Care was taken to select pumps that would not pass contaminating vapors, especially oil vapors, to the charcoal beds. An oilless rotary pump was used for runs with a flow of two liters per minute or greater. With lower flows, excessive heating of the pump occurred and a diaphragm pump was substituted. Flow past the pump was controlled by a needle valve; then a three way valve gave access to a mercury manometer, allowing measurements of the pressure drop across the remainder of the system.

Twice, with fresh chemicals in the drying beds, the charcoal beds plugged with water vapor. The moisture source was traced to a small leak of undried air around the shaft of the rotary pump. Completely sealing the pump appeared impractical, but a small tube containing ascarite and anhydrous magnesium perchlorate placed downstream from the pump was found to remove the entrained moisture satisfactorily.

The Charcoal Beds

Three containers for charcoal beds were prepared and used in the test system. The first, fabricated from brass pipe, held a charcoal bed 46.5 centimeters long with a diameter of 3.81 centimeters. A pipe fitting was soldered on each end and pipe caps were attached to connect to the test system. Charcoal was held in the bed by perforated metal disks across the inlet and outlet; polyurethane foam was packed between these disks and the outlets to prevent contamination of the system by charcoal dust. Figure 6 is a schematic diagram of this and the other two beds.

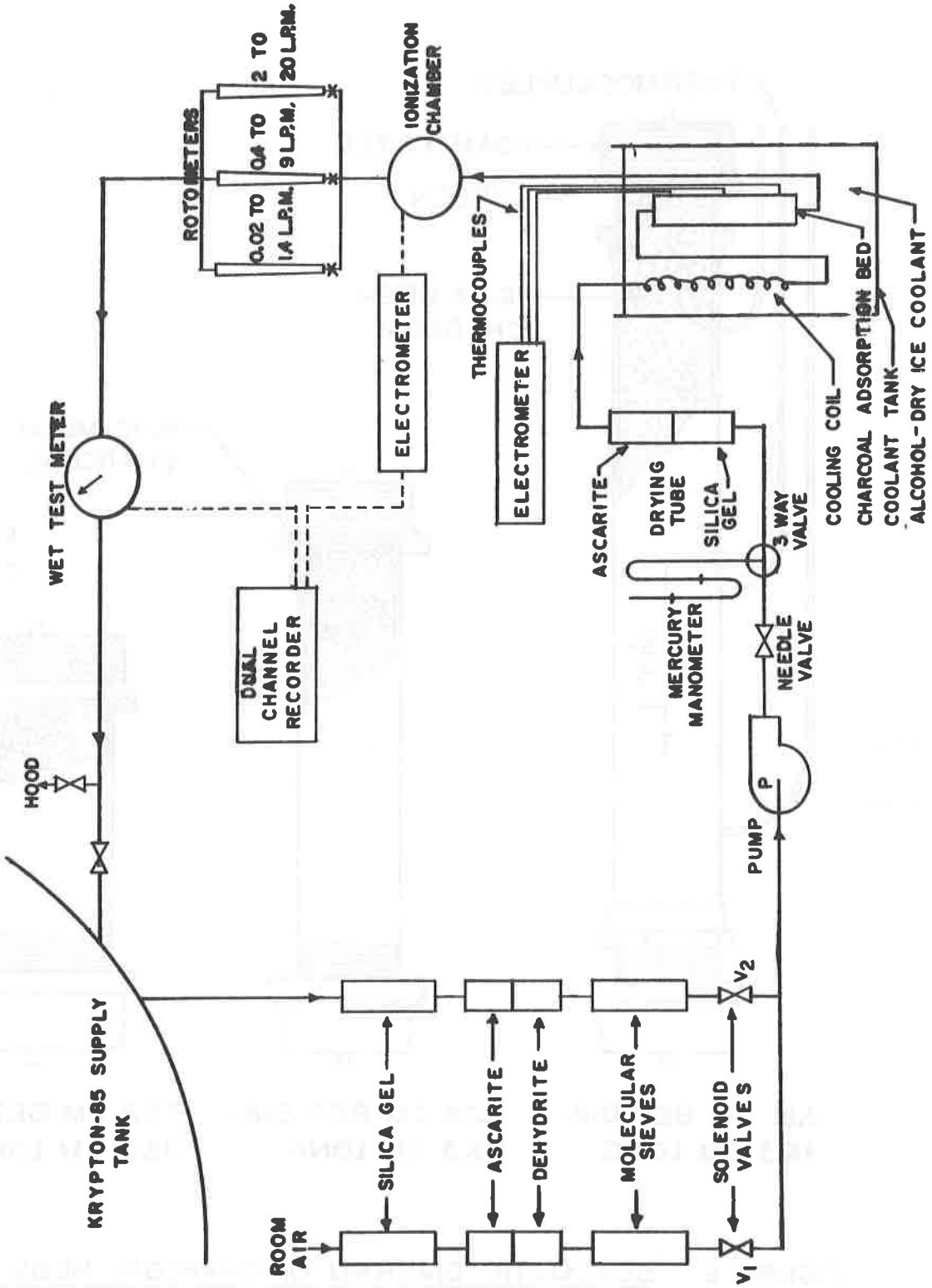

FIGURE 5 SCHEMATIC DIAGRAM OF THE TEST SYSTEM

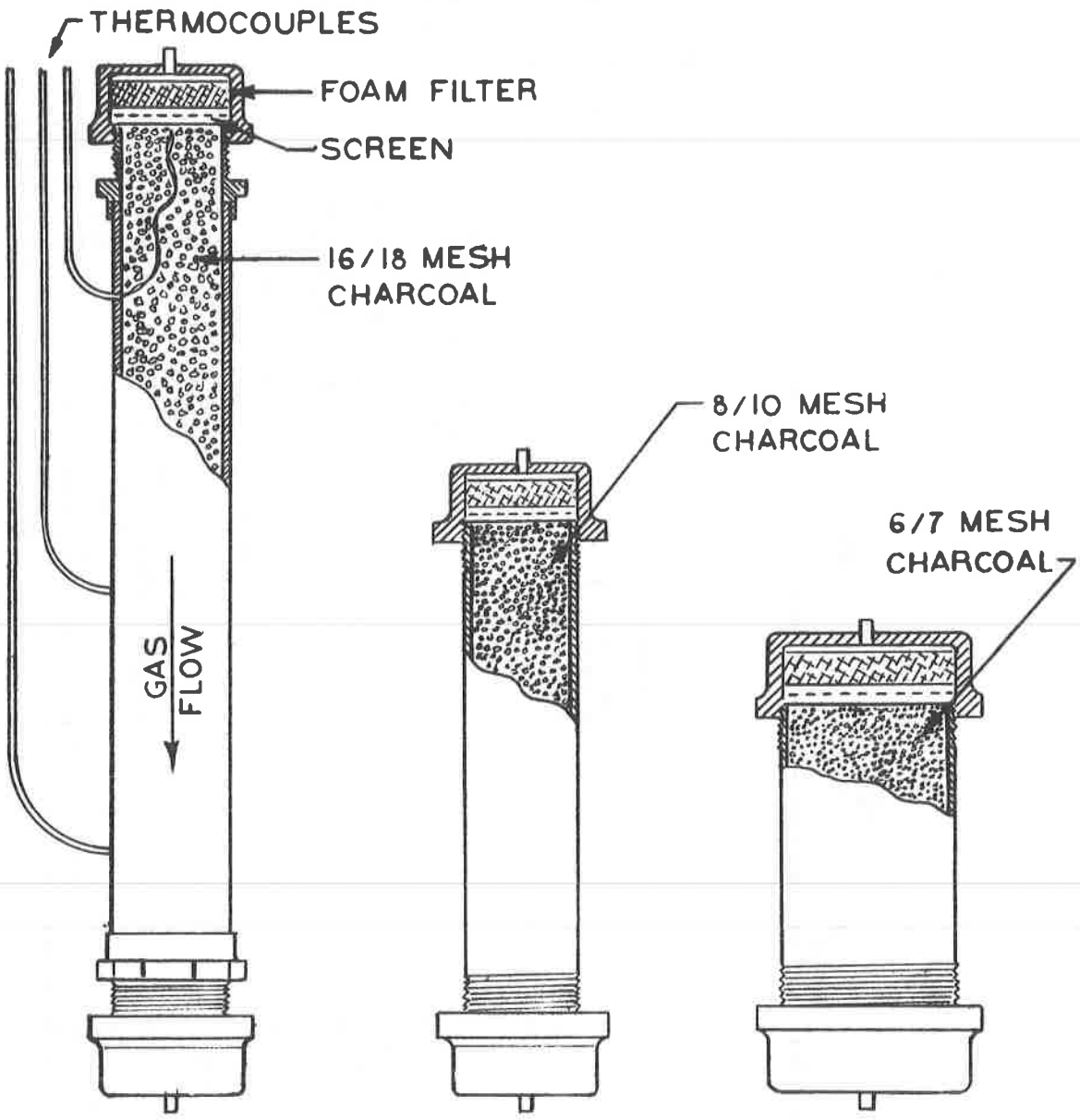

FIGURE 6 SCHEMATIC DIAGRAM OF CHARCOAL BEDS USED IN THE TEST SYSTEM

Three chromel-alumel thermocouple wells were inserted into the 3.81 centimeter bed. The upper thermocouple, placed at the juncture of the charcoal granules and the entrant air, could detect any temperature changes brought about by insufficient cooling of the entrant gases.

The 16/18 mesh (U.S. Series) charcoals in the 3.81 centimeter bed have a mean diameter of 0.11 centimeter. The ratio of bed diameter to mean particle diameter, 3.81 cm/0.11 cm = 35, was sufficient to reduce wall effects to a negligible factor. Wall effects might become important if larger charcoal granules were placed in this bed. Therefore two additional bed containers were prepared using steel pipe. One could hold a bed 28.3 centimeters long, with a diameter of 5.08 centimeters, and the other could hold a bed 12.8 centimeters long, with a diameter of 7.62 centimeters. The ratios of bed diameter to mean particle diameter were 23 for the 8/10 mesh charcoal used in the 5.08 centimeter bed and 25 for the 6/7 mesh charcoal used in the 7.62 centimeter bed. Thermocouples were omitted in these two beds because the temperature in the first bed varied less than a degree from bath temperature under test conditions.

As proper packing to avoid channels is an important factor, the same procedure was followed in filling each bed. Charcoal was poured to within one-half inch of the brim and the pipe tapped with a hammer to settle the charcoal. As much additional charcoal was added as possible.

The threads of the end caps were sealed with a self vulcanizing silicone rubber, RTV 102*. This material was found to be impermeable to alcohol and water and remained sufficiently plastic after a series of runs at dry ice temperatures to be removed easily by hand or light wrench pressure.

The beds were placed in a twelve-inch diameter tank containing an alcohol-dry ice coolant mixture. No runs were made until thermal equilibrium was attained, which for the 3.75 bed required approximately three hours; longer equilibration times were allowed for the other beds. During a test run air from the pump passed through a cooling coil, made of 1/4 inch copper tubing immersed in the coolant bath, directly to the charcoal beds.

Effluent Gas Analysis

Effluent gas from the charcoal beds passed out of the coolant bath to a 500 milliliter flow-through Cary** ionization chamber. The size of this chamber represented a compromise between larger chambers of greater sensitivity and smaller chambers of more rapid response. The detector was a Cary Model 31 vibrating reed electrometer fitted with a resistor turret switch having 10^8, 10^{10}, and 10^{12} ohms input resistance. Voltage across the ionization chamber was held at 135 or 270 volts. For some runs at higher velocities the higher voltage was necessary to prevent a loss of a significant fraction of ions from the ionization chamber.

Air from the ionization chamber passed through one of three rotameters in parallel. These three rotameters had a combined response range of 40 to 20,000 milliliters per minute and were used for rough flow control during the runs.

---

* General Electric Company

**Applied Physics Corp., Monrovia, California.

For a more accurate measurement of flow, the air from the rotameter section was passed through a wet test meter. Each full turn of the main shaft of the wet test meter indicated passage of 3.0 liters. A potentiometer attached to the main shaft produced a voltage proportional to the angle of turn of this shaft, providing a continuous reading to a fraction of liter of the total gaseous throughput. The outputs from the potentiometer and from the ionization chamber were recorded on a Texas Instruments* Model 75-222 Dual Channel Recorder. Air from the wet test meter was passed back to the krypton tank or vented to the atmosphere depending on its radionuclide concentration.

To prevent leakage, every connection in the test system downstream from the charcoal beds was coated with epoxy cement and tested for tightness. The only connection not coated was the high pressure seal between the adsorption bed and the copper tubing leaving the bed. The pumps, known to have a small leakage were placed before the beds. Any air picked up by the pumps was forced through both the beds and the flowmeters, resulting in a minimum error in the subsequent analysis of the breakthrough curves.

EXPERIMENTAL RESULTS

Five series of adsorption and desorption runs were made to determine the height equivalent of a transfer unit for the transport of krypton-85 in an air carrier through a charcoal adsorbent at 195°K. Of these five series, three were made with coconut base charcoal and two with petroleum base charcoal. The bed dimensions for each series are given in Table 1 along with the source and mean diameter of the charcoal adsorbent particles.

The number of transfer units for each run was determined by the following geometrical construction. A tangent was drawn to the breakthrough curve at the point X_1, where the concentration reached one-half the final value, and extended to X_2, on the base line of the breakthrough curve (see Figure 7).

The number of transfer units in the bed is

$$N = \frac{\pi}{2} \left(\frac{X_1}{X_2 - X_1}\right)^2 \qquad \text{Equation 3.1}$$

This construction is based on the slope of the integral Gaussian curve at the midpoint, and has the theoretical advantage that the slope at this point is not strongly affected by the unsymmetrical behavior found with a smaller number of transfer units. Similar results are obtained from a construction given by Glueckauf.[4]

This estimate of transfer units is subject to error in practice. The experimental breakthrough curves are not mathematically smooth curves and drawing tangents to these curves in a general area of inflection is at least partially subjective. A small error in the slope of the tangent leads to a much greater error in the estimate of transfer units. The experience of this

---

*Texas Instruments, Inc., Houston, Texas.

FIGURE 7

ANALYSIS OF BREAKTHROUGH CURVES

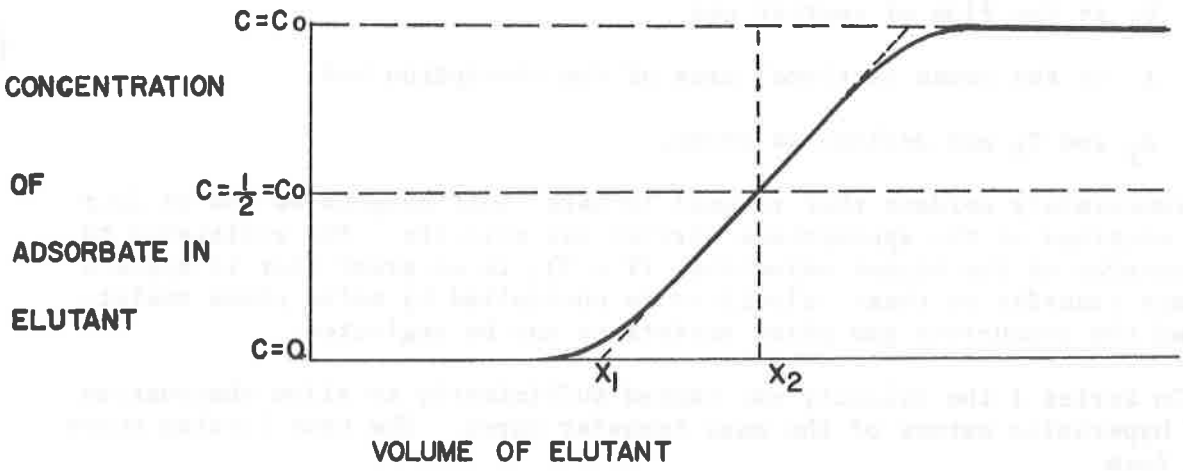

investigator in repeatedly drawing tangents and estimating transfer units suggests that these estimates are accurate to about $\pm$ ten percent for Series 1, and 2, $\pm$ 20 percent for Series 3 and 4, and $\pm$ 30 percent for Series 5.

A regression analysis of the breakthrough curves could yield considerable improvement in the estimates of the number of transfer units.

As would be expected, the adsorption data are heavily weighted with points taken before the effluent concentration reached half the final concentration and the desorption data are equally overweighted with points taken after the effluent concentration dropped below half the initial concentration. At the time of this writing this regression analysis had not been completed.

Figures 8 through 10 give the reduced height of a transfer unit for the test Series 1 through 5. The abscissa in these graphs, the reduced superficial velocity, v, is a modified Peclet number defined as:

$$\frac{V_t \quad d_p}{A \quad D_f}$$

Where: V_t is the flow of carrier gas

A is the cross sectional area of the adsorption bed

d_p and D_f are defined as above.

It is immediately evident that reduced transfer unit heights as low as four may be obtained at the appropriate carrier gas velocity. The resistance to mass transfer at the higher velocities ($V > 3$), is so great that it appears that mass transfer at these velocities is controlled by solid phase resistance and the concurrent gas phase resistance may be neglected.

In Series 1 the velocity was varied sufficiently to allow observation of the hyperbolic nature of the mass transfer curve. The best fitting curve of the form

$$h = \frac{a}{v} + b + cv \qquad \text{Equation 3.2}$$

has the constants $a = 0.57$, $b = 2.59$, and $c = 0.49$. If the interparticle void volume of the adsorbent bed is assumed to be 0.50 of the total bed volume, the v_i, the reduced interparticle velocity is twice as great as the reduced superficial velocity, v. In terms of v_i, the constants for

$$h = \frac{a_i}{v_i} + b_i + c_i v_i \qquad \text{Equation 3.3}$$

are $a = 1.14$, $b_i = 2.59$, and $c_i = 0.25$.

These constants may be correlated with the Van Deemter equation as

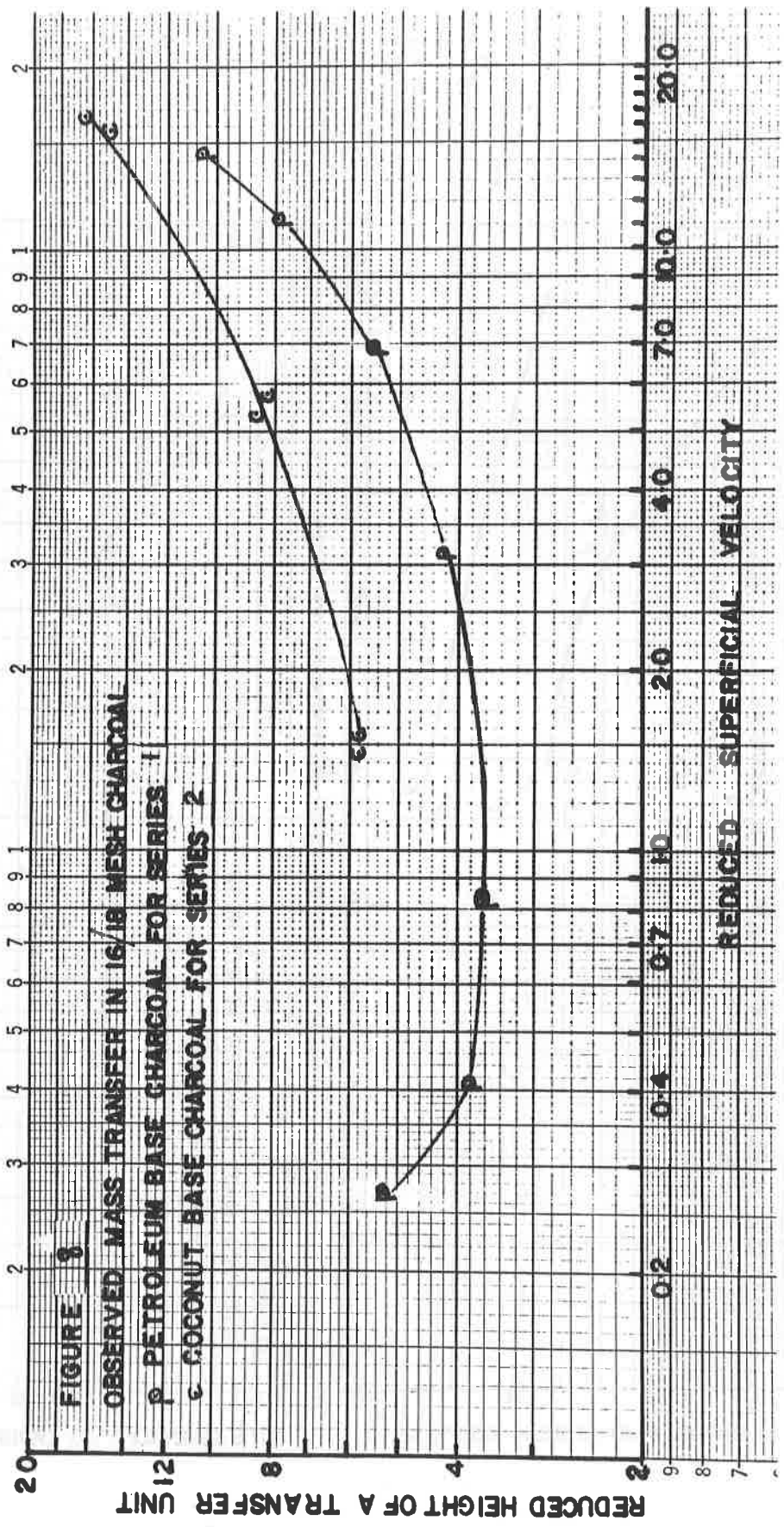
FIGURE 8
OBSERVED MASS TRANSFER IN 16/18 MESH CHARCOAL
P PETROLEUM BASE CHARCOAL FOR SERIES 1
C COCONUT BASE CHARCOAL FOR SERIES 2
REDUCED HEIGHT OF A TRANSFER UNIT
REDUCED SUPERFICIAL VELOCITY
20
12
8
4
2
0.2
0.4
0.7
1.0
2.0
4.0
7.0
10.0
20.0

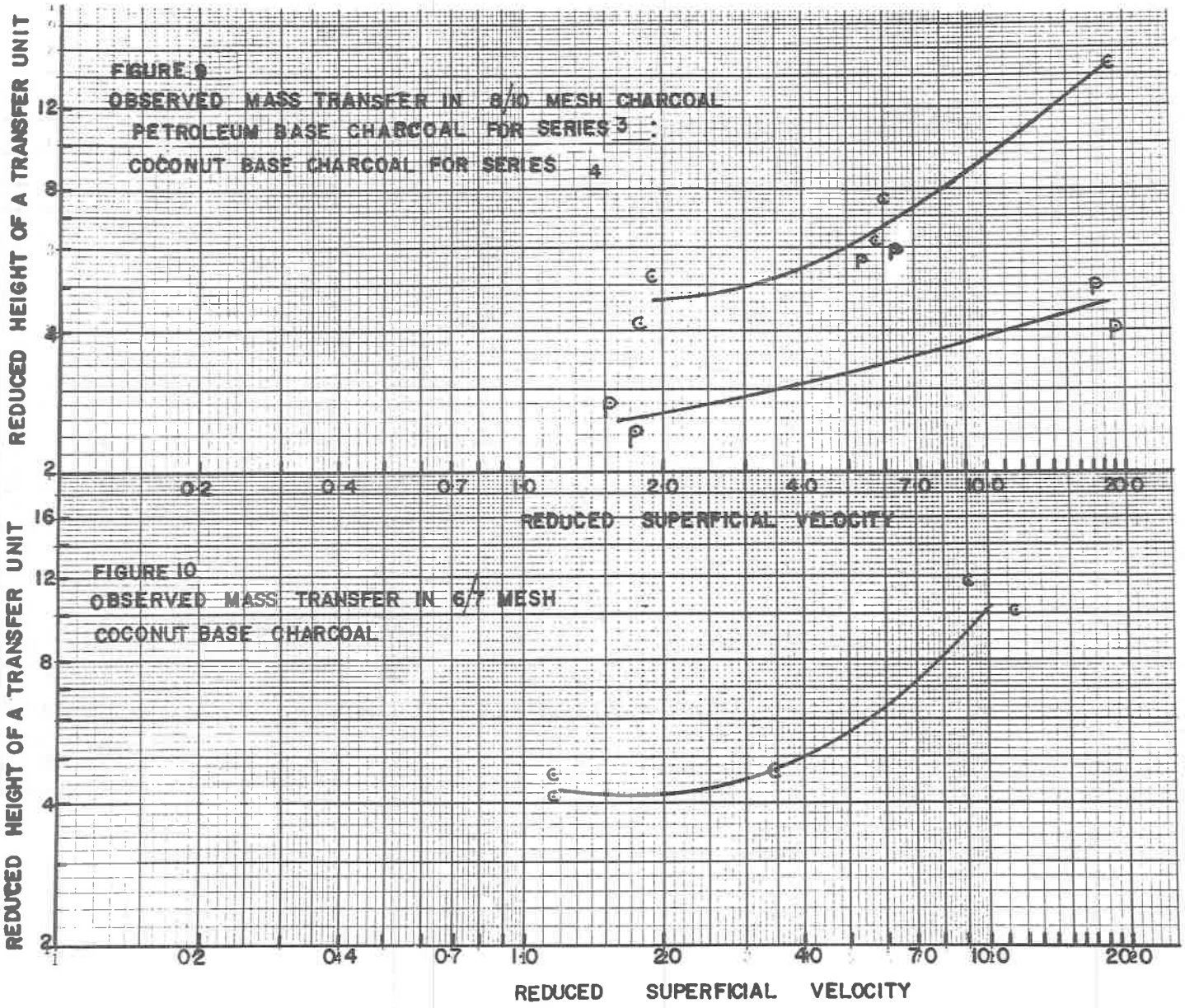
FIGURE 9
OBSERVED MASS TRANSFER IN 8/10 MESH CHARCOAL
PETROLEUM BASE CHARCOAL FOR SERIES 3 :
COCONUT BASE CHARCOAL FOR SERIES 4
REDUCED HEIGHT OF A TRANSFER UNIT
REDUCED SUPERFICIAL VELOCITY
0·2
0·4
0·7
1·0
2·0
4·0
7·0
10·0
20·0
FIGURE 10
OBSERVED MASS TRANSFER IN 6/7 MESH
COCONUT BASE CHARCOAL
REDUCED HEIGHT OF A TRANSFER UNIT
REDUCED SUPERFICIAL VELOCITY

$$a_i = 2\gamma \qquad \text{Equqtion 3.4 a}$$

$$\therefore \gamma = 0.57$$

$$b_i = 2\lambda \qquad \text{Equation 3.4 b}$$

$$\therefore \lambda = 1.30$$

$$c_i = \frac{D_f \; k'}{2^{\,2} D_s \; (k' + 1)^2} \qquad \text{Equation 3.4 c}$$

The values for γ and λ are in good agreement with the rough estimates made earlier. The coefficient c_i, is sufficiently high to confirm that it is the solid phase resistance rather than the gas phase resistance which is controlling at the higher velocities. The solid phase diffusion coefficient, D_s, can be calculated from Equation 3.4 c. Assuming

$c_i = 0.25$ (Values obtained from Test Series I)

$k' = 260$

$d_f = 0.067$ (Extrapolated from Reference 5)

then $D_s = 0.00005 \text{ cm}^2 \text{ sec}^{-1}$.

Other series of runs were conducted over a more restricted range of velocities, but they indicate that:

1. There is appreciably less resistance to mass transfer for krypton in the petroleum base charcoal than in the coconut base charcoal.

2. Mass transfer for krypton in the larger charcoal granules may be calculated using similar constants for c_i in equation 3.3.

The results presented here show that mass transfer of krypton in charcoal adsorption beds can be correlated with known physical mechanisms. This conclusion can be tested by extending the mass transfer measurements to other carrier gases and to a greater range of temperatures and velocities.

TABLE 1

Observed Mass Transfer of Krypton-85 in Charcoal Beds at 195°K

Series 1

16/18 Mesh Petroleum Base Activated Charcoal (Columbia Grade ACC, Lot H-412-14)
Nominal Particle Diameter: 0.11 ± 0.01 cm.
Bed Diameter: 3.81 cm.
Bed Length: 46.5 cm.

Run Number	Flow of Carrier Gas, liters per minute (NTP)	Reduced Superficial Velocity	Number of Transfer Units	Height of a Transfer Unit, cm.	Reduced Height of a Transfer Unit
1a	0.16	.27	80	0.58	5.2
2a	0.31	.51	108	0.42	3.8
3a	0.50	.82	115	0.40	3.6
4a	----	----	---	----	---
5a	1.90	3.12	96	0.48	4.4
6a	4.12	6.8	75	0.62	5.6
7a	6.99	11.5	54	0.86	7.8
8a	9.08	14.9	40	1.18	10.8

Series 2

16/18 Mesh Coconut Base Activated Charcoal (Barneby-Cheney #513)
Nominal Particle Diameter: 0.11 ± 0.01 cm.
Bed Diameter: 3.81 cm.
Bed Length: 46.5 cm.

Run* Number	Flow of Carrier Gas, liters per minute (NTP)	Reduced Superficial Velocity	Number of Transfer Units	Height of a Transfer Unit, cm.	Reduced Height of a Transfer Unit
1a	0.95	1.57	73	0.64	5.8
d	0.93	1.53	72	0.64	5.8
2a	3.43	5.7	50	0.92	8.4
d	3.22	5.3	48	0.96	8.8
3a	10.00	16.5	26	1.82	16.6
d	9.73	16.0	28	1.64	15.0

*a = adsorption of krypton 85
d = desorption of krypton 85

Series 3

8/10 Mesh Petroleum Base Activated Charcoal (Columbia Grade ACC, Lot H-412-14)
Nominal Particle Diameter: 0.22 ± 0.02 cm.
Bed Diameter: 5.08 cm.
Bed Length: 28.3 cm.

Run Number	Flow of Carrier Gas, liters per minute (NTP)	Reduced Superficial Velocity	Number of Transfer Units	Height of a Transfer Unit, cm.	Reduced Height of a Transfer Unit
1a	0.84	1.56	44	0.64	2.8
d	0.90	1.68	53	0.54	2.4
2a	3.08	5.7	23	1.24	5.6
d	3.34	6.20	23	1.26	5.8
3a	9.70	18.0	26	1.08	5.0
d	9.17	17.0	21	1.24	6.0

Series 4

8/10 Mesh Coconut Base Activated Charcoal (Barneby-Cheney AC L7399)
Nominal Particle Diameter: 0.22 ± 0.02 cm.
Bed Diameter: 5.08 cm.
Bed Length: 27.3 cm.(container not completely filled)

Run Number	Flow of Carrier Gas, liters per minute (NTP)	Reduced Superficial Velocity	Number of Transfer Units	Height of a Transfer Unit, cm.	Reduced Height of a Transfer Unit
1a	0.97	1.80	30	0.92	4.2
d	1.03	1.92	23	1.18	5.4
2a	3.14	5.83	20	1.40	6.4
d	3.25	6.04	16	1.66	7.6
3a	9.85	18.4	8.5	3.22	14.6

Series 5

6/7 Mesh Coconut Base Activated Charcoal (Barneby-Cheney AC L7399)
Nominal Particle Diameter 0.31 ± 0.025 cm.
Bed Diameter: 7.62 cm.
Bed Length: 12.8 cm.

Run Number	Flow of Carrier Gas, liters per minute (NTP)	Reduced Superficial Velocity	Number of Transfer Units	Height of a Transfer Unit, cm.	Reduced Height of a Transfer Unit
1a	0.99	1.16	9.3	1.38	4.4
d	0.98	1.14	10.0	1.28	4.1
2a	3.04	3.51	8.8	1.44	4.6
d	----	----	---	----	---
3a	7.3	8.5	3.6	3.56	11.4
d	9.21	10.9	4.4	2.90	9.4

Symbol Table

A	Cross-sectional area of adsorption bed, cm^2
a, b, c	Coefficients for Equation 3.2
a_i, b_i, c_i	Coefficients for Equation 3.3
C	Concentration of adsorbate in carrier gas
C°	Inlet concentration of adsorbate in carrier gas
C'	Derivative of concentration with respect to distance from the inlet
D_f	Coefficient for diffusion of adsorbate through carrier gas, cm^2 sec^{-1}
D_s	Coefficient for diffusion of adsorbate through adsorbent, cm^2 sec^{-1}
d_p	Average diameter of adsorbent particles, cm
H	Height equivalent of a transfer unit, cm
h	Reduced height equivalent of a transfer unit
k'	Ratio of adsorbate in adsorbent, at equilibrium, to adsorbate in the carrier gas
L	Length of adsorbent bed, cm
N	Number of mass transfer units
Sm	Schmidt number for adsorbate in carrier gas
t	Time following introduction of adsorbate, sec
V_i	Interparticle velocity of carrier gas
V_t	Flow of carrier gas, ml sec^{-1}
v	Reduced superficial velocity (Peclet number based on superficial carrier gas velocity)
v_i	Reduced interparticle velocity (Peclet number based on interparticle carrier gas velocity)
X_1, X_2	Points on the breakthrough curve defined in Figure 7
x	Distance from inlet of adsorbent bed, cm
γ	Tortuosity factor for gas diffusion
λ	Geometric mixing factor for eddy diffusion
$\sigma_{C'}^2$	Variance in C', cm^2
w	$= x - (k' + 1) V_i t$, convenient parameter for Equation 1.2, cm.

REFERENCES

1. Knox, J. H., and McLaren, L.
A New Gas Chromatographic Method for Measuring Gaseous Diffusion Coefficients and Obstructive Factors.
Analyt. Chem. 36, 1477, (1964)

2. Wilke, C. R., and Hougen, O. A.
Mass Transfer in the Flow of Gases Through Granular Solids Extended to Low Modified Reynolds Numbers.
Trans. Am. Inst. Chem. Engrs. 41, 445 (1945)

3. Van Deemter, J. J., Zuiderweg, F. J., and Klinkenberg, A.
Longitudinal Diffusion and Resistance to Mass Transfer as Causes of Nonideality in Chromatography.
Chem. Eng. Sci. 5, 271 (1956)

4. Glueckauf, E.
Theory of Chromatography. Part 9. The "Theoretical Plate" Concept in Column Separations.
Trans. Faraday Soc. 51, 34 (1955)

5. Reist, P. C., Thesis for Sc.D. Degree.
The Disposal of Radioactive Krypton-85 in Porous Media.
Harvard University (1965)

DISCUSSION

KOVACH: Did you check any correlation between the pore structure and the differences obtained between the cocoanut shell and petroleum base material to correlate the mass transfer data? The base in raw materials doesn't justify any variation.

UNDERHILL: No, we haven't but there are some results by, again, going back to an earlier paper in which was reported the factor C in terms of obtaining it in a different type of study. In that study, waves of gas were passed through an adsorption column and the conditions of the waves were stabilized. There was an attempt to correlate the results with a mean diameter. The results are still in the process of analysis and we would like to try correlating the work here with the four lengths and mean diameters of the calculation. I think it can be done from the type of information obtained.

KOVACH: I would like to caution you, if you check that data, you will have to use both mercury penetration and nitrogen pore volume measurements.

UNDERHILL: Two diameters were given; one of the range of angstroms and the other in the range of millimeters.

STANDARDIZED GENERATION OF VAPOR-PRODUCED SODIUM AEROSOLS AND THEIR BEHAVIOR

By

R. L. Koontz, C. T. Nelson, and L. Baurmash

Atomics International
A Division of North American Aviation, Inc.

ABSTRACT

A method for generating reproducible sodium aerosols in gas media of known composition is required in order to establish growth phenomenon and measurement techniques for particulates produced from a sodium fire following a primary-coolant spill in a sodium cooled reactor.

Sodium aerosols have been produced by reacting sodium vapor in the presence of nitrogen with various mixtures of nitrogen and air. By suitable variation of the conditions of generation, the concentration and distribution of the aerosols produced have been studied. These distribution data are presented as measured by different sizing techniques, and are compared to those produced by liquid sodium-air reaction.

INTRODUCTION

In the safety analysis of sodium-cooled fast reactors fueled with plutonium, it is postulated that potentially serious dispersions of fuel, fission products, and sodium may occur under certain major accident conditions. Thus, the study of the phenomenology of sodium aerosol production, the release characteristics of the associated materials, and the ultimate design of adequate engineering safeguards to limit the consequences of such accidents are necessary. Aerosols generated during sodium fires may consist of sodium, its oxides, fission products, and reactor fuel mixtures of Pu and U compounds. Because of the nature of a sodium fire and the changes which occur to the initial distribution of the aerosol throughout its lifetime, it is of importance to be able to evaluate the capabilities of the aerosol sizing devices.

Certain types of instruments require that the concentration and particle size be constant over long periods of time. Reproducible sizes are required indefinitely. It is also pertinent to be able to produce heterogeneous aerosols which simulate the material produced during a sodium fire.

This paper describes research in the generation of sodium and sodium oxide aerosols consisting of spherical particles of narrow size distribution. The sodium aerosols are produced by a condensation technique, and the oxide is produced by reacting vapor-laden nitrogen with air (oxygen).

*Work performed for U.S. Atomic Energy Commission under Contract AT(11-1)-GEN-8

EXPERIMENTAL APPARATUS

The sodium and sodium oxide aerosols are generated by using a sweep gas-evaporation technique with nitrogen as the sweep gas. A simplified sketch of the generator and associated equipment is shown in Figure 1. The generator consists of a 2-in.-diameter quartz tube which is placed in an electric tube furnace, 18 in. long. A boat filled with sodium is placed inside the quartz tube. A cross tube is attached to the generator tube through which the reactant gases flow. An additional heater is placed around the generator tube at the intersection with the cross tube to eliminate condensation of the sodium vapor prior to mixing with the reactant gas. The temperatures of the sodium in the boat, furnace, and heater near the tee are controlled and normally maintained at 1000°F. Various combinations of sweep gas and reaction gas flows were tried, resulting in a "standard blend" at a flow of 0.5 ℓ/min for the sweep gas and 3.0 ℓ/min for the reactant gas. This combination of temperature and gas flow appeared to produce the approximate particle concentration and size distribution which give a reasonable sample time and concentration, and correspond to typical sizes obtained over steady-state sodium fires in low oxygen environments.

The flowrates of the nitrogen sweep gas and reactant gas, which can be either nitrogen or air or their mixtures, are controlled through a manifold of 7 flowmeters of various sizes. By proper valving, many combinations of flows are available, ranging from a few cc/min to 36 ℓ/min. The sweep gas can be filtered (0.1 μ millipore) if necessary, and the oxygen can be removed if desired by flowing through a hot copper coil which is filled with copper mesh. The N_2 sweep gas is heated in the furnace as it enters the vapor region to minimize condensation above the molten metal. The gas and vapor flow along the evaporation tube to the cross tube, where the vapor reacts with air which enters from one arm of the cross-tube; or the vapor may be condensed if the air in the cross-tube is replaced by nitrogen. The evaporation tube is reduced in size before joining the cross-tube to minimize the possibility of diffusion of air into the vapor region during certain flow conditions. The sodium vapor or sodium oxide proceeds to a 6 by 8-in. sampling chamber. The present chamber is made from glass so as to serve as a viewing chamber. Observations show that the sodium particles rise to the top of the chamber with the hot gas prior to being swept out of the sample chamber. Figure 2 shows the laboratory model which was fabricated.

The resulting temperature profile in the generator is shown in Figure 3. The temperature along the horizontal axis of the generator shows that the gas rises to a temperature of 1000°F over the boat area, and remains constant until the reaction zone is reached, at which point the temperature drops to approximately 700°F. A temperature profile of the cross-tube shows that the reactant gas rises from ambient to 700°F, and gradually decreases in temperature to a value of 10 to 15°F above ambient at the lower outlet ports of the sampling chamber. There is a slight difference in temperature in the reaction region when air is used instead of N_2.

Particle-size distribution measurements were made with an electrostatic precipitator (ESP), modified Lovelace impactor, and modified Andersen impactor.[1] The particle size distribution from the ESP samples is obtained with the aid of an electron microscope and a Zeiss particle-size analyzer. The impactors classify aerosols according to aerodynamic diameter. The sodium is analyzed by means of a Coleman flame photometer.

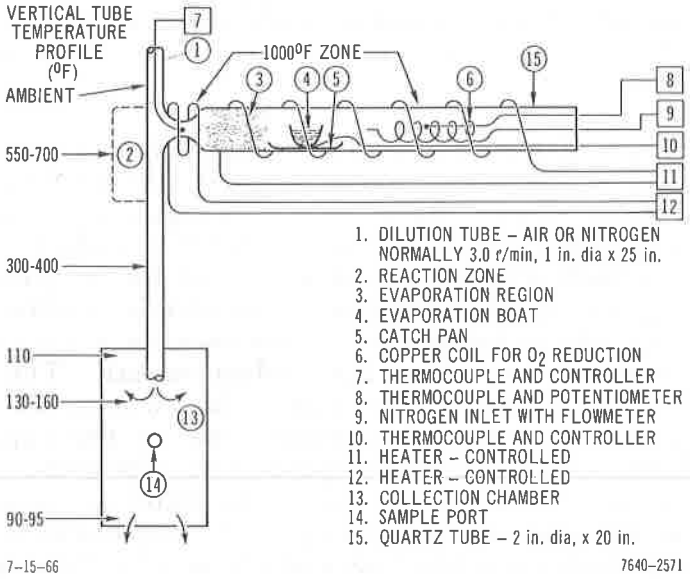

Figure 1. Particle Generator Diagram

PARTICLE GENERATOR

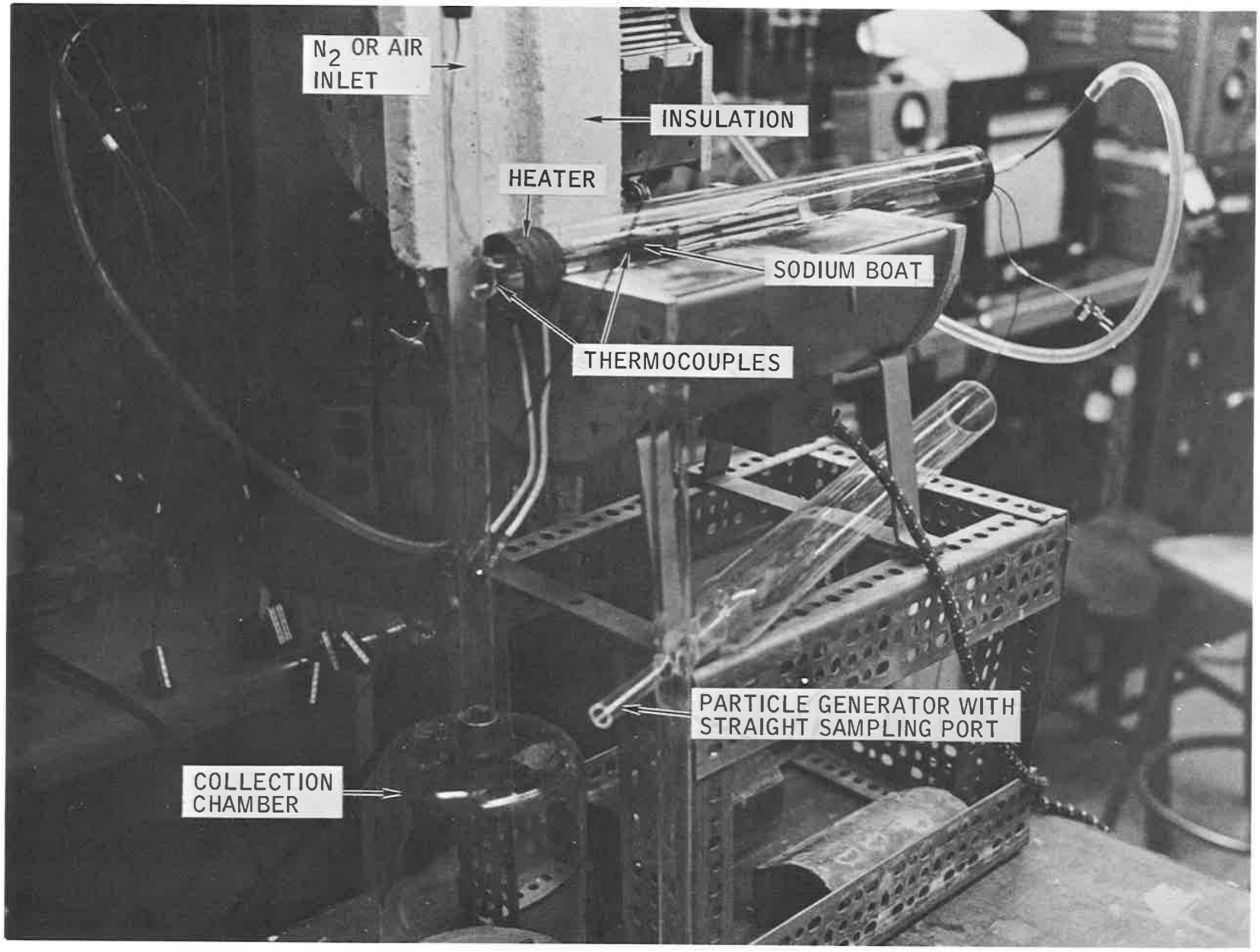

Figure 2. Particle Generator

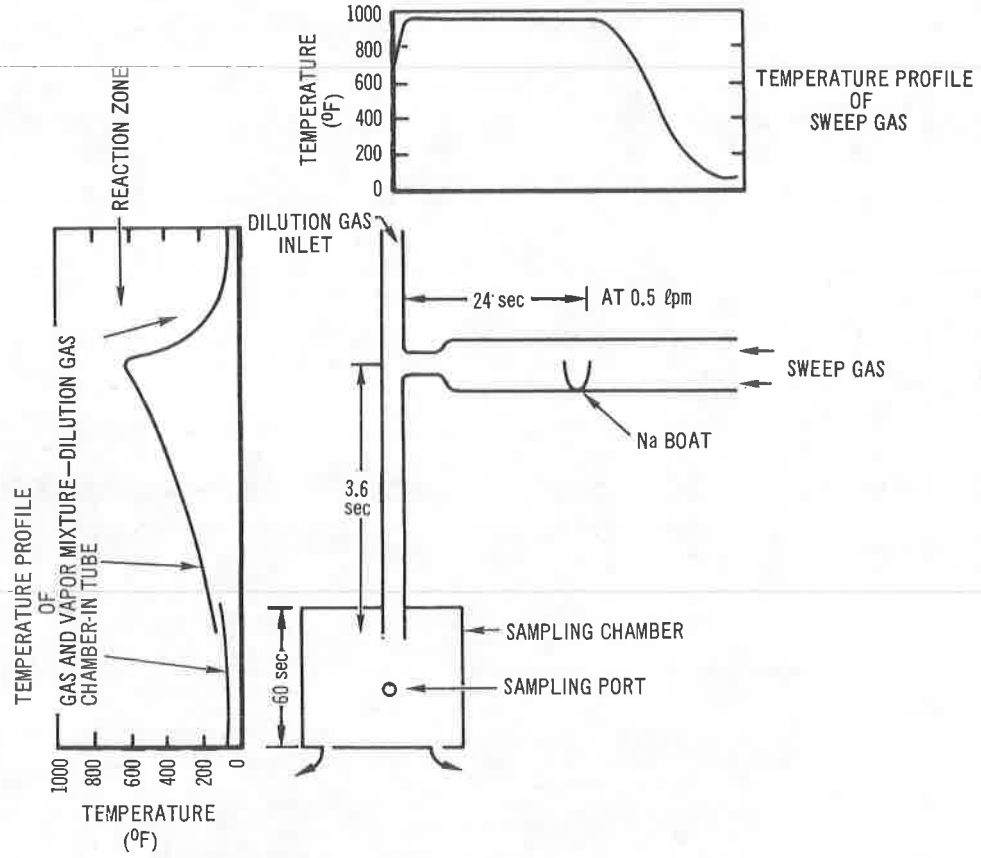

Figure 3. Temperature Profile of Particle Generator

EXPERIMENTAL RESULTS AND CONCLUSIONS

The following discussion represents some of our preliminary conclusions regarding performance of the generator. Data are presented in Table 1 in terms of the 50% aerodynamic diameter (AED) obtained from impactors.

Size vs Concentration

Under constant-flow conditions, there is a fixed time interval from the reaction zone, where the vapor is condensed or oxidized, to the sample region, which represents the life time of the aerosol from its formation to its measurement. If the initial size is very small, then from agglomeration theory

$$d^3 = \frac{6CKt}{\pi\rho} \quad , \qquad \ldots(1)$$

where

d = diameter in cm

C = concentration in $\mu g/cc = \rho V$

t = time

V = particle mass density μ^3/cm^3

K = agglomeration constant $cm^3/p\text{-}sec$

ρ = density in $\mu g/cc$.

Thus, the expected difference in growth between Run 6 and Run 5 in Table 1, where the concentration ratio is ~0.5/0.06 = 8.35, is

$$\frac{d(\text{Run 5})}{d(\text{Run 6})} = (8.35)^{1/3} = 2.0 \ .$$

The measured ratio of median AED is 2.2 which is in good agreement with 2.0. An indication of the dependence of median size of condensed sodium on concentration can be seen from Runs 1, 3, and 4 where, at a constant temperature, the flow of N_2 over the evaporation boat is decreased. This has two effects on concentration: (1) it decreases the evaporation rate, and (2) it results in an increase in the dilution when the vapor mixes with the N_2. The dilution factor is defined as

$$\frac{Q_{(N_2)} + Q'}{Q_{(N_2)}} \quad ,$$

where Q' is the flow of N_2 or air in the cross tube, and Q_{N_2} is the flow over the sodium. Runs 3 and 4 were conducted with a larger surface area of sodium in the evaporation region, and also represent condensation growth rather than coagulation.

Initial Size and Growth

As the sodium temperature is decreased below 900°F, (Runs 6, 7, and 8) the concentration is further decreased; however, one observes that the 50% size does not decrease. This is consistent with the elementary agglomeration theory, which simply states that if the concentration is small (~0.03 to 0.003 $\mu g/cc$), then the time t for the vapor air reactants to increase to a

TABLE 1

PARTICLE GENERATOR PERFORMANCE SUMMARY

Run Number	AED 50%	σ	$Q_{(N_2)}$* (ℓpm)	$Q'_{(N_2)}$* (ℓpm)	$Q'_{(air)}$* (ℓpm)	Na Temperature (°F)	MMD† (μ)	Relative Concentration (μg/cc)
1	2.5 - 2.8	1.85 - 1.95	0.5	3.0	0	1000	2.5 - 2.8	0.5
2	1.1 - 1.4	1.67	0.5	3.0	0	900	1.1 - 1.4	0.06 - 0.09
3	1.5 - 1.8§	1.9 - 2.4	0.27	3.0	0	1000	1.5 - 1.8	0.2 - 0.4††
4	1.0§	1.9	0.075	3.0	0	1000	1.0	0.18††
5	0.95 - 1.1	1.5 - 1.6	0.5	0	3.0	1000	0.66	0.4 - 0.5
6	0.45	2.0 - 2.3	0.5	0	3.0	900	0.30	0.06
7	0.54	2.25	0.5	0	3.0	800	0.36	0.03
8	0.4 - 0.63	1.6 - 2.7	0.5	0	3.0	720	0.27 - 0.42	0.003
9	0.73**	1.5	0.5	0	3.0	1000	0.49	0.4
10	4.0**	2.2	0.5	0	0	1000	4.0	1.8
11	—	—	0.3	—	3.0	—	—	0.35
12	—	—	0.5	—	3.0	—	—	0.52
13	—	—	1.0	—	3.0	—	—	0.63

*$Q_{(N_2)}$ = Sweep gas flow in liters per minute.

Q' = Dilution or reactant gas in liters per minute.

†MMD = AED/$\sqrt{\rho}$, ρ = 1, for $Q'_{(N_2)} + Q_{(N_2)}$, and σ = 2.27 when $Q_{(N_2)} + Q'_{(air)}$ are used.

§I^{131} release studies AED activity median diameter and sodium AED are the same.

**Sample taken vertical tube outlet with sampling chamber removed.

††Increased boat area.

PHOTOGRAPH OF PARTICLES GENERATED DURING RUN 1

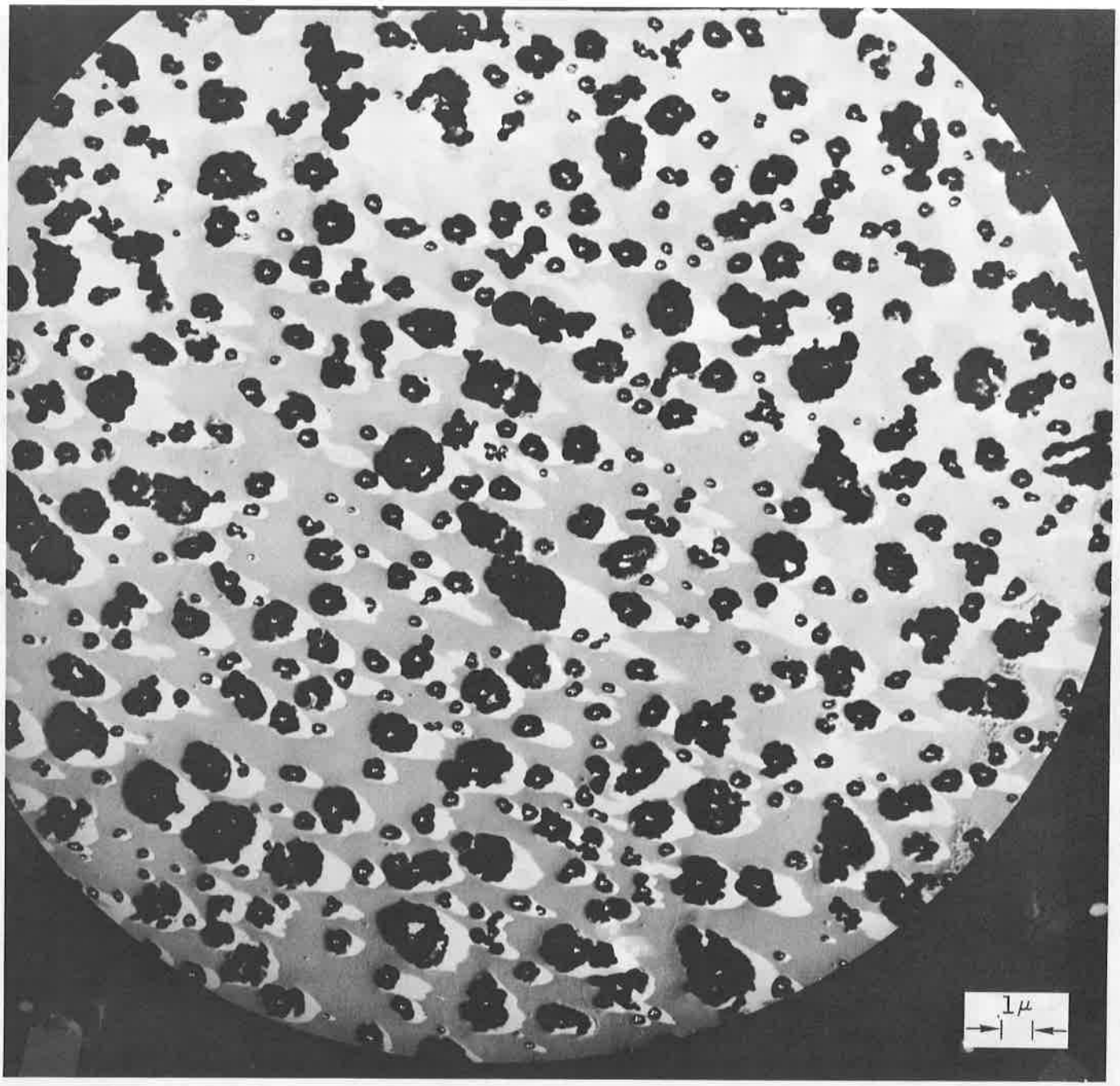

Figure 4. Electron Microscope Photograph of Particles Generated during Run 1 (Table 1)

PHOTOGRAPH OF PARTICLES GENERATED DURING RUN 5

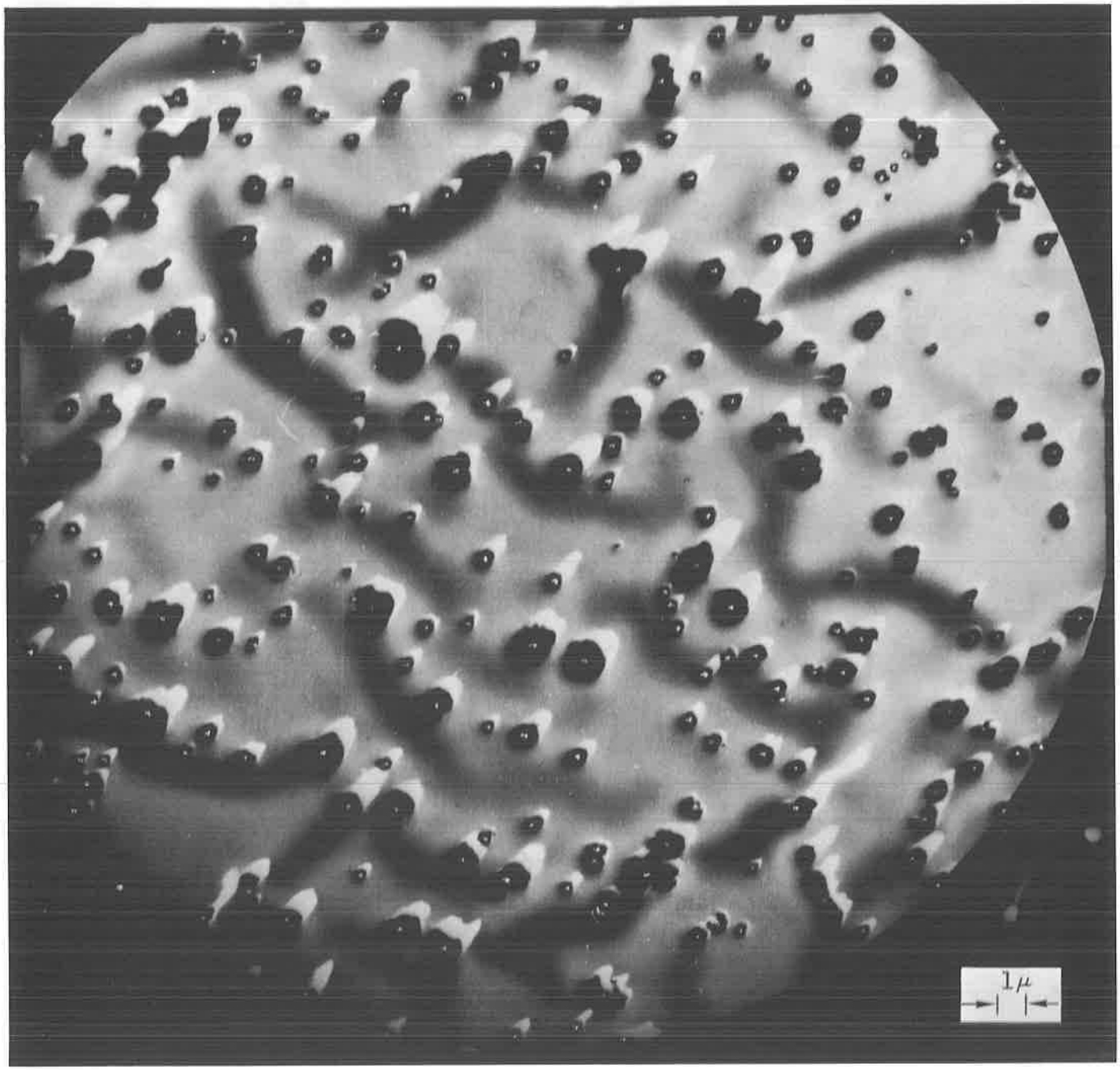

Figure 5. Electron Microscope Photographs of Particles Generated During Run 5 (Table 1)

larger size is much greater than it is at 0.5 μg/cc (see Equation 1). By utilizing the agglomeration code discussed in Reference 2, an attempt will be made to compute what the initial size must have been.

Another indication that the size of the particles is increasing can be noted from Run 9, where a sample is obtained before it enters the sample region. The aerosol life is ~3.5 seconds at this time. The sample chamber capacity flow relation is such that it takes about 30 sec for the gas and particles to reach the sample position where the sample in Row 5 was obtained. Thus, a growth in diameter from 0.73 to ~ 1.0 μ occurs in ~30 sec.

Vaporization Rate and Vapor Growth

The concentration C in Cμg/cc measured in the sampling chamber can be used to compute the concentration over the evaporation boat and thus the evaporation rate. Runs 11 through 13 show the variation of concentration with flow. If one computes $C_o(\mu g/cc)$ over the boat for the lower flowrates, then

$$C_o = C\left[\frac{Q_{(N_2)} + Q_{Air}}{Q_{(N_2)}}\right] = 3.7\,\mu g/cc \quad .$$

This is consistent with the vapor pressure of sodium at 1000°F.

Run 10 showed a very large particle size when 0.5 ℓ/m of N_2 was flowed through the entire system. This growth is associated with condensation at higher concentrations of vapor and an increase in the growth time of ~7 (the ratio of total flow).

It is generally accepted that the rate of increase of radius of a condensing particle[3] is proportional to $t^{1/2}$, while that of agglomeration materials is $t^{1/3}$; and thus one might expect larger particles of condensed droplets to exist after a given time. This is shown to be the case when Runs 1 and 2 are compared with Runs 5 and 6.

Distribution vs Size

In the reactions of sodium vapor with air-N_2 mixtures, the largest median AED have the smallest geometric standard deviations. This is consistent with the agglomeration theory presented in Reference 2, in which it is shown that a highly dispersed aerosol narrows in distribution as it agglomerates.

Iodine Release Studies

The generator as designed can easily be used to study release characteristics of fission products in sodium. Preliminary iodine release experiments have been conducted in the particle generator. Approximately 1500 ppm of NaI containing 2.4 mc I^{131} was mixed with sodium and placed in the evaporation boat. The sodium was raised to a temperature of 1000°F and purified N_2 was swept over the boat. Two experiments were performed with sweep gas flows of 75 cc/min and 270 cc/min. The dilution N_2 gas was maintained at 3ℓ/min. Results from the initial two tests indicate that the distribution coefficient for the I^{131} was approximately unity; e.g., the ratios I/Na in the liquid and vapor phases are equal. Additionally, the radioactive median aerodynamic diameter and the sodium median AED was the same. These experiments are summarized in Runs 3 and 4 of Table 1.

TABLE 2

COMPARISON OF AEROSOL CHARACTERISTICS

Conditions from Table 1	Density (gm/cc)	CMD	MMD	σ	AED Median Computed	AED Median Measured	σ
Run 1	1.0	1.0	2.74* 2.30†	1.8 1.7†	2.74 2.30†	2.5 - 2.8	1.85 - 1.95
Run 5	1.0	0.8	1.37 1.1*	1.54 1.5	1.37 1.1	0.95 - 1.1	1.5 - 1.6
Run 5	2.27	0.8	1.37 1.1*	1.54 1.5	2.06 1.7	0.95 - 1.1	1.5 - 1.6

*Computed from Hatch[4]

†Computed from ΣnD^3

Electron Microscope Studies

Count median diameters (CMD) were obtained from counting on a Zeiss particle size analyzer. Samples were obtained from electrostatic precipitator samples which were then photographed in an electron microscope. The correlation of the CMD median with the impactor AED is possible if one knows the density of the material which is airborne. Thus, mass median diameters (MMD) is defined as the diameter of a sphere having the same settling velocity as the particle and having the same density as the bulk material from which the particle is made. The AED is defined as the diameter of a sphere having the same settling velocity as the particle and a density equal to one.

Table 2 shows typical comparisons of aerosol characteristics from ESP and impactors. Row 1 of Table 2 shows that reasonable agreement is obtainable if there is no doubt as to the density of the material. There is little difference in the mass median diameter computed from the typical Hatch[4] relation

$$MMD = (CMD) \exp(3 \ln^2 \sigma)$$

and that computed by summing the diameter cubed (ΣnD^3). Rows 2 and 3 represent the reaction of the sodium vapor with air. The true density of Na_2O is 2.27 gm/cc; however, the aerosol which is produced may not be pure sodium oxide but rather in some cases surfaced oxidized sodium droplets. If one makes this assumption, then Run 2 of Table 2 shows good correlation with impactors. Run 3 represents the normal assumption that the aerosol produced in sodium fires is Na_2O. Here the agreement is poor. Figures 4 and 5 show electron microscope photographs of the particles generated under conditions described in Runs 1 and 5 of Table 1, respectively.

SUMMARY

In summary, a sodium aerosol generator has been built to produce aerosols useful in evaluating many types of sizing devices. The generator has the capability of producing particulates similar to those created initially in a sodium fire, and can be utilized for obtaining fundamental information on sodium aerosol characteristics.

REFERENCES

1. C. T. Nelson, L. Baurmash, and R. Koontz, "Techniques for Sampling Sodium Smoke and Fission Products," Ninth AEC Air Cleaning Conference (September 1966)

2. P. Spiegler and R. Koontz, "Evaluation of Equations that Govern Coagulation of an Aerosol by Means of an Electronic Computer," Ninth AEC Air Cleaning Conference (September 1966)

3. "The Physical Chemistry of Aerosols," Disc. of Faraday Soc. (1960)

4. T. Hatch, J. Frank. Inst., 215, 27 (1933)

TECHNIQUES FOR SAMPLING SODIUM SMOKE AND FISSION PRODUCTS

By

C. T. Nelson, L. Baurmash, and R. L. Koontz

Atomics International
A Division of North American Aviation, Inc.

ABSTRACT

Various sampling techniques are described which allow one to characterize the aerosols produced from sodium fires in a controlled environment test chamber. By using plating and fallout deposition samplers combined with Cascade impactors, electrostatic precipitators, and millipore air samplers, studies are made of the spatial and temporal behavior during the production, dispersion growth, and removal of the suspended particulates. The role of each sampling technique in verifying analytical models is discussed.

INTRODUCTION

Potentially serious dispersions of materials, such as plutonium, fission products, and sodium, are postulated to occur as a result of a primary coolant sodium fire following certain major accidents in a sodium-cooled fast reactor. Research on sodium fires is thus needed to provide data from which to formulate a method for characterizing the various processes occurring in the course of a sodium coolant accident. This paper gives consideration to the various techniques for sampling sodium smoke and fission products which are released to the environs.

Techniques for sampling aerosols which contain foreign contaminants of lower allowable concentrations, such as fission products and fissile material, make sizing particle distributions by electron microscopy an inadequate tool. Additionally, techniques which characterize an aerosol at only one time and place will not describe it completely, unless the particle concentration and sizes are so small that no further change in the distribution will occur.[1]

This paper describes a number of empirical approaches which have been used at Atomics International to characterize the matter released from sodium in an environment of nitrogen with a low oxygen and humidity content.

SODIUM FIRES LABORATORY TEST CHAMBER

A laboratory test chamber has been used to study the dynamic size and concentration characteristics of an aerosol produced by the reaction of hot sodium with atmospheres of varying oxygen content. The 40 ft^3 chamber,

*Work performed for U.S. Atomic Energy Commission
under Contract AT(11-1)-GEN-8

3 ft in diameter by 7 ft high was designed in two sections and is capable of withstanding 15 psig. Figure 1 shows the chamber in the upright position, encircled with the various penetrations, sampling and monitoring equipment. Figure 2 shows the chamber in the loading position. The chamber is hinged to the bottom plate and is tilted in the horizontal position for ease of access. All internal walls are coated with an epoxy resin which has resulted in a surface which is easily cleaned and durable. The photograph shows the type of equipment which is installed in the bottom plate, such as the burn pot, heater, miniature flood light, and automatic fallout sampler. Sodium burn pots of 2 to 6 inches in diameter have been used in various experiments. The lid of the pot is remotely connected to the outside of the vessel allowing the pot to be covered or uncovered as desired. Thermocouples are immersed in the sodium for temperature monitoring and control. The oxygen content is determined by means of a Hays Recording Analyzer with periodic checks using a manual Beckman Oxygen Analyzer. The temperature distribution inside the chamber is monitored with thermocouples and a multipoint recorder. Aerosol sampling positions are located at varying heights above the fire and at varying distances from the axis of the chamber in order that concentration and size measurements can be made. The indexing mechanisms for the automatic wall and ceiling plating samplers are both mounted externally with the drive shafts penetrating the wall. These samplers together with the fallout sampler are controlled by a dual channel controller. There are four windows in the chamber wall for observations of the burning sodium and the resultant aerosol.

PARTICULATE CHARACTERIZATION TECHNIQUES

Samplers used in these experiments can be divided into two types: deposition samplers and aerosol samplers. Deposition samplers have been built to automatically collect samples of wall plating, ceiling plating, and floor deposition. High concentrations >> 1μg/cc are easily measured. Aerosol samplers are used manually to collect spot samples for particle size and concentration measurements.

The ceiling and wall deposition sampler (Figure 3) consists of a twelve-position table containing deposition discs, each of which is rotated into sampling position upon command from a programmer. A shaft which penetrates the chamber wall positions the sampling head near the chamber axis. The indexing motor is located outside the chamber (Figure 1).

The floor deposition sampler (Figure 4) in its present configuration includes the indexing motor. This sampler contains 24 sampling positions and therefore is on a different sampling cycle than wall or ceiling samplers. The additional 12 positions are exposed by means of another sample port. During the first 12 sample positions the outer sample port is open, but as the indexing motor rotates the table from Sample 12 to Sample 13, a shutter is released which closes the outer port and opens the inner port providing an additional 12 samples. Stainless steel discs for cumulative sampling are attached to the ceiling, walls, and floor by magnets. These samples are removed at the completion of the experiment and analyzed for total deposition.

Aerosol samplers which are used only to obtain concentration data are pre-washed membrane filters, with 0.2μ pore size, and three midget impingers (in series), using water as the collecting medium.

Cascade impactors are used to collect samples for particle size measurements and to obtain concentration data. Multijet and single jet impactors have been used in these studies. The 7-stage, 400-jet impactor supplied by A. A. Andersen[2] was originally used for these experiments with a membrane filter

LABORATORY TEST CHAMBER

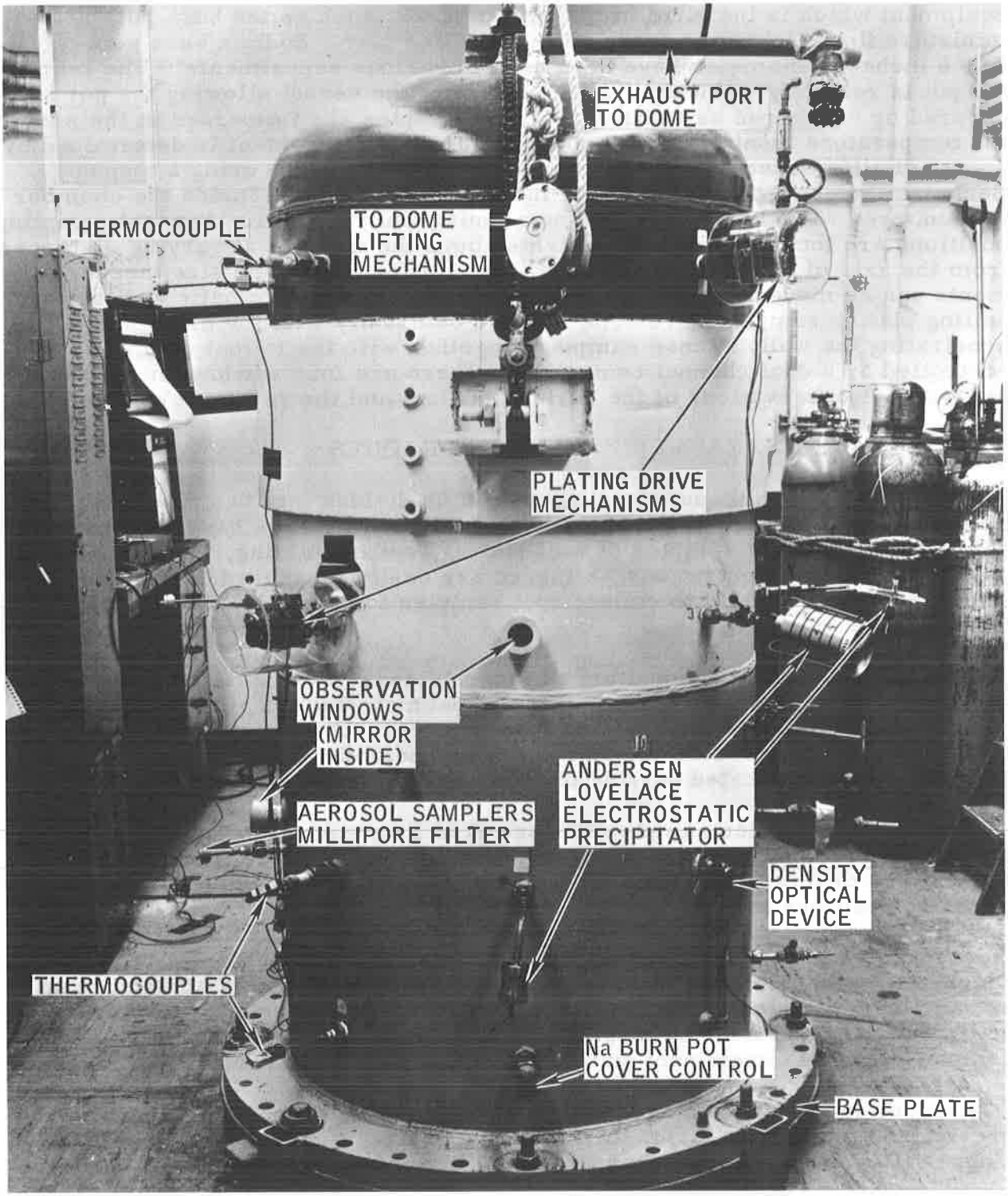

Figure 1. Laboratory Test Chamber

INSIDE VIEW OF SODIUM FIRES TEST CHAMBER

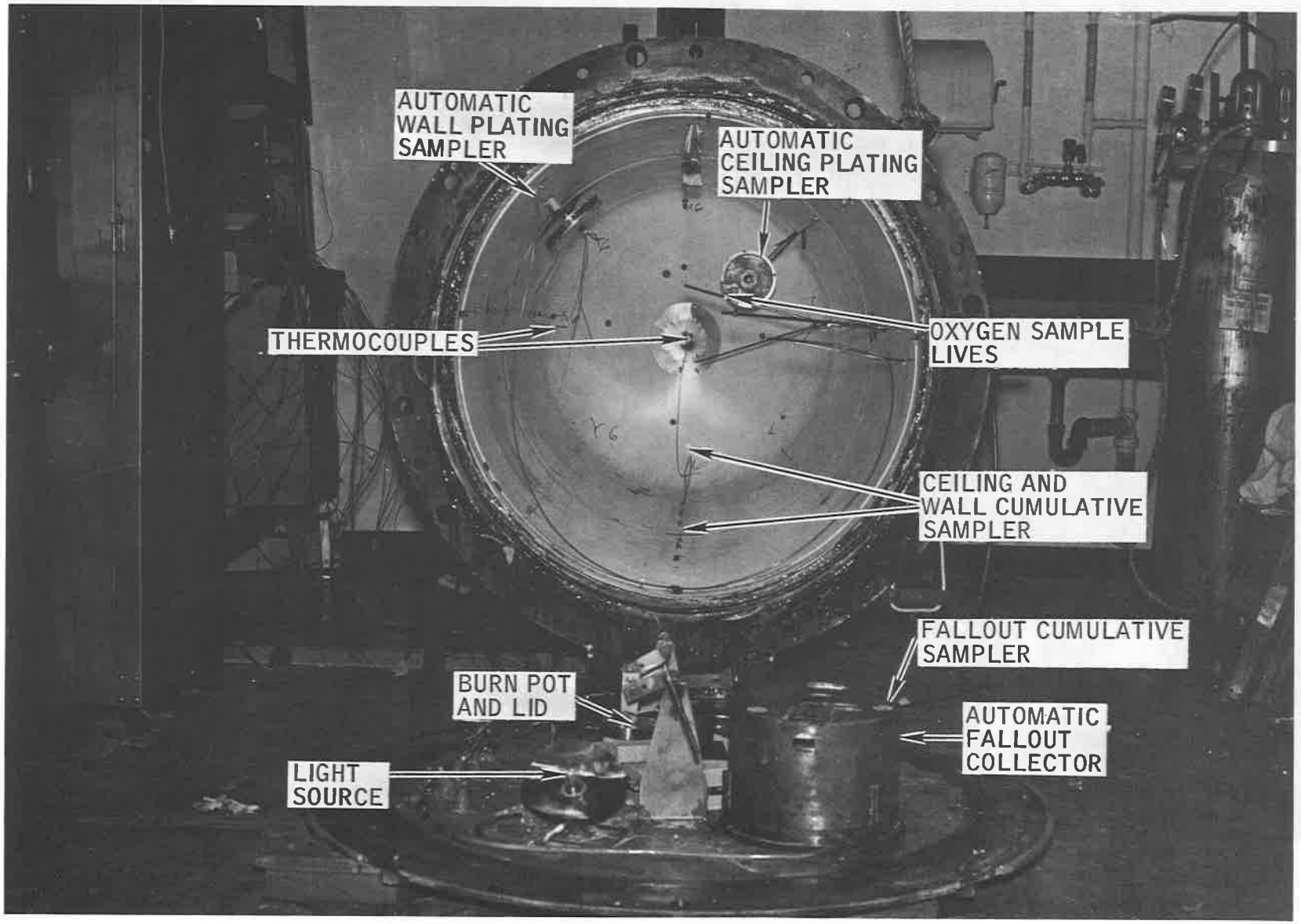

Figure 2. Inside View of Sodium Fires Test Chamber

CEILING DEPOSITION SAMPLER

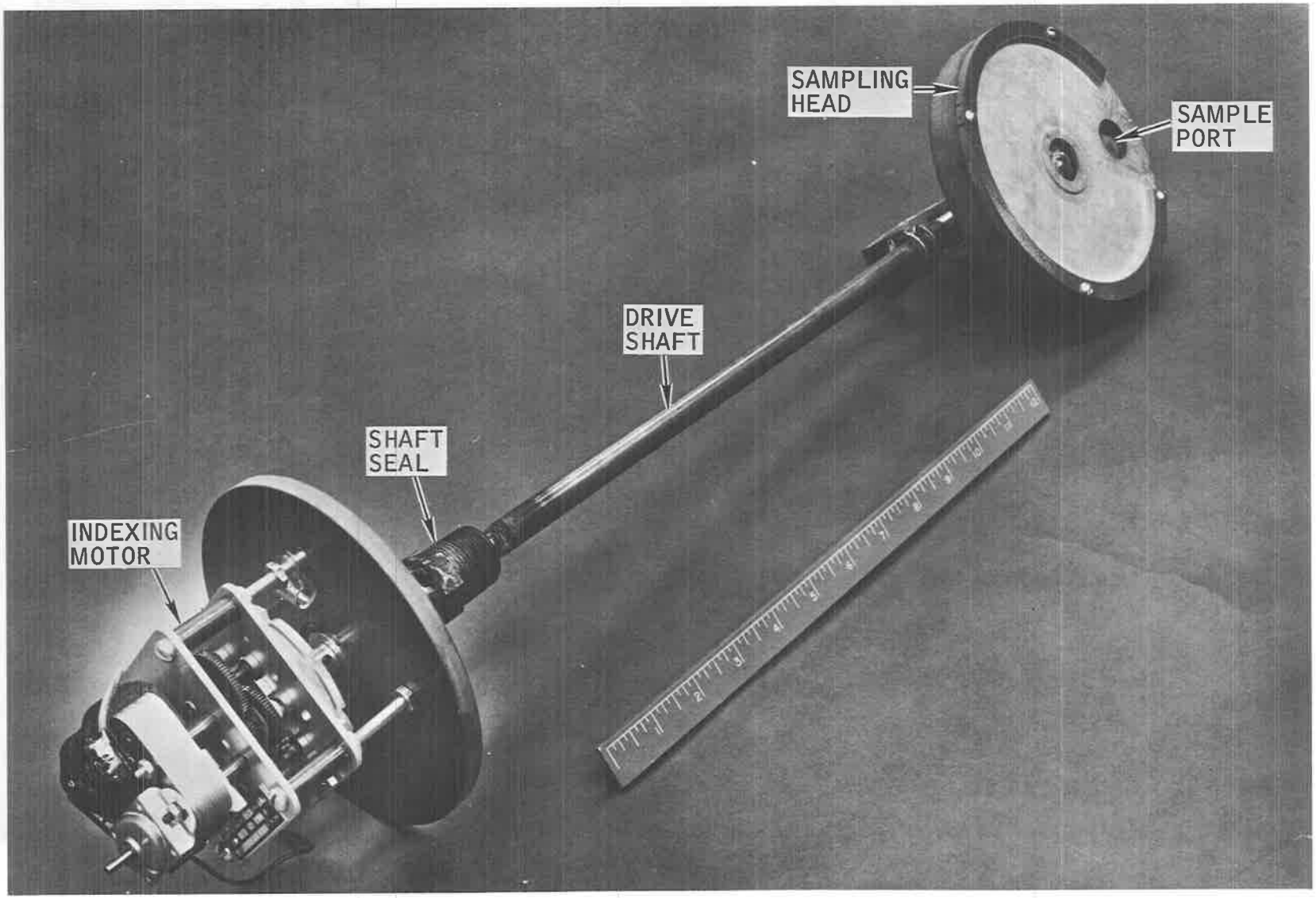

Figure 3. Ceiling Deposition Sampler

WALL AND FLOOR DEPOSITION SAMPLERS WITH EXTERNAL PROGRAMMER

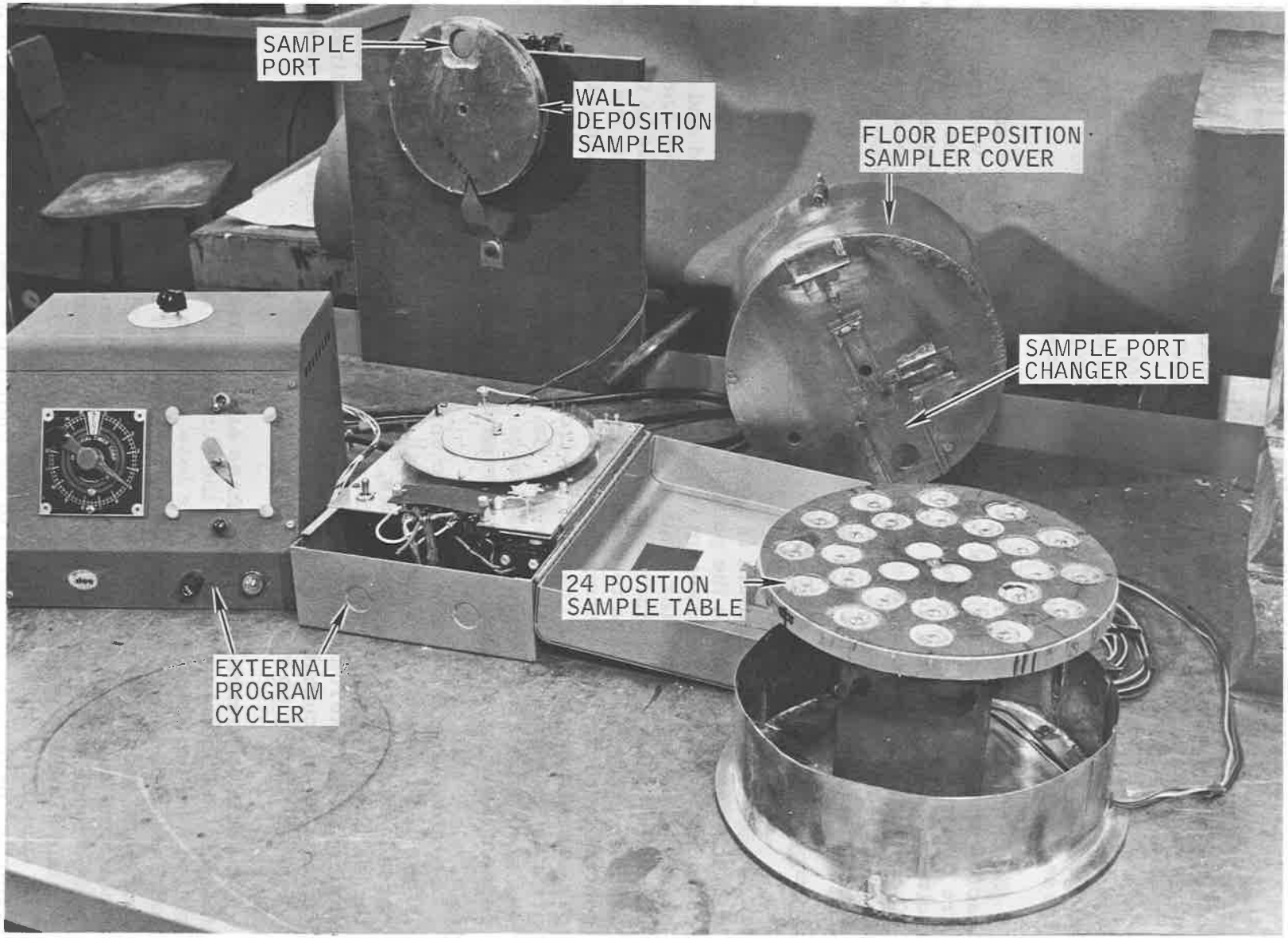

Figure 4. Wall and Floor Deposition Samplers with External Programmer

eighth-stage. However, the required flowrate of 1 cfm was unsatisfactory. Therefore, a 5-jet and 10-jet impactor were used in later studies (Figure 5) at flowrates 1/80 and 1/40 of that for the original unit. One 400-jet impactor was also modified by masking all the jets in each stage except 10 in a 45-degree sector (Figure 5). After loosening the retaining springs, proper rotation of each stage allows eight samples to be taken on each slide. This modification, called "sidewinder," and the other modified Anderson samplers were used with stage constants, based on aerodynamic equivalent diameters.[3]

A single-jet, 7-stage impactor (Figure 6), based on the design of Mercer,[4] was also used in these studies. This unit is an in-line impactor with an 8-stage membrane filter. The flowrate was maintained at about 100 cc/min for these experiments, but could be varied as desired.

Since photographic samples were needed for comparative sizing with impactor samples, a point-to-plane electrostatic precipitator was made (Figure 6) using the design of the University of Rochester.[5] The applied high voltage was set at 7000 volts and the sample flowrate was either 35 cc/min or 70 cc/min. Samples were collected on 200-mesh electron microscope grids for electron microscopy. Photographs would then be sized by means of a Zeiss Particle Size Analyzer to obtain distribution data.

EXPERIMENTAL PROCEDURE

A known weight of sodium is placed in the burn pot. The sodium is flushed with nitrogen after which the pot is closed with a lid and installed in the test chamber. A lifting mechanism is then engaged to the pot lid and the chamber closed. Immediately after sealing, the chamber is evacuated and filled with nitrogen. After the sodium is heated and the test chamber is in thermal equilibrium, oxygen is added to the chamber atmosphere to raise the oxygen concentration to the predetermined value. The oxygen level, humidity, and temperature of the internal chamber environment are continuously monitored just prior to and during the experiment. In one experiment, the chamber pressure was also monitored. An optical device has now been added so that changes in concentration can be directly observed during a test.

Sodium oxide is released into the environment as a result of oxidation and is carried to the top of the ~7-ft-high vessel by the hot gas mixture where it spreads out, plates, agglomerates, and settles. Cool gas passes down near the walls and creates a turbulent or stirred and homogeneous particulate environment. Aerosol, wall plating, and fallout samples are obtained on a continuous and cumulative basis during the test. The experiment is stopped when practically no mass remains airborne.

In addition to measuring the mass and its distribution in the gas phase, a material balance is obtained for the sum of the mass settled, suspended and plated as a function of time. The loss of oxygen is used to compute the total oxidized sodium and the residue in the burn pot is analyzed for the weight of oxide and sodium which remains. Thus, the sodium collected on the walls, floor, and ceiling represent the released sodium, and a simple comparison can be made to the sodium equivalence of consumed oxygen. The oxide which remains in the pot plus that on the walls allow one to make a material balance. The sum of the masses collected during the observation period of the automatic sampling devices is compared to the cumulative samples located throughout the chamber. Air samples are collected with electrostatic precipitators, millipore filters, and impactors at various heights and positions.

FOUR TYPES OF ANDERSEN IMPACTOR SAMPLERS

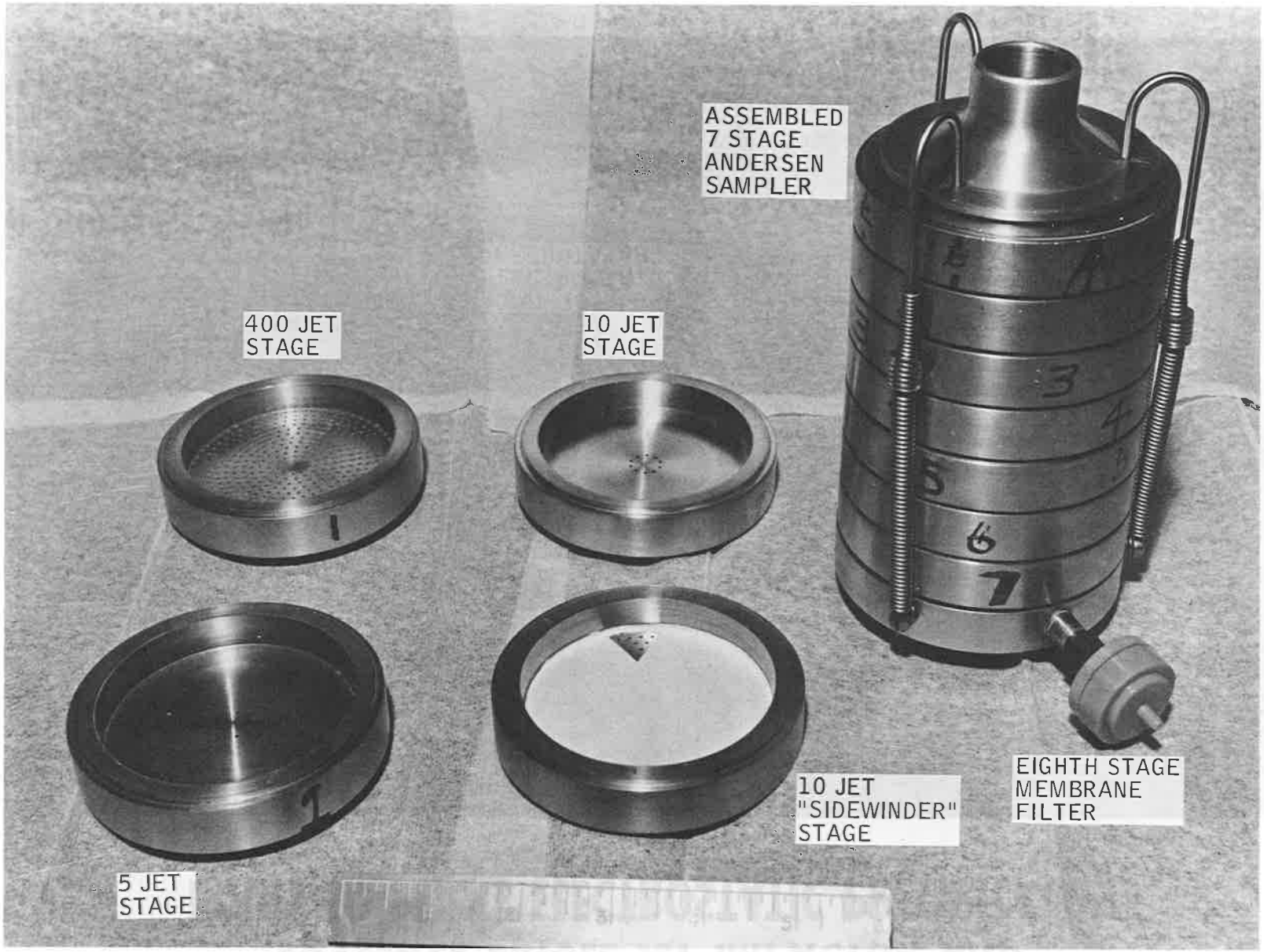

Figure 5. Four Types of Andersen Impactor Samplers

LOVELACE SINGLE JET IMPACTOR AND POINT-TO-PLANE ELECTROSTATIC PRECIPITATOR

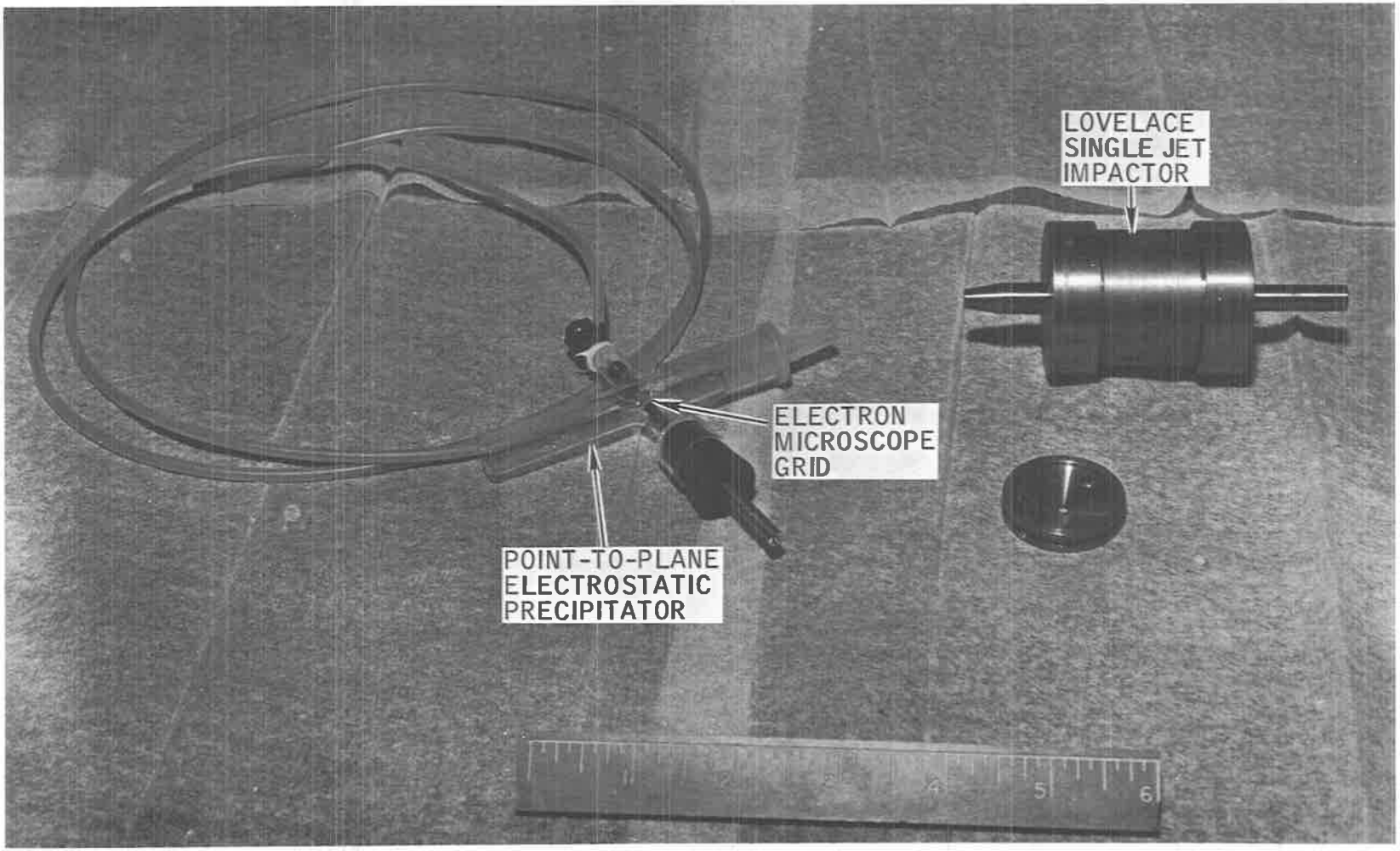

Figure 6. Lovelace Single Jet Impactor and Point-to-Plane Electrostatic Precipitator

EXPERIMENTAL RESULTS

A simplified equation, for an equivalent "monosize" distribution, is presented to describe the relationship between the various removal mechanisms in the test chamber. The objective of the experiments are clearly to observe the empirical coefficients and relate them to an analytical model.

Let

$$\frac{dV}{dt} = S - \lambda V - \beta V \qquad \ldots(1)$$

and

$$\frac{dN}{dt} = S' - KN^2 - \lambda N - \beta N \qquad \ldots(2)$$

where

V = particle mass density per unit volume of gas, μ^3/cm^3

N = particle number density, part/cm^3

λ = settling removal time constant, 1/sec

β = wall plating removal time constant, 1/sec

K = agglomeration constant

S and S′ = source term, P/cm^3-sec or μ^3/cm^3-sec.

K, λ, and β are functions of the particle size, and the particle radius, r, is related to the particle volume V as $r(t) = [3V/4\pi N(t)]^{1/3}$. As mentioned previously, the experimental observations include:

1) V(t), volume suspended particles

2) $\int \lambda V dt$, volume settled particles

3) $\int \beta V dt$, volume plated particles

as well as r(t) and σ, the radius and distribution of the suspended material vs time.

By observing r, σ, and V(t), one can compute N(t) the number of particles in suspension. Techniques have been developed, but not used as yet, to measure the size distribution which plates or settles as a function of time.

Table 1 presents a summary of three experiments performed in the laboratory test chamber.

The automatic deposition samplers described were used to measure the mass of material deposited in fixed time intervals during a sodium oxide aerosol experiment in the laboratory test chamber. By adding the accumulated mass for each observation period, it was possible to compare the total mass on the plating devices to the mass which deposited on a fixed slide located near the automatic samplers. These techniques gave very nearly the same value, thus verifying the adequacy of the samplers. Figure 7 shows the relative mass accumulated on the floor and walls as a function of time.

In Tests 2 and 3, the air concentration vs time and the total deposition was measured at three different heights. The concentrations and amounts deposited

Table 1

LABORATORY TEST CHAMBER DATA

Parameter	Test 1	Test 2	Test 3	Test 4
Area fire pot (ft^2)	0.031 ($29\ cm^2$)	0.031 + leak ($29\ cm^2$)	0.2 + leak ($185\ cm^2$)	0.031 ($29\ cm^2$)
Na temperature (°F)	1000	1000	1140 to 900	1000
Initial O_2 (%)	4.0	2.45	3.9	4.0
Released Na_2O as (gm Na) (leaving pot)	3.4	3.3	73.0	3.6
Fraction Na deposited				
Ceiling	0.32	0.32	0.01	0.02
Wall	0.24	0.31	0.12	0.34
Floor	0.45	0.37	0.87	0.64
Unreleased oxide found in pot as (gm Na)	6.7	10.0	leaked	6.4
Release fraction of oxidized Na	0.34	0.25	0.43	0.35
Burn rate (lb Na/hr-ft^2-%)-K'	0.92	-	0.92 and 0.43	-
Half-time for wall plating (min)	45	47	54	37
Wall plating rate during half-time I(μ gm/min-cm^2)	0.076	0.10	0.80	0.2
C, air conc. at 10 min (μ gm/cc)	1.7	1.7	22	2.0
Half-time for floor deposition (min)	64	55	40	37
Equiv. diameter of particles (μ) for $T_{\frac{1}{2}}$ (Stokes)	2.0	2.2	2.6	2.7
Effective wall plating distance δ (μ)	1.6	1.2	1.2	0.7

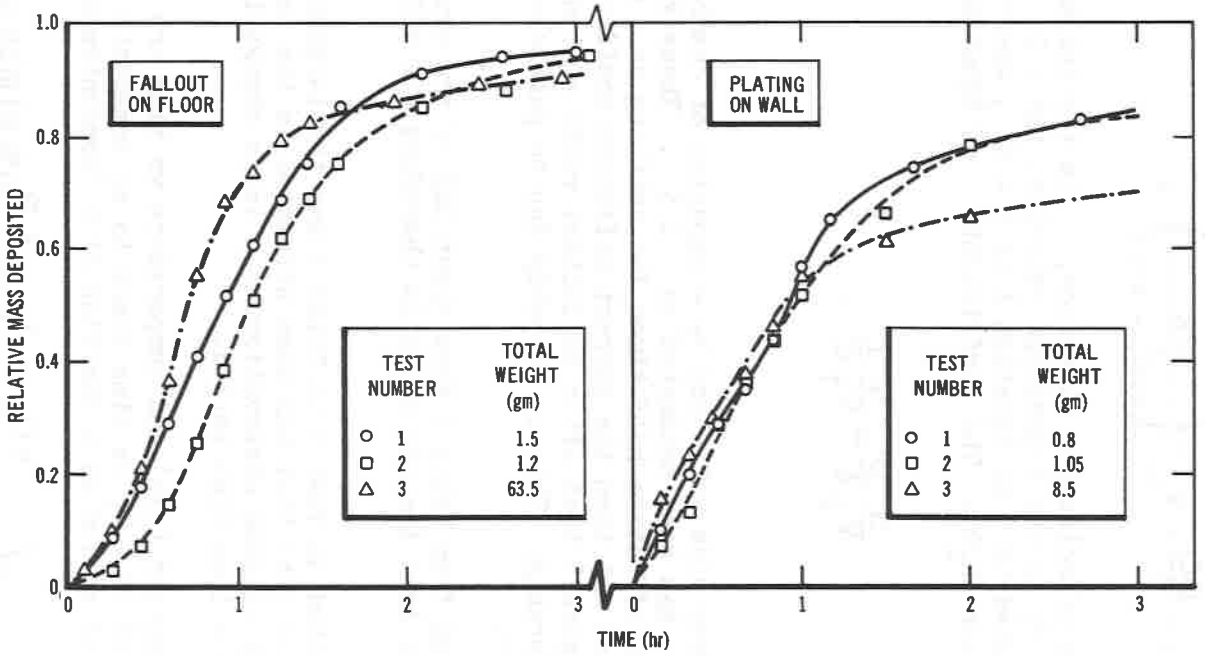

Figure 7. Plating and Fallout Data – Laboratory Test Chamber

were the same as these heights, thus verifying that stirred settling was occurring.

The deposition rate on the walls is related to the intensity of convection and to diffusion. Fuks[6] expresses this as

$$I = \frac{DC}{\delta} = V_D C \left(\frac{\mu g}{cm^2 - sec} \right) ,$$

where D is the coefficient of molecular dissusion, is the thickness of a thin layer close to the walls, V_D is the deposition velocity, and C is the concentration in g/cc. C is related to V of Equation 1 as C = V , where is the density of aerosol (2.27 for Na_2O). The coefficient of Equation 1 is equal to:

$$\frac{S}{V_T} \frac{D}{\delta} = \frac{S}{V_T} \frac{I}{C} ,$$

where S = surface of chamber side walls and V_T = capacity of chamber. For these three experiments, has been estimated as 1.5 . These values are estimated by utilizing the effective half-times for settling as a means of computing a mean particle size and then the correct diffusion coefficient. It is interesting to note in Figure 7 that after an initial rapid plating rate, the process slows down considerably. This is probably due to particle size increase and concentration decrease.

It should also be noted from Table 1 that about 34% of the oxidized sodium leaves the pot and escapes into the air which is therefore the effective fraction released.

The experiment designated as Test 3 in Table 1 was the largest (pounds of sodium consumed and area of pot) that has been attempted in the laboratory test chamber. As such, it allowed observation of a large change in the initial oxygen concentration over a long time period.

The data for oxygen content (v/o) and temperature vs time are presented in Figure 8. The linearity of ln % O_2 vs time leads to an immediate analysis of the burning relationship of sodium as a function of O concentration; i.e.,

$$- \frac{dw}{dt} = \varphi w = K \left(\frac{lb\ O_2}{ft^2 - \%O - hr} \right) \frac{A(ft^3)\ P_o(\%\ O)\ W(lb\ O_2)}{W_o(lb\ O_2)}$$

where

P_o = percent of O_2 present initially

W_o = initial pounds of O_2

K = oxygen depletion rate constant for pot of Area A ft^2 (the value of K' is shown in Table 1, where K' = 2.9 K)

BURNING RATE DATA vs TIME IN LABORATORY TEST CHAMBER

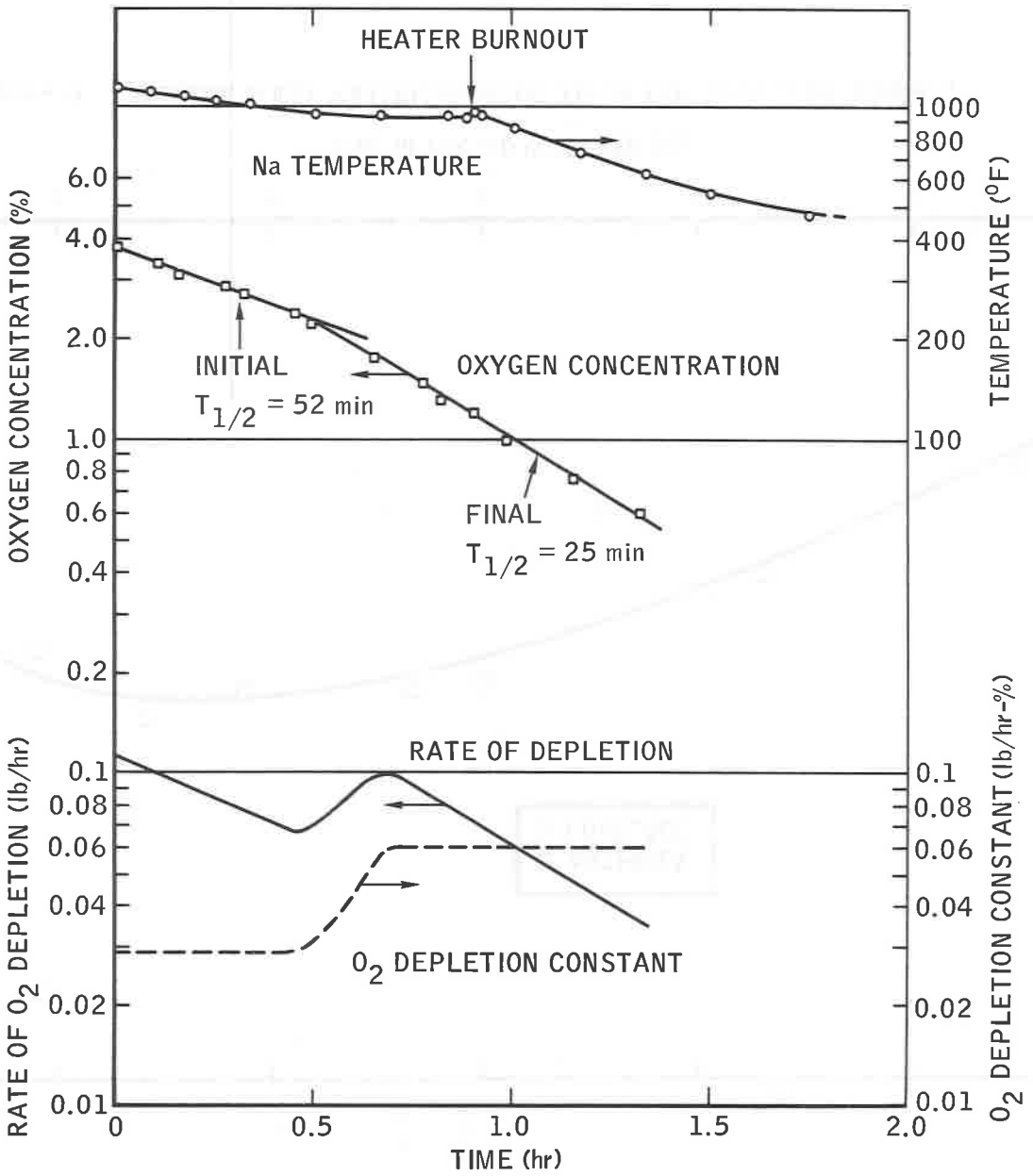

Figure 8. Burning Rate Data vs Time in Laboratory Test Chamber

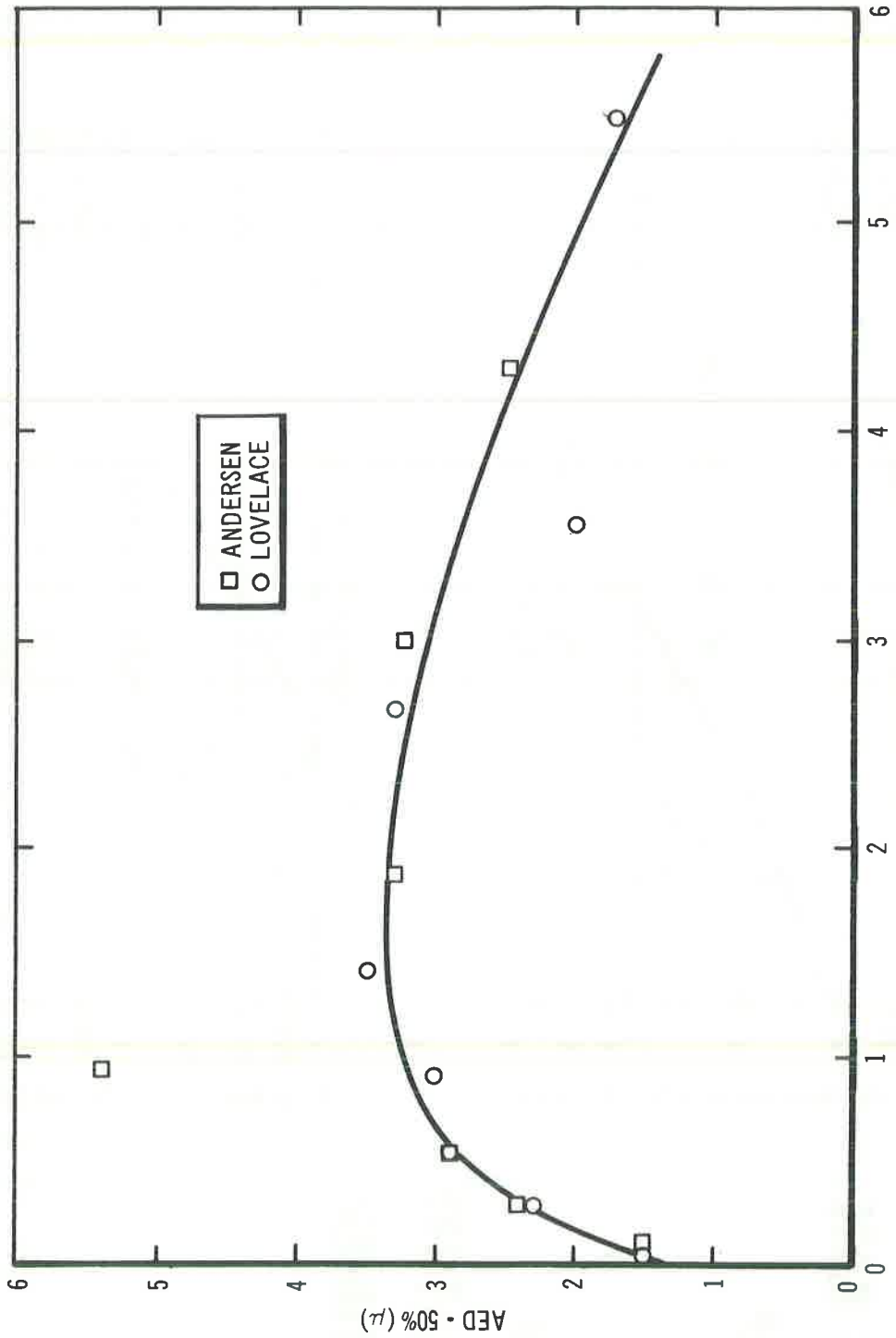

Figure 9. Median AED Variation with Time for Test 2 of Table 1

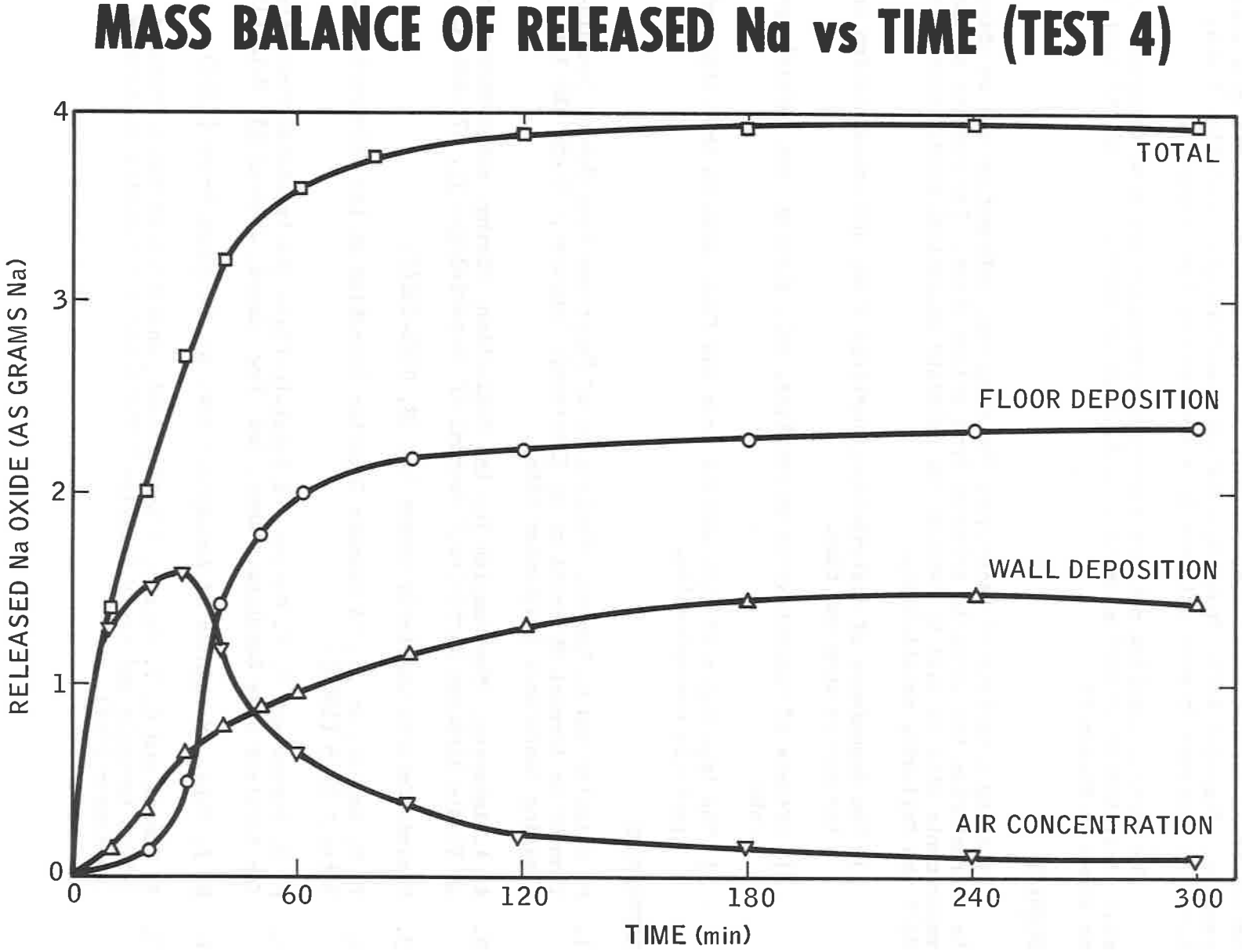

Figure 10. Mass Balance of Released Na vs Time (Test 4)

Fair agreement between size distributions obtained with the electrostatic precipitator (ESP) and impactors have been obtained with a particle generator.(7) However, a typical experiment in the laboratory test chamber leaves much to be desired as far as agreement between the two techniques is concerned. The importance of agreement has to do with the ultimate objective of characterizing the sizes of the associated fission products which are released during sodium fires. Impactors can be used for this purpose but optical methods (ESP) cannot. Figure 9 shows the median aerodynamic diameters (AED) obtained from two different detectors as a function of time for Test 2. The other experiments give similar results. Computed AED's from count median diameters give a similar trend; i.e., an increase in size followed by a decrease as time proceeds.

The various sampling methods described previously are used to obtain the mass distribution of sodium oxide as a function of time in the 40 ft^3 test vessel, as shown in Figure 10.

SUMMARY

By using a variety of techniques for sampling, information can be obtained to characterize the aerosols released from sodium fires. The results of these experiments will be used to develop and validate analytical models which predict the following relationship:

1) The dependence of distribution, particle size, and concentration on the source term and time.

2) Effects of concentration on settling, wall plating, and particle growth rate.

3) The importance of wall surface area and floor area on the suspended particle concentration.

REFERENCES

1. P. Spiegler and R. Koontz, "Evaluation of Equations that Govern Coagulation of an Aerosol by Means of an Electronic Computer," Ninth AEC Air Cleaning Conference (September 1966).

2. A. A. Andersen, "New Sampler for the Collection, Sizing, and Enumeration at Viable Airborne Particles," Journal of Bacteriology, 76, 471-484, (1958).

3. Hazards Control Quarterly Report No. 18, UCRL-12167.

4. T. T. Mercer, et al, "A Cascade Impactor Operating at Low Volumetric Flow Rates," LF-5 (1962).

5. P. E. Morrow and T. T. Mercer, "A Point-to-Plane Electrostatic Precipitator for Particle Size Sampling," Amer. Ind. Hyg. Assoc. Journal 25, 8-14 (1964).

6. N. A. Fuks, "Mechanics of Aerosols," Rev. Ed. Pergamon Press (1964).

7. R. Koontz and C. T. Nelson, "Standardized Generation of Vapor-Produced Sodium Aerosols and their Behavior," Ninth AEC Air Cleaning Conference (September 1966).

SODIUM AEROSOL AND ITS FILTRATION

by

P. Himot, F. J. Viles, Jr., J. Sullivan, and M. W. First

Department of Industrial Hygiene
Harvard School of Public Health
Boston, Massachusetts 02115

ABSTRACT

Accidental loss of coolant from a sodium cooled nuclear reactor can result in rapid vaporization and burning of the metal to produce an airborne fume. Restrictions on the quantity discharged to the atmosphere require 99% removal to prevent a health hazard in the surrounding environment. In this study various configurations of graded, deep bed filters were tested to evaluate their application for controlling such fumes and to determine their maximum filter loading capacity. The pack included 2-inch-deep beds of stainless steel fiber media followed by 2-inch-deep beds of glass fiber media and a pleated absolute filter. Fiber sizes ranged from 1000 to 2.0 microns, face velocities ranged from 5 to 40 fpm, and the units were operated up to a total resistance of 20 i.w.g. With proper design and operation, it was shown that a total filter storage of approximately 0.75 pound of sodium per square foot could be obtained with greater than 99% by weight of sodium fume (average MMD of 1.5 microns) being retained in the deep bed filter pack. No iodine, as elemental iodine or sodium iodide, penetrated the filter pack when the sodium melt contained 3.5 ppm iodine as sodium iodide.

SODIUM AEROSOL AND ITS FILTRATION

I. INTRODUCTION

The use of liquid metal coolant in nuclear reactors may lead to contamination problems if spills or leaks occur during high temperature operation. In the event of a coolant loop rupture, large quantities of molten metal will be released to form a dense fume of metal oxide in the containment vessel atmosphere. To prevent vessel rupture and leakage to the atmosphere, release of overpressure must occur with retention of particulate matter and radio-iodine. Minimum filter requirements are 99% removal of particles and iodine from an exhaust gas stream containing up to 30 lbs. of sodium without exceeding a resistance of 20 i.w.g. across the entire filter at a maximum exhaust flow rate up to 1000 cubic feet per minute and maximum temperature of 250°F. Oxygen concentration may reach 2%. Under these conditions, the fume may be liquid (melting point of sodium is 203°F) or solid; when solid, it may be condensed sodium metal or sodium oxide. Sodium metal retained on the filter may change physical state as filtration proceeds and may oxidize if oxygen enters the filter container.

II. EXPERIMENTAL PROCEDURE

A. Test Apparatus

Tests were performed with the equipment shown in Figure 1. It consisted of a sodium melting and vaporization vessel, a heating system, a blower to circulate the carrier gas, and a filter holder. Controls were installed to regulate carrier gas flow rate and temperature of the molten sodium. Ports were placed at numerous locations for temperature and differential pressure measurements, aerosol sampling, and the addition and measurement of oxygen in the nitrogen carrier gas.

Oil pumped nitrogen was supplied to the system from an oil-sealed spirometer of 20 cubic feet capacity. The spirometer was filled from tanks of compressed gas. So that leakage would be outward, a positive pressure of not less than 0.5 i.w.g. was maintained at the inlet to the blower (lowest pressure location within the system) by placing weights on the spirometer bell. The gas volume in the spirometer was self adjusting, keeping the system at a uniform pressure. For most tests, the filtered gases were recirculated, but it was possible to operate the apparatus as a single pass system. Aerosol was generated by passing up to 25 CFM of gas tangentially across the surface (0.23 $ft.^2$) of molten sodium maintained at 800° to 1100°F. Temperature, measured with a thermocouple inserted into the melt, was kept constant with electric heaters connected to a temperature controller.

The system was designed with a gas recirculating loop that by-passed the sodium pot so the gas and sodium could be preheated separately. The filter holder was a 1-foot diameter cylinder, 2 feet in length, with a filter face area of 0.78 square feet. Face velocities in excess of 30 feet per minute were produced by reducing the filter cross section. The final filter stage for all tests was

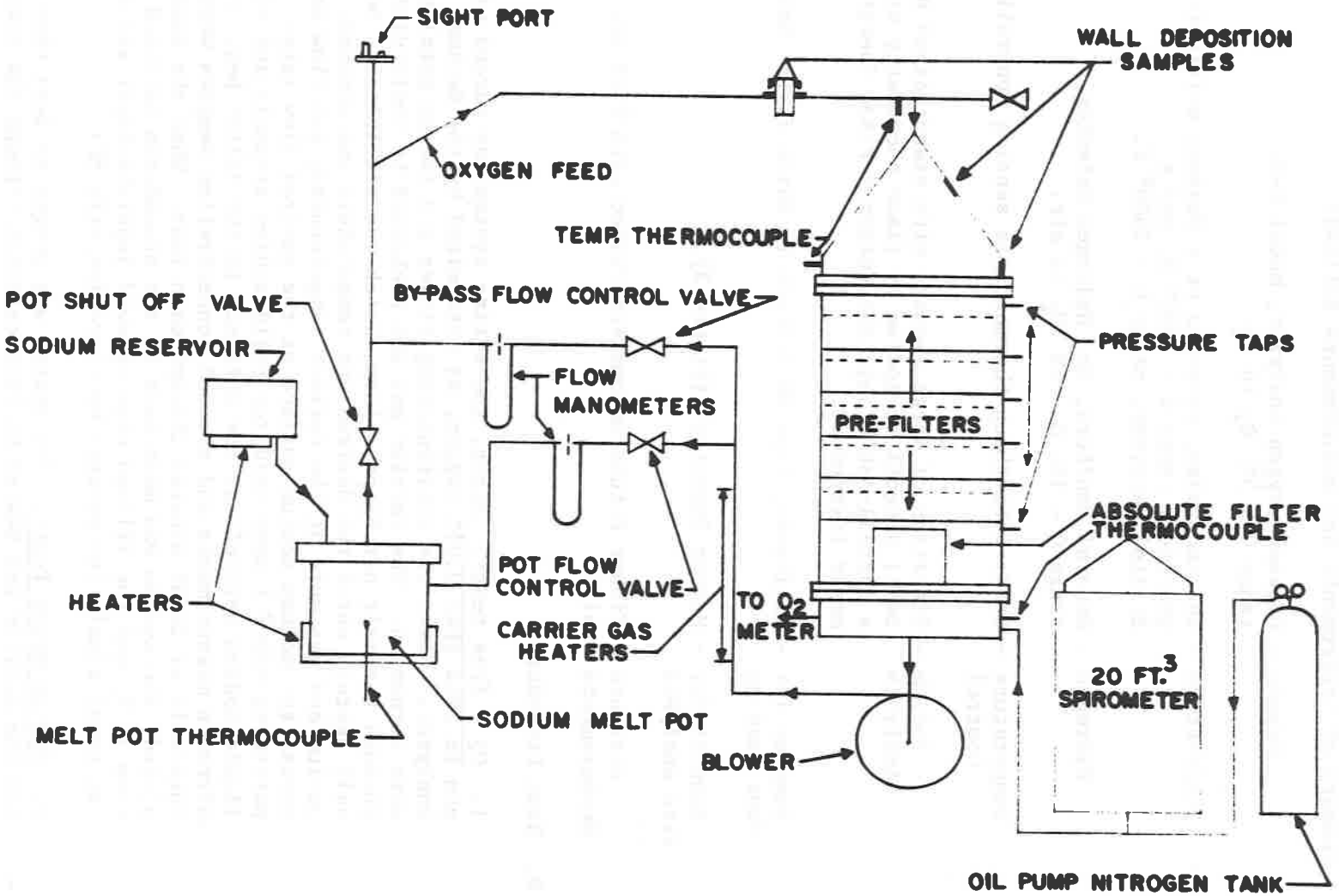

FIGURE 1. SODIUM FUME TEST APPARATUS.

an all-glass absolute filter, either as flat sheets of paper (0.78 sq. ft.) or as an 8" x 8" x 6" pleated filter (10.5 sq. ft. of paper). Sampling and wall pressure taps were placed at 2-inch intervals along the length of the cylinder wall. Tabs were used inside the cylinder to support the filter retaining screens.

A summary of instruments and measurements follows:

Oxygen - Beckman oxygen analyzer, Model C-2, range 0 - 5% O_2 in N_2.

Temperature - Thermocouples, recorded on a Foxboro multipoint recorder, range 0 - 1000° F, and a Bristol recorder, range 0 - 2500° F.

Hydrogen - General Monitors, Co. Hydrogen Detector, range 0 - 1%, 0 - 5% H_2 in air.

Temperature Control - Leeds & Northrup thermocouple sensing controller.

Sodium Analysis - Titration of large amounts with standardized HCl. Small amounts of sodium by flame photometry with a Jarrell-Ash Atomic Absorption / Flame Spectrometer instrument.

Samples for fume loading - Millipore, type HA filters in Unico filter holders.

Samples for size analysis - Mercer Impactor[1] (Figure 3).

Pressure Measurements - Fisher U-tube manometers filled with 0.78 sp. gr. oil.

B. Test Procedures

1. O_2 - free tests. First, the entire system was purged with nitrogen to less than 0.01% oxygen, as determined by the Beckman oxygen analyzer. Next, the recirculating blower and sodium metal heaters were turned on. The carrier gas was preheated by recirculating it through the melt pot by-pass loop, which was electrically heated by wall heaters until the desired gas temperature was reached. When sodium and gas were at the correct temperatures, gas flow was directed across the molten sodium surface at the desired flow rate. Gas temperatures <200° F were used for solid sodium aerosols and >210° F for liquid sodium aerosols at the entrance to the filter bed. Filter resistance measurements and aerosol concentration samples were taken at intervals of 20-30 minutes through each test. When the test was completed, the system was made safe by the procedures outlined in Section II D, and the filters were removed layer-by-layer and analyzed for total alkali (as sodium) by titration with HCl.

2. Sodium Oxide Tests. The system was purged to less than 2% oxygen and the carrier gas heated by recirculation through the heated by-pass loop until a filter inlet temperature of 120° F was obtained.

Aerosol generation was started by opening the melt pot shut-off valve and flowing 0.5-1.0 CFM of oil pumped nitrogen from storage tanks tangentially across the sodium melt (Figure 2). The main gas stream was circulated through the by-pass loop by the blower and make-up oxygen was injected into the main gas stream three feet above the melt at a controlled rate to keep the oxygen concentration, measured at the exit of the filter train, between 1 and 2%. (When the main gas flow, containing 1-2% oxygen in nitrogen, was directed across the surface of the melt, it caused such rapid local oxidation and local fume deposition that the feed line plugged at the gas entry point.) After the test, the sodium on the filters was reacted as outlined in Section II D and individual layers analyzed for sodium.

3. Iodine Tests. A sodium mixture containing 3.5 ppm iodine by weight as sodium iodide was prepared and samples taken to determine the uniformity of the mixture. Tests were performed in a 1-2% oxygen atmosphere and samples were taken up- and downstream of the filter pack. Upstream Millipore filter samples and downstream copper beads samples were analyzed for iodine.[2]

4. Wall Deposition. Wall deposition tests were conducted concurrently with filter tests by placing pieces of five-mil steel shim stock in the horizontal 2-inch pipe, the vertical cone, and the vertical 12-inch pipe, as shown in Figure 1. Care was taken to obtain intimate contact between the back of the deposition strip and the pipe to prevent deposition on the back of the plaques. The plaques were recovered at the conclusion of the test and analyzed for sodium by flame spectrophotometry.

C. Sampling and Analytic Methods

Aerosol samples for measuring fume loading were obtained up- and downstream of the test filters through 0.30-inch diameter sampling probes and filtered on HA Millipore filters in holders located outside the test filter holder. Probes were faced into the aerosol stream and moved across the diameter of the test filter section during sampling.

After sampling, the Millipore filters were washed in distilled water and the solution analyzed for sodium content with a flame spectrophotometer capable of detecting 0.1 μg sodium in a 1-ml. sample. Examination of the probes showed deposition of less than 0.5% of the sodium collected on the sample filter. Blank analysis of HA Millipore filters showed negligible sodium.

Test filter deposition was determined by removing each layer, washing it with distilled water, and titrating the solution with HCl to a pH of 3.5-5.0 with brom-cresol green indicator.

Size analyses of the fume were made with the aid of Mercer impactors.[1] The impaction surfaces were analyzed by washing with 1 ml. of distilled water and determining the sodium content in the solution by flame spectrophotometry. Figure 3 is a photograph of a disassembled Mercer impactor. Stage efficiency calibrations were determined from the correlations provided by Mercer.[1]

Iodine was analyzed colorimetrically using a method based on the catalytic reduction of cerric ions by iodide. Sensitivity was 0.002 μg of iodine in 5 ml. of solution.[2]

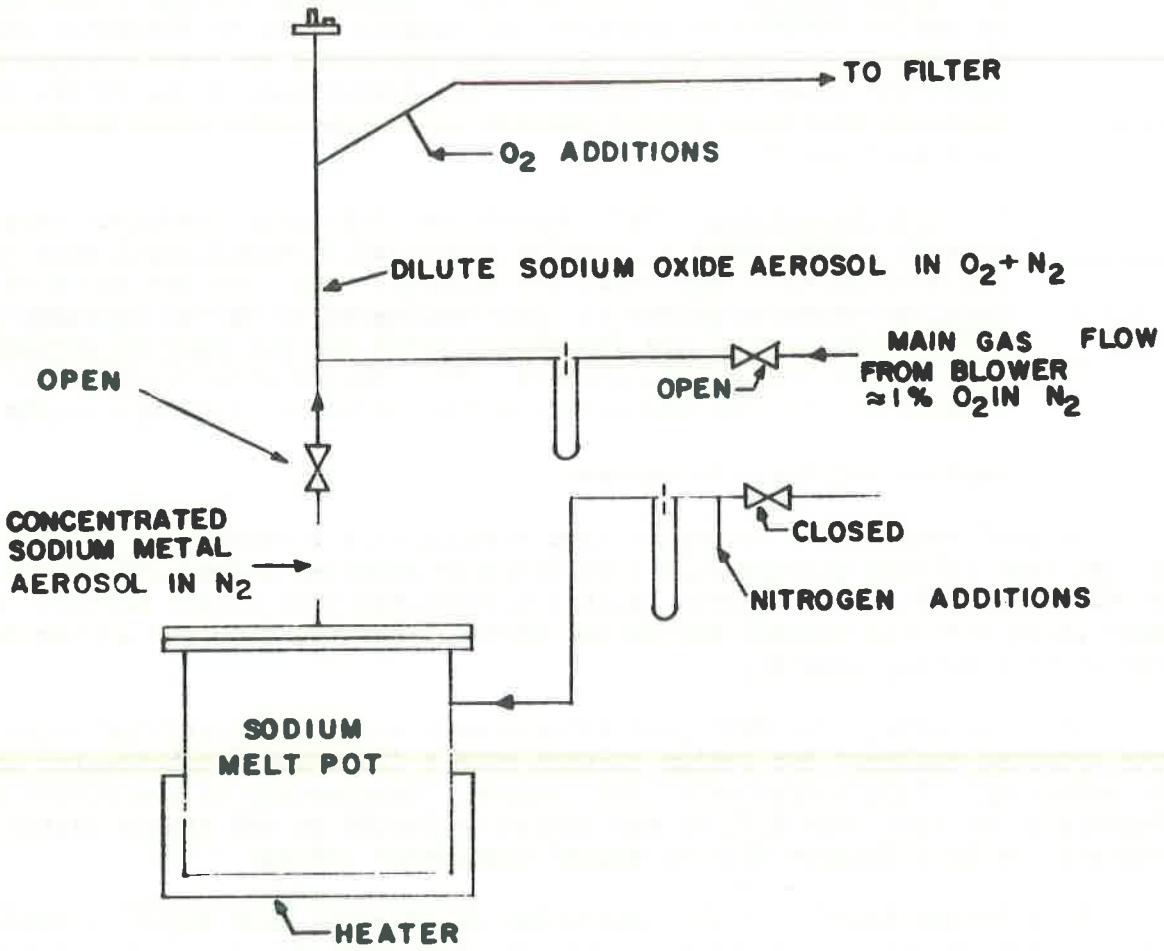

FIGURE 2. ARRANGEMENT OF APPARATUS FOR GENERATING A SODIUM OXIDE AEROSOL.

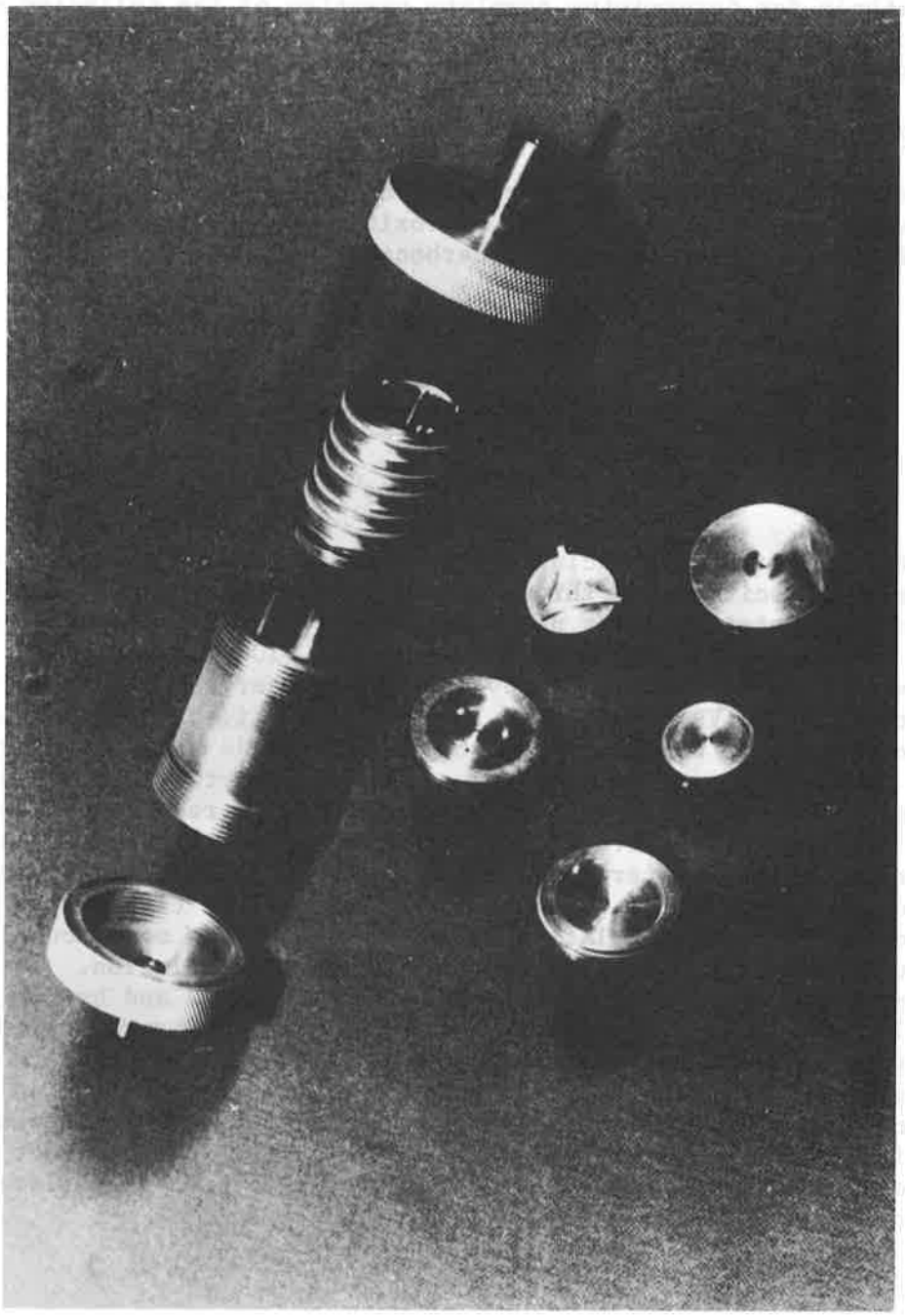

FIGURE 3. MERCER IMPACTOR DISASSEMBLED.

D. Reaction of Sodium Stored in Filters and on Walls of Apparatus

Prior to opening the filter packs used for the collection of aerosols of sodium metal (liquid or solid), sodium oxide, and sodium peroxide, the deposited material was converted to a stable monovalent salt, such as carbonate, to eliminate fire and explosion hazards. A description of the following techniques for reacting elemental sodium (Procedure A) or the oxide and peroxide (Procedure B) includes methods for determining complete reaction of the collected material prior to opening the filter pack. These procedures also include measurements used to assess control of the reactions involved.

Procedure A

This method is based on (a) the reaction of sodium (as liquid or solid) with water vapor to form sodium hydroxide, and (b) the reaction of hydroxide with carbon dioxide to form carbonate.

$$2Na + 2H_2O = 2NaOH + H_2$$

$$2NaOH + CO_2 = Na_2CO_3 + H_2O$$

$$2Na + H_2O + CO_2 = Na_2CO_3 + H_2$$

The arrangement for producing these reactions is shown in Figure 4 (line A). Nitrogen is recirculated through the filter pack by means of a blower. The system is maintained under positive pressure by a continuous nitrogen feed and a system bleed. The main nitrogen line (10-15 liters/min, line A) is saturated at room temperature by passing it over water in a series of three 20-liter flasks (VP of water at 73° F = 23 mm; i.e., 3% H_2O vapor by volume). Carbon dioxide is added to this stream to provide a 2% concentration by volume. At intervals, a part of the stream is directed into a flask containing air and the probe of a hydrogen gas detector. A response on the meter indicates generation of hydrogen and incomplete conversion of sodium to hydroxide or carbonate. After the reaction is completed, no hydrogen will be detected. Because of the large volume of the filter test system and the high rate of recirculation relative to the system bleed, occasionally the system is flushed of all residual nitrogen without recirculation. This is done by closing the system between nitrogen feed and bleed, and by purging the recirculation blower and increasing the nitrogen feed rate. After a negligible hydrogen reading is obtained, the gas is again recirculated to permit hydrogen concentration buildup to disclose if unreacted sodium is still present. When no additional hydrogen is detected by this technique, the reactions are assumed to be complete. This has proven correct in all instances. Measurements are made continuously to assure complete absence of oxygen from the system during this procedure.

Procedure B

When oxygen is present during production of sodium aerosols, oxide formation occurs. Some peroxide is produced also when oxygen is in excess of sodium fume concentrations. Decomposition of peroxide is essential, particularly when organic filter media or organic binders are used. Experiments have shown that carbon dioxide in air or nitrogen will decompose sodium peroxide according to the following reactions:

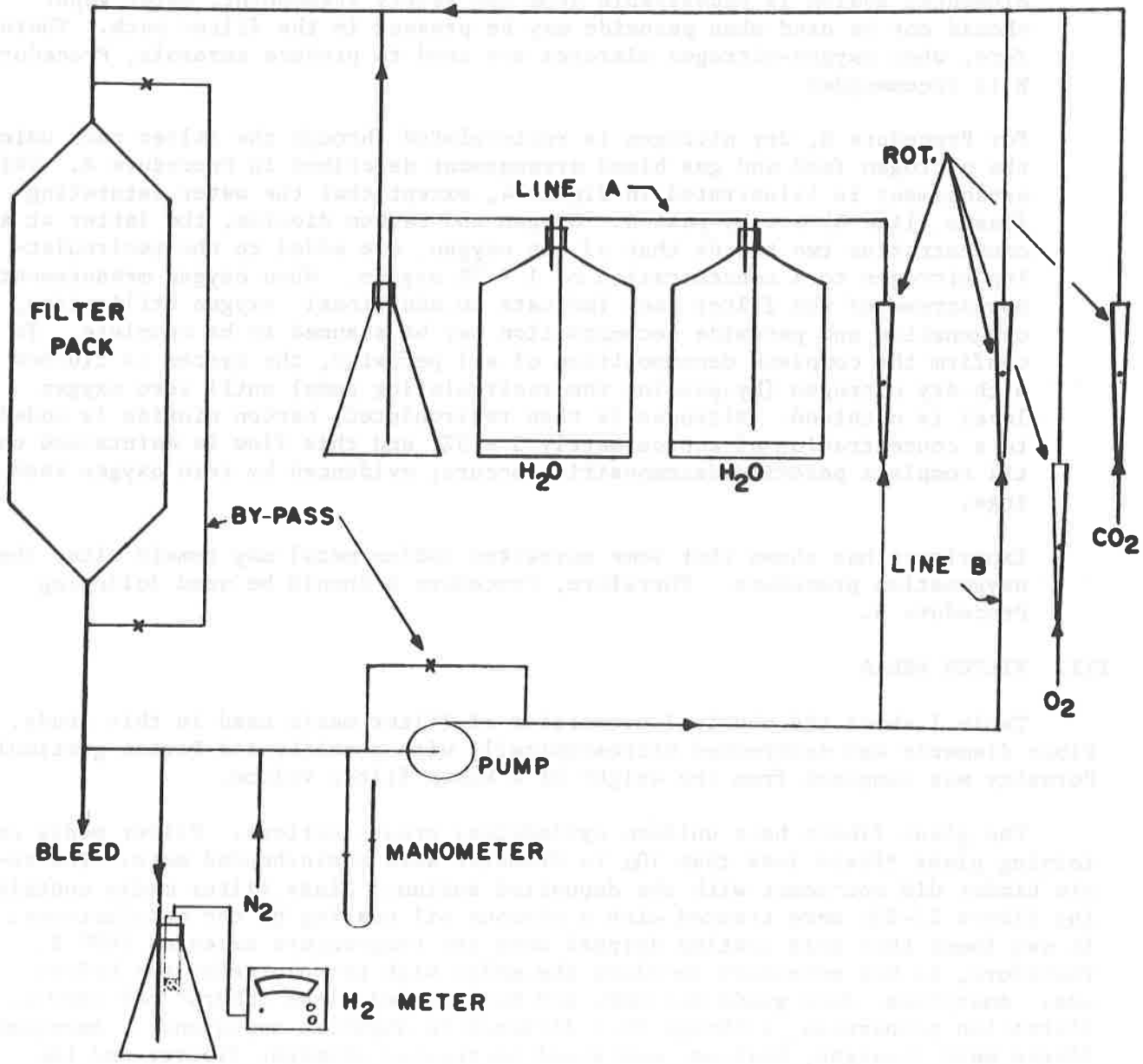

FIGURE 4. APPARATUS FOR REACTING SODIUM IN FILTER.

$$Na_2O_2 + CO_2 = Na_2CO_3 + 1/2\ O_2$$

In addition, water vapor will decompose sodium peroxide according to the following reactions:

$$Na_2O_2 + H_2O = 2NaOH + 1/2\ O_2$$

$$Na_2O_2 + H_2O = Na_2O + H_2O_2$$

As noted previously, when unreacted sodium is present, water vapor will produce hydrogen. As the presence of both O_2 and H_2 in a system containing elemental sodium is undesirable from the safety standpoint, water vapor should not be used when peroxide may be present in the filter pack. Therefore, when oxygen-nitrogen mixtures are used to produce aerosols, Procedure B is recommended.

For Procedure B, dry nitrogen is recirculated through the filter pack using the nitrogen feed and gas bleed arrangement described in Procedure A. This arrangement is illustrated in Figure 4, except that the water saturating flasks (line B) are by-passed. Oxygen and carbon dioxide, the latter at a concentration two thirds that of the oxygen, are added to the recirculating nitrogen to a concentration of 1 - 3% oxygen. When oxygen measurements downstream of the filter pack indicate no additional oxygen utilization, oxygenation and peroxide decomposition may be assumed to be complete. To confirm the complete decomposition of all peroxide, the system is flushed with dry nitrogen (by-passing the recirculating pump) until zero oxygen level is obtained. Nitrogen is then recirculated, carbon dioxide is added to a concentration of approximately 3 - 5%, and this flow is maintained until complete peroxide decomposition occurs; evidenced by zero oxygen readings.

Experience has shown that some unreacted sodium metal may remain after the oxygenation procedure. Therefore, Procedure A should be used following Procedure B.

III. FILTER MEDIA

Table 1 shows the physical properties of filter media used in this study. Fiber diameter was determined microscopically with a calibrated Porton graticule. Porosity was computed from the weight of a known filter volume.

The glass fibers have uniform cylindrical cross-sections. Filter media containing glass fibers less than 10μ in diameter were resin-bonded mats. The resin binder did not react with the deposited sodium. Glass filter media containing fibers 25-35μ were treated with a viscous oil coating by the manufacturer. It was found that this coating dripped when the temperature exceeded 200° F. Therefore, it was necessary to clean the media with trichloroethylene before use. Amerglass, fine grade Roll-mat, and K115 curled glass fibers[3] had similar filtration properties, although they differed in physical appearance. Amerglass fibers were straight; Roll-mat contained corrugated straight fibers; and the K115 filters were composed of curled fibers. Amerglass and fine grade Roll-mat were supplied in blanket form; whereas K115, a bulk fiber, had to be hand packed.

Steel wool media of all grades have fibers of polygonal cross-section, usually triangular,[4] and a wide range of fiber sizes. Manufacturers' standards

TABLE 1

Filter Media

Medium	Average Fiber Diameter (μ)	Fiber Diameter Range (μ)	Bulk Density (lbs/ft3)	Porosity (% voids)	Supplier
Stainless mesh	1000	115-1000	15 - 30	94 - 98	Volks Limited
#3 Steel wool	95	40- 200	2 - 8	98.4-99.7	American Steel Wool Mfg. Co.
Rollmat, Coarse fiber	85	20- 250	0.5-2.0	98.7-99.6	American Air Filter Corp.
Stainless Wool, Coarse	76	30- 130	2 - 8	98.4-99.7	American Steel Wool Mfg. Co.
Stainless, Wool, Medium	62	20- 90	2 - 8	98.4-99.7	American Steel Wool Mfg. Co.
Dynel (24 Denier)	49		0.9	98.8	Union Carbide Corp.
#2 Steel Wool	47	23- 91	2 - 8	98.4-99.7	American Steel Wool Mfg. Co.
U-Trim-It	40		2.2	98.6	Owens Corning Corp.
Amerglass	32		.25-7.0	98.5-99.8	Owens Corning Corp.
Rollmat, fine fiber	28	16- 65	.4 -2.0	98.5-99.7	American Air Filter Corp.
K115, curled glass	27	23- 32	1.5-6.0	96 -99	Owens Corning Corp.
#1 Steel Wool	26	16- 65	2-8	98.4-99.7	American Steel Wool Mfg. Co.
PF334	7	2- 14	.5-2.0	98.5-99.6	Owens Corning Corp.
PF018	7		.46	99.7	Owens Corning Corp.
FM011	2.5		.43	99.7	Owens Corning Corp.
MSA, type B	2.5	1.2- 10	10	93.5	Mine Safety Appliance Corp.
AAF 50	1.5		.45	99.7	American Air Filter Corp.
FM 004	1.5		.47	99.7	Owens Corning Corp.
PF105	1.2		.31	99.8	Owens Corning Corp.
Absolute filter paper 1106B	<1				Mine Safety Appliance Corp.
Pleated absolute filter	<1				Flanders Filter, Inc.

for both stainless and standard steel wool are contained in Federal Specification FF-S-740A.

Stainless corrugated steel mesh was made from threads containing 12 strands of 0.004-inch-diameter wire. It was supplied in the form of a flattened corrugated tube 6 inches wide. For our experiments, it was used in the form of flat sheets or as a pad in which the mesh was formed into 3-inch strips and spiral-wound to 12-inch diameter.

Dynel, a synthetic organic material, was used for NaK studies conducted several years ago[5], but although used for some early tests, it was considered unsafe in contact with peroxide and molten sodium and was discarded. In addition, it was thought that the maximum recommended operating temperature, 250° F, was unsuitable. Similar considerations led to the rejection of all organic filter media.

IV. RESULTS

A. Solid Aerosol (<200° F), Oxygen Free

The particle size-retention characteristics of clean filter media are dependent on fiber size and packing density. The finer the fiber and greater the packing density, the better the retention of small particles. As the filter becomes loaded, its collection efficiency increases and finally cake filtration begins.

In one test, clean stainless steel mesh (1000μ diameter) filters had negligible resistance to flow and collected 16% of the fume (Table 3), with a resistance rise of 0.12 i.w.g. However, the same medium collected 53% of the aerosol in Test 55 (Table 4) with a resistance rise of 15.4 i.w.g. In the latter test high resistance cake filtration occurred.

At first, the steel mesh composed of 50 - 200μ fibers was a poor filter (i.e., less than 5% efficiency), but as the fibers became coated with sodium fume, the efficiency increased until it reached 80% with cake filtration.

Clean filters composed of 30 μ diameter fibers packed 3 lbs/cu.ft. to a depth of 6 inches have been shown to collect 50% of particles with 0.7 μ mass media diameter (MMD) and a superficial face velocity of 10 fpm.[3] Using these materials in deep beds, it was found that overall collection efficiencies of greater than 90% could be obtained for a combination of filter and cake filtration.

Filters containing <10 μ diameter fibers collected 90% of particles greater than 0.5 μ MMD. Fume was stored largely on the surface and high resistance cake filtration resulted in collection of only 0.01-0.03 pounds of sodium per square foot of filter area for a 20 i.w.g. resistance rise.

Resistance increases of individual layers composing the filter pack are plotted in Figures 5-8 with increasing filtration time and total sodium collected. The distribution of sodium in the filter packs for these tests is shown in Tables 2 - 5.

In Test 49, both Amerglass (1.0 lb/ft^3) and K115 (1.5 lb/ft^3) fibers collected over 40% by weight of the aerosol particles (Table 2). However, each medium did its major collecting at a different time during the test. This may

TABLE 2

Fume Deposition Within Filter Bed, Test 49.

Media Composition	Packing Density lbs/ft^3	Thickness (in.)	Face Velocity (fpm)	Pressure in i.w.g. initial	final	Δ P	Total Fume Deposited (lbs/ft^2 face area	C_R *
Amerglass	1.0	1.5	42.8	.05	9.75	9.7	0.088	
K115	1.5	3	42.8	.08	4.0	3.9	0.077	
K115	3.0	3	42.8	.20	.70	.50	0.014	
PF334	2.0	3	42.8	1.0	1.70	.70	0.013	
Absolute	Pleated	6.0	42.	.16	.20	.04	- -	
Total				1.5	16.3	14.8	0.192	1.8

Filter inlet temp. Range °F 140 - 200

Sodium Pot temp °F 980
MMD = 1.60 μ σ_g = 2.4

* C_R = i.w.g. resistance/lbs fume per sq. ft. of filter surface/ft. per min. filtering velocity. Based on 42.8 fpm, 14.8 i.w.g. ΔP, 0.192 lbs fume.

TABLE 3

Fume Deposition Within Filter Bed, Test 51.

Media Composition	Packing Density lbs/ft^3	thickness (in)	Face Velocity (fpm)	Pressure (i.w.g.) Initial	Final	ΔP	Total fume Deposited (lbs/ft^2 face area)	C_R*
Flat Stainless Mesh	--	1.0	13.5	.05	.12	.12	0.041	
Amerglass	.5	1.5	13.5	.05	13.2	13.2	0.105	
Amerglass	1.0	1.5	13.5	.05	3.2	3.2	0.058	
K115	1.5	3.0	13.5	.05	.16	.16	0.040	
K115	3.0	3.0	13.5	.10	.19	.09	0.013	
Absolute	Pleated	6.0	42.0	.17	. .32	.15	--	
Total			13.5	.30	17.2	16.9	0.257	4.8

Filter Inlet Temp Range °F 165 - 195
Sodium Pot Temp. °F 1070
MMP = 2.07 σ_g = 1.90

* C_R = i.w.g. resistance/lbs fume per sq. ft. of filter surface/ft per min. filtering velocity. Based on 13.5 fpm, 16.9 i.w.g. ΔP, 0.257 lbs. fume.

TABLE 4

Fume Deposition Within Filter Bed, Test 55

Filter Composition	Media Packing Density lbs/ft^3	Thickness (in.)	Face Velocity (fpm)	Pressure in i.w.g. initial	final	Δ P	Total Fume Deposited (lbs/ft^2 face	C_R * area
Flat Stainless	30	1	13.5	< .05	15.4	15.4	0.254	
#3 Steel wool	3.5	1.5	13.5	< .05	0.1	.1	0.063	
#3 Steel wool	5.0	1.5	13.5	< .05	1.5	1.5	0.046	
#2 Steel wool	5.0	1.5	13.5	< .05	0.25	.2	0.067	
K115	1.5	1.5	13.5	.06	2.60	2.5	0.028	
K115	3.0	1.5	13.5	.05	0.25	.2	0.021	
Absolute	pleated	6	42	.19	0.7	.5	--	
Total				.35	20.8	20.4	0.478.	3.2

MMD = 1.92 μ; σ_g = 2.35

Filter inlet temp °F 160 - 190

Sodium pot temp °F 990

* C_R = i.w.g. resistance/lbs. fume per sq. ft. of filter surface/ft. per min. filtering velocity
Based on 13.5 fpm., 20.4 i.w.g. ΔP, o.478 lbs. fume

Test 58

Table 5 Fume Deposition Within Filter Bed

Filter Composition	Packing Density #/ft³	Thickness (in)	58 a – Velocity (fpm)	Pressure in i.w.g. initial	final	ΔP	Total Deposited lbs/ft² face area	58 b – Velocity (fpm)	Pressure in i.w.g. initial	Final	Δ P	Fume Deposited #/ft2	58 c – after pulse – Velocity (fpm)	Pressure in i.w.g. initial	final	ΔP	Total Fume Deposited lbs/ft² face area
Coiled Stainless Steel Mesh	29	3	13.5	<0.05	0.13	0.13	0.123	6.7	0.09	12.83	12.74	0.354	6.7	10.30	18.00	7.70	0.363
Flat Stainless Mesh	29	1	13.5					6.7					6.7				0.057
#3 Steel Wool	4.5	3	13.5	<0.05	0.35	0.35	0.075	6.7	0.17	0.17	0.23	0.080	6.7	0.23	0.23	0.0	0.080
Coarse Stainless Steel Wool	4.8	3	13.5	<0.05	2.38	2.38	0.080	6.7	1.15	1.15	0.00	0.087	6.7	1.15	1.15	0.01	0.087
#2 Steel Wool	4.5	1.5	13.5	<0.05	0.11	0.11	0.035	6.7	0.05	0.06	0.01	0.035	6.7	0.06	0.06	0.0	0.035
K115	1.5	1.5	13.5	0.09	15.80	15.70	0.066	6.7	4.99	4.57	-.42	0.066	6.7	0.39	0.39	0.0	0.066
K115	3.0	1.5	13.5	0.05	0.56	0.51	0.025	6.7	0.23	0.30	0.07	0.025	6.7	0.14	0.14	0.0	0.025
Absolute	Pleated	6	42	0.16	0.59	0.43	--	21.0	0.30	0.27	0.03	--	21.0	0.25	0.26	0.01	--
Total			13.5	0.31	19.92	19.61	0.403	6.7	6.98	19.41	12.43	0.655		12.52	20.22	7.70	0.72

MMD = 1.57 μ σ = 2.85

Filter inlet temperature = 195°F
Sodium pot temperature = 1000°F

58 a, C_R = 3.6 Based on 13.5 fpm., 19.6 i.w.g. ΔP, 0.403 lbs. fume
58 b 7.3 " " 6.7 fpm., 12.4 i.w.g. ΔP, 0.252 lbs. fume
58 c 17.7 " " 6.7 fpm., 7.7 i.w.g. ΔP, 0.066 lbs. fume

be seen in Figure 5. First, K115 (1.5 lb/ft^3) was a high retention layer for about 50 minutes; then the Amerglass layer became the major fume retention layer and it increased in resistance from 2 to 9.7 i.w.g. in 20 minutes. After 55 minutes and until the end of the test (70 minutes), Amerglass was removing particles principally by cake filtration. This is indicated by a rapid increase in the resistance of this layer and a reduction in the rate of resistance increase of the K115 (1.5 lb/ft^3) during the same time period. The existence of cake filtration was confirmed by a layer of sodium carbonate observed on the surface of the fibers when they were removed from the filter holder.

Test 51 (Figure 6) indicates cake filtration more clearly when, after 70 minutes, the resistance of the 1.0 lb/ft^3 Amerglass remained steady, while the resistance of the 0.5 lb/ft^3 Amerglass, ahead of it in the filter pack, increased rapidly. Gas flow was stopped after 80 minutes and then restarted. During the last 25 minutes of test, the increase in resistance of the 1.0 lb/ft^3 Amerglass was caused by leakage past the 0.5 lb/ft^3 Amerglass when its support screen ruptured slightly.

Most of the fume was retained by the 1.0 lb/ft^3 Amerglass in Test 49 and by the 0.5 lb/ft^3 Amerglass in Test 51 (Tables 2 and 3). The medium collecting the most fume during Test 55 (Table 4) was the stainless mesh, the first layer. It collected 0.25 lbs. per ft^2 of face area.

Figure 7 helps to explain the way fume collection occurred. First, fume penetrated to the absolute filter. Then after 40 minutes, the efficiency of the K115 (1.5 lb/ft^3) fiber bed had increased sufficiently to protect the absolute filter. After 100 minutes the #3 grade steel wool (5 lb/ft^3) increased in efficiency sufficiently so that no further resistance increases occurred in the K115 medium. After 160 minutes the stainless steel layer accumulated enough fume to become a good filter and from 180 minutes to termination of the test, it collected 99% of the sodium (determined by interstage sampling) and increased to a final resistance of 15.4 i.w.g. This kind of data analysis shows where and when major resistance increases occur and is of assistance in selecting filter components to give maximum fume storage with minimum resistance rise.

A number of methods were investigated to increase the storage capacity of a filter pack. The first method was to decrease filtration velocity after operating it at test velocity until it reached 20 i.w.g. A second method was to move the bed by stopping and restarting flow (Test 58). In Test 58 (Table 4 and Figure 8) approach velocity was reduced to one half after a resistance rise of 20 i.w.g. This resulted in a 62% increase in the holding capacity of the bed. Figure 8 indicates that for the K115 layer the decrease in resistance was greater than 50%. After 20 i.w.g. filter resistance was reached at the reduced flow, gas flow and fume generation were stopped for one minute and then resumed. This produced a movement of the filter layers and disturbed the filter cakes, resulting in a resistance reduction across the 1.5 lb/ft^3 K115 layer from 4.5 to 3.0 i.w.g. This mode of operation permitted an 18% increase in fume storage capacity. A second pulse, produced in a similar manner, resulted in only 3% filter life extension. From these experiments it may be concluded that (a) reductions in velocity and (b) disturbances to the filter cake may be used to extend filter life.

Figure 9 (Test 58) shows a photo of reacted sodium deposited on coiled and flat stainless mesh media. It was noted that there is a cake on the coiled filter, while the flat medium has deposition within the filter.

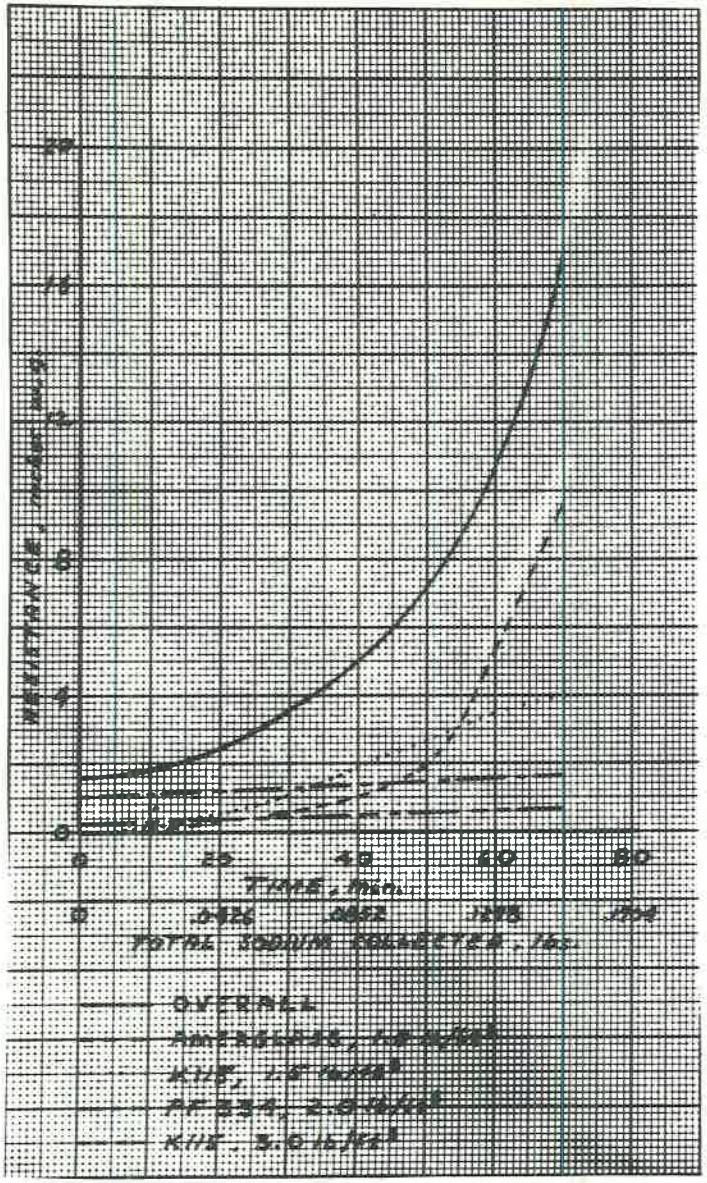

FIGURE 5. TEST 49, RESISTANCE OF FILTER BED DURING LOADING WITH SOLID SODIUM AT 42.8 F.P.M. FACE VELOCITY.

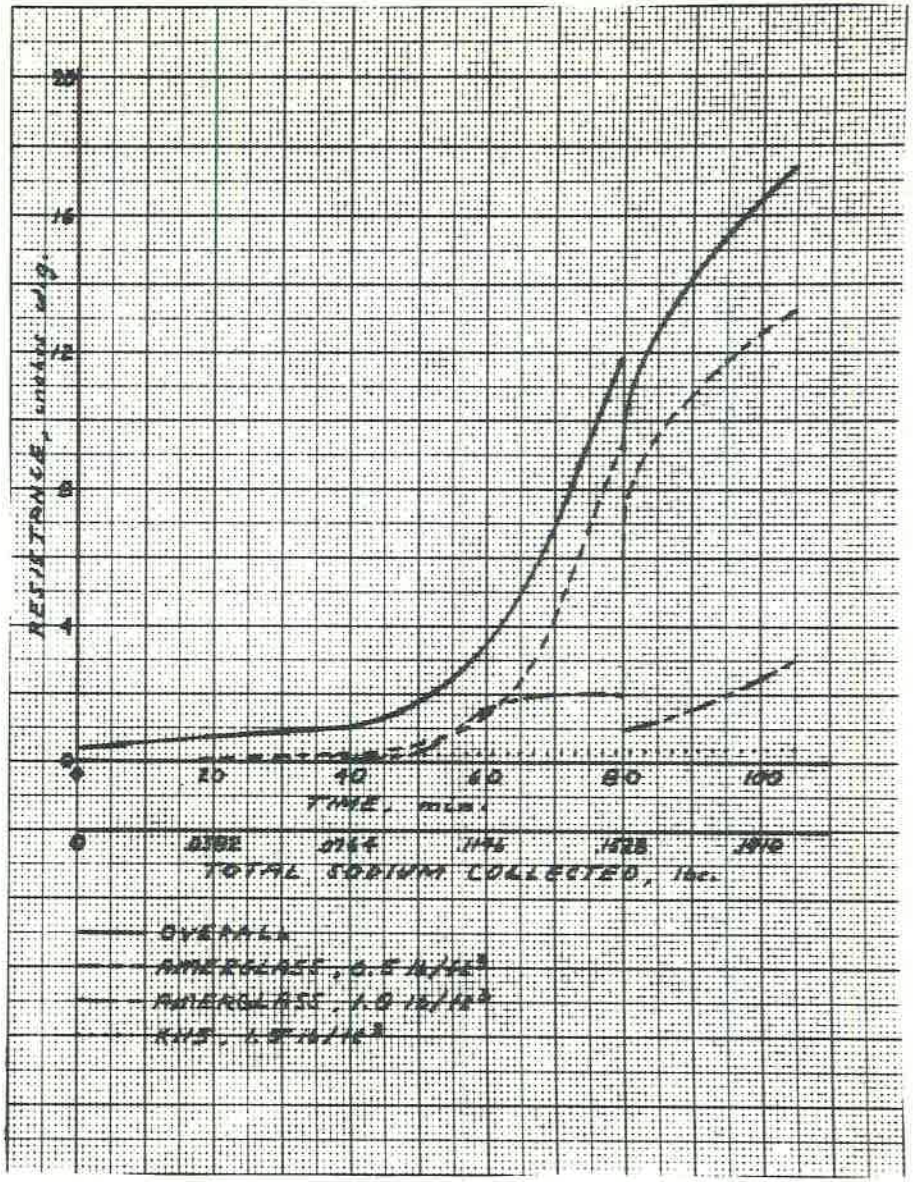

FIGURE 6. TEST 51, RESISTANCE OF FILTER DURING LOADING WITH SOLID SODIUM AT 13.5 F.P.M. FACE VELOCITY.

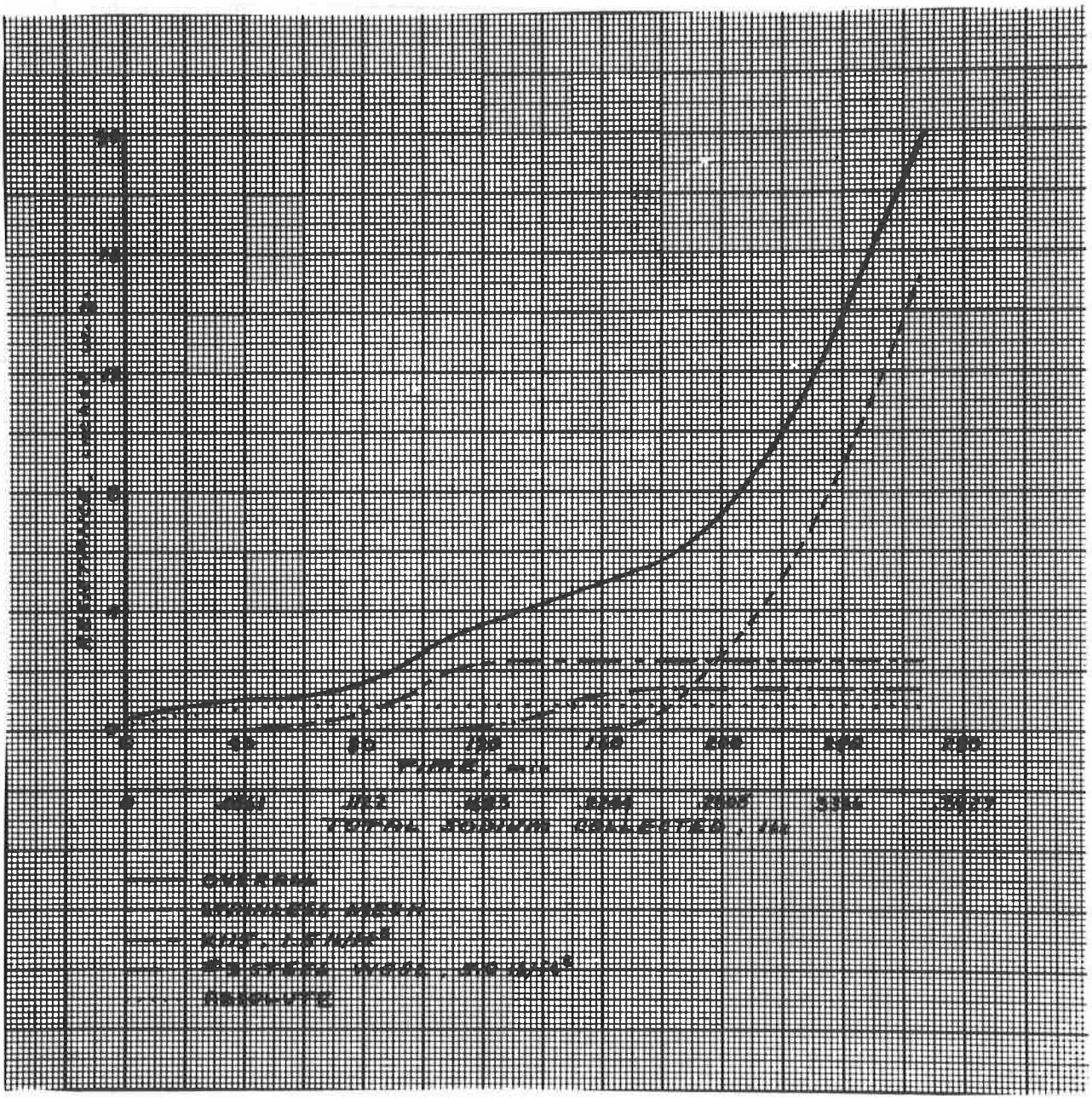

FIGURE 7. TEST 55, RESISTANCE OF FILTER BED DURING LOADING WITH SOLID SODIUM FUME AT 13.5 F.P.M. FACE VELOCITY.

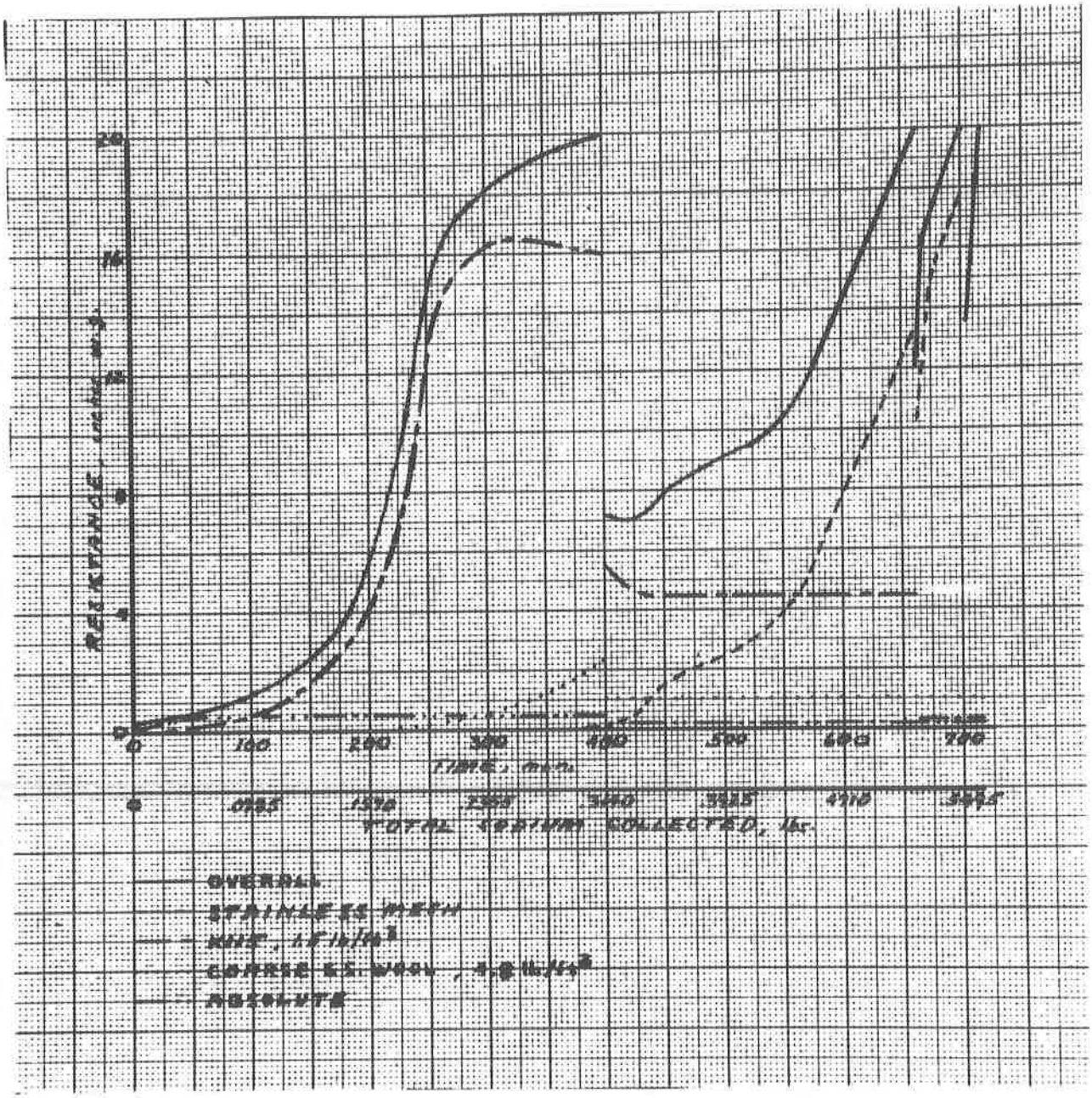

FIGURE 8. TEST 58, RESISTANCE OF FILTER BED DURING LOADING WITH SOLID SODIUM FUME AT 13.5 AND 6.7 F.P.M. FACE VELOCITIES.

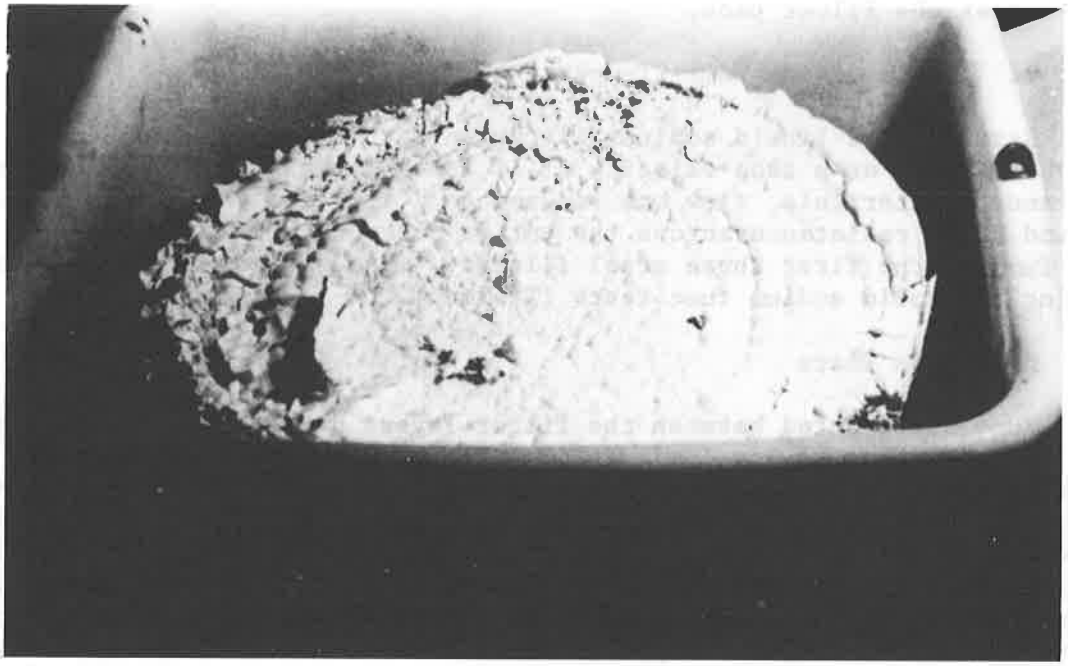

COILED MESH, 3" DEPTH

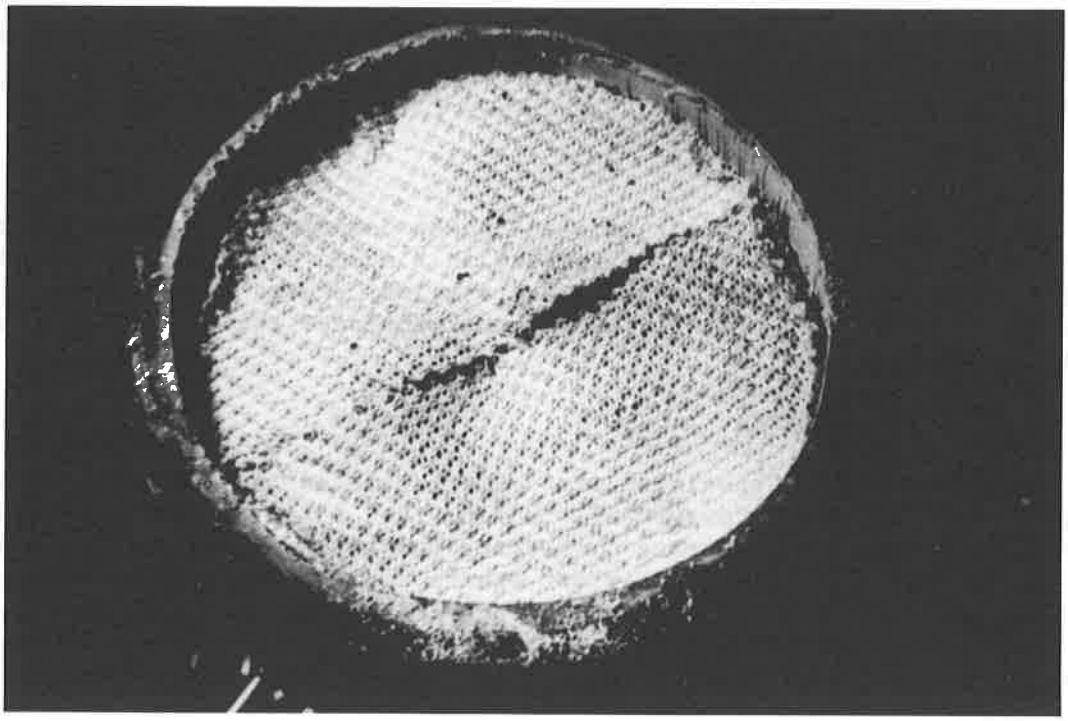

FLAT MESH, 1" DEPTH

FIGURE 9. STAINLESS MESH FILTERS, TEST 58.

The resistance coefficient C_R (inches water resistance per lb. fume collected per sq. ft. of filter surface per fpm velocity) combines basic filter parameters to determine overall filter pack merit. The smaller the C_R number, the better the filter pack.

B. Liquid Sodium Fume (Temperature >210° F)

Results of a liquid sodium filtration test are shown in Table 6. The filter was tested at a face velocity of 14 fpm and was operated to 20 i.w.g. resistance. After this, flow was reduced to 7 fpm face velocity and testing continued until resistance across the entire pack reached 16 i.w.g. with most of the fume on the first three steel filters. This was similar to what occurred during the solid sodium fume tests (Table 5).

C. Oxide Tests

Fume distributed between the filter layers during this test as shown in Table 7. Because of low loadings during the latter part of the test, it was necessary to continue this test over a 3-day period to reach a resistance of 20 i.w.g. Filtration was halted at 75 and 405 minutes (Figure 10). The absolute filter resistance increased during the first 25 minutes to 2 i.w.g. During the first 75 minutes, when the fume loading was high, the majority of the fume deposited in the first two layers (stainless mesh and #3 steel wool), which collected, respectively, 34.4% and 37.9% of the sodium. The large percentage collected within the #3 steel wool indicates that the MMD of the particles was smaller than in Test 58 or that sodium oxide particles penetrate coarse fibers more easily, possibly because of density and shape factor differences.

Reduction of gas flow from 12.8 fpm to 6.4 fpm and stopping and starting flow produced only an 13.7% increase in total loading when resistance was allowed to rise to 20 i.w.g.

D. Iodide Tests

Analyses of iodine vapor samples[2] taken downstream of the absolute filter indicated less than 0.002 μg of iodides in 2 cubic feet of gas. Particulate iodine, analysed on upstream Millipore samples, showed background iodine levels (0.002 μg) indicating that iodine did not penetrate the filter pack as vapor or particulates.

E. Wall Deposition

Results of wall deposition tests are tabulated in Table 8. Aerosols were oxygen-free except for test 60-62. During test 63-64 the sodium particles were maintained in the liquid state by keeping temperature above 210° F. The greatest deposition (pounds deposited per square foot of wall surface per pound of sodium generated) occurred when oxide particles were present. Liquid and solid sodium particles deposited at about the same rate (Table 8). The deposition rate increased with velocity.

F. Aerosol Size Characteristics

The particle MMD varied from 1.0 to 2.6 microns with a geometric standard deviation (σ_g) of 1.9 to 4.5. There appeared to be no correlation of aerosol

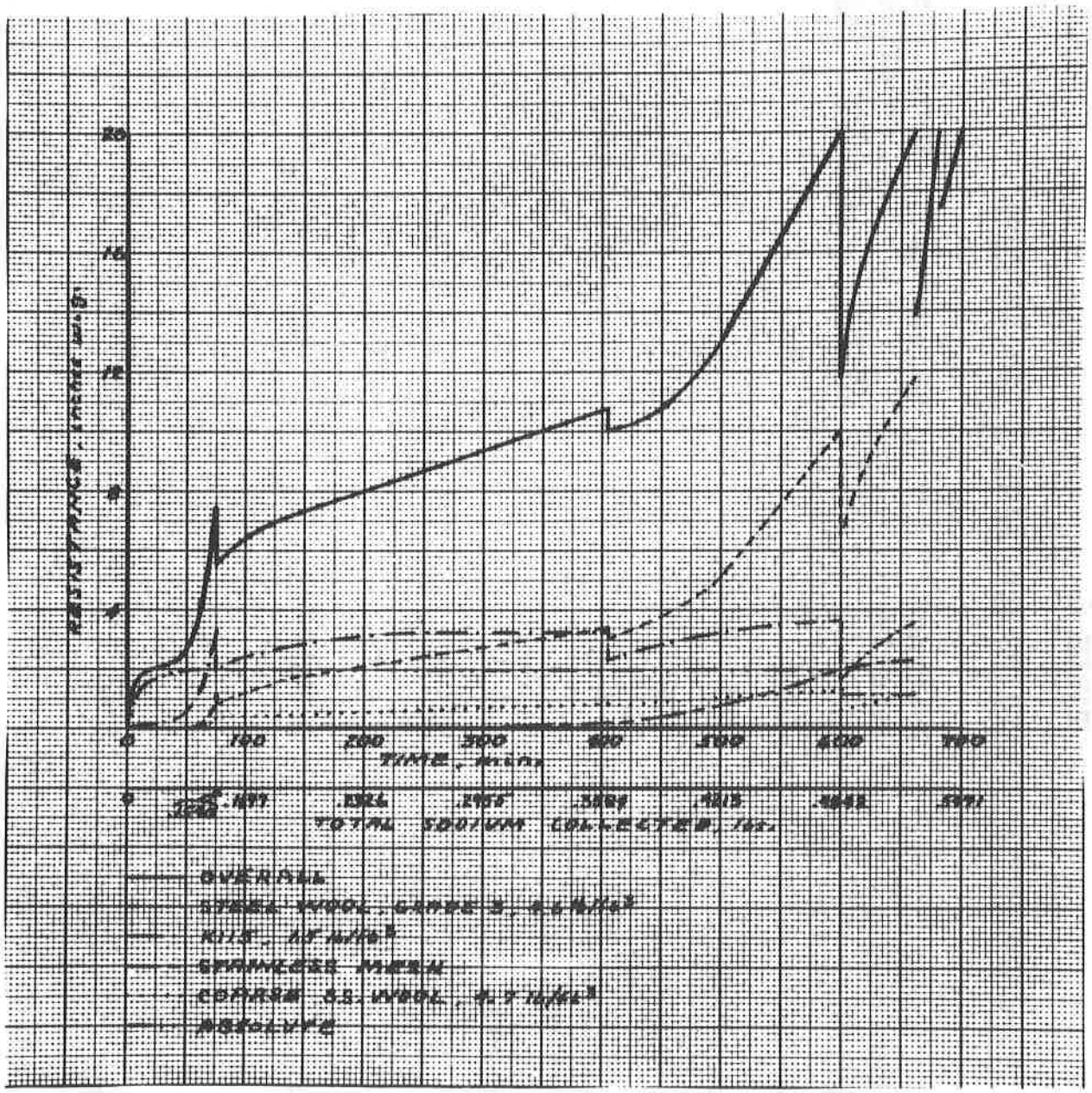

FIGURE 10 RESISTANCE BUILD UP, SODIUM OXIDE FUME.

TABLE 6

Fume Deposition Within Bed Liquid Sodium Fume

Filter Composition	Packing Density (lbs/ft^3)	Thickness (in.)	Total Fume Deposited (lbs/ft^2 face area)
Stainless mesh coil	29	3.0	0.550
Stainless mesh flat	29	1.0	0.387
#3 Steel wool	4.5	3.0	0.196
Coarse stainless steel wool	4.8	3.0	0.055
#2 Steel wool	4.6	1.5	0.038
K115	1.5	1.5	0.060
K115	3.0	1.5	0.009
Absolute	pleated		----
			1.295

Fume MMD = 1.42 μ; σ_g = 2.45

Filter inlet temp. = 200 - 230°F.

Melt pot temp. = 1115°F.

TABLE 7

Oxide Fume Deposition Within Filter Bed

Test 60 - 62

Composition	Filter Packing Density (lbs/ft³)	Thickness (in.)	Filtration Velocity (fpm)	Pressure, (i.w.g.) Initial	Final	ΔP	Fume Deposited (lbs/face area)	C_R	Velocity (fpm)	Initial	Final	ΔP	Cumulative fume deposited (lbs/face area)	C_R
Coiled Stainless Mesh	29	3.0	12.8	<.05	2.0	2.0	0.197		6.4	1.75	3.75	2.0	0.148	
Flat Stainless Mesh	29	1.0	12.8						6.4				0.092	
#3 Steel Wool	4.6	3.0	12.8	<.05	10.1	10.1	0.234		6.4	8.60	11.1	2.5	0.266	
Steel Wool, Coarse	4.8	3.0	12.8	<.05	1.4	1.4	0.065		6.4	.60	1.30	.7	0.074	
#2 Steel Wool	4.9	1.5	12.8	.06	.73	.67	0.040		6.4	.37	.41	.04	0.040	
K115	1.5	1.5	12.8	.09	3.74	3.65	0.051		6.4	2.07	2.13	.06	0.0514	
K115	3.0	1.5	12.8	<.05	.14	.14	0.027		6.4	.08	.08	___	0.027	
Absolute	pleated	6.0	40	.45	2.22	1.77	-----		20	1.25	1.90	.64	___	
Total				0.6	20.2	19.7	0.614	2.5	6.4	14.7	20.7	6.0	0.698	11.1*

Filter Inlet Temperature 130 °F

Sodium Pot Temperature 1050 °F

* Based on 6.4 fpm, .084 lb/ft² fume, 6.0 i.w.g. ΔP

TABLE 8

Wall Deposition - Sodium Fume

Test No.	Location	Local Vel. (fpm)	Local Temp (°F)	Exposure Time (min.)	Collection Area (Sq. in.)	Total Na Collected (mg)	Deposition Rate (lb/min/ft²)	Deposition Rate (lb/ft²/lb generated)
47	12" Pipe	42.8	130/215	180	4	2.12	9.3×10^{-7}	17.5×10^{-4}
	Cone	125	"	180	4	1.20	5.3×10^{-7}	9.9×10^{-4}
48/49	12" Pipe	42.8	140/200	88	4	2.0	18.1×10^{-7}	23.9×10^{-4}
	cone	125	"	88	4	0.7	6.3×10^{-7}	8.3×10^{-4}
51	12" Pipe	13.5	165/200	105	3.75	11.2	90.2×10^{-7}	46.8×10^{-4}
	cone	39.5	"	105	3.75	0.7	5.6×10^{-7}	2.9×10^{-4}
52	Cone	39.5	140/210	100	3.75	3.50	29.6×10^{-7}	12.9×10^{-4}
	12" pipe	13.5	"	100	3.75	3.61	30.5×10^{-7}	13.2×10^{-4}
53/54	Cone	39.5	140/190	160	3.75	1.96	10.4×10^{-7}	9.6×10^{-4}
	12" pipe	13.5	"	160	3.75	2.09	11.1×10^{-7}	10.0×10^{-4}
58	Cone	39.5/19.5	195	709	4.30	7.56	7.8×10^{-7}	9.9×10^{-4}
	2" pipe	485/242	195	709	5.95	79.5	59.8×10^{-7}	75.3×10^{-4}
60/61	Cone	39.5/19.5	110/140	695	5.95	16.3	12.5×10^{-7}	15.9×10^{-4}
62	2" pipe	485/242	110/140	695	5.95	25.4	194×10^{-7}	24.7×10^{-4}
63/64	2" pipe	485/242	200/260	675	5.95	179	166×10^{-7}	93.7×10^{-4}

TABLE 9

Impactor Size Data

Test No.	Melt Temp.	MMD (μ)	Geometric Std. Dev.
14	1080	1.30	2.45
15	1080	1.16	2.09
16	1060	1.20	1.90
17	1080	1.65	2.75
18	1060	1.45	1.80
19	1060	1.26	2.05
21	1070	1.28	3.60
22	980	1.40	4.40
23	1010	1.34	3.80
25	840	1.27	4.10
26	735	1.15	3.77
27	885	1.27	3.37
28	825	1.20	3.16
29	725	1.20	3.25
30	700	1.17	4.50
33	995	1.00	2.7
34	1045	1.20	2.08
35	1075	1.65	2.10
37	875	1.35	3.50
38	900	1.20	2.50
42	800	1.59	2.70
43	880	1.40	2.30
44	870	1.10	2.80
47	985	1.80	3.16
49	980	1.40	2.60
50	990	1.87	1.90
51	1060	2.07	1.90
52	1060	1.82	2.13
53	850	1.42	4.40
54	995	2.50	3.00
55	990	1.92	2.35
56	1000	2.60	3.00
58	1000	1.57	2.85
59	1075	1.44	2.03
63/4	1115	1.42	2.45

size with melt pot temperature, state of the aerosol (liquid or solid), or gas flow rate. A large geometric standard deviation indicates very wide size distribution. Tests 21 through 38 were performed using a single gas pass through the system and venting the aerosol. All other data are the result of samples taken during filter tests. Tests 59 and 63/4 were with liquid sodium; all others were solid. These data are presented in Table 9.

V. CONCLUSIONS

A deep bed filter pack constructed of 2-inch-deep layers of 1000, 500, 250, 125 and 60 μ diameter stainless steel fibers packed 4-5 lbs/ft^3, plus two 2-inch layers of 30 and 15 μ glass fibers 15 lbs/ft^3, plus a pleated absolute filter, can collect and store 0.75 lbs. of sodium and sodium oxide fume per square fott of filter face area. Filter resistance reached 20 i.w.g. when operated at 10 fpm face velocity. Reductions in filter face velocity extend filter life and provide low resistance with high fume storage capacity. The efficiency of these filter packs is >99% for all particles.

REFERENCES

1. T. T. Mercer, A Cascade Impactor Operating at Low Volumetric Flow Rates, USAEC Report LF-5, Lovelace Foundation for Medical Education and Research, Dec. 1962.

2. F. J. Viles, In-Place Iodine Removal Efficiency Test, 9th Air Cleaning Conference, Harvard Air Cleaning Laboratory, Sept. 1966.

3. A. G. Blasewitz, Filtration of Radioactive Aerosols, USAEC Report HW-20847, Hanford Works, April 1951.

4. L. E. Browne, Steel Wool, Steel, Feb. 25, 1946.

5. R. Dennis, Fibrous Filters for NaK Fume Removal, USAEC Report NYO 4811, Harvard Air Cleaning Laboratory, May 1960.

CHARACTERISTICS OF THE AEROSOL PRODUCED FROM BURNING PLUTONIUM

H. J. Ettinger, W. D. Moss and H. Busey*
Los Alamos Scientific Laboratory
Los Alamos, New Mexico

*Present Affiliation
Douglas Aircraft Company
Santa Monica, California
June 1966

ABSTRACT

Safety analysis of sodium-cooled, plutonium-fueled, fast reactor plants must be concerned with the possibility of fires involving these materials. Design of an air cleaning system for such a facility requires basic data defining the aerosol characteristics of sodium and plutonium released during a fire.

Size characteristics of the aerosol produced during plutonium fires were determined for different atmospheres ranging from 20.8% oxygen, 79.2% nitrogen to 0.5% oxygen, 99.5% nitrogen. Plutonium-cobalt-cerium alloy, and alpha- and delta-phase plutonium metal were burned. Data were obtained to estimate the fraction of plutonium alloy airborne during a plutonium fire. Fires simulating a reactor accident involving both fuel and coolant defined the relative airborne concentration of plutonium and sodium.

I. Summary

1. The aerosol collected directly above burning chips of plutonium-cobalt-cerium alloy (57.7% plutonium) showed the following size characteristics.

Count Median Diameter (C.M.D.) : 0.04 - 0.09 microns (μ)

Geometric Standard Deviation (σ_g): 1.24 - 1.54

Mass Median Diameter (M.M.D.) : 0.05 - 0.14 μ

2. The aerosol collected directly above burning metallic plutonium turnings (alpha- and delta-phase) showed the following size characteristics.

C.M.D.: 0.02 - 0.06 μ

σ_g: 1.24 - 1.76

M.M.D.: 0.03 - 0.13 μ

3. Oxygen concentration of the burning atmosphere does not affect the particle size of the aerosol produced from burning plutonium metal or alloy.

4. When plutonium-cobalt-cerium alloy is burned under reduced oxygen conditions, the fraction airborne ranges from 1.8×10^{-7} to 38.8×10^{-7} depending on burn temperature and oxygen concentration.

5. Fires involving plutonium alloy and sodium produce airborne particulates with a plutonium-sodium ratio ranging from 0.34 to less than 0.008%. The high initial ratio is rapidly reduced as the molten sodium blankets the release of plutonium.

II. Introduction

Safety analysis of sodium-cooled, plutonium-fueled, reactor plants must consider the possibility of a fire involving these materials during the maximum credible accident (M.C.A.). To provide design criteria for the plant air cleaning system and to evaluate any potential hazard due to release of radioactive particulates, basic data defining the aerosol characteristics of sodium and plutonium produced during an M.C.A. fire are required.[1]

A test program determined the size characteristics of the aerosol produced during plutonium fires. Since a system of this type may be operated at reduced oxygen conditions, aerosol parameters were determined for fires in which the atmosphere consisted of various oxygen-nitrogen mixtures ranging from 20.8% to less than 0.5% oxygen.

Data were also obtained defining the percent of burned plutonium airborne during a fire, and the relative concentrations of airborne sodium and plutonium resulting from a fire involving both reactor fuel and coolant.

III. Plutonium Aerosol

A. Background.

Several investigators have attempted to determine the aerosol characteristics of airborne plutonium produced from fires. Carter[2,3] found an aerodynamic M.M.D. of 8.5 to 9.7 μ when sampling with a cascade impactor. He confirmed these values by autoradiography of fallout samples. Using cascade impactors, Stewart[4] found M.M.D.'s (unit density) ranging from 1 to 16 μ. He suggested a single particle size distribution to define the airborne plutonium aerosol. This aerosol had an M.M.D. of approximately 1.5 μ. Sherwood[5] used autoradiographic techniques on filter paper samples to evaluate the particle size of airborne plutonium in radiochemical laboratories. He found the airborne plutonium generally attached to inactive particles of dust. Using autoradiography, Moss[6] found an M.M.D. of 0.14 to 0.65 μ when sampling for plutonium outside the glove boxes in metal fabrication areas.

They estimated the size of plutonium aerosols by relating the number of tracks arising from a particle of plutonium to the mass. It was evident from these data that the best way to view and characterize these small plutonium aerosols was by electron microscopy.

The present test was designed to characterize the aerosol present just above a plutonium fire. The air sampler selected collected the aerosol directly on E.M. grids and permitted the use of electron microscopy to evaluate any submicron aerosol produced.

B. Procedures.

Because of the toxicity of plutonium, all burning apparatus and sampling equipment had to be located in a glove box, and all sampling manipulations carried out through glove ports. Approximately 50 to 100 grams of plutonium or plutonium-cobalt-cerium alloy were burned in a tantalum dish which fitted inside the copper burning pot shown in Fig. 1. Special oxygen-nitrogen gas cylinders were prepared, and each cylinder analyzed using a gas chromatograph. The various oxygen-nitrogen gas mixtures were supplied just above the tantalum dish holding the plutonium, to evaluate the effects of oxygen concentration on aerosol characteristics. Thermocouple holes in the copper base plate permitted measurement of the burning pot temperature. Relative humidity within the glove box was consistently below 25 ppm.

Since the air sampler could not be used outside the glove box after completion of the experiment because of contamination, a relatively inexpensive sampler was desirable. The all-glass, point-to-plane electrostatic precipitator (E.S.P.) shown in Fig. 2 was used. This sampler permits aerosol collection directly on carbon-coated electron microscope (E.M.) grids. The unit is operated at a flow rate of 5 liters per minute and a high voltage potential of 9,000 to 10,000 volts a.c. provided by a conventional neon-lamp transformer. Previous work[7] has shown that this sampler has representative aerosol collection characteristics comparable to those defined by several thermal and electrostatic precipitators. Figure 3 shows the E.S.P. just above the plutonium burning pot inside the glove box. The distance between the burning pot and the E.M. grid was 23 centimeters.

After sampling, the E.M. grid was removed from the glove box and monitored for alpha activity to estimate the quantity of plutonium collected. The grids were then alpha-counted and shadowed with chromium or platinum at 30°. Electron micrographs were obtained from random grid openings.

All electron micrographs (enlarged photographically to 50,000X) were sized on the basis of equivalent area (projected diameter)[8] using the Zeiss Particle Size Analyzer,* and the data obtained were plotted on log-probability paper.[9]

Count median diameter (C.M.D.) and geometric standard deviation (σ_g) were determined graphically. Mass median diameter (M.M.D.) was calculated using the Hatch and Choate[10] equation which also assumes a log normal distribution, Log M.M.D. = Log C.M.D. + 6.9 $\text{Log}^2 \sigma_g$.

*Carl Zeiss (mfgr.) Particle Size Analyzer, Model TGZ-3.

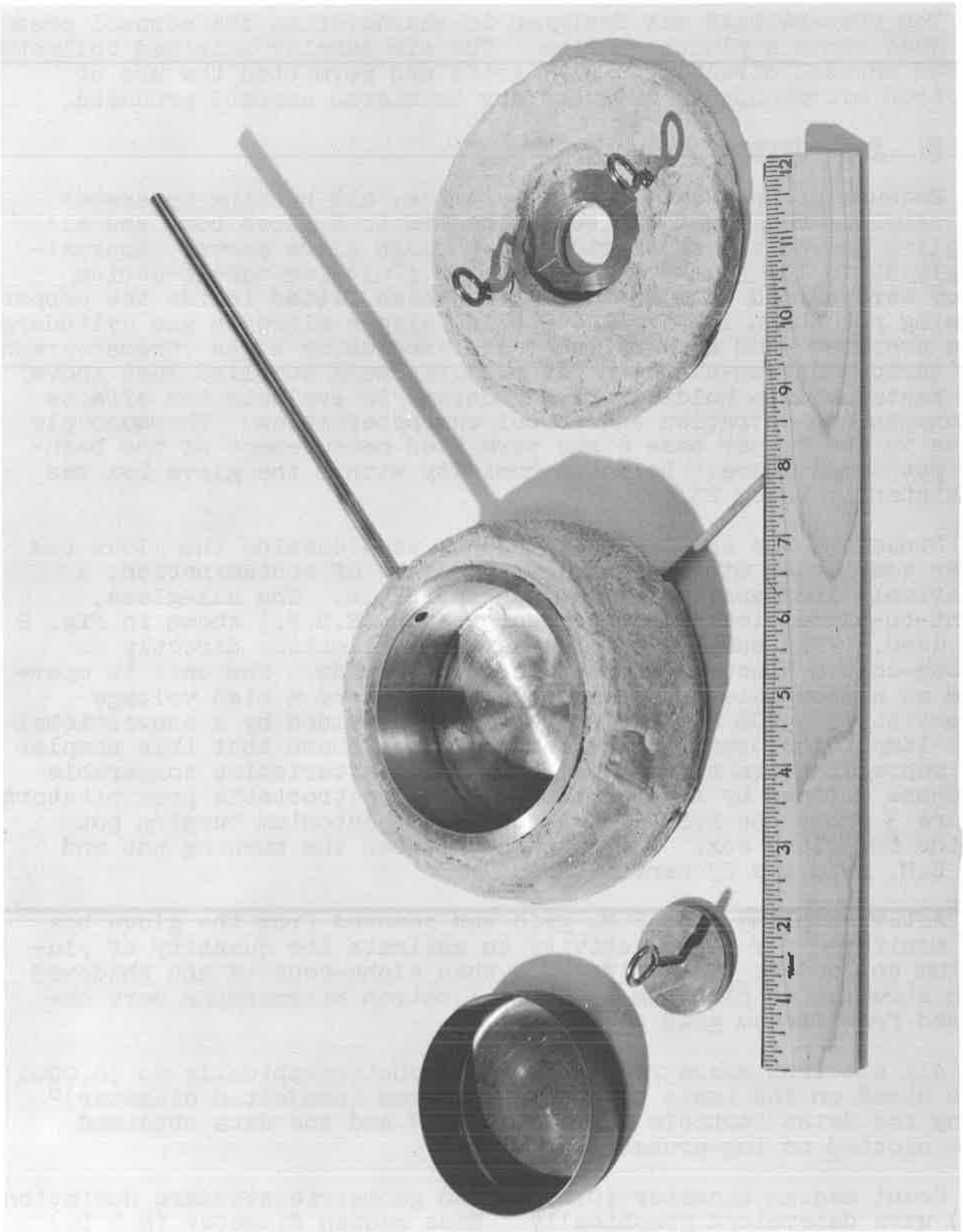

Fig. 1 Copper Burning Pot with Tantalum Dish.

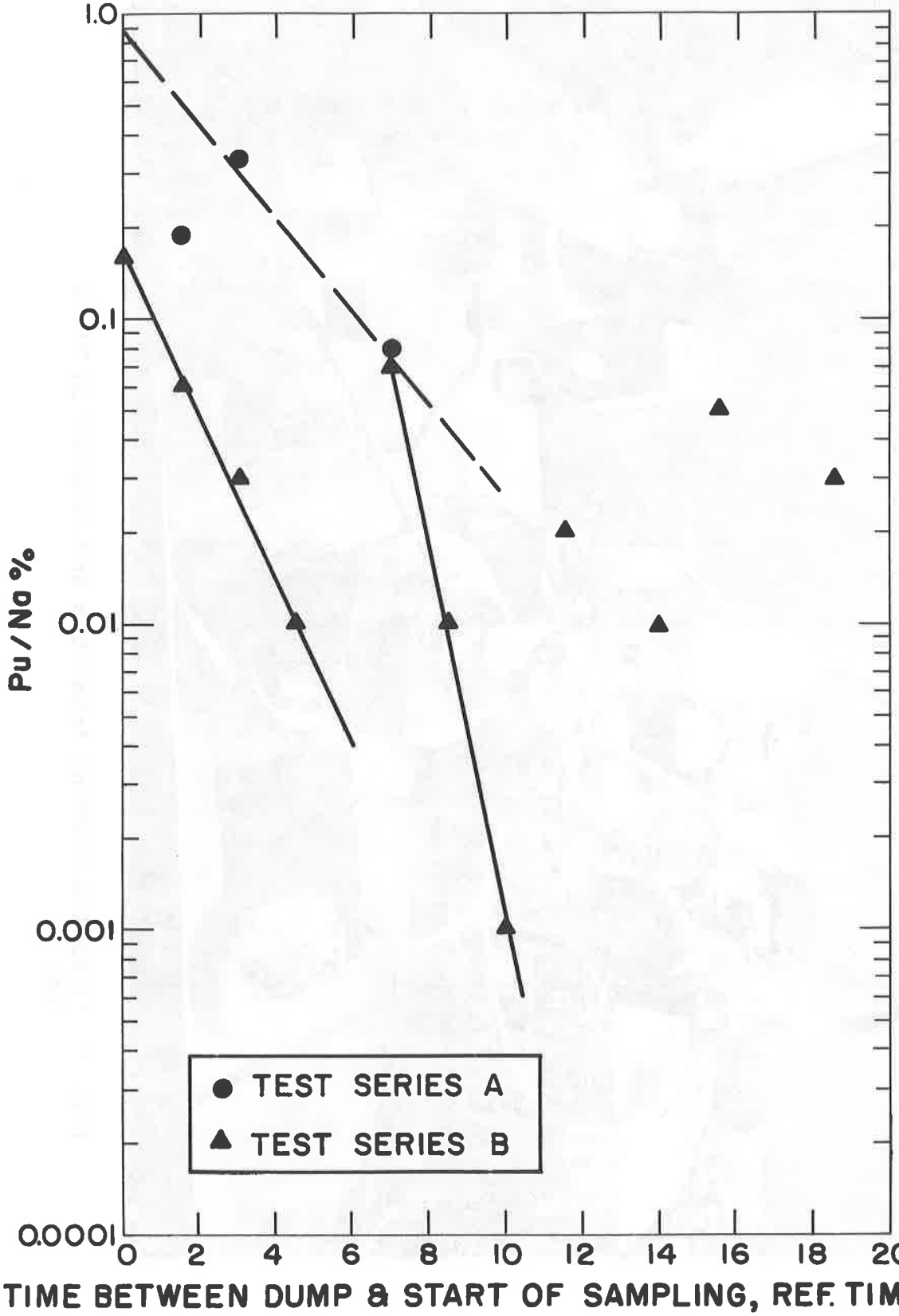

Fig. 2 Point-to-Plane Electrostatic Precipitator.

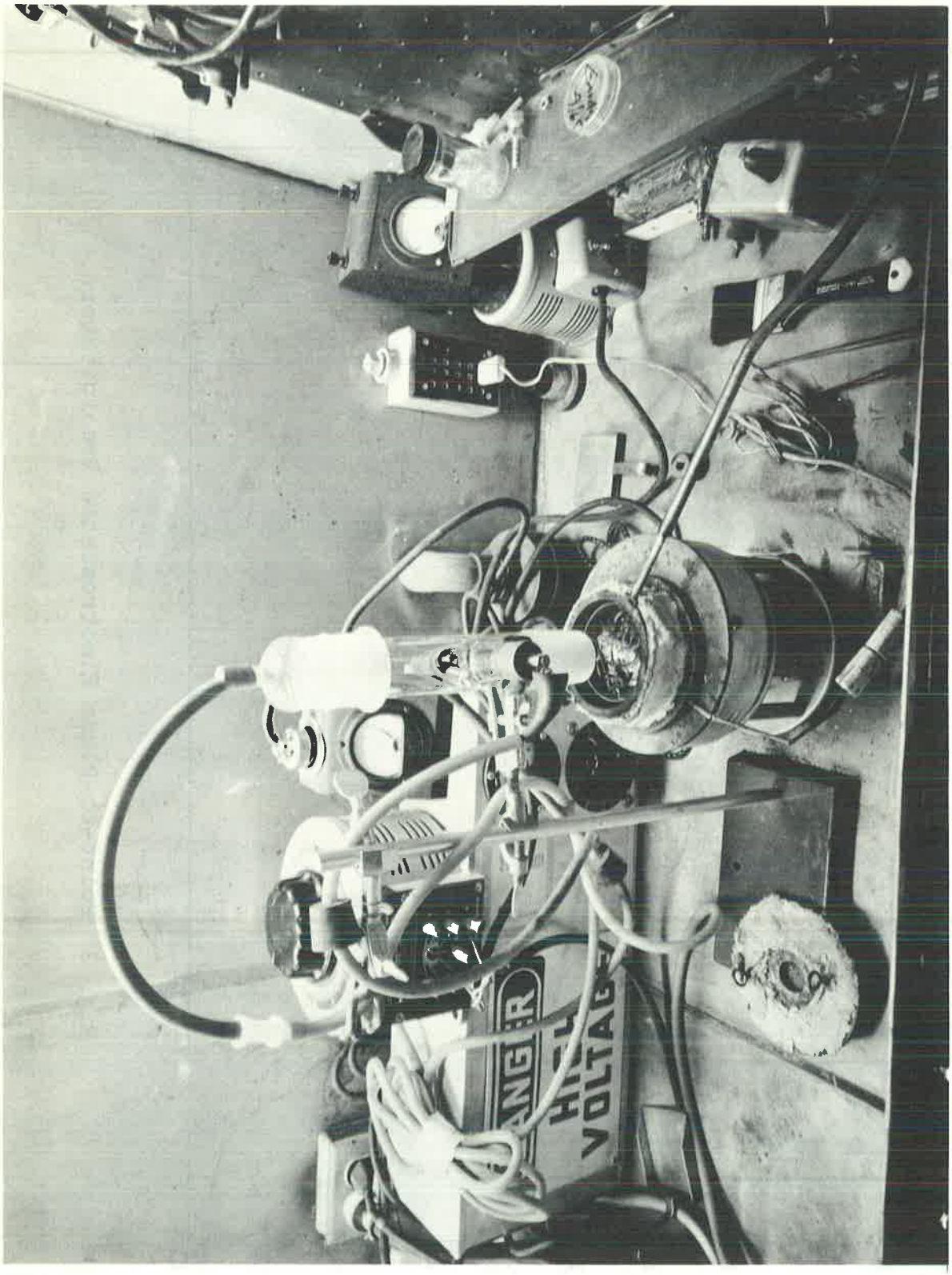

Fig. 3 Plutonium Burning Apparatus and Sampler in Glove Box.

C. Results.

Table I summarizes the aerosol characteristics from burning plutonium-cobalt-cerium alloy (57.7% plutonium) and plutonium metal (alpha- and delta-phase). In all instances the C.M.D. was below 0.1 μ and the M.M.D. below 0.15 μ. Aerosol size was independent of oxygen concentration. The aerosol C.M.D. produced from burning alpha- and delta-phase plutonium was somewhat smaller then that resulting from burning the alloy.

The small particle size (C.M.D. of 0.02 to 0.09 μ) shows that careful attention must be given to the design of air cleaning systems if these materials must be handled.

Figure 4 shows the typical aerosol collected when plutonium alloy or metal was burned at four different oxygen concentrations. Since the plutonium aerosol C.M.D. was as small as 0.02 μ, it was feared that the platinum or chromium deposited on the E.M. grid during shadowing might present an artifact. Figure 5 shows a grid platinum shadowed on both sides at a magnification of 50,000 times. The single large particle (approximately 0.5 μ) is due to background material within the glove box. This was verified by air samples obtained when no burning was taking place. The material deposited during shadowing presents no background problem.

Several of the samples collected during burning of delta-phase plutonium showed small amounts of a relatively large chain-structured aerosol. This aerosol was not present in samples taken when burning plutonium-cobalt-cerium alloy or alpha-phase plutonium. The possibility that gallium present in delta-phase plutonium produced this chain-structured aerosol was investigated. Figure 6 shows the aerosol produced from burning gallium metal. Figure 7 shows the chain-structured material present when delta-phase plutonium was burned. Because of this similarity, the chain-structured material was omitted when sizing the aerosol collected from burning delta-phase plutonium.

IV. Airborne Plutonium

To fully evaluate the potential hazard from a plutonium fire, it is necessary to estimate what fraction of the material burned would be airborne. Stewart[4] has found that from 2.1×10^{-2} to 6×10^{-5} of burned plutonium metal or alloy is airborne. His tests were conducted under oxygen concentrations at or above 20.8% with nitrogen constituting the remainder of the burn atmosphere. A limited test program was carried out at Los Alamos to obtain similar information for reduced oxygen conditions.

Plutonium-cobalt-cerium alloy (2.0 grams) was placed in the tantalum boat located in the center of the quartz tube shown in Fig. 8. Oxygen-nitrogen gas mixtures ranging from 0.4 to 2.76% oxygen flowed over the tantalum boat at a velocity of approximately 300 feet per minute. This gas velocity was selected to simulate conditions during a postulated M.C.A. No attempt was made to evaluate the effect of varying gas velocity past the burning plutonium alloy. After a combustion furnace was brought to temperature, the quartz tube was positioned in the furnace and the entire gas mixture passing over the plutonium was sampled with an AA Millipore filter. This closed-system test procedure guaranteed collection

TABLE I

PLUTONIUM AEROSOL CHARACTERISTICS

Material Burned	Oxygen Content (%)	Temperature (°C)	C.M.D. (μ)	σ_g	M.M.D. (μ)
Pu-Co-Ce	20.8	550-575	0.04	1.24	0.05
Pu-Co-Ce	8.8	500-550	0.08	1.45	0.13
Pu-Co-Ce	1.7	510	0.08	1.54	0.14
Pu-Co-Ce	0.49	505	0.09	1.41	0.13
None	20.8	25	---	---	---
Pu (α phase)	20.8	575	0.02	1.33	0.03
Pu (α phase)	8.8	525	0.05 0.03	1.72 1.49	0.13 0.05
Pu (α phase)	1.7	500	0.06 0.03	1.64 1.76	0.13 0.08
Pu (α phase)	0.49	495	0.06	1.46	0.09
None	20.8	25	~ 0.5-0.6	---	---
Pu (δ phase)	20.8	550	0.04	1.24	0.05
Pu (δ phase)	10.6	525	0.05	1.38	0.06
Pu (δ phase)	2.67	505	0.04	1.55	0.07
Pu (δ phase)	0.55	500	0.03	1.47	0.05

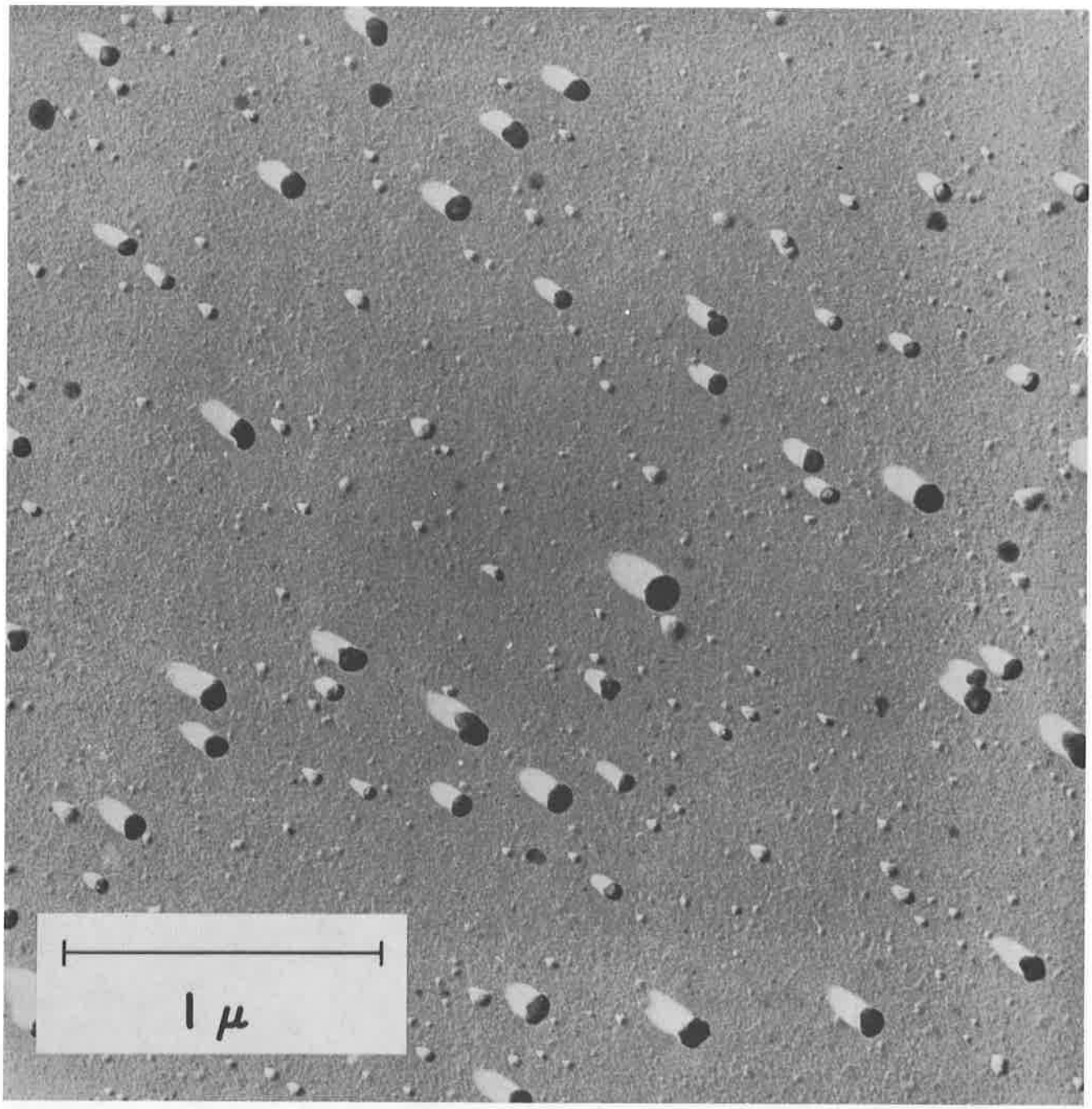

Fig. 4 Aerosol Produced by Burning Plutonium Metal (α phase) in 1.7% Oxygen. Shadowed With Platinum at 30°. Typical for All Plutonium and Oxygen Conditions Tested.

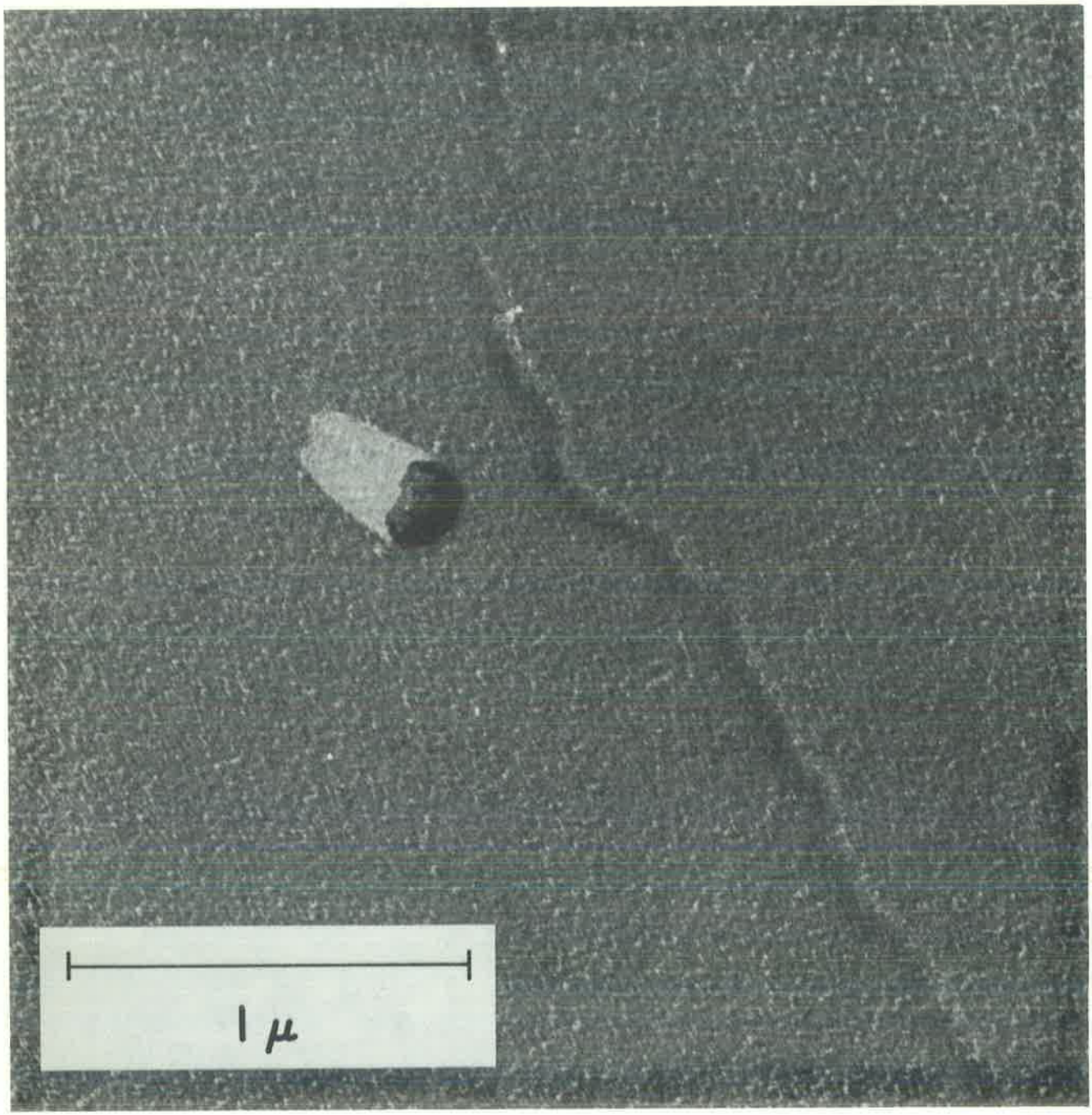

Fig. 5 Electron Microscope Grid Double Shadowed with Platinum.

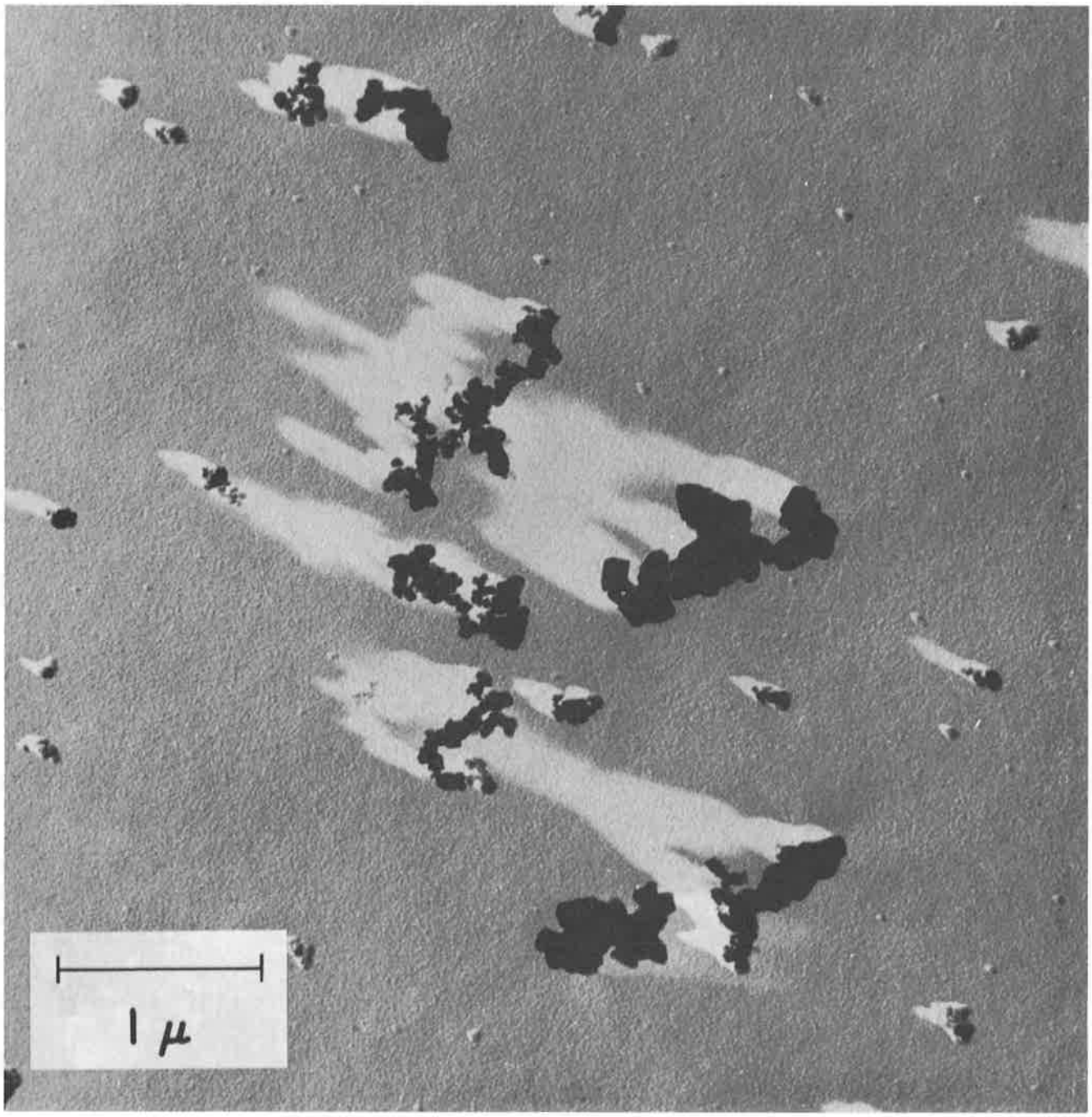

Fig. 6 Aerosol Produced by Burning Gallium Metal. Shadowed with Platinum at 30°.

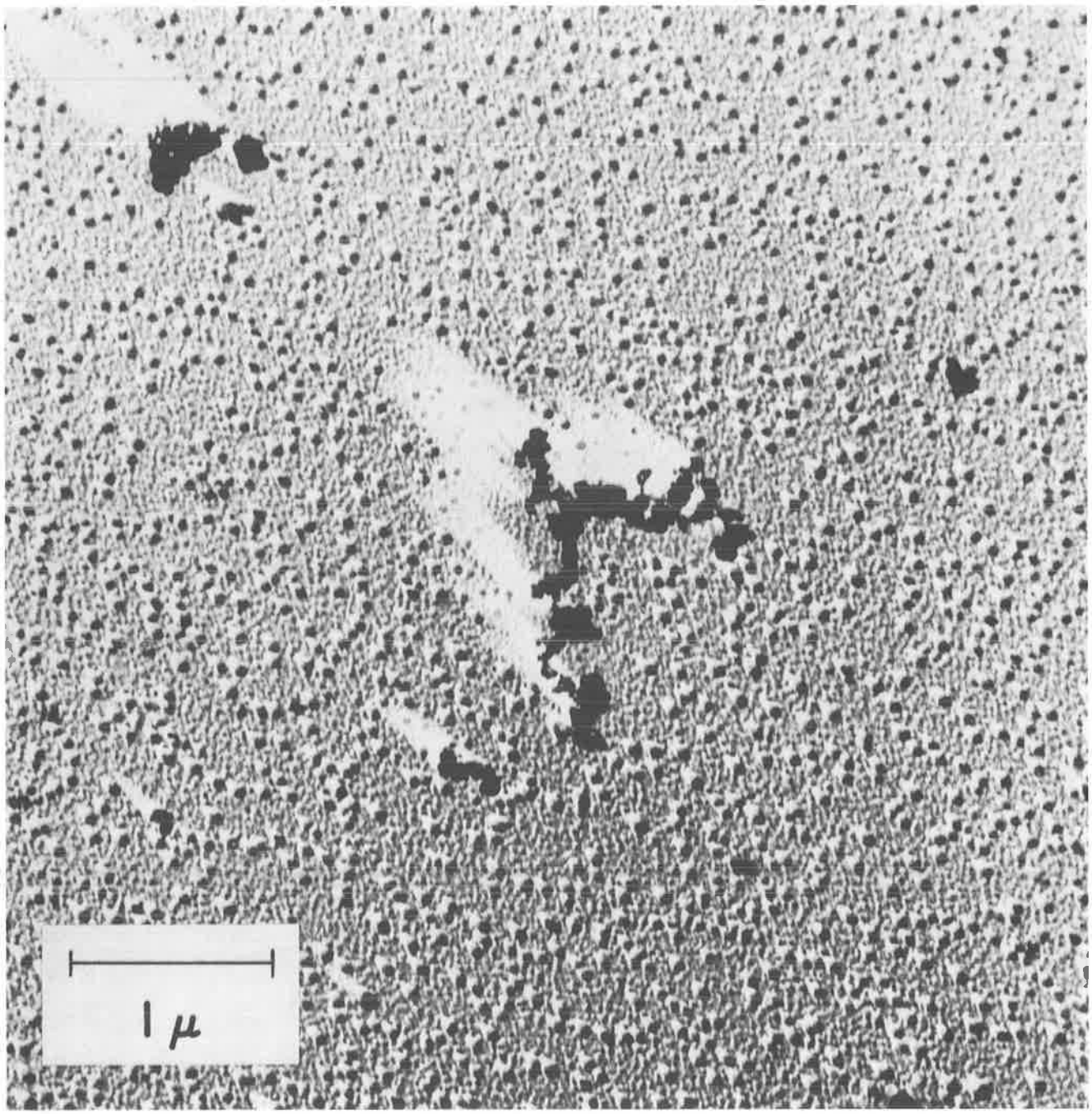

Fig. 7 Aerosol Produced by Burning Delta-Phase Plutonium. Shadowed with Platinum at 30°.

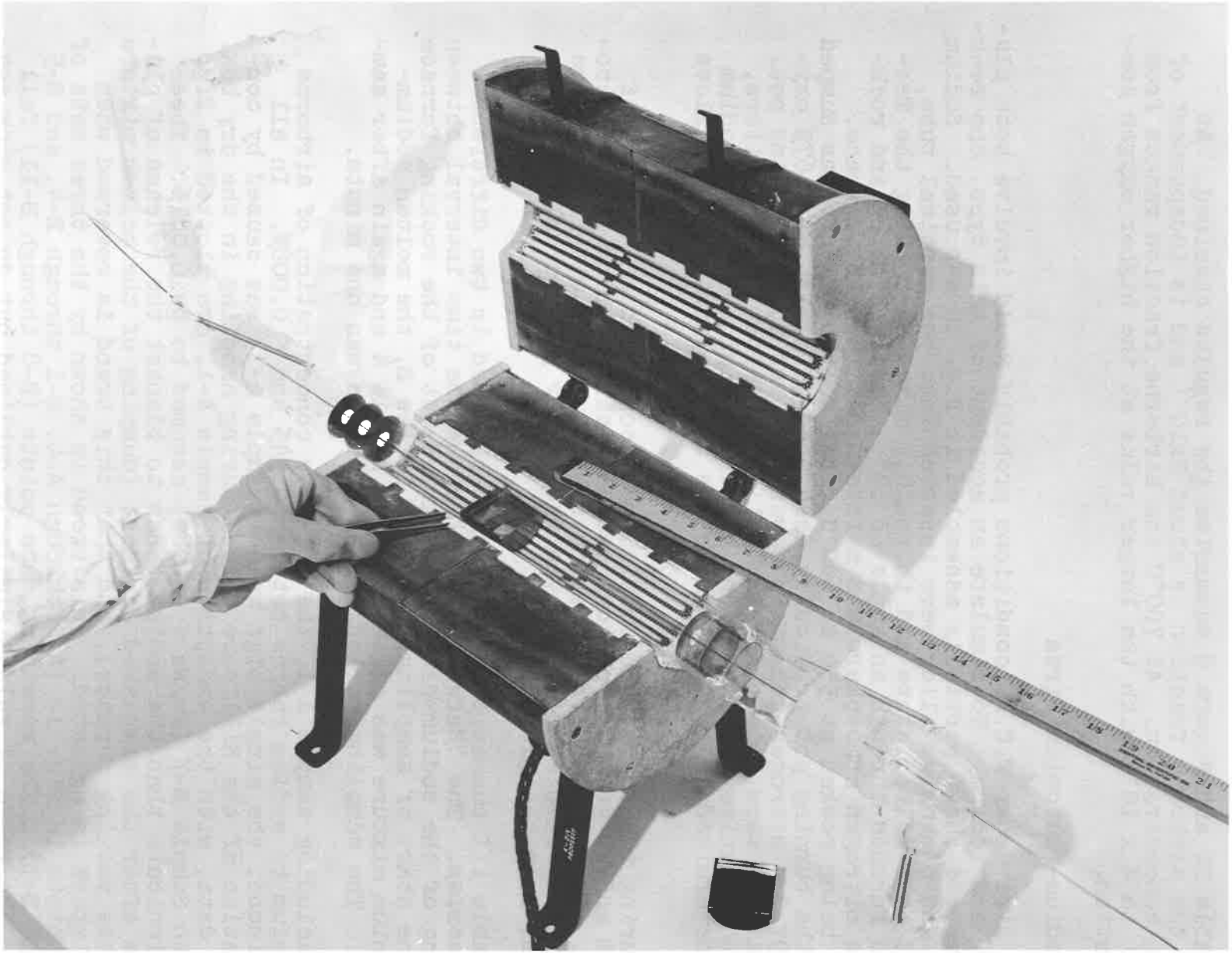

Fig. 8 Quartz Tube Used to Determine Fraction of Plutonium Airborne During Fire.

of all airborne particulate material. There was no attempt to compensate for plate-out on any surfaces between the tantalum boat and the sampling Millipore filter. The Millipore filters were alpha-counted to determine what fraction of the original 2.0 grams of alloy was airborne.

Table II and Figure 9 summarize the results obtained. At 500°C the airborne fraction is about 2×10^{-7} and is independent of oxygen concentration. At 700°C the airborne fraction ranges from 4×10^{-7} to 4×10^{-6} with the larger value at the higher oxygen concentration.

V. Sodium-Plutonium Fires

A fire under M.C.A. conditions probably would involve both plutonium and sodium. To simulate an accident of this type, the rocking furnace shown partially assembled in Fig. 10 was used. Sodium metal and plutonium alloy were inserted into the vertical tube, heated to a molten state and thoroughly mixed by rocking the Tee-shaped furnace through an angle of 60°. During heating and rocking, a nitrogen atmosphere was maintained within the furnace. After being rocked at 550 to 600°C., the molten mixture was dumped into the burning pot previously described (Fig. 1). A 2.67% oxygen, 97.33% nitrogen gas mixture was supplied to the burning pot. Air samples were obtained using Millipore filter field monitors, and the relative concentrations of airborne plutonium and sodium were determined. Figure 11 shows the test apparatus in the glove box.

During the tests, the initial melt consisted of 45 grams of sodium and 20 grams of plutonium-cobalt-cerium alloy (57.7% plutonium). To minimize contamination from plutonium within the glove box, filter samples were removed from their plastic holder after removal from the glove box.

Table III summarizes the results obtained in two different test series. The "Reference Time" shows the time interval between dumping of the sodium-plutonium mixture out of the rocking furnace and the start of sampling. In Test Series B, the molten sodium-plutonium mixture was agitated after sample 4 and again after sample 8. The sampling period for each sample was one minute.

Excluding sample A-1, the relative concentration of airborne plutonium to sodium ranges between 0.34% and < 0.008%. In all likelihood, the single high value (sample A-1) was caused by contamination of the Millipore filter during handling in the dry box. These data, with the exception of sample A-1, are plotted in Fig. 12 with Sample B-7 (Pu/Na < 0.008%) assumed to be 0.001%. These data indicate that the sodium tends to blanket the release of plutonium after the simulated accident (dumping of the molten mixture from the rocking furnace), and that this trend is reversed when the mixture is agitated. This trend is shown by the three sets of data points in Fig. 12 (A-2 through A-4, B-1 through B-4, and B-5 through B-7). The remaining data points (B-8 through B-11) fall within the range of values similarly outlined but do not show any consistent trend.

TABLE II

FRACTION PLUTONIUM AIRBORNE DURING FIRE

Oxygen Concentration (%)	Temperature (°C)	Fraction Pu Airborne
1.9	700	38.8×10^{-7}
0.4	700	4.2×10^{-7}
2.76	500	1.9×10^{-7}
0.5	500	1.8×10^{-7}

TABLE III

RELATIVE AIRBORNE CONCENTRATION OF PLUTONIUM AND SODIUM

Test Series	Sample Number	Reference Time (min.)	Sodium Collected (mg)	Plutonium Collected (mg)	Pu/Na (%)
A	1	0	0.96	0.194	20.2
	2	1.5	1.08	0.002	0.19
	3	3.0	1.20	0.004	0.34
	4	7.0	9.34	0.007	0.08
B	1	0	1.06	0.0017	0.16
	2	1.5	1.42	0.0008	0.06
	3	3.0	1.49	0.0005	0.03
	4	4.5	3.16	0.0002	0.01
	5	7.0	2.31	0.0014	0.06
	6	8.5	4.79	0.0005	0.01
	7	10.0	0.38	< 0.00003	< 0.008
	8	11.5	1.91	0.0004	0.02
	9	14.0	2.00	0.0001	0.01
	10	15.5	1.46	0.0007	0.05
	11	18.5	1.68	0.0005	0.03

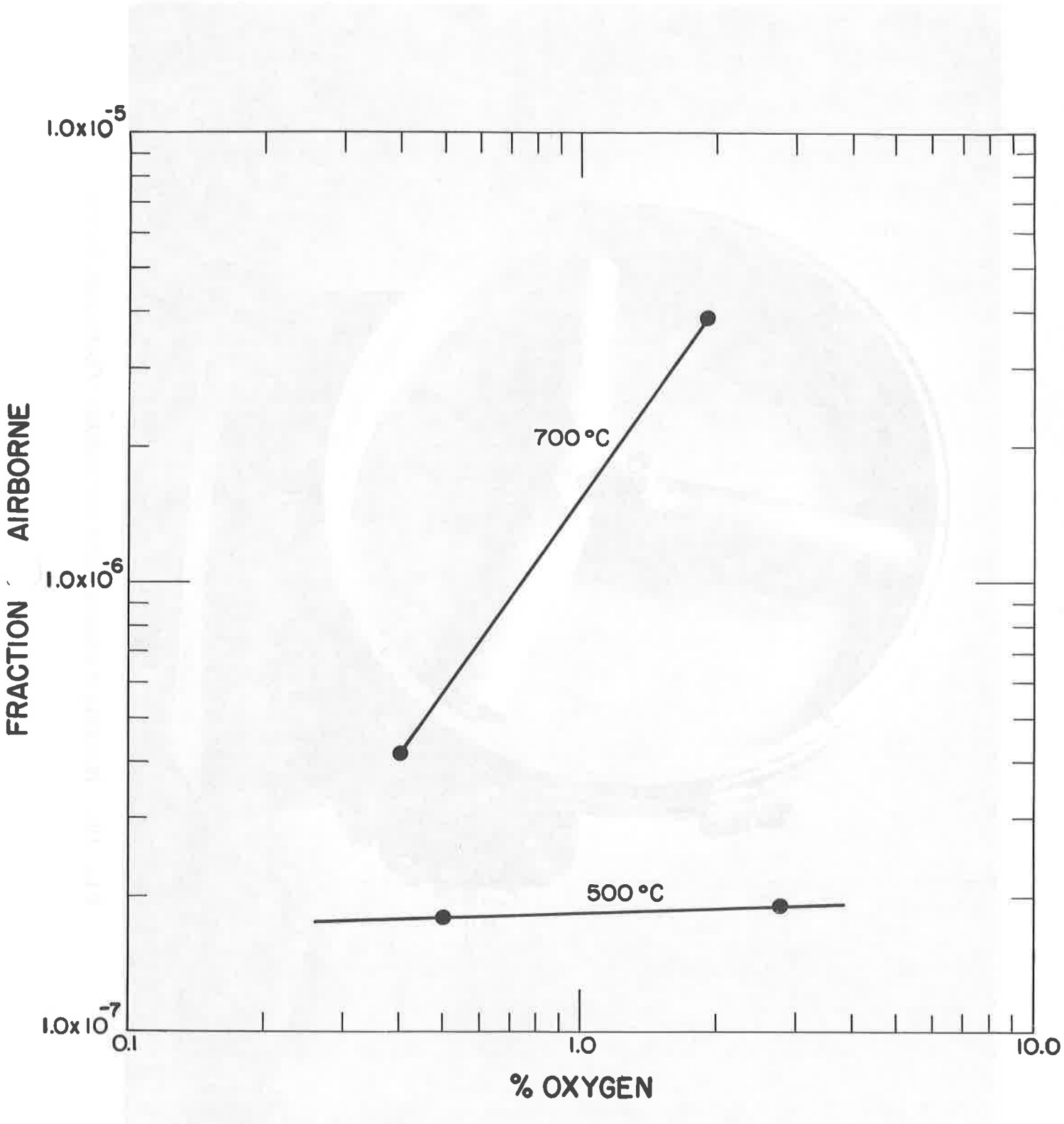

Fig. 9 Fraction of Plutonium Airborne During Fire as Function of Burn Temperature and Oxygen Concentration.

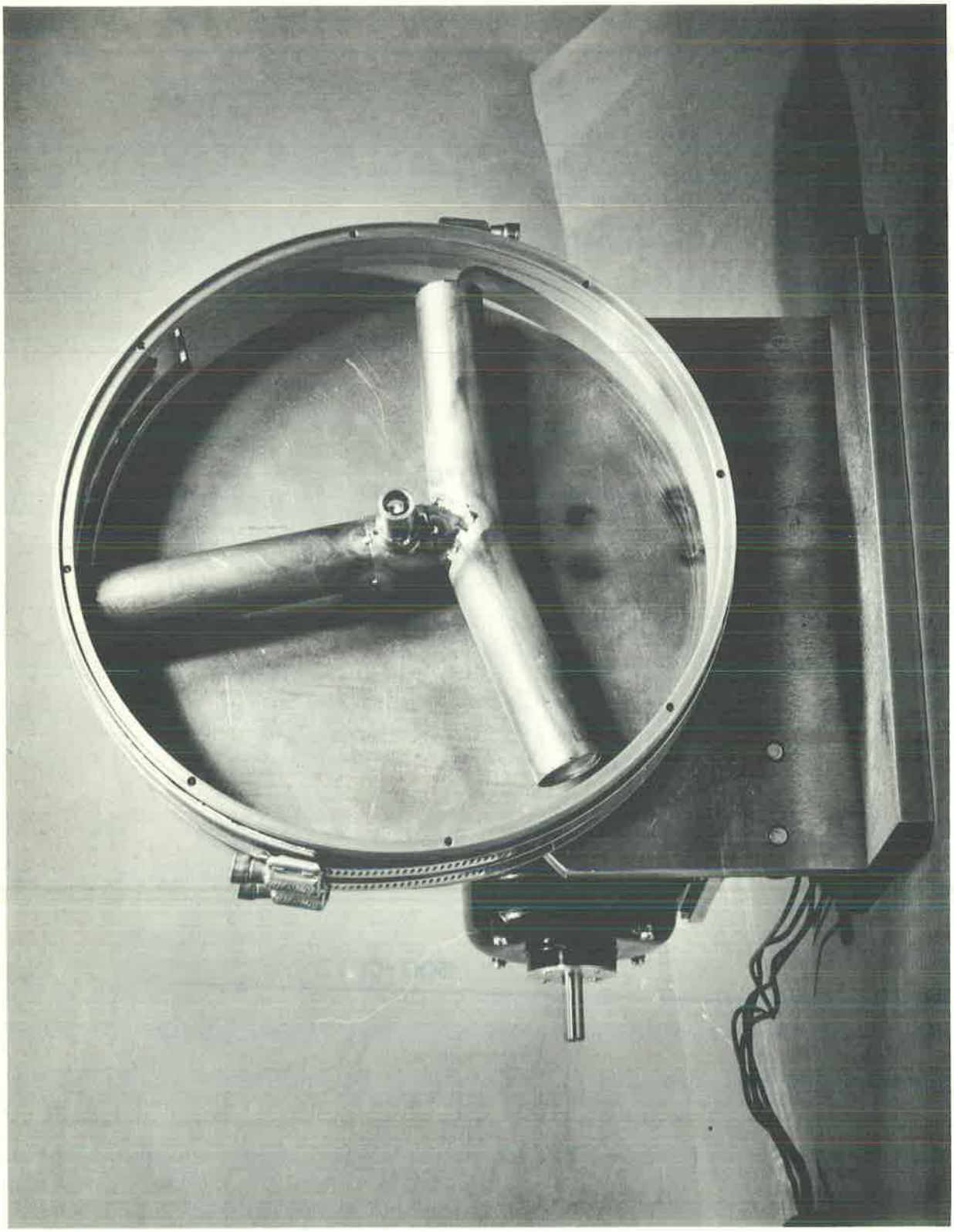

Fig. 10. Rocking Furnace Used for Sodium-Plutonium Fires

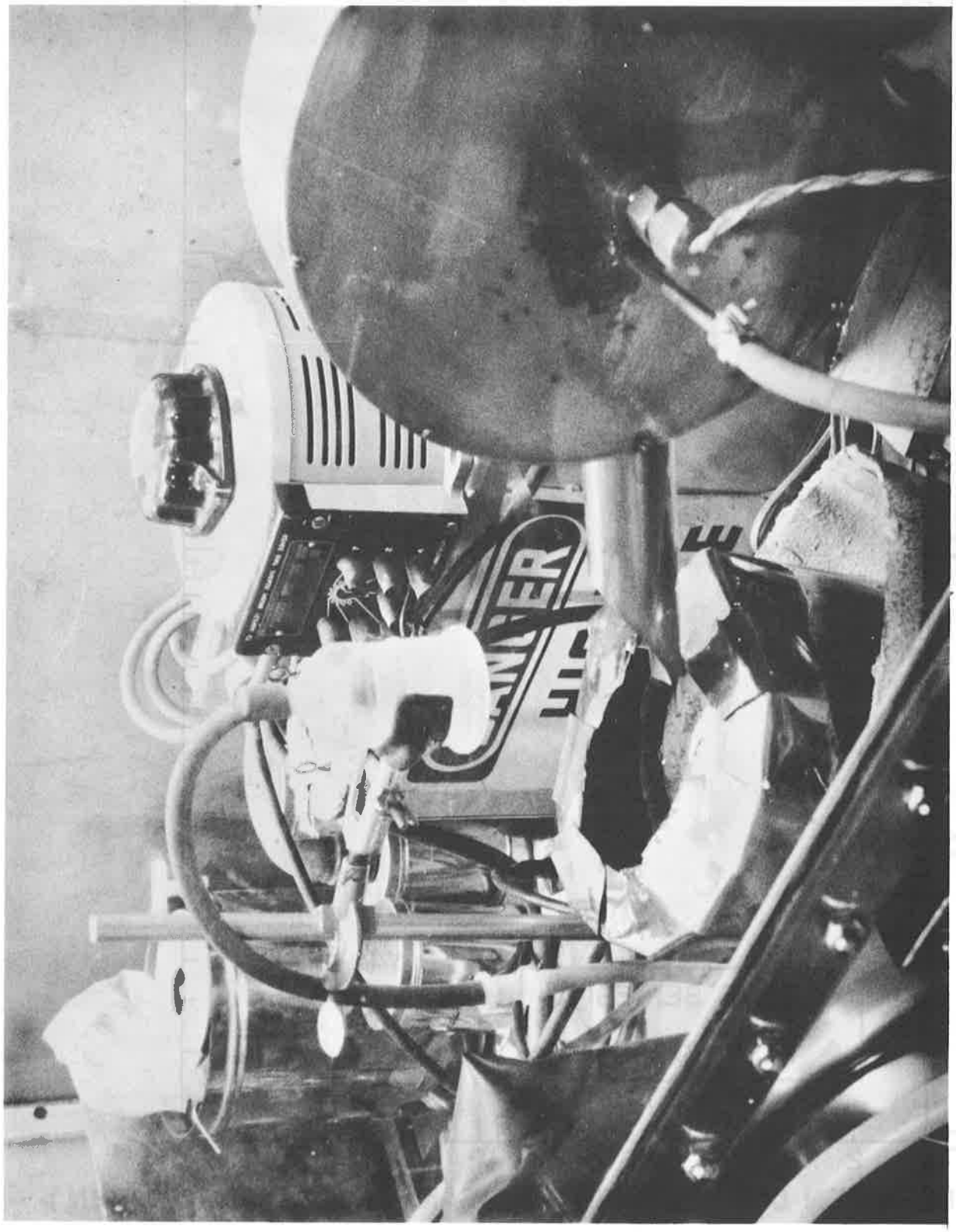

Fig. 11 Test Setup in Glove Box For Sodium-Plutonium Fires.

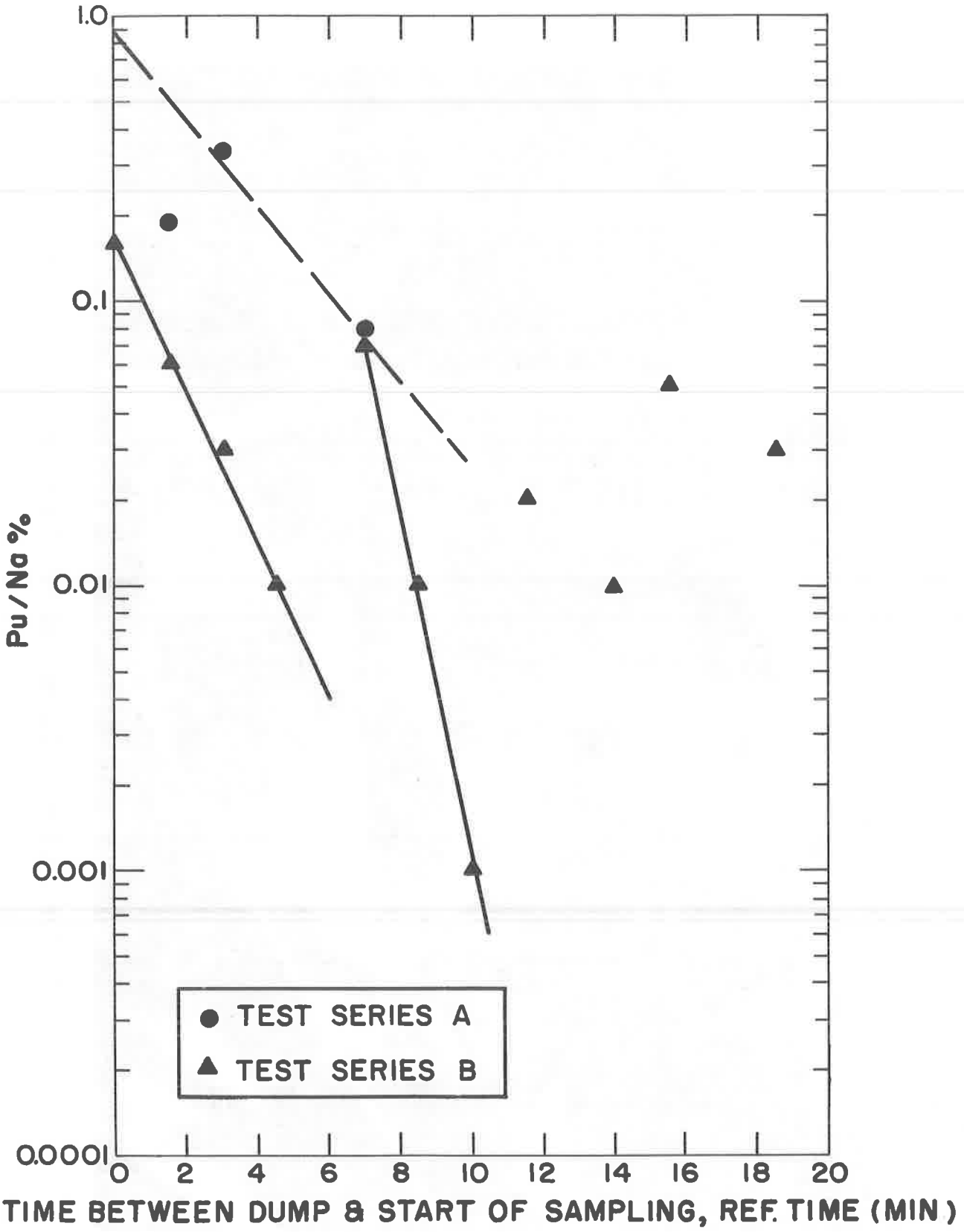

Fig. 12 Relative Airborne Concentration of Sodium and Plutonium as Function of Time After Dumping Melt from Rocking Furnace.

REFERENCES

1. H. J. Ettinger, W. D. Moss and H. Busey, Characteristics of the Aerosol Produced From Burning Sodium and Plutonium, U.S. A.E.C. Report, LA-3491, Los Alamos Scientific Laboratory, February 1966.

2. R. F. Carter, Ignition of Plutonium, Part 2, Particle Size Distribution Measurements, British Report, AWRE-O-49/58, December 1958 (Official Use Only).

3. R. F. Carter, B. Foy, and K. Stewart, Particulate Material Formed by the Oxidation of Plutonium, British Report, AERO/CONF./8, November 1960.

4. K. Stewart, The Particulate Material Formed by the Oxidation of Plutonium. Progress in Nuclear Energy, Series IV, Vol. 5, Technology, Engineering and Safety, MacMillan Co., New York, 1963.

5. R. J. Sherwood, and D. C. Stevens, Some Observations on Nature and Particle Size of Airborne Plutonium in the Radiochemical Laboratories, Harwell, British Report, AERE-R-4672, November 1963.

6. W. D. Moss, E. C. Hyatt, and H. F. Schulte, Particle Size Studies on Plutonium Aerosols, Health Phys. J., 5, 212 (1961).

7. H. J. Ettinger, and S. Posner, Evaluation of Particle Sizing and Aerosol Sampling Techniques, Am. Ind. Hyg. Assoc. J., 26, No. 1, 17 (Jan-Feb 1965).

8. G. Herdan, Small Particle Statistics, 2nd ed., p. 26, Elsevier Publishing Company, New York, 1960.

9. G. C. Whipple, The Element of Chance in Sanitation, J. Franklin Inst. 182, 37, 205 (1916).

10. T. Hatch, and S. P. Choate, Statistical Description of the Size Properties of Non-Uniform Particulate Substances, J. Franklin Inst. 207, 369 (1929).

DISCUSSION

CHEEVER: What consideration did you make of the residence time of the aerosol before air cleaning would take place?

ETTINGER: We did not try to compensate it; we tried to sample it, directly above the fire, setting up a system in order to calculate the size and the function of time and some sort of an air screen. However, we cancelled that approach.

HEYSE: The absolute filter in the system was identified as a completed Flanders' element. Do you know what the media was for an especially high temperature?

ETTINGER: The conventional one.

LAUBEN: When speaking of released fractions of plutonium, was this based on the initial charge?

ETTINGER: Yes.

LAUBEN: In other words, it is not based on the amount burned or you did not make an attempt on that?

ETTINGER: No, it is based on it. We thought we had burned to completion. We weighed out two grams accurately; in fact, we burned the sample and got a milligram and we calculated the ratio of that. We did burn it to what we judged to be the completion.

FULLER: Mr. Himot, I would like to ask you, what is your technique for measuring the velocity, in particular where it was less than 50-feet per minute?

HIMOT: We measured the velocity in the inlet pipe to the sodium burning pot with an orifice plate and manometer and then computed the flow through the filter by measuring the temperature of the gas entering the filter; thus we computed the velocity through the filter.

MISHIMA: I have a couple of questions. First, during the initial experiment, where you were burning plutonium in the pot, do you know what the velocity of the air over the burning plutonium was?

ETTINGER: I do not remember what the air flow was coming in that inlet. I can say that we were not very critical about that. It probably ranged from 5 to 25 meters per minute in a four-inch diameter burning pot, but I never calculated it and I never did really worry about it.

MISHIMA: What was the length of the run? What was the period of release time?

ETTINGER: I do not remember, off-hand. We started with 2 grams and although I do not remember how long, but we did burn to completion. I couldn't even give you an estimate, without looking up the data.

LAWROWSKI: I would like to thank you first of all for the air-borne plutonium. I do have several comments about the pressure drop through the filters in Mr. Himot's paper.

There are really two phases that you go through; the viscous flow, in which there is a pressure drop with the flow, and then in the last stages, in which the pressure builds up and the filter plugs a little. Then comes the transfer over to turbulent flow and then perhaps you are working in between.

When you reduce the flow by a factor of three, you can then essentially take a look at its equivalent pressure drop; it goes down by a factor of almost 8 to 10, because it is to about 1.8 power, and this has some bearing on the paper this morning. For flow across filters, you may be kidding yourself as to the amount that you can really put on a filter before you really plug it, because towards the end you are probably just closing up the last few holes.

I really do not know, myself, what the mechanism of flow is in that filter, because there is no nice, clean flow path. So that this seems to be a real scramble.

GREENFIELD: Did either of you by any chance collect your distributions to see how well they were represented, thus justifying your computations?

ETTINGER: We did not check these analytically. We did find that the pots were almost perfect, remarkably so, considering the small place in which we were working.

HIMOT: We took our samples and generally we found the size range of the sodium aerosol about 1-1/4 to 2-1/2 microns. With all of the data that we had, we still couldn't find out what were the controlling parameters within the ranges in which we worked.

PORTABLE SMOKE PHOTOMETER

by

H. H. Hunter and R. I. Mitchell
Battelle Memorial Institute
Columbus Laboratories

INTRODUCTION

In the evaluation of absolute filters it is necessary to challenge them with an aerosol and measure the concentration of the aerosol before and after it passes through the filter. The present procedure is to measure these aerosol concentrations with a smoke photometer which determines concentration by measuring the amount of light scattered by the aerosol particles. The amount of light scattered is proportional to the number of particles of a given size in the view volume of the instrument. The purpose of our research program is to miniaturize the smoke photometer and to increase its reliability by the use of semiconductors in place of vacuum tubes.

To date, the electronics portion of the instrument has been completed and will be described in this paper. The optics portion of the instrument is still under development.

Work performed under AEC Contract No. W-7405-eng-92.

ELECTRONICS OF THE PHOTOMETER

The electronics of the smoke photometer consists of two sections, (1) the photometer and its power supply and (2) the constant-intensity light and its associated power supply.

The function of the photometer is to produce an electrical signal proportional to the light reflected from particulate matter in the test volume of the penetrometer. The light reflected from the test volume is proportional to the quantity of material or to the concentration of material in the test volume. Thus, the output of the photometer is proportional to the concentration of particulate matter in the air being sampled.

The function of the constant-intensity light is to illuminate the test volume of the instrument and provide light that can be reflected from airborne particles as an indication of the particle's relative size. It is important that the intensity of the primary illumination be constant so that variations in the intensity of the reflected light are due solely to variations in the quantity of particulate material in the test volume. Otherwise, an uncertainty would exist as to whether a variation in reflected light was due to a change of particle concentration or to a change in the primary illumination.

Figure 1 shows the electronic circuitry of the smoke photometer. The photometer is in the upper portion of the figure, while the constant-intensity light source is in the lower portion.

Figure 2 is a photograph of the electronic portion of the completed prototype instrument. It is built into a case 8 x 9 x 22 inches in size and is easily carried. The unit weighs 21 pounds.

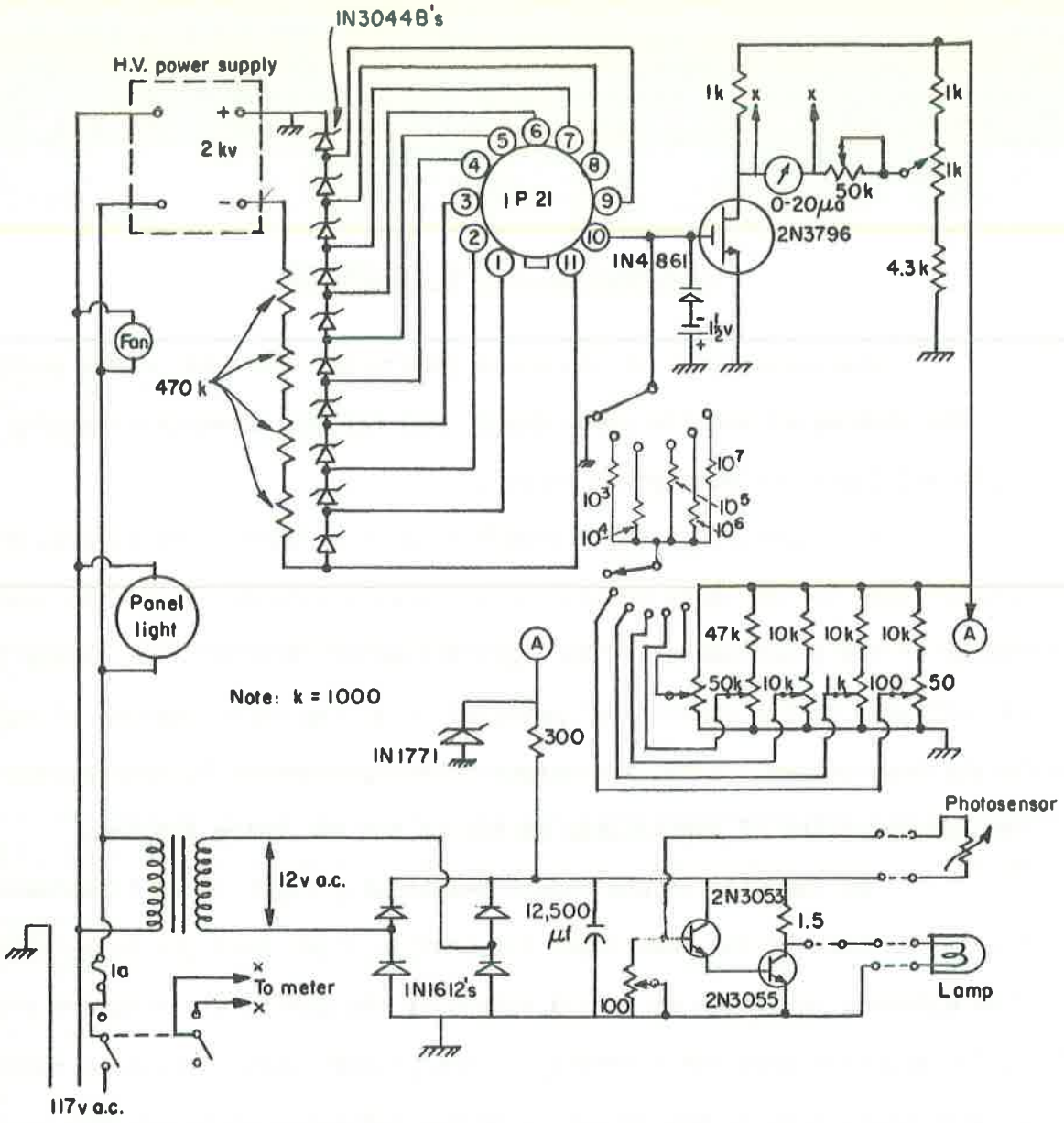

FIGURE 1. CIRCUIT OF PHOTOMETER AND CONSTANT-INTENSITY LIGHT SOURCE

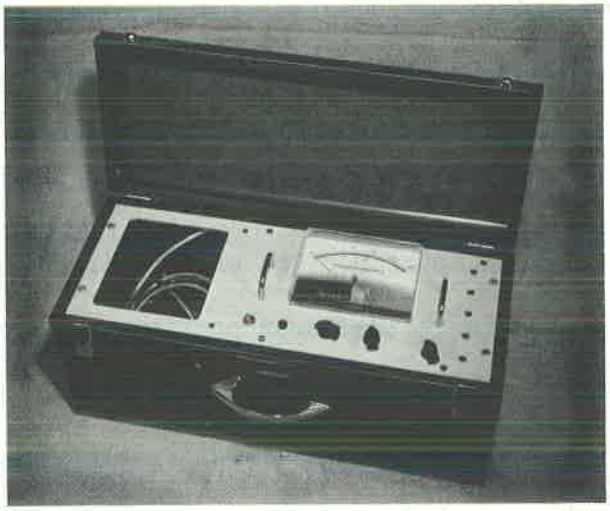

FIGURE 2. PHOTOGRAPH OF THE ELECTRONIC PORTION OF THE SMOKE PHOTOMETER

Photometer and Power Supply

The photometer is composed of (1) a photomultiplier tube and its regulated power supply and (2) an amplifier and readout meter, together with its associated power supply.

Photomultiplier Tube

A Type 1P21 photomultiplier tube was used. It was hoped that the spectral response of the photosensor could be matched with the spectral output of the incandescent light source, but available photomultiplier tubes that have a peak response in the desired spectral region were found to have a relatively low sensitivity. For instance, the Type 7102 photomultiplier has a peak response of 8000 Å, near the red end of the spectrum, and a typical sensitivity of 0.45 ampere/lumen. The Type 1P21 photomultiplier has a peak at about 4000 Å, near the blue end of the spectrum, and a typical sensitivity of 80 amperes/lumen. The Type 1P21 photomultiplier appeared to be a better tube for this application because its sensitivity is higher, even though its spectral response does not match well with the light source.

When stable operation of a photomultiplier is required, it is necessary that the various electrode potentials of the tube be closely controlled. Conventionally, the electrode potentials applied to a photomultiplier are obtained from a resistive voltage divider supplied by a suitable high-potential source. With this system, a compromise must be made. For instance, if the resistance of the voltage divider was made high in order to keep its power dissipation low, electrode currents

caused by a change in the light viewed by the photomultiplier would cause a change in the potentials applied to the various tube elements. Such potential changes would affect the operation of the photomultiplier so that its output current would not be directly proportional to the input illumination. This would be undesirable, because the response of the tube would no longer be linear. The situation could be improved considably by decreasing the resistance of the voltage divider, but this would cause increased power dissipation in the voltage divider and require a larger power supply.

To avoid the difficulties described above, a series of zener diodes was used to maintain constant the various electrode voltages applied to the photomultiplier in spite of variations in illumination viewed by the tube or variations in supply voltage. The zener diodes in the photometer are operated conservatively and should give long life.

The high-voltage power supply chosen is a commercial unit* which supplies an output of 2000 volts. By using a 2000-volt power supply, only 1000 volts of which is required by the tube, and dissipating the excess voltage in the limiting resistors, the input line voltage can vary over a wide range with little effect on the potentials applied to the photomultiplier. In practice, the line voltage can vary from 100 volts to 130 volts with practically no affect on the performance of the photomultiplier. This is an important feature if the instrument is to be used in an industrial rather than a laboratory environment.

---

* The unit used is a Type HV20-502M manufactured by Plastic Capacitors Inc., Chicago, Illinois.

Photometer Amplifier

The output current of the photomultiplier varies from a maximum of about 10^{-4} ampere to less than 10^{-9} ampere. Because of the small currents involved, an indicating meter could not be used directly. Thus, an amplifier was required which has a high input impedance in order that it not affect the operation of the photomultiplier. In the past, vacuum tubes have been used for this purpose. Although ordinary bipolar transistors do not have a sufficiently high input impedance, a relatively new semiconductor device, known as a field-effect transistor, or FET, met the requirements.

The amplifier was designed and built using an insulated gate FET* in a half bridge. Output current of the photomultiplier is passed through a suitable load resistor, and the potential developed across this resistor is used to drive the amplifier.

It is of interest at this point to note the arrangement of the load resistors for the photomultiplier, which also represent the input of the amplifier. In the past it has been common practice to use several resistors in series as the load for the photomultiplier. These resistances were chosen so their sum would produce the desired photomultiplier load for the most sensitive range. The output for the less sensitive ranges was taken at the junctions of the various resistors. A disadvantage of this technique is that, if light intensities to be measured vary over several orders of magnitude, as they do in a smoke photometer, the potential drop

---

* The unit used is a Type 2N3796 manufactured by Motorola Semiconductor Products Inc., Phoenix, Arizona.

across the load resistors must vary by the same ratio. For instance, if the maximum output potential is chosen to be 0.01 volt on the most sensitive range and the light intensity is expected to vary over four orders of magnitude, the maximum potential across the entire load resistor on the least sensitive range will be 100 volts. In effect, the voltage drop across the load resistor reduces the last-dynode-to-anode potential of the photomultiplier, and a reduction of only a few volts is enough to adversely affect the linear operation of the photomultiplier. Obviously, a reduction of, say, 100 volts can greatly impair the proper operation of the photomultiplier.

The technique used in the photometer described here was to use a separate load resistor for each range of interest. The load resistors were chosen to give a maximum potential drop of 0.1 volt. On the least sensitive range it was desired to limit the anode current of the photomultiplier to 100 microamperes as specified by the manufacturer. Thus, from Ohm's law, the load resistor is

$$R = \frac{E}{I} , \tag{1}$$

where

R = load resistor, ohms

E = potential drop across load resistor = 0.1 volt

I = anode current of photomultiplier = 10^{-4} ampere

Therefore,

$$R = \frac{0.1}{10^{-4}} = 1{,}000 \text{ ohms}, \tag{2}$$

and the load resistor on the least sensitive range is 1,000 ohms. For decade ranges of greater sensitivity, the load resistors are, progressively, 10^4, 10^5, 10^6, and 10^7 ohms. These are the values used in the instrument.

By limiting the voltage drop across the anode resistor of the photomultiplier to 0.1 volt, the change in the nominal last-dynode-to-anode potential of 100 volts is only 0.1 percent on any sensitivity range, which has little affect on the photomultiplier operation.

It will be noted from the circuit diagram (Figure 1) that provisions were made to supply an adjustable bias voltage to the input of the amplifier on the various sensitivity ranges. This allows cancellation of the input potential due to dark current in the photomultiplier and to signals caused by stray light in the optical portion of the instrument. This bias potential is adjusted for each range.

Power to operate the photomultiplier amplifier is obtained from the power supply of the constant-intensity light source. A zener diode is used to regulate the voltage applied to the amplifier.

Figure 3 shows the response of the photomultiplier and its amplifier to light of various intensities. It is apparent that the output of the system is proportional to the input illumination; the system is linear. While its response was being measured, the photomultiplier was enclosed in a metal shield electrically connected to the photocathode. A small hole in the shield was arranged so it could be covered by a neutral-density filter, which was an optical step wedge. The anode load resistance was 1,000 ohms for the test.

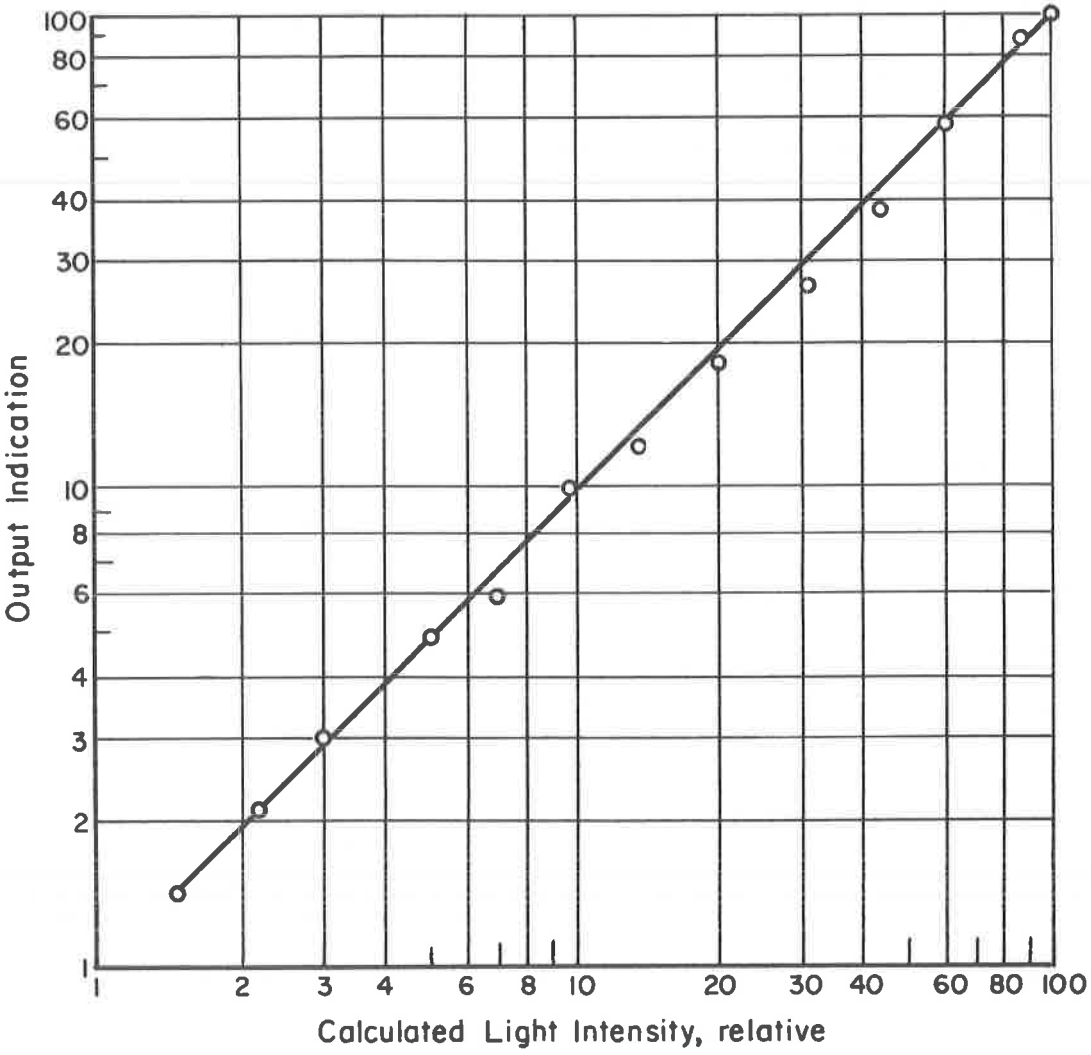

Figure 3. RESPONSE OF THE PHOTOMULTIPLIER AND AMPLIFIER TO LIGHT

CONSTANT-INTENSITY LIGHT AND POWER SUPPLY

The purpose of the light source for the photometer is to provide illumination for the test volume of the instrument. This illumination must be of constant intensity, so that variations in the light reflected from airborne particles in the test volume result solely from variations in the particle concentration.

The intensity of illumination from an incandescent lamp can be regulated by viewing the lamp with a suitable photosensor and using the output of the photosensor to control the current supplied to the lamp.

A shunt regulator was chosen for this application because it did not require the lamp current to pass through the regulator transistor. A series regulator was studied briefly, but its performance was not as good as that of the shunt unit. A two-stage d-c amplifier using transistors is driven by a photoresistor which views the lamp. Output of the amplifier controls the electric current through the lamp.

The circuit of the constant-intensity light source is shown in Figure 1. The photosensor* is physically mounted to the optical system so that it can view the lamp. The lamp is a special type supplied with the Bausch and Lomb optics. The 100-ohm variable resistor in the base circuit of the 2N3053 transistor controls the nominal current through the lamp. It is adjusted to a lamp current of 1.9 amperes.

Figure 4 shows the relative light output of the lamp as a function of applied line potential for three different lamp currents. Output of the

---

* The photosensor is a cadmium sulphide unit, a Type NSL-532HP produced by National Semiconductors Ltd., Montreal, Canada.

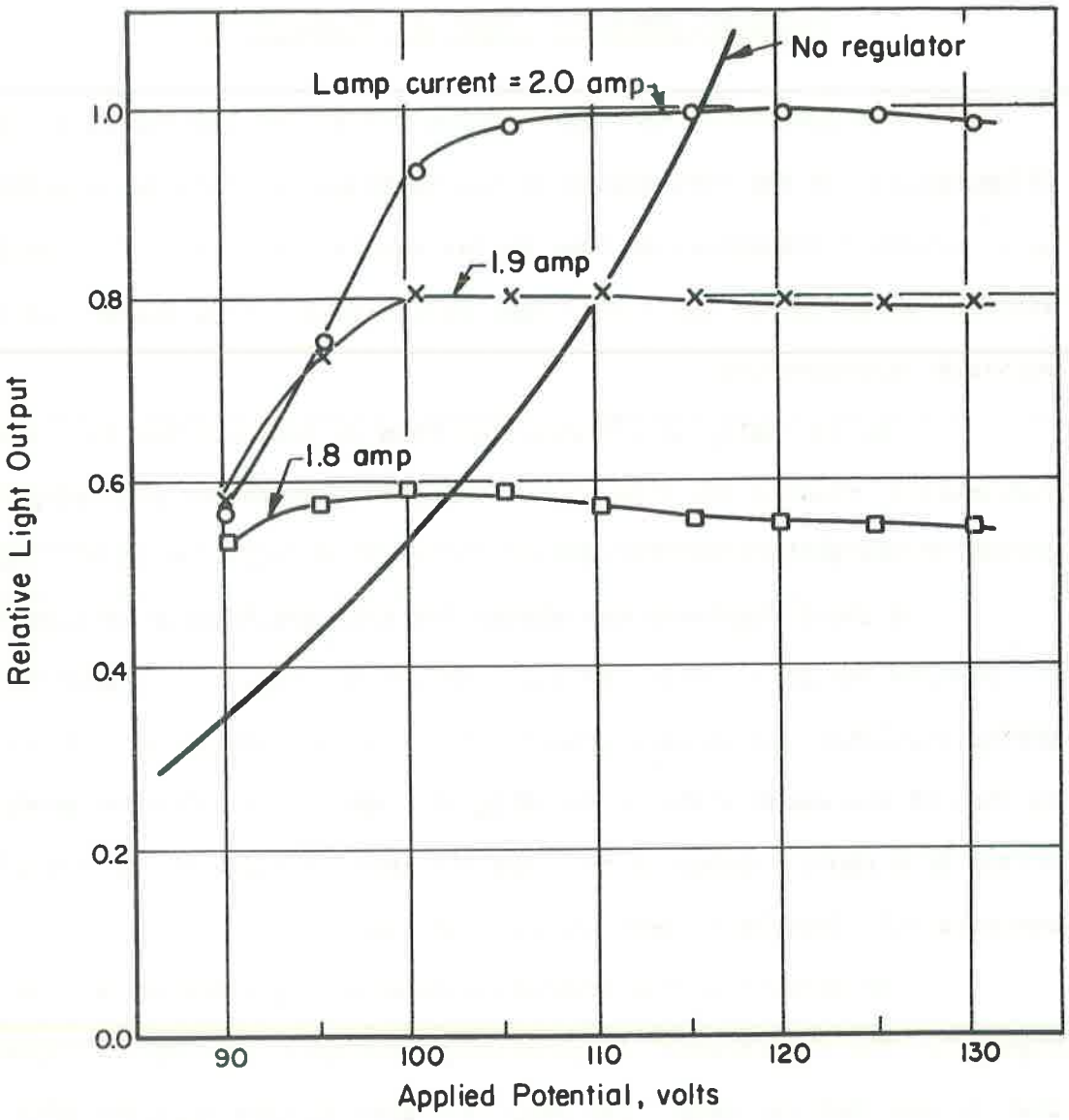

FIGURE 4. RELATIVE OUTPUT OF LIGHT SOURCE AS A FUNCTION OF APPLIED LINE POTENTIAL WITH AND WITHOUT REGULATOR

incandescent lamp with no regulator is shown for comparison. For these tests, light intensities were measured with a laboratory photometer. Rated current for the lamp used is 2.0 amperes. In the instrument, however, the lamp is operated at a current of 1.9 amperes. This slight reduction in operating current decreases the light output of the lamp somewhat, but increases the lamp life considerably and allows better regulation of the light output. At a nominal lamp current of 1.9 amperes, the lamp intensity is within $\pm$ 1.4 percent of the nominal value when the line potential is varied from 100 volts to 130 volts. With no regulation, the intensity variation over this range would be more than 100 percent.

OPTICS SYSTEM

In an attempt to miniaturize the smoke photometer, yet maintain its overall sensitivity, it was decided to modify the optics portion of the Bausch and Lomb 40-1 particle counter. In this device the aerosol flows through a high-intensity light beam and the light scattered by the particles is collected by a first surface parabolic mirror. This light is then focused by a lens onto the photocathode of the photomultiplier tube.

Because this optical system was designed as a particle counter, there is essentially never more than one particle in the view volume at one time. Attempts to increase the size of the view volume have resulted in an extremely large increase in the amount of stray light, which reduces the overall efficiency of the unit. Increasing the aerosol volume flow rate has not increased its overall sensitivity.

We have looked at some other optics systems and we feel that it would be difficult to make much of an improvement in the overall optic

system of the NRL penetrometer described by Knudson and White(*). Our final instrument will be very similar, except that the aerosol will pass through a disposable light cell that can be discarded if the instrument becomes contaminated with radioactive material.

SUMMARY

A solid-state photometer has been designed and constructed. This photometer has a linear response and is suitable for use with conventional optics used in smoke penetrometers. The instrument uses solid-state devices rather than vacuum tubes, and requires no warm-up time. Preliminary results indicate that its sensitivity is comparable to existing vacuum-tube units.

The instrument also has a constant-intensity light source in which the light intensity varies only ± 1.4 percent when the line potential varies from 100 volts to 130 volts.

The optics portion of the instrument is still under development and needs further modification.

(*) "Development of Smoke Penetration Meters", H. W. Knudson, and Locke White, U. S. Naval Research Laboratory Report No. P2642, 14 September, 1945.

DISCUSSION

STEINBERG: When you mentioned the optic system, which you have not included, you refer to the scattering chambers, will you eventually include the scattering chamber in this cabinet?

HUNTER: Probably not in this one, but we will have a two-suitcase deal.

STEINBERG: I was very curious as to how you got 21 pounds, without any transformers.

HUNTER: There are some transformers.

STEINBERG: You have regular transformers for power supply?

HUNTER: Yes. All electronic parts of the unit are in the suitcase. In fact, better than half of the volume and the weight is the constant intensity light source, because the power supply for this is considerably larger and heavier than the power supply of the photometer.

STEINBERG: What did you intend putting in the other suitcase?

HUNTER: The optics, the blower and the air sampling part of the instruments.

STEINBERG: You will have a vacuum source in it?

HUNTER: Yes.

JAMES A. YOUNG: I missed a point, and I hope that you will clarify it for me. In the modified circuit for the 1P21, does this enable you to remove the requirement for a filter in the incident light, to lower this level on the 100% scale, as we do in the Naval Research Laboratory type instrument?

HUNTER: Do you mean this plate with the holes in it?

JAMES A. YOUNG: Yes.

HUNTER: We have used such a filter in our L type optics. We did not use such a filter here.

JAMES A. YOUNG: But you would require it in the NRL type light scattering chamber.

HUNTER: It depends upon the maximum concentration. If the concentration gets high enough, you will require such a filter.

ZPPR ROOF SAND FILTRATION OF URANIUM, PLUTONIUM AND URANINE AEROSOLS

C. L. Cheever
D. R. McFee
J. Sedlet
T. L. Duffy

Argonne National Laboratory

ABSTRACT

The accident filtration system for Argonne National Laboratory's proposed Zero Power Plutonium Reactor consists of a sand and gravel roof followed by HEPA filters. Filtration efficiency tests were run with uranium, plutonium, and uranine aerosols to predict the effectiveness of this system for containment of plutonium fume. Penetration of uranium and plutonium fumes through 30 inches of sand ranged from .0004 to .02%. With the backup HEPA filters the overall penetration of plutonium fume from a reactor accident should not exceed .0001%. Results indicate that uranine aerosol will be satisfactory for in-place testing of the sand and gravel roof.

INTRODUCTION

Filtration tests have been carried out by the Industrial Hygiene and Safety Division of Argonne National Laboratory (ANL) to assist the Idaho Division in their preliminary safety analysis of ANL's Zero Power Plutonium Reactor (ZPPR). The ZPPR is to be built at the National Reactor Test Station (NRTS) in Idaho. It will have a sand and gravel roof and over this roof a metal shell building housing high efficiency particulate air (HEPA) filters. This combination will serve as a high volume filtration system to minimize escape of airborne plutonium while relieving gas pressure from the cell in the improbable event of a major reactor accident. A cross section sketch of the ZPPR is shown in Figure 1. The sand and gravel roof will serve as a heat sink as well as a filter thereby protecting the HEPA final filters. This system offers the advantage of lower cost than that of a conventional containment structure.

Our filtration tests were to evaluate the effectiveness of the proposed filtration system rather than to obtain information for system design. Uranium, plutonium, and uranine aerosols were selected for testing purposes.

Uranium fume was used as a test aerosol because of its similarity to plutonium fume and because its much lower health hazard permitted collection of experimental data with considerably less effort and time expenditure than with plutonium.

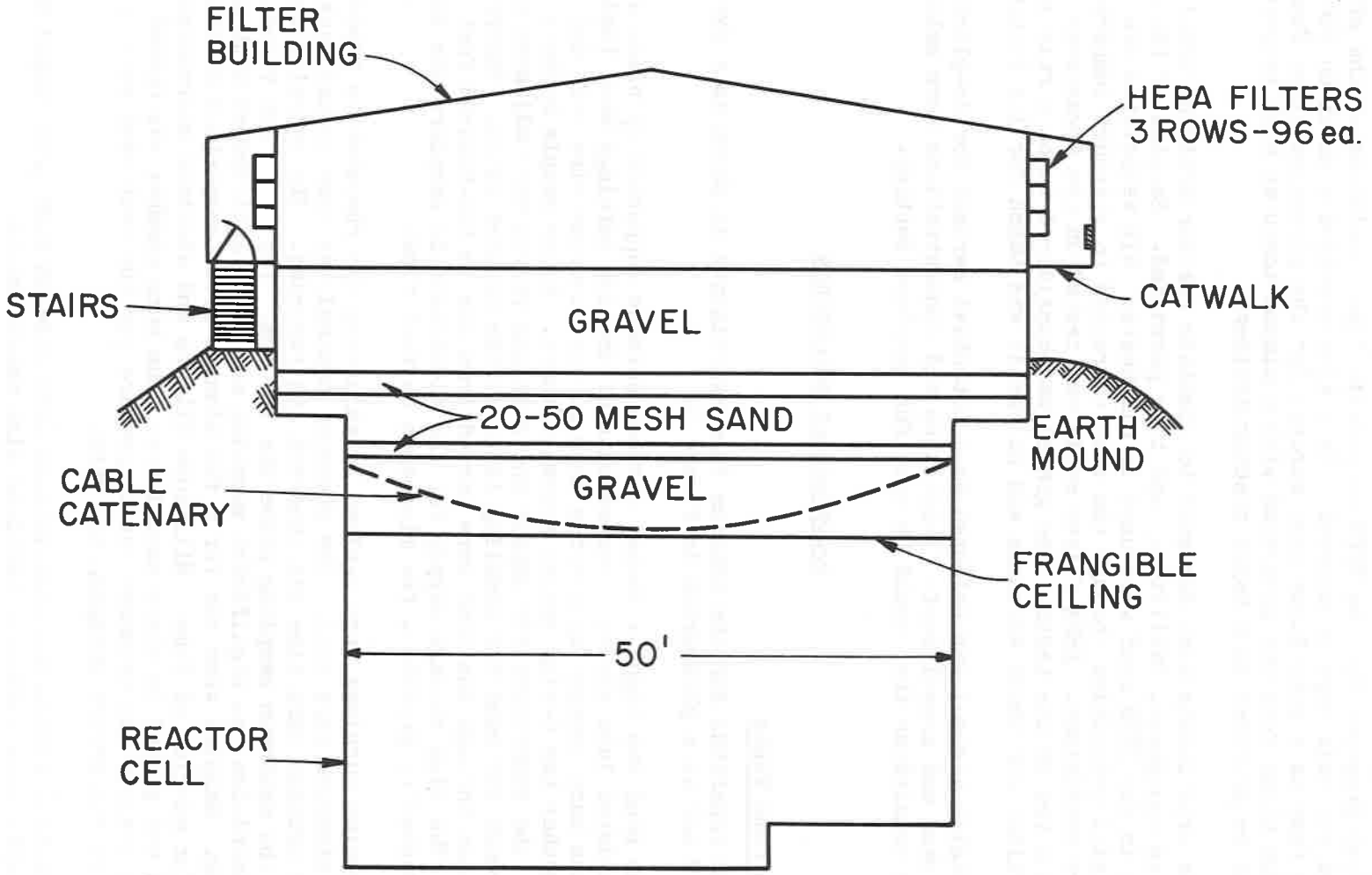

Figure 1. ZPPR Cross Section Sketch

The uranium fume tests were designed to simulate pressure conditions in the event of a major accident. Test pressures included those calculated from the design basis accident and up to the pressure above which the sand and gravel roof would begin to lift. In this way, sand filtration was studied over and above the range of flow rates that were postulated for accident conditions.

The uranium experiments were followed by tests using fume from the plutonium alloy fuel proposed for the ZPPR to provide direct evidence of the efficiency of the sand for this type of aerosol. This also provided a check on the use of uranium fume as a substitute test aerosol for the plutonium alloy fume. The plutonium alloy fume was generated with a plasma torch at high temperatures such as might be produced in a major reactor accident.

The experiments were designed to simulate reactor accident conditions in so far as equipment, facilities, and time permitted. Samples of the sand proposed for use in the ZPPR roof were used in all tests. All velocities are listed as superficial velocities through the sand corrected to standard temperature and pressure conditions. HEPA filter media was tested on the downstream side of the sand in a few of the tests. The gravel was considered to be a relatively inefficient filter for these aerosols and no credit was taken for its filtration effect.

Uranine aerosol was selected as a potential aerosol for in-place testing of the sand and gravel roof. Velocities and concentrations were selected to include conditions that could be used for in-place testing.

EXPERIMENTAL PROCEDURES

Uranium Fume Tests

The apparatus for the uranium fume experiments is shown as a sketch in Figure 2 and as a photograph in Figure 3.

The sand was tightly packed between screens supported by brass disks which were soldered into place. Gram amounts of uranium turnings were loaded into the glass burn chamber by placing them on the nichrome wire coil and then bolting together the O-ring sealed access flanges. After sample holders had been loaded, the compressed air supply and sampling valves were adjusted to force air through the sand and sampling lines at the desired rates. Superficial velocities through the sand were varied from one to two-hundred feet per minute (fpm). The high voltage supply for the electrostatic samplers was turned on and adjusted to provide a few microamps current flow.

Uranium turnings were ignited by adjusting the rheostat to produce red heat on the nichrome wire coil. The rheostat control was then turned back to zero and the uranium burn time was observed and recorded. The velocity through the tip of the upstream sampling probe was 120 fpm. For these low velocities and small particles, no significant sampling error was anticipated with non-isokinetic sampling. Samples were run for a few minutes after completion of the burning to allow for purging of fume. Millipore filters and electron microscope grids were removed and placed in clean containers. The burn chamber was opened and the uranium residue was vacuumed out to prepare for the next test run. A series of tests was run before changing the sand.

Electron microscope observations were made on each grid sample and some photographs were taken for particle size measurements.

Millipore filter samples were treated slowly with hot concentrated nitric acid and small amounts of 50% hydrogen peroxide as necessary. After destruction

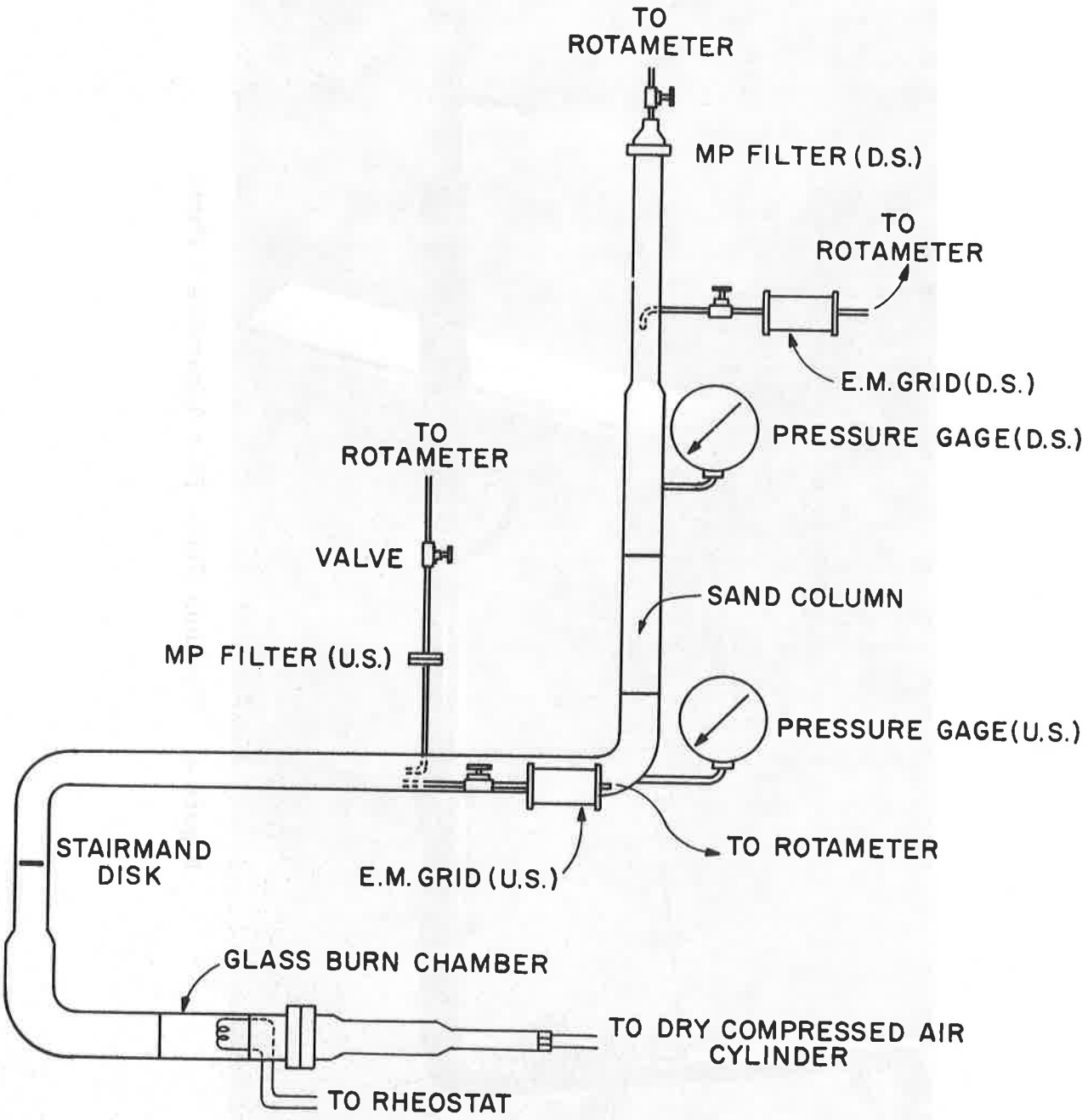

Figure 2. Uranium Fume Test Apparatus - Schematic

Figure 3. Uranium Fume Test Apparatus - Photo

of organic material and careful evaporation to dryness the samples were dissolved in 4N nitric acid with heating. The amount of uranium present was determined fluorometrically using the procedure of Schwartz et al[1] and the sodium fluoride-lithium fluoride flux reported by Centanni[2] et al. All analyses were done in triplicate and quenching was evaluated for each.

Plutonium Fume Tests

The plutonium filtration tests were conducted by generating fume inside a small enclosure and drawing it upward through a stack containing the sand filters. The test system is shown as a sketch in Figure 4 and Figure 5 is a photograph of the small enclosure. Except for the 30 inch sand column, samples were collected isokinetically on Millipore filters upstream and downstream of the sand to determine the percentage penetration. For 30 inches of sand the amount of fume recovered from the sand filter and from the downstream total airflow filters were used for efficiency calculations. Fume was electrostatically precipitated onto electron microscope grids in three tests and examined with the electron microscope.

The fume was generated by feeding the plutonium alloy fuel as a powder smaller than 200 mesh (<74 microns) into the plasma torch along with the argon which forms the plasma. A measured volume of powdered fuel containing about 0.1 gram of plutonium was fed into the torch during each test. The temperature of the plasma was in excess of 3100°C. Oxygen was fed into the fume enclosure within the nitrogen atmosphere glove box at a rate calculated to give a synthetic air containing 20.8% oxygen.

The 6 inch sand filters were arranged in three 2 inch segments of sand packed between sixty mesh brass screens. The 30 inch sand filter consisted of the three 2 inch segments of sand followed by four 6 inch segments. Only four tests (at 1, 4.8, 13.2, and 28.3 fpm) were conducted on the 30 inch deep sand filters. These tests were run simultaneously with all four stacks mounted above the fume enclosure and drawing from the common fume source. HEPA filter media followed by a Millipore filter was used as a final filter for all systems.

The superficial velocity through the sand was varied from 1 to 133 fpm. Test times ranged from one-half to eight minutes, with the shortest periods being used for the highest test velocities.

Following completion of each test the system was disassembled. Samples and sand segments were bagged out of the glove box and transferred to clean containers for analysis.

The plutonium content of all samples was determined by measuring the alpha activity. Millipore filter samples that contained less than about 5×10^5 disintegrations per minute (dpm) were counted directly in a zinc-sulfide alpha scintillation counter. Millipore filters too active to be counted directly and all the HEPA filters were dissolved and the solutions diluted to known volumes. Aliquots of the solutions were evaporated to dryness and counted in 2-pi, gas-flow, proportional counters. Millipore filters were dissolved by treatment with hot, concentrated nitric acid and 50% hydrogen peroxide containing a few drops of hydrofluoric acid. The samples were then diluted to volume with 3N nitric acid. HEPA filters were dissolved by treatment with a mixture of hydrofluoric, hydrochloric, and perchloric acids. The solution was evaporated to fumes of perchloric acid to remove the hydrofluoric acid, and then diluted to volume with 6N hydrochloric acid.

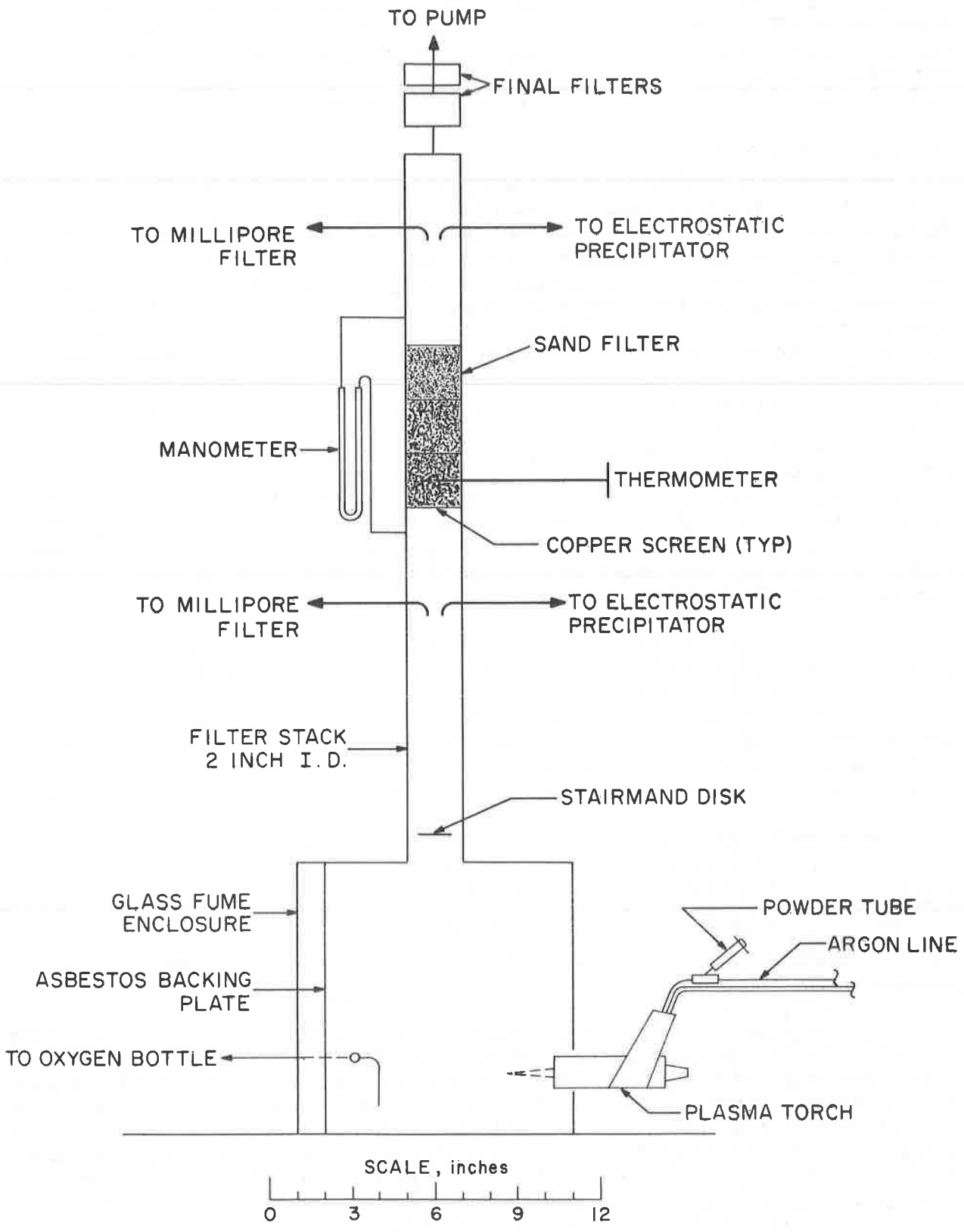

Figure 4. Plutonium Fume Test Apparatus - Schematic

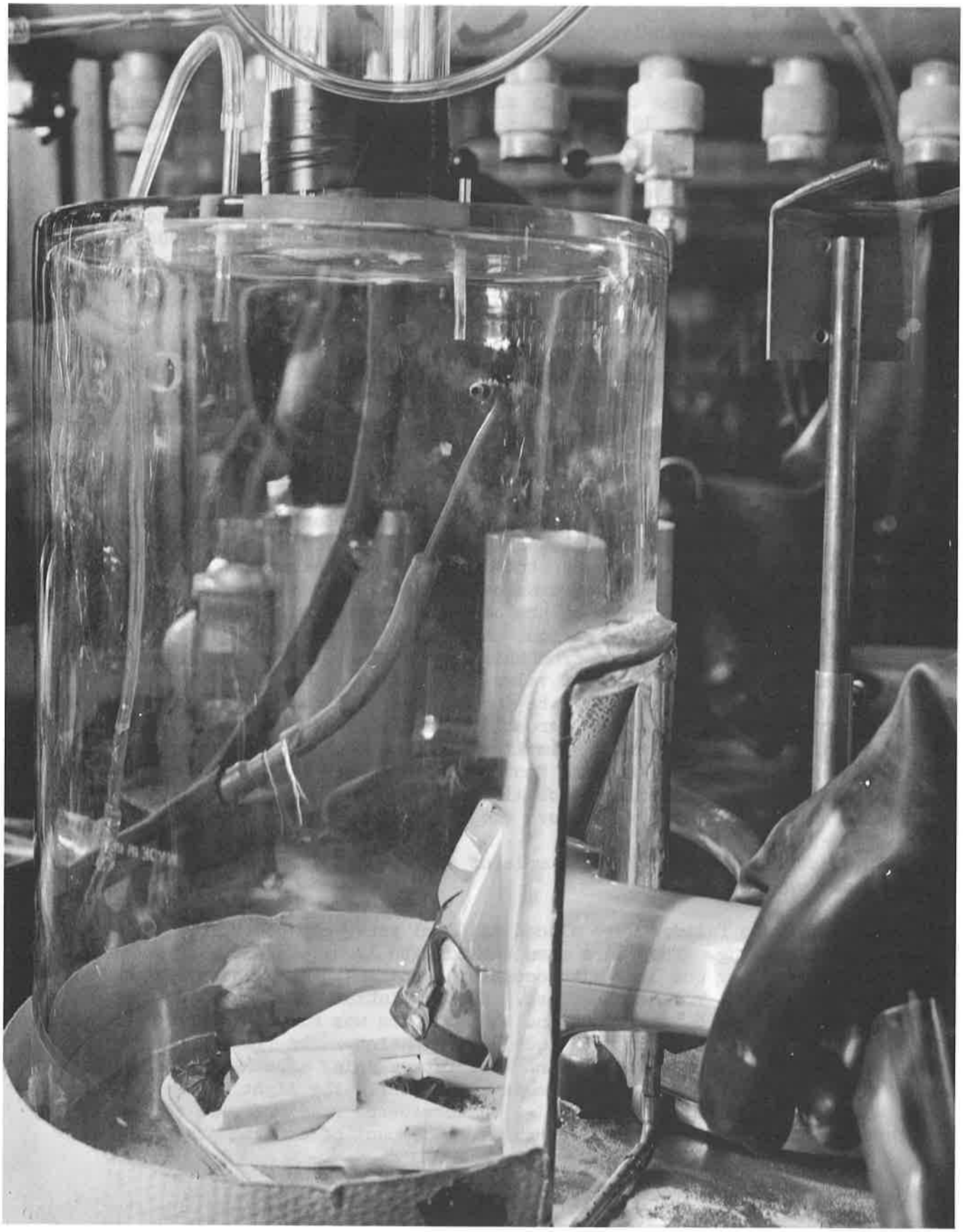

Figure 5. Plutonium Fume Test Apparatus - Photo

Brass screens were analyzed by dissolving them in nitric acid, and counting aliquots of the solution.

All sand samples were thoroughly mixed before analysis. Samples containing less than about 1.5×10^6 dpm/g were analyzed by counting a weighed aliquot (1.5 to 3 g) spread uniformly over a 2 inch diameter planchet in a zinc-sulfide alpha scintillation counter. Corrections for self-absorption were made by counting, under identical conditions, weighed samples of sand to which had been added known amounts of plutonium. Sand samples too active to be counted directly were diluted by weight with unused sand, mixed well, and counted as described above. Several sand samples of intermediate activity were counted directly and then by dilution to check this procedure.

Several methods were used to test the validity of the results. These included calibration of both types of counters with the same standard, duplication of each procedure and count, and the determination of plutonium in some sand and filter samples by counting directly and by counting of aliquots of the dissolved samples. On the basis of these tests it is believed that the accuracy of the analytical results at the 90% confidence level is $\pm 5\%$.

Uranine Aerosol Tests

Uranine tests were run with the same system used for the uranium fume tests, Figures 2 and 3, except that the lower horizontal portion of this apparatus was removed. Uranine aerosol was generated by a Pen-i-sol nebulizer containing a 0.5 percent by weight solution of uranine in water. The generating pressure was set at 10 psig. The output of the nebulizer was mixed with 2 cfm of dry cylinder air inside a 20 liter carton. A small diaphragm pump was used to pick up a portion of the air flowing from this carton and to force it through the sand column. A bleed off line and valve on the discharge side of the pump provided for regulating the flow rate through the sand column. Tests were also run with further dilution of the aerosol to simulate concentrations for in-place testing of the ZPPR roof. Sampling and data recording were as described for the uranium tests. At the one foot per minute flow rate, sampling time was increased to several hours to obtain amounts of uranine on the downstream Millipore sample that were well above the lower detection limit.

An electron microscope grid sample of the upstream aerosol was observed after each test.

The Millipore filters were placed in 50 ml screw-cap centrifuge cones using forceps for handling. They were then washed with 10 ml of deionized water and allowed to stand for one hour with occasional shaking. An aliquot was removed and added to a 10 ml volumetric flask. After dilution to volume 1 ml of phosphate buffer, pH 8, was added and the solution was mixed. A water blank and a reagent blank were run with each determination. The fluorescence of the solution was measured at constant temperature using a Beckman DU spectrophotometer equipped with a fluorescence attachment. The light filter system used was that recommended by C. Sill[3]. Fluorescence readings were compared to those of a standard curve to determine the amount of uranine present.

MATERIALS AND EQUIPMENT

All Tests

The sand used for these studies was from the Central Facility gravel pit at the NRTS in Idaho. The ANL Idaho Division supplied the sand as samples

meeting the specifications proposed for the ZPPR. The sand was washed and screened to a specification requiring 98% to pass through a 20-mesh screen and less than 2% to pass through a 50-mesh screen. As compacted in the columns the sand contained approximately 35% void space. Sand grains were irregular in shape.

Millipore filters were type AA, 0.8 micron pore size, from the Millipore Filter Corporation.

The electrostatic precipitator samplers were fabricated by our own group. One electrode consisted of an electron microscope grid mounted on the end of a brass rod. The opposing electrode consisted of a hypodermic needle positioned to provide a 1 inch gap. The two electrodes were supported opposite one another in either a glass or plastic cylindrical chamber and were connected to a Mine Safety Appliances Company's Model 48317 Electrostatic Sampler Power Supply.

Uranium Fume Tests

Most of the test system was fabricated of standard copper tubing and fittings with the joints soldered. See Figures 2 and 3. The sand column was 2 inches in diameter for the 29.5 inches of sand depth and 1 inch in diameter for the 6 inches sand depth. The glass burn chamber was made by butting and fusing together the glass ends of two Housekeeper type glass-to-copper seals. The entire system was assembled and tested for leaks at 13 psig using a soap solution.

The depleted uranium consisted of turnings about 0.001 inch thick by 0.015 inch wide.

Air was supplied from cylinders of dry compressed air.

Plutonium Fume Tests

The apparatus including the fume enclosure, the stacks, and sampling devices were all enclosed in a nitrogen atmosphere glove box. Pumps and flow measuring rotameters were located outside of the glove box. These were protected by Millipore filters placed at the connection of the equipment with respective sampling and system lines inside the box. See Figures 4 and 5.

The plasma torch was a Model SG-3 ADJ purchased from the Giannini Plasmadyne Corporation, Santa Ana, California. The plasma gas was argon.

The alloy used for generation of the fume was the 24.3% plutonium, 73.2% uranium and 2.5% molybdenum fuel proposed for the ZPPR. The fuel was ground in a helium atmosphere glove box and passed through a 200-mesh screen.

Uranine Aerosol Tests

The test system was essentially the same as that used for the uranium fume tests. The uranine (disodium fluorescein) was obtained from Eastman Organic Chemicals Company.

The Pen-i-sol nebulizer was a No. 211G obtained from the Hudson Oxygen Therapy Sales Company, 2801 Hyperion Avenue, Los Angeles, California.

A twenty liter cardboard container was used for mixing the aerosol and dry dilution air.

A DeVilbis Corporation's diaphragm pump, Model 501, was used to force the uranine aerosol into the test system under pressure.

RESULTS

Uranium Fume Tests

Figure 6 is an electron micrograph of an upstream sample of uranium fume. The magnification is shown by the 1 micron mark. This sample indicated a count median diameter of .07 micron and a standard geometric deviation of 2.5. The downstream sample of uranium fume for the same test after penetration through 6 inches of sand showed a similar but slightly smaller size composition.

Table 1 lists data and results from tests on 6 inches of sand. The percent penetration at various test velocities is plotted in Figure 7. Penetration ranged from .22 to 1.45 percent over the velocity range of 5 to 200 fpm. Penetration appears to peak at an intermediate velocity of around 60 fpm. Data and results for 29.5 inches of sand are given in Table 2 and the percent penetration versus velocity is shown in Figure 8. The highest penetration of .015 and .013% occurred at the lower test velocities of 1 and 10 fpm respectively.

Plutonium Fume Tests

Data and results from these tests are summarized in Table 3. Figure 9 is a plot of the penetration versus velocity for 6 inches of sand. Maximum penetration through 6 inches of sand appears to occur at about 60 fpm. The plot of penetration versus velocity for 30 inches of sand is shown in Figure 10. The maximum penetration result of .02% occurred at a velocity of 4.8 fpm.

Penetration by fume which had passed through preceeding 6 inch segments of sand ranged from about 13% in the second 6 inch segment to a maximum of about 84% in subsequent segments.

Penetration through 30 inches of sand followed by HEPA filter media ranged from $.002 \times 10^{-4}\%$ to $1.6 \times 10^{-4}\%$ with an average of $.63 \times 10^{-4}\%$ in four tests.

Penetration of HEPA filter media ranged from .006% to 1.4% with an average of .46% penetration by fume which had passed through 6 inches of sand in six tests and from .003% to .99% with an average of .40% penetration by fume which had passed through 30 inches of sand in four tests.

Upstream fume collected on electron microscope grids showed a high degree of agglomeration. However, there were also many discrete particles. Agglomerates ranged in length from .04 to 1 micron. Discrete particles ranged from .02 to .06 microns in diameter. Because of limitations placed on the alpha activity to be inserted in the microscope it was necessary to view many fields for particle size determinations.

Uranine Aerosol Tests

Table 4 lists data and results from tests to determine penetration through 29.5 inches of sand. A plot of the percent penetration versus velocity for these tests is shown in Figure 11. Penetration ranged from .0012 to .0052% and averaged .0029%. An average penetration of .0021% was found in three tests at one foot per minute, the velocity proposed for in-place

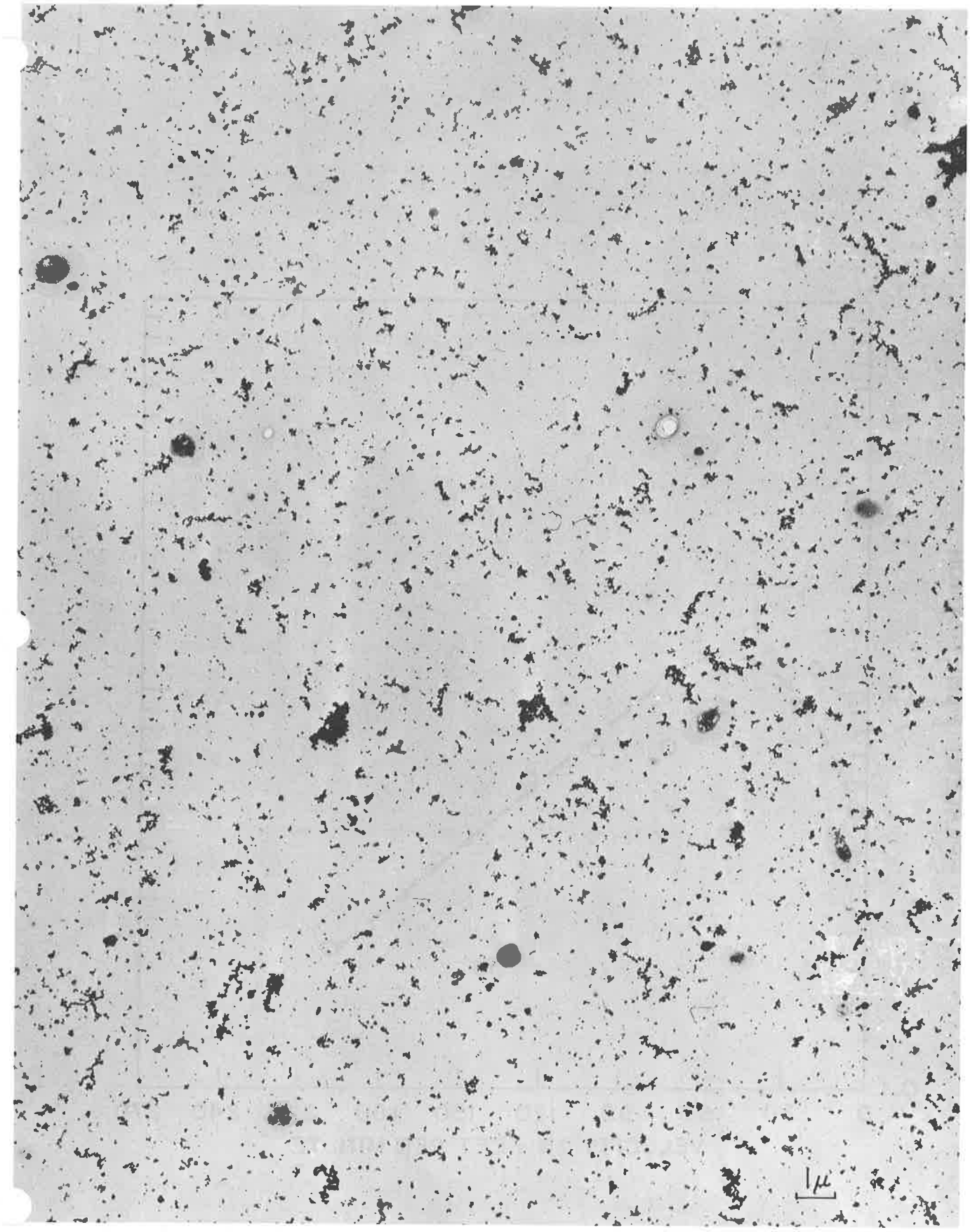

Figure 6. Uranium Fume - Electron Micrograph

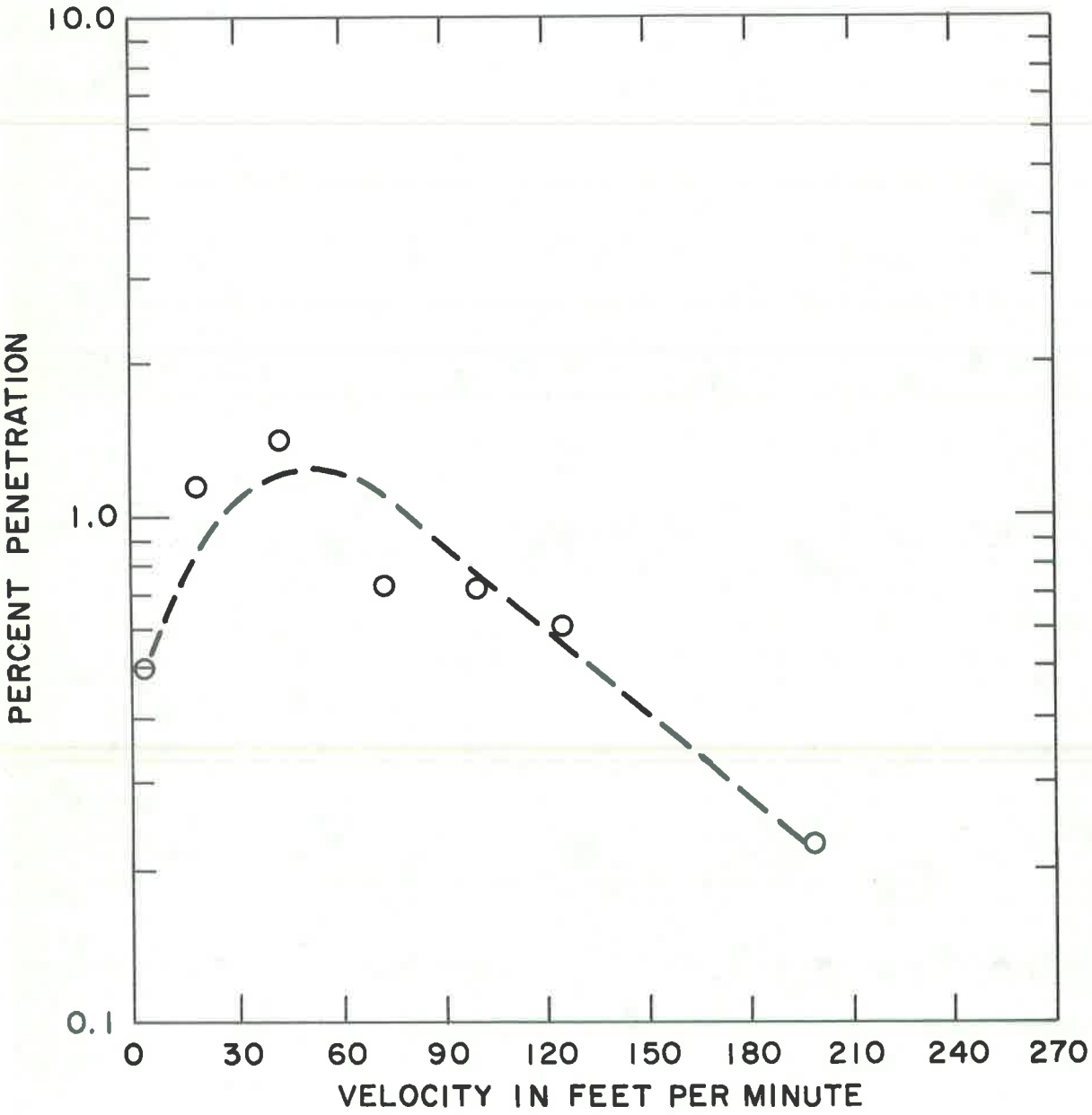

Figure 7. Uranium Fume Penetration vs. Velocity through 6 inches of sand

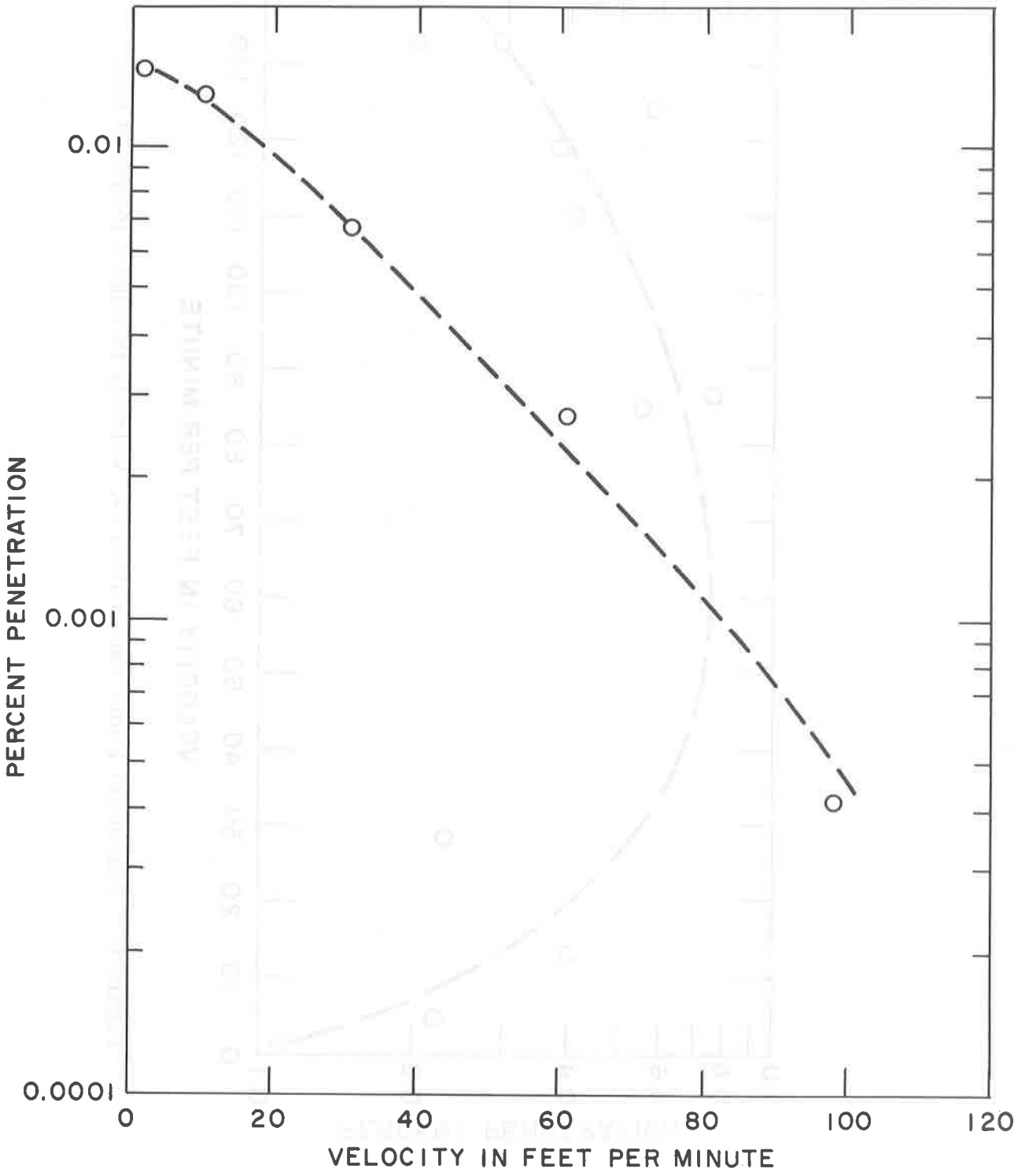

Figure 8. Uranium Fume Penetration vs. Velocity through 29.5 inches of sand

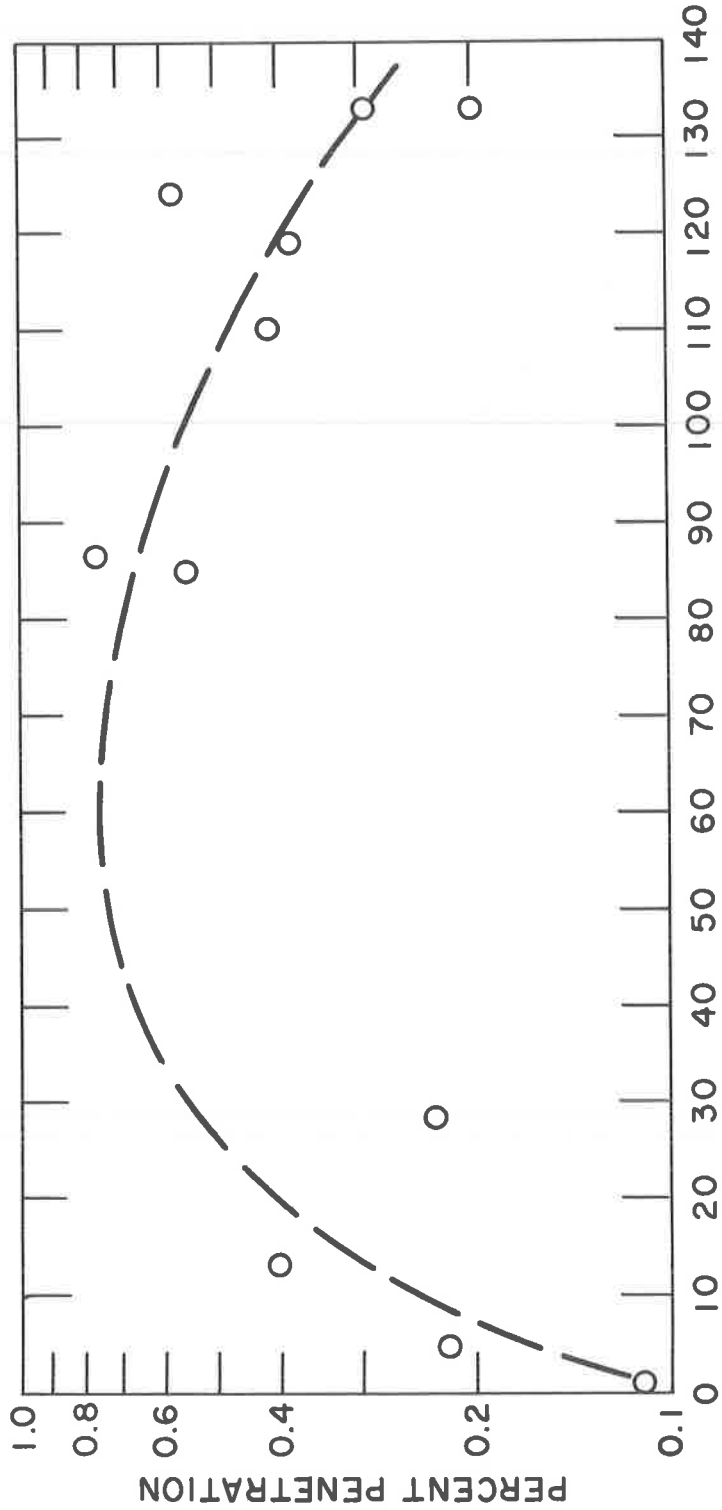

Figure 9. Plutonium Fume Penetration vs. Velocity through 6 inches of sand

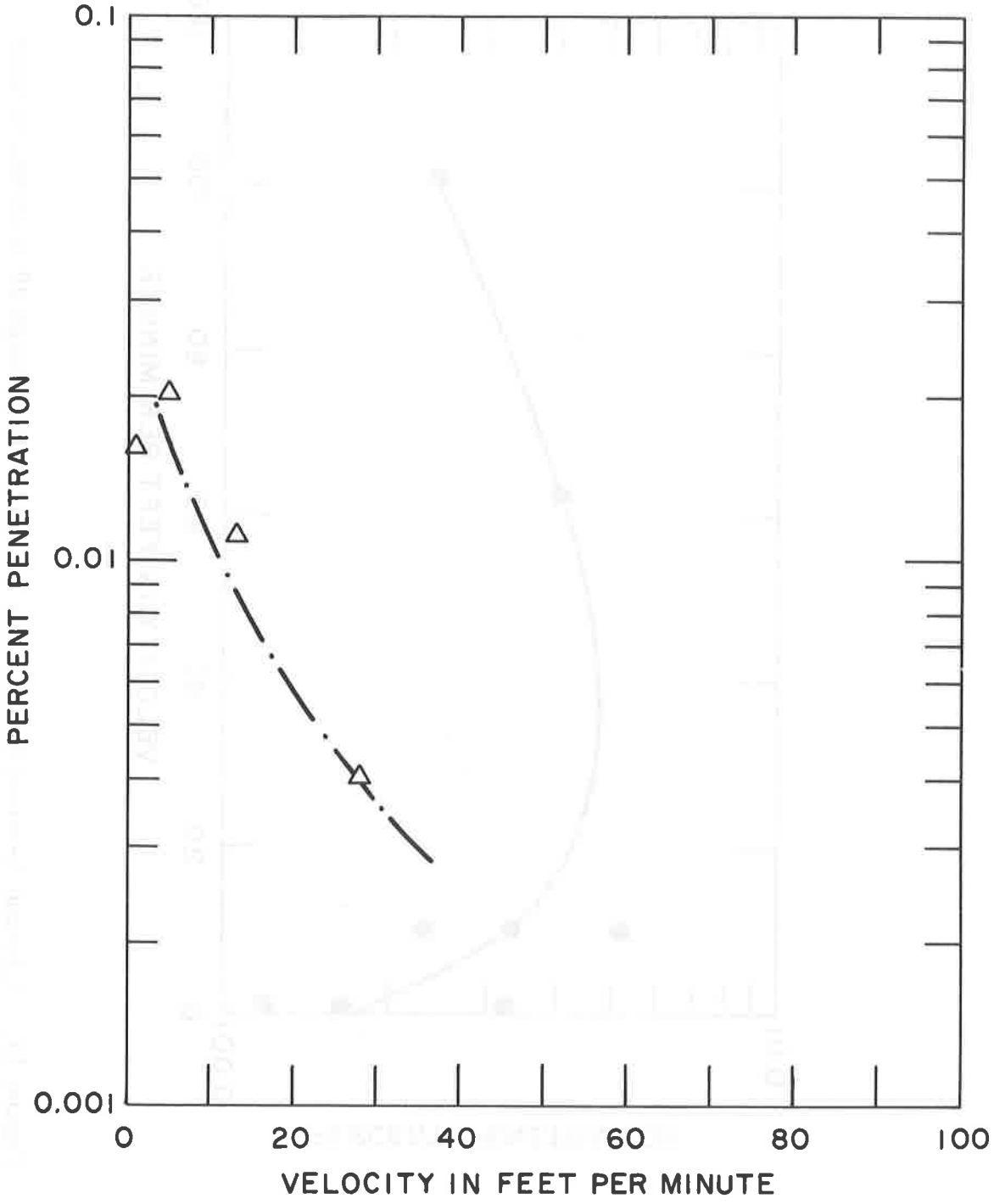

Figure 10. Plutonium Fume Penetration vs. Velocity through 30 inches of sand

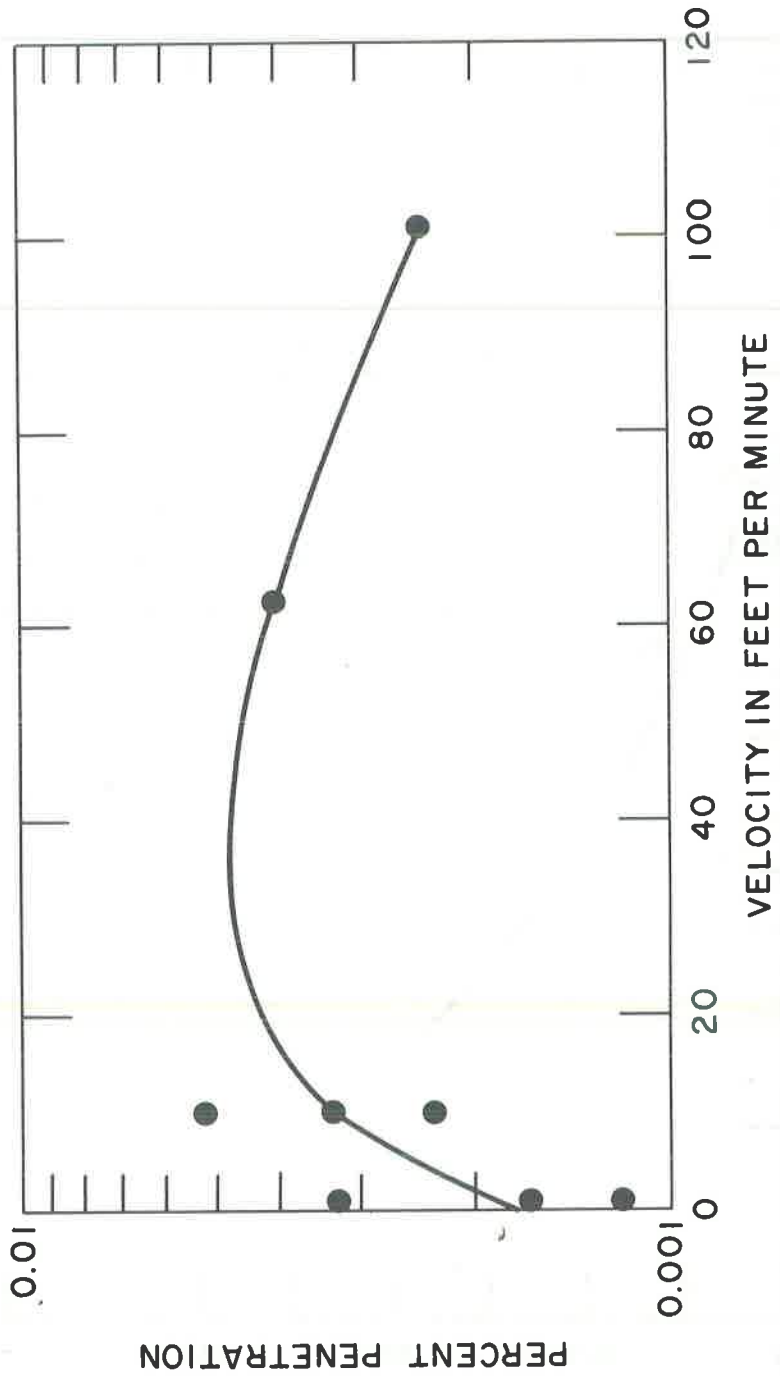

Figure 11. Uranine Aerosol Penetration vs. Velocity through 29.5 inches of sand

TABLE 1

URANIUM FUME TESTS: SIX INCHES OF SAND

Superficial Velocity, fpm	Pressure Drop Through Sand cm. Hg.	Upstream Concentration μg U/ft^3	Percent Penetration
5	.6	156	.50
20	2.3	102	1.16
43	5.2	100	1.45
72	8.4	38	.72
100	12.2	46	.72
125	16.5	44	.61
153	20.2	79	1.00
200	28.5	21	.22

TABLE 2

URANIUM FUME TESTS: 29.5 INCHES OF SAND

Superficial Velocity, fpm	Pressure Drop Through Sand cm. Hg.	Upstream Concentration μg U/ft^3	Percent Penetration
1.3	.7	303	.015
10.0	5.3	147	.013
30.5	15.3	249	.0069
60.8	31.1	386	.0027
98.0	48.2	678	.00042

TABLE 3

PENETRATION OF SAND BY PLUTONIUM FUME

Superficial Velocity, fpm	Upstream Concentration $\mu gPu/ft^3$	Percent Penetration of 6" Depth	Percent Penetration of 30" Depth
1	2,950	.11	.016
4.8	3,120	.22	.020
13.2	2,806	.40	.011
28.3	2,379	.23	.004
85.1	1,230	.55	----
86.5	1,234	.76	----
110	3,516	.41	----
119	1,335	.38	----
124	2,095	.58	----
133	2,291	.29	----
133	6,334	.20	----

TABLE 4

URANINE AEROSOL TESTS: 29.5 INCHES OF SAND

Superficial Velocity, fpm	Upstream Concentration $\mu g/ft^3$	Percent Penetration
1.0	452	.0033
1.0	200	.0012
1.0	345	.0017
10.0	25.7	.0052
10.0	21.6	.0033
10.0	160	.0023
62.4	15.7	.0041
101.0	204	.0024

testing of the sand and gravel roof.

An electron micrograph of a sample of upstream uranine aerosol is shown in Figure 12. The magnification is indicated by the one micron scale mark. Particle sizing from this sample indicated a count median size of .1 micron and a standard geometric deviation of 2.16. The calculated mass mean diameter was .59 micron.

DISCUSSION

The penetration versus velocity data for uranium fume and for plutonium fume showed close agreement. Penetration of uranine aerosol was within an order of magnitude of results obtained from the uranium and plutonium fume tests. These comparisons are illustrated in Figure 13 as a composite graph of penetration through a nominal 30 inches of sand versus velocity for the three test aerosols.

In both the uranium and plutonium fume penetration tests with 6 inches of sand the velocity for maximum penetration appeared to be near the middle of the test range, about 60 fpm. Penetration of these fumes through a nominal 30 inches of sand apparently peaks at the low end of the velocity test range. Though not well defined, this peak occurs between zero and 10 fpm. The shift of the maximum penetration to lower velocities for the increased depth of sand is believed to be due to a change in the relative importance of removal mechanisms as the particle size composition changes with passage through the sand.

We have plotted percent penetration versus velocity which was our controlled variable. However, we recognize that velocity was not the only variable as fume concentration and particle size composition of the fume were not constant.

In the uranium fume studies where a number of tests were run before changing the sand, the velocity testing sequence was staggered to prevent systematic bias of penetration versus velocity results by fume loading in the sand.

Uranine aerosol appears to be suitable for in-place testing of the ZPPR sand and gravel roof. It offers high sensitivity with fluorescence measurements down to 3×10^{-4} µg of uranine from a Millipore filter sample. Its hygroscopic nature is a drawback but it has been successfully used for in-place testing. Penetration of uranine aerosol at a superficial velocity of one foot per minute through a nominal 30 inches of sand was within an order of magnitude of that of uranium and plutonium fume. This provides a guideline for interpretation of in-place testing results.

CONCLUSIONS

1. Penetration of plutonium fume through the ZPPR accident filtration system should not exceed .0001%. Penetration of plutonium fume through the sand filter should not exceed .02%.

2. Uranine aerosol appears to be suitable for in-place testing of the ZPPR sand and gravel roof.

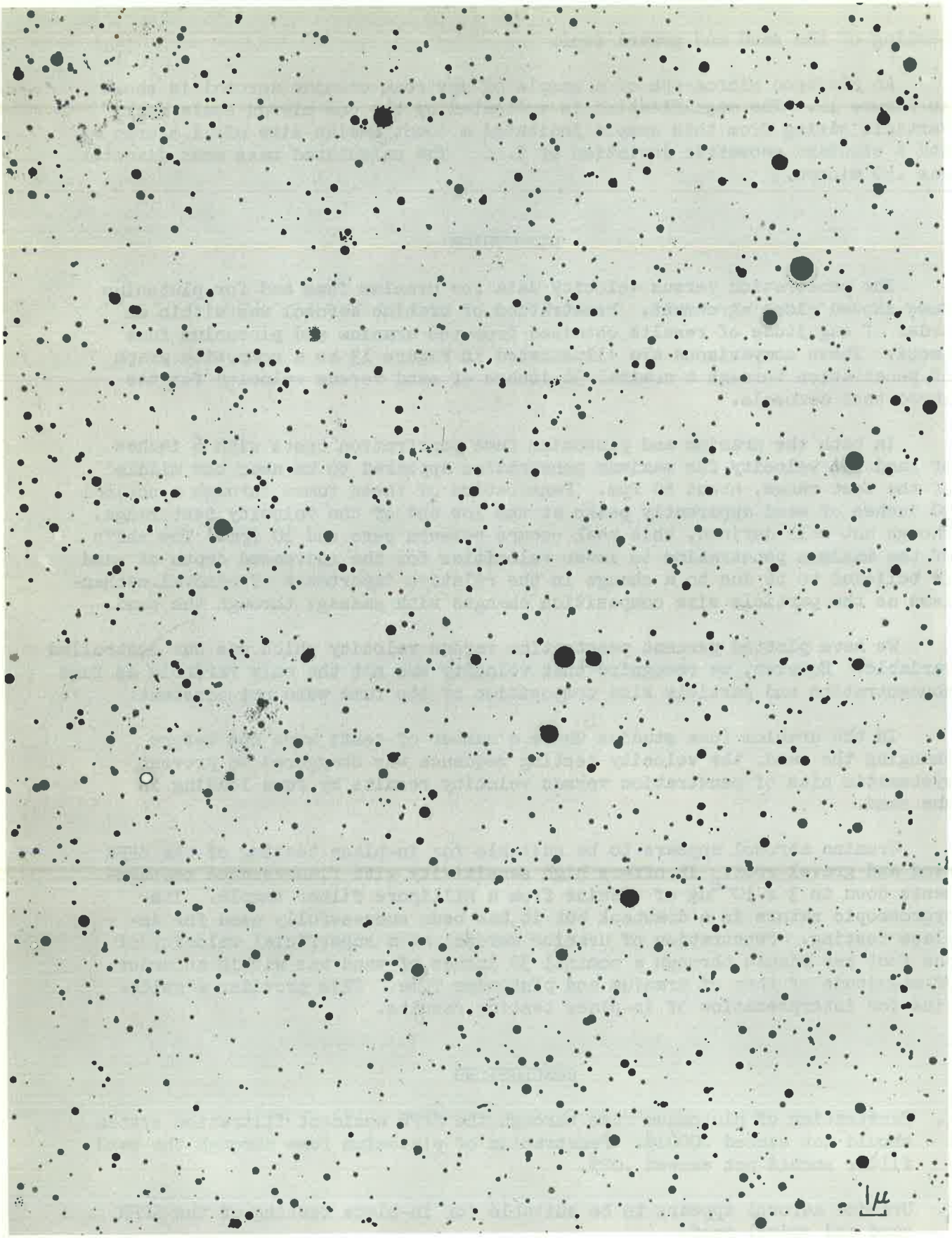

Figure 12. Uranine Aerosol - Electron Migrograph

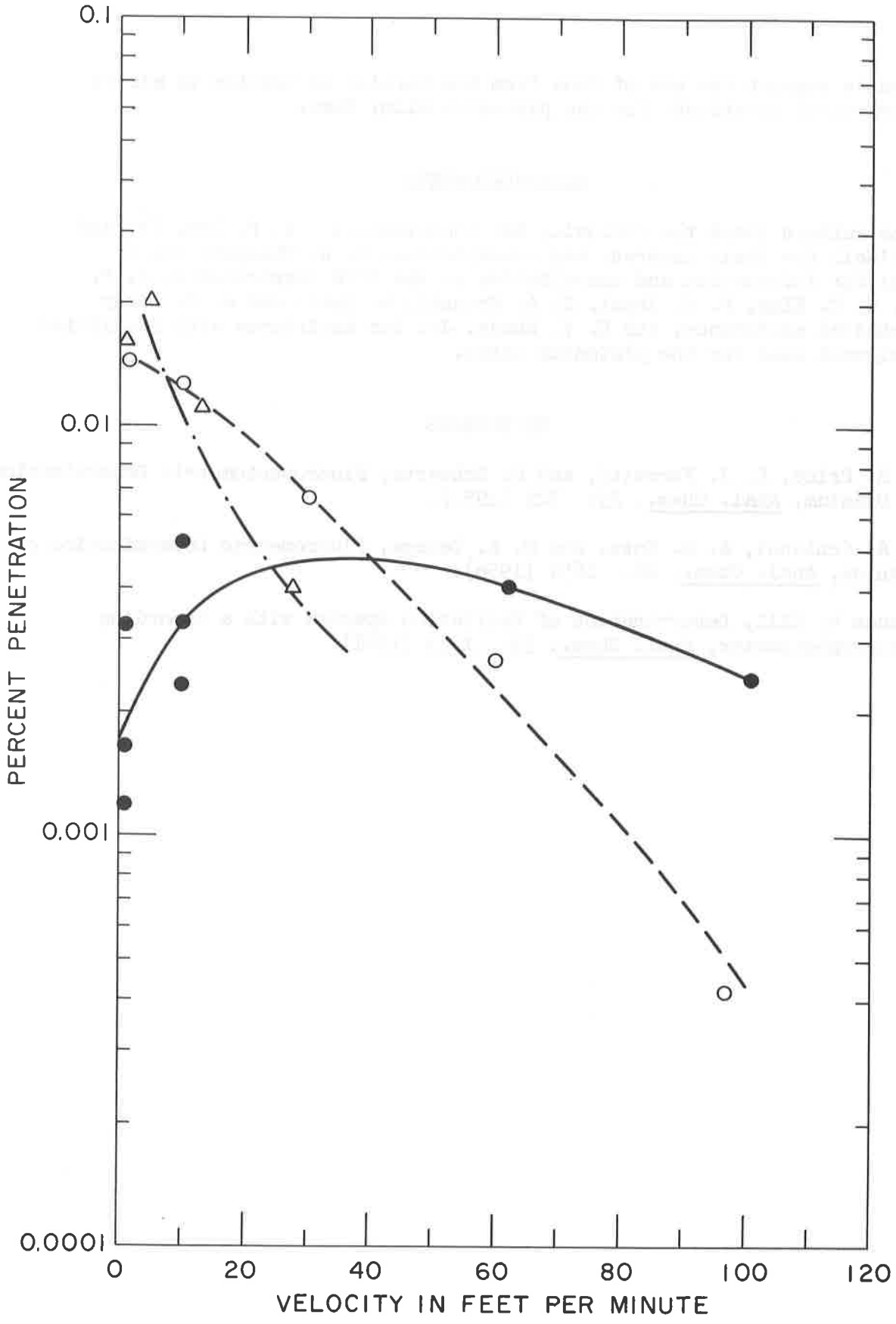

Figure 13. Composite of Uranium, Plutonium, and Uranine Penetration through nominal 30 inches of sand

3. Results support the use of fume from the burning of uranium in air as a practical substitute for the plutonium alloy fume.

ACKNOWLEDGMENTS

The authors thank the following ANL contributors: J. F. Ege, Jr. and D. P. O'Neil for their interest and consultation; F. W. Thalgott and H. Lawroski for information and consultation on the ZPPR requirements; R. P. Hetzel, G. C. King, F. S. Iwami, J. A. Wronski, M. Haas, and A. E. Lissy for technical assistance; and H. V. Rhude, Jr. for assistance with facilities and equipment used for the plutonium tests.

REFERENCES

1. G. R. Price, R. J. Ferretti, and S. Schwartz, Fluorophotometric Determination of Uranium, Anal. Chem., 25: 322 (1953).

2. F. A. Centanni, A. M. Ross, and M. A. DeSesa, Fluorometric Determination of Uranium, Anal. Chem., 28: 1651 (1956).

3. Claude W. Sill, Determination of Excitation Spectra with a Recording Spectrophotometer, Anal. Chem., 33: 1579 (1961).

THE DESIGN, TEST AND USE OF THE BROOKHAVEN NATIONAL LABORATORY (BNL) REACTOR BYPASS FILTER FACILITY*

R. O. McClintock
Health Physics Division
Brookhaven National Laboratory
Upton, New York

ABSTRACT

The purpose of the BNL Reactor Bypass Filter Facility is to provide improved air cleaning in the event of a fuel element failure at either the Brookhaven Graphite Research Reactor (BGRR) or the High Flux Beam Reactor (HFBR). It also provides sufficient air cleaning to allow the use of air cooling as a method of combating a graphite fire at the BGRR. For normal BGRR cooling, approximately 365,000 ft^3/min. is required. Although the filters provided are sufficient for normal operation, additional cleaning is required for fuel rupture and graphite fire situations. This system was therefore designed to accommodate 100,000 ft^3/min. with high filtering efficiency under emergency conditions.

The bypass filter facility contains ninety-six 24 in. x 24 in. x 11.5 in. absolute filters backed by a like number of activated charcoal filters. Each filter combination has a capacity of 1,000 ft^3/min. at a face velocity of 70 ft/min. with a pressure drop of less than 1 in. of water. Under normal operation the facility is closed off so that the cooling air passes directly to the stack. A description of the valving design and procedures will be presented.

Each filter unit was tested for both particulate efficiency and iodine retention. The particle efficiency test used DOP smoke and the iodine test was made using ^{128}I vapor. In-place tests were conducted using DOP and the radioactive effluent from the BGRR during a graphite annealing run. All tests showed the facility to be over 99.98% efficient for particle removal while at the same time removing 99.9% of the detectable iodine vapors.

*Research carried out at Brookhaven National Laboratory under contract with U.S. Atomic Energy Commission.

Introduction

The purpose of the Brookhaven National Laboratory's Reactor Bypass Filter Facility is to provide improved air cleaning in the event of a fuel element failure at either the Brookhaven Graphite Research Reactor (BGRR) or the High Flux Beam Reactor (HFBR). It also provides sufficient air cleaning to allow the use of air cooling as a method of combating a graphite fire in case one should occur at the BGRR.

The BGRR is an air cooled, graphite moderated, enriched uranium fueled research reactor. The reactor core consists of a graphite cube 25 ft. on a side constructed from over 60,000 individual pieces of graphite. The fuel elements each contain 15 grams of 93% enriched uranium. The fissionable material is a uranium-aluminum alloy slab covered on the top and bottom by aluminum sheets at least 20 mils thick with the edges welded all around. The reactor is cooled by air drawn through the core by three 1,000 hp. fans. The air is precleaned by glass fiber filters before passing through the core. The exit air then passes through deep pocket woven-glass fiber filters whose efficiency is only 80% for particulates in the 0.3 micron range and is released at the top of a 320 ft. stack.

Under normal conditions the present air cleaning is satisfactory. Although small amounts of radioactive contamination are generated in the cooling air by activation of impurities in the air, the levels produced fall well below the Radiation Protection Guides for both occupational and non-occupational situations. Extensive on and off-site monitoring programs at BNL indicated that about 25 curies of short half life particulate activity and 130 millicuries of ^{131}I are released per month from the reactor stack. Off-site environmental surveys[1] show that even under the worst meteorological conditions these releases will remain well below the Radiation Protection Guides.

Possible Reactor Accidents

Although the normal release of radioactive material to the environment is very low, an analysis of maximum possible reactor accidents

indicates the need for improved reactor air cleaning. A study conducted at BNL[2] postulated an accident which could involve a meltdown of up to four fuel elements and which could release as much as 400 curies of ^{131}I. Against assuming the worst possible meteorological conditions and assuming that no countermeasures were taken, this could conceivably result in a thyroid dose to humans in excess of 200 rads. Although countermeasures such as withholding milk from the public, selected temporary evacuation, etc., are planned, it was felt that an improved air cleaning capability was appropriate for upgrading control of airborne contamination.

A second possible accident involving the release of large amounts of radioactive materials is a graphite fire in the reactor core. Emergency procedures and equipment have been provided for shutting down the fans, blocking the graphite openings, and introducing carbon dioxide within the confined area[3]. Graphite oxidation and heat transfer studies conducted by the BNL Metallurgy Division have indicated that the most effective means of combating a graphite fire is by cooling the graphite with air[4]. Since the air can now be cleaned, air cooling of the graphite can be used as an emergency procedure for combating a graphite fire.

The second BNL reactor connected to the Bypass Filter Facility, the HFBR, is a D_2O cooled and moderated, enriched uranium fueled research reactor. As with the BGRR ordinary air cleaning is satisfactory under normal operating conditions. The building exhaust, 12,000 ft^3/min., comes mainly from the building air with smaller amounts from hoods, experimental facilities and process off-gas lines. The reactor itself is not connected to the building air exhaust except through a system which, during reactor depressurization, releases off-gases through two charcoal iodine filters to the building exhaust system. The building exhaust passes through a bank of absolute filters, silver-plated copper mesh iodine filters, and then up the reactor stack.

As with the BGRR, a review of potential accidents indicates that improved air cleaning would be beneficial. The maximum credible accident taken from the HFBR Safety Analysis Report[5], indicates that here too thyroid exposures in excess of 200 rad are possible. Again this assumes all equipment and procedures malfunction, no countermeasures are taken and the worst meteorological conditions prevail. Since these possibilities for accidents do exist, although the chance of their occuring seems very small, it is only prudent to improve the air cleaning capability in the event of a fission product release from either the BGRR or the HFBR.

Construction

The Bypass Filter Facility is located below ground to the east of the fan house, parallel to the BGRR air discharge duct (see Fig. 1). It is approximately equidistant from both reactors and next to the reactor stack. The building is constructed of reinforced concrete with a minimum wall thickness of 12 in. The roof is constructed of reinforced concrete with six removable covers over the filter racks. Access ports were provided to the filter area and all valves. Prefilter and postfilter sampling ports were installed in the system to facilitate the testing program.

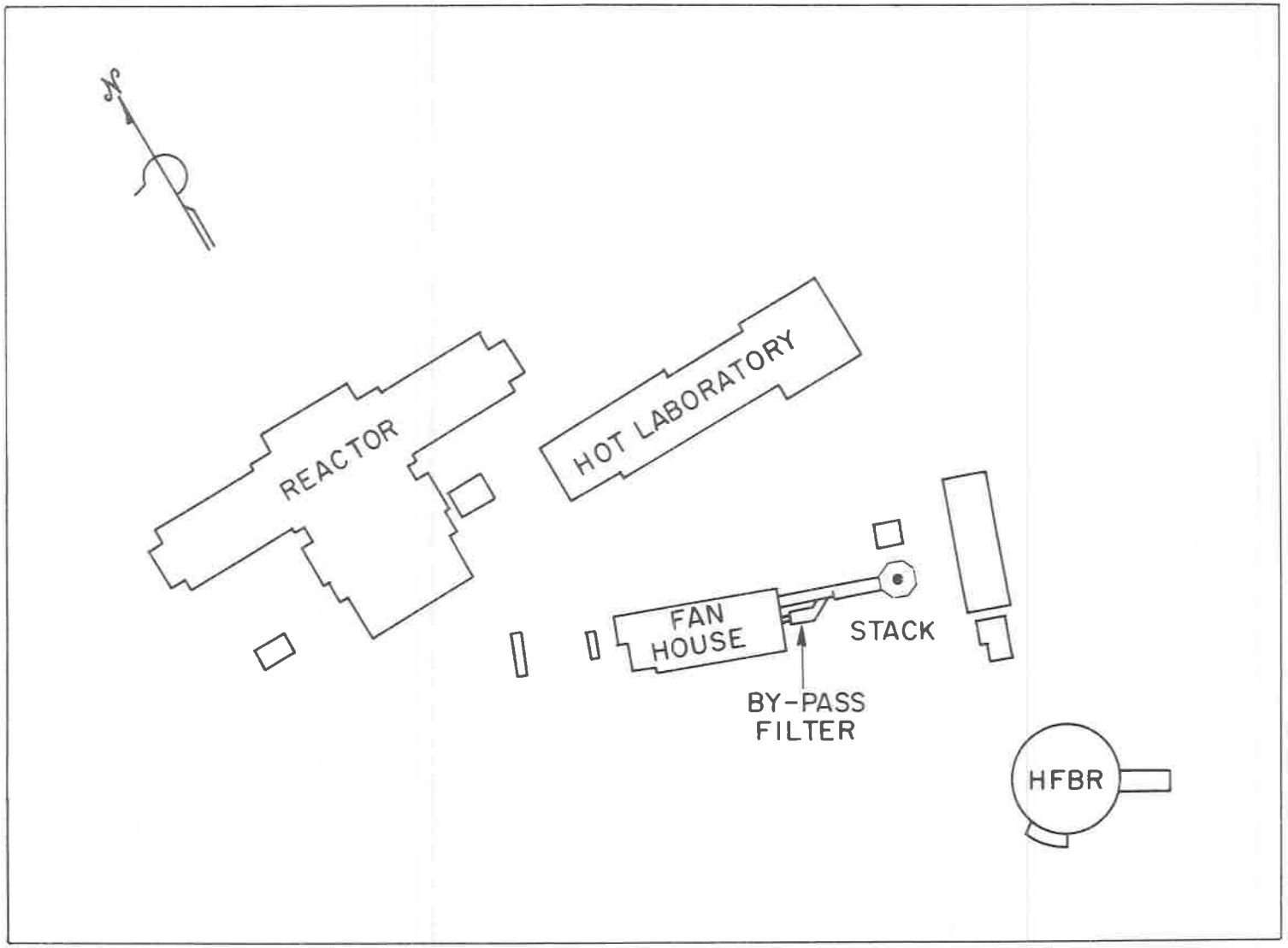
N
REACTOR
HOT LABORATORY
FAN HOUSE
STACK
BY-PASS FILTER
HFBR

FIGURE 1

The filter racks consist of ninety-six 24 in. x 24 in. x 11.5 in. absolute filters backed by a like number of activated charcoal filters. The facility is designed to filter approximately 100,000 ft^3/min., thus each filter combination has a capacity of 1,000 ft^3/min. The face velocity at each filter is 70 ft./min. with a pressure drop of less than 1 in. of water.

The absolute filters use cadmium-plated carbon steel frames bolted together with glass fiber membrane filter media. The carbon steel frames were used instead of wood frames for greater fire protection and to lower the cost of decontamination and waste disposal of the filter units if they become highly contaminated. The filters are of non-combustible material and were designed to withstand a surface pressure of 6 in. of water, and 75% relative humidity. All filter units are gasketed against steel framing, using a silicone rubber sealant. The charcoal filters for removing iodine are flow rated the same as the absolute filters and the filter medium is a hard, activated cocoanut shell carbon in natural grain form. The grain size distribution is from 0.039 in. to 0.131 in. with packing such that there are no straight-through holes. The frames are also cadmium-plated carbon steel with silicone rubber gaskets.

Construction of the facility presented no unusual problems although special care was taken during the installation of the filters themselves. Previous communications[6] have indicated that improper installation and filter damage during installation are the two important reasons for poor efficiency of a filter system. Therefore, each set of filters was set in place, individually tightened and visually inspected for damage. Only two filters showed visible damage after installation and these were removed, retested, and replaced.

Operation

The downstream duct (see Fig. 2) of the facility is connected to the reactor stack by means of an air expansion joint. The upstream BGRR connection is joined to a 48 in. diameter discharge pipe from the Number 5 BGRR cooling fan. The upstream HFBR connection is joined to a 30 in. diameter inlet air duct from the HFBR building exhaust line. Quick opening butterfly valves are installed at all connections.

During normal conditions valves Number 1 through 4, as seen in Fig.2, are closed and Number 5 is open. The Number 5 cooling fan is not operated at this time, the exhaust air from the BGRR passes through fans Number 1, 2 and 3. To filter the BGRR effluent valves Number 1 and 4 are closed, Number 5, 2 and 3 are open. Reactor cooling fans Number 1, 2 and 3 are turned off and Number 5 is turned on. To filter the HFBR effluent valves Number 1, 2 and 5 are closed and Number 3 and 4 are open. Reactor cooling fan Number 5 is turned off.

Filter Testing Program

A filter testing program was initiated to accomplish three purposes. First, the filters were to be individually tested by the manufacturer and by BNL after delivery to assure that all filters met specifications and that no damage was done in shipment. After installation any filters

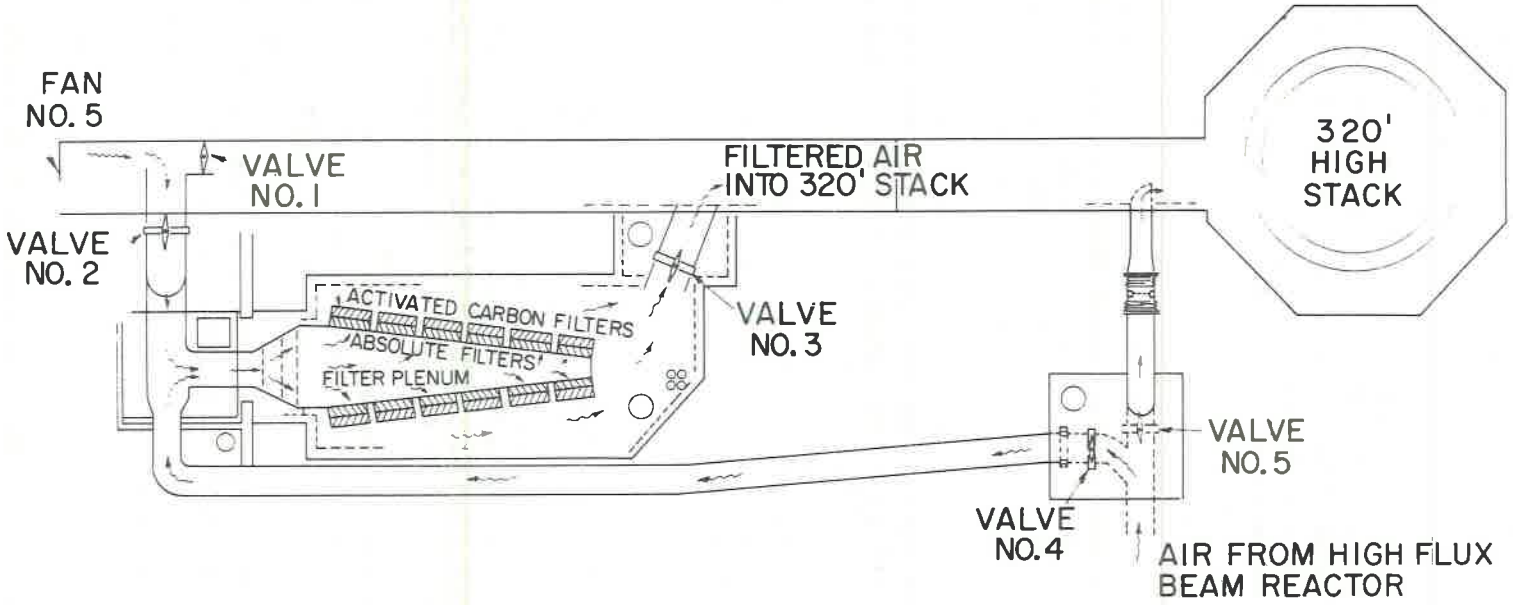

BYPASS FILTER FACILITY

FIGURE 2

showing signs of physical damage were to be retested and replaced if necessary. Second, the filters were to be tested in place periodically, to assure that the initial installation was satisfactory and to assure continued satisfactory system performance. Finally, from the above tests the efficiency of the system was determined to assist in emergency planning.

The manufacturer's test, to meet AEC specifications for filter efficiency, used standard DOP test aerosol methods, and the test for the activated carbon filters used chemical methods. Upon arrival at BNL, approximately 10% of the filters were tested using the equipment pictured in Fig. 3. Test methods and equipment are similar to those reported in previous Air Cleaning Conferences. The filters were placed in the system with special care to assure no leakage around the gaskets. Smoke was generated using BNL-fabricated Model II NRL-type DOP smoke generators. Baffle plates were installed in the system to assure complete mixing of the smoke, and sample ports were located to allow sampling over any portion of the filter. The smoke was drawn through the filter using a 1,000 ft^3/min. blower fan. Finally the smoke was measured using an aerosol photometer. All filters tested were 99.98% efficient or better.

Approximately 10% of the charcoal filters were tested using the same test stand. After the filter was in place one-half gram of stable iodine was irradiated in the BGRR pneumatic tube facility. The resultant ^{128}I was vaporized in the filter test stand using the same mixing conditions used during the DOP test. Prefilter and postfilter samples were taken by drawing 1 ft^3/min. through two small charcoal traps. These traps were then counted on a 100 channel analyzer and the relative sizes of the 0.45 MeV ^{128}I peaks were compared. The results in all cases showed 99.9% of the detectable iodine vapors were removed. It is recognized that some small error is introduced by using a sample collection medium that is the same as the filter medium. The tests did, however, prove the filters were uniformly good with no leaks and will be used as a basis for comparison with future tests. It is also interesting to note that several silver-plated copper mesh filters of the same size, which are also used at other installations at BNL for removing iodine, were tested using the same procedure. The results indicated only 94% to 97% removal of the detectable iodine vapors .

After installation the filter system was tested for the removal of particulates and iodine vapor. This test was conducted during a BGRR annealing run. The purpose of these runs is to heat up the reactor and cause a controlled release of Wigner energy[7]. To do this the air cooling on the reactor is cut back and valved through the bypass filters. During these runs approximately 100 millicuries of particulate contamination and radioactive iodine vapors are produced in the air stream. Although these amounts are small, they were large enough to be used to test the filters. Prefilter and postfilter samples were drawn through a Millipore absolute filter and a charcoal trap at a rate of 1 ft^3/min. The samples were then counted and compared. The results showed greater than 99.98% removal of the detectable particulate contamination and 99.9% of the radioactive iodine vapors.

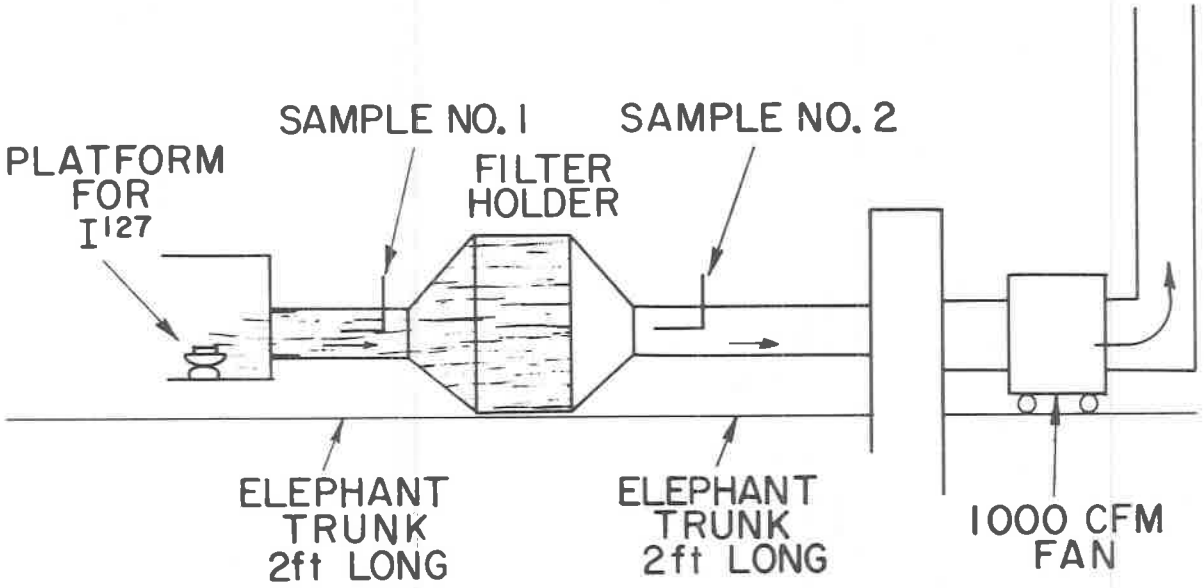
PLATFORM FOR I127
SAMPLE NO. 1
FILTER HOLDER
SAMPLE NO. 2
ELEPHANT TRUNK 2ft LONG
ELEPHANT TRUNK 2ft LONG
1000 CFM FAN

FIGURE 3

Summary

Although the facility has been in operation for over a year there are no significant operational data to report. Since its installation the Bypass Filter Facility has been used only for two routine operations, the HFBR fuel discharging and BGRR anneal. Even in these cases it was used for an emergency safeguard rather than for air cleaning. Although there has not been, and hopefully will never be, any emergency need for the facility, it has allowed the Reactor Division to improve their procedures and thus produce more effective emergency planning.

References

1 A. P. Hull, "1963 Environmental Radiation Levels at Brookhaven National Laboratory", Report BNL-915, May 1964

2 A. P. Hull and M. E. Smith, "An Evaluation of the Environmental Significance of a Postulated Fuel Element Failure Incident at the Brookhaven Graphite Research Reactor", Report BNL-819, August 1963

3 "BGRR Operations Procedures Manual", Chapter III, p. 26-8, Brookhaven National Laboratory, July 1964

4 D. G. Schweitzer, G. C. Hrabak, R. M. Singer, "Oxidation and Heat Transfer Studies in Graphite Channels", Vols. I, II, III, IV, and V, from the Proceedings of the Fifth Conference on Carbon, 1962

5 "Final Safety Analysis Report on the Brookhaven High Flux Beam Research Reactor", Report BNL-7661, p. 14-1 to 14-58, April 1964

6 E. C. Parrish, Oak Ridge National Laboratory, personal communication, 1963

7 M. Fox, and R. W. Powell, "The Annealing of the Graphite Moderator Structure in the BNL Reactor", Report BNL-275, January 1954

CONTINUOUS SAMPLER-MONITOR

FOR FISSION PRODUCTS IN CONTAMINATED ATMOSPHERES

R. E. Schindler
Idaho Nuclear Corporation

ABSTRACT

The Continuous Sampler-Monitor is being developed for use in sampling fission product concentrations in the containment building atmosphere during the Loss of Fluid Test. A spray scrubber, placed in the containment atmosphere, washes nearly all of the iodine and other condensible fission products from a continuously drawn atmosphere sample leaving essentially only rare gas fission products in the gas stream. The gas and liquid streams then flow outside the containment building for separate monitoring of their gross gamma activity.

A Continuous Sampler-Monitor (CSM) is being developed for use in sampling the containment building atmosphere to determine the fission product concentrations during the Loss of Fluid Test (LOFT). The CSM, for which a schematic flowsheet is shown in Figure 1, uses a scrubber located in the containment building to sample continuously the atmosphere and to separate the fission products into two streams which flow separately through the containment wall to radiation monitors and samplers located outside the building. The scrubber, located in the containment atmosphere to avoid problems with fission product plateout on long sampling lines, washes nearly all of the condensible fission products out of the atmosphere sample into a liquid stream, leaving essentially only rare gas fission products in the gas stream. The scrubbing of the atmosphere sample allows the condensible and ingestible fission products - primarily iodine - to be monitored apart from the more active but less hazardous (less ingestible) rare gases. The radiation monitors and sampling stations are located outside the containment building where the background radiation is moderate and the equipment is accessible. Gross gamma monitors on each sampling line will provide a continuous record of the gross condensible and rare gas fission product activities in the containment atmosphere. Samples

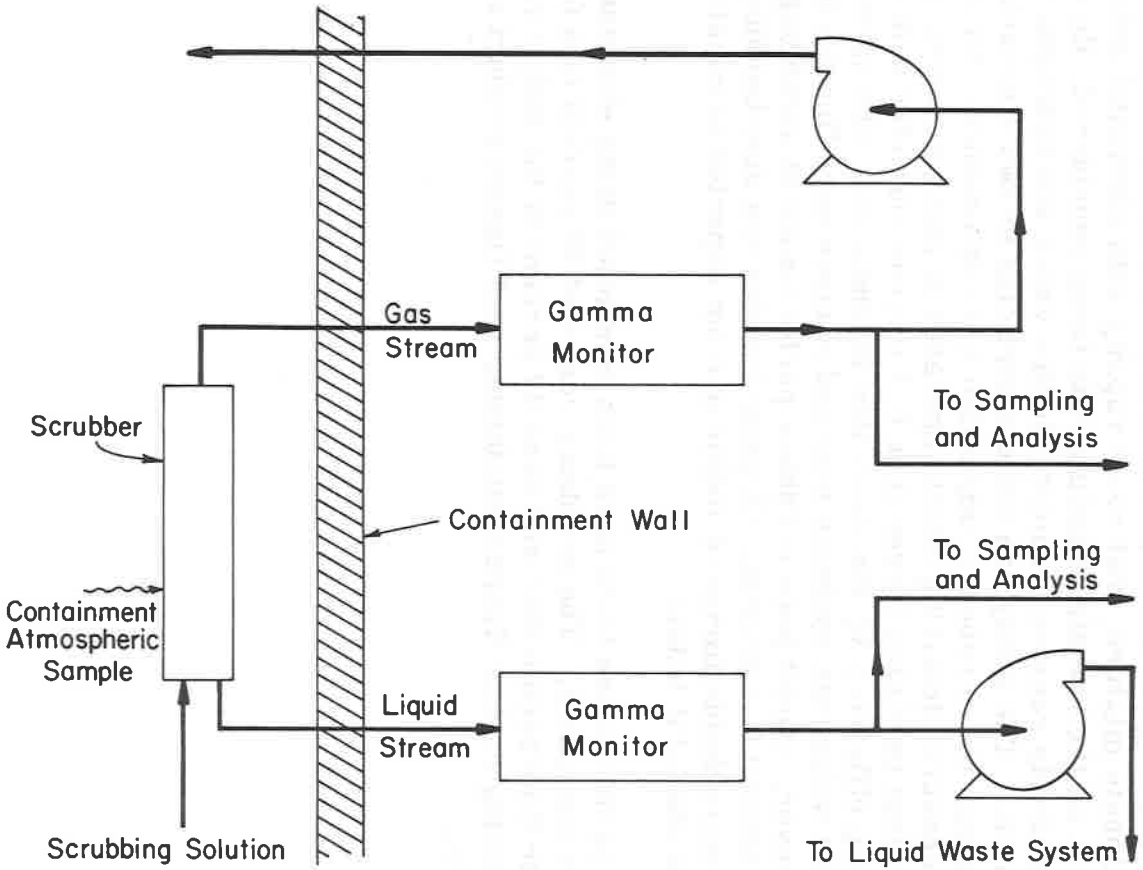

Figure 1

CONTINUOUS SAMPLER-MONITOR

SCHEMATIC FLOW SHEET

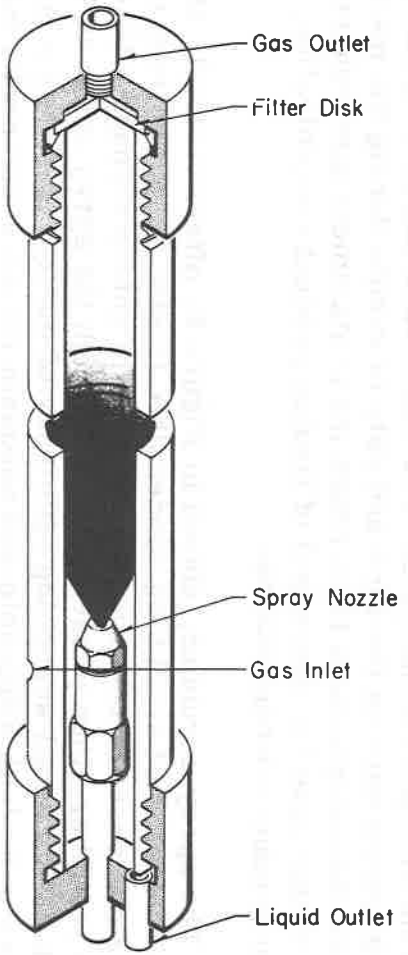

Figure 2

SPRAY SCRUBBER

taken from each stream will be analyzed for the major isotopes using spectrum stripping techniques. The Continuous Sampler-Monitor will provide useful data on the time and rate of events during the meltdown - the time fission products first reach the containment atmosphere, the rates of increase (or decrease) of fission product concentration, and peak fission product concentrations.

The spray scrubber, shown in Figure 2, offers a simple and potentially effective means of scrubbing condensible fission products from the containment atmosphere. The atmosphere sample enters through a hole in the side of the scrubber, then passes upward through the spray and a de-entrainment device. An overall scrubbing efficiency of ninety percent is a goal which appears to be both attainable and adequate for scrubber performance.

Iodine, the fission product of greatest concern, can be released in at least four forms: elemental iodine vapor, hydrogen iodide, organic iodides, and adsorbed on particulate matter. There are several solutions, such as a caustic thiosulphate mixture, that react rapidly with elemental iodine and hydrogen iodide. At the low air sampling rate being considered, these solutions quantitatively remove elemental iodine vapor and hydrogen iodide from an air sample. The spray can collect particles by two mechanisms as they pass through the scrubber: impaction and coalescence. By using a small swirl pressure atomizing nozzle operated at high pressure, the scrubber can collect particles larger than 0.3 micron diameter with the desired scrubbing efficiency by the impaction mechanism. The spray also forms a fine mist which can coalesce with and remove very fine particles. One would, however, expect poor scrubber performance in scrubbing particles with diameters around 0.1 micron. Organic iodides are also troublesome; however, the unscrubbable forms of iodine are not expected to constitute a large fraction of the total iodine.

Scrubber performance tests have been conducted using elemental iodine vapor and fluorescein dust. The scrubber removed 98 percent of a 0.55 micron diameter fluorescein dust and over 99 percent of the iodine vapor. Tests are continuing on fine fluorescein dusts, real fission product releases, and methyl iodide.

DISCUSSION

THOMAS: Are you going to use impregnated charcoal to take care of the iodide problem?

McCLINTOCK: The iodine filters as installed do not contain the impregnated charcoal. The bypass facility was completed before the magnitude of the methyl iodide problem was apparent. Impregnation of the charcoal will be considered.

THOMAS: Well, probably somebody has to say whether or not the impregnation is worthwhile. To me, it looks like it is worthwhile.

FULLER: Do you have a regular program of testing your system? You mentioned only exercising it two times in one year, of testing the valves and the functioning of the system.

McCLINTOCK: We pre-test it, and test for iodine removal and DOP on an annual basis. The mechanical operation of the system is tested on a monthly basis.

THAXTER: If I heard you correctly, you spoke of 25 curies per month release as a maximum. Is that under normal operating conditions?

McCLINTOCK: Yes.

THAXTER: To what kind of activity are you referring?

McCLINTOCK: Well, there are two types. The majority is the activity of impurities in the air stream from smoke and dust, et cetera, and then there is a small amount of fresh fission product activity that comes from surface contamination on the fuel element.

We have fairly strict surface contamination specifications down to 1 microgram per square foot. Even these small amounts will allow this kind of monthly activity on the stack, when you are talking about the large amount of fuel element surface area presented to the cooling air flow.

THAXTER: What happens to the argonne-41?

McCLINTOCK: There are 14,000 curies a day of argonne-41 going out the stack. I was talking about the short-lived particulate and the iodine activities.

KEIGHER: I have two questions. First, I assume you prefer to buy metal frame filters for fire protection. Were these filters purchased before the listing available in January 1965?

McCLINTOCK: Yes; this was three years ago.

KEIGHER: Secondly, did these filters go through one of the AEC filter testing stations?

McCLINTOCK: No; they did not. We did our own testing in the laboratory and in place.

FILTER TESTING PROGRAM

ATOMIC ENERGY OF CANADA LIMITED

by

F. Panchuk and W. Rachuk
ATOMIC ENERGY OF CANADA LIMITED
Chalk River Nuclear Laboratories
Biology and Health Physics Division
Radiation and Industrial Safety Branch

ABSTRACT

At the Chalk River Nuclear Laboratories air exhausted from equipment, systems and areas which may act as sources of air-borne radioactive particulate matter is cleaned with high-efficiency particulate air filters.

A program of checking the integrity of filters and filtration systems was initiated in 1964. The basic equipment and technique used are those developed by the U. S. Atomic Energy Commission, the U. S. Naval Research Laboratory and the Oak Ridge National Laboratory.

The filter test rig and mobile equipment fabricated for laboratory and field use at Chalk River Nuclear Laboratories are described as are typical filter installations. The tests themselves are described and the results are summarized. Field tests have shown that the performance of the self-contained filters commonly in use at Chalk River Nuclear Laboratories has been excellent. However, with open faced filters, unless the installation was carefully designed and maintained, excessive penetration could occur.

1. INTRODUCTION

In 1964 a filter testing program was initiated by the R.&I.S. Branch at the Chalk River Nuclear Laboratories of Atomic Energy of Canada Limited. Prior to that time high-efficiency particulate filters were not tested either as received or in place and operating. Samplers were used at exhaust stacks and outlets to measure releases of radionuclides to the atmosphere and this was the only check made on the effectiveness of air cleaning systems.

When the feasibility of conducting in-place filter tests was established by the Oak Ridge National Laboratory, it was decided to establish a filter testing program at the Chalk River Nuclear Laboratories. It was also decided to use equipment and techniques developed jointly by the United States Atomic Energy Commission, the Oak Ridge National Laboratory, and the United States Naval Research Laboratory.

All filters are now tested before installation and filtration systems with filters in place are tested periodically.

Two years of testing show that:

1. defective filters are found on pre-installation tests;
2. filtration systems using self contained filters show excellent test results;
3. many systems using open faced filters do not have the filtering efficiency required.

2. HIGH EFFICIENCY PARTICULATE FILTERS

High efficiency particulate air filters provide a minimum filtering efficiency for 0.3 micron size particles of 99.97% when no damage or manufacturing defects are present. They are specified

at the Chalk River Nuclear Laboratories for all ventilation exhaust systems serving radioactive or potentially radioactive areas.

In addition, high-efficiency particulate air filters are used on decontamination vacuum cleaners.

Figures 1 to 7 inclusive illustrate some of the models in use at the Chalk River Nuclear Laboratories.

3. DESCRIPTION OF THE TEST

The test consists of passing a poly-disperse liquid aerosol of dioctyl-pthalate (DOP) through the filter or filtration system. The efficiency is calculated from the concentrations of particles measured upstream and down stream of the filter(s) with a forward light scattering photometer.

The filtering efficiency is determined as follows:-

$$\text{Filtering Efficiency} = 100 - \left\{\frac{C_2}{C_1} \times 100\right\} \text{ per cent}$$

Where C_2 = concentration of particles downstream

C_1 = concentration of particles upstream

This test only approximates the test performed by filter manufacturers as the particle size is not controlled and therefore is not monodisperse. The aerosol generator used was developed by the United States Naval Research Laboratory who found that true monodispersions are not required to ascertain filter performance. Imperfections, damage or by-pass leakage result in penetration which is generally so much greater than penetration of the actual filter media that a closely controlled particle size is not essential.

4. BASIC EQUIPMENT REQUIRED

The basic equipment required for conducting tests

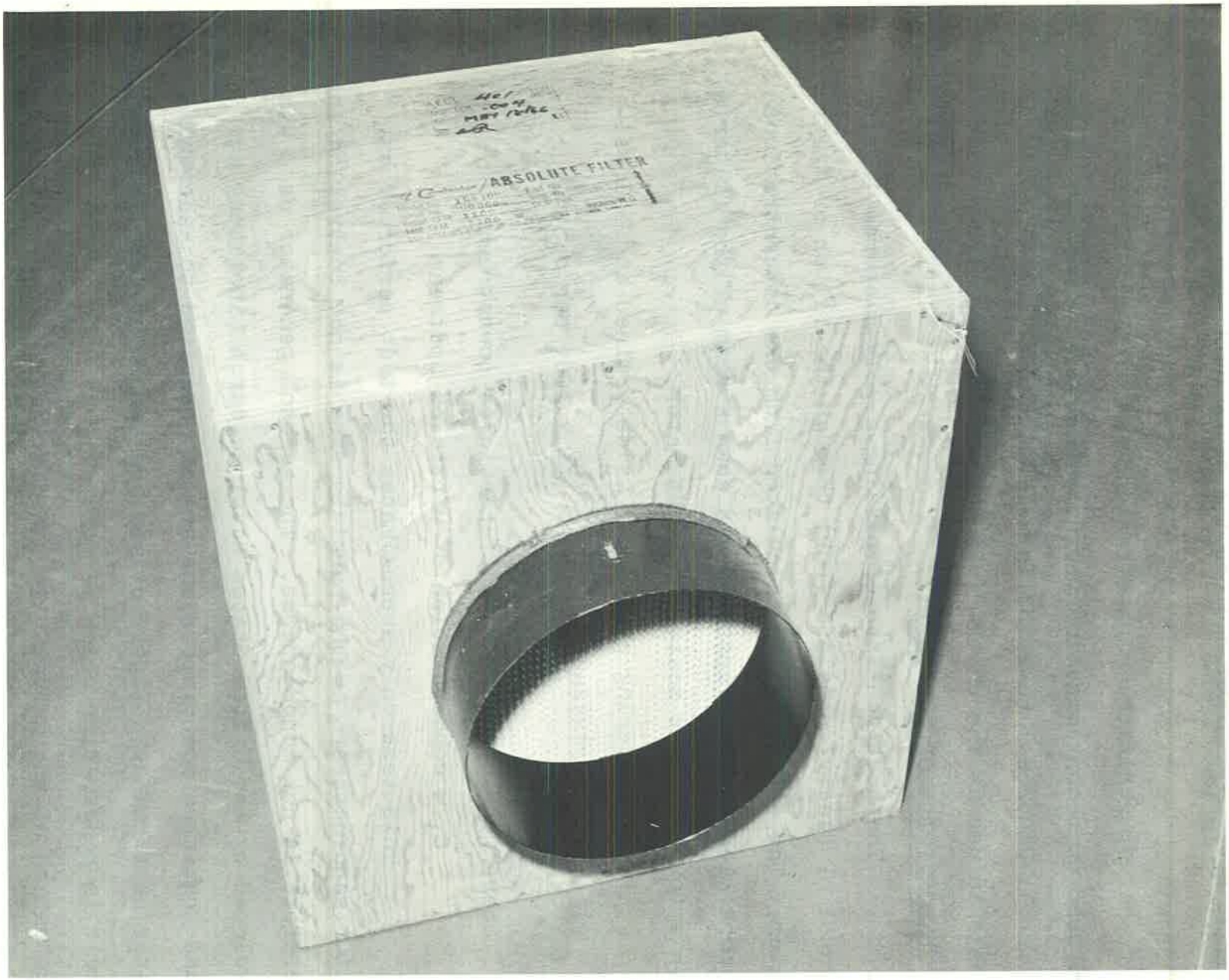

FIG. 1

Self Contained 1000 cfm High-Efficiency Particulate Air Filter

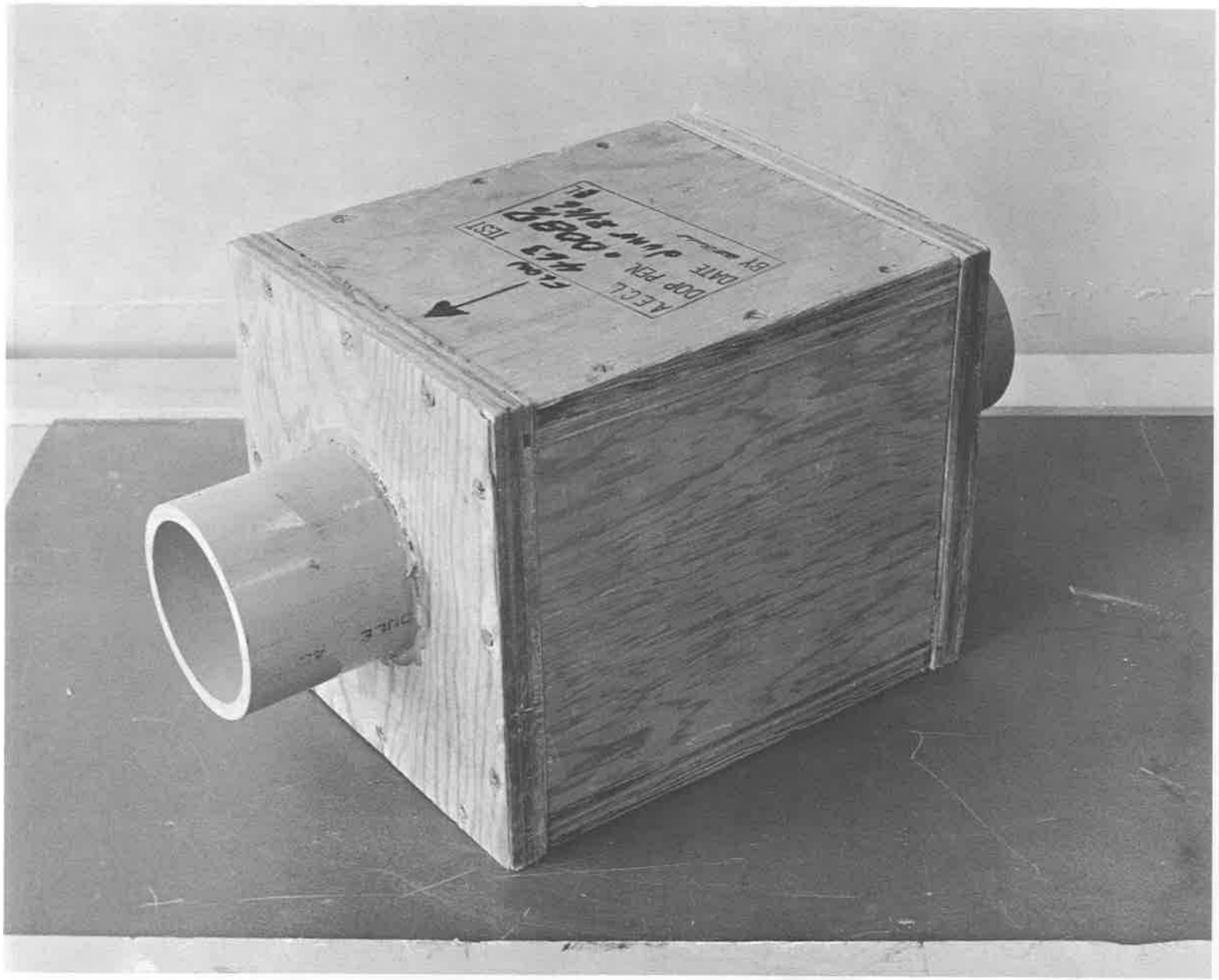

FIG. 2

Self Contained 25 cfm High-Efficiency Particulate Air Filter

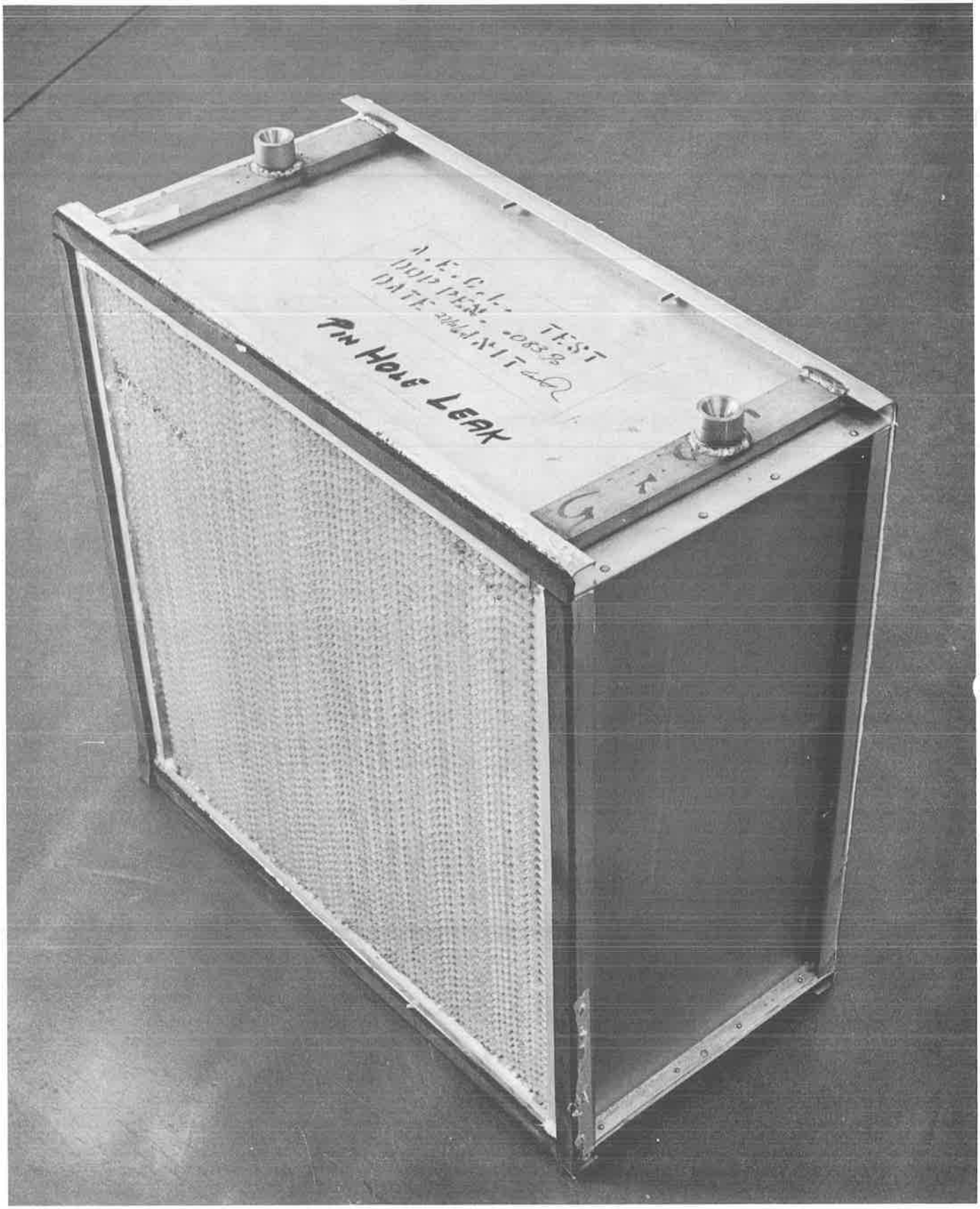

FIG. 3

Open Faced 1000 cfm Fire Resistant High-Efficiency Particulate Air Filter

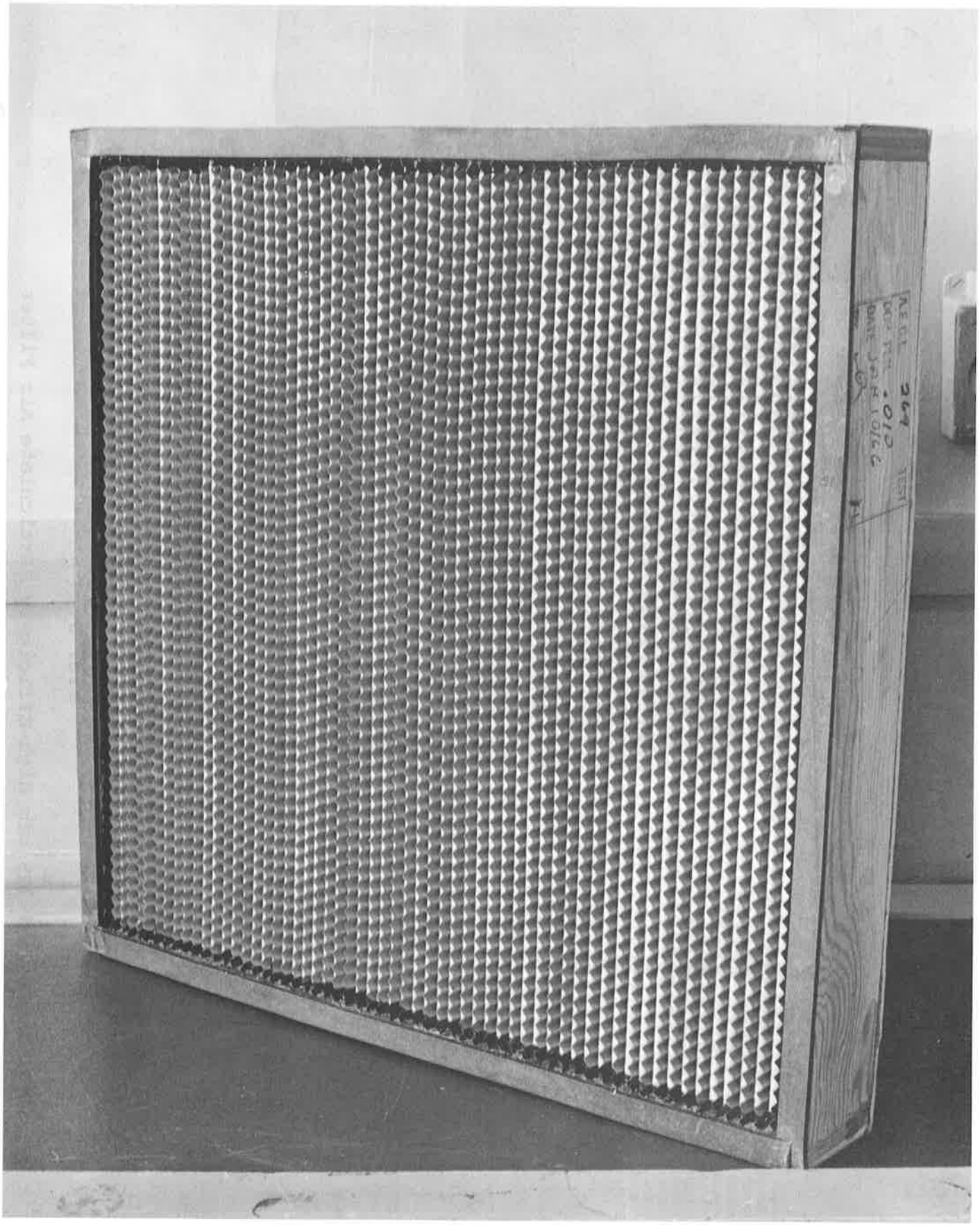

FIG. 4

Open Faced 250 cfm High-Efficiency Particulate Air Filter

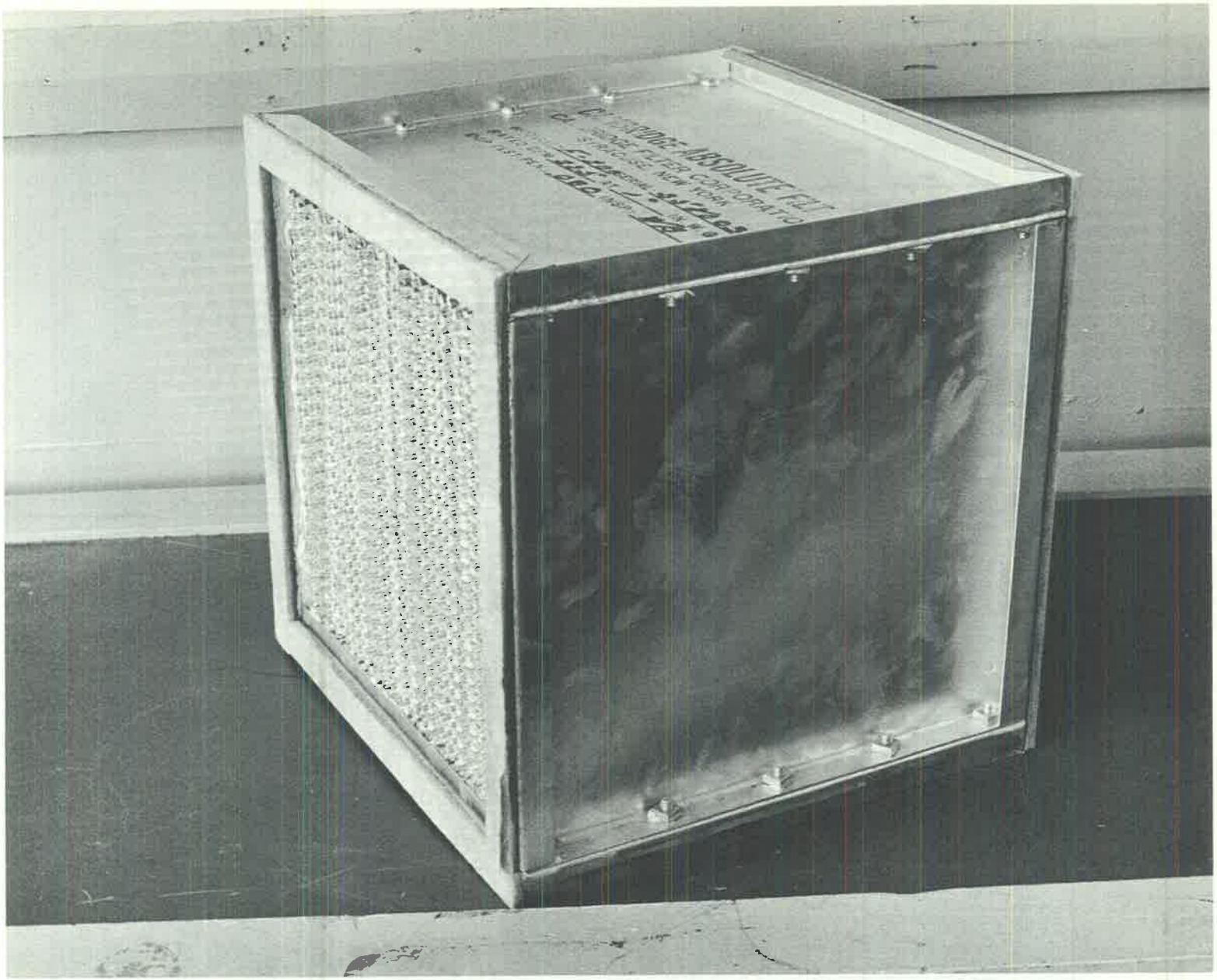

FIG. 5

Open Faced 225 cfm High-Efficiency Particulate Air Filter

FIG. 6

Open Faced 250 cfm High-Efficiency Particulate Air Filter with Self Contained Adaptors

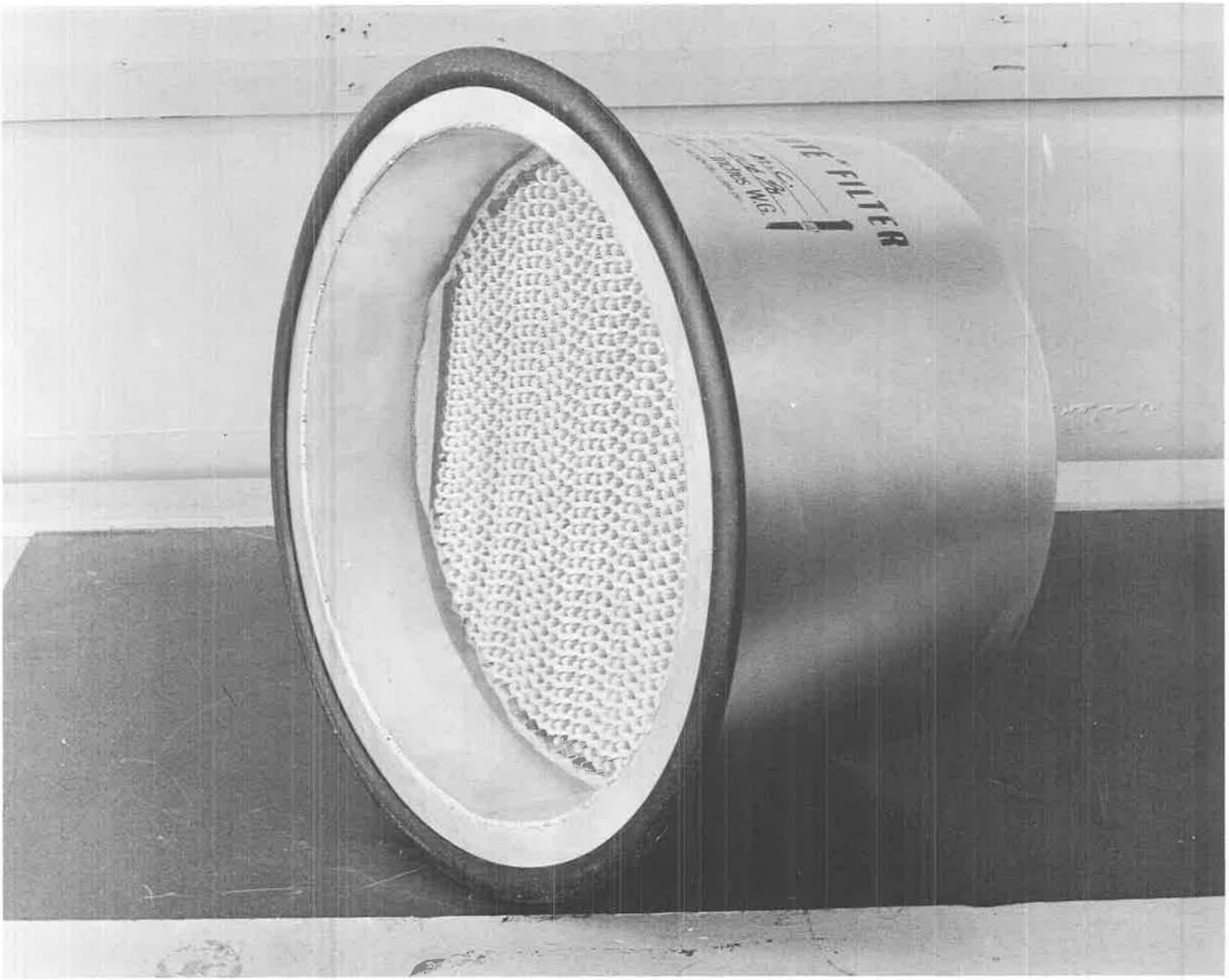

FIG. 7

Vacuum Cleaner High-Efficiency Particulate Filter

consists of the following:

(1) A forward light scattering photometer

(2) A percent penetration indicating amplifier

(3) A constant intensity light source

(4) A vacuum pump for sampling

(5) An aerosol generator

The first four items are shown in Fig. 8, and Fig. 9 shows a small capacity adjustable air operated aerosol generator.

4.1 Forward Light Scattering Photometer

A cross section of a forward light scattering photometer is shown in ORNL-LR-DWG77999, Fig. 10.

Parrish and Schneider describe its operation as follows:

"The air sample containing the DOP aerosol particles is drawn into the chamber, passes through a pair of open-ended cones apex to apex and is then discharged. The optical system in front of the light source is such that the beam of light forms a hollow cone, the center of which is a cone of darkness. The lens and the phototube at the opposite end of the chamber are located within the diverging cone of darkness; thus only light which is forward scattered from particulate matter in the cone of light reaches the phototube."

Many models and types of photometers are available but the one selected for use at the Chalk River Nuclear Laboratories is a copy of the instrument designed and developed by the U.S. Naval Research Laboratory. The percent penetration indicating amplifier is a U.S. Naval Research Laboratory development also.

4.2 Constant Intensity Light Source

The constant intensity light source is provided by an

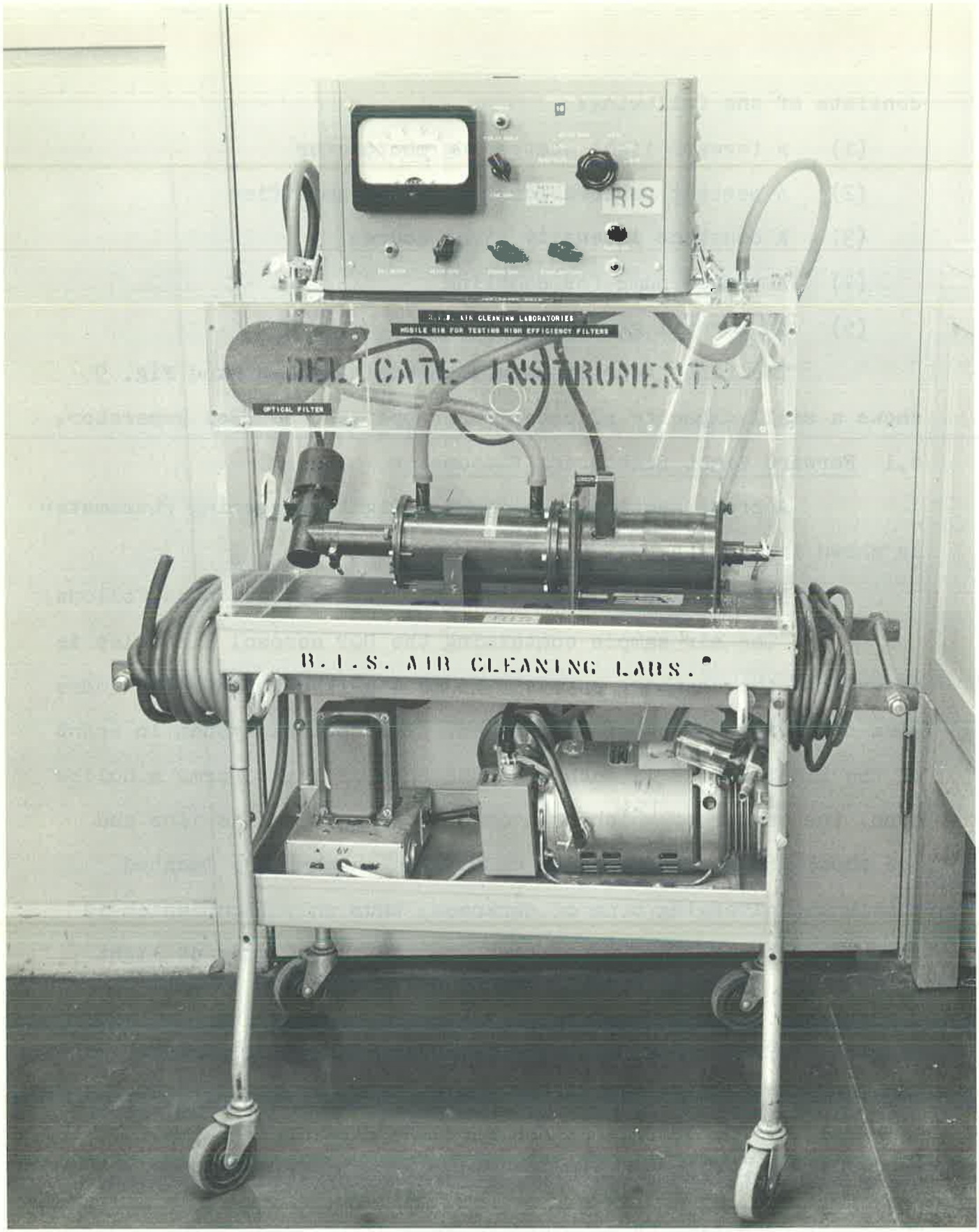

FIG. 8

Portable Instrument and Sampling Pump Console

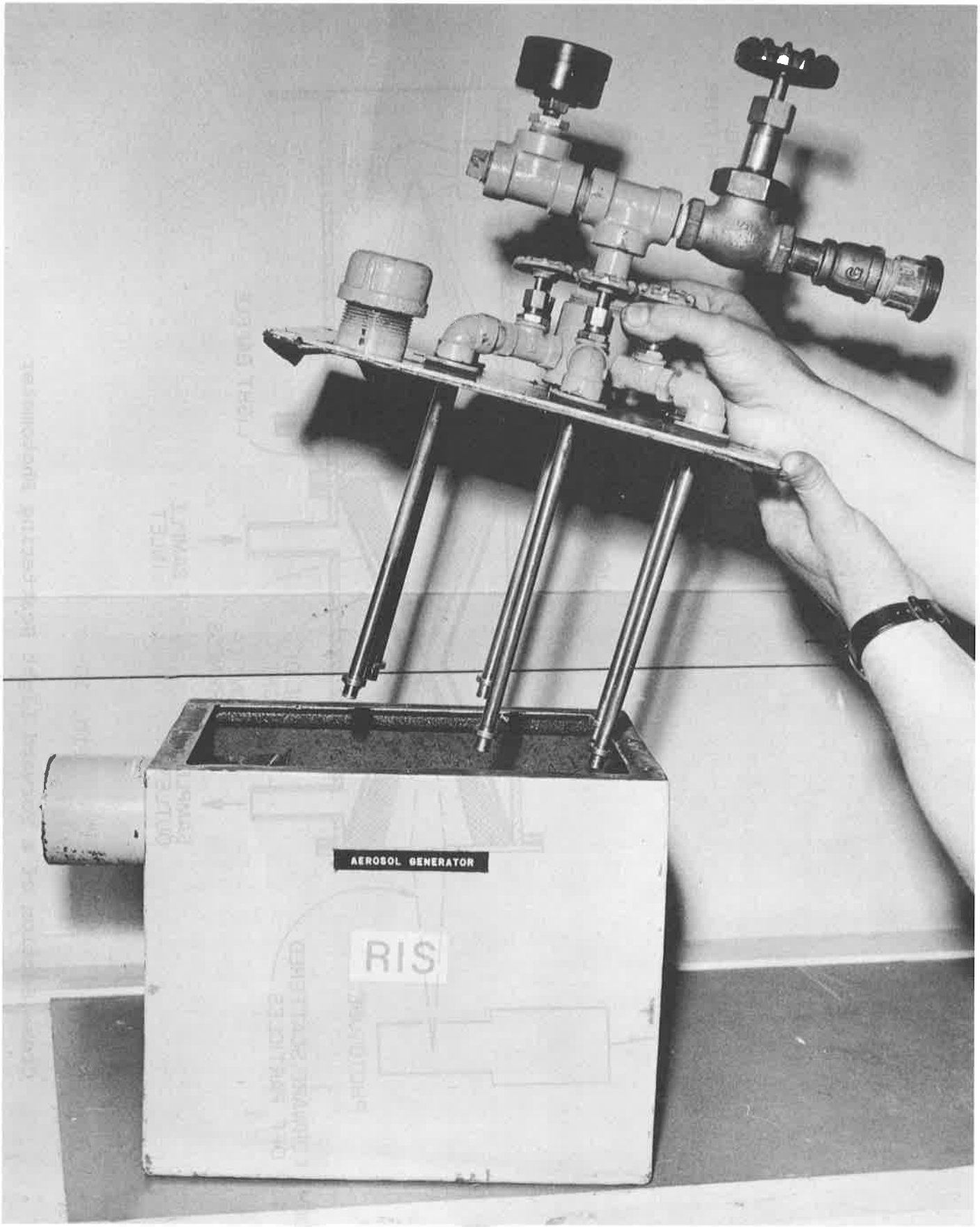

FIG. 9

6-Nozzle Adjustable Air Operated Aerosol Generator

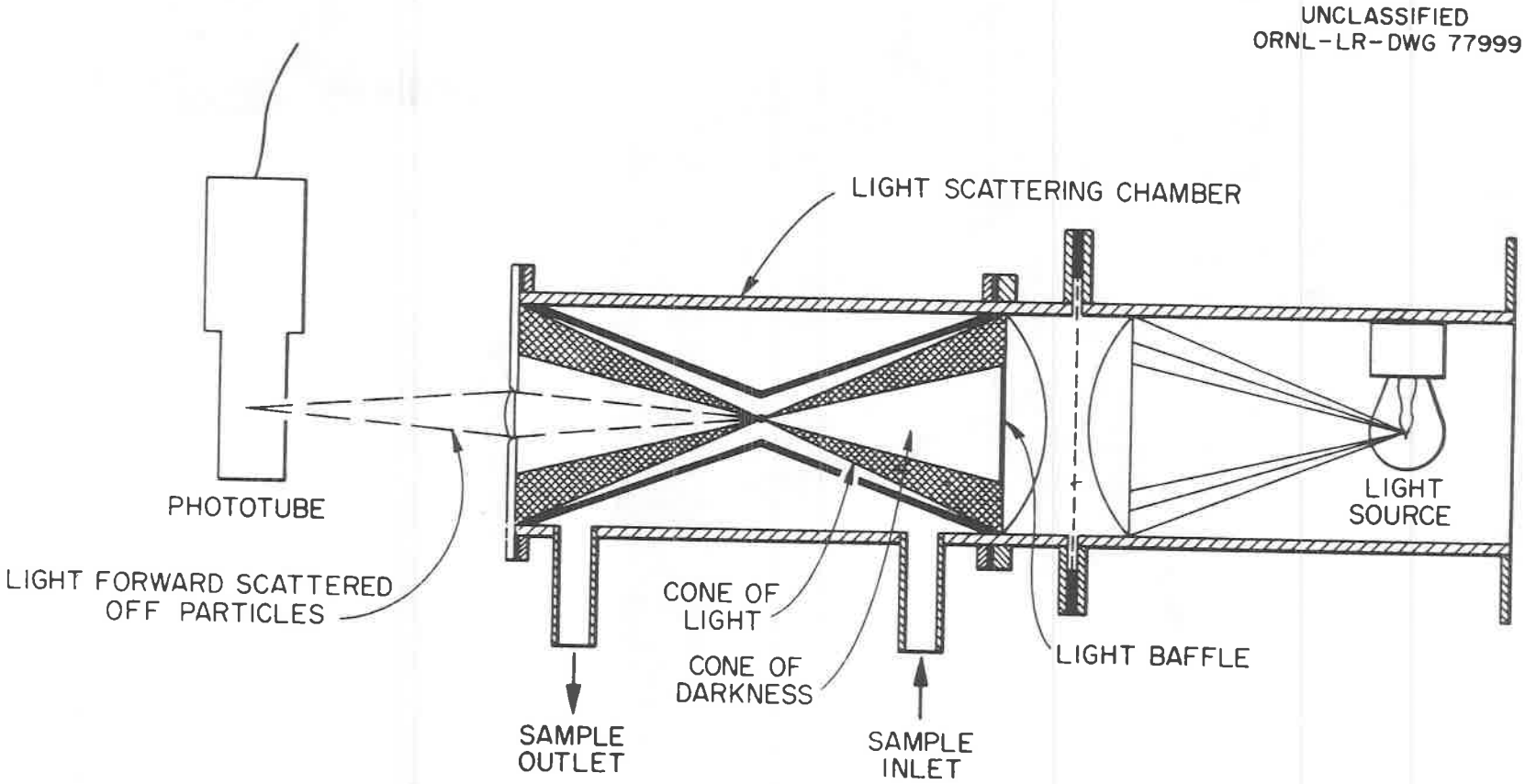

FIG. 10

Cross Section of a Forward Light Scattering Photometer

automotive light bulb and a commercially available constant voltage transformer.

4.3 Vacuum Sampling Pump

The vacuum sampling pump is a commercially available model generally used on air sampling apparatus.

4.4 Air Operated Aerosol Generator

The air operated DOP aerosol generator was developed by the U. S. Naval Research Laboratory. It consists of a number of atomizer nozzles submerged about 1 inch in liquid dioctyl-pthalate and connected to a low pressure (20-30 psi) air supply.

The improved model of atomizer nozzle (Fig. 11) was assembled into aerosol generators with capacities suited to our needs.

5. LABORATORY TEST EQUIPMENT

In addition to the basic equipment described above, a rig was required for testing new filters.

Fig. 12 shows the laboratory instrument console and the upstream portion of the filter test rig with a self contained filter in place. Flow adjustment is provided by the manual damper at the inlet to the test rig and mixing is provided by Stairmand discs* located on each side of the filter and ahead of the sampling points. Free wheeling propellor fans have also been installed in the duct to provide additional mixing. The air pressure for operating the aerosol generators is controlled by a pressure reducing valve.

---

* A Stairmand disc consists of a disc of similar shape to the section of duct, located centrally in a duct with an area equal to one half the duct area. This device is used to provide mixing in the air stream.

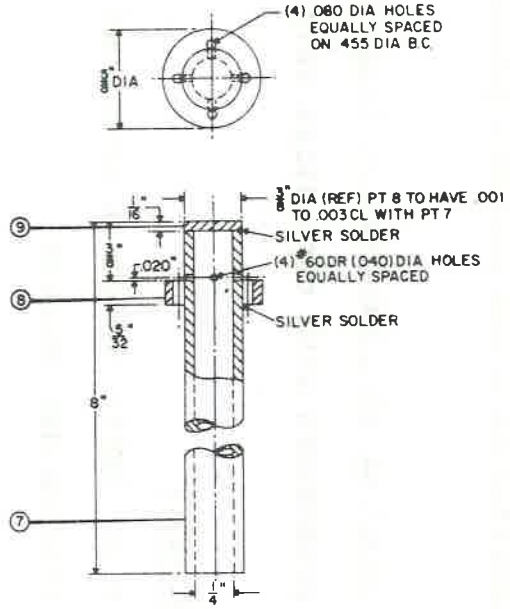

FIG. 11

Naval Research Laboratory Improved Atomizer Nozzle

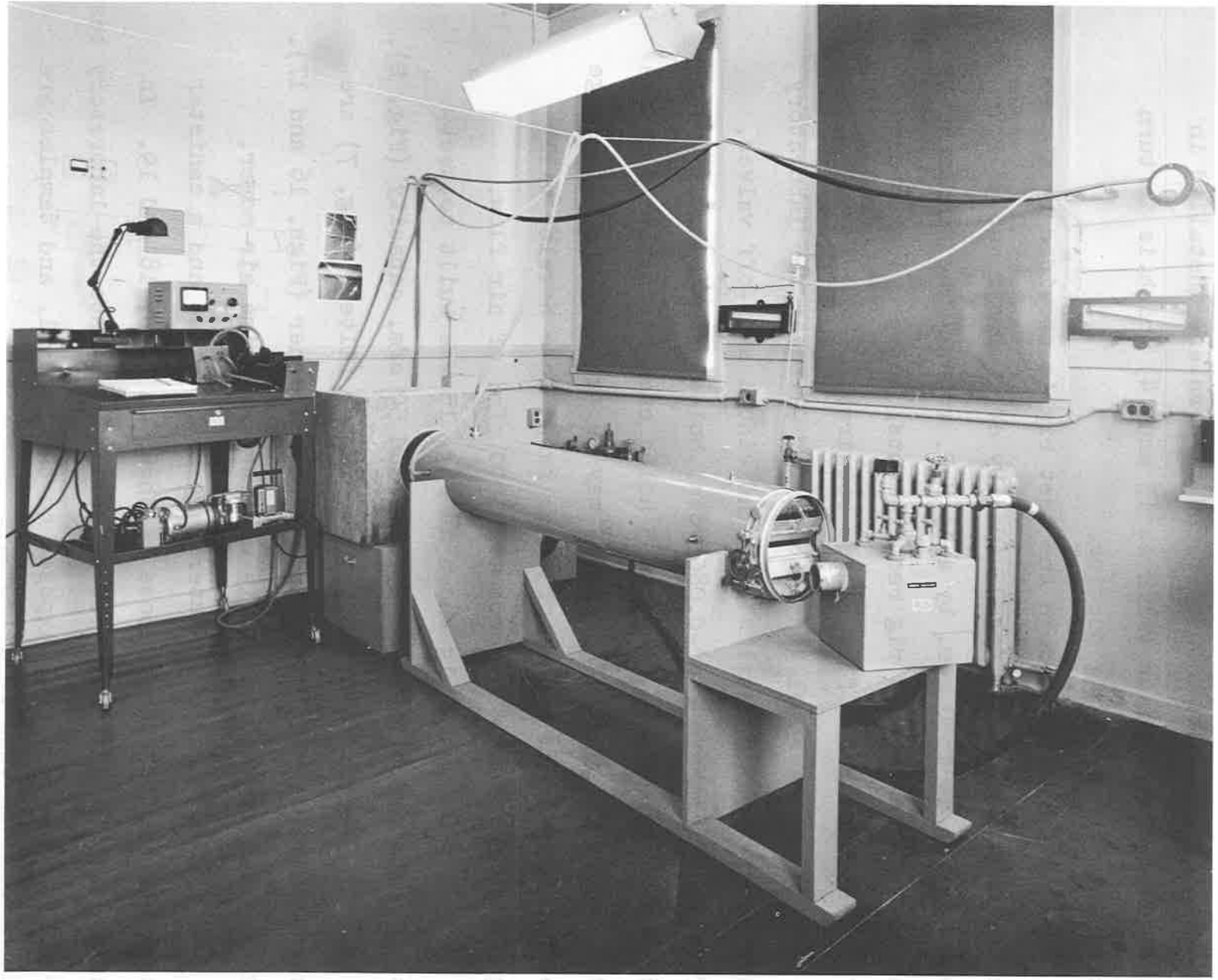

FIG. 12

Laboratory Filter Test Rig

Self contained filters are installed directly into the test rig ducting. Open faced filters are installed in the filter test holder (Figures 13 and 14) which is in turn tied into the test rig ducting.

Air flow through the test rig is provided by a centifugal fan with a rated capacity of 1060 cfm. at 3" P_s when driven at 1530 rpm. by a $1\frac{1}{2}$ H.P. motor. The fan capacity actually exceeds test rig requirements, but provides steady flow throughout the flow ranges required.

The aerosol generator (Fig. 9) built for laboratory use consists of 6 nozzles with individual shut-off valves. Three nozzles have four-0.080" dia. holes each (Fig. 11), while the other three have 1, 2 and 3 holes each respectively. Thus the amount of aerosol generated may be matched to a wide range of air flows. As a rule of thumb two-4 hole nozzles will generate sufficient aerosol for 1000 cfm. of air flow.

The small rig shown in Fig. 15 was built to test self contained filters of 25 cfm. and 50 cfm. capacity (Fig. 2).

Decontamination vacuum cleaner filters (Fig. 7) are tested after installation in a vacuum cleaner (Figs. 16 and 17). The vacuum cleaner itself is used as the prime air mover.

Respirator canisters are also tested and a canister test holder for this purpose is shown in Figs. 18 and 19. In this case the canister test holder is tied into the laboratory test rig with the canisters exposed to the aerosol, and samples are drawn through them at rated flow.

6. FIELD TEST EQUIPMENT

Dollies are used on field equipment to make it as portable as possible.

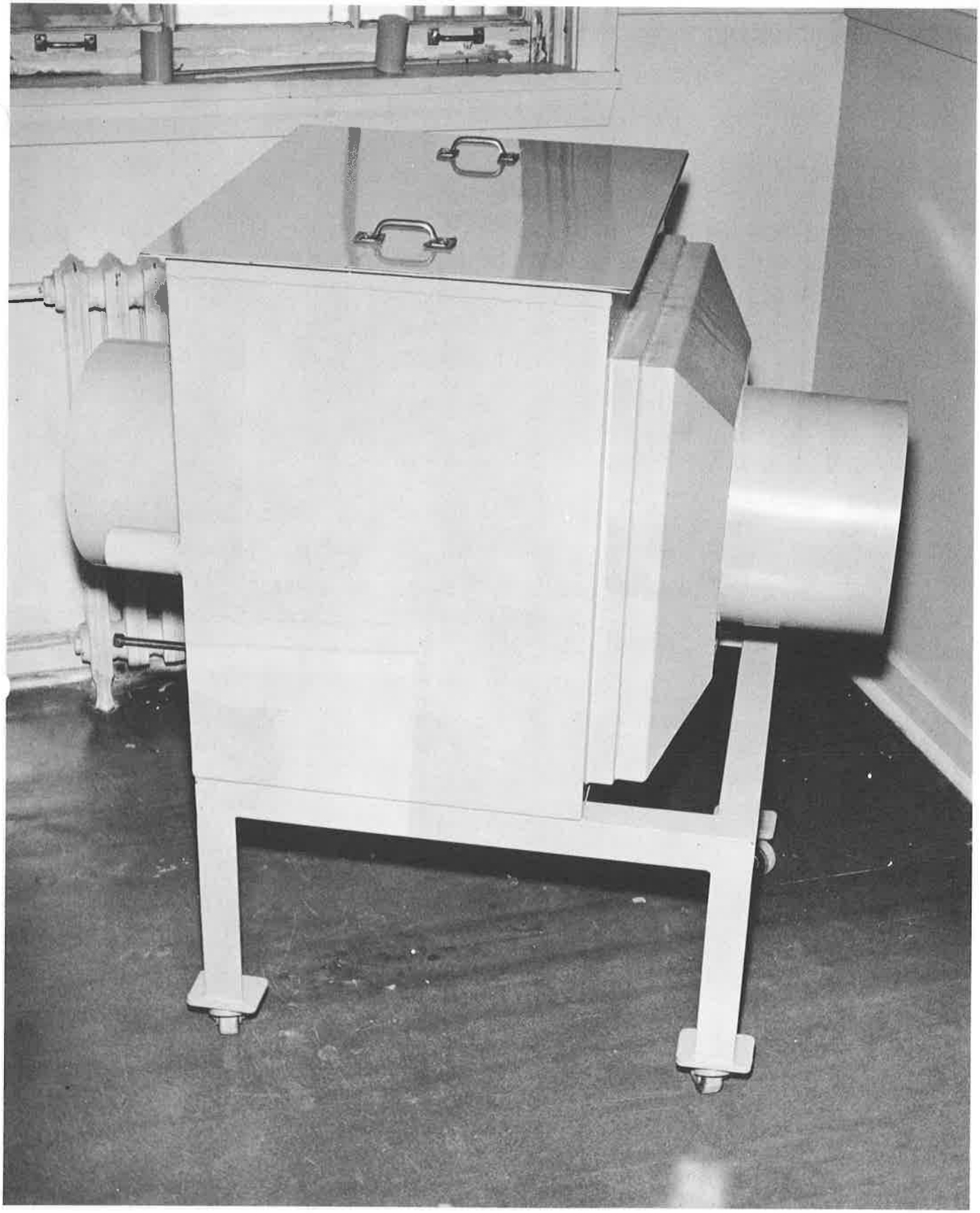

FIG. 13

Side View of Open Faced Filter Test Holder

FIG. 14

Top View of Open Faced Filter Test Holder

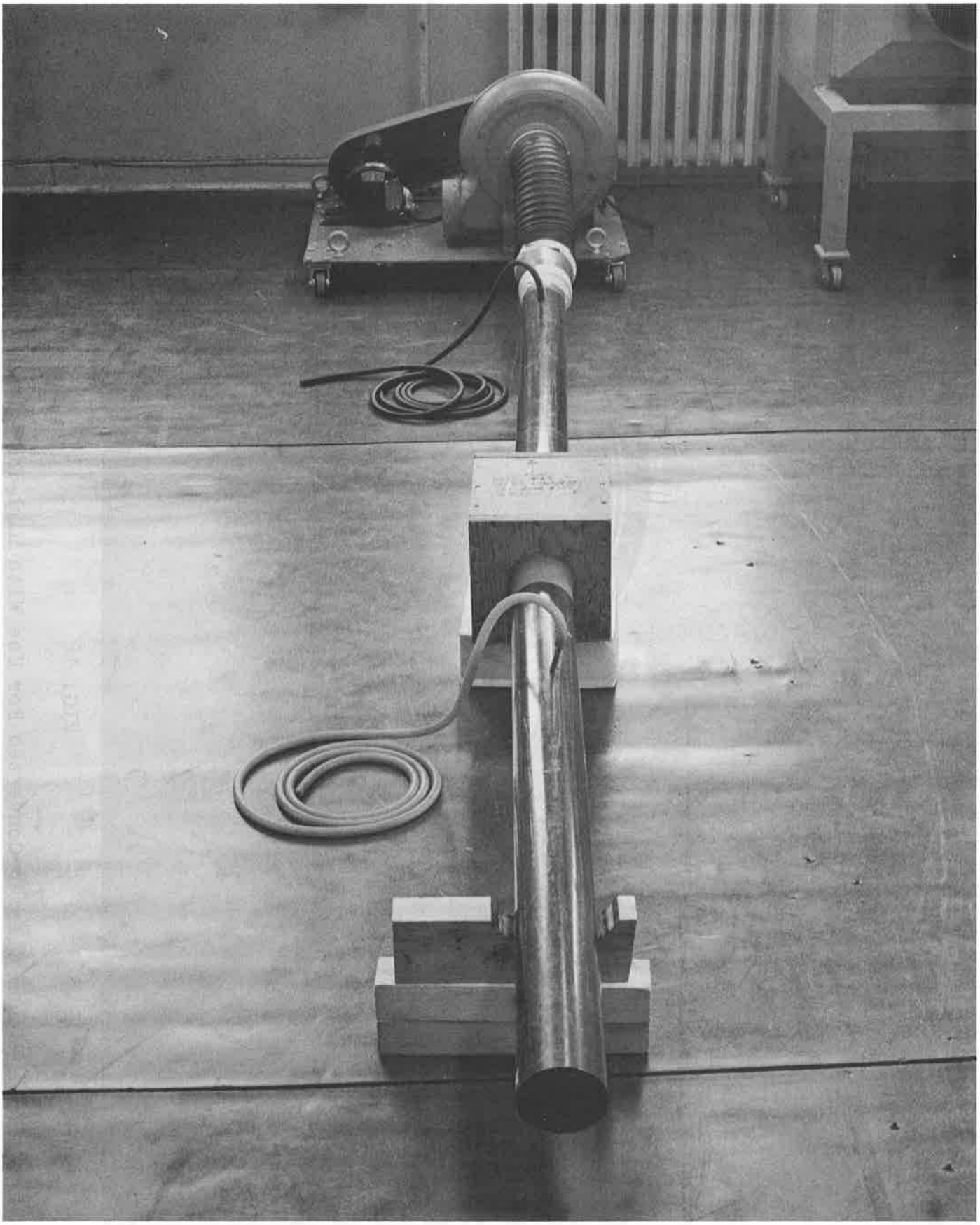

FIG. 15

Small Filter Test Rig for Filters up to 50 cfm Capacity

FIG. 16

Industrial Type Vacuum Cleaner Converted For Use With High-Efficiency Particulate Filter

FIG. 17

Assembled Vacuum Cleaner with High-Efficiency Particulate Air Filter

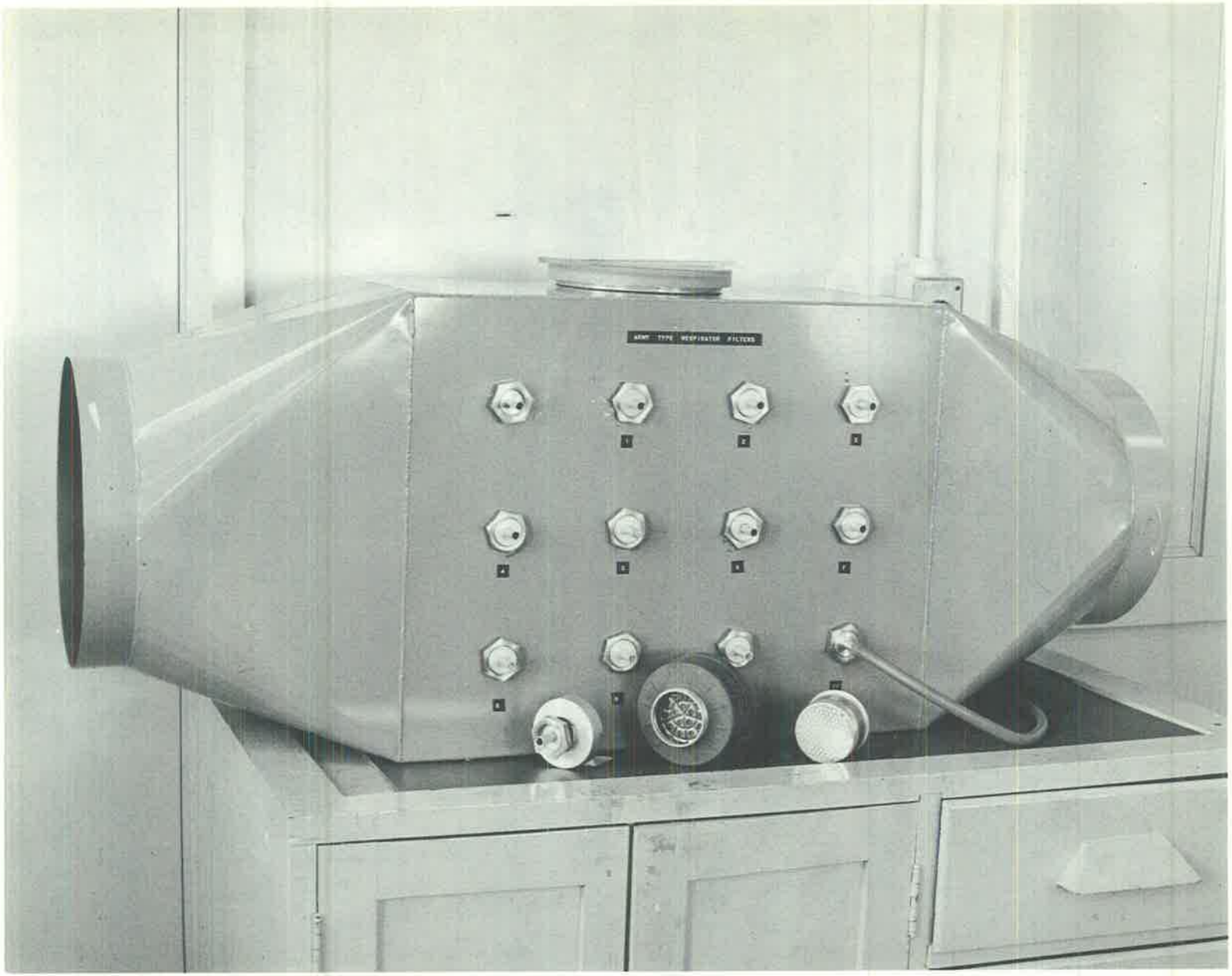

FIG. 18

Side View of Respirator Canister Test Holder

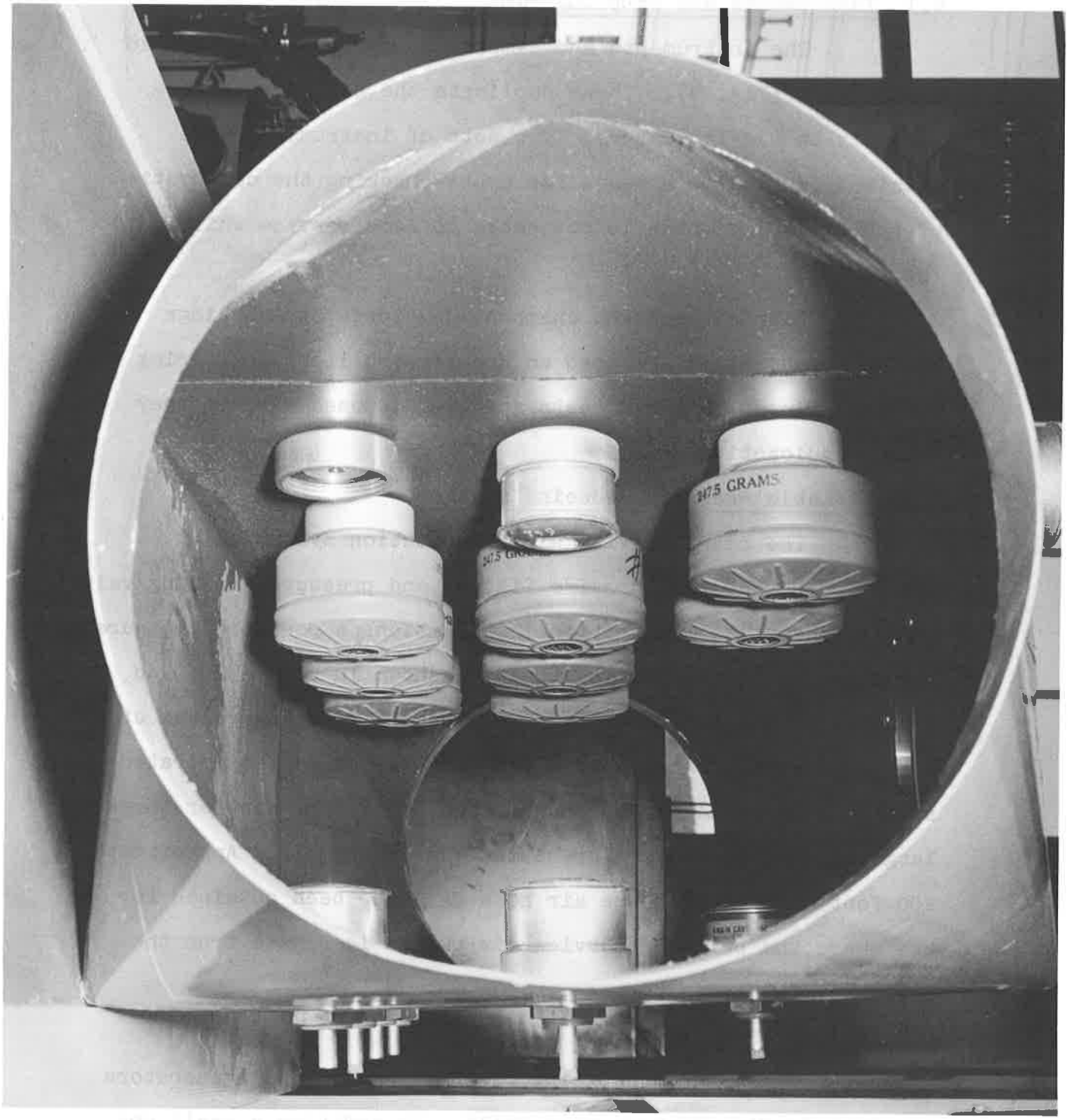

FIG. 19

Inside View of Respirator Canister Test Holder

6.1 Instruments and Sampling Pump

The instruments and sampling pump have been mounted on one unit (Fig. 8). These duplicate the set located permanently in the laboratory. Two sets of instruments were obtained to provide a means for cross-checking the calibration of the field set which is subjected to hard service while in the field.

Disposable light chambers developed at Oak Ridge National Laboratory are used on the forward light scattering photometer used in field tests and are disposed of when they become radioactive.

6.2 Portable Pressure Reducing Station

The plant service air distribution system is at 100 psi. Rather than provide filters and pressure reducing valves at all exhaust air filtration installations a portable pressure reducing station was built. This is shown in Figure 20. and consists of an air filter and two pressure reducing valves of different size. The pressure reducing valves can be operated singly or in parallel and can provide sufficient air for three large aerosol generators operating simultaneously. Approximately 200 feet of high pressure air hose has also been obtained for use where the building service air outlet is remote from the filter installation.

6.3 Aerosol Generators

Three large capacity (12 nozzles) aerosol generators as shown in Fig. 21 have been built. In addition a small one similar to that shown in Fig. 9 has been built for field use. Figure 22 illustrates one of large capacity which has been made

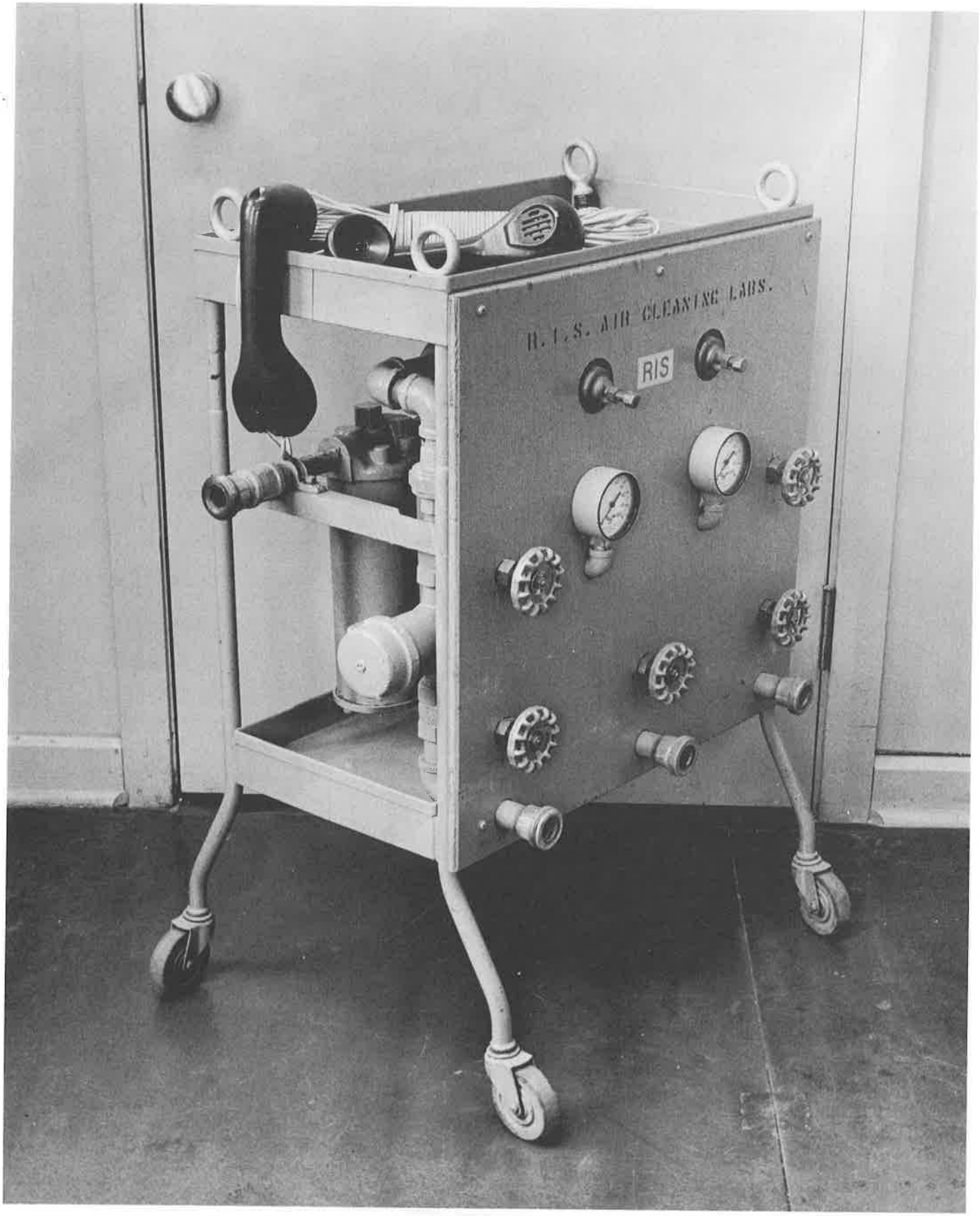

FIG. 20

Portable Air Pressure Reducing Station

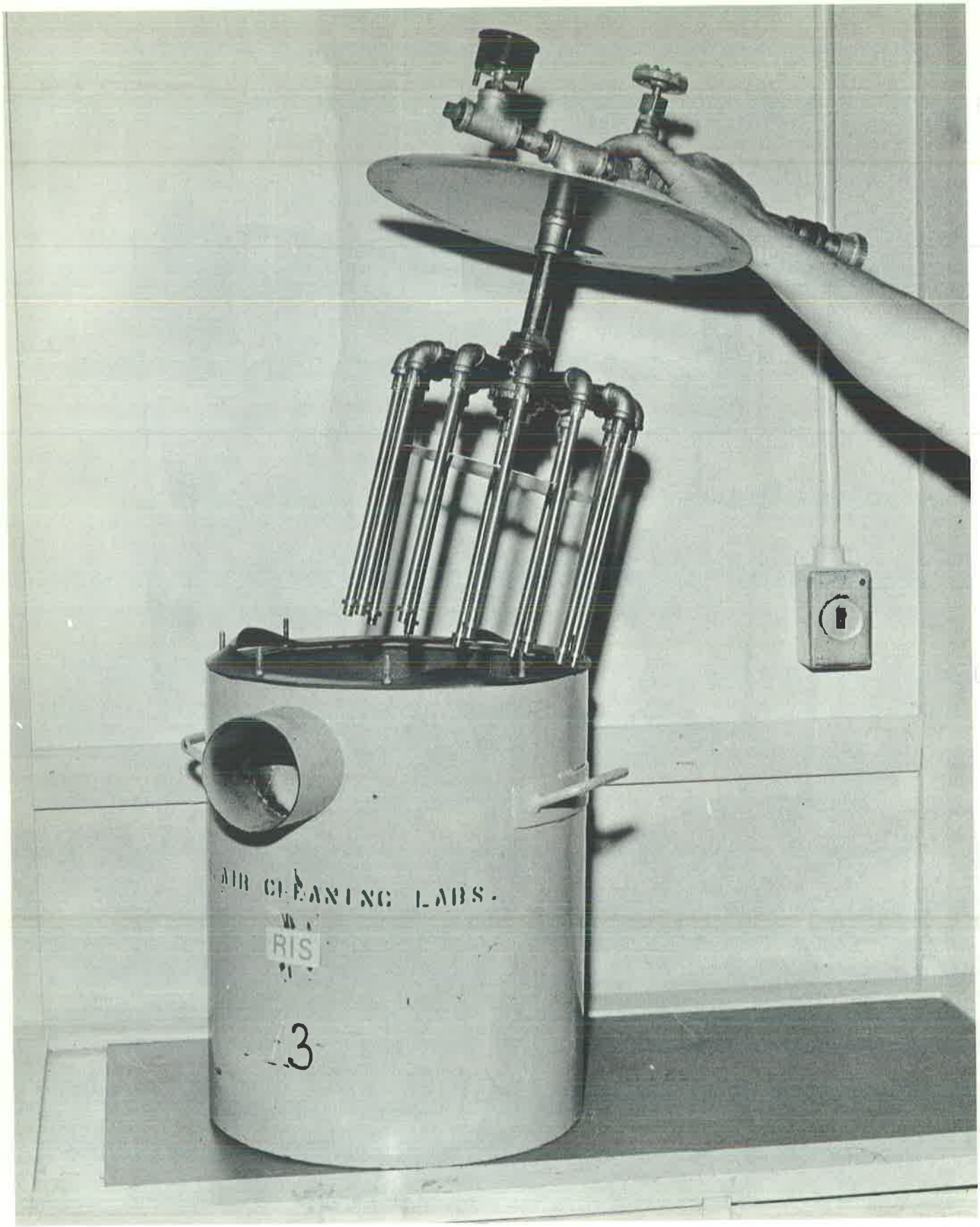

FIG. 21

12-Nozzle Air Operated Aerosol Generator

adjustable through a wide range by using a stop valve on each nozzle. It also is equipped with a separate pressure reducing valve, filter and trolley.

Flexible ducting is used to carry the aerosol from the generators to the ventilation system air stream. Fig. 23 shows three large aerosol generators and the portable pressure reducing station connected to a ventilation exhaust system under test.

7. IN-PLACE TESTS

The technique used to test new filters in the laboratory test rig is also used for field in-place tests. However, the essentials readily available in the laboratory such as good sampling points, adequate mixing and convenient aerosol inlets are seldom provided in ventilation exhaust systems when they are constructed.

Where sampling points are not adequate a traverse is taken across the duct and estimates of the average concentration are made. Where adequate mixing cannot occur adjacent to the filters, the aerosol is injected as far as possible upstream of the filters to facilitate upstream mixing, and sampled downstream after the fan where mixing by the fan has occurred. Where aerosol injection points are not readily available, these have been installed on the duct runs.

In-place tests are carried out on systems having a wide range of capacities. Fig. 24 shows a single self contained filter installed on a fume hood, while Fig. 25 shows a bank of six self contained filters. Fig. 26 shows a bank of eighteen self contained filters on a reactor exhaust system.

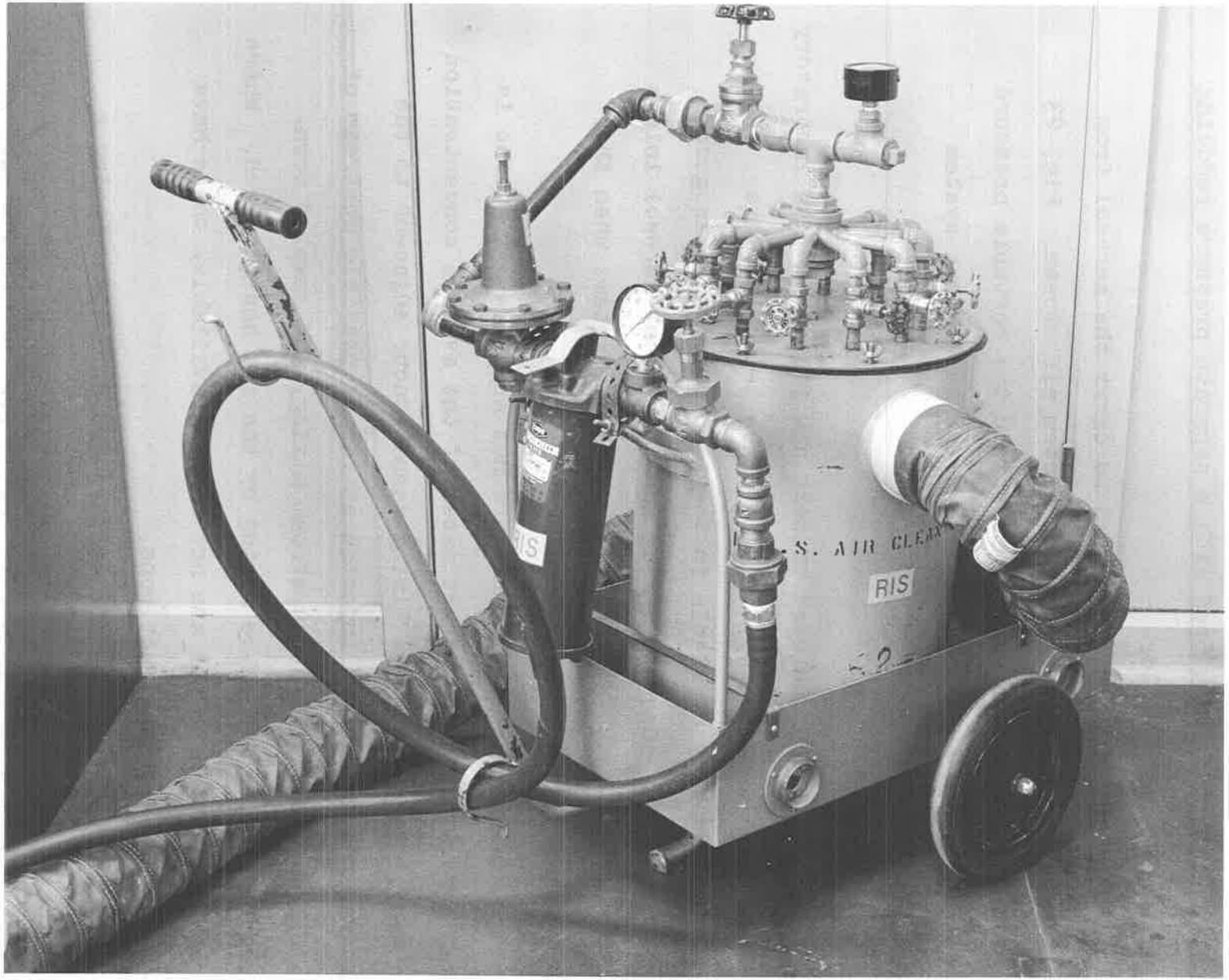

FIG. 22

12 Nozzle Adjustable Air Operated Aerosol Generator c/w Trolley, Filter and Pressure Reducing Valve

FIG. 23

Aerosol Injection Point on a Large Reactor Filter Installation

FIG. 24

Single Self Contained Filter Installation on a Fume Hood

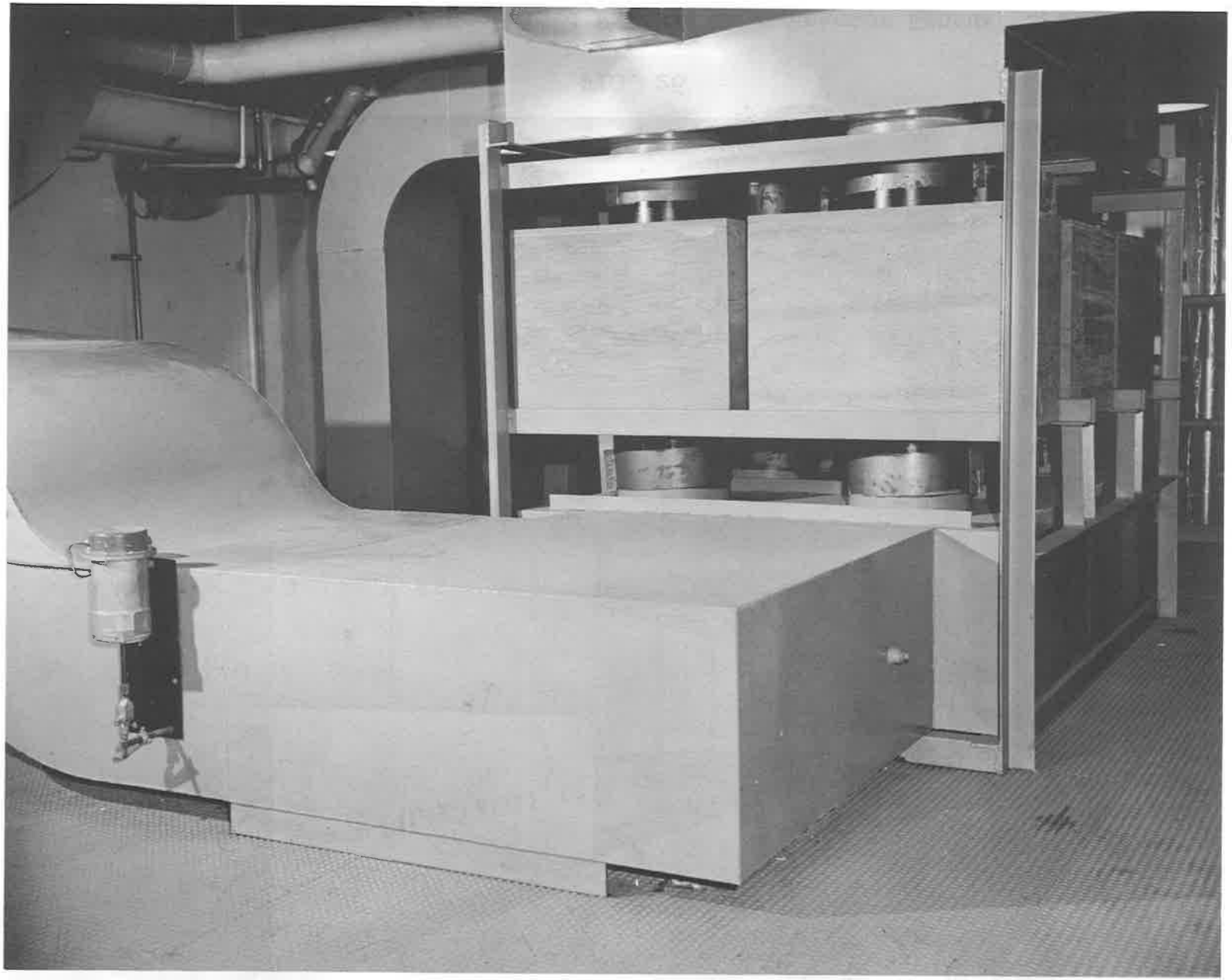

FIG. 25

Multiple Self Contained Filter Installation

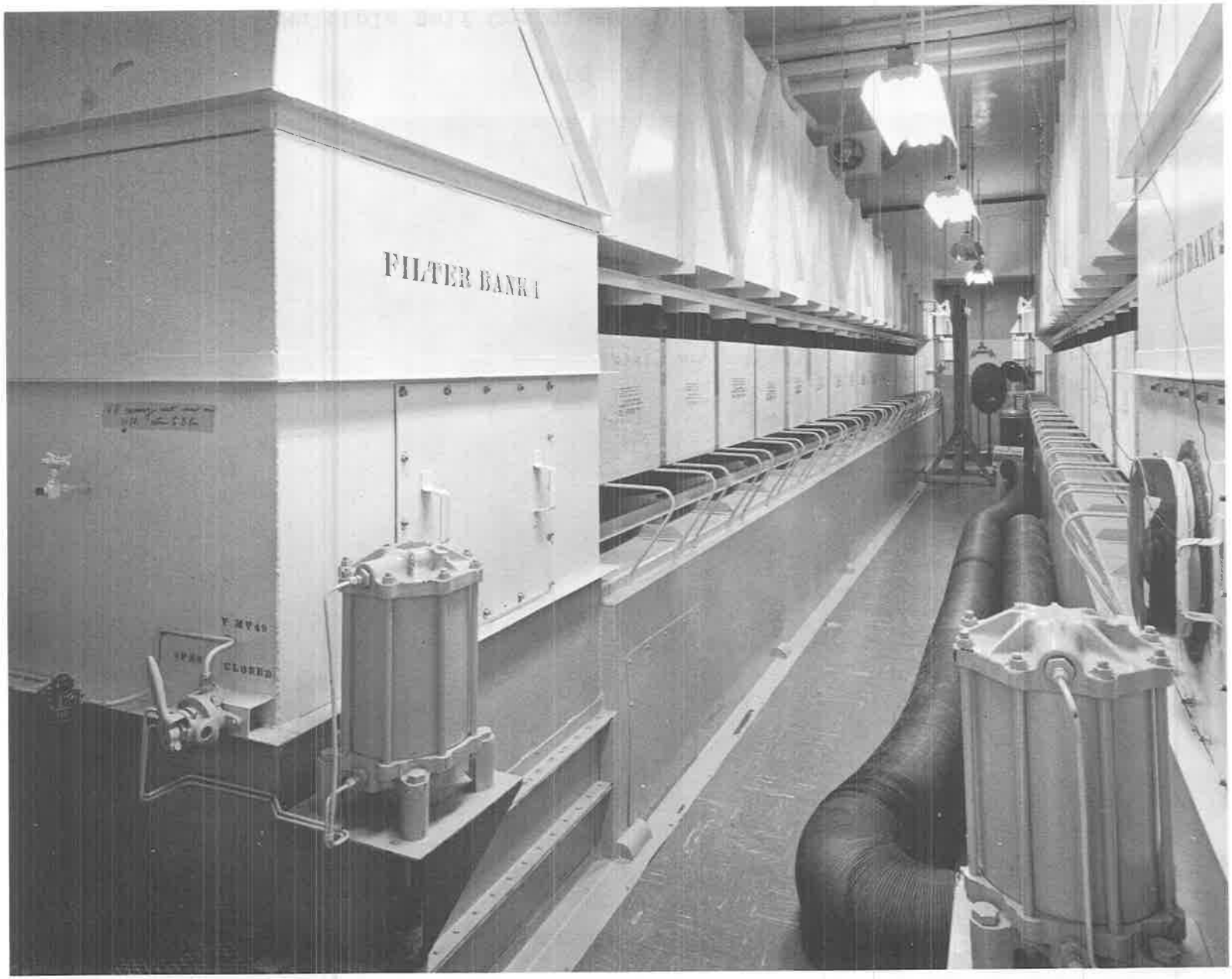

FIG. 26

Large Bank of Self Contained Filters on a Reactor Exhaust System

During a test, the efficiency of the whole filter bank is measured. Then as an added check, the concentration of DOP downstream of each filter is measured to determine whether any filter is defective.

The use of self-contained filters limits points of leakage to either the media or the seal between the media and the filter frame and in most cases results in a system which is relatively easy to test.

8. TEST RESULTS

Table 1 shows results of tests done on new high-efficiency particulate air filters since the program was begun. The percentage of defective filters in the case of the 135 cfm. open faced vacuum cleaner filters was high, and was due to a welding defect in the filter casing of almost all of the filters in one shipment. About five per cent of the most commonly used ventilation filters, the 1000 cfm. self contained fire resistant type, were defective when received.

Table 2 shows results of the first in-place tests on systems using self contained ventilation filters. The filters in many of these installations were new and proven by test to be good. This was reflected in the field test. Unless a self-contained filter is damaged during installation it will show a penetration equivalent to that during the pre-installation test. The excessive DOP penetrations found on the one-filter systems ranged from 0.072% to 1.5%. The highest penetration was observed on the ventilation exhaust system for a steam cleaning decontamination process. Direct exposure of the filter to steam resulted in the failure.

TABLE 1

RESULTS OF TESTS ON NEW HIGH-EFFICIENCY PARTICULATE AIR FILTERS

Filter Type	Capacity (cfm.)	Construction	Application	No. Tested	No. *Defective
Self-Contained (Fig. 2)	50	Fire Resistant	Ventilation	30	nil
Self-Contained (Fig. 1)	600	Fire Resistant	Ventilation	15	2
Self-Contained (Fig. 1)	1,000	Fire Resistant	Ventilation	230	12
Open-Face (Fig. 4)	250	Fire Resistant	Ventilation	2	nil
Open-Face (Fig. 3)	1,000	Fire Proof	Ventilation	10	1
Open-Face (Fig. 7)	135	Fire Proof	Decontamination	17	8
** Self-Contained (Fig. 6)	250	Fire Proof	Decontamination	33	2

* Filter defective when DOP penetration > 0.03%.

** These are open faced filters (Fig. 4) converted to self contained at CRNL.

TABLE 2

RESULTS OF FIRST IN-PLACE TESTS ON
VENTILATION SYSTEMS USING SELF CONTAINED FILTERS

No. of Filters in each Bank	No. of Banks Tested	No. of Banks with Excessive* DOP Penetration	No. of Defective Filters
1	112	5	5
2	8	nil	**1
4	7	nil	nil
5	3	nil	nil
6	1	nil	nil
8	3	nil	nil
10	3	nil	nil
12	4	nil	nil
18	4	nil	nil

* Penetration excessive when it exceeds 0.05%.

** The Filter Bank had an acceptable penetration but on checking individual filters one was defective (> .03%).

Results of the first in-place tests on ventilation systems using open faced filters are shown in Table 3. DOP penetrations were highest on the one-filter installations, and most of these systems were on hot cells where contamination release is generally high. Inadequate clamping devices which resulted in poor gasket seals caused the leaks. DOP penetration was also high on the banks of eight filters. In this case four 1000 cfm. open faced filters are assembled as is shown in Fig. 27, and two such assemblies are used in parallel. Leakage paths were found between individual filter units as well as at the main gaskets of the filter assembly. Modifications are being carried out on the systems with excessive DOP penetration.

9. CONCLUSIONS

The performance of systems using self-contained filters has been excellent, but that of some systems using open faced filters was not. In order to insure that the efficiency of high-efficiency particulate air filters is achieved on installation and maintained during use, a filter testing program is essential.

This program should include:-

1. Pre-installation tests to identify filters with manufacturing defects and/or transportation and handling damage.
2. In-place tests to determine whether filters have been damaged during installation and whether gasket seals (if used) are satisfactory.
3. In-place tests at appropriate intervals to demonstrate that the systems remain satisfactory.

TABLE 3

RESULTS OF FIRST IN-PLACE TESTS ON
VENTILATION SYSTEMS USING OPEN FACED FILTERS

No. of Filters in each Bank	No. of Banks Tested	No. of Banks with Excessive DOP Penetration	Maximum DOP Penetration Found
1	16	16	14.0%
4	6	4	0.13%
8	4	4	0.45%
12	1	nil	0.043%
16	2	nil	0.020%

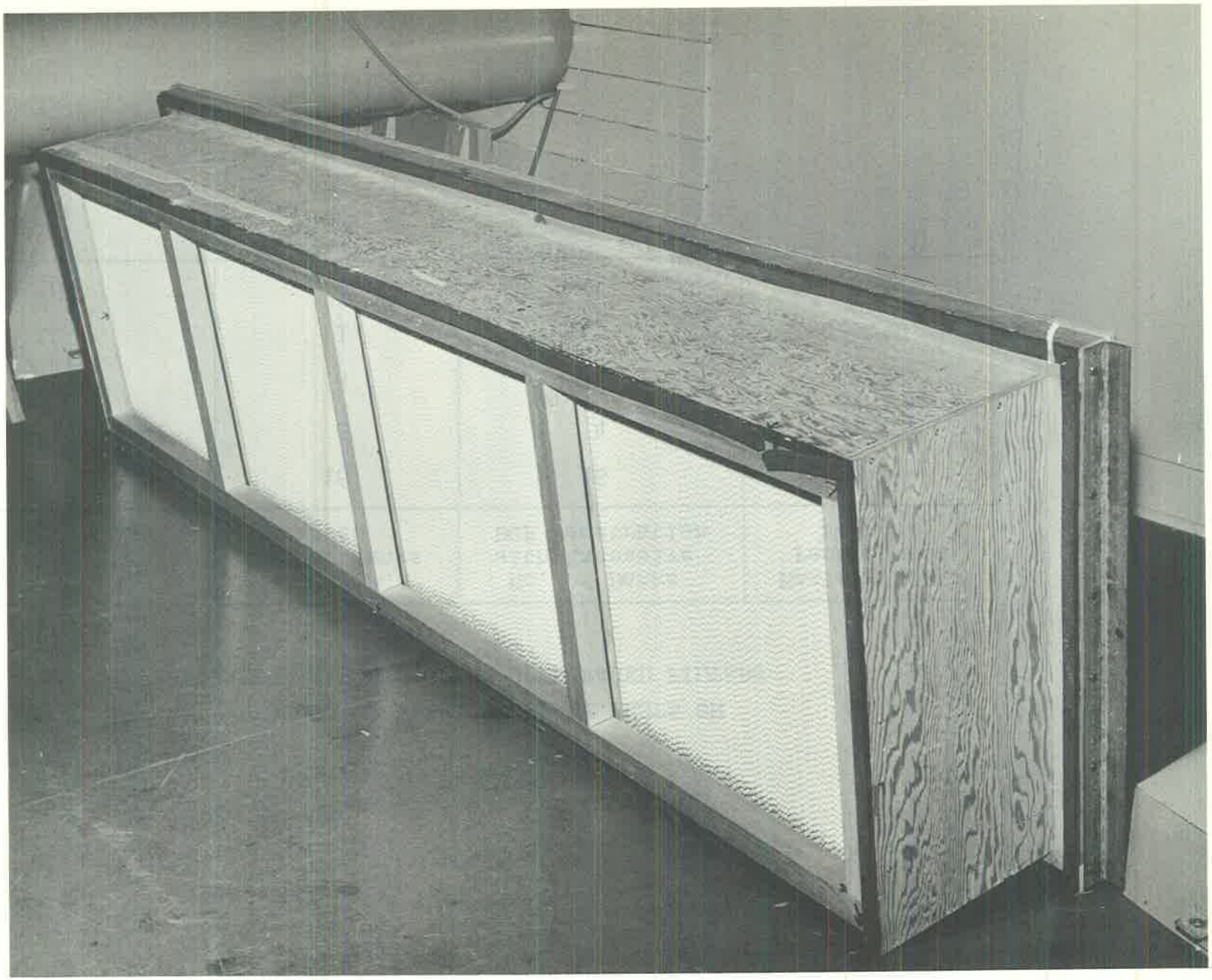

FIG. 27

Assembly Containing Four 1000 cfm. High-Efficiency Particulate Air Filters

10. ACKNOWLEDGEMENTS

The authors gratefully acknowledge the assistance received from the following during the initial stages of the filter testing program:

1. Mr. Humphrey Gilbert, Division of Operational Safety, United States Atomic Energy Commission.
2. Mr. J. Thomas and Staff, Filter Testing Workshop, N.Y.O., Health and Safety Laboratory, United States Atomic Energy Commission.
3. Messrs. E. C. Parrish and R. W. Schneider, Inspection Engineering Department, Oak Ridge National Laboratory.
4. Mr. J. A. Young, United States Naval Research Laboratory.

REFERENCES

1. E. C. Parrish and R. W. Schneider, Tests of High-Efficiency Filters and Filter Installations at ORNL. 1963, ORNL-3442.
2. W. H. Echols and J. A. Young, Studies of Portable Air-operated Aerosol Generators. 1963, NRL Report 5929.
3. Inspection, Storage, Handling, Installation of High-Efficiency Particulate Air Filter Units. TID-7023, Division of Technical Information, USAEC.

DISCUSSION

ETTINGER: What I would like to ask is on the in-placed filters, what penetration do you consider excessive in requiring corrective measures?

PANCHUK: .05%.

ETTINGER: Could I ask how you came up with that number? Was it just taking the 99.97% filter efficiency and downgrading, or did you have another basis for selecting .05% as the allowable penetration in-place?

PANCHUK: This is the number that was indicated by Oak Ridge as the acceptable one for in-place tests and we just followed suit.

TESTING OF AIR CLEANING SYSTEMS - TESTING OF THE COMPONENTS - IN-PLACE TESTS

by F. Billard and J. Brion

Commissariat à l'Energie Atomique,
Fontenay-aux-Roses, France

The reliability of air cleaning systemps is dependent on the testing they are submitted to. Althrough in-place tests are the most important as they act as final tests upon achieved plants, component tests are necessary too. They allow detection of defective units before they are installed, partition of unit defects from mounting defects and they are more sensitive. For similar reasons, material tests are most useful.

The various tests are described, about aerosol filters for one part, iodine trap for the other.

The checked features are : materials nature, units sizes, efficiency, air resistance, flammability, humidity resistance, temperature resistance, adsorbent friability etc...

On iodine trapping systems, small check traps, working in by-pass with the main trap are periodically subjected to efficiency tests. This control allow to cut down the in-place tests frequency, particuliarly when poisoning from organic vapours is to be feared.

INTRODUCTION

The safety of nuclear plants where their surroundings are concerned is largely founded on the efficiency of air cleaning systems. However the efficiency of these devices can be reduced, sometimes drastically, by a number of factors : defective elements, incorrect mounting, deterioration as a result of clogging, poisoning by vapours, ageing of materials, etc...

It is therefore necessary to institute a systematic procedure of testing the devices installed.

In addition, in order to eliminate defective elements before mounting and to differentiate between the defects of the element and those of the fitting, while at the same time improving the sensitivity of the measurements, one must check the elements themselves.

Finally it is desirable for similar reasons to test the main component of the element.

To establish the procedure for these tests, three documents or sets of documents must therefore be drawn up :

1°) A general paper giving details of the inspection procedure : the tests necessary, the stage of manufacture or delivery at which they are carried out, the percentage of elements involved, steps to be taken on the basis of the results etc...

2°) Technical notes describing each test in detail.

3°) A technical accounts and specifications book containing, for a given order, details of the characteristics demanded and their tolerances.

Only the technical side of the procedure will be described here. The only two types of cleaning system considered are folded paper aerosol filters and activated charcoal iodine traps.

I - TESTING OF FILTERS

As mentioned above, this procedure is divided into three parts :

- testing of the filter paper
- testing of the filter element
- testing of the complete filter installed on the site.

1.1 - Testing of the filter paper

The filter manufacturers test their filter papers systematically and a simple check is necessary. Samples of paper are taken from the rolls already inspected and the following characteristics are checked :

- superficial specific weight
- tensile strength
- pressure drop
- efficiency.

The first involves simple weighing of samples of paper with a water content around an average value.

The tensile strength if tested on a special small machine which indicates the breaking load and the elongation of samples 15 mm. wide and 200 mm. long.

For the pressure drop measurement the air passage speed through the sample is about the nominal speed in industrial use, i.e. 1 cm/s.

There are many methods of measuring the efficiency of air filters : the methylene blue method, the sodium flame method, the polydispersed DOP method, the monodispersed DOP method etc... In order to give comparable results the method adopted must be equally applicable whether testing the filter paper or checking the filter in situ. This condition excludes the monodispersed DOP method. The polydispersed DOP method has the disadvantage that a high concentration is necessary upstream from the filter, giving poor reproducibility of the measurements as a result of coalescence phenomena which vary in degree according to the arrangement of the circuit tested. Our choice is the uranine aerosol method studied by L. SILVERMANN (1) and K.T. WHITBY (2-3) chiefly notable for its high sensitivity ; the principle of this method is as follows.

A liquid aerosol is produced by pulverisation of a 1 °/₀ aqueous uranine solution. Droplets of diameter greater than 2 μ are removed by an impactor . After evaporation in a heating tube and dilution with dry air, a solid aerosol of maximum diameter around 0.5 μ is obtained. Samples upstream and downstream from the filter tested are taken on filters which are then washed, and the washing solution are tested by fluorimetry. The method is so sensitive that a measurement obtained on the downstream sample is equal to twice the ''background'' for a sample of air one cubic metre in volume taken behind a filter of 10 000 efficiency (99.99 °/₀), with a solid aerosol concentration upstream of only 4 μ/m^3, i.e. a liquid aerosol emission equivalent to 0.4 mg/m^3.

1.2 - Testing of the filter elements

A filter unit can be used within a fairly wide range of flow-rates, but the results of certain tests are dependent on the conditions chosen. If the element is used with a high flow-rate the installation occupies less space and therefore investment costs are lower, but on the other hand maintenance costs are higher since the elements must be replaced more frequently. It is logical therefore to refer the standard unit flow-rate or nominal flow-rate to the volume of the element.

For the smallest element currently used in France this nominal flow-rate is taken as 100 m^3/h. The corresponding value for the 600 x 600 x 300 mm. element is 1 400 m^3/h.

The testing of filter elements involves checking the following characteristics :

- as a reminder, general aspect (dimensions of the frame, number of folds, aspect of the joint, of the paper, protection etc...), and pressure drop ;
- clogging ;
- non-inflammability ;
- resistance to water ;
- resistance to temperature ;
- mechanical strength ;
- efficiency.

The lifetime of a filter is generally limited by clogging, this being very variable from one type of filter to another and depending essentially on the area of paper available in a given volume and also on the way in which the paper is folded.

The clogging of a filter is determined by operating it under conditions similar to normal working conditions, i.e. in a natural atmosphere. The pressure drop is read periodically, at the same time as the accumulation of atmospheric dusts, and in this way the filter clogging curve cas be established. Unfortunately this method is very slow, and we are attempting to work out an artificial method of rapid clogging which would be representative of the natural process.

The non-inflammability of air filters is not easily defined, and we are obliged to divide so-called non-inflammable filters into different categories on the basis of the following criteria (4) :

- flame propagation,
- smoke production,
- release of incandescent fragments,

- release of stored dusts,
- preservation of a high degree of efficiency.

For the test, the filter is mounted on a circuit where it can operate at the nominal flow-rate. The flame of a gas burner, of defined dimensions and temperature, is held in contact with the filter for one minute and the effects observed are recorded. If smoke is produced, its abundance is detected by means of an aerosol photometer. Any lowering of efficiency is determined with the same apparatus by measurements made before and after the test with an aerosol obtained from a smoke-producer.

When a filter is used with liquid aerosols there is a danger that, besides the inevitable but reversible clogging, there will be a permanent deterioration of the efficiency, pressure drop and mechanical resistance properties as a result of a change in the paper texture. For this reason a simplified check is made by immersion followed by measurement of these characteristics.

The heat resistance of a filter is checked by a simple test wich consists of placing it in an oven for 24 hours ; the correlation between the testing temperature and the temperature limit in permanent operation is established by means of preliminary comparative tests in an oven and on a circuit at high temperature.

It is useful to chek the mechanical resistance of air filters, in other words the maximum flow-rate they can filter without breaking, since on the basis of this characteristic their behaviour can be predicted in the event of accidental over-pressure, in a reactor hall for example. This test is carried out by mounting the filter unit on a circuit where it can operate to breaking point, at a flow-rate increasing regularly from the nominal value to a value 40 times greater.

1.3 - Testing of filtration systems in situ

The testing of filtration systems on the site simply involves checking the pressure drop and the efficiency.

The uranine efficiency testing method is quite suitable because of its high sensitivity. It is possible in fact to test large units, of several hundred thousand cubic metres per hour, from a single portable generator. However the measurement is seldom performed under such good conditions as with the filter elements because of the difficulties generally involved in the choice of aerosol introduction and sampling points.

2 - TESTING OF IODINE TRAPS

As with aerosol filters, this procedure is divided into three parts :

- testing of the adsorbent material, i.e. activated charcoal ;
- testing of the adsorbing element ;
- testing of the trap installed on the site.

2.1 - Testing of the activated charcoal

Unlike filters, which are in common use in industry, activated charcoal for the construction of iodine traps is ordered for a specific purpose. However it can only be manufactured in minimum quantities greater than those needed to equip a plant, and it is therefore ordered and tested in separate batches.

The properties tested are :

- the density
- moisture content
- granulometry
- pressure drop
- friability
- pH
- ignition temperature
- efficiency with respect to molecular iodine
- efficiency with respect to methyl iodide.

Activated charcoal is sold by weight, but in filling a trap the volume is the factor defined. It is therefore important to check its density and moisture content.

The granulometry of an activated charcoal must be checked as a fundamental parameter of its efficiency towards iodine (5). It is also necessary to verify that the proportion of fine grains is not great enough to cause clogging of the sieve which holds the charcoal.

In measuring the pressure drop of a charcoal it is important to define the material used, particularly the device for compressing the charcoal and the type of charcoal-holder.

The friability of an activated charcoal is a mechanical resistance property to be taken into consideration. Elements filled with a friable charcoal do not stand up well to transportation, handling and vibration during operation. The measurement is carried out by rotation of a perforated cylinder containing a given quantity of charcoal and a metal block. The proportion of charcoal dust produced defines the friability.

To avoid corrosion of metal components, the pH of the activated charcoal must be checked by soaking in water and measuring the final pH of this water.

Since in the event of a reactor accident the gaseous effluent which must be purified before discharge often becomes very hot, the ignition temperature of the charcoal must be known and checked. To do this, air or carbon dioxide is passed at progressively increasing temperature through a charcoal sample placed in an insulated tube.

The efficiency of activated charcoal towards iodine is obviously an essential characteristic. The means of generating iodine 131 must be carefully studied. The original method was to oxidize a dry deposit of iodine 131-labelled alkaline iodide with dry hot air (600 to 800°C) (6). However at this temperature the measurements were perturbed, probably by the formation of an unstable gaseous compound of silicon and iodine. This is why, in the new process, iodine 127 is introduced not as iodide but in the form of vapour mixed with the air sweeping the radioactive iodide deposit. In this way iodine 131 is liberated by isotopic exchange at room temperature.

Since English and American researchers have shown (7 to 15) the existance of the methyl iodide form and the possibility of trapping it with impregnated charcoal, the need arises to test such charcoal with methyl iodide. Iodine 131-labelled gaseous methyl iodide is produced by reaction of dimethylsulphate on potassium iodide (16) after a process used by COLLINS, then let in a circuit containing air 90 °/₀ relative humidity. The methyl iodide emission lasts 15 minutes and the total duration of the test is four hours. The reference traps are made up of layers of coke charcoal impregnated to 5 °/₀ with triethylenediamine.

2.2 - Testing of the adsorbing elements

For the manufacture of the elements the quantity of activated charcoal necessary is taken from the batch already checked for delivery to the manufacturer.

After construction a percentage of the elements, varying with the size of the batch, is taken for testing.

Besides being examined for conformity with regard to dimensions, systems for keeping the charcoal compressed, shielding, joints etc... the following characteristics are checked :

- pressure drop
- efficiency towards iodine
- resistance to shock and vibration.

It does not seem strictly necessary to measure the efficiency towards methyl iodide, since in principle the efficiency-to-iodine measurement is enough to establish that the charcoal, already tested with methyl iodide, is being correctly employed. We feel therefore that we can dispense with it and thus avoid the installation of a high-humidity conditioning system on the high flow-rate testing bench used.

Since the efficiency of a trap is bound up with the way in which the charcoal is packed, it is important that this packing is not disturbed in spite of shocks during handling or any vibration in the course of operation. The element tested is therefore subjected to shocks from a vibrating machine, in different positions, then its efficiency towards iodine is checked.

2.3 - Testing of iodine trap units in situ

The testing of fitted iodine traps simply involves checking the efficiency towards molecular iodine, since the methyl iodide test would have little significance in view of the practical impossibility of conditioning to high humidity the air passing through the trap tested.

The molecular iodine check in situ is carried out according to the method already described for activated charcoal. A strong, leak-proof portable iodine source is used, smaller in volume and weight than the original model (6), of capacity 3 curies.

Experience shows that fairly frequent tests are necessary - several per year - on iodine traps installed on a circuit in permanent operation. The efficiency of activated charcoal towards iodine is affected by certain vapours, particularly those given off from paint. In order to cut down the frequency of tests in situ, always costly and often a hindrance to the running of the reactor, one or two small reference traps are installed on branch lines off the main trap and they can be easily removed from time to time for an efficiency check in the laboratory.

CONCLUSION

Although the methods briefly described for the testing of fitters and iodine traps can only be developed and improved as techniques progress by a C.E.A. Laboratory, well acquainted with air cleaning problems, it seemed important nevertheless that an organization completely independent of the C.E.A. and of the manufacturers should be given charge of the testing.

However because of the high quantities of radioiodine handled it was necessary to make an exception for the in situ checks on iodine traps, which will be handled by the health physics departments of nuclear Centres. For all the other tests we have approached the Centre d'Etudes de Prévention who have acquired the necessary training, and we therefore hope that they will soon be in systematic operation at the C.E.A.

REFERENCES

1 - Burgess, Silverman and Stein : ''A new technique for evaluating respirator performance''

2 - K.T. Whitby and C.M. Peterson : ''Electrical neutralization and particle size measurement of dye aerosols''
Ind. and Engry. Chem. Fund. 4, 66

3 - K.T. Whitby, D.A. Lundgren and C.M. Peterson : ''Homogeneous aerosol generators''
Int. J. Air Wat. Poll., 1965 Vol 9, pp. 263-277

4 - C.E.A., Service Technique d'Etudes de Protection : ''Critères de comportement au feu des filtres à air'', 16 mai 1966

5 - F. Billard, G. Chevalier et J. Pradel : ''Résultats obtenus dans la recherche des caractéristiques de piégeage de l'iode 131 par les charbons actifs'', Colloque International sur la Pollution Radioactive des Milieux Gazeux, Saclay, novembre 1963

6 - J. Pradel, G. Chevalier, F. Billard, J. Miribel : ''Méthode d'essai des pièges à iode équipant les circuits de ventilation des réacteurs'', Congrès Health Physics Society, New York 1963 - Note CEA N°455, 1963

7 - D.H. Atkins, A.E.J. Eggleton : ''Iodine compounds formed on release of carrier-free iodine 131'', A.E.R.E.-M-1211, 1963

8 - A.C. Chamberlain : ''Physical chemistry of iodine and removal of iodine from gas streams'', Report of Aerosol Group part 1 - A.E.R.E.-R.4286, 1963

9 - G.W. Parker, G.E. Creek, W.J. Martin, C.J. Barton : ''Fission product retention in reactor confinement systems - Efficiency of the ORR confinement system'', O.R.N.L. 3591, 1964

10 - R.D. Collins and J.J. Hillary : ''Some Experiments relating to the behavior of gasborne iodine'', Int. Symp. on Fiss. Prod. Release and Transp., Oak Ridge, April 1965

11 - D.A. Collins, R. Taylor and L.R. Taylor : ''The removal of methyl iodide from reactor effluent gases'', Int. Symp. on Fiss. Prod. Release and Transp., Oak Ridge, April 1965

12 - R.E. Adams and W.E. Browning Jr. : ''Removal of iodine compounds from air systems by activated charcoal'', Int. Symp. on Fiss. Prod. Release and Transp., Oak Ridge, April 1965

13 - D.A. Collins, R. Taylor and W.D. Yuille : ''Sampling and characterization techniques used in the study of iodine release from irradiated fuel elements'' Int. Symp. on Fiss. Prod. Release and Transp., Oak Ridge, April 1965

14 - A.W. Castleman, Jr, I.N. Tang and H.R. Munkelwitz : ''Chemical state of iodine released from irradiated fuel into steam'', Int. Symp. on Fiss. Prod. Release and Transp., Oak Ridge, April 1965

15 - W.E. Browning, Jr, R.E. Adams, R.D. Ackley, M.E. Davis and J.E. Attrill : ''Identity, Character and chemical behavior of vapors forms of radioiodine'', Int. Symp. on Fiss. Prod. Release and Transp., Oak Ridge, April 1965

16 - H.R. Diffey, C.H. Rumary, M.J.S. Smith and R.A. Stinchcombe : ''Iodine clean-up in a steam suppression system'', Appendix - Int. Symp. on Fiss. Prod. Release and Transp., Oak Ridge, April 1965

DISCUSSION

CHEEVER: Would you describe your uranine aerosol generator?

BRION: We use the one described by Professor K. T. Whitby, a collision atomizer. It is the same as the one described in British Standard Specification No. 2831, I think, and we have to add an impactor to remove the large particle, and we made a mixture with dry air to evaporate the droplets.

THOMAS: Are there anymore questions on this paper?

I would like to ask one question. Did you tell me that you intend to have your carbon beds impregnated with one of the amines to take care of methyl iodide?

BRION: Yes, I did, and we are strongly thinking about that, but it is not only a technical matter; there is an economical point of view concerning the choice of the impregnant. Of course, when it is safety, you cannot be stopped by money considerations, but for the choice of the impregnant when you have several solutions, you may consider their cost.

RIVERS: Have you reported on, in any detail, your experience in operation of iodine removal carbon units in reactor situations?

BRION: In fact, there is such a report, but not a recent one titled "Methode d'essaides des pieges a iode equipant les circuits, de ventilation de reacteurs" par J. Pradel, G. Chevalier, F. Billgard and J. Miribel, CEA No. 455, 1963.

ON-SITE TESTING OF FILTERS WITH SPECIAL REFERENCE TO SOLID AEROSOLS

Hans Flyger
H. C. Rosenbaum

Research Establishment Risö
Danish Atomic Energy Commission

Abstract

A lithium flame photometer test is proposed for on-site testing of filter installations. The lithium test is intercalibrated with the standard Sodium Flame Test. The spraying time needed to introduce the lithium salt into a ventilation system is considered inconvenient for systems handling more than 10^5 m^3/h. For such systems photoelectric particle counters can be used with the dust naturally present in the local atmosphere. Where the dust level is too low, Aitken nuclei can easily be artificially generated in sufficient amounts. The relation between filter evaluation by such particle counting and by lithium measurements is established.

INTRODUCTION

The on-site testing of installed filters presents problems which are generally absent from the techniques involved in the laboratory testing of filter elements.

In the laboratory a small filter element or system can be treated as a single unit and the test set-up arranged so that the efficiency of the unit appears in the results as the ratio between truly representative

samples of particle concentrations taken before and after the test unit.

In on-site testing the very physical layout might make it impossible to carry out determinations equivalent to those on the laboratory scale. Usually large filter banks are dealt with, containing one or more dust filters and the same number of absolute filters. These filter banks are installed to accommodate one or more large ventilation channels servicing an entire building section. The air flow in these channels is of the order of thousands to tens of thousands of cubic metres per hour.

It is intended to discuss some of the laboratory methods available for measuring the effectiveness of filters and to show how one of these methods can be adapted to accommodate the on-site evaluation of filter installations.

DISCUSSION OF SOME STANDARD LABORATORY FILTER TESTS IN RELATION TO ON-SITE TESTING

An estimation of the performance of a highly efficient filter is made on the basis of an experiment in which a cloud of particles in the micron range, moving at a certain velocity, is passed through the filter and the ratio between the concentrations of particles in the air before and after the filter is determined.

The experimental techniques discussed here involve the use of an inhomogeneous test cloud consisting of solid particles with an approximate mean size of about 0.5 microns.

Two examples of the employment of an inhomogeneous test cloud are the British standard tests the Methylene Blue Test[1] and the later developed Sodium Flame Test[2].

Both tests involve an atomizer which delivers a spray from a solution of methylene blue or sodium chloride. The spray is dried in an evaporation tube, thus forming a particulate cloud with particles of about 0.5 microns.

A common feature of the Methylene Blue and the Sodium Flame Test is that the attainment of reliable results depends on a most careful control of the atomizer air-flow system.

In the Methylene Blue Test a subjective comparison is made of the stain intensities on two filter papers sampling the air on either side of the test filter. The air sample from before the filter is obtained within a few seconds by means of a small hand pump, while the collection of an air sample from behind the filter takes about half an hour for highly efficient test filters. For a test filter with a penetrability of 0.02% the unfiltered volume of methylene-blue cloud may have to be about 12 ml (drawn evenly with

a hand pump) as compared with 60 litres of the filtered cloud, so that the two stain intensities lie close together for reliable comparison. In a comparable situation the lithium-flame test requires one or two litres for a sufficient sample to be gathered. The lithium test[4] is further free of subjective approximations, and the lithium amounts sampled before and after the test filter are measured quite independently of each other.

The Sodium Flame Test requires an even more carefully controlled atomizer air-flow system as no air sample is taken before the filter, the efficiency of the latter being evaluated only by measurement of the concentration of sodium in the air after the filter. The measurement is made by means of a specially designed flame photometer that can analyse a continuous air stream. The instrument has to be calibrated anew every time it is to be used, by allowing a diluted sample of the unfiltered test gas to enter the flame. In an on-site test, the required calibration equipment, which may involve the use of two flow metres and a mixing bottle for each decade the unfiltered test gas is diluted, is very inconvenient. In some, not uncommon, cases the section before a filter bank is in fact isolated from the effluent side by the wall in which the filter bank has been installed. In such cases it may prove impossible to connect the calibration equipment to the flame apparatus.

To avoid such difficulties, an essential specification for on-site equipment is that the sampling units before and after the test filter must be independent of each other. The equipment for the lithium flame test fulfils this demand and avoids the tedious task of repeated calibration of an air-flow system.

The hardware required for the construction of the sodium flame photometer is not among standard production items and must therefore be produced by each individual laboratory from the Porton specifications[3]. Any type of quality flame photometer may be used for the lithium test.

The application of the lithium flame test on-site will be discussed later in connection with a practical example.

The basic scheme of the lithium flame photometer test is briefly as follows:

A two per cent aqueous solution of Li_2SO_4 is atomized by a Collison atomizer (see Fig. 1). The spray is diluted with prefiltered dry air in an evaporation tube, which thus yields a diluted particulate stream of Li_2SO_4 crystals. The stream enters a mixing chamber where a few litres per minute is tapped and past through a membrane filter. A portion, or all, of the remaining flow is passed through the filter to be tested. The effluent air enters a second mixing chamber identical with the first, and an appro-

Modified Collison Atomizer

The design allows the atomizer to be used for small quantities of radioactive solutions. The cap design ensures complete tightness of the system.

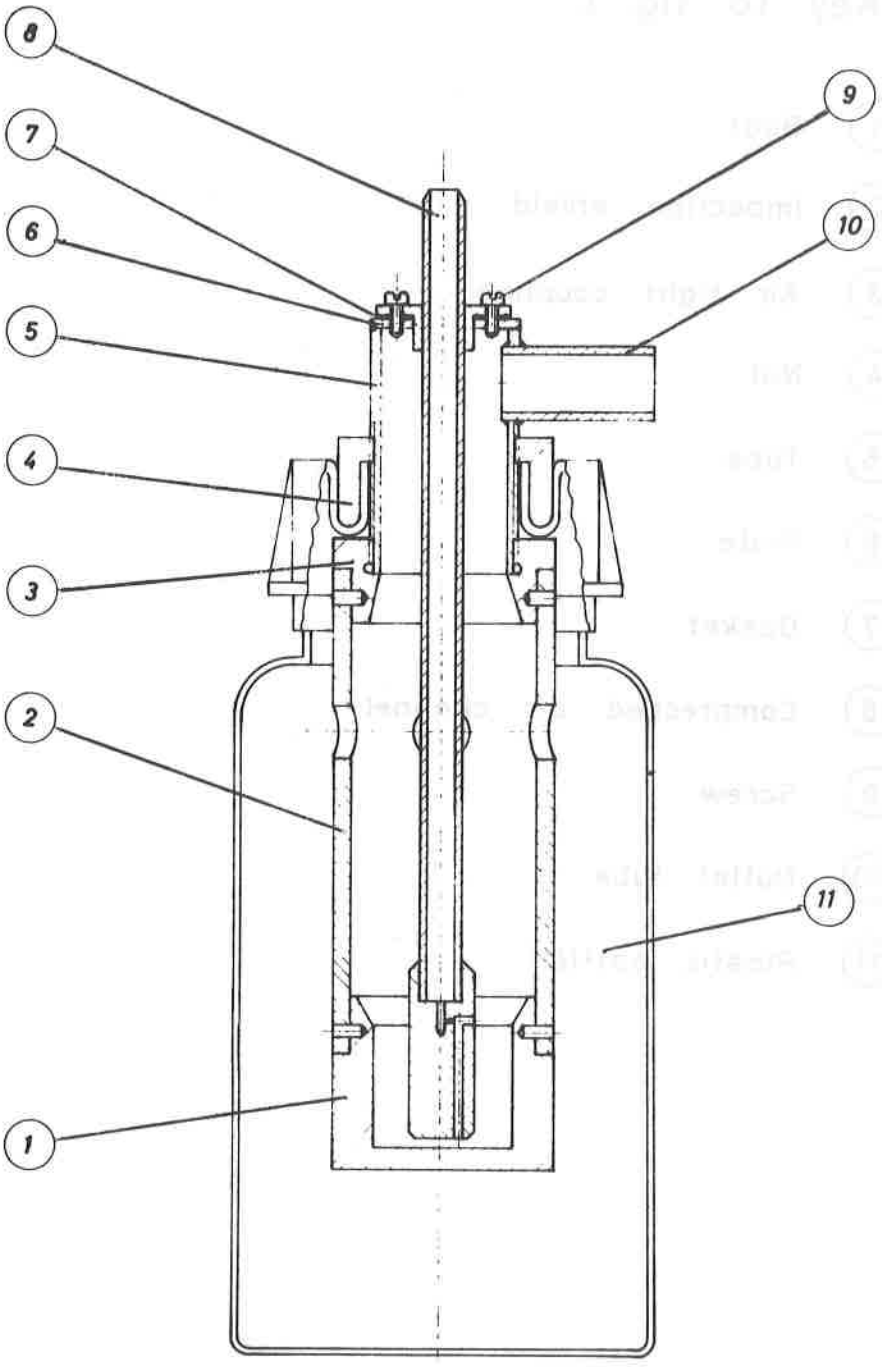

Fig. 1.

Key to fig. 1.

(1) Boat

(2) Impaction shield

(3) Air tight coupling

(4) Nut

(5) Tube

(6) Plate

(7) Gasket

(8) Compressed air channel

(9) Screw

(10) Outlet tube

(11) Plastic bottle

priate amount of the flow is tapped and passed through a second membrane filter. The membrane filters are then processed chemically, and two solutions are produced in which concentrations of lithium as low as 0.0002 γ/ml can be detected with a quality flame photometer.

The ratio between the lithium contents of the two solutions is then, after compensation for differences of air volumes sampled, a measure of the effectiveness of the test filter.

That lithium has been chosen as a tracer substance for sodium though a flame photometer is about ten times as sensitive to sodium as to lithium is due to the relative rarity of lithium in laboratory surroundings and the ease with which it is measured on a flame photometer because of the lack of interference from other alkali metals present[5].

In coastal areas, concentrations of NaCl in the air[6] of up to 20.000 ug NaCl per m^3 have been measured.

A set of membrane filters rubbed over various surfaces at this laboratory were processed for lithium determinations on a photometer capable of detecting 0.0002 γ Li/ml in the 5 ml solutions used. In no case was any lithium found.

The inapplicability of sodium a tracer component is further emphasized by the variations of the amounts of sodium found on fresh membrane filters. If an amount of sodium large enough to allow us to neglect the variation in the sodium content of the filters should be sampled from the air after the filter to be tested, it would in practice mean that sodium would be much less sensitive than lithium as a tracer component.

The mean size by mass of the Li_2SO_4 particles was not measured, but the atomizers employed in all the experiments deliver NaCl particles of a mean size by mass of 0.6 microns from a 2% NaCl solution.

Electron microscopy reveals that Li_2SO_4 crystals appear as elongated rhombic forms unlike the cubic NaCl crystals from a Sodium Flame Test cloud.

As the original atomizer made from the Porton specifications was of steel, it was reconstructed in a hard plastic to avoid corrosion. At the same time the containment was changed, the glass jar originally used being replaced by a plastic bottle to avoid the difficulties of tightening the screw-lid. For radioactive tracer experiments, in which the amount of radioactivity applied in the atomizer should not exceed what is necessary for the experiment, a special beaker was attached to the bottom of the impaction shield. In this case the holes in the impaction shield should be closed to avoid waste of liquid.

1. Methylene Blue Particulate Test for Respirator Filters. British Standard No. 2577 (1955).

2. Sodium Flame Particulate Test. Chemical Defence Experimental Establishment, Porton Down, Salisbury, Wilts, England. Porton Specification No. 1632 A.

3. Drawing No. 6536, Sodium Flame Test Equipment. Chemical Defence Experimental Establishment, Porton Down, Salisbury, Wilts.

4. H. Flyger, H.C. Rosenbaum. A Lithium Flame Photometer Test for Highly Efficient Filters. J. Am. Ind. Hyg. Ass. 26 (1965).

5. T.F. Borovik-Romanova. Mutual Influence of Alkali Metals in their Determination by Flame Photometry. Bull. Acad. Sci. USSR No. 7: 955 (1962).

6. R.M. Moyerman, K.E. Shuler. The Concentration of Contaminant Alkali Salts in Ground-Level Air. Science 118: 512 (1953).

CALIBRATION OF THE LITHIUM TEST WITH THE SODIUM FLAME TEST AND POLLAK COUNTINGS

In order to determine what differences a filter might display between a sodium chloride cloud and a lithium sulfate cloud, a series of investigations were made. The importance of such inter-calibration is apparent as the Sodium Flame Test is a standard test widely used by filter manufacturers.

The intercalibration was carried out by spraying 2% solutions of Li_2SO_4 and NaCl into the open end of a cylindrical conduit of diameter 8 cm leading to the test filter. From the latter the conduit continued to a larger conduit in which a ventilation fan drew the air. The air flow through the test filter was measured by a flow meter of the rotameter type and controlled by adjusting a valve opening into the large conduit.

The cylindrical conduit from inlet to test filter was about 8 metres long and contained two baffle plates. It had a sharp bend two metres from the test filter.

A before-filter tap-hole was situated after the bend and an after-filter tap-hole about 8 metres from the test filter, after a baffle plate.

The atomizer was of the type shown in Fig. 4. An aluminium pot contains three atomizers of the collison type, made from the Porton specifications. The atomizers are interconnected by a distributor plate allowing a general feed of compressed air to them of about 7 atmospheres. In order

Portable Atomizer for On-Site Testing

The three atomizer elements included are equivalent in structure to the element used in the Collison Atomizer shown in fig. 1.

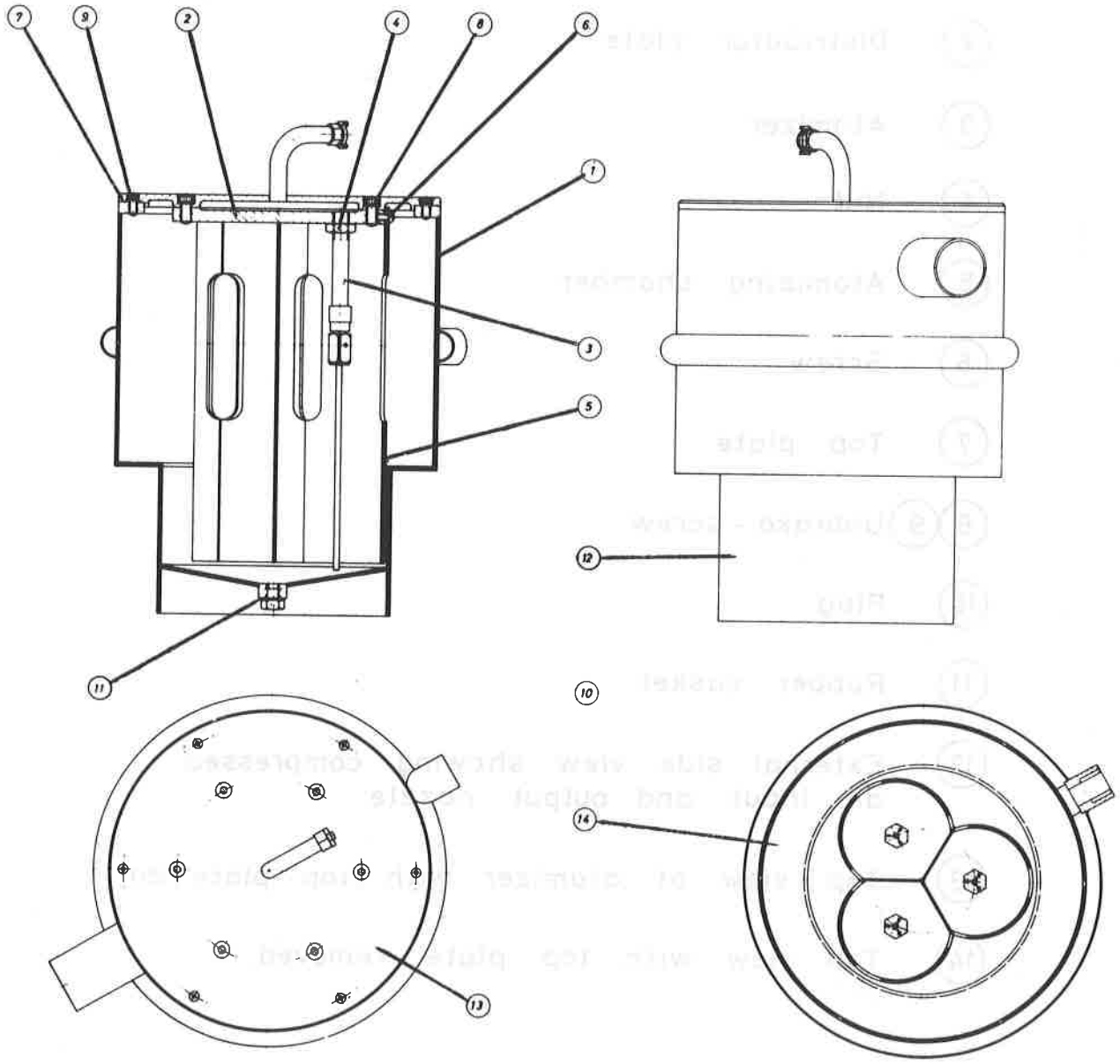

Fig. 4.

Key to fig. 4.

(1) Aluminium container

(2) Distributor plate

(3) Atomizer

(4) Nut

(5) Atomizing chamber

(6) Screw

(7) Top plate

(8) (9) Unbrako - screw

(10) Plug

(11) Rubber gasket

(12) External side view showing compressed air input and output nozzle.

(13) Top view of atomizer with top plate on.

(14) Top view with top plate removed.

to obtain an efficient impingement of the atomized liquid, the atomizers are surrounded by a special baffle-plate arrangement allowing an equally efficient impingement of the droplets from all sides. Fast evaporation of the droplets and an improved yield of lithium crystals are obtained by the addition of an air flow through a range of small holes placed along the circumference of the aluminium pot. The extra air is distributed on the holes by means of a circular tube welded to the outside of the pot.

The total output from the atomizer pot was measured at about 8 ml liquid/min. With a compressed-air flow at 7 atm and an auxiliary evaporation air flow of about 100 l/min the consumption of compressed-air is 252 l air (760 mm Hg)/min.

The NaCl solution was spiked with 24 Na so that the test-filter penetration could be measured directly by counting of the activities sampled from the air before and after the filter.

The lithium measurements were made by the method mentioned previously. The details of this method are described in the following section.

The test filters comprised the types 33, 44, 55 manufactured by the British filter manufacturing company Vokes Ltd. The manufacturer's penetration ratings for the filters in the above order were 25%, 2% and 0.05%. The filters were tested at a flow rate of 850 litres per minute.

In addition to these tests the natural particles found in the building were drawn through the test filters.

The before and after particle concentrations were determined by means of two Pollak counters[7] operating from the two tap-holes.

The penetration of these natural aerosols is shown together with the results of the inter-calibration.

The purpose of using the Pollak counters is to demonstrate the relation between the mass penetration of the lithium and sodium salts and the particle-number penetration of the natural aerosol.

In cases where the natural particles found in the air are present in concentrations too low to be measured accurately after passage through a highly efficient filter, particles can be generated artificially by inflating a large rubber balloon with particles from a filament over which a boat of TUFNOL is suspended. Within a short time a large reservoir can in this way be loaded with a very high particle concentration.

The particles generated in this way have a diameter of about 10^{-5} cm provided that during the glowing process the air around the Tufnol boat is only circulated by the free convection from the heat developed. If forced convection is applied, the diameter of the particles may fall in the range of 10^{-6} to 10^{-7} cm.

A test with a 66 type filter (manufacturer's rating 0.1% penetration) displays the so-called pinhole effect, see Fig. 2. The effect, when present, can easily be ascertained by means of a Pollak counter as well as by a lithium test as the penetration appears to decrease with increasing air speed through the filter. The pinhole effect may dominate the performance of a filter.

Whether there were actual pinholes in the filter material or pinhole leaks due to damage or faulty installation, was not determined. It can only be said that the unit did not function according to the manufacturer's specifications.

7. A. L. Metnieks, L. W. Pollak. Instruction for the Use of Photoelectric Condensation Nucleus Counters. Geophys. Bull. 16 (1959).

PREPARATION OF THE FLAME-PHOTOMETER SOLUTIONS FOR THE DETERMINATION OF LITHIUM ON MEMBRANE FILTERS

It has been determined that a Göttingen membrane filter of 50 $mm^{\varnothing}$ of the type MF can be dissolved under gentle heating in 1 ml conc. HNO_3. If this solution is diluted with H_2O to 5 ml, a Zeiss flame photometer of the type PF 5 is able to detect the presence of 0.003 γ/ml Li. It has been found that the response of the photometer to these solutions is not linear in the range 0.003 γ/ml Li to 0.03 γ/ml Li. Further, the responses are quite unstable.

In order to increase the sensitivity of the photometer readings, the addition of 1 part of acetone to 4 parts of the final solutions was tried.

A membrane filter was dissolved in 1 ml concentrated HNO_3 in a 5 ml measuring flask by heating gently over a bunsen flame and shaking. The solution was allowed to cool to room temperature. 1 ml of distilled water was added, and the solution was allowed to cool to room temperature. An appropriate amount of Li in aqueous solution was added (see below). 1 ml of acetone was added. A white precipitate formed. Distilled H_2O was added up to the 5 ml mark, and the flask was shaken thoroughly. The contents were then filtered through a Whatman glass-fibre filter, and the clean effluent was set aside in another 5 ml measuring flask. On account of the constant formation of gas from this solution it is advisable to leave the flasks only lightly covered.

For measurements on the flame photometer a range of standard solutions were prepared. As an appropriate amount of Li, the following quantities of a 3 γ Li/ml solution were added to the measuring flasks: 5, 10,

Plot of Results from Tests with Filter 66

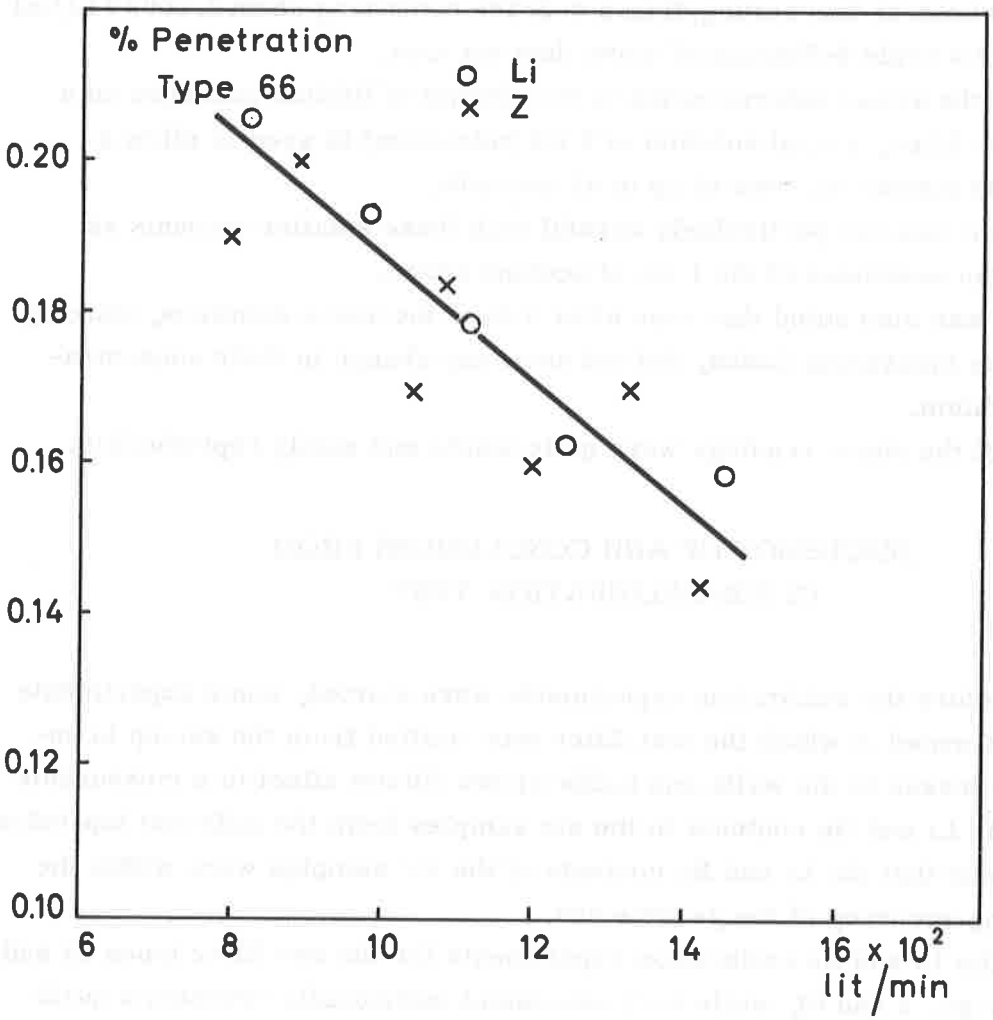

Fig. 2

20, 25, and 50 ul, giving standard solutions of 0.003, 0.006, 0.012, 0.015, and 0.03 γ Li/ml. The null solution was obtained by eliminating the addition of Li. The measurements on the flame photometer are shown in Fig. 3.

In order to ascertain whether any of the lithium was lost in the precipitate, a new calibration row was made in which the aliquots of 3 γ Li/ml sol. were added in the final step after filtration.

The measurements on the flame photometer are shown in Fig. 3.

In addition to these tests, one was performed in which the photometer was set at its maximum sensitivity and the null solution adjusted to zero on the scale. In this case the 0.003 γ Li/ml sol. read 25 units on the scale.

If the instrument is assumed to respond approximately linearly to these solutions at this setting, then a solution containing about 0.0002 γ Li/ml would give a scale deflection of more than one unit.

In the actual determination of the amount of lithium adsorbed on a membrane filter, a total solution of 5 ml (minimum) is used to allow a reasonable measuring time of up to 45 seconds.

One must be particularly careful with these smaller amounts as regards the exactness of the 1 ml of acetone added.

It was also noted that even after 7 days the above solutions, standing open in the measuring flasks, did not show any change in their concentration of lithium.

All the above readings were quite stable and easily reproducible.

DISCUSSION OF AND CONCLUSIONS FROM INTER-CALIBRATION TEST

Before the calibration experiments were started, some experiments were performed in which the test filter was omitted from the set-up to ensure that losses to the walls and baffle plates did not affect to a measurable degree the Li and Na contents in the air samples from the different tap-holes. It was found that the Li and Na contents of the air samples were within the measuring accuracy of the gasometers.

The Li and Na calibration experiments for the two filter types 55 and 44 (see Figs. 5 and 6), while very consistent individually revealed a qualitative shift in the Li - Na ratio of penetrability of the two filters. The shift was somewhat surprising and could not be explained by means of the filtration theory. The filters were consequently reinstalled, and the calibration experiments were repeated. Figs. 8 and 9 display the results. Comparing

Fig. 3

Calibration Curves for Zeiss PF5 Flame Photometer
Air pressure = 1ato., Acetylene pressure = 90 mm W

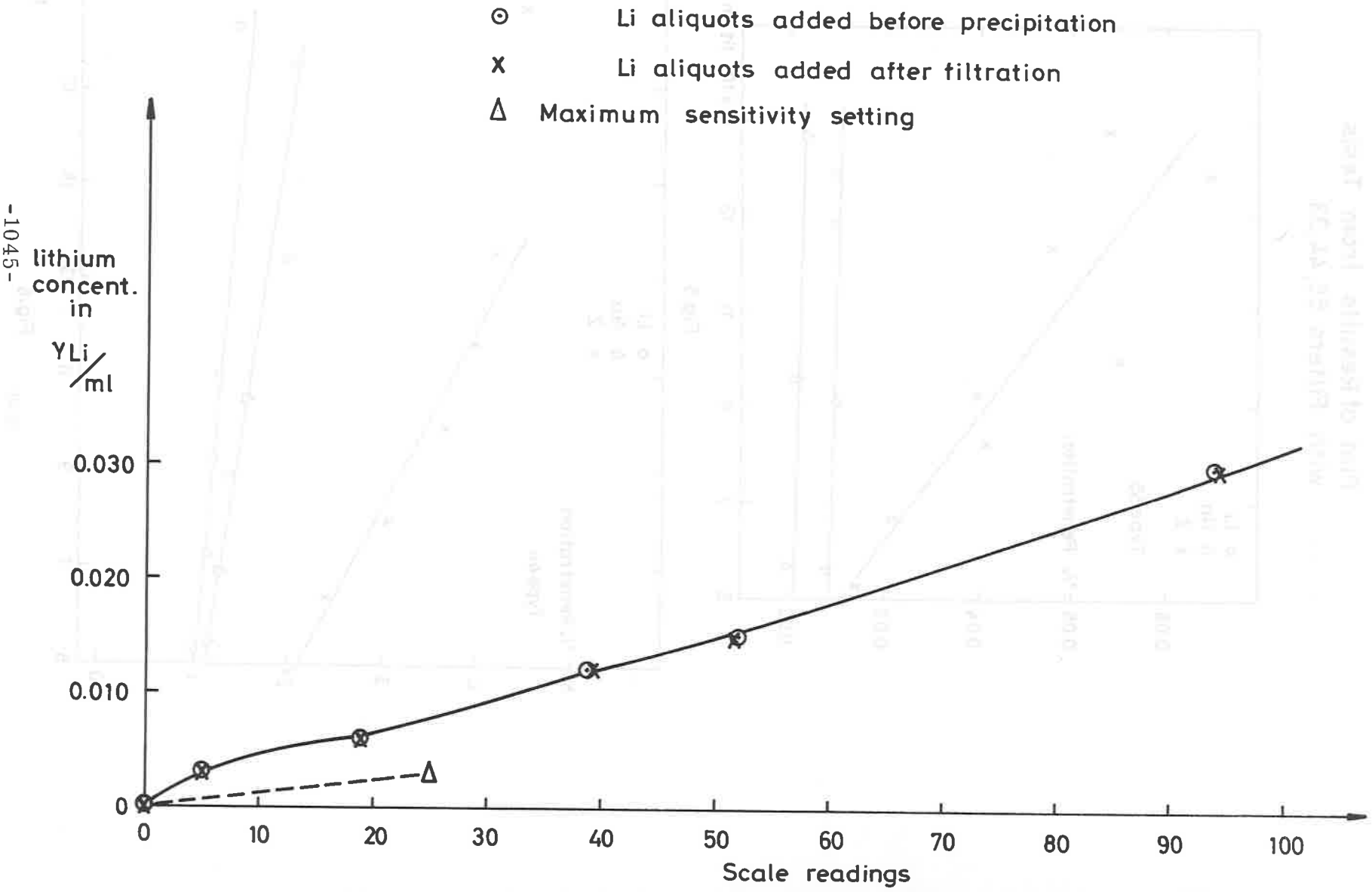

Plot of Results from Tests with Filters 55, 44, 33

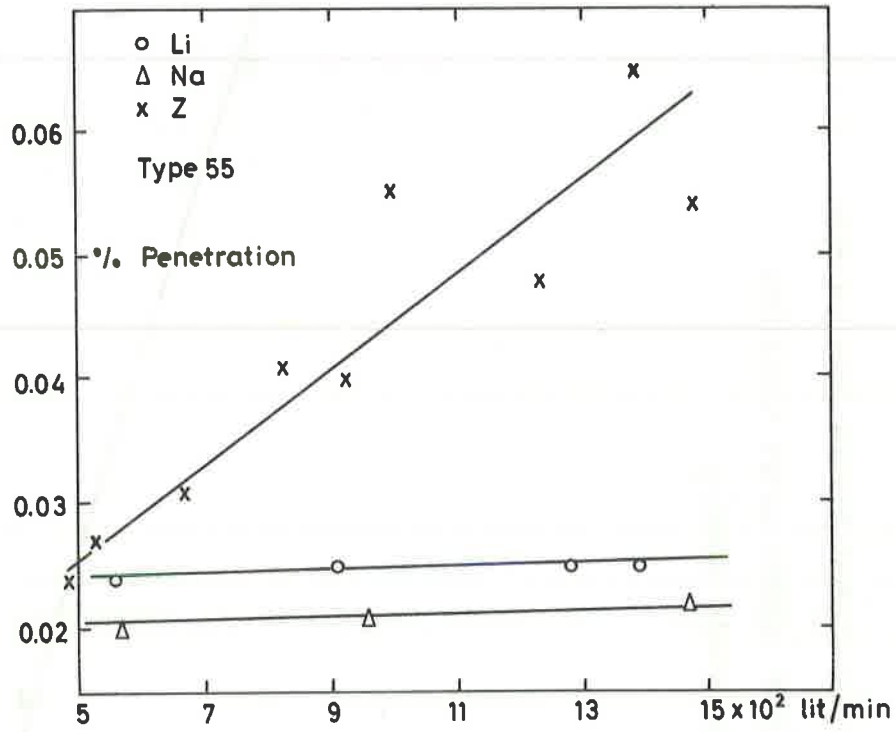

Fig.5

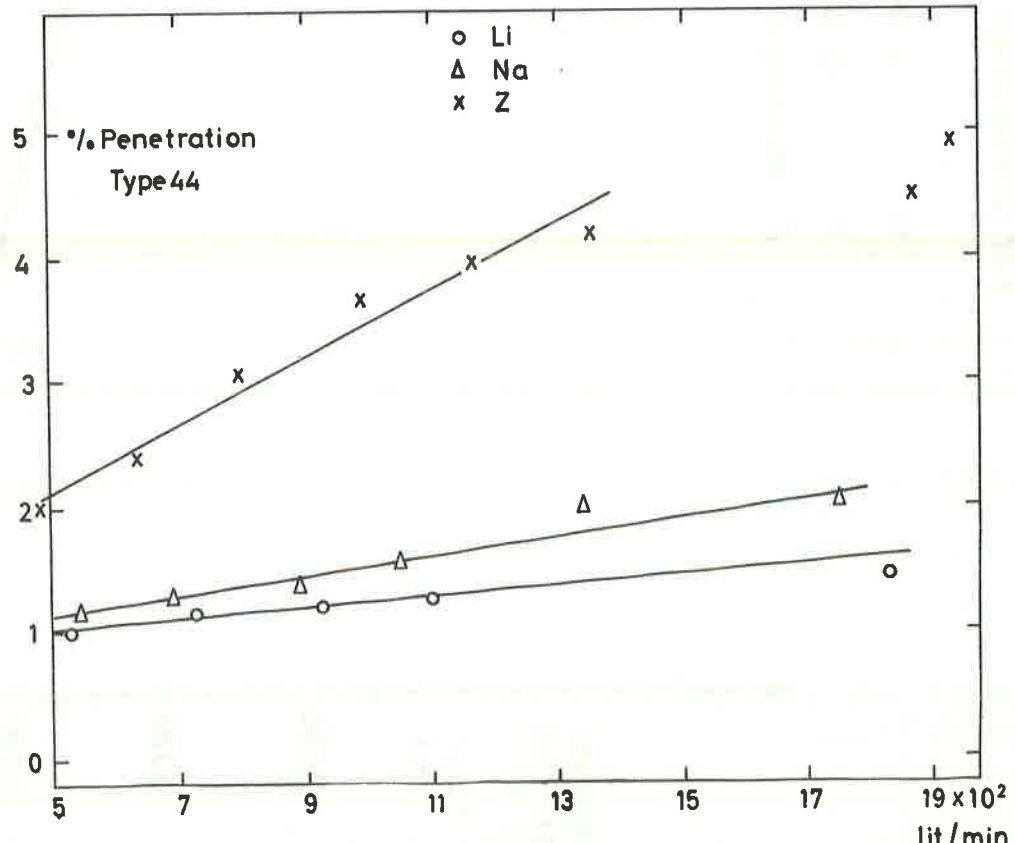

Fig.6

the results from Fig. 5 with those from Fig. 8 and the results from Fig. 6 with those from Fig. 9, we notice the same qualitative shift in the Li - Na ratio of penetrability, but in this particular case it is not related to a shift in filter type, but connected with the same individual filter. These observations made us look for an uncertainty in the radioactive counting technique involved in the estimation of the $_{24}$Na.

The after filters from the $_{24}$Na tests were measured on two different types of counters, a G - M counter in cases in which the activities to be measured were well above the background of the counter, and an anti-coincidence gas-flow counter when the activities were weaker. The before filters were all measured with a G - M counter.

The ratio of effectiveness between these two counters was found to vary from 6.5 to 8.5, and this must be regarded as an inherent uncertainty in the relative positions of the lithium to the sodium curves from test to test.

Thus it cannot be concluded from Figs. 5-9 that lithium sulphate and sodium chloride are filtered significantly differently by the test filters used.

The conclusion is therefore that, according to our measurements a given filter of the type 33, 44 or 55 does not discriminate between Li_2SO_4 particles and NaCl particles, and that the Li_2SO_4 test is equivalent to the NaCl test.

The Pollak counter curves, on the other hand, lie consistently relative to the lithium and sodium curves as shown.

DISCUSSION OF AN EXAMPLE OF AN ON-SITE TEST

A simple example of a large installed filter system is that cleansing the ventilation air of the reactor building DR 3 at Risö.

The installation consists of a single ventilation channel, cross section about 1 m^2, in which the flow is 6000 m^3/h. In this duct a primary dust filter and an absolute filter are installed. The underpressure in the channel is about 80 mm H_2O before the primary filter and about 150 mm H_2O after the absolute filter.

At a point about six metres from the face of the primary filter a cloud of droplets atomized from a 2% Li_2SO_4 aqueous solution is sprayed into a tap-hole. At a point between the primary and the absolute filter another tap-hole is connected to a piston pump which draws about 20 litres per minute from the channel air through a membrane filter.

Further downstream, about ten channel diameters from the end face

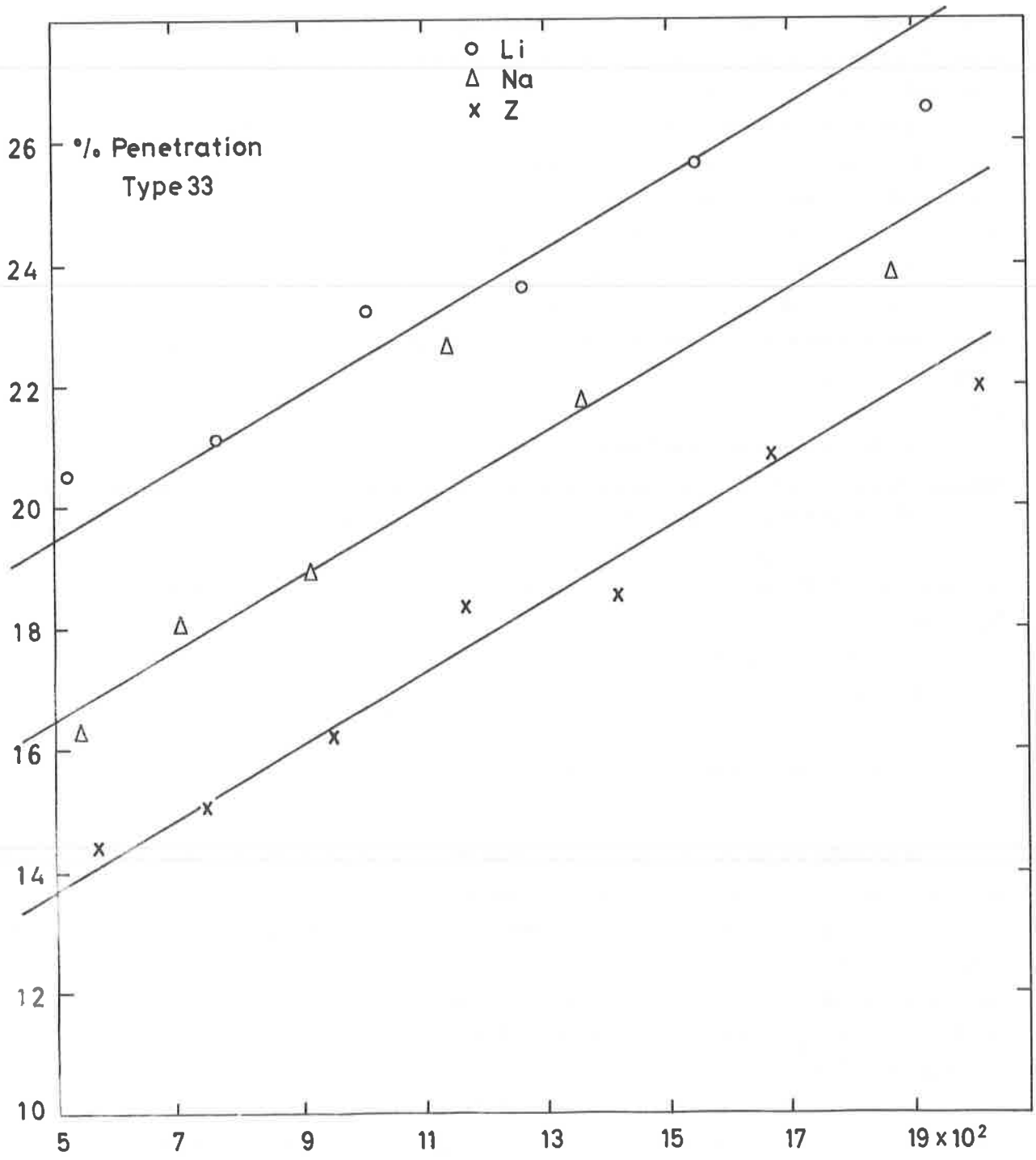
o Li
Δ Na
x Z
% Penetration
Type 33
26
24
22
20
18
16
14
12
10
5
7
9
11
13
15
17
19 x 10²

Fig.7

Repetition of Tests with Filters 44, 55 after Removal and Reinstallation

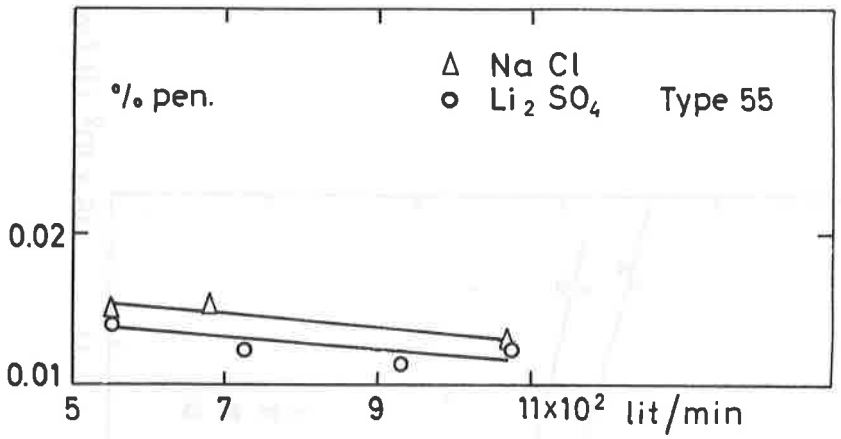

Fig. 8

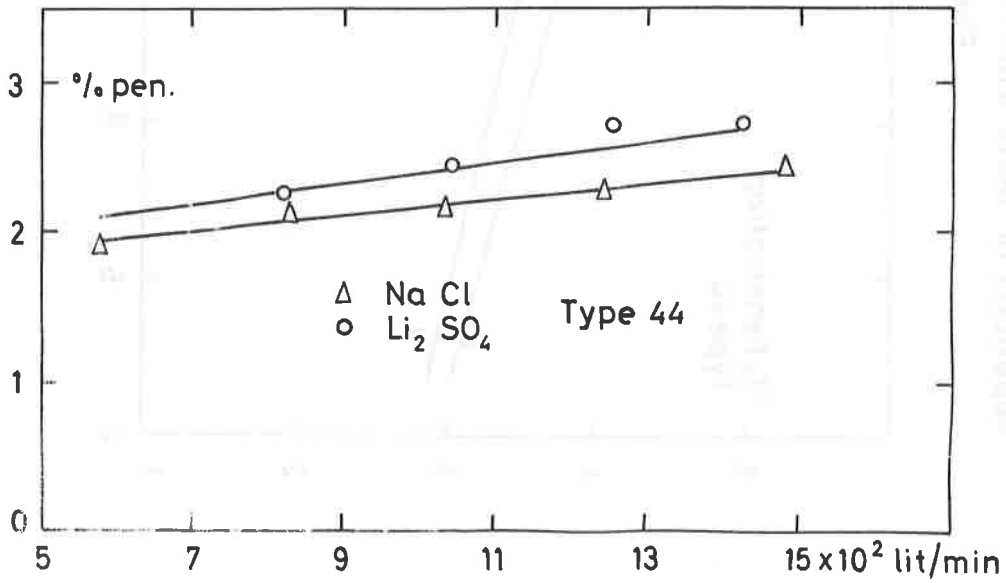

Fig.9

Repetition of Tests with Filter 44 Demonstrating the Start Phenomenon

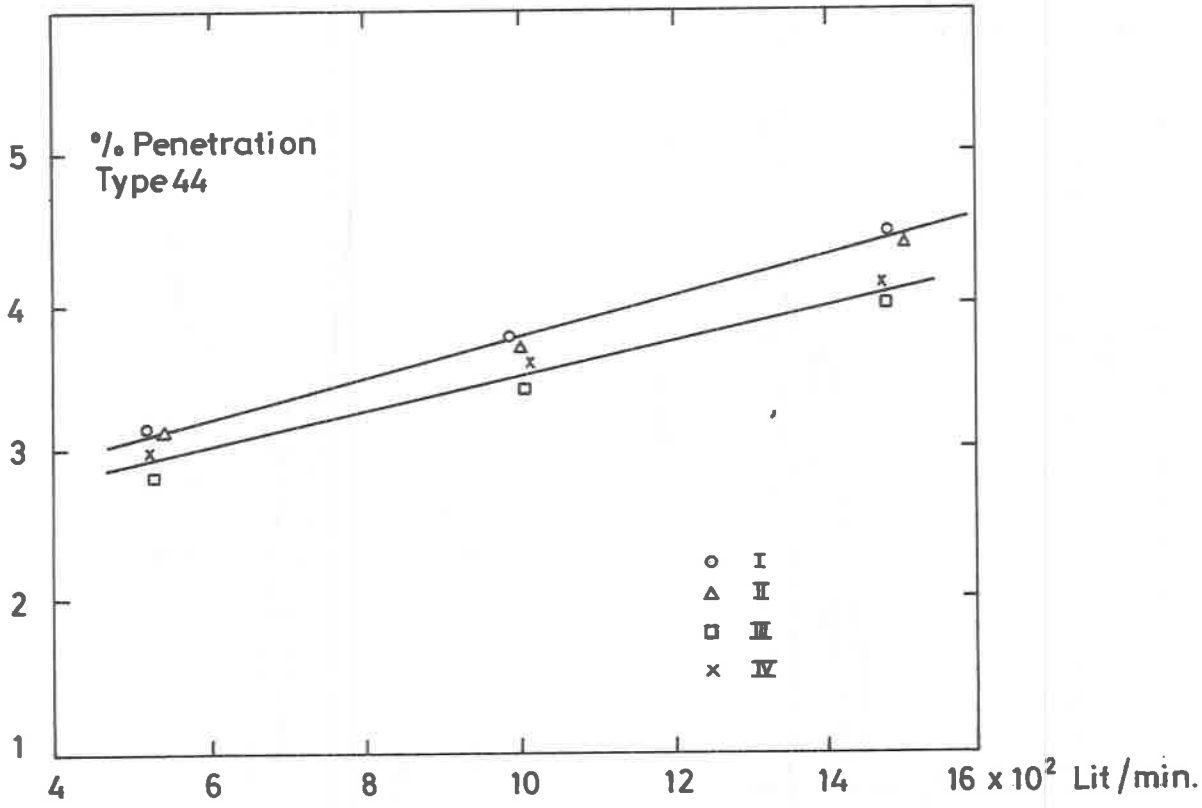

Fig. 10

Flow Diagram of the Modified EEL Flame Photometer

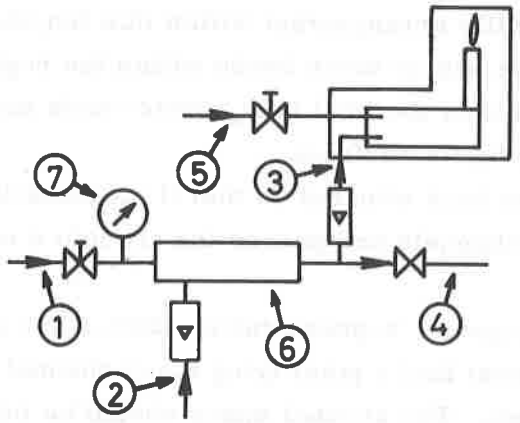

① Compressed Air Supply
② Test Air Input
③ Test Air Mixture
④ Shunt
⑤ Burner Gas Input
⑥ Ejector Pump
⑦ Manometer

Fig. 11

of the absolute filter and round a gradual right-angle bend in the channel, a final tap hole draws 20 litres per minute of air through a membrane filter.

The flow of sampled air is monitored by two flow meters of the float type, and the air volumes are measured by two gasometers.

The atomizer used was of the type shown in Fig. 4. Four runs were performed, and the results were as follows: trial 1: 0.69%, trial 2: 0.70%, trial 3: 0.10%, and trial 4: 0.60% penetration.

The variation in these results illustrates a basic aspect of site testing.

In order to be certain that an air sample taken from a channel is representative of the total air flow passing through the channel at that point, one has to be sure that any tracers in the air are homogeneously distributed within the channel at that point, i.e. that the stream has been thoroughly blended.

According to recent determinations[8], thorough mixing in such a conduit is assumed for points lying more than 30 channel diameters downstream of a source of contamination or the effluent face of a filter, and that only if there is some baffle arrangement within this length.

If the conduit has one or more bends within the region from the point of injection of the aerosol to the final hole, these bends might, if sufficiently acute be effective as baffle surfaces.

Consider a filter bank situated so that it cleanses the air coming from a few ventilation channels and passes the air into a common exhaust channel.

If one wishes to gather representative after-filter samples from the exhaust channel, one must find a point lying many channel diameters downstream of the filter bank. The aerosol spray should be introduced, if possible, so far upstream of the filter bank that the concentration of lithium-chloride particles is homogeneous across the face of the filter bank. A before-filter sampling hole could then be made near the face of the filter bank.

If these points exist and are accessible, the above procedure can yield a measurement of the efficiency of the filter bank as a whole.

An on-site test that fulfilled the above requirements was carried out on the same filter at the DR 3 reactor.

In this case the aerosol from a $_{24}$Na spiked 2% NaCl solution was introduced into one of the inlets of a ventilation duct in the reactor hall itself.

The tap-hole for the before filter was situated just before the primary filter face and the after tap-hole about 15 metres downstream of the absolute filter; the length of conduit in between had four sharp bends.

According to the NaCl test cloud, the penetration was 0.06%.

The atomizer used was a modified Collison delivering 15 ml of solution per hour.

A total of 10 mC $_{24}$Na was sprayed into the ventilating system in order to ensure good after-filter measurements. The spraying time was 6 hours.

The same DR 3 filter bank could have been evaluated by means of a 2% Li_2SO_4 solution atomized by the portable atomizing unit capable of delivering 8 ml solution per min. The total number of litres to be sampled by the after filter in order to ensure a good flame-photometer reading was calculated at about 80.

The same test was performed on an auxiliary filter unit situated in parallel to the first filter. The penetration according to the Na^{24} Cl test cloud was 0.10%.

A test was then performed with the Pollak counters, the natural aerosol from the reactor hall being utilized for purposes of comparison.

The first filter displayed a particle-number penetration of 0.12%, twice that of the NaCl cloud.

The auxiliary filter displayed a particle-number penetration of 0.25%, $2\frac{1}{2}$ times that of the NaCl cloud.

The particle count in the reactor hall was of the order of 250,000 particles/cm^3, and sometimes much higher. This high concentration might be found in most reactor halls and is probably due to the high level of ionizing radiation emanating from various research arrangements around the reactor.

The particles in such aerosols can be expected to have a diameter of about 10^{-7} cm.

8. S.E. Smith, P.A. White. Design of Radioactive Filtration Systems. Nucl. Eng. June (1962).

DISCUSSION OF AND CONCLUSIONS FROM INTER-CALIBRATION TEST

Before the calibration experiments were started, some experiments were performed in which the test filter was omitted from the set-up to ensure that losses to the walls and baffle plates did not affect to a measurable degree the Li and Na contents in the air samples from the different tap-holes. It was found that the Li and Na contents of the air samples were within the measuring accuracy of the gasometers.

The Li and Na calibration experiments for the two filter types 55 and 44 (see Figs. 5 and 6), while very consistent individually revealed a qualitative shift in the Li-Na ratio of penetrability of the two filters. The shift was somewhat surprising and could not be explained by means of the filtration theory. The filters were consequently reinstalled, and the calibration experiments were repeated. Figs. 8 and 9 display the results. Comparing the results from Fig. 5 with those from Fig. 8 and the results from Fig. 6 with those from Fig. 9, we notice the same qualitative shift in the Li-Na ratio of penetrability, but in this particular case it is not related to a shift in filter type, but connected with the same individual filter. These observations suggest an uncertainty in the radioactive counting technique involved in the estimation of the ^{24}Na.

The after filters from the ^{24}Na tests were measured on two different types of counters, a G-M counter in cases in which the activities to be measured were well above the background of the counter, and an anti-coincidence gas-flow counter when the activities were weaker. The before filters were all measured with a G-M counter.

The ratio of effectiveness between these two counters was found to vary from 6.5 to 8.5, and this might have been a source of uncertainty in the relative positions of the lithium to the sodium curves from test to test.

Thus it cannot be concluded from Figs. 5-9 that lithium sulphate and sodium chloride are filtered significantly different by the test filters used.

In order to eliminate the possible effect of counting error, a new series of the same experiments with the same 44-filter was performed in which all the counting was done on a single scintillation counter. The shifts between the effectivity curves from test to test for both sodium and lithium were found to be the same as those observed previously. Therefore it was concluded that the counting technique was not a cause of this apparent shifting.

There were two other possibilities that might each lead to such variations. It was possible that the atomizer mechanism somehow varies; or that the filter itself undergoes a true variation in effectivity during the test series.

If a variation in the atomizer mechanism were responsible for the shifts then one could hope to observe such variations by taking effectivity measurements before and after stopping and starting the atomizer again.

If there is an intrinsic variation in the filter itself from test to test then one could try to force such variations by varying the airflow through the filter from extreme to extreme and seeing if a given effectivity determination taken before and after these impressed flow changes holds the same value.

It was shown that no significant shifts were present due to the

starting and stopping of the atomizer, or due to the raising and lowering of the flow from nearly zero to maximum flow (1600 lit./min.), but that there was a shift measured when the air flow was completely stopped then started again.

The shift in this latter case was, for the 44 type filter, from a penetrability of 4.85% to a penetrability of 4.50%, at a flow of 1000 lit./min.

In order to confirm the existence of such a 'start phenomenon', whereby a filter's effectivity may change each time the air-flow through it is stopped and started again, two experiments were performed.

A test cloud of ^{24}Na spiked NaCl was used on the 44-filter.

The points on each curve were determined as the air flow was increased from zero to maximum and back to zero again.

The shift between the two curves shown in Fig. 10 indicate the existence of the start phenomenon.

The conclusion is therefore that, according to our measurements a given filter of the type 33, 44 or 55 displays a start phenomenon that dominates any discrimination of these filters between Li_2SO_4 and NaCl particles. The Li_2SO_4 test is therefore practically equivalent to the NaCl test.

The Pollak counter curves, on the other hand, are consistent relative to the lithium and sodium curves as shown.

DISCUSSION OF AN EXAMPLE OF AN ON-SITE TEST

A simple example of a large installed filter system is that cleansing the ventilation air of the reactor building DR 3 at Risö.

The installation consists of a single ventilation channel, cross section about 1 m^2, in which the flow is 6000 m^3/h. In this duct a

primary dust filter and an absolute filter are installed. The underpressure in the channel is about 80 mm H_2O before the primary filter and about 150 mm H_2O after the absolute filter.

At a point about six metres from the face of the primary filter a cloud of droplets atomized from a 2% Li_2SO_4 aqueous solution is sprayed into a tap-hole. At a point between the primary and the absolute filter another tap-hole is connected to a piston pump which draws about 20 litres per minute from the channel air through a membrane filter.

Further downstream, about ten channel diameters from the end face of the absolute filter and round a gradual right-angle bend in the channel, a final tap-hole draws 20 litres per minute of air through a membrane filter.

The flow of sampled air is monitored by two flow meters of the float type, and the air volumes are measured by two gasometers.

The atomizer used was of the type shown in Fig. 4. Four runs were performed, and the results were as follows: trial 1: 0.69%, trial 2: 0.70%, trial 3: 0.10%, and trial 4: 0.60% penetration.

The variation in these results illustrates a basic aspect of site testing.

In order to be certain that an air sample taken from a channel is representative of the total air flow passing through the channel at that point, one has to be sure that any tracers in the air are homogeneously distributed within the channel at that point, i.e. that the stream has been thoroughly blended.

According to recent determinations [8], thorough mixing in such a conduit is assumed for points lying more than 30 channel diameters downstream of a source of contamination or the effluent face

of a filter, and that only if there is some baffle arrangement within this length.

If the conduit has one or more bends within the region from the point of injection of the aerosol to the final hole, these bends might, if sufficiently acute, be effective as baffle surfaces.

Consider a filter bank situated so that it cleanses the air coming from a few ventilation channels and passes the air into a common exhaust channel.

If one wishes to gather representative after-filter samples from the exhaust channel, one must find a point lying many channel diameters downstream of the filter bank. The aerosol spray should be introduced, if possible, so far upstream of the filter bank that the concentration of lithium chloride particles is homogeneous across the face of the filter bank. A before-filter sampling hole could then be made near the face of the filter bank.

If these points exist and are accessible, the above procedure can yield a measurement of the efficiency of the filter bank as a whole.

An on-site test that fulfilled the above requirements was carried out on the same filter at the DR 3 reactor.

In this case the aerosol from a ^{24}Na spiked 2% NaCl solution was introduced into one of the inlets of a ventilation duct in the reactor hall itself.

The tap-hole for the before filter was situated just before the primary filter face and the after tap-hole about 15 metres downstream of the absolute filter; the length of conduit in between had four sharp bends.

According to the NaCl test cloud, the penetration was 0.06%.

The atomizer used was a modified Collison delivering 15 ml

of solution per hour.

A total of 10 mC ^{24}Na was sprayed into the ventilating system in order to ensure good after-filter measurements. The spraying time was 6 hours.

The same DR 3 filter bank could have been evaluated by means of a 2% Li_2SO_4 solution atomized by the portable atomizing unit capable of delivering 8 ml solution per min. The total number of litres to be sampled by the after filter in order to ensure a good flame-photometer reading was calculated at about 80.

The same test was performed on an auxiliary filter unit situated in parallel to the first filter. The penetration according to the $^{24}NaCl$ test cloud was 0.10%.

A test was then performed with the Pollak counters, the natural aerosol from the reactor hall being utilized for purposes of comparison.

The first filter displayed a particle-number penetration of 0.12%, twice that of the NaCl cloud.

The auxiliary filter displayed a particle-number penetration of 0.25%, $2\frac{1}{2}$ times that of the NaCl cloud.

The particle count in the reactor hall was of the order of 250,000 particles/cm^3, and sometimes much higher. This high concentration might be found in most reactor halls and is probably due to the high level of ionizing radiation emanating from various research arrangements around the reactor.

The particles in such aerosols can be expected to have a diameter of about 10^{-7} cm.

CONCLUDING REMARKS

The question arises as to the significance of the efficiency measured in these ways. It is not the inherent penetrability of the adsorbing material in the individual filters that is of principle interest here since it is always specified by the manufacturer. What is the concern here is the performance of the installed units, and the importance of measuring the overall effectiveness of the bank is that such a determination can reveal a malfunction in the filter bank, e. g. a badly installed filter or a leak in one of the filters due to transport damage. It is the detection of faults and anomalies in a filter bank that is of primary interest in an on-site test.

When the results of an on-site lithium test indicate that the manufacturer's specifications are not fulfilled by the installation as a whole, one knows exactly the extent of the failure because the lithium test is directly comparable with the Sodium Flame Test used by the manufacturer.

Thus one is in a position to quantitatively evaluate the performance of a filter installation by direct comparison with the figures offered by the manufacturer as to the expected performance of the unit.

In other words, the lithium on-site test represents an easy way of comparing the actual efficiency of a filter installation in operation with the efficiency attainable according to the manufacturer's test.

The spraying time needed to introduce sufficient amounts of lithium salts into a ventilation system sets a practical upper limit to the utilization of a lithium salt as a tracer in very high capacity systems.

For example, in a ventilating system through which the flow is 100,000 m^3/h and whose filter bank shows a penetration of 0.01%, it would be necessary to sample about 8,000 litres on the after filter. This figure is based upon the output of the portable atomizer unit mentioned previously. The time of sampling based upon a sampling rate of 20-50 l/min through a 5 cm diameter membrane filter would be from 7 to 3 hours.

For these very high capacity systems a counting by Pollak counters, of the natural particles found before and after the filter bank is a reliable indication of the integrity of the filter bank.

Allowance must be made for the difference between the effectiveness of a filter bank as determined by Pollak counting and the effectiveness as an expression of mass concentrations before and after the filter bank. This difference is demonstrated and established by the inter-calibration curves (Figs. 5-9).

These curves are valid only for filters in which the pinhole effect is not significant.

In cases where it is possible to vary the air flow through a filter bank and thus demonstrate the existence of a pinhole effect by Pollak counting, the effectiveness thus obtained converges with the effectiveness as measured by the lithium and sodium methods.

Fig. 2 demonstrates this convergence.

When the results of such a test indicate that there is a leak somewhere in the filter bank, it might be desirable to determine the exact location of the defect (if it cannot be tolerated from a safety point of view). This can be done by injecting the lithium particle cloud into the input channel and then scanning the back surface of

each filter with a flexible probe introduced through a hole in the conduit wall. The air injected into this probe, e.g. by means of an ejector, is passed directly into a flame, and the intensity of the lithium line is registered on a photometer.

In this way a continuous profile of the lithium in the effluent air is obtained, and any leak will reveal itself as a deflection on the photometer scale.

In this procedure the lithium concentrations due to a leak are very high, and thus it suffices to use a cheap and simple flame-photometer device. Such a system has been constructed by modifying a cheap, commercially available flame photometer (Evans Electroselium Ltd.).

Fig. 11 is a flow diagram of the EEL flame photometer as adapted for use as a leak detector.

At the most sensitive setting a scale deflection of 10 units ($\sim$ 1.5 cm) is obtained from a channel concentration of 1.2×10^{-2} γ Li/lit. air.

We wish to thank P.O. Heidemann for his help in planning and drawing the atomizer assemblies shown in Figs. 1 and 4.

IN-PLACE TESTING OF CHARCOAL FILTER BANKS

AT AMES LABORATORY RESEARCH REACTOR (ALRR)

C. A. Gukeisen and K. L. Malaby
Ames Laboratory, Iowa State University

ABSTRACT

The air exhaust system at the ALRR is described. An experimental program was conducted to develop an appropriate in-place iodine test for the charcoal filter banks. Three techniques were tested; namely, (1) spectrophotometric analysis, (2) neutron activation, and (3) iodine-131 tracer. Comparisons of the testing results and experience are enumerated with comments and recommendations. The neutron activation and the iodine-131 tracer techniques proved to be the most appropriate methods for in-place iodine testing of the ALRR charcoal filter banks.

INTRODUCTION

The Ames Laboratory Research Reactor, ALRR, is a 5-MW heavy water moderated and cooled reactor operated by Ames Laboratory at Ames, Iowa. Highly enriched MTR-type fuel elements are utilized, and the reactor confinement is a conventional concrete building. Purpose of the reactor, which began full power operation in July, 1965, is to supplement the research capabilities for the staff at Ames Laboratory and Iowa State University. An elaborate air exhaust system, Figure 1, is required to safeguard the health and safety of persons outside the reactor exclusion area during normal reactor operation and also in event of an emergency involving the release of radioactivity, such as the postulated loss-of-coolant accident.

AIR EXHAUST SYSTEM

During normal reactor operation, three ventilation systems exhaust building air through the stack; namely, (1) Basement Exhaust System, (2) Main Floor Exhaust System, and (3) Irradiated Air Exhaust System. The latter system draws 800 scfm of room air through the experimental facilities, thereby isolating the prime source of gaseous activity, and passes the air through a particulate filter prior to stack discharge. The 4300-scfm Main Floor Exhaust System also passes air through a tier of particulate filters, whereas the large amount of air exhausted by the Basement Exhaust System for building temperature control is not filtered. Exhaust air during normal operation does not pass through charcoal filters in order to preserve the filters for any emergency. A slight negative

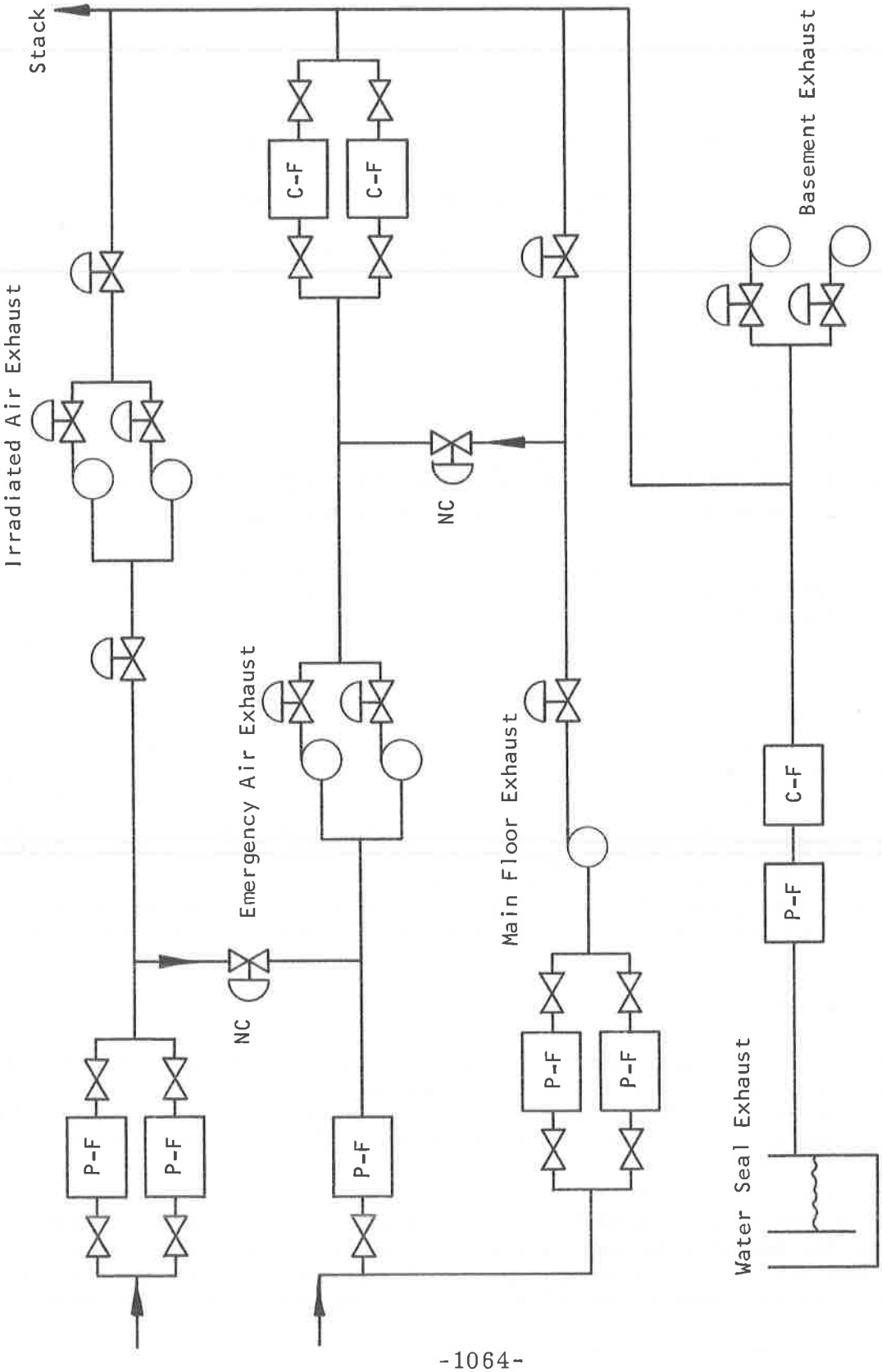

Figure 1. ALRR Air Exhaust System

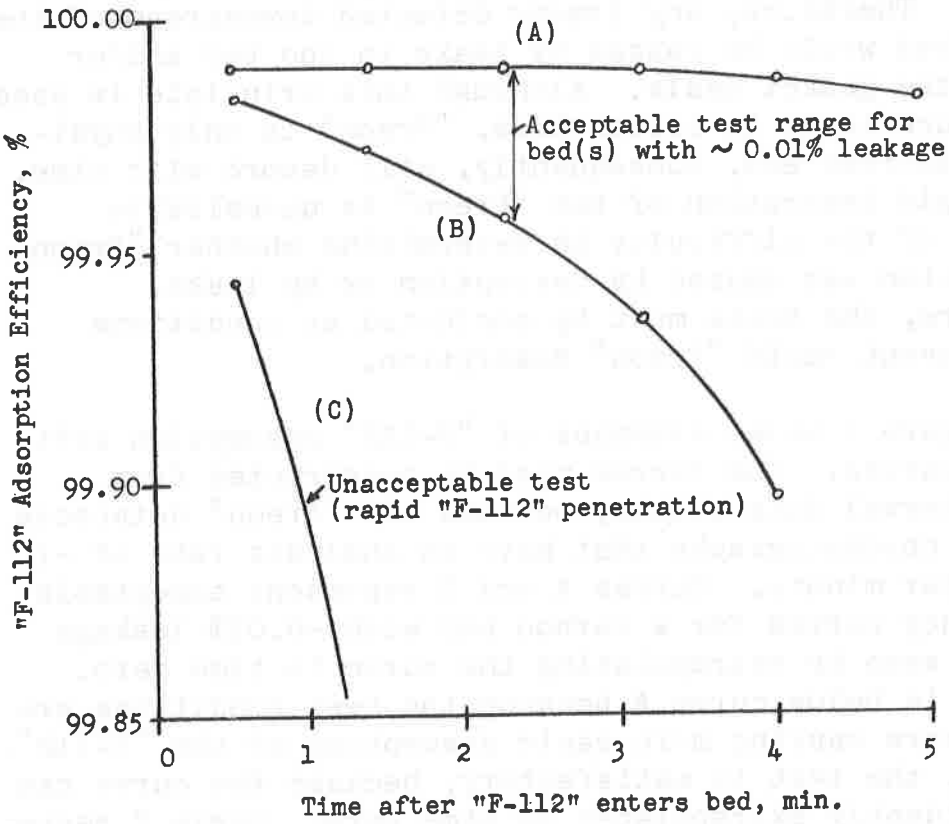

FIG. 1 ACCEPTABLE AND UNACCEPTABLE "F-112" TESTS

LEAK TEST DEVELOPMENT

Leakage in a carbon bed can be determined from the concentration of the tracer in the flowing air upstream of the test bed and the concentration of the tracer in the flowing air downstream of the test bed if the carbon at test conditions removes essentially all (~99.99%) of the tracer in the air flow that does pass through the carbon. Therefore, any tracer detected downstream of the carbon bed would be caused by leaks in the bed and/or around the gasket seals. Although this principle is used to measure leaks in carbon beds, "Freon" is only physically adsorbed and, consequently, will desorb with time. Very rapid desorption of the "Freon" is undesirable because of the difficulty in determining whether "Freon" penetration was caused by desorption or by leaks. Therefore, the tests must be conducted at conditions that prevent rapid "Freon" desorption.

Figure 1 shows examples of "F-112" adsorption efficiency curves. The curves must be constructed from time-interval data points, because the "Freon" detectors are gas chromatographs that have an analysis rate of ~1 sample per minute. Curves A and B represent acceptable efficiency curves for a carbon bed with ~0.01% leakage flow as seen by extrapolating the curve to time zero. Curve B is below curve A because the test conditions are more severe causing more rapid desorption of the "F-112". However, the test is satisfactory, because the curve can be confidently extrapolated to time zero. Curve C represents an unacceptable test, because the "F-112" desorbed too rapidly to permit confident extrapolation.

"Freon" compounds were evaluated for improved adsorption characteristics on new carbon using small-scale carbon beds[2-4]. Based on this work, "F-112" was selected as the tracer for in-place leak testing. Used carbon in both small-scale and full-size beds were then used to further evaluate "F-112".

The tests of small-scale carbon beds show that new and used carbon are significantly different. Tests at air velocities of 70 ft/min with carbon containing up to 25% sorbed water were satisfactory for new carbon.

INTRODUCTION

Halogen vapor (principally ^{131}I) that might be released accidentally into the buildings of Savannah River Plant (SRP) reactors would be removed by normal, routine flow of the exhaust ventilation air through carbon beds. Performance of the beds is a function of the efficiency and capacity of the carbon for removing iodine from the air and of leakage in or around the beds that would prevent air from contacting carbon. Carbon efficiency and capacity are measured in small-scale laboratory tests of carbon samples, but leakage measurements on small beds are not meaningful. Techniques using "Freon"* have been developed, however, for measuring leakage in banks of full-scale beds in installed position. Additional work is needed to establish if "Freon" tests have value in measuring efficiency or capacity of carbon.

New carbon beds are tested for leaks by a nondestructive technique in which "Freon-12" is used as a tracer.[1] The "F-12" technique is limited to testing new carbon beds with air flow at a maximum velocity of 20 ft/min and with carbon containing no more than 5% sorbed water. Used carbon beds cannot be tested because adsorbed impurities cause the "F-12" to desorb too quickly (in less than one minute) for a definitive measurement of a leak path.

Although each carbon bed is proof-tested before installation, a standardized nondestructive test was required that would be generally applicable for in-place leak testing of installed, used carbon beds. A new test was developed in which the limitations imposed on air velocity and sorbed water were reduced significantly by substituting the less-volatile "F-112" for "F-12"[2,3,4]. This paper discusses the development, application, and results of an in-place leak test of used carbon beds installed in the SRP confinement system.

---

* "Freon" and combinations of "Freon-" or "F-" with numerals are Du Pont's registered trademark for its fluorinated hydrocarbons.

IN-PLACE NONDESTRUCTIVE LEAK TEST FOR IODINE ADSORBERS*

by

D. R. Muhlbaier

Savannah River Laboratory
E. I. du Pont de Nemours & Co.
Aiken, South Carolina 29801

ABSTRACT

A nondestructive in-place test for detecting leaks in a bank of installed carbon beds with "Freon-112"** tracer was developed by the Savannah River Laboratory and demonstrated in the reactor confinement facilities of the Savannah River Plant. Leakage flow (flow that bypasses the carbon) of 0.01% of the total air flow through the beds is detected readily. Installed carbon beds with about 2 years exposure to exhaust air flow in the confinement system were evaluated successfully with the test. An equation was also developed that correlates the conditions for "F-112" testing of carbon beds of different design.

---

* The information contained in this article was developed during the course of work under Contract AT(07-2)-1 with the U. S. Atomic Energy Commission.

** "Freon" and combinations of "Freon-" or "F-" with numerals are Du Pont's registered trademark for its fluorinated hydrocarbons.

sensitivity of these methods adequate? It may or may not, depending on the condensation nuclei concentration and the sensitivity of the instrument. If the air is over the sea, perhaps you will get too low a concentration. I think the methods are all right if they turn out to be sensitive enough.

DISCUSSION

HILLARY: We did some experiments some years ago using molecular iodine to test charcoal beds. We found it very difficult to get the iodine to the bed because of its plating out on steel pipe work. Can I ask Mr. Gukeisen, does he know if the iodine reached the charcoal bed?

GUKEISEN: Yes, we do. First of all, from radioactivity, there was none measured on the duct work; also, how else could iodine get to the upstream sample? There was quite a distance between where we inserted the iodine and where we measured it, although there was some distance from these upstream samples to the charcoal, but we were afraid of this at first because we had no idea whether our techniques would work, and at first we weren t getting concentration. That is what we thought had happened, but we just didn't put enough iodine in.

THOMAS: Maybe you put enough in until finally the rate of desorption was equal to the rate of adsorption. Mr. Brion?

BRION: I would like to add a comment about what you say to answer to Mr. Hillary, as we have done a lot of in-place tests with iodine 131, and at first we did not have any iodine 127 added. Actually, we get more than 90% of the iodine we have filled the generator with, according to the upstream sampling. With these conditions, we found that half of the iodine might be lost in the circuit tested especially when it has a delay chamber.

We are now using much more iodine 127, with iodine 131 because of the efficiency which is a function of concentration, and we are trying to keep closely to the concentration you may get in case of an accident.

THOMAS: In other words, you are using the I-127 to prevent too much plate out of the I-131.

BILLINGS: Condensation nuclei should provide a useful tool for certain in-place testing problems. The atmosphere contains a sufficient number so that generation is unnecessary. Nuclei counters are available from General Electric Company and from a small firm in the Boston area. Another approach for in-place tests would be to use the radon and thoron daughter decay. The daughters attach to small particles in the atmosphere and a good sample for counting purposes can be obtained in a reasonable time. Carl Lindeken did some work on this approach a few years ago, using natural aerosols and natural radioactivity.

THOMAS: All right; thank you for your comments regarding the condensation nuclei and radon daughters. We have done work on radon daughters and we find in the test of a defective filter you get the same effect as you do with the DOP. The method is okay. Also, I think the condensation nuclei method should be correct. The only question in my mind, is the

iodine compounds that were released by the iodine generators.

The technique using iodine-131 as a tracer provided results with the greatest sensitivity, whereas the spectrophotometric technique provided the least sensitivity, especially with the presence of air-borne dust particles. However, the use of radioactive iodine-131 demanded greater precaution to minimize the danger of contamination. Charcoal samplers were preferred to the liquid bubblers for reasons of convenience and accuracy.

CONCLUSIONS

From the experience gained by the experimental testing program, either the neutron activation or the radioactive iodine-131 tracer techniques shall be used for the annual verification that the ALRR charcoal filter banks are not deteriorating with respect to iodine adsorption capabilities. Iodine vapor shall be produced by the oxidation of sodium iodide by potassium dichromate, and the samplers shall consist of the appropriate activated charcoal. A test should be developed to check the methyl iodide adsorption capabilities of the charcoal filter banks; however such a test shall be for informative purposes only, not as an annual filter test.

REFERENCES

1. E. F. Conti, USAEC - Chicago Operations Office, Memorandum to D. M. Gardiner, October 1964.

2. G. W. Parker and N. J. Horton, Oak Ridge National Laboratory, personal communication, June 1966.

4. Analyze the samples with a multi-channel analyzer, RIDL Nanolyzer Model 24-1.

Similarly to the test procedure used for spectrophotometric analysis, iodine vapor was released to the air stream by bubbling compressed air through the iodine solution, air blanks were obtained for analytical purposes, and several sample bubblers were operated in series to determine the percentage of breakthrough. Test results indicated iodine adsorption efficiencies of 99.3 - 99.4% for the Emergency Exhaust filter banks and 99.9% for the Water Seal Exhaust filter bank. Sensitivity of this neutron activation technique was very high, and there was no problem of collecting a detectable concentration of iodine in the downstream samplers. However, only 25 - 40% of the sample line iodine was trapped in the first sampler of dibutyl phthalate, thereby causing some inaccuracies concerning the actual amount of sample line iodine.

Iodine-131 Tracer

Another technique[2], which is frequently used in laboratory work with fission product iodine, is as follows.

1. Generate iodine vapor containing iodine-131 tracer by oxidation of sodium iodide.

2. Collect samples with activated charcoal.

3. Analyze the charcoal samples with a multi-channel analyzer.

Approximately 10 millicuries of iodine-131 as sodium iodide was used for testing each filter bank. This tracer was added to a mixture of nonradioactive sodium iodide and potassium dichromate which was heated to induce oxidation and to release iodine vapor directly to the air stream. The samplers contained activated coconut charcoal, Barnebey-Cheney Type 727, which is impregnated with potassium iodide and elemental iodine. Test results indicated iodine adsorption efficiencies greater than 99.99% for both filter banks in the 4300-scfm Emergency Exhaust System.

SUMMARY

Tabulated results of the indicated iodine adsorption efficiencies for the three charcoal filter banks by the three experimental techniques are listed below.

Indicated Iodine Adsorption Efficiencies

	Spectrophotometric	Neutron Activation	I-131
Emer. Exhaust, Top Bank	99.2%	99.3%	>99.99%
Emer. Exhaust, Bottom Bank	99.3%	99.35%	>99.99%
Water Seal Exhaust	99.8%	99.95%	---

The lower efficiencies evident by the spectrophotometric and neutron activation techniques are postulated to be the result of some generation of organic iodine compounds due to the presence of methyl chloroform and methyl alcohol as source solutions. No analysis was done to determine what form or amount of organic

EXPERIMENTAL IODINE TESTING

Three techniques were developed for indicating the iodine-removal efficiencies of in-place charcoal filter banks. To minimize plateout, the iodine-generating and sampling apparatus were constructed of glass, porcelain, or stainless steel. Full-length sampling probes were located upstream and downstream of each filter bank, plus between the first and second filter tiers. The sampling flowrate for each sampler was checked periodically with the same rotometer. All testing was conducted at room air temperature and humidity; i.e., 75°F and 50% humidity. The three techniques devised for iodine testing are enumerated in detail.

Spectrophotometric Analysis

A technique suggested by Dr. Leslie Silverman, Harvard University School of Public Health, consisted of the following.[1]

1. Generate iodine vapor from iodine crystals dissolved in methyl chloroform.
2. Collect samples in a 5% potassium iodide solution.
3. Analyze the samples with a Beckman DU Spectrophotometer utilizing a wave length of 352 mμ.

Iodine vapor was injected into the air stream by bubbling compressed air through the iodine solution. It was noted that the solubility of iodine crystals in methyl chloroform was low; i.e., approximately 2 grams per liter.

The relatively low sensitivity by the spectrophotometer for iodine in solution (0.2 μg/ml) and the relatively high air stream flowrates posed the problem of experimentally optimizing conditions for a low sample volume and a high sampling flowrate until a detectable iodine concentration was collected in the downstream samples. Also, the sampling procedure was conducted initially without an iodine source to obtain air blanks for assessing what residual iodine and other materials were present in the airstream that would interfere with the analytical technique. To determine the amount of breakthrough of iodine past a sample bubbler, several bubblers were operated in series.

Test results indicated iodine adsorption efficiencies of 99.2 - 99.3% for the Emergency Exhaust filter banks and 99.8% for the Water Seal Exhaust filter bank. The major problems confronted with this spectrophotometric technique were the presence of dust particles suspended in the sampling solution and the rapid vaporization of iodine from the sampling solution. Only 10 - 15% of the sample line iodine passed through the first bubbler.

Neutron Activation

Another technique which appeared feasible is as follows.

1. Generate iodine vapor from iodine crystals dissolved in methyl alcohol.
2. Collect samples in dibutyl phthalate.
3. Irradiate the samples with neutron flux.

pressure of 0.2" w.c. is constantly maintained inside the 500,000-ft^3 building to assure inward leakage.

In the event of high exhaust air activity, high radiation level, or low coolant level, all normal ventilation systems would be automatically shut down and isolated. An Emergency Exhaust System fan immediately would pass 500 scfm of air through a charcoal filter bank before discharge through the stack. If reactor decay heat or other energy sources cause the building pressure to exceed atmospheric pressure, the Main Floor Exhaust System would automatically pass an additional 4300 scfm through the charcoal filter bank until the pressure within the building is reduced below atmospheric. If the building pressure were to exceed a positive 1.5" w.c. as the result of a catastrophic release of energy, approximately 1500 scfm of air would pass through the particulate and charcoal filter banks contained in the Water Seal Exhaust System. This system was designed to operate inherently without mechanical movement or electro-pneumatic signals.

FILTERS

Single tiers of 2-ft. x 2-ft. high-efficiency particulate filter cells are incorporated in all exhaust systems, excluding the Basement Exhaust System. The maximum air velocity through any filter is 250 fpm. Prior to installation, each filter cell is checked by means of a dioctylphthalate (DOP) smoke test to verify the specified minimum efficiency of 99.95% for removal of 0.3-micron smoke particles. After installation of the cells inside the ductwork, each tier is tested again with DOP smoke to check for faulty gaskets and framework.

Three tiers in series of Dorex-Type 42C charcoal cells, manufactured by Conner Engineering Corporation, are incorporated in both filter banks in the Emergency Exhaust System and the single filter bank in the Water Seal Exhaust System. Each cell provides a 3/4-inch bed thickness of activated charcoal for a total $2\frac{1}{4}$-inch thickness per bank. The maximum air velocity through any filter cell is 100 fpm. Following installation of the charcoal filter cells, Freon-12 was injected upstream of each tier to check for any gross leakage past the holding frames, gaskets, and structural frame by means of a flame detector. This gross leakage test, plus subsequent visual observation, gave evidence of a poor construction job; thus a substantial modification was required to provide a completely welded frame assembly, a more durable clamping device, and a closed-cell gasket material. Also, access doors were provided between all filter tiers to allow for visual examination of the in-place gaskets.

TESTING OF AIR EXHAUST SYSTEM

The air exhaust system is tested periodically to assure that the internal filtering of air discharged from the reactor building will be performed properly regardless of the situation. Operation of all fans and isolation valves is checked prior to each reactor startup, and the water level in the Water Seal Exhaust System is monitored once per shift. Once a year the particulate filter tiers shall be checked with the standard DOP smoke test, and the charcoal filter banks shall be checked with an iodine vapor test.

An experimental program was required to develop an appropriate in-place iodine test for the charcoal filter banks. Of prime importance was the indicated iodine-removal efficiency of each bank to verify the required 99.9% efficiency as specified in the Hazards Summary Report for ALRR.

But used carbon (15 months service in a reactor ventilation system) could not be satisfactorily tested at 50 ft/min velocity and only 6.0% sorbed water. These results showed that both velocity and water content of carbon must be significantly reduced to test used carbon. Full-size carbon beds were tested to define more accurately the limits for testing used carbon.

Tests of full-size SRP beds showed that the "F-112" adsorption efficiency of carbon is gradually reduced with service. This effect is caused by the loss of adsorption sites due to the adsorption of trace impurities in the ventilation system air. Thus, used carbon must be tested at a lower water content to compensate for the loss in active sites. Reduction in face velocity also provides more time for "Freon" to adsorb. The effect of the carbon service on the "F-112" adsorption characteristics is summarized in Table 1. By comparing the test conditions and efficiencies of new carbon and carbon with 7 and 15 months service in C Reactor, it is apparent that less severe test conditions (lower velocity and/or lower water content) are required to test older carbon. Loss in "F-112" adsorption efficiency will probably continue with increased carbon service as indicated by the "F-112" test results of K Reactor carbon with 2 years service. The conditions used for "F-112" testing of SRP carbon beds with ~$2\frac{1}{2}$ years service are 10 ft/min air velocity and <4% sorbed H_2O.

Under humid conditions, heating the ambient air before it passed through used carbon beds improved "Freon" adsorption. Air with a dew point of <20°C was heated to 50°C and passed through carbon to reduce the water content to <4%. When SRP carbon beds were tested, heaters were installed upstream of the carbon beds and the air flow was reduced.

In-place "F-112" test of installed carbon beds did not significantly affect the iodine adsorption efficiency of the carbon. Carbon exposed 15 months in the C Reactor ventilation system and containing up to 0.33 mg of sorbed "F-112" per gram of carbon (equivalent to at least one "Freon" test) was evaluated. Tests with air or steam-air

TABLE 1

"F-112" Efficiency of Full-Size Carbon Beds

Carbon	Test Conditions: Air Velocity, ft/min	Test Conditions: Sorbed Water, %	Test Conditions: Temp., °C	Desorbed Before Test(a)	Upstream "Freon" Conc., ppm	Efficiency at 4 min, %(b)
New	70	22.4	23	-	10	99.85
P Reactor	30	16.6	21	No	10	99.98
(15 months)	35	15.9	23.5	No	10	99.92
C Reactor	25	9.1	28	Yes	10	99.87
(7 months)	20	5.6	33	Yes	10	99.99+
	25	6.9	36	Yes	10	99.99
	25	2.0	46	Yes	10	99.99+
C Reactor	20	20.7	31	No	20	99.5
(15 months)	20	4.3	31	No	10	99.94
	20	2.0	40	No	20	99.99+
K Reactor	20	4.0	32	Yes	10	99.5
(2 years)	15	4.7	32	Yes	20	99.68
	15	2.0	43.5	Yes	20	99.98

(a) Desorption was effected by purging carbon with air at ~90°C for at least 20 hours.

(b) An acceptable test efficiency is 99.9+% at 3 to 5 minutes after "Freon" injection.

mixtures showed that the removal efficiency for elemental iodine was 99.9+%. The carbon was not desorbed prior to the tests, and the results are comparable with those reported[6] for used SRP carbon with no "F-112". Desorption of the more volatile impurities (e.g., nitric oxide) from the used carbon prior to the iodine test improved the efficiency for iodine removal (99.99+%) even with carbon containing up to 0.73 mg "F-112" per gram of carbon (equivalent to at least two "F-112" tests). The carbon was desorbed with air at 80 to 95°C for 2 hours. Table 2 summarizes the iodine tests of used carbon containing "F-112".

"Freon-112" is physically adsorbed and therefore can be desorbed from activated carbon. Desorption of "F-112" from SRP-type activated carbon is very slow under the conditions recommended for in-place leak testing. Desorption of "F-112" from activated carbon is enhanced by high temperature and high water content (Table 3). The desorption times and conditions are applicable to new carbon beds with loadings of ~0.4 to 0.8 mg "F-112" per gram of carbon. The "F-112" was adsorbed on the front of the carbon bed and desorbed by driving the "F-112" through the bed and out the back, except where noted. The ease of desorption of a given quantity of "Freon" increases with increased "Freon" loading. Air velocity also affects "F-112" desorption time, but its influence was not studied.

IN-PLACE LEAK TEST OF INSTALLED CARBON BEDS

Figure 2 is a diagram of the equipment for testing installed carbon beds at SRP. Only three connections to the filter compartment are required. One connection at the top of the compartment is used for the "F-112" injection. The other two connections are for sampling.

The "Freon" injection apparatus consists of a reservoir containing liquid "F-112" and an injection tube made of thin-walled stainless steel. The stainless steel tubing is used as a resistance heater to vaporize the "F-112" before injection in the filter compartment. The tubing is insulated electrically from the "Freon" reservoir and filter compartment. The reservoir is pressurized

TABLE 2

Iodine Tests of Used Carbon Exposed to "F-112"(a)

"F-112" Loading, mg "F-112"/g Carbon	Carbon Desorbed(b)	Iodine Carrier	Iodine Removal Efficiency,%
0.18	No	Air	99.92
0.18	No	Steam-Air	99.98
0.33	No	Air	99.94
0.73	Yes	Air	99.99+
0.73	Yes	Steam-Air	99.99+
0.73	Yes	Steam-Air	99.99

(a) The carbon was removed from C Reactor after 15 months exposure in the ventilation system.
(b) Desorption of the carbon was effected by exposure to flowing air at 80 to 95°C for 2 hours.

TABLE 3

Desorption(a) of "F-112" from New Carbon(b)

"F-112" Desorption, %	Air Conditions			Desorption Time
	Velocity, ft/min	Relative Humidity, %	Temp., °C	
>95	70	<3	100	3 weeks
>95	70	75+	30	3 weeks
~90	70	<3	130+	5 days
~70	70	55 to 65	30	10 days
~1	70	<40	30	1 day
>95	70(c)	<3	95	3 days

(a) The "F-112" was desorbed from the opposite side from which it was first adsorbed except where noted.
(b) Data for new small-scale carbon beds with ~0.4 to 0.8 mg "F-112" per g carbon at starting conditions.
(c) The "F-112" was desorbed from the same side of the bed from which it was first adsorbed.

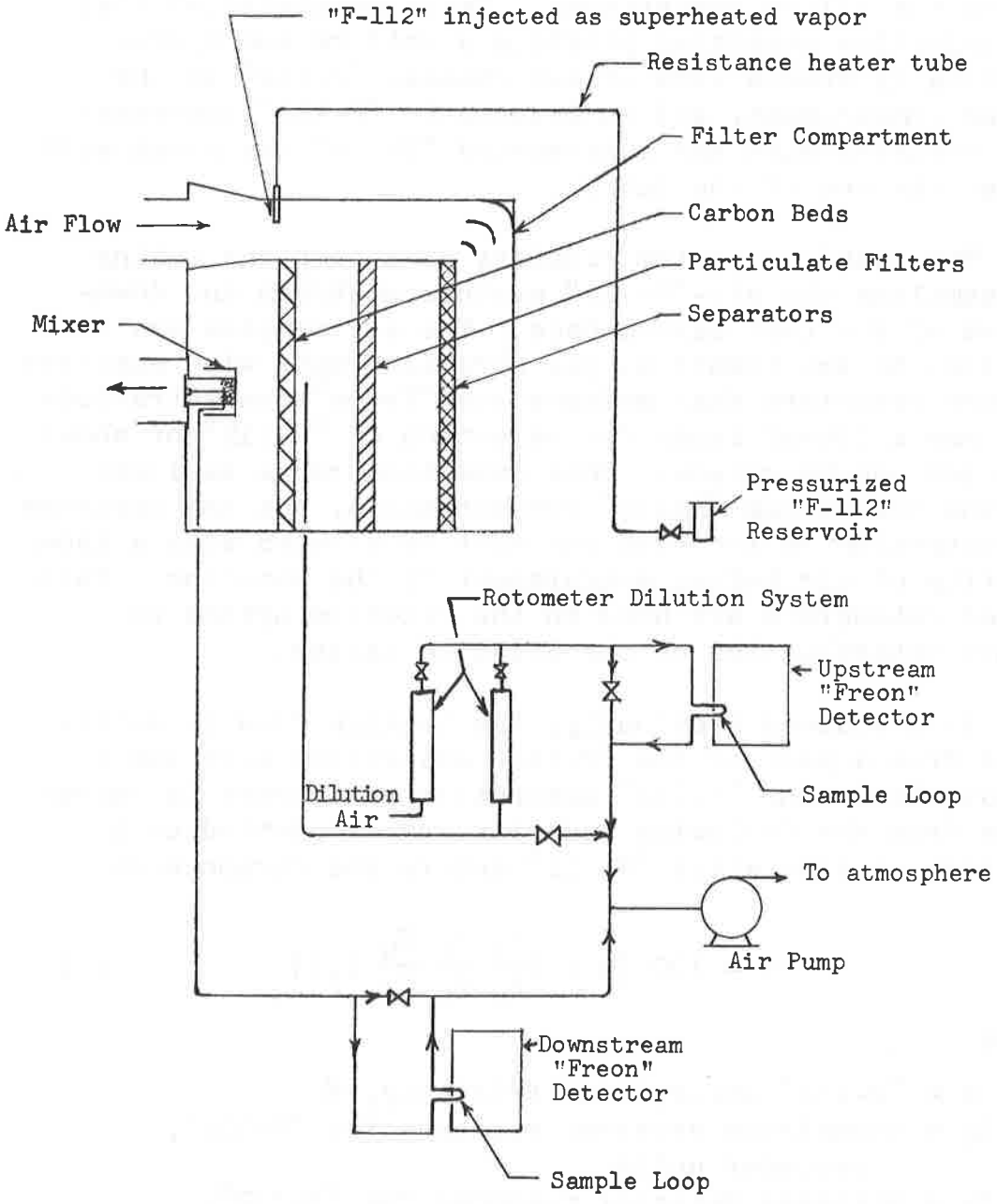

FIG. 2 DIAGRAM OF EQUIPMENT FOR TESTING INSTALLED SRP CARBON BEDS

with nitrogen that forces liquid "F-112" into the heated tubing where it is vaporized and superheated before it enters the filter compartment. Tests demonstrated that the injection apparatus provides a uniform and hydrodynamically stable flow of superheated "F-112" to the filter compartment, and no detectable "F-112" condensation occurred when the superheated "F-112" was mixed with air at the end of the tube.

The sampling system consists of a pump and tubing for sampling the air-"F-112" mixture upstream and downstream of the test carbon beds. The air samples are supplied to two identical gas chromatographs with electron capture detectors that measure the "Freon" concentrations; each has a linear range for detection of "F-112" of about 1 to 100 ppb by volume. This detection range is ideal for the downstream "Freon" concentration, but the upstream concentration is too high and must be diluted with a known quantity of air before measurement by the detector. Calibrated rotameters are used in the dilution system to permit determination of the dilution factor.

As discussed previously, the leakage flow is determined from a plot of the "F-112" adsorption efficiency versus time. The "F-112" adsorption efficiency is calculated from the following equation and is plotted as a function of time after "F-112" enters the carbon bed:

$$\epsilon = 100 \left[1 - \left(\frac{R_d}{R_u} \frac{1}{f_d} \frac{C_u}{C_d} f_c\right)\right] \qquad (1)$$

where

ϵ = "F-112" adsorption efficiency, %
R_d = downstream detector response for "F-112", recorder units
R_u = upstream detector response for "F-112", recorder units
f_d = dilution factor of sample from upstream carbon bed to upstream detector, dimensionless constant
C_u = upstream detector response to standard calibration solution, recorder units per microliter

C_d = downstream detector response to standard calibration solution, recorder units per microliter

f_c = calibration conversion factor, dimensionless constant

During the "F-112" leak test, it is not necessary to know the absolute values of the following: tracer concentrations; air flow through the carbon beds; or calibration of the "Freon" detectors. However, an estimate of the air flow is necessary to set the upstream tracer concentration at 10,000 to 20,000 times the minimum downstream detector response to detect leaks of 0.01% of the total flow.

Relative calibration of the detector is accomplished by injecting a solution of "F-112" in hexane onto the chromatograph column.* The solution contains a given mass of "F-112" per unit volume (e.g., 10^{-11} g "F-112"/µl of hexane). The response of both detectors to the same "F-112"-hexane solution is determined in recorder units per microliter ($R_u/\mu l$).

Equation 1 contains two constants. The dilution factor (f_d) converts the relative "F-112" concentration measured by the upstream detector to the relative value upstream of the test carbon beds. f_d is equal to the dilution ratio of the rotameter dilution system (e.g., if dilution ratio = 500:1, f_d = 500).

The second constant of Equation 1 is the calibration conversion factor (f_c) which converts the relative "F-112" calibration determined from the "F-112"-hexane mixture to the relative "F-112" calibration in a "F-112"-air mixture. This factor is needed because "F-112" is detected in air during the leak test and not in hexane. Although the detectors respond equally to equal masses, whether in air or hexane, the ratio of mass injected to the detectors by

* This is a standard chromatographic technique. The hexane is used to dilute the "F-112" and enable injection of very small quantities of "F-112".

each method is not necessarily equal. For the "F-112"-hexane method, the ratio of mass injected to each detector was set equal to one (1 µl for upstream detectors per 1 µl for downstream detector). For the "F-112"-air calibration, the volume of sample injected depends on the volume of the sample loop (Figure 2). For example, the sample volume may equal 0.60 ml on the upstream detector and 0.50 ml for the downstream detector. The calibration conversion factor would then be 0.60/0.50 or 1.20.

For a definitive measurement of leakage flow through carbon beds, the upstream "Freon" concentration must be nearly uniform across the face of the carbon beds and the sample removed downstream of the beds for "Freon" analysis must be representative of a nearly uniform mixture. Otherwise, a significant leak might not be detected.

Mixing tests in a SRP filter compartment showed that the upstream mixing was satisfactory when "F-112" was injected near the influent nozzle with no device to promote mixing; mixing was within ±7% of the calculated mixed-mean concentration. Downstream mixing tests showed that a single point sampler and a single mixing orifice installed in the compartment effluent nozzle were unsatisfactory. Consequently, a multiorifice mixer was developed and used in conjunction with a multipoint sampler. The system was installed in the compartment effluent nozzle for a leak test. Tests of the mixer and multipoint sampler showed a maximum variation of ±10% from the calculated mixed-mean "F-112" concentration downstream of the carbon beds.

Measurement of the percentage leakage flow during in-place leak tests of SRP carbon beds can be predicted with a standard deviation of ±9%* when all errors in measurements of the "F-112" concentrations are combined. The errors result from incomplete mixing, both upstream and downstream, and variation in calibration of the "Freon" detectors and dilution rotameters.

* ±9% for 0.1% leakage (±20% for 0.01% leakage).

LEAK TEST RESULTS

The technique and equipment previously described were successfully demonstrated on banks of carbon beds installed in C Reactor at SRP[5]. The "F-112" adsorption efficiency for five compartments is shown in Figure 3, and the leakage flow is summarized in Table 4. The average leakage flow for all five compartments was <0.03% of the total air flow.

Compartment No. 3 required two tests because the first test showed leaks of ~0.2% due to several loose mounting bolts. After the bolts were tightened, the leakage flow was 0.04%, well within the acceptable range.

APPLICATION

The "F-112" leak test was developed to measure leakage flow through carbon beds installed in reactor confinement systems. The test was successfully demonstrated at SRP. The test can be used to evaluate beds of different design and different carbons. Figure 4 shows a diagram for the application of the "F-112" leak test to a typical carbon bed installation. "F-112" is injected upstream of the test carbon beds and far enough away so that thorough mixing of air and "F-112" will occur before reaching the carbon beds. A mixed sample can be obtained downstream by installing a mixing device or by removing a sample downstream of the exhaust fan. However, if the "F-112" must travel a significant distance before reaching the sample point, the system should be checked to make certain that no significant "F-112" is adsorbed by the duct and that a representative sample reaches the sample point. Otherwise, an error could be introduced in measuring the leakage flow. In the tests at SRP, there was no significant "F-112" adsorption on the duct between the carbon beds and the sample point. Adsorption upstream of the carbon beds was of no concern, because the "F-112" concentration was measured immediately upstream of the carbon beds.

Significant "F-112" adsorption on the sample lines must be avoided to ensure that a representative sample

TABLE 4

Measured Leaks in Carbon Beds Installed in C Reactor Confinement System

Filter Compartment	Leakage Flow, %
2	0.05
3	0.04
4	0.01
5	<0.01
6	<0.01
Average	<0.03

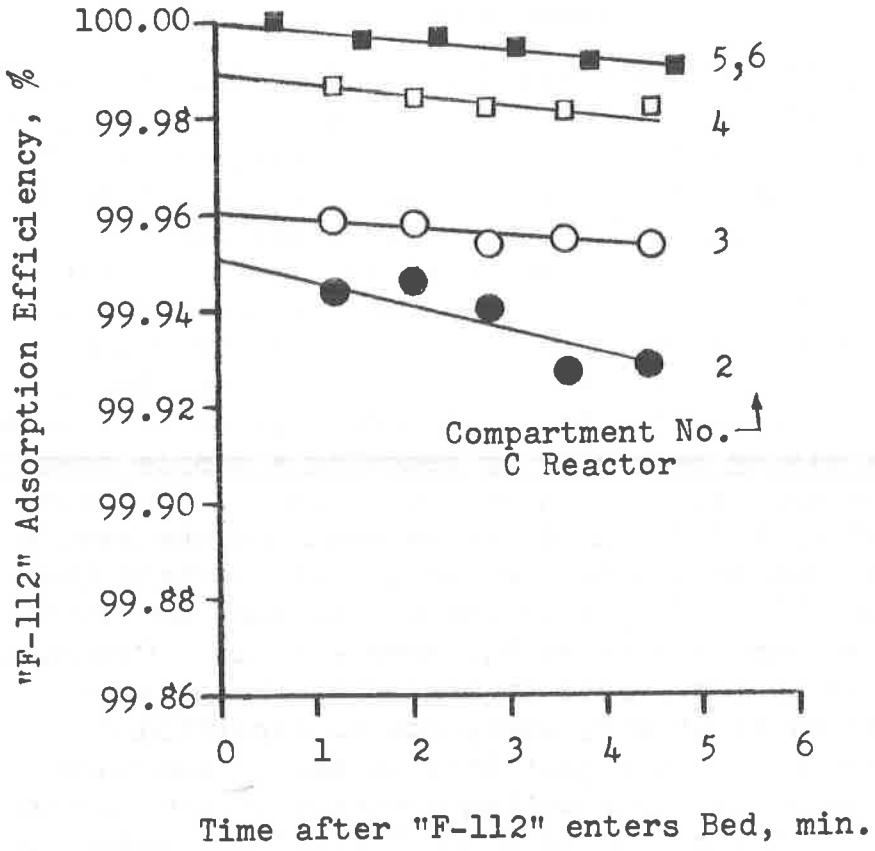

FIG. 3 "F-112" EFFICIENCY OF BANKS OF INSTALLED SRP CARBON BEDS

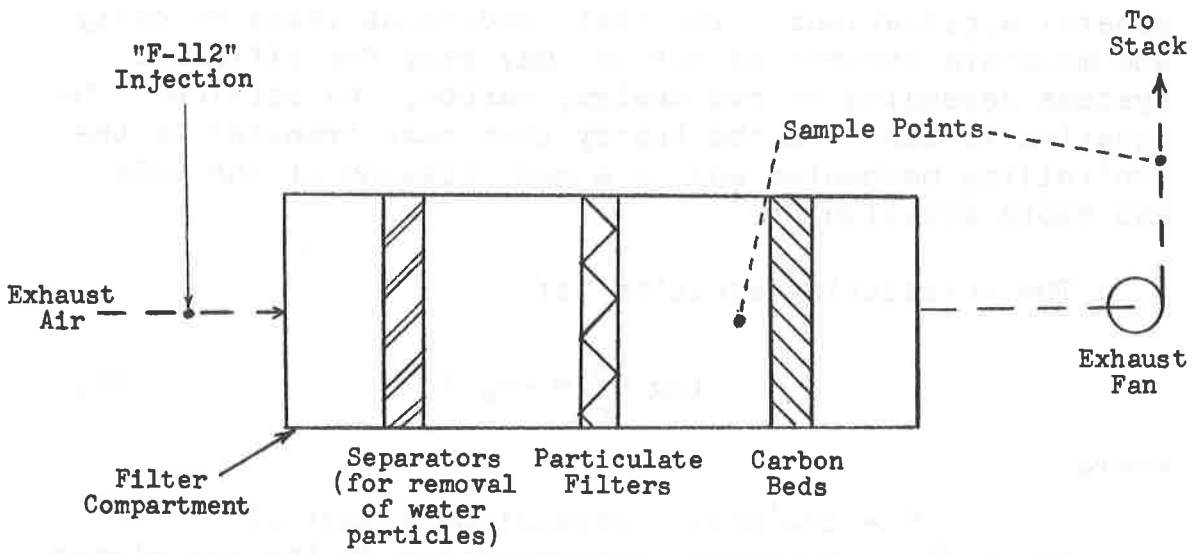

FIG. 4 DIAGRAM OF EQUIPMENT FOR "F-112" LEAK TESTING OF TYPICAL CARBON BED INSTALLATIONS

reaches the detectors. Both the line material and transit time are important factors. Tubing materials such as stainless steel, "Teflon"*, and glass are satisfactory for conveying "F-112"-air samples to the detector. Sample transit times ≤ 5 seconds are satisfactory.

An equation was developed to predict the maximum test conditions with "F-112" tracer for new carbon beds for general applications. The test conditions (face velocity and moisture content of carbon) may vary for different systems depending on bed design, carbon, and service. The equation is based on the theory that mass transfer is the controlling mechanism and is a modification of the Dole and Klotz equation[6,7].

The correlating equation is:

$$\text{Log } \frac{C_b}{C_o} = -c_2 \, K \qquad (2)$$

where

$K = XyA'p/\phi G$ (correlating K factor)

$\text{Log } C_b/C_o$ = adsorbate concentration in the gas stream downstream of carbon bed divided by upstream concentration, in consistent units**

c_2 = constant (3.2×10^{-3} g/cm^2-sec)**

X = bed depth, cm

y = fractional free outer surface area of the carbon (i.e., the fraction of outer surface area that contains no adsorbed gases)

A' = maximum effective outer surface area of the carbon (i.e., no adsorbed gases on the carbon), cm^2/g

p = average packing density of carbon, g/cc

ϕ = shape factor for carbon bed geometry

G = mass velocity of gas stream, g/cm^2-sec**

* Registered trademark of E. I. du Pont de Nemours & Co.

** "F-112" vapor in air at 20 to 30°C and to 75% relative humidity in this work.

Equation 2 was verified experimentally with "F-112" tests of new small-scale carbon beds (shape factor ϕ = 0.90) with the following range of variables:

X = 1.3 to 5.1 cm
y = 0.08 to 0.44
A' = 41 to 100 cm^2/g
p = 0.52 to 0.63 g/cc*
Dp** = 0.11 to 0.30 cm
G = 12 to 41 x 10^{-3} g/cm^2-sec (21 to 70 ft/min)

Both coconut shell and bituminous base carbons were used in the correlation and no significant differences were observed. The upstream "F-112" concentration (C_o) was 20 ppm (by volume in air) in all tests.

The variables Dp and A' were estimated as 0.15 cm and 75 cm^2/g, respectively, for Type 416 carbon*** (used at SRP) and related to other carbon (assuming the same sphericity) by the following equation:

$$\frac{A_1'}{A_2'} = \frac{\rho c_2}{\rho c_1} \times \frac{Dp_2}{Dp_1} \qquad (3)$$

where

ρc = apparent density of carbon particle (by Hg displacement), g/cc

The average diameter of the carbon particles (Dp) was estimated by a sieve analysis of the carbon[8].

Water was the adsorbate that occupied most of the carbon's surface area during the tests, because nearly all the tests were conducted with humid air. The surface area that was available to adsorb "F-112" was assumed as the external surface area not occupied by moisture. The frac-

* These packing densities represent firmly packed carbon beds.
** Dp is average particle diameter.
*** Product of Barnebey-Cheney Co.

tional free area of all carbons tested was related to the quantity of adsorbed water by the following equation:

$$y = \frac{W-Z}{W} \qquad (4)$$

where

W = minimum wt % water on carbon to occupy all adsorption sites
Z = wt % water on carbon at time of test

Equation 4 is based on the assumption that y is a linear function of Z. This assumption is probably valid when no multilayer adsorption occurs. Values of W of 33, 36, and 40 wt % were evaluated in the correlating equation; 40 wt % water produced the least scatter in the data.

The data for 1.3-cm-thick beds tested with the larger carbon particles (0.30 cm) showed penetrations higher than predicted by Equation 2. In these tests, the bed thickness to particle diameter ratio (X/Dp) was probably too low to prevent "F-112" from channeling through the bed. Thus, the following limit was imposed on this ratio:

$$\frac{X}{Dp} \geq 8.5$$

As previously stated, Equation 2 was developed for laminar flow (Reynold's Number less than 40). However, data with Reynold's Numbers up to 70 were correlated adequately.

The data correlated by Equation 2 are shown in Figure 5. The correlation has a standard deviation of ~10% in the K factor for the range of "F-112" penetration most accurately measured (0.01 to 0.3%). Scatter in the data was due to variations in the properties of the different types of carbon (differences in sphericity, packing density, water isotherm, and base materials).

The data correlated by Equation 2 were obtained from tests of new carbon. The correlation is also probably applicable for used carbon, because mass transfer should

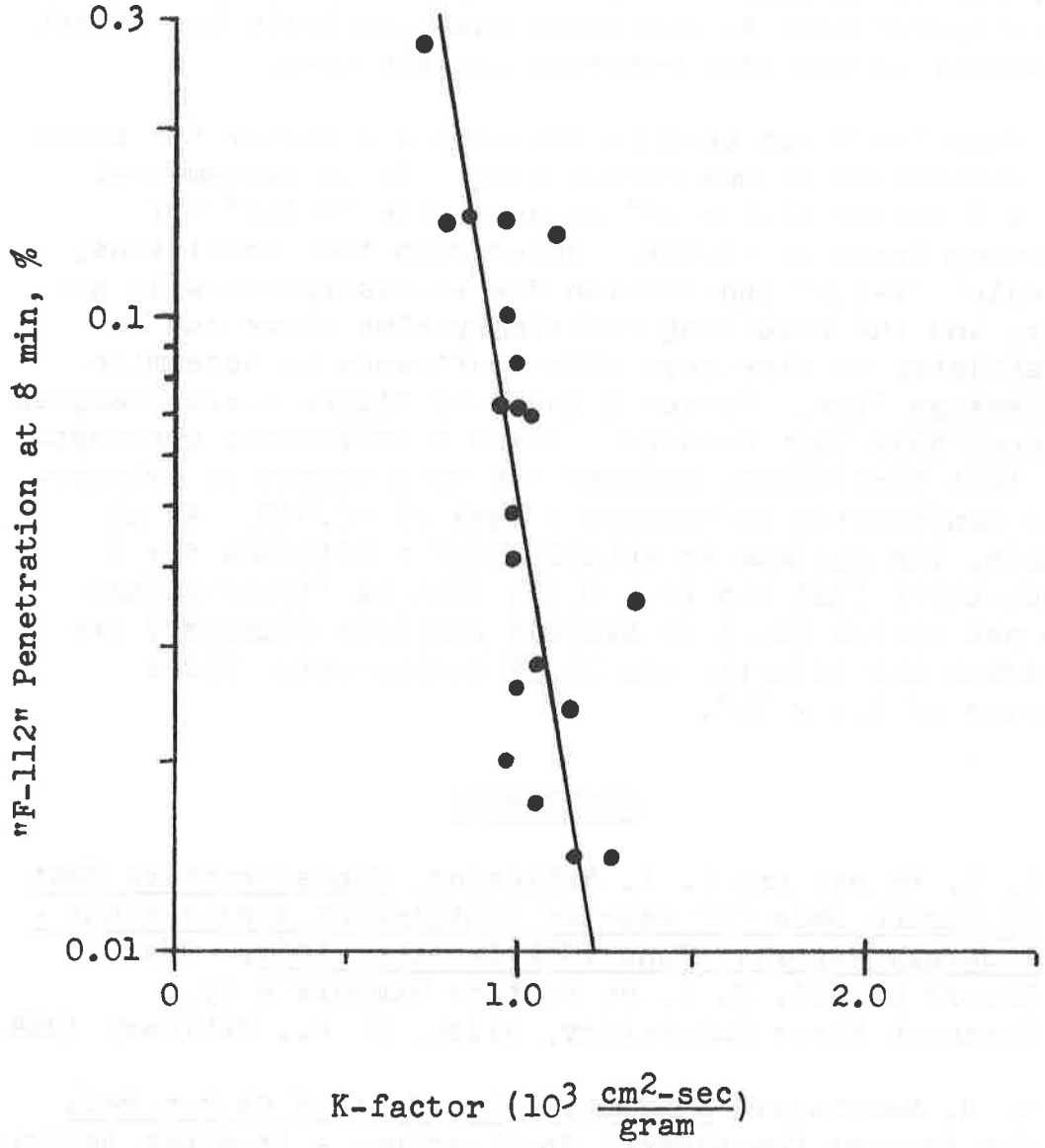

FIG. 5 CORRELATION OF "F-112" PENETRATION OF ACTIVATED CARBON BEDS

still be the controlling mechanism. Used carbon contains sorbed impurities that reduce the free external surface area, but sufficient data are not yet available from the full-size SRP beds to determine quantitatively the effect of service on the free external surface area.

Equation 2 was used to evaluate a K factor for known test conditions of new carbon beds. It is recommended that a K factor $\geq 1.1 \times 10^3$ be used with "F-112" for detecting leaks of ~0.01%. Under such test conditions, excessive "F-112" penetration due to desorption will not occur, and the resulting efficiency-time curve can be extrapolated to time zero with confidence to determine any leakage flow. Curves A and B of Figure 1 are examples of acceptable test results. Curve C represents unacceptable test conditions, because the data cannot be extrapolated confidently to measure a leak of ~0.01%. As an example, the maximum acceptable test conditions for a 1-inch-thick flat bed ($\phi = 0.90$) that is firmly packed with new carbon (0.15 cm average particle diameter) are 35 ft/min air velocity and 31.5% sorbed water for a K factor of 1.1×10^3.

REFERENCES

1. A. H. Peters and D. R. Muhlbaier, Nondestructive Test of Carbon Beds for Reactor Containment Applications - Progress Report: June 1962-December 1963, USAEC Report DP-870, E. I. du Pont de Nemours & Co., Savannah River Laboratory, Aiken, S. C., February 1964.

2. D. R. Muhlbaier, Nondestructive Test of Carbon Beds for Reactor Containment Applications - Progress Report: January-March 1964, USAEC Report DP-910, E. I. du Pont de Nemours & Co., Savannah River Laboratory, Aiken, S. C., September 1964.

3. D. R. Muhlbaier, Nondestructive Test of Carbon Beds for Reactor Containment Applications - Progress Report: April-June 1964, USAEC Report DP-920, E. I. du Pont de Nemours & Co., Savannah River Laboratory, Aiken, S. C., November 1964.

4. D. R. Muhlbaier, Nondestructive Test of Carbon Beds for Reactor Containment Applications - Progress Report: July-September 1964, USAEC Report DP-950, E. I. du Pont de Nemours & Co., Savannah River Laboratory, Aiken, S. C., April 1965.

5. D. R. Muhlbaier, Nondestructive Test of Carbon Beds for Reactor Confinement Applications - Progress Report: October 1964-January 1966, USAEC Report DP-1053, E. I. du Pont de Nemours & Co., Savannah River Laboratory, Aiken, S. C., June 1966.

6. M. Dole and I. M. Klotz, Sorption of Chloropicrin and Phosgene on Charcoal from a Flowing Gas Stream, Ind. Eng. Chem. 38, 1289 (1946).

7. B. W. Gamson, G. Thodos, and D. A. Hougen, Heat Mass and Momentum Transfer in the Flow of Gases Through Granular Solids, Trans. Am. Inst. Chem. Engrs. 39, 1 (1943).

8. G. G. Brown, et al., Unit Operations, p. 16, Wiley, New York, 1950.

IN-PLACE IODINE FILTER TESTING

J. H. Swanks

Oak Ridge National Laboratory*

ABSTRACT

A series of in-place iodine filter tests was performed on the charcoal iodine filters at the High Flux Isotope Reactor. Two sets of charcoal filters were tested - the first for elemental iodine retention and the second for methyl iodide and elemental iodine retention. This paper presents the results of those tests and discusses the conclusions drawn from those results.

INTRODUCTION

At the Oak Ridge National Laboratory charcoal filters are used in various air-decontamination systems which must prevent releases of radioactive iodine to the atmosphere; and, as integral parts of those systems, the charcoal filters must be reliable components whose efficiencies are known. In order to determine these efficiencies, in-place tests are performed on the filters immediately after their installation and periodically thereafter.

The purpose of this paper is twofold. The first is to consider these tests with respect to the general techniques, problems, and limitations involved with special emphasis on methods of obtaining and analyzing the data. The second purpose is to emphasize the necessity for performing the in situ experiments. It is erroneous to assume that the mere installation of a set of properly designed and pretested filters is adequate; because manufacturing techniques, installation procedures, filter loading or poisoning, and other factors significantly affect efficiencies.

In general, the efficiency tests, as performed at ORNL involve releasing a radioactive isotope of iodine into a system at some point upstream from the filter unit being tested. Then samples of the air-iodine mixture are withdrawn into small charcoal-filled sampling traps from points upstream and downstream from the

*Operated by the Union Carbide Corporation for the U. S. Atomic Energy Commission.

filter unit. The radioactive iodine content of the traps is determined by spectral analysis techniques, and each filter unit's efficiency is derived from the amount of radioiodine collected by the two sampling traps.

A series of these iodine filter tests was performed on the charcoal filters at the High Flux Isotope Reactor (HFIR). The following description of those tests illustrates the methods used in testing at ORNL and the conclusions that may be drawn from the tests.

DESCRIPTION OF HFIR TESTS

The HFIR employs two separate systems for the disposal of radioactive gases and for cleaning air which might become contaminated.[1] As the primary element in the dynamic containment system, the special building hot exhaust (SBHE) system provides a method for the filtering and subsequent disposal of large amounts of possibly contaminated air. Each of two separate segments of the SBHE draws 14,500 cfm of air from areas of the reactor building which contain potential sources of radioactive gases. In general, the SBHE system handles large quantities of low-concentration effluents.

The second system, the hot off-gas (HOG) system, is actually a radioactive-gas-disposal unit which handles normal gaseous releases from the subsystems of the reactor such as the cooling system and from experiment facilities. It is designed to handle small amounts of high-concentration effluents and is itself made up of two components: the closed hot off-gas (CHOG) and the open hot off-gas (OHOG) systems. The CHOG serves pressurized facilities, whereas the OHOG serves only unpressurized ones. The maximum flow in each component is 500 cfm.

Air from the SBHE and HOG systems passes through separate underground filter assemblies and is then forced up a 250-ft stack. Each system has three parallel filter assemblies or units (Figure 1). Under normal conditions any two of the assemblies may be used, so that the third is in a standby condition. Manually operated dampers are used to regulate and control the path of flow. The two filter systems are very similar and consist of Fiberglas prefilters, absolute filters, silver plated copper wool filters, two charcoal iodine absorbers in series, and another bank of absolute filters. Two main differences exist between the two systems. The higher capacity SBHE system has a series arrangement of two banks of twelve single charcoal filters in a 3 x 4 array; the HOG system has only two single filters in series in each unit. The other difference is that the SBHE system has conventional 24-in. x 24-in. pleated-type charcoal filters and the HOG systems have an arrangement of canister-type charcoal filters. The total flow rates are equivalent to about 1240 cfm per single filter in the SBHE system and 25 cfm per canister in the HOG system.

The HFIR operating limits[2] require that the iodine filters be tested at the time of installation and semiannually thereafter. The tests described herein are those performed after the installation of the first two sets of SBHE system filters. The first set was tested with elemental iodine, and the second set was tested with methyl iodide as well as elemental iodine. The first SBHE filters had nominally 1/2-in. thick activated charcoal beds contained between perforated sheet metal plates, cadmium plated to inhibit corrosion. The HOG filters were canisters having 3/4-in. thick beds of activated charcoal.

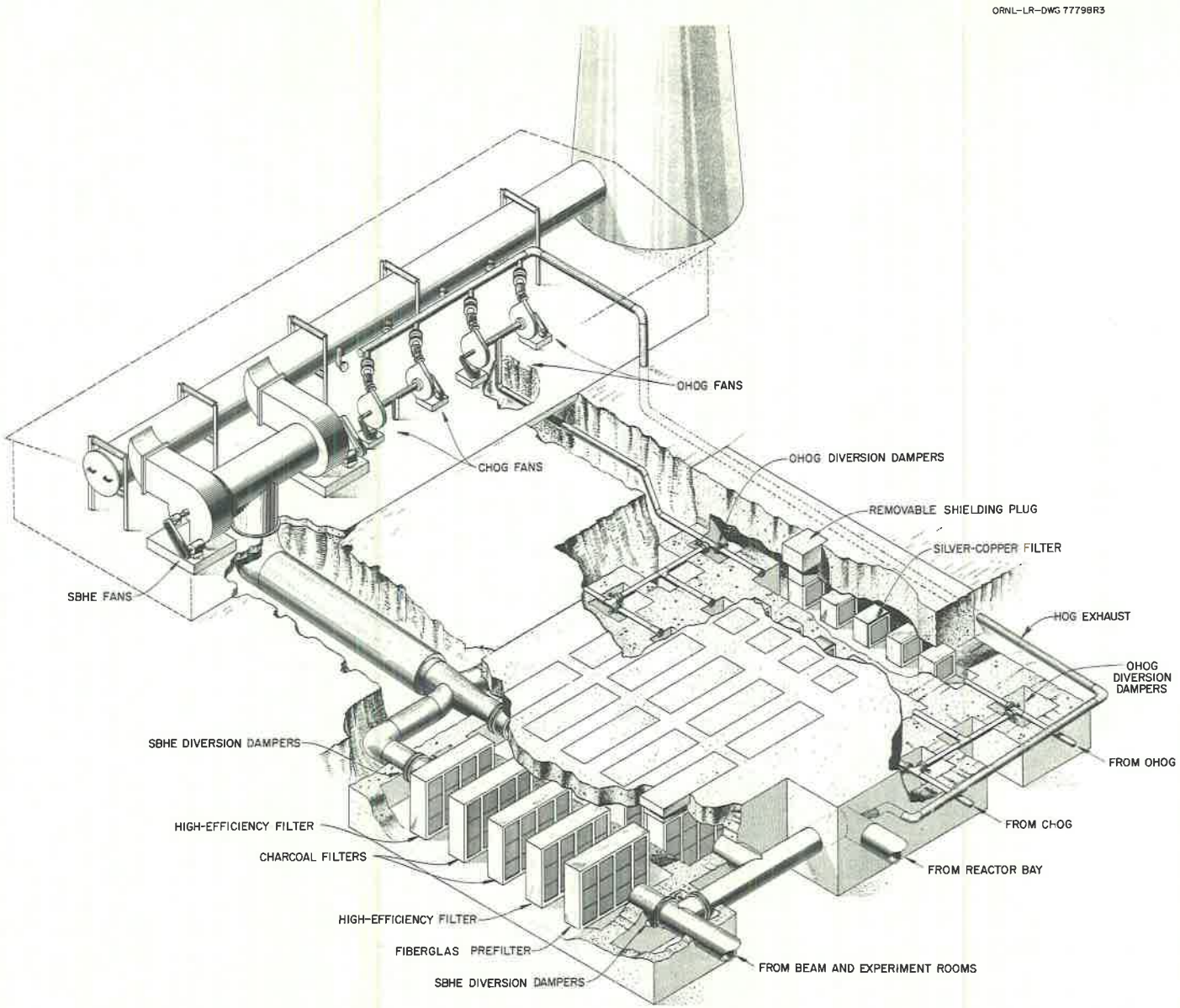

Fig. 1. SBHE and HOG Filter Systems

Iodine-131 was chosen as the radioactive isotope to be used in the tests because, due to its 8.05-day half-life, there would be no real hurry to remove and analyze the traps. For the tests on the SBHE system filters, 100 mg of stable ^{127}I traced with 30 mc of ^{131}I were used. For the HOG tests, the same amount of carrier was used, but it was traced with only 15 mc of ^{131}I.

The iodine sources were obtained from the ORNL Isotopes Division as elemental iodine crystals which were contained in a glass ampoule. The ampoule was placed into the apparatus shown in Figure 2. This container served a twofold purpose. It protected the ampoule from breakage during transit to the testing facility, and it served as an apparatus with which to inject the iodine into the system being tested.

The injection tube was mounted in a glovebox which contained the rest of the injection system (Figure 3) and the injection tube was connected to the system to be tested. For the conditions existing at the HFIR, it was decided that no exact requirements would be placed on the injection rate but that the iodine should be injected at a reasonably constant rate over a period of about 15 minutes while normal flow and temperature conditions were maintained in the system being tested. In order to release the iodine vapors into the system, a small air flow was established through the injection tube. Then the thin-wall tubing of the injection tube was mashed thereby breaking the glass ampoule. The air flow which had been previously established swept the iodine vapors from the crushed ampoule into the system being tested. By gradually varying the flow rate, the rate of injection was kept fairly constant; and, after the injection period, only an insignificant amount of the iodine remained in the tube.

The air streams were sampled with sampling traps like those shown in Figure 4. Activated charcoal was used as the iodine absorber. All of the other parts of the samplers were made of glass and stainless steel with the exception of rubber O-rings used on each end of the glass pipes. The larger traps were used during the tests on the SBHE system from which 14.5-cfm samples were drawn. The smaller traps were used for the tests on the HOG system from which 1.5 cfm samples were drawn. In both systems the samples were withdrawn immediately upstream and downstream from the filter assemblies through the sampling tubes which extended to the centerline of the duct. It was assumed that complete mixing of the air and iodine had taken place upstream from the first sampling point and that the samples withdrawn were of the average concentration. Samples were drawn simultaneously and continuously during the entire injection period and for approximately two hours after the injection was begun. Thus any iodine that came off the filters during this two hours was detected in addition to that which passed through the filters during the injection period.

After the sampling period, the traps were removed and disassembled for analysis. The charcoal was removed from the traps and divided into small quantities. Then the inside of the traps were swabbed to remove any charcoal dust and iodine that might have deposited on the surfaces. The individual charcoal samples and the swabs were placed in petri dishes and counted separately with a gamma spectrometer. The radioiodine content of each sample was then determined, and the total for the entire trap was obtained by summing the activities of the components.

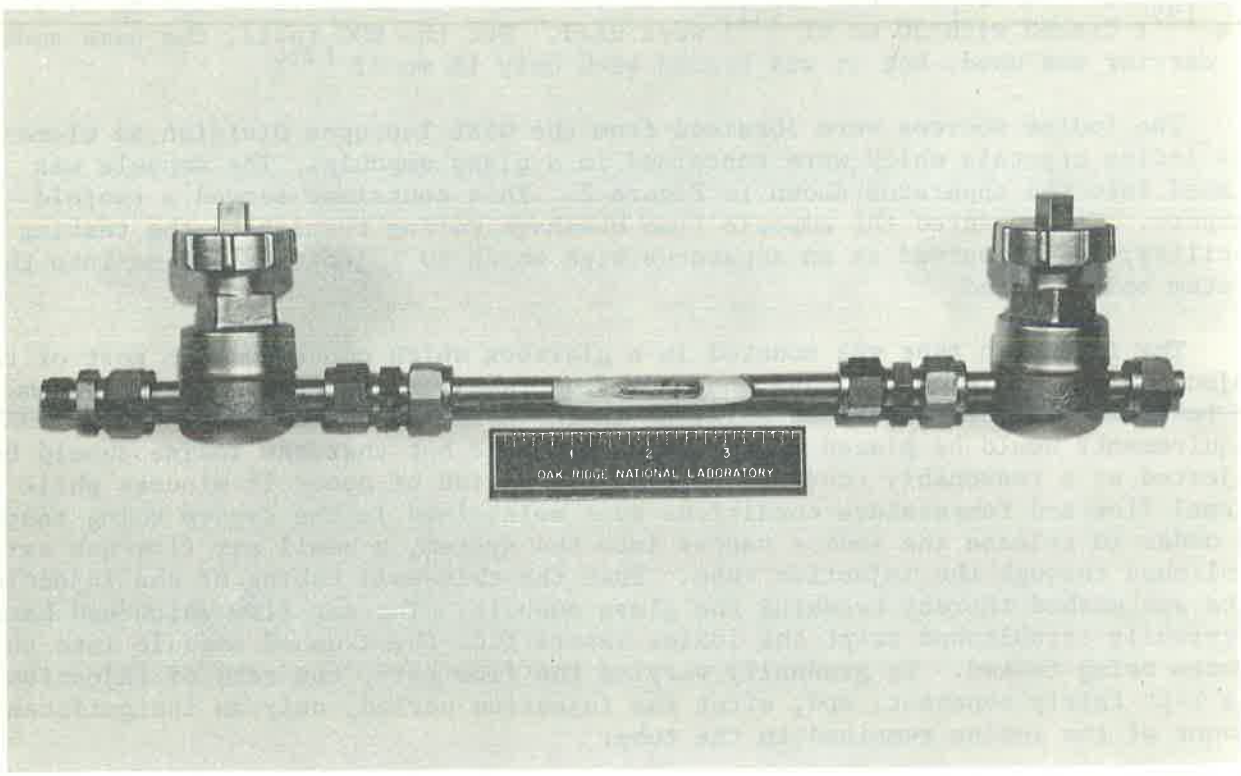

Fig. 2. Injection Tube with Iodine Ampoule

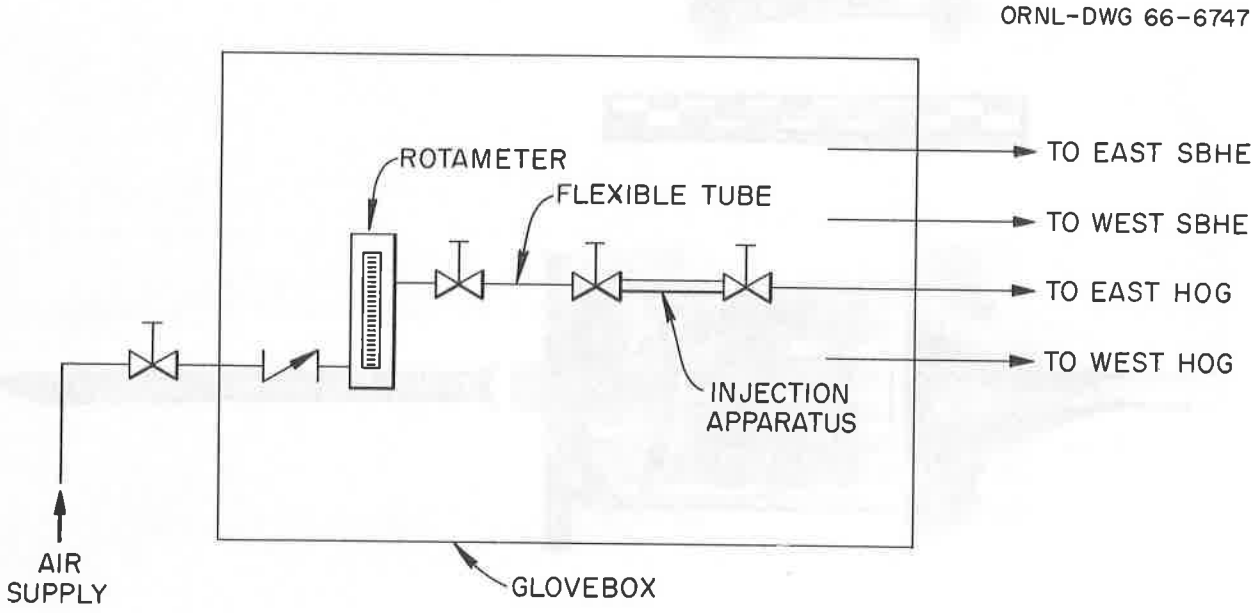

Fig. 3. Iodine Injection System

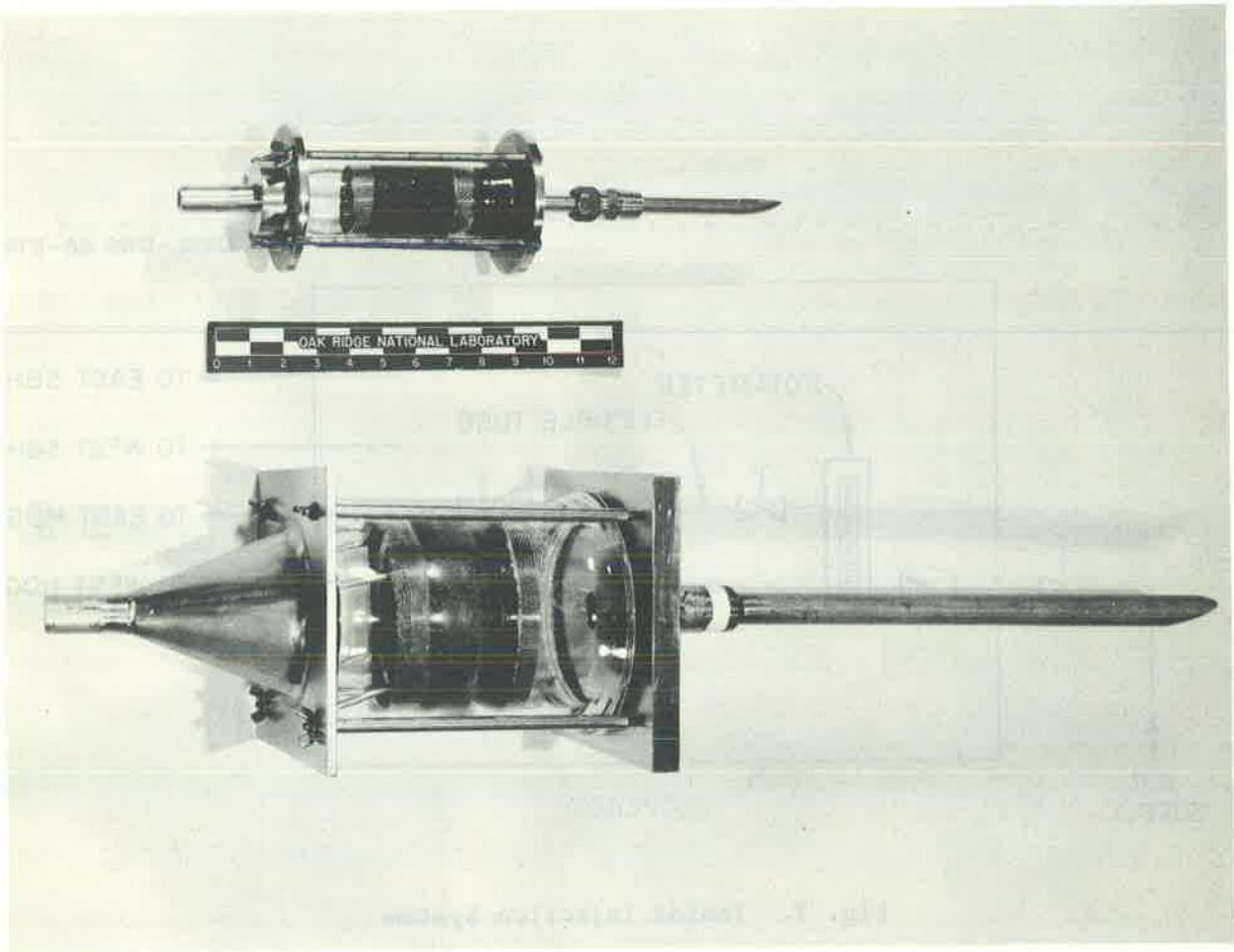

Fig. 4. Sampling Traps

The results of the first series of tests are given in Table 1. The indicated decontamination factor (DF) is the simple ratio of the upstream to downstream iodine concentrations and is related to the efficiency by the following relation:

$$\text{Efficiency} = 1 - \frac{1}{DF}$$

Table 1. Results of First Test of 1/2-Inch-Thick Filters

System Tested	Iodine Removal Efficiency (%)	Decontamination Factor (DF)
East SBHE	99.06	106
Standby SBHE	99.62	260
West SBHE	99.40	166
East HOG	99.98	4120
Standby HOG	99.98	3700
West HOG	99.99	8200

Upon examination of the results of these tests it was concluded that the HOG filter systems performed satisfactorily and that no modification or further testing of those systems was necessary. However, the fact that the efficiencies of the SBHE systems' filters were so low caused some concern, for it was felt that their efficiencies should be on the order of 99.8% or greater. In order to check the results of the first tests, another test was performed on the east bank of SBHE filters. The results of this test were:

Efficiency = 98.9%
DF = 92

In order to determine the cause of the low efficiencies, the filters were removed from their compartments and inspected. Several large openings were observed around the framework of the filters, so a large portion of the air stream had been bypassing the filters.

The leaks around the filters were sealed, the filters were replaced in their compartments, and more tests were performed. The results indicated in Table 2 were obtained from those tests. As may be noted here, sealing the leaks improved the system efficiency somewhat, but the efficiencies were still lower than desired.

Table 2. Results of Second Test of 1/2-Inch-Thick Filters

System Tested	Iodine Removal Efficiency (%)	Decontamination Factor (DF)
East SBHE	99.65	263
Standby SBHE	99.75	397
West SBHE	99.77	442

In order to determine whether or not the fault lay in the thickness of the charcoal filters, a comparison was made between the results of tests run on two 1/2-in.-thick HFIR charcoal filters and two 3/4-in. filters which were available. Identical conditions were maintained while running the tests of the two types of filters and the results shown in Table 3 were obtained.

Table 3. Results of Comparison Tests

System Tested	Iodine Removal Efficiency (%)	Decontamination Factor (DF)
1/2-in. filters	99.67	303
3/4-in. filters	99.94	1730

Due to the low efficiencies of the 1/2-in.-thick filters and due to a study regarding the methyl iodide hazards at the HFIR,[3] it was decided to replace the 1/2-in.-thick filters with a new set of thicker filters. The new filters are made of perforated stainless steel with an impregnated activated charcoal filler which is nominally 1 1/8-in. thick.

Two types of iodine retention tests were performed on the new filters. They were first tested for elemental iodine retention using the same procedures that were used while testing the set of 1/2-in.-thick filters. In addition, the new filters were tested for methyl iodide retention. The sampling and analytical techniques for the methyl tests were identical to those used in the elemental tests, but the injection procedure had to be modified somewhat. The same quantity of iodine was used as in the elemental tests except that it was in the form of methyl iodide and was contained in a stainless steel U-tube. In order to obtain a fairly uniform release rate, the U-tube was installed in the injection apparatus, a delay tank was connected to the downstream side of the U-tube, and the tank was connected to the system to be tested. A very small air flow was established through the U-tube so that methyl iodide vapor moved into the delay tank and then slowly flowed from the tank into the system being tested.

During the test on the west SBHE filters, the elemental iodine and methyl iodide tests were run simultaneously by using elemental iodine-131 and methyl iodide-130. By using both of the isotopes, only one injection and sampling was necessary. Spectral analyses of the samples allowed one to distinguish between the ^{130}I and ^{131}I isotopes during the analyses. The results of the test are presented in Table 4.

Table 4. Test Results of Stainless Steel Filters in West SBHE

Type of Test	Iodine Removal Efficiency (%)	Decontamination Factor (DF)
Elemental Iodine	98.55	69
Methyl Iodide	47.37	1.9

Considering these results, it was obvious that something was wrong with the system because the original, thinner filters performed more efficiently than these.

The filters were inspected in place, and no leaks were evident. They were then removed from their compartments, disassembled, and opened for examination. Upon removal of the tops of the filters, the problem was seen immediately; the charcoal had settled to such an extent that numerous air gaps had formed at the top of the filters. A typical settled filter is shown in Figure 5. The filters were refilled with the same type of charcoal, reinstalled in their compartments, and retested. The results of the tests of all the SBHE systems are given in Table 5.

Table 5. Results of Tests of Stainless Steel SBHE Charcoal Filters

System Tested	Iodine Removal Efficiency (%)		Iodine Decontamination Factor	
	Elemental	Methyl	Elemental	Methyl
East SBHE	99.994	99.97	17,300	3,580
Standby SBHE	99.994	99.97	16,100	3,850
West SBHE	99.995	99.98	20,300	4,200

The absolute accuracy of the results of these tests is somewhat questionable, for the activities in the downstream samplers were quite low. However, the results are definitely conservative and the systems are at least as efficient as these results indicate.

These tests illustrate that the filters perform quite satisfactorily for both elemental iodine and methyl iodide. It, of course, still remains to be seen how the filters will behave as the charcoal ages.

CONCLUSIONS

Considering the results of the tests performed at the HFIR, several general conclusions may be drawn.

If iodine test results indicate that a filter unit is inefficient, it remains then to decide whether the inefficiency is due to poor charcoal filter design, air leaks around the filters, loading and poisoning of the filters, or some other fault. In other words, the mere fact that a test indicates a low unit efficiency does not necessarily mean that the filters themselves are inefficient. They may indeed be, but one must carefully inspect the system to determine what fault or combination of faults causes the inefficiency. Generally, as far as the results of the tests are concerned, no distinction can be made as to what type of fault exists.

In-place filter tests are the only reliable method of determining whether a system will perform as it was designed; however, the methods and procedures used in performing those tests are essential in obtaining valid, reliable results

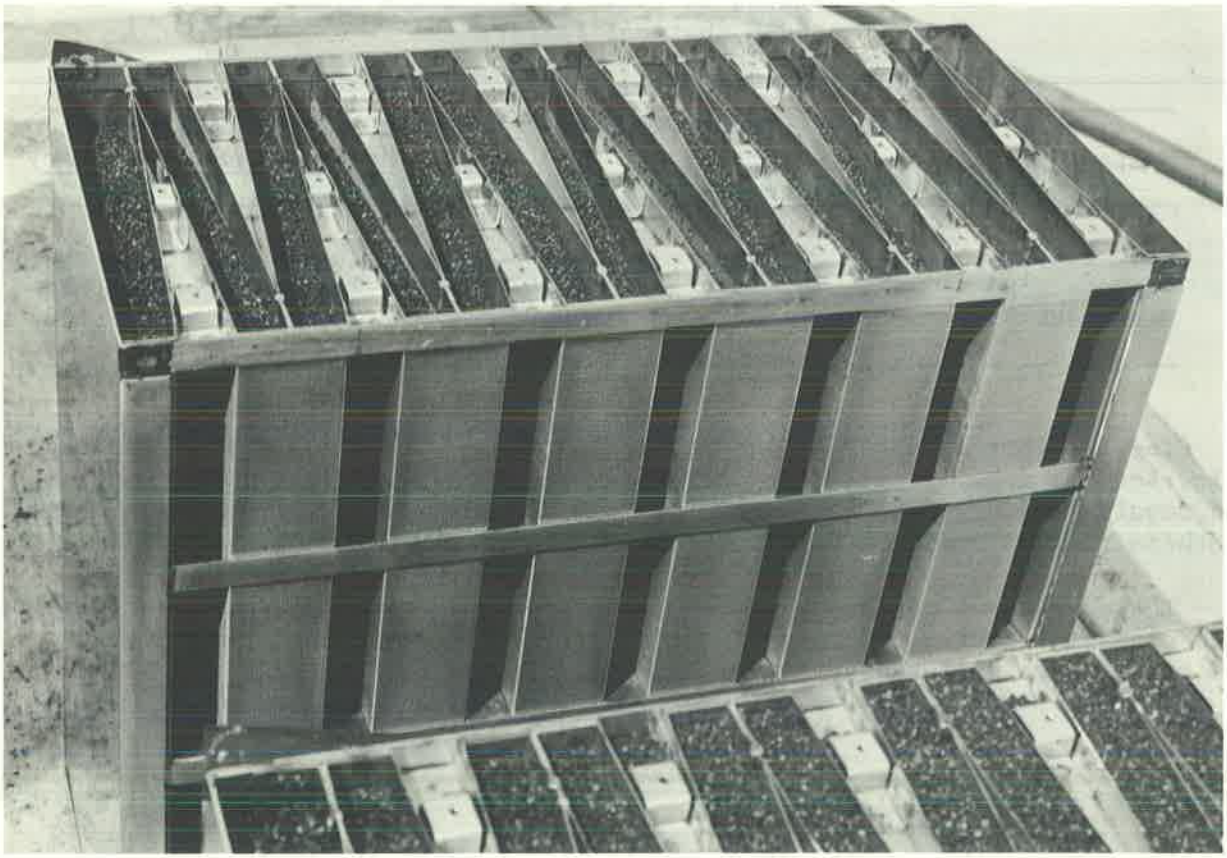

Fig. 5. An SBHE Filter in Which Charcoal had Settled

which are necessary to evaluate an installed system properly. Tests performed under conditions different from those normally present in a system or with poor regard for injection and sampling procedures are of questionable value and may lead to erroneous conclusions.

It must be recognized that various chemical forms of iodine may exist in a system, and the capability of a filtration system for removing one of these forms does not insure its capability for removing another. Systems to be tested must, therefore, be investigated to determine what chemical forms of iodine might be present and then the appropriate tests may be performed.

If the filter system is required to have a definite capability, then it is imperative that the system actually be tested in situ in order to guarantee that capability. Furthermore, periodic tests should be performed to determine whether or not the system maintains its capability.

Acknowledgement

The author wishes to acknowledge the assistance of R. E. Adams of ORNL in establishing testing criteria and procedures.

REFERENCES

1. F. T. Binford and E. N. Cramer (Eds.), The High Flux Isotope Reactor: A Functional Description, Vol. 1, USAEC Report ORNL-3572, Oak Ridge National Laboratory, May 1964, Rev. March 1, 1965.

2. Operating Safety Limits for the High Flux Isotope Reactor (HFIR), (100 Mw Maximum Power), USAEC Report ORNL-TM-1532, Oak Ridge National Laboratory, May 16, 1966.

3. R. E. Adams, W. E. Browning, Jr., W. B. Cottrell, and G. W. Parker, The Release and Adsorption of Methyl Iodide in the HFIR Maximum Credible Accident, USAEC Report ORNL-TM-1291, Oak Ridge National Laboratory, October 1, 1965.

DISCUSSION

THOMAS: I would like to remark that the Freon test tells you if the carbon bed is properly installed; whether one has leaks or other troubles. I think this is quite an important paper. Mr. Hillary?

HILLARY: Before my question, I would like to say that we are inclined to test charcoal beds, as was indicated in one of my papers, with methyl iodide itself. It seems to be most effective.

I would like to ask whether there is any permanent retention of Freon on the charcoal and, if there is, is this likely to effect the iodine adsorption efficiency?

MUHLBAIER: No, it does not effect the iodine adsorption efficiency. There may be a small degree of retention of the Freon, but it is difficult to measure this and tests of the iodine efficiency with carbon containing as much as four times the normal Freon loading of the in-place in the test has shown no effect on the iodine efficiency of the carbon.

THOMAS: Let me make sure of one point. Besides the Freon test, you also removed carbon beds from your big banks and test them individually with iodine from time to time; don't you?

MUHLBAIER: That is correct.

THOMAS: You see, they are really checking both leaks and charcoal capacity. Another question?

BRESLIN: Would it be possible to avoid the use of two Freon detectors by some kind of upstream and downstream sequential sampling?

MUHLBAIER: Well, certainly that would be possible. It would require further restrictions on the test conditions so that you would have adequate time to have the single detector analyze both samples. It would double the time in the test, essentially, so that we would be concerned with desorption of Freon, possibly half again as long.

PETERS: I would like to elaborate on Dave's last answer. In some applications, it is quite possible that only one detector would be required without any measurement at all of the upstream concentration. Once you assure yourself that you are injecting sufficient Freon upstream, then the actual upstream concentration is relatively unimportant as far as determination of the leakage flow; and again, the upstream Freon concentration is important where you are trying to detect a leakage flow of .01% as compared to 0.1% or one percent. It depends on the actual application and requirements of the system.

THOMAS: Thank you. I would like to have more discussion about this paper, but we are already a half hour behind time.

ETTINGER: I have a question regarding the test you ran where you later found that the leakage was caused by settling of the charcoal. In your first slide, you showed a 98% efficiency on elemental iodine and 40% on methyl iodide. You attributed this to settling and actual leakage. Why should you have much more direct passage through voids by the elemental iodide as compared to the methyl iodide?

VILES: That is a good question. I hope you can answer that one.

SWANKS: I have no answer for that.

At any rate, you showed us that you have got to be careful about carbon settling out from the top of its container.

PETERS: I would like to make two comments. And I will try to keep them brief. It is fairly obvious that if you used Savannah River specifications for your carbon beds, you did not get beds that look like ours at all. The mechanical design of the ORNL bed is quite different from the SRP bed.

VILES: The other question I have, were your beds installed with the pleats vertical?

SWANKS: They are installed with pleats vertical. They have a one-inch solid section at the top to prevent air channeling around the top of the filters; however, the settling was below that.

PETERS: Even so, we found a number of years ago, with beds installed vertically with a non-perforated section of an inch, that this is not enough, because with 24 inches of carbon in a vertical direction it is possible to get settling much more than an inch.

In regards to your difference in efficiency between the iodine and the methyl iodide, I wonder if this may not be due to sampling problems downstream of the carbon banks?

Really, what I am asking is, are your efficiency determinations the efficiency of the system, the efficiency between the sampling points, or the efficiency of the carbon beds themselves? Did you take precautions to ensure that you mix the sample downstream quite thoroughly? As an example, you could remove a single filter from the edge of a large manifold bank of filters, and if you have a single point sampler in the middle of that duct, you could miss the relatively large leak entirely. In other words, we found mixing efficiencies as low as 10% with the single point sampler in a large system.

SWANKS: I will agree to that point; that is, that there are sampling problems. However, I think in our system, at least with the type of ducting and filtration system as it exists, there is no question about the mixing downstream of the filters themselves. These tests measured the filtration between the sampling points.

IN-PLACE IODINE REMOVAL EFFICIENCY TEST

by

F. J. Viles, Jr. and L. Silverman†

Harvard Air Cleaning Laboratory
Harvard School of Public Health
Boston, Massachusetts 02115

A B S T R A C T

The application of iodine removal units in the ventilation systems for nuclear power reactors requires a sensitive means for periodic in-place testing of their performance. This study involved the application of iodine-127 as a tracer for such tests and the associated development of (a) a sampling technique which assures its collection at 100% efficiency, and (b) an ultra-sensitive analytical technique for its analysis. Investigations showed that 1 inch depth beds of 1 to 2 mm diameter clean electrolytic copper beads provided collection efficiencies greater than 99% for air velocities up to 120 fpm and for iodine loadings up to 0.1 milligram per sq. cm. of copper surface. An analytical technique, based on the iodine catalytic reduction of ceric ions, proved reliable and adaptable to in-place testing. The analytical procedure is accurate for amounts of iodide ranging from about 0.002 µg up to 0.12 µg (assuming a 5 ml test sample).

† Deceased

INTRODUCTION

The application of iodine removal units (charcoal beds) in ventilation facilities for nuclear reactors requires a means for periodic in-place testing of these devices to assure their adequate performance at all times. Iodine-127 is an ideal vapor tracer for this test since it is an isotope of the element for which the removal device is required and is non-radioactive. In addition, repeated use of iodine-127 for in-place testing may improve the efficiency of the unit for the removal of radioiodine by providing a significant amount of stable iodine for isotopic exchange.

The amounts of iodine used for in-place tests should be small so that repeated tests will not significantly affect the capacity of the removal unit for all isotopes of iodine. It has been proposed[1] that 1 gram of iodine-127 per hour per 1000 cfm be used as a specification for periodic in-place iodine removal efficiency tests. This would result in an average concentration of 0.057 ppm of I_2 up-stream of the unit. For a 99.9% removal efficiency (downstream concentration = 5.7×10^{-5} ppm I_2), only 0.06 microgram would be present in a 100 liter downstream sample. The first requirement, therefore, for an in-place test is an ultra-sensitive method of analysis for iodine-127. A second requirement is a highly efficient sampler for these low concentrations. Such a device must meet the following requirements: (1) the sampler must be free of any iodide contamination; (2) the materials or chemicals used must not interfere with the analysis; and (3) the entire sample collected must be recoverable for analysis.

This paper briefly discussed the development of (1) an ultra-sensitive analytical procedure for iodine and iodide and (2) a sampling technique which assures 100% collection and recovery of iodine at low concentrations and which is adaptable to the analytical method.

REVIEW OF SENSITIVE ANALYTICAL METHODS FOR IODINE

The most sensitive methods of chemical analysis for iodine are based on its properties as a catalyst, notably: a) oxidation of NN' tetra methyl-diaminodiphenylmethane (tetrabase) by chloramine T[2]; b) reduction of ceric sulfate by sodium arsenite[3,4,5,6], and c) reduction of ferric ferri-cyanide by sodium arsenite[7]. These reactions proceed at extremely slow rates or not at all except when catalyzed by iodide ions. In the tetrabase reaction, the chloramine T oxidizes iodide to iodine which then returns to iodide by oxidizing tetrabase to a blue quinoidal compound. The other two methods involve

the reduction of ceric or ferric ions when they oxidize iodide to iodine, which is then reduced back to iodide by arsenite ions. In the ferric method, the reaction rate, which is related to iodine concentration, is indicated by the extent of the formation of the blue complexes of ferro ferricyanide and ferric ferrocyanide. In the ceric method, determination of the reacted ceric ions (cerous ions) after a specified period of time provides a correlation for the iodide concentration present.

Preliminary studies of the tetrabase reaction revealed instability of color with rapid changes from intense blue to blue green, then to yellow green and ultimately to green yellow, the latter a weak color of poor sensitivity. Stabilization of the initial intense blue color by using 50:50 alcohol and water solutions was partially successful, but results were inconsistent from day to day even with freshly prepared reagents. The general acceptance of ceric sulfate methods, as indicated by citations in the literature on iodide analysis, led to further investigation of its application for in-place testing.

IODIDE ANALYSIS BY CATALYTIC REDUCTION OF CERIC IONS

The chemical reactions involved in this method are 1) reduction of ceric to cerous ions by iodide oxidation to iodine and 2) reduction of iodine back to iodide by oxidation of arsenite to arsenate ions. Reactions are:

$$2\ Ce\ IV + 2\ I^- = 2\ Ce\ III + 2\ I^\circ$$

$$2\ I^\circ + As\ III = 2\ I^- + As\ V$$

$$2\ Ce\ IV + As\ III = 2\ Ce\ III + As\ V$$

The reactions are performed in a solution specified in acid and chloride (NaCl or NH_4Cl) normalities. The chloride is used to suppress foreign ion interference and stabilize the reaction rate. The net reduction of ceric by arsenite ions is related to reactant concentrations, iodide concentration, temperature and time.

The technique used by Miller and Schneider[4] involved stopping the catalyzed reduction of ceric ions, after a stated period of time, by addition of a specified amount of standardized Mohr's salt (ferrous ammonium sulfate) to reduce the remaining unreacted ceric ions. The amount of ferrous ions (depending upon normality) remaining, after this step, is equivalent to the ceric ions reduced by the original iodine catalyzed reduction and is determined by back titration with standard ceric solution. For the conditions of the test (temperature, time and reagent concentrations), this amount of reduced ceric ions is related to the iodide concentration which is established by means of known iodide standards.

Discrepancies in preparation of iodine standards led to conclusions that errors could occur by improper application of standardized Mohr's solution in this procedure. As mentioned in the ferric ferricyanide test for iodine, the ferric ion is catalytically reduced by iodide in the presence of arsenite ions.[7] In the Miller-Schneider ceric sulfate method, the ferric ions, produced by oxidation of ferrous ammonium sulfate from the unreacted ceric ions, would be catalytically reduced to ferrous ions by iodide and arsenite present in the test. These additional ferrous ions would require additional ceric sulfate in back titration and would therefore indicate an iodide concentration greater than that present.

Difficulties created by this latter problem and also the required use of large amounts of glassware, which increased the problem of contamination, led to the determination of ceric ion reduction by colorimetric measurement of the highly colored ceric ions.

The colorimetric procedure still retained some of the inadequacies of the titration technique, namely 1) unknown variable iodide contamination in blanks which necessitated accurate standardization curves for each set of sample analyses, and 2) need for analysis of contaminants (organics, etc.) which would reduce ceric ions by a one step non-catalytic process. The latter had to be determined prior to iodide analysis by test without arsenite (which is required only for the catalytic iodide reduction) so that extra ceric salt could be added for the iodide test to assure the correct amount available for the iodide reaction. In addition, accurate standardization of the ceric reagent was required so that correct amounts were available for the iodide test.

To eliminate many of these inadequacies, the procedure of Lein and Schwartz[6] was adopted with modifications. This method makes use of the reaction rate and its relation to iodide concentration to obtain a standard calibration curve.

If the concentration of all but one of the reactants (I^-) are increased by relatively enormous proportions, pseudo first order reaction conditions will prevail. Thus:

$$- d(\text{Ce IV})/dt = k\,(I^-)\,(\text{Ce IV})$$

$$- \ln(\text{Ce IV}) = k\,(I^-)\,t + C$$

and

$$\ln(\text{Ce IV})_1 - \ln(\text{Ce IV})_2 = k\,(t_2 - t_1)\,(I^-)$$

or $\Delta \log (Ce\ IV) / \Delta t = k^1 (I^-)$, (a)

A plot of T (transmission) vs log (Ce IV) yields an S-shaped curve which is linear in the middle portion (~ 30% - 65% T.) (Figure 1). For this straight portion of the plot:

$$T = -m \log (Ce\ IV) + c$$

$$\Delta T = m\ \Delta \log (Ce\ IV)$$

or $$m^1\ \Delta T = \Delta \log (Ce\ IV)$$

Substituting (a) above into this equation,

$$m^1\ \Delta T / \Delta t = k^1 (I^-)$$

and finally $\Delta T / \Delta t = K (I^-)$

Thus, the concentration of iodine is proportional to the ratio of the change in transmission to change in time, $\Delta T / \Delta t$, as long as ΔT is in the linear portion of the transmission curve for ceric ion concentration.

In contrast to other methods, the above depends on the reaction rate constant, which for specified conditions is invariable. Only intervals of time and transmittance are required, not absolute values and not necessarily the values at the initiation of the reaction. Since a change in concentration is measured, accurate standardization of the ceric ion is not required. Details of the procedure are presented in the Appendix to this report.

IODINE VAPOR SAMPLING STUDIES

Beds of clean electrolytic copper beads were used as samplers for the iodine (Fig. 2 - Appendix). Numerous studies involving approximately 1 inch depth beds of 1 - 2 mm diameter beads have demonstrated greater than 99% collection for air velocites as high as 120 ft. per minute and for iodine loadings to 0.1 milligram per sq. cm. of copper surface[8]. A discussion of the preparation and application of the bed samplers is presented in the Appendix.

Determination of the iodine concentration downstream of the removal unit is the most significant analysis in an in-place test. For arrangements where a known amount of iodine can be injected immediately upstream of the removal unit and with

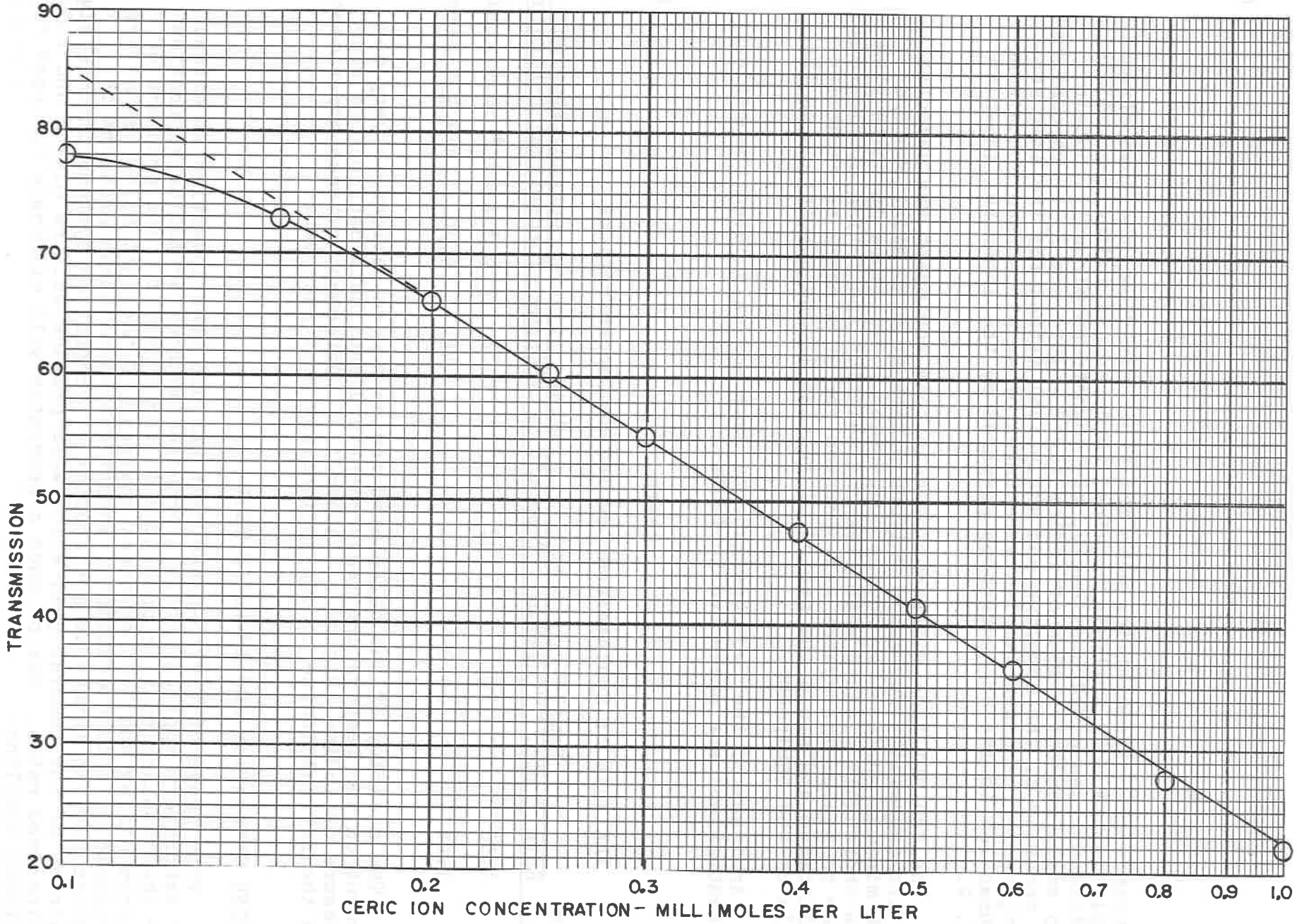

FIGURE 1. CALIBRATION CURVE OF CERIC ION SOLUTION AT 400 MμL WITH A KLETT COLORIMETER.

assurance of uniform mixing with the known air flow, the down stream sample is the only analysis required to determine iodine removal efficiency. As noted previously, the downstream air will contain very small concentrations of iodine (10^{-3} - 10^{-5} ppm I_2). To confirm the accuracy of the sampling and analytical method for the in-place test, copper bead bed samples were taken of an air stream containing a known low iodine concentration prepared by the apparatus shown in Fig. 2.

The venturi type mixer employed in this equipment was selected for its capability for rapid uniform mixing at high dilutions and with minimum surface for iodine adsorption. All lines in the system were thoroughly cleaned with cleaning solution and fuming nitric acid prior to test. The system was operated for 30 minutes to establish equilibrium and avoid the period of initial iodine adsorption on the walls of the equipment.

Analyses of the two runs made to date and calculated theoretical concentrations are presented in Table 1.

TABLE 1

Analysis of Synthesized Low Iodine Concentrations.

Test No.	Sample		Iodine		Concentrated ppm	
	Rate / min.	Time-Min	Temp (°C)	VP(ppm)	Theoretical	Determined
1	1.01	10	2	52	6.3×10^{-3}	6.4×10^{-3}
2	1.02	10.25	1	46	5.25×10^{-3}	5.5×10^{-3}

The accuracy of the calculated iodine concentrations is very dependent on the temperature measurement and available data on the vapor pressure of iodine (Figure 1 - Appendix). Agreement between experimental and theoretical iodine concentrations was most acceptable.

IODINE GENERATION FOR IN-PLACE TEST

This phase of the in-place test has not been investigated except for laboratory applications. A proposed method for iodine generation for the in-place test is presented in the Appendix. The problems of uniform mixing and iodine losses upstream of the unit to be tested are mentioned in this discussion. Investigation of these problems is planned for the future as are studies of generation systems immediately upstream of the removal unit which will provide uniform mixing and known iodine feed rates. Use of such a generator will eliminate the need for upstream sampling.

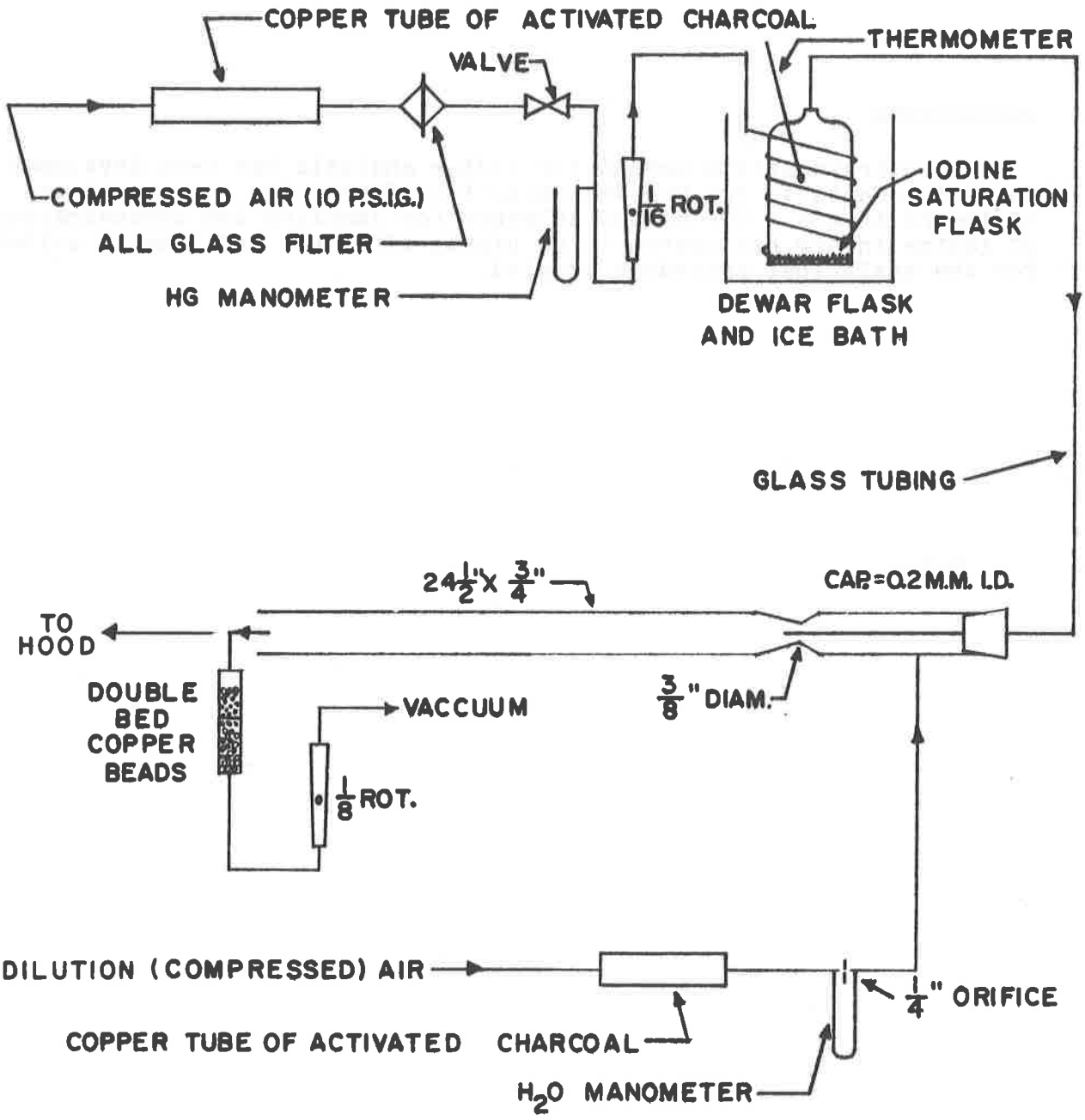

FIGURE 2. PREPARATION OF KNOWN IODINE CONCENTRATIONS.

CONCLUSIONS

An ultrasensitive method for iodide analysis has been developed which is adaptable for the determination of very low concentrations of iodine in air. The method selected for sampling low concentrations of iodine in air has proven to be highly efficient and ideally suited for the analytical procedure adopted.

REFERENCES

1. Personal Communication - Mr. Harold Bernard, Division of Reactor Development, U.S. Atomic Energy Commission, Washington, D. C. Sept. 1965.

2. Jungreis, Ervin and Gedalia, Itzhak: Ultramicro Determination of Iodine in Drinking Water on the Basis of Feigl's Catalytic Reaction, Mikrochim Acta 1, 145, 1960.

3. Sandell, E. B. and Kolthoff, I. N., Chronometric Catalytic Method for the Determination of Micro Quantities of Iodine. J. Amer. Chem. Soc. 56, 1426, 1934.

4. Miller, A. D. and Schneider, L. A.: Determination of Micro Amounts of Iodine in Natural Waters by a Catalytic Method, Zhurnal Anditicheskoi Khimii, 18, 371, 1963.

5. Malmstadt, H. V. and Hadjicoannou, T. P.: Ultramicrodetermination of Iodine by a Rapid Automatic Reaction-Rate Method. Analytical Chemistry 35, 2151, 1963.

6. Lein, Allan and Schwartz, Meina, Ceric Sulfate- Arsenious Acid Reaction in Microdetermination of Iodine. Anal Chem. 23 1507 - 1510, 1951.

7. Gremlin, R. and Virtanen, A. I.: A sensitive Colour Reaction for the Paper Chromatographic Detection of Iodide, Iodinated Tyrosines and Thyronines, Acta Chem. Scand. 13: 1469, 1959.

8. Viles, F. J. and Silverman, L., Progress Report, July 1964 - Sept. 1965. Air Cleaning Laboratory, Harvard School of Public Health, NYO - 841 - 4 (not yet published).

APPENDIX

PROCEDURE FOR IN-PLACE IODINE REMOVAL EFFICIENCY DETERMINATIONS

by

F. J. Viles, Jr. and L. Silverman

Harvard Air Cleaning Laboratory
Harvard School of Public Health

Boston, Mass. 02115

PROCEDURE

This procedure has been developed for in-place efficiency testing of iodine removal units employed in the ventilation clean-up and release systems for nuclear power reactors such as that in use on the N. S. Savannah. It consists of three parts, namely: (1) Generation of Iodine in System, (2) System Air Sampling, and (3) Analytical Procedure.

GENERATION OF IODINE IN SYSTEM

Concentrations of iodine 127 in the ventilation system are prepared by feeding iodine-saturated air at room temperature into the system well upstream of the test section. Known concentrations can be determined from measured system flow and iodine-saturated air feed rates, assuming no other sources of iodine in the system. The feed air should be pre-filtered through high efficiency glass or membrane media and coconut shell charcoal to eliminate iodine removal by adsorption on particles or reaction with organic vapors. If preferred, cylinder compressed air may be used without the above precleaning. Prior to saturation with iodine, the feed air is metered by conventional means (rotameter, orifice meter, etc.).

Air is saturated with iodine by passing it over iodine crystals in a series of three or more flasks sized so that one air change or less per minute occurs for each flask. The entire bottom of each flask should be covered with iodine crystals and the inlet feed air should impinge on the surface of the iodine crystals without iodine particle release. Iodine-saturated air may be obtained also by passing air consecutively through two or more beds of iodine crystals supported on glass frits. Iodine particle release should be avoided by employing suitable bed velocites. In both types of generators, a thermometer is used in the last unit to establish saturation temperature. High efficiency binder-free filters are employed downstream of the generator to remove any particulate iodine that may become airborne in the process. The feed system from the iodine generator to the system tested should be constructed of non-adsorbing materials such as clean glass or pre-oxidized stainless steel.

Based on the release of 1 gram of iodine into the system in one hour and an iodine vapor pressure of 430 ppm (0.327 mm Hg) at 25°C (Figure 1), the required feed flow rate is 3.75 liters of iodine saturated air per minute. This rate of iodine feed will result in an average concentration of 0.057 ppm of I_2 in a 1000 cfm system. If the flask type generation is employed for saturating the feed air with iodine, three or more 4 liter flasks in series should be used. The bed type generation should utilize two or more 350 ml fritted bottles (60 mm frit diameter.)

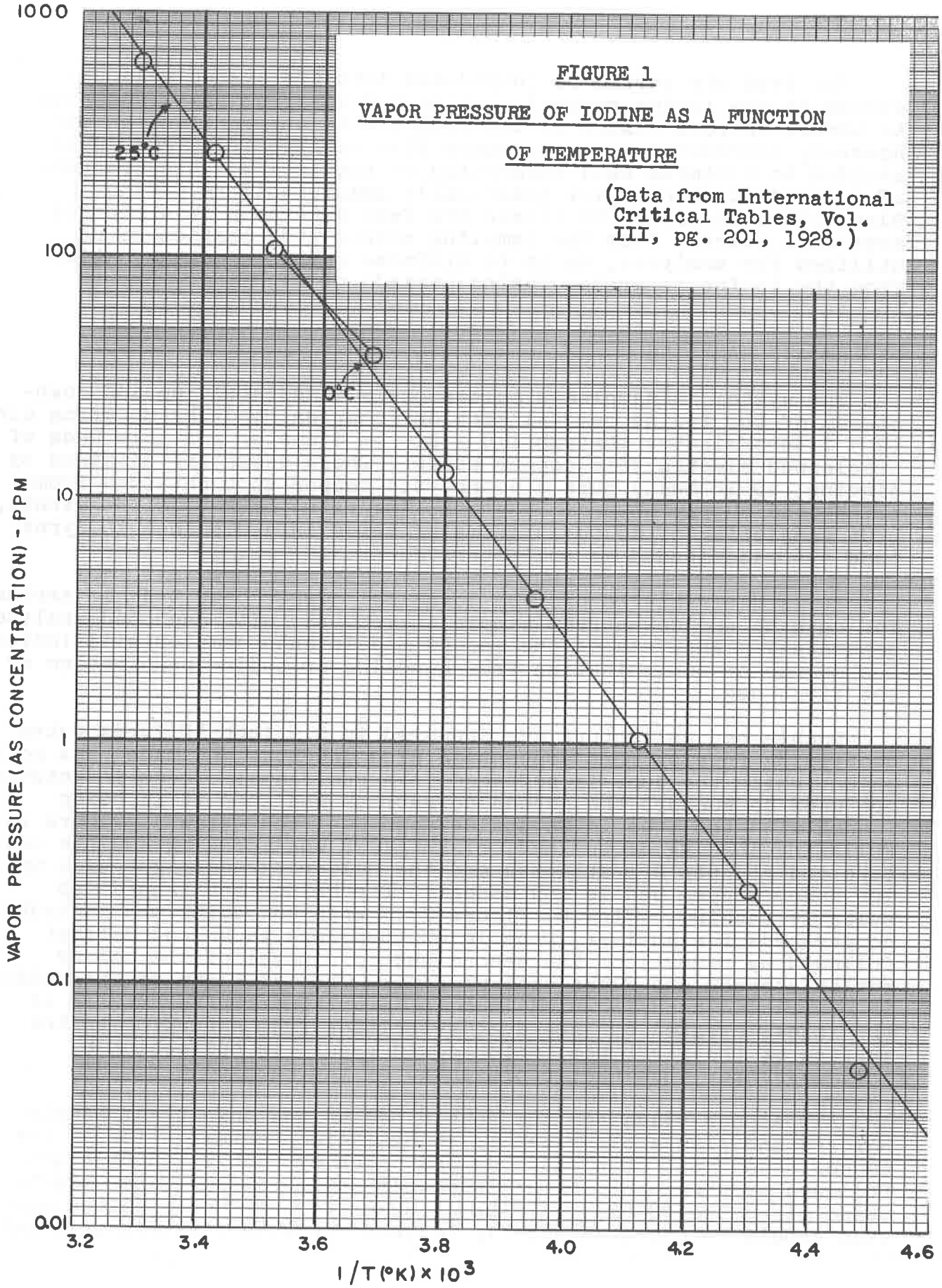

FIGURE 1

VAPOR PRESSURE OF IODINE AS A FUNCTION OF TEMPERATURE

(Data from International Critical Tables, Vol. III, pg. 201, 1928.)

The feed air should be introduced into the system well upstream of the iodine removal section and upstream sample station to assure uniform mixing of the iodine with the ventilation air. However, introduction at excessive distances upstream should be avoided to minimize wall absorption of the iodine. The presence of a few duct elbows will practically assure uniform mixing. Also, it is desirable to locate the feed generator in a room or area well removed from the sampling points and location to be utilized for analyses, so as to minimize possible contamination from the iodine generator during periods of handling.

SYSTEM AIR SAMPLING

The system is sampled simultaneously immediately up and downstream of the iodine removal section (charcoal bed) by metering air (2-5 liters/minute) through 1.0 - 2.0 mm diameter particle beds of precleaned electrolytic copper beads. These beads are obtained by sieving (10-18 mesh) pure electrolytic copper shot obtained from scientific supply houses. For sampling rates of 2-5 liters/minute, beds consisting of 15 to 20 grams of beads in a 0.5 inch ID Pyrex tube are recommended as collectors.

It is desirable to use two identical copper bead beds in series for both up and downstream sample collectors, with each bed analyzed separately. Analysis of the second bed in each sampler will indicate the degree of contamination from handling or iodine penetration of the first bed.

Double bed collectors are prepared in 0.5 inch ID Pyrex tubes containing four or more concentric side indentations made by a pointed object while the tube is softened in a gas flame. These indentations are used to support the second downstream bed when it is being loaded with the tube in an upside down position (View A, Figure 2). Following loading of the bed, clean glass wool packing and the outlet tube and stopper are attached and the holder turned right side up. The upper copper bed is now added to the holder and tapped for suitable packing, (View B, Figure 2). When unloading the separate copper beds for analyses, the inlet (top) bed is unloaded first followed by removal of the second bed by removal of the holder outlet stopper and glass wool packing. The inlet end of the holder is restricted to 2/16 - 1/4 inch ID to prevent air turbulence at the inlet, created by high duct velocities from extending to the surface of the first bed, which could result in collection of iodine greater than that represented by the sampled air.

All copper beads for the double bed up and downstream sample holders and also a blank bed to check iodine contamination in the copper beads must be cleaned as one batch by washing in 6N NH_4OH followed by thorough rinsing in double demineralized water (Barnstead mixed Bed #8902). Old beads suspected of iodine contamination should be digested briefly (etched) in dilute nitric acid and

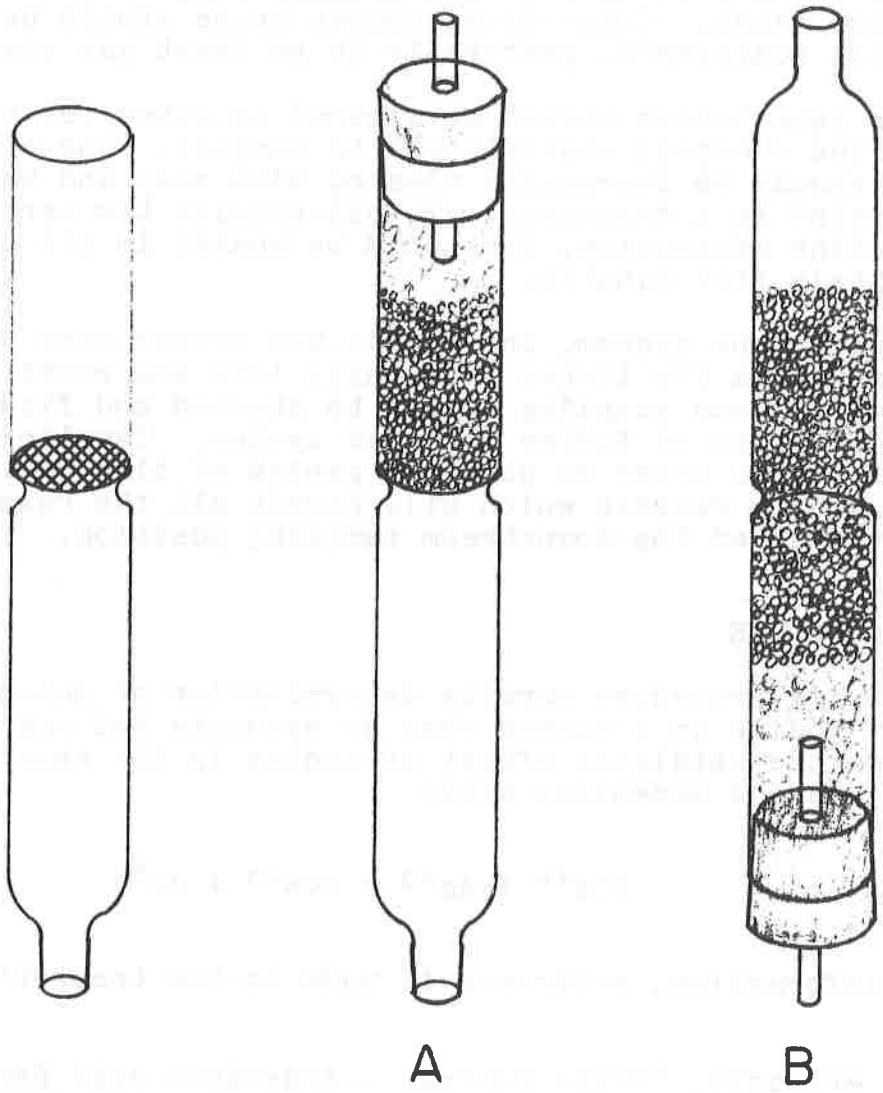

FIGURE 2. COPPER BEAD IODINE SAMPLER (TO SCALE)

rinsed prior to final washing with 6N NH_4OH. Following draining of the final water rinse, the beads should be dried immediately by washing a few times with acetone and passing dry, charcoal cleaned air through the beads. Clean dried copper beads should be stored in closed glass containers, preferably in an inert gas atmosphere.

The Pyrex tube holder should be cleaned as noted for all glassware used in the chemical analysis of the samples. The stainless steel screen should be thoroughly cleaned with soap and water, rinsed, and dried in a desicator. To pre-oxidize the screen for negligible iodine adsorption, it should be heated in air to 600°C for approximately five minutes.

When sampling the system, the double bed copper bead collectors should be inserted a few inches vertically into the ventilation duct or wall. Simultaneous sampling should be started and flows adjusted prior to the addition of iodine into the system. Sampling flows should be terminated after an adequate period of time following cessation of iodine release which will permit all the released iodine to have passed the downstream sampling position.

ANALYTICAL PROCEDURE

The following procedure permits determination of sub-microgram quantities of iodine in a manner that is accurate and reproducible. It is based on the catalytic effect of iodine in the reaction between ceric ions and arsenious acid:

$$2Ce^{+4} + As^{+3} = 2Ce^{+3} + As^{+5}$$

For further information, reference is made to the theoretical treatment below:

Lein and Schwartz, "Ceric Sulfate - Arsenious Acid Reaction in Microdetermination of Iodine", Anal. Chem., 23: 1507-10, 1951.

A. Discussion

This analysis is based on measurement of the ratio of the change in per cent transmission of residual ceric ions (ΔT) to reaction time (Δt) which is proportional to the iodine content of the sample. Since the Klett-Summerson Photoelectric Colorimeter is utilized in this analysis, Table 1 is a conversion table for Klett Readings to % transmission. It must be noted that the linearity of this relationship holds true for transmission readings between 20% and 65% (Klett Readings from 350 to 93). Therefore, readings below or above these limits must be discarded.

TABLE 1

CONVERSION OF KLETT READINGS TO PER CENT TRANSMISSION

Klett	%T	Klett	%T	Klett	%T	Klett	%T	Klett	%T	Klett	%T
50	79.4	100	63.1	150	50.1	200	39.8	250	31.6	300	25.1
51	79.1	101	62.8	151	49.9	201	39.6	251	31.5	301	25.0
52	78.7	102	62.5	152	49.7	202	39.4	252	31.3	302	24.9
53	78.3	103	62.2	153	49.4	203	39.3	253	31.2	303	24.8
54	78.0	104	61.9	154	49.2	204	39.1	254	31.0	304	24.7
55	77.6	105	61.7	155	49.0	205	38.9	255	30.9	305	24.6
56	77.3	106	61.4	156	48.7	206	38.7	256	30.8	306	24.4
57	76.9	107	61.1	157	48.5	207	38.6	257	30.6	307	24.3
58	76.6	108	60.8	158	48.3	208	38.4	258	30.5	308	24.2
59	76.2	109	60.5	159	48.1	209	38.2	259	30.3	309	24.1
60	75.7	110	60.3	160	47.9	210	38.0	260	30.2	310	24.0
61	75.5	111	60.0	161	47.6	211	37.8	261	30.1	311	23.9
62	75.2	112	59.7	162	47.4	212	37.7	262	29.9	312	23.8
63	74.8	113	59.4	163	47.2	213	37.5	263	29.8	313	23.7
64	74.5	114	59.2	164	47.0	214	37.3	264	29.6	314	23.6
65	74.1	115	58.9	165	46.8	215	37.2	265	29.5	315	23.4
66	73.8	116	58.6	166	46.6	216	37.0	266	29.4	316	23.3
67	73.4	117	58.3	167	46.3	217	36.8	267	29.2	317	23.2
68	73.1	118	58.1	168	46.1	218	36.6	268	29.1	318	23.1
69	72.9	119	57.8	169	45.9	219	36.5	269	29.0	319	23.0
70	72.4	120	57.5	170	45.7	220	36.3	270	28.8	320	22.9
71	72.1	121	57.3	171	45.5	221	36.1	271	28.7	321	22.8
72	71.8	122	57.0	172	45.3	222	36.0	272	28.6	322	22.7
73	71.4	123	56.8	173	45.1	223	35.8	273	28.4	323	22.6
74	71.1	124	56.5	174	44.9	224	35.6	274	28.3	324	22.5
75	70.8	125	56.2	175	44.7	225	35.5	275	28.2	325	22.4
76	70.5	126	56.0	176	44.5	226	35.3	276	28.0	326	22.3
77	70.2	127	55.7	177	44.3	227	35.2	277	27.9	327	22.2
78	69.8	128	55.5	178	44.1	228	35.0	278	27.8	328	22.1
79	69.5	129	55.2	179	43.8	229	34.8	279	27.7	329	22.0
80	69.2	130	55.0	180	43.6	230	34.7	280	27.5	330	21.9
81	68.9	131	54.7	181	43.4	231	34.5	281	27.4	331	21.8
82	68.6	132	54.4	182	43.2	232	34.4	282	27.3	332	21.7
83	68.2	133	54.2	183	43.0	233	34.2	283	27.2	333	21.6
84	67.9	134	54.0	184	42.8	234	34.0	284	27.0	334	21.5
85	67.6	135	53.7	185	42.7	235	33.9	285	26.9	335	21.4
86	67.3	136	53.5	186	42.5	236	33.7	286	26.8	336	21.3
87	67.0	137	53.2	187	42.3	237	33.6	287	26.7	337	21.2
88	66.7	138	53.0	188	42.1	238	33.4	288	26.6	338	21.1
89	66.4	139	52.7	189	41.9	239	33.3	289	26.4	339	21.0
90	66.1	140	52.5	190	41.7	240	33.1	290	26.3	340	20.9
91	65.8	141	52.2	191	41.5	241	33.0	291	26.2	341	20.8
92	65.5	142	52.0	192	41.3	242	32.8	292	26.1	342	20.7
93	65.2	143	51.8	193	41.1	243	32.7	293	25.9	343	20.6
94	64.9	144	51.5	194	40.9	244	32.5	294	25.8	344	20.5
95	64.6	145	51.3	195	40.7	245	32.4	295	25.7	345	20.4
96	64.3	146	51.0	196	40.6	246	32.2	296	25.6	346	20.3
97	64.0	147	50.8	197	40.4	247	32.1	297	25.5	347	20.2
98	63.7	148	50.6	198	40.2	248	31.9	298	25.4	348	20.1
99	63.4	149	50.4	199	40.0	249	31.8	299	25.2	349	20.0
										350	20.0

The analytical procedure has been adapted to the determination of iodine collected on copper beads. The procedure is accurate for iodide concentrations from about 0.002 to 0.004 µg up to 0.12 µg (assuming a 5 ml test sample.)

B. Apparatus

This procedure has been developed using the Klett-Summerson Photoelectric Colorimeter with a number 40 filter (400 mµ) and with approximately thirty curvettes (Klett Standard, 15 x 150 mm., graduated at 5 and 10 ml.

Also required are a constant temperature water bath set for 20°C. and a stopwatch.

C. Preparation of Reagents.

All reagents are prepared with single distilled, double demineralized water which will be referred to simply as water throughout this procedure. Tap water and distilled water will be referred to as such when appropriate.

7N H_2SO_4: To a two liter volumetric flask containing about one liter of water, slowly add 389 ml of concentrated H_2SO_4 (DuPont - 98%) and dilute with water to the mark at water bath temperatures.

0.2N Arsenious Acid ($HAsO_2$): This reagent may be prepared in two ways: (1) in a clean 400 ml beaker, dissolve 19.8 grams of As_2O_3 (Fisher cert. A. C. S.) in 120 ml of hot 1N NaOH (Fisher cert. A.C.S. - 40.0 gm. of NaOH per liter of solution). Dilute with water to about 250 ml, acidify with 3.6N H_2SO_4 (100 ml of concentrated 98% acid per liter of solution) until just acid to litmus paper, and dilute with water to two liters in a volumetric flask. (2) Add 25.98 grams of sodium Meta arsenite ($NaAsO_2$) to a 2 liter volumetric flask and dilute to the mark with water. The first technique has demonstrated minimum iodide contamination and is the one recommended.

3N NH_4Cl: This reagent is prepared by adding one liter of 6N HCl to one liter of 6N NH_4OH. This particular method of supplying the required chloride ions for analysis was chosen since the method for removing the collected iodine from the copper beads utilizes the latter two reagents. The 6N HCl is prepared by adding 1032 ml of 36% HCl to about 500 ml of water and diluting to two liters in a volumetric flask. The 6N NH_4OH is prepared by adding 800 ml of 30% NH_4OH to about 1000 ml of water and diluting to 2 liters in a volumetric flask. Both the NH_4OH and the HCl must be standardized. The suggested method of standardization of the HCl is by titration against pure sodium carbonate utilizing methyl orange as the indicator.

The sodium carbonate is prepared by heating sodium bicarbonate in an oven 290-300°C overnight. The NH_4OH is then standardized against the standard 6N HCl.

0.01 $(NH_4)_2Ce(NO_3)_6$ in 3.6 N H_2SO_4: Using a weighing bottle, weigh by difference exactly 10.965 gm. of ceric ammonium nitrate (G. Frederick Smith Co. - dried at 110°C for two hours) into a two liter volumetric flask, dissolve in 3.6N H_2SO_4 and dilute with the same solvent to the mark at the water bath temperature. The resulting solution should be exactly 0.01N in ceric ion; if desired, however, this may be checked by the following titration:*

Weigh by difference exactly 0.021 to 0.023 gm. of primary standard sodium oxalate (Fisher cert. A.C.S.-Sorensen) into a 250 ml erlenmeyer flask, add 15 ml of concentrated HCl, 5 ml of 0.005M ICl (0.813 gm of ICl per liter of solution), and dilute with distilled water to 100 ml. Heat the solution to 50°C using a thermometer as a stirring rod. Add one drop of 0.025M ferroin indicator and titrate with the ceric ammonium nitrate solution, maintaining the temperature between 50-60°C. The endpoint is very sharp and the color change is from pink to pale blue. A pale blue color should remain for one minute. Iodine monochloride can be obtained in pure form; ferroin indicator solution can be obtained commercially prepared as the 0.025M solution; both can also be prepared in the laboratory. A blank should also be run.

Calculations:

$$\text{Normality CeIV} = \frac{\text{wgt. sodium oxalate}}{\text{meq. wgt. sodium oxalate} \times \text{vol. } Ce^{+4}}$$

$$= \frac{\text{wgt. sodium oxalate}}{0.067 \times \text{vol. } Ce^{+4}}$$

Note: This standardization is not necessary if a standard curve is run each time new reagents are prepared.

Iodine Standard (10 mg/ml I^{-1}): Add 1.3071 gm of KI (Fisher cert. A.C.S.) to 100 ml volumetric flask and dilute to the mark with water. This solution is stable only for one week. To prepare 0.1 µg/ml standard, dilute the 10 mg/ml standard 1:100 and then 1:1000. This weaker standard is stable for a maximum of one day and should be freshly prepared before use.

* Willard, Furman, Bricker, Elements of Quantitative Analysis, Fourth edition, D. Van Nostrand Co. Inc., Princeton, N. J., 1966.

All iodine reagents should be kept clear of the analysis area in order to minimize the risk of contamination.

D. Procedure

1. Standard Curve

A Standard curve should be run before attempting an analysis of a series of analyses. This curve should include at least four points, at least one blank, and at least one organic blank. The suggested iodide standards are 0.02 µg, 0.05 µg. 0.07 µg, and 0. 10 µg, which are prepared from the 0.1 µg/ml I^{-1} standard using micropipettes.

The standards are preliminarily prepared as follows, in clean Klett tubes:

Reagent Blanks: Add 2.0 ml of $7\underline{N}$ H_2SO_4,
2.0 ml of $0.20\underline{N}$ $HAsO_3$,
1.6 mg of $3\underline{N}$ $N\overline{H}_4Cl$,
3.4 ml of water.
Mix and set in water bath at 20°C for 10 min.

Organic Blanks: Add 2.0 ml of $7\underline{N}$ H_2SO_4,
1.6 ml of $3\underline{N}$ $N\overline{H}_4Cl$,
5.4 ml of water
Mix and set in water bath at 20°C for 10 min.

Standard Samples: Add 2.0 ml of $7\underline{N}$ H_2SO_4,
2.0 ml of $0.20\underline{N}$ $HAsO_3$,
1.6 ml of $3\underline{N}$ $N\overline{H}_4Cl$,
x ml of standard KI solution,
(3.4 - x) ml of water.
Mix and set in water bath at 20°C for 10 min.

Standards are mixed with miniature stirring rods which are allowed to remain in the Klett tubes while cooling in the water bath.

At the prescribed intervals, one ml of $0.01\underline{N}$ Ce^{+4} is added to each Klett tube. The solutions are mixed once more and the stirring rods are removed. The time of completion of mixing is noted. A Klett reading of each standard, blank, and sample should be taken 5 minutes after the completion of mixing. Therefore, if 0.75 minutes are allowed for each Klett reading, a series of 6 samples may be run in succession. Of course, after reading the first series on the Klett, a second and a third series may be run, if necessary.

At a Δt of 30 minutes after the initial reading, the final Klett reading should be taken. Thirty minutes was found to be the optimumm time for reproducibility of the standard curve. To obtain the standard curve, the Klett readings should be converted to per cent transmission (%T) utilizing Table 1. The ΔT is then determined and divided by Δt.

The value ($\Delta T/\Delta t$) is then plotted against µg of I^{-1} on arithmetic paper. The standard curve appears in Figure 3. Experimental data for this curve appears as Table 2. The amount of Iodine in the blank is then determined graphically as shown in Figure 3.

(2) Iodine Analysis

The wash solution from the copper beads will have a volume of 25 ml and contains 24 meq. (milliequivalents) of Cl^{-1} (see Section E below). The maximum sample aliquot for this analysis is 5 ml. which contains the desired chloride concentration of 4.8 meq. Therfore, when 5 ml of sample are analyzed, no additional chloride need be added. However, when less than 5 ml of sample are analyzed, additional NH_4Cl must be added to provide the required 4.8 meq [(ml x 3N NH_4Cl) = 3(ml) meq Cl^{-1} : ml = 1/3(required meq)].

When analyzing iodine samples, at least one reagent blank and at least one organic blank for each sample must be run. It is also suggested that standards be run as a check on the standard curve. The latter are prepared as presented previously. Iodine samples are prepared in duplicate along with a sample organic blank for each sample.

Sample organic blanks are prepared as follows in clean Klett tubes:

Add 5 ml of sample,
2 ml of 7N H_2SO_4,
2 ml of water,
Mix and set in water bath at 20°C for 10 minutes.
Add 1 ml of Ce^{+4} . Mix and note time.

Iodine samples are prepared as follows in clean Klett tubes:

x ml of sample,
(5-x)(0.32) ml of 3N NH_4Cl,
2 ml of $HAsO_2$
2 ml of 7N H_2SO_4
Bring volume of sample up to 9 ml with water (i.e. add ml H_2) = (5-x ml 3N NH_4Cl or ml H_2O = 3.40-0.68x).
Mix and set in water bath at 20°C for ten minutes
Add 1 ml of Ce^{+4}
Mix and note time.

Samples are then analyzed on the Klett as before

(3) Determination of Iodine in the Bead Samples

The determination of Iodine in the bead samples is based on the standard curves, both corrected for the blank and the uncorrected curve. The $\Delta T/\Delta t$ for each of the samples is determined and the iodine

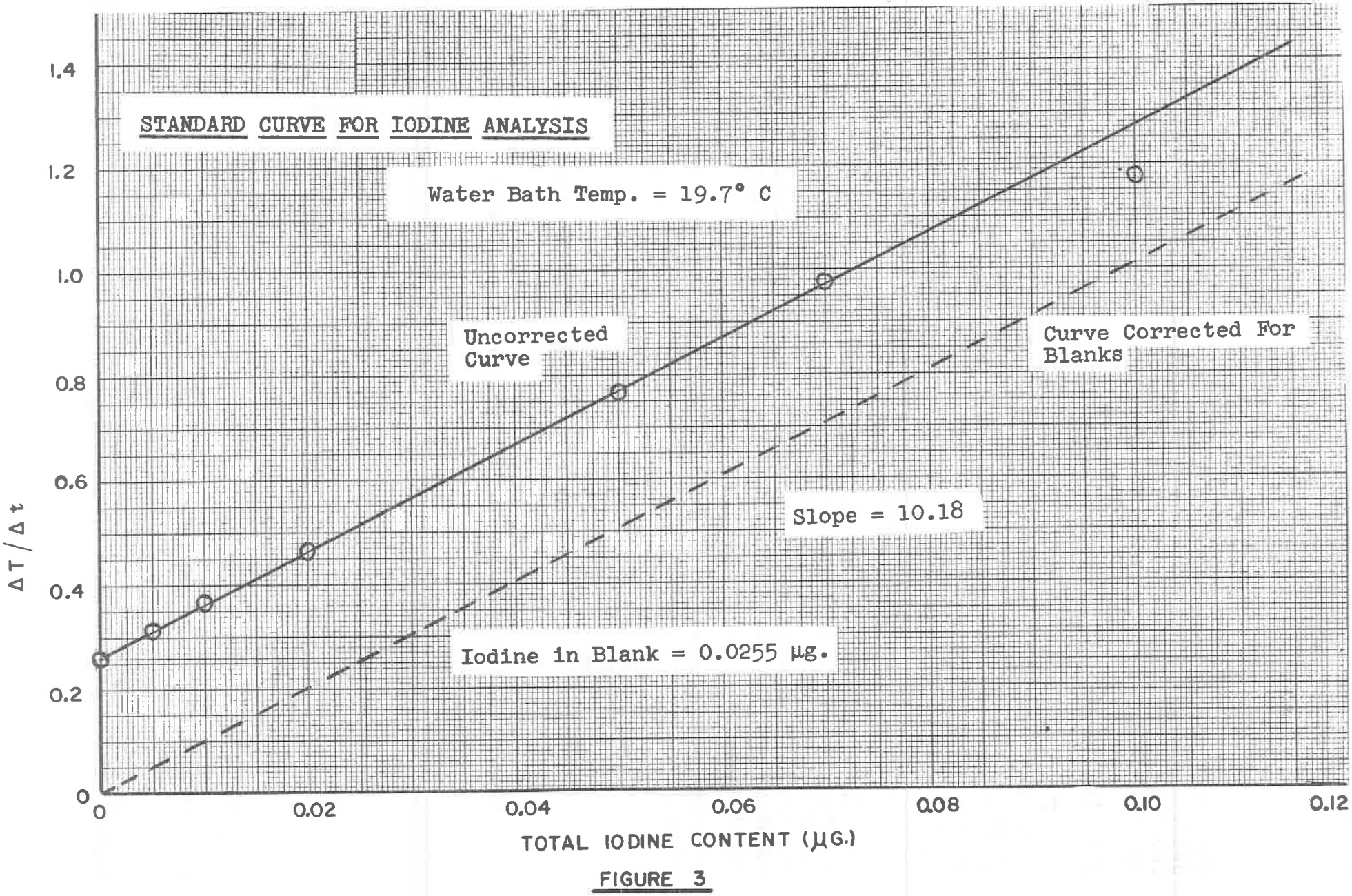
STANDARD CURVE FOR IODINE ANALYSIS
Water Bath Temp. = 19.7° C
Uncorrected Curve
Curve Corrected For Blanks
Slope = 10.18
Iodine in Blank = 0.0255 µg.
ΔT / Δt
TOTAL IODINE CONTENT (µG.)
0
0.2
0.4
0.6
0.8
1.0
1.2
1.4
0.02
0.04
0.06
0.08
0.10
0.12

FIGURE 3

TABLE 2

DATA FOR STANDARD CURVE DETERMINATION

SAMPLE	TIME CE IV ADDED	TIME OF READING	KLETT READING	%T	TIME OF READING	KLETT READING	%T	ΔT	$\Delta T / \Delta$ time
Org-Bl	0.00 min	5.00 min	337	21.2	35.00 min	337	21.2	0.0	0.0
Blank	0.75 "	5.75 "	325	22.4	35.75 "	260	30.2	7.8	0.260
0.005µg	1.50 "	6.50 "	322	22.7	36.50 "	247	32.1	9.4	0.313
0.01 µg	2.25 "	7.25 "	325	22.4	37.25 "	238	33.4	11.0	0.367
0.02 µg	3.00 "	8.00 "	315	23.4	38.00 "	214	37.3	13.9	0.464
0.05 µg	3.75 "	8.75 "	307	24.3	38.75 "	162	47.4	23.1	0.770
0.07 µg	10.00 "	15.00 "	299	25.2	45.00 "	132	54.4	29.2	0.973
0.10 µg	10.75 "	15.75 "	270	28.8	45.75 "	96	64.3	35.5	1.18

content is obtained from the corrected curve. The iodine content of the reagent blank from the corrected curve is then subtracted from this value which yields the iodine content of the sample. If there is a significant organic blank, its $\Delta T/\Delta t$ value is determined from the corrected standard curve, and the corresponding equivalent iodine content is found. This value is subtracted from the previous iodine content value and the result is the true iodine content of the sample. The iodine content of the entire wash solution is then calculated.

An analysis should also be performed on a known weight of beads from the same batch as those used in the analysis but which were not used to collect the iodine, in order to determine the background iodine content of the beads. This amount of iodine, corrected for bed weight should be deducted from the iodine determined in the sample to determine the correct amount of iodine collected by the copper bead bed. It should be noted that no background iodine is found in properly prepared electrolytic copper beads.

E. Removal of Iodide from Copper Beads.

Place the copper beads from each bed in a separate 25 ml beaker and add 4 ml of 6N NH_4OH (or equivalent, i.e., 24 meq NH_4OH) to dissolve the CuI_4. Swirl and transfer the wash solution to a clean 25 ml volumetric flask. Rinse the beads three times with 4 ml of water, swirling vigorously each time, and adding the washings to the volumetric flask. Then add 4 ml of 6N HCl (or equivalent, i.e., 24 meq HCl) to the beads; swirl and transfer the wash solution to the volumetric flask. At this time the blue color of the copper ammonium complex should disappear. Wash the beads with 4 ml of water transferring the wash solution to the flask. Then fill the flask to the mark with water. Five ml of this solution is then equivalent to the desired chloride concentration.

(1) Upstream Sample

Sampling at a rate of 2 liters of air per minute will result in a collection of 71 µg of I_2 in the upstream sample based on the iodine generation procedure described previously. (1 gm of I_2 released in one hour in a 100 cfm system.)

$$\frac{10^6 \times 2 \times 60}{1000 \times 28.3 \times 60} = 71 \text{ µg}$$

where 28.3 = liters/cu.ft.

In order to obtain an aliquot containing an iodide concentration suitable for analysis, 2 ml of the 25 ml total bead wash solution is diluted to 25 ml with water in a standard volumetric flask. A 1 ml aliquot of this latter solution is added to another 25 ml volumetric flask, 8 ml of 3N NH_4Cl (or its equivalent) solution is added and the solution made up to 25 ml with water. A 5 ml volume of this solution is analyzed according to the procedure. The amount of iodide in this latter sample is 0.0455 µg

$$71 \times \frac{2}{25} \times \frac{1}{25} \times \frac{5}{25} = 0.0455 \text{ µg}$$

(2) Downstream Sample

Assuming an iodine removal efficiency of 99.9% by the iodine removal unit, the downstream sample will have collected 0.071 µg of iodine for a sampling rate of 2 liters per minute, or 0.177 µg for a sampling rate of 5 liters per minute. A 5 ml aliquot of the 25 ml total bead wash solution will contain 0.0142 and 0.0355 µg of iodine, respectively. Air sampling rates of 2 liters per minute would permit determination of removal efficiencies ranging from >99.986 to 99.29% based on an analytical range of 0.002 to 0.1 µg of iodide per 5 ml aliquot. Similarily, a sampling rate of 5 liters per minute would result in a removal efficiency range of >99.9944 to 99.72%.

F. Notes

(1) All glassware (pipettes, Klett Tubes, Beakers, flasks, bottles, etc.,) should be cleaned with 30% fuming nitric acid (Mallinckrodt) and rinsed a minimum of six times with water, before each use.

(2) Clean, inverted 5 ml beakers should be kept on the Klett tubes at all times during a run in order to reduce the possibility of contamination from the ambient air.

(3) All reagent solutions, including the water, should be kept in the water bath to maintain a temperature of 20°C.

(4) Klett tubes are dried prior to use in an oven at 110°C for a minimum of 20 minutes. They are immersed in the water bath before the addition of the reagents, and removed from the bath only to mix the solutions and to take the Klett readings.

(5) Use pipettes adapted with automatic dispensing units to add reagents, touching only the tip of the pipette to the Klett tube about one fourth of an inch above the 10 ml mark. The iodine samples, added with lambda pipettes, may be added below the mark with little difficulty.

(6) Test solutions should be mixed with only properly cleaned small stirring rods.

(7) The Klett Colorimeter should be calibrated before each run. Set the scale at 54 for a 0.0001M Ce IV solution with the slit adjustment knob and at 330 for a 0.001M Ce IV solution with the zero adjustment knob. The solutions are prepared with 2 ml of 7N H_2SO_4, the appropriate amount of 0.01N CeIV and brought up to 10 ml with water. Several adjustments are usually necessary before the instrument is correctly calibrated. This procedure enables one to carry out the analysis in the most accurate region of the Klett.

(8) Once the iodide has been dissolved from the copper bead bed, the solution should be analyzed within a few hours (i.e., the same day) to minimize the adsorption of the iodide ion on glass surfaces. If the analysis cannot be completed within this period, the copper beads should not be washed for removal of iodine until adequate time is available to complete the analysis. The copper beds can be kept (sealed) for a matter of days without loss of iodine.

(9) Water baths at 20°C can be prepared by using a mix of cold and warm tap water. Once obtained at 20°C, the heat gained by the bath from ambient temperatures above 20°C is offset by the heat losses due to water evaporation and the bath usually remains at 20°C $\pm$ 1°C for the period required for analysis.

DISCUSSION

HILLARY: Firstly, in a previous paper, you described the method for the analysis of low concentrations of methyl iodide. This might suggest a similar test procedure based on inactive methyl iodide? Secondly, how did you cross-check between the analytical method for methyl iodide (using say, caustic alkali breakdown) with the aqueous phase iodine method?

VILES: Let me answer your second question. Yes, we have used this technique for the analysis of methyl iodide. In some of our earlier work before we had completed a satisfactory calibration of the chromatograph, we had to do something to get the show on the road, so to speak, and not wait for the chromatographic studies, so we developed this method for the determination of methyl iodide in air.

What we did was adopt the method of chlorinated hydrocarbon analysis, which dates back to 1937, I believe, and apply this procedure to catalytically combust and decompose methyl iodide into elemental iodine and hydrogen iodide. The gases were absorbed in sodium carbonate solution which was then analyzed for total iodine by the ceric sulfate method. The only disadvantage of this technique is the time required to flush a sample through combustion units, drain out the solution, wash out the absorbing column beads, and set up the solution for analysis.

Now, the first question?

HILLARY: Using the methyl iodide method developed for low mass concentrations, does this suggest you can use methyl iodide inactively?

VILES: Yes.

HILLARY: As an in-situ test?

VILES: Yes, for example, you may be concerned about methyl iodide penetration in an in-place test. If you want to perform such a test, there is no reason why you couldn't generate methyl iodide concentrations as presented and analyze by the method just described.

IN PLACE TESTING FOR IODINE REMOVAL EFFICIENCY USING AN ELECTRONIC DETECTOR

W. G. Thomson - Todd Shipyards Co.
R. E. Grossman - USAEC

ABSTRACT

Technical specifications of the N. S. Savannah require quarterly qualifications of the air cleaning systems for ability to remove iodine. Such required periodic testing can be accomplished at low cost using an electronic detector-recorder that is sensitive to elemental iodine vapor concentrations of one part in a billion parts of air. This test method has proven satisfactory in maritime service aboard the N. S. Savannah although a careful laboratory type operating technique is required. The combination of equipment and operating technique has qualified the air cleaning system with good correlation to move expensive, tedious, and time consuming tests using radioiodine 131.

Conclusion and Recommendations

The testing of air cleaning systems at nuclear facilities for ability to remove radioactive iodine has required use of either Iodine 131 and on-site gamma counting or stable iodine very carefully sampled and quantified using thermal neutron activation analysis. When performed at Galveston, Texas, using materials from and equipment at the Oak Ridge National Laboratory these techniques cost $3000 and $2000 respectively for each test. While these costs are high but not prohibitive, the tests themselves are impractical for a nuclear power merchant ship seeking admission to both domestic and foreign ports.

The electronic detector-recorder cost $2400 for the set with insignificant operating costs. Presently available data indicate the tests to be accurate within $\pm$ 0.025% with iodine vapor concentrations of one part per billion parts of air. This allows qualification of the air cleaning systems with a good degree of accuracy. Testing the duplicate systems aboard the N. S. Savannah takes about 6 hours.

Test Requirements of N. S. Savannah Air Cleaning System

Technical specifications of the N. S. Savannah (1) require that the reactor space ventilation charcoal adsorbers be tested quarterly for assurance that they have factors of at least 1000 for the removal of iodine from the ventilation stream. However, it is impossible to obtain a representative sample of air across the charcoal alone. Therefore, the iodine vapor injection point upstream of the adsorber and the sampling point downstream of the adsorber encompass the entire removal system rather than just the charcoal, and all iodine removal efficiencies will relate to the total system.

Original Test Procedures

The reactor space ventilation system has been tested using either a radioactive or normal iodine with thermal neutron activation analysis techniques. (2)

The radioiodine method requires special preparations and precautions including handling short half life material which present difficulties in scheduling availability of Iodine 131 to meet a shipping schedule. Uncontrollable local port conditions such as weather or labor strife may force the ship to alternate routes with attendent risk of being in violation of technical specifications. In addition to the possibility of being unable to perform the test, each test costs about $3000.

The use of stable iodine injection and sampling followed by thermal neutron activation analysis, costing about $2000 per test, has not proven satisfactory. It has been almost impossible to obtain laboratory conditions of sampling equipment purity under shipboard conditions. Losses incurred during shipment to a source of thermal neutrons further reduce the use of the techniques. (3) Finally, the one to three week time lapse between time of test and obtaining the test results is not suitable for a nuclear power reactor with the potential for entering many centers of population.

Alternative Techniques Sought

The stated difficulties and costs associated with the established methods led to investigations of alternative techniques. Various sniffer tubes designed to give a visual measure of iodine concentration by color change were investigated but discarded for lack of sensitivity, lack of reproducibility, and lack of recordable proof of the iodine concentration detected.

Other techniques ranging from classical chemistry to gas chromatography were investigated but discarded because of personnel, equipment, or financial requirements in addition to questionable suitability in the maritime environment.

The most promising of the techniques investigated was that using an electronic detector-recorder designed as an oxidant detector by the Mast Development Company, Davenport, Iowa. (4)

Test Method Development

In the development program the smallest concentration of iodine which could be indicated was first determined. Test apparatus for this purpose was procured and installed in the RSVS system as shown in Figure 1. Air is passed over iodine crystals at ambient temperatures and the resulting mixture is injected into the 1000 CFM air stream at a location upstream from the fan. The Mast instrument samples the ventilation stream downstream of the fan. Numerous runs using this apparatus have established the smallest iodine concentration discernible by the Mast instrument to be about one volume of iodine vapor per billion volumes of air (1 vppb).

This lowest determinable concentration sets the requirements of the rest of the system. The iodine concentration downstream of the charcoal adsorbers must still be above the threshold sensitivity (1 vppb) of the Mast instrument. Therefore, the iodine vapor concentration upstream of the charcoal adsorbers must be at least 1000 times the threshold concentration, since the iodine vapor concentration must be reduced a thousandfold in passing through the charcoal adsorbers (i. e. iodine removal efficiency of at least 99. 9%). Use of an upstream concentration of 10, 000 rather than 1000 times the threshold sensitivity results in greater test accuracy. This (10, 000) upstream vapor concentration requires one gram of iodine vapor per 335 cubic feet of air or, since the iodine is to be added to a 1000 CFM air stream, the addition of about three grams of iodine per minute.

Ultimate Sensitivity of Test

Initial work on this equipment indicated that while it had the potential for determining removal factors it more likely would be useful for frequent routine testing of system integrity; an awareness of filter penetrations or gasket failure. (5)

Later work showed that oxidant detection of one vapor part per billion is obtainable. This includes instrument sensitivity to other oxidants normally found in air such as nitrogen oxides and ozone. Methyl iodide, considered typical of the organic forms of iodine, has no affect upon the detection sensitivity of the instrument or technique. (6) (7)

Equipment Arrangement

The overall location of the test equipment and the ventilation system with respect to the reactor compartment is shown in Figure 2. It is to be noted that

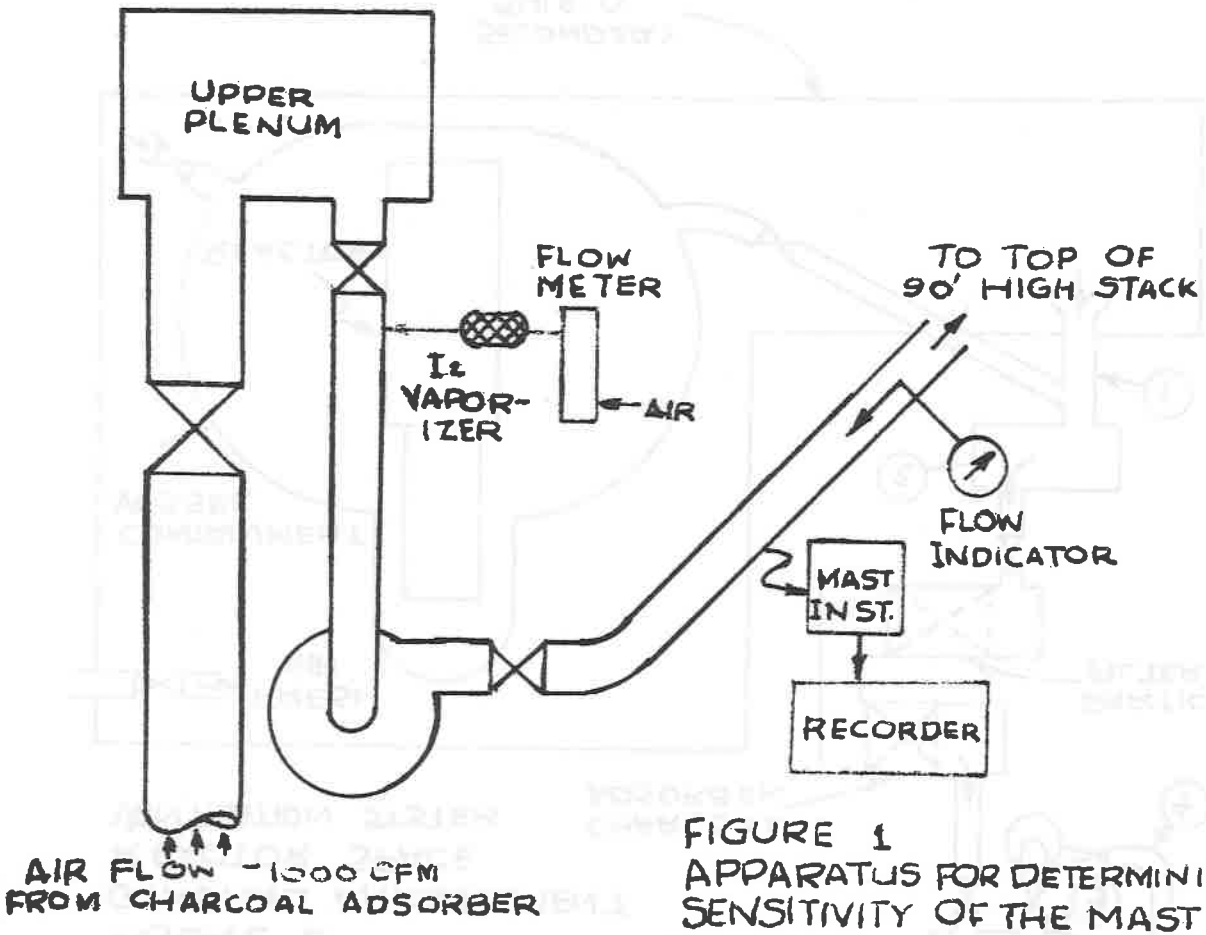

FIGURE 1
APPARATUS FOR DETERMINING SENSITIVITY OF THE MAST INST. TO IODINE VAPOR

FIGURE 2.
GENERAL ARRANGEMENT
REACTOR SPACE
VENTILATION SYSTEM

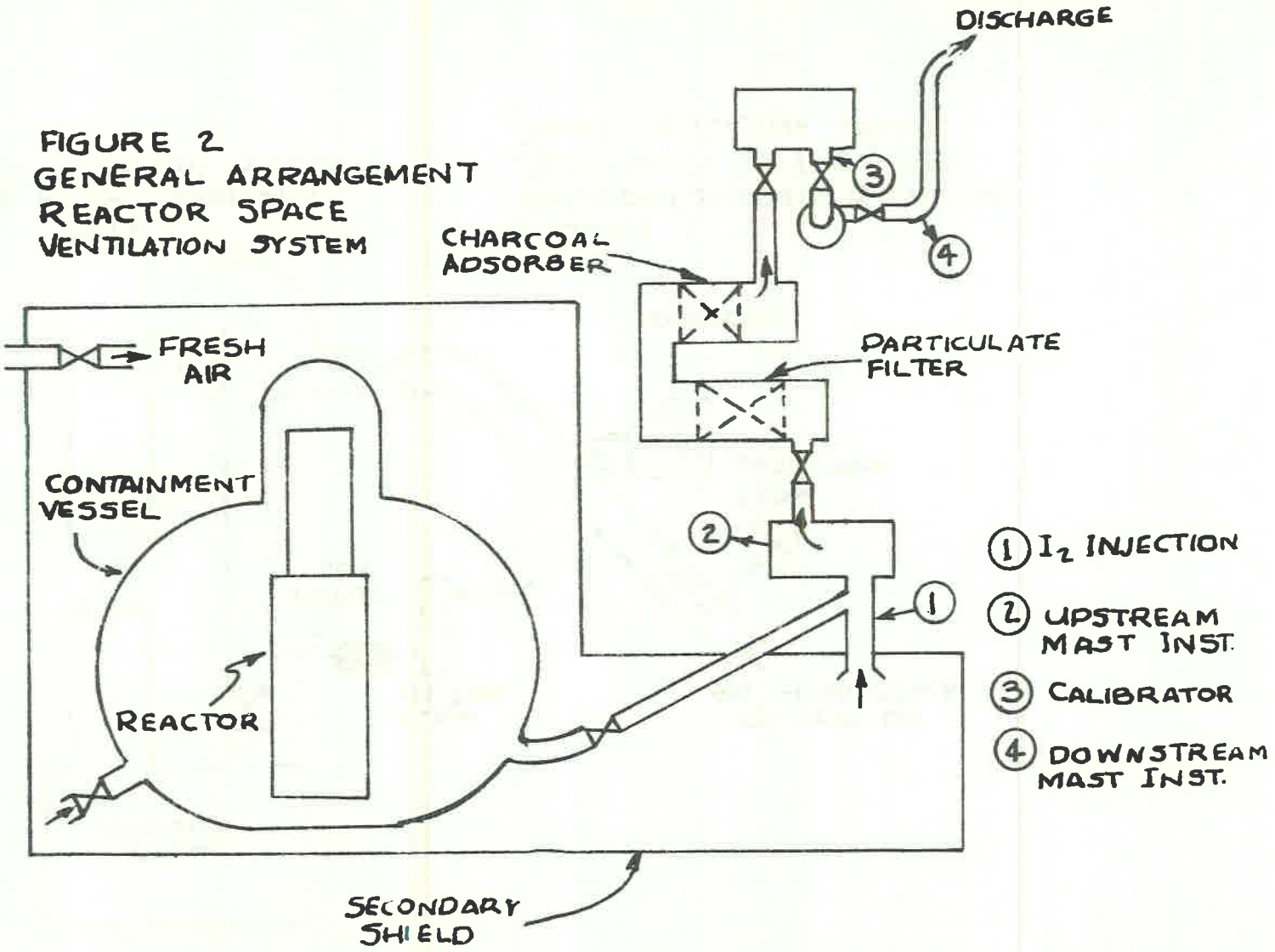

the reactor compartment is kept at a slight negative pressure with respect to both the containment vessel and the surrounding shipboard areas. This insures that any air leakage will be into the reactor compartment and exhausted through the air cleaning system.

The equipment arrangement consists essentially of four items. First is an apparatus for vaporizing and injecting 3 grams of iodine vapor per minute into the ventilation system. Second is a Mast instrument to monitor the upstream concentrations of iodine vapor. Third is an apparatus for the addition of a very small quantity of iodine vapor to the downstream ventilation stream to be used for checking and calibrating the downstream Mast instrument, item number four. This arrangement was chosen primarily on the basis of simplicity and ease of installation.

Location of the test apparatus on the ventilation system is as shown in Figure 3.

The injector is mounted on the ductwork a short distance above the air intake. The upstream Mast instrument samples the lower plenum.

The use of a single instrument for detection of iodine vapor samples both upstream and downstream of the RCVS was considered impractical. The time lag for switching and purging sample lines, the risk of accidental cross-contamination, and the probability of plate-out and desorbtion from long sample lines made the use of a detailed calibration system for two separate instruments preferable.

The sample point is far enough (10 duct diameters) from the injection point to insure good mixing of the iodine vapor and air. The calibration injector is mounted on the ductwork between the upper plenum and the fan. The air and iodine vapors are thoroughly mixed in passing through the fan. This permits taking a sample for the downstream Mast instrument a short distance from the fan.

Operation

Figure 4 is a view of the calibrator assembly. The flow meter has a range of 5 to 600 cc/minute. Air passes from the flow meter via the flexible plastic tubing to the flow regulating needle valve. From this control the air is filtered through the glass wool and sintered glass plate to the iodine crystal bed. Here it becomes saturated with iodine vapor. The mixture of air and iodine vapors passes through the forward sintered glass plate and on into the ventilation stream.

The static pressure inside the ductwork is about 6 inches below atmospheric pressure. This slight vacuum provides the force required for pulling the air through the apparatus.

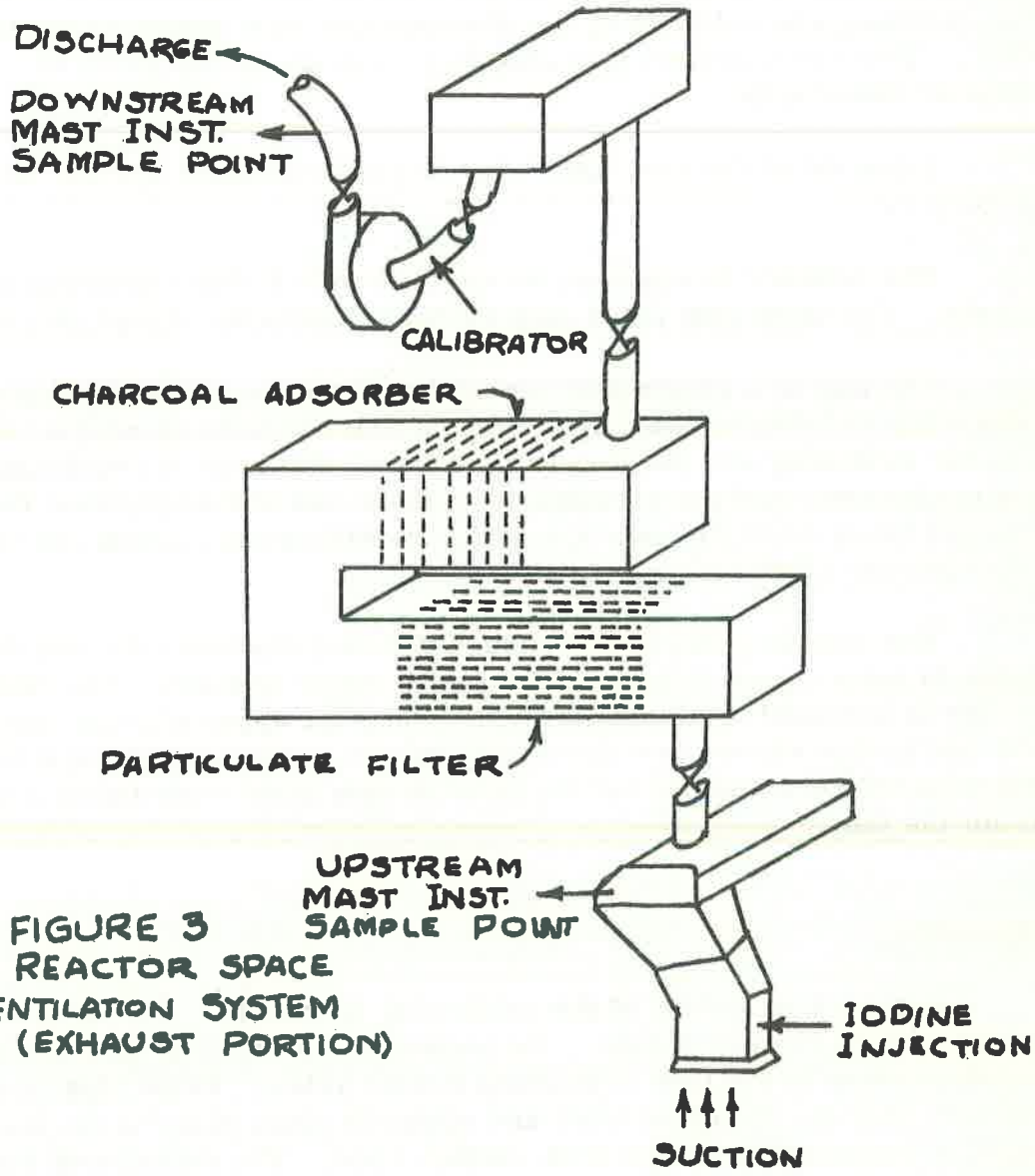

FIGURE 3
REACTOR SPACE VENTILATION SYSTEM (EXHAUST PORTION)

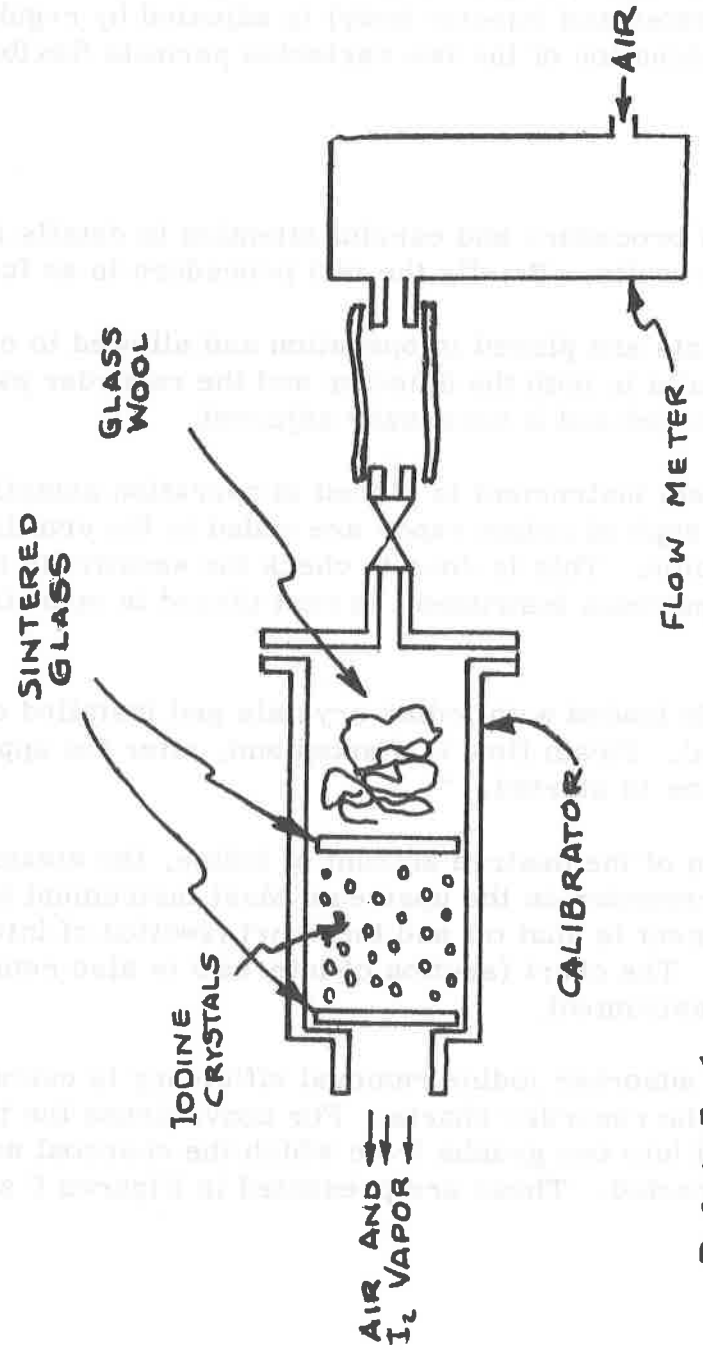

FIGURE 4
CALIBRATOR ASSEMBLY

The injector is shown in Figure 5. This device is similar in operation to the calibration injector, the principle difference being a much higher rate of iodine injection. This apparatus is steam jacketed. The combination of the higher temperature from the steam jacketing (higher iodine vapor pressure), and a larger air flow, results in a greatly increased vaporization rate. Air for the injector is supplied from the ship's air system. The mixture of air and iodine vapor is injected into the 1000 CFM air stream.

The air flow is adjusted by means of the regulating valve; the temperature of the system (preheater and injector body) is adjusted by regulation of the steam pressure. The combination of the two variables permits flexibility of operation.

Test Procedure

A definite test procedure and careful attention to details is required to achieve significant results. Briefly the test procedure is as follows:

Both Mast instruments are placed in operation and allowed to come to equilibrium, The electronic circuits in both the detector and the recorder parts of the Mast instruments are checked and if necessary adjusted.

The downstream instrument is placed in operation sampling ventilation system air. A few vppb of iodine vapor are added to the ventilation system via the calibration injector. This is done to check the sensitivity of the downstream instrument. The upstream instrument is next placed in operation sampling the lower plenum.

The injector is loaded with iodine crystals and installed on the ductwork at the "D" deck level. Steam flow is started and, after the apparatus is at temperature, air flow is started.

After injection of the desired amount of iodine, the steam and air flows are stopped. The recorder on the upstream Mast instrument is allowed to peak and then the instrument is shut off and the chart (section of interest) is removed from the recorder. The chart (section of interest) is also removed from the downstream Mast instrument.

The charcoal adsorber iodine removal efficiency is calculated from the operations log and the recorder charts. For convenience the test parameters have been combined into two graphs from which the charcoal adsorber efficiency can be directly extracted. These are presented in Figures 6 and 7.

Test Results

Several of the tests in the early development period resulted in no data or else data known to be in error. These runs are not tabulated in this report. Data presented in the last half of Table I are from consecutive runs.

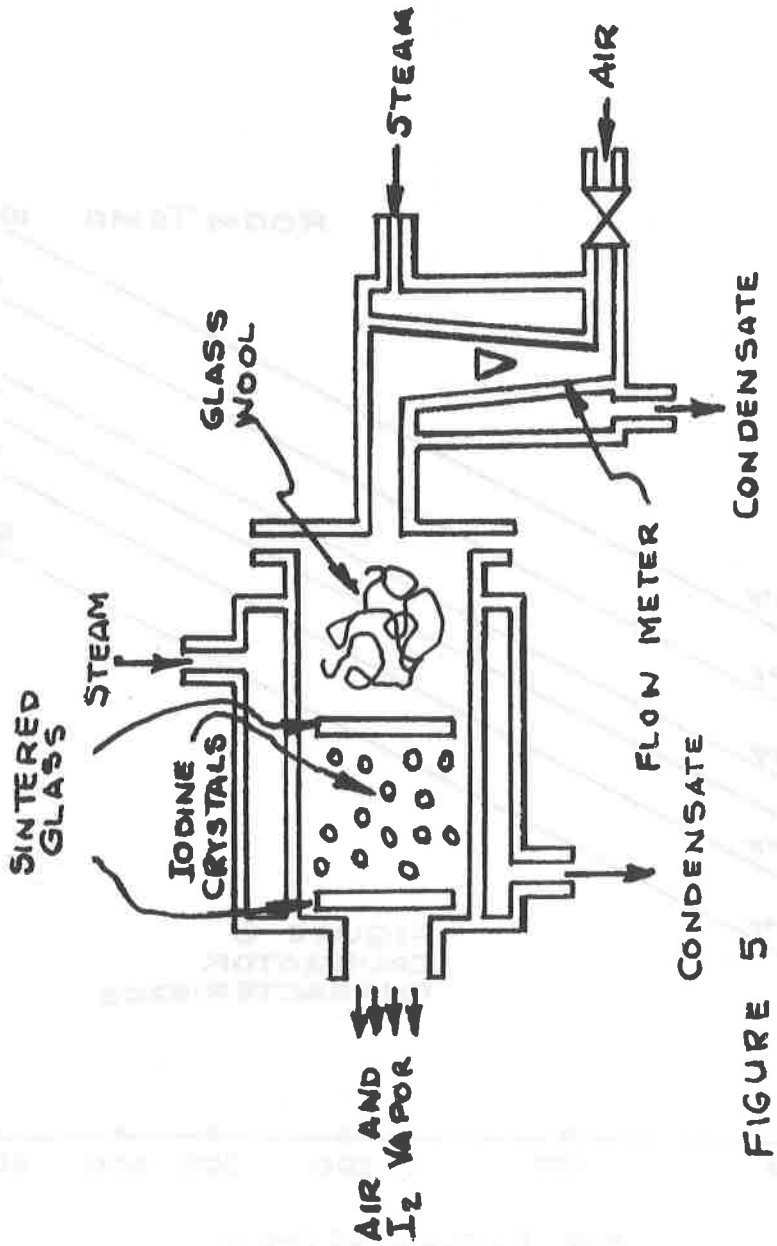

FIGURE 5
INJECTOR
ASSEMBLY

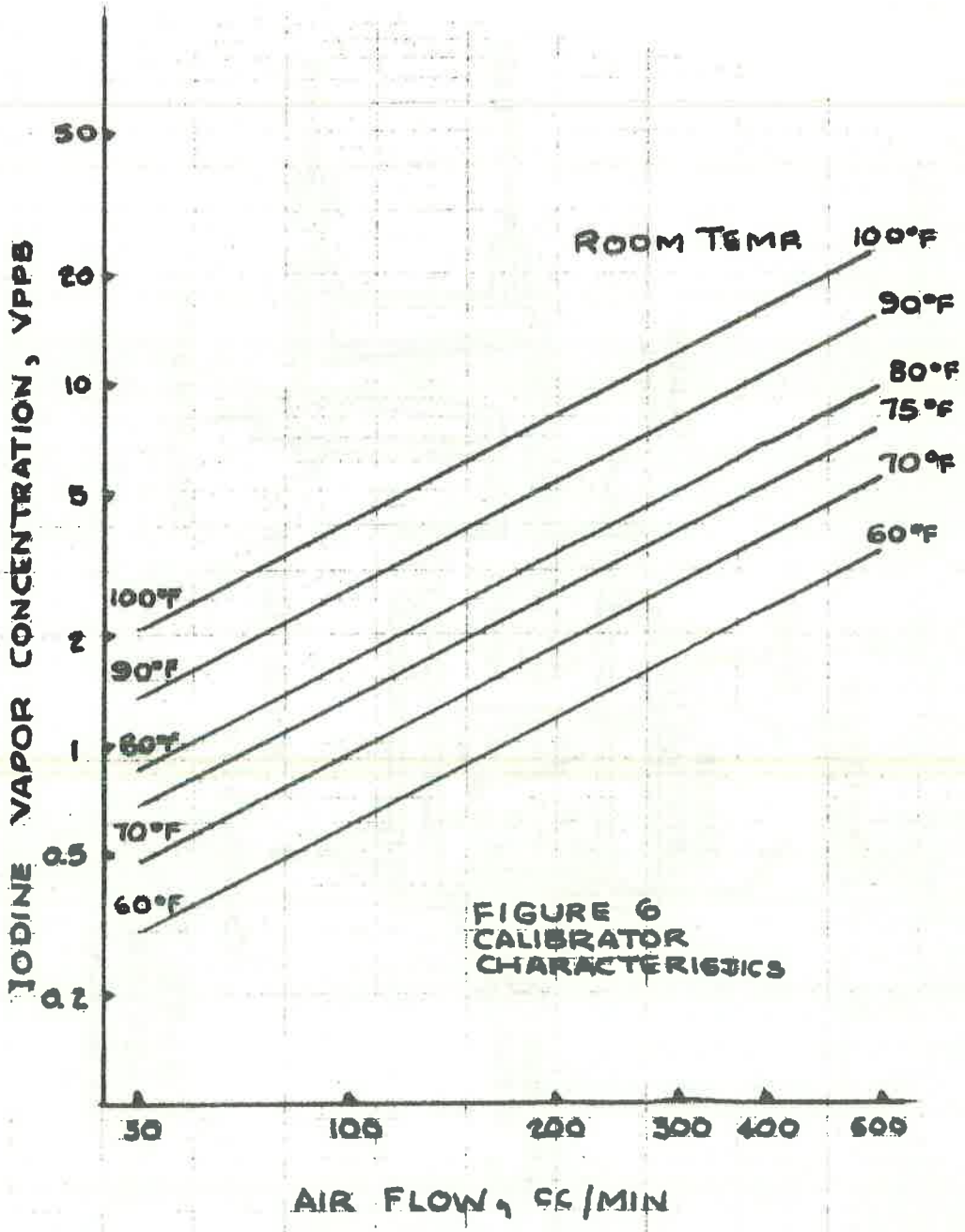

FIGURE 6
CALIBRATOR
CHARACTERISTICS

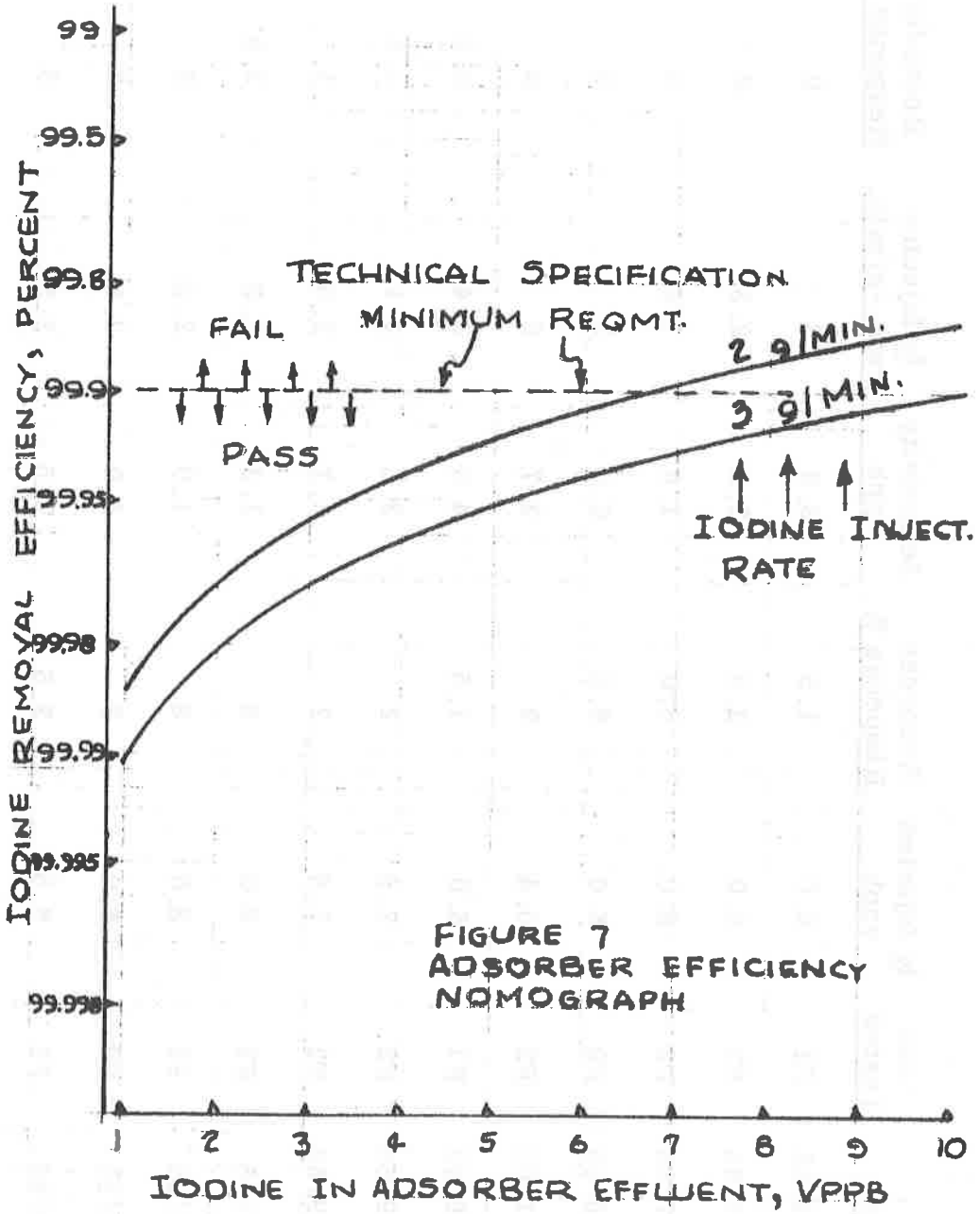

FIGURE 7
ADSORBER EFFICIENCY
NOMOGRAPH

TABLE I

CHARCOAL ADSORBER TEST RESULTS

Date	Unit Tested	I_2 Injected vppb	Recorder Response %	Sensitivity vppb	I_2 Injector rate--g/min.	Recorder Response %	vppb I_2	I_2 Removal Efficiency %
6/11/65	F2	5.0	1.5	3.3	3	0	0	100-0.005
6/17/65	F2	8.0	3.5	2.3	2.3	2	4.6	99.94±0.014
6/17/65	F2	8.0	5.0	1.6	1.8	3	4.8	99.92±0
6/18/65	F2	6.0	6.5	0.9	3	5	4.6	99.955±0.005
6/21/65	F2	5.4	2	2.7	6	4	10.8	99.948±0.009
6/28/65	F1	6.0	1.5	4.0	2.4	1.5	6	99.925±0.025
6/29/65	F2	7.5	2	3.8	2.1	1.5	5.5	99.922±0.025
6/29/65	F2	7.5	2	3.7	2.5	1	3.7	99.956±0.021
7/1/65	F2	8.0	6	1.3	2.5	3.5	4.5	99.946±0.008
7/1/65	F2	8.0	8	1.0	2.5	2	2	99.976±0.006
7/2/65	F2	6.0	2	3.0	2.5	2	6	99.928±0.017
7/7/65	F2	6.5	2.5	2.5	2.5	3	7.8	99.907±0.013
7/7/65	F2	13.0	8	1.6	3	2	3.2	99.968±0.008

TABLE II

CHARCOAL ADSORBER TEST RESULTS

(RADIOIODINE 131)

DATE	UNIT	IODINE REMOVAL* EFFICIENCY, %
1/5/65	F1	99.997
1/6/65	F2	99.985
5/30/65	F1	99.984
5/31/65	F2	99.983
7/5/65	F1	99.934
7/5/65	F2	99.988

*Average of 4 individual values

The variation in efficiency on consecutive runs is believed to be largely due to varying amounts of ozone or nitrogen oxides in the ventilation stream. This material interferes with operation of the Mast instrument. The welding being performed in the containment vessel during the test period was probably the major contributor to the varying ozone or nitrogen oxide concentrations.

Sample Calculations

A typical set of sample calculations follows.

Iodine from Calibrator
- Temp. of Iodine crystals 90° F
- Air flow rate 500 cc/minute
- Iodine vapor concentration in vent stream, refer to figure 6 - 13 vapor parts per billion

Downstream Mast Instrument (see section of chart)
- Background 24%
- Background + I_2 from calibrator (13 vppb) = 32%
- 13 vppb = 32-24 = 8%
- Sensitivity of instrument = $\frac{13 \text{ vppb}}{8\%}$ = 1.6 vppb/%
- Background + 13 vppb + adsorber leakage = 34%
- Leakage = 34-32 = 2%
  = 2% x 1.6 vppb/% = 3.2 vppb
- Leakage considering reproducibility of Mast instrument
  = $3.2 \pm \frac{1.6}{2}$ = 2.4 to 4.0 vppb

Injection Rate $\cong$ 3 g/min (see section of chart)
- Refer to Figure 7
- air cleaning system efficiency (2.4 vppb) 99.976%
- air cleaning system efficiency (4.0 vppb) 99.960%

or

- air cleaning system efficiency ($3.2 \pm \frac{1.6 \text{ vppb}}{2}$ = 99.968 ± 0.008%)

(1) Technical specification of N. S. Savannah - STS-9

(2) R. E. Adams - W. E. Browning, Jr., Iodine Vapor Adsorbtion Studies for the N. S. Savannah Project, USAEC Report ORNL-3726 Oak Ridge National Laboratory, February 1965

(3) E. H. Dewell, Babcock & Wilcox Company, personal communication, 1964

(4) G. M. Mast & H. E. Saunders Research and Development of the Instrumentation of Ozone Sensing ISA transactions Volume I, No. 4, October 1962

(5) R. E. Grossman - W. G. Thomson N. S. Savannah Ventilation System Filter Testing USAEC TID-20426

(6) R. P. Denise, R. E. Grossman, W. G. Thomson, unpublished data, February 1964

(7) R. G. Kling, Mast Development Company, personal communication, 1965

DISCUSSION

FIRST: Mr. Belter, do you have any statements you wish to make at this time?

BELTER: Are there other comments anyone would wish to make at this time? Do you think we have covered fairly well the entire field of radioactive air pollution control?

Some of you may wish to give this some additional thought, and if you have any further ideas on this subject I would appreciate your writing them down and sending them to us in AEC, either to myself or Mr. Bernard, in the Division of Reactor Development and we will be very happy to consider any suggestions you may have which would increase the effectiveness of this type of conference.

FIRST: In some of the previous conferences we have had progress reports from various sites; we did not have them this year. I would be interested to know whether this is a topic which we ought to include in future air-cleaning conferences.

BELTER: That was one of the items I mentioned, thinking in terms of our normal operating experience at the various AEC sites. During the other eight conferences, we devoted a lot of time to this aspect.

Do any of you think that it is important to allow more time for presenting air cleaning operational experience at future meetings? (No response.) No one appears to have any strong feelings on this subject. Perhaps over the past 15 years that area has been pretty well covered.

FIRST: I was thinking more in the way of on-going research projects. We are not quite ready for a formal presentation in that the work is in progress. Partial results are available which people might be interested in hearing about while awaiting the final. This is the type of progress report I had in mind.

BELTER: Not just operational experience.

FIRST: Yes, just to make the meeting current on what's going on.

BELTER: Yes.

BURCHSTED: I would like to comment. As far as ORNL is concerned, we would be more interested in new experience more than we would be in a reporting of the past, especially those that have been covered in previous meetings.

BELTER: Some new or significant aspect of air-cleaning operations?

BURCHSTED: Current topics, but those that are new since the previous conference and that have not been previously reported.

BILLINGS: I wonder what the feelings would be from the people who use this or have to use this who come into the business, so to speak, in terms of taking a look at possibly a bibliographic cross-indexing for filters, iodine filters, radioactive plutonium and so forth. Is there any need for this?

BELTER: You mean by going over the entire Proceedings of the Conference?

BILLINGS: At this one time.

BELTER: Of previous conferences? Does anyone wish to comment on Dr. Billings' suggestion here? Is there a need for this sort of thing with our operating and research groups?

BURCHSTED: Doesn't all of this material wind up in Nuclear Science Abstracts sooner or later?

BILLINGS: Not if it has already been abstracted and could be indexed.

BELTER: It is abstracted in NSA and also in the different journals, such as the Nuclear Safety Journal and Nuclear News, as well as the regular TID distribution. The Nuclear Safety Information Center at Oak Ridge is indexing most of this material anyway.

BERNARD: That is just what I was going to mention so I will just add the fact that Oak Ridge is now in the process of summarizing their research in air cleaning that has gone on in the last several years and undoubtedly would include the applicable information from the past air-cleaning conferences.

BELTER: Another part of the Oak Ridge National Laboratories, dissemination of information on nuclear safety, and of course this is one of the more important aspects of it.

Are there any other comments?

MURROW: I would like to have those who can, send in questions on areas of interest, such as operating problems, research, or special problems, ahead of time, and set up work sessions in some smaller rooms. Questions would be put in and anyone who had any experience or suggestions would answer. Discussions of problems, partial solutions or good solutions to problems would be of interest to those attending. Even knowing who was working on specific problems would be useful for future reference and contacts.

BELTER: We have attempted to do that sort of thing in an informal way at the Harvard Air Cleaning Laboratory. Our group and Humphrey Gilbert

have attempted 6 to 9 months before holding a conference to obtain some kind of general views from people in the field, who are involved in research and in operations, on what should be included in the conference.

MURROW: I was thinking more of getting the people together to provide an opportunity for informal talks at the conference.

BELTER: At the conference itself?

MURROW: Yes. Instead of papers, perhaps a half-day could be programmed where a number of different general subjects could be discussed without any formal papers. Anyone who was interested in that subject or has had some experience or has problems could attend. More or less a bull-session instead of a formal paper presentation. A knowledgeable "referee" would be necessary in each session.

BELTER: Would you have more than one group like this going at a time?

MURROW: Yes, I think so.

BELTER: There is a problem with doing that because many of our people have interests in two or three or four of the groups that might be going on simultaneously.

MURROW: That's very true, but I believe that most of the organizations are represented here by several people. They could decide who would attend specific sessions in order that most aspects could be covered for each organization.

BELTER: Right. We attempted something like that during the meeting in 1963. It wasn't getting together in a separate room or anything like that, but we did have several panels at that time, if you recall, to cover four or five subjects of a major interest in which the panel leaders just gave brief descriptions of their experience in this area and then opened up the meeting for informal discussion. One person has suggested that we should lengthen our coffee breaks; there is a lot of merit to this suggestion because this is a time when people could get together for small group meetings without necessarily having to be away from the sessions; in other words, lengthen the coffee breaks to 45 minutes or an hour. I don't know whether this would mean cutting down on the number of papers, but you can see we are really overwhelmed with papers this year. As you know, there is a wealth of information that is developed on this subject in a two year and possibly three-year period; but, if any of you have some further ideas on this, we certainly would be pleased to receive them in the mail. Jot them down and send them to us.

Do any of you have suggestions where we might possibly hold a meeting of this type probably in the late summer or early fall of 1968?

KEIGHER: Hanford has excellent facilities for a technical conference now, with our new federal building, 300-seat auditorium, cafeteria, and improved motel facilities within walking distance of the federal building. The Hanford Project has every facet of the air-cleaning activities and we always have large representations at AEC Air Cleaning Conferences; so, on behalf of the Richland Operations Office and our many contractors at Hanford, I do invite your attendance in the fall of 1968. If there are some questions please ask. Hanford has never hosted the Air Cleaning Conference, I might add.

BELTER: Fine. Anybody else care to throw something in the hopper?

SILBERBERG: I would like to recommend for consideration the Los Angeles area, and Atomics International, Division of North American, would be pleased to serve as a host for the 1968 conference. The facilities in the Los Angeles area are excellent for holding such a meeting, and this would also give the conference an opportunity to visit with us at our sodium fires test laboratory and large modeling test installation, which, hopefully, will be in operation in 1968. With the interest increasing in the Fast Breeder field, I think it would be advantageous to hold the conference in the L. A. area in conjunction with a tour of sodium air cleaning facilities.

OPEN END SESSION

FIRST: For this session all presentations will be brief and they will be open for discussion from the floor.

Mr. Birney Fish will open the proceedings with his presentation.

FISH: In addition to the important air cleaning parameters which have been discussed by the various speakers, there are two other economically and operationally important factors. These are: retention and removal.

One may assume that particles stick after deposition, but whether they do or not depends upon the balance of the forces acting upon them. We have two papers related to particle adhesion that will be coming out in the literature sometime within the next several months and I would like to give you a preview of our results.

One area of interest is the adhesion force that is due to capillarity. Various people have described some aspects of this force in their publications, and I will outline the basic points only briefly at this time.

Most of you are probably familiar with the Kelvin equation relating to the partial pressure over a curved liquid surface. The expression for the total pressure discontinuity was derived by Laplace long ago, and it is written in terms of the surface tension γ of the liquid layer and the total curvature, (the sum of the reciprocals of the principal radii of curvature passing through the point on the surface where you are determining the discrepancy in the pressure).

For the capillary that is formed between a sphere and a plane, the surface is a surface of revolution about the axis of contact between the sphere and the plane. The meridian curve is concave inward, so that one radius terminates outside of the surface and is taken to be negative. The other radius is the normal of the meridian curve at the point in question and always terminates on the axis of rotation which is normal to the plane at the point of contact.

It can be shown that, for relative humidities less than 100%, the normal of the meridian curve is larger than the radius of curvature, thus the total curvature $\left(\frac{1}{n} - \frac{1}{r}\right)$ is negative, hence the pressure drop, $\Delta P = \gamma \left(\frac{1}{n} - \frac{1}{r}\right)$, is negative.

Just using this simple model, the handbook values for the partial pressure, the molecular weight, etc., for a 43 micron diameter glass bead on a glass surface, we predicted that the maximum force at 100% relative humidity would be 3.43 dynes, and we observed, using a centrifuge, 3.23 dynes. These are very significant forces in that they represent something like 17,000 times the force of gravity.

That is rather good agreement; however, at low relative humidity (31%), this simple model predicts a ridiculously small force (0.00017 dynes) compared with the observed maximum force (1.08 dynes). Fortunately, we have recognized what should have been obvious to previous authors writing on this subject. A rather plausible modification of the simple model will lead us to assume that the greatest pressure drop you can have under atmospheric conditions is one atmosphere, i.e., the lowest pressure you can expect to find inside the liquid layer is zero.

That would lead to a prediction that the min-max force on a 43 micron glass bead is greater than 0.5 dynes which is in much better agreement with the observed force. We are working on the details of the model now, so it will be a few months before that will be in shape to publish; however, we are reporting the experimental data in the literature as soon as we can. Also, we are reporting the fact that we see an aging effect. In theory, one would predict that it takes a finite time for water molecules to diffuse into the capillary region; thus, the layer will take a finite time to grow to its final maximum size.

We have observed that the force required to remove glass particles shows this growth effect, reaching a maximum after considerable periods of time. We also have time-lapse photography showing the growth of the capillary between two spheres.

It takes on the order of twenty-four hours for the maximum force to be obtained. The time is somewhat shorter for high relative humidity, but still a finite length of time is required.

The other area of our interest is in electrostatic forces. A lot of people "nod their heads in the direction of electrostatic forces" whenever they come across something that seems unusual in their data. There is a strong temptation to blame what we don't understand on electrostatics.

We wanted to look at the details of some of these electrostatic forces, and see to what extent it is legitimate to say that they are responsible. In addition, of course, electrostatic forces are important because they are the only adhesive forces that are effective over long enough distances to induce deposition on a particular spot. If there is a charged spot on a surface and a particle comes close enough, (if the electric field gradient is strong enough it can be a neutral particle or even one having the same sign charge), the most likely site of deposition is the charged spot.

The only possibility for a repulsive force is the case of a conductive particle on a charged, conductive surface; the particle will pick up the same sign charge as the surface, resulting in a net repulsive force.

People have made all sorts of speculations about this mechanism, even to the extent that the image charge attraction will overcome the repulsive component leaving a net attraction.

It turns out that you can't solve the sphere-on-a-plane geometry analytically, although you can solve the problem for a hemisphere on a plane.

The solution for the hemisphere shows that the electric field along a radius vector is a function of the angle θ between that radius and the perpendicular thru the center of curvature, and the magnitude is three times the field on the plane far away from the hemisphere, $E_{hs} = 3E_p \cos\theta$. From this, one can calculate the force, knowing the field, or the surface charge density, on the plane.

One can calculate also the force for a flat flake, but, for a sphere, it was necessary to resort to an analog solution. We now have a solution to the problem and the two factors that are of interest to this meeting are the force on the sphere and the perturbation of the field. The field at the top of the sphere is normal to the sphere, and is $\pi^2/2$ times the field over the plane out, away, from the sphere.

As to what constitutes a conductive particle, it is seen that almost all particles are conductive in the sense that, if you are willing to wait a short time, the charge will redistribute itself and the particle will behave as if it were conductive.

In regard to deposition of particles on the surface, the field at the top of the particle is roughly five times the field out away from the particle. Thus, if electric charge is effective in influencing deposition, and another particles comes along, guess where it is going to deposit? Obviously, the preferred deposition site near the first particle is on top of the first particle and so on, forming a chain directed away from the surface. When the chain grows long enough, it acts as a fiber and some of the later particles deposit on the fiber forming little off-shoots. We plan to follow this effect further by studying additional geometries including a sphere and a chain of spheres (and other shapes) on a cylinder.

The solution for the field along a radius of the sphere is a function of the angle θ between the radius and the vertical thru the center of the sphere, thus $E_S = \pi^2/2\ Ep \cos^4\theta/2$. The net force, which you can calculate from this function, is always repulsive. In terms of the surface density of charge on the plane σp , the radius of the sphere r, and the permittivity ϵ of the surrounding medium, the force is given by

$$F = \frac{\pi^5}{15\epsilon} r^2 \sigma_p^2 .$$

It should be noted that, if the surface relaxation time for the sphere-plane capacitor is such that the electric charge will redistribute itself sooner than the capillary liquid layer can grow, the particle may be repelled from the surface. Of course, both things can happen. One can have the capillary attractive force growing faster than the electrical repulsive force. I will conclude by saying that this is as far as we have gone. We are also beginning to study contact potential adhesion which is always an attractive force.

FIRST: Thank you very much, Mr. Fish. This dissertation is now open for discussion, and, exercising the Chairman's prerogative, I will ask the first question. You mentioned that the maximum force of capillarity was developed in twenty-four hours. What percentage would be developed in one minute?

FISH: Not much with respect to the final force that is attained. The one minute force depends upon the relative humidity, being much greater at 100% than at 30%. The rate of increase in force is, itself, a function of relative humidity so that twenty-four hours is really a round-house average. The time ranged from about ten hours for equilibrium to something like 80 hours in one case where the moisture content of the air was very low.

FIRST: This wouldn't have much effect on the retention of particles, since presumably, the entraining force would be immediate upon contact, whereas the capillarity force you are talking about would take a substantial amount of time to develop. Something else must be holding the particles, immediately after contact.

FISH: Yes, there are several other forces. You can list quite a catalog of adhesive forces.

FIRST: Are there any questions or comments from the floor?

GIESEKE: Do you have any idea how the magnitude of this force compares with the London-van der Waals forces?

FISH: In order of magnitude, greater than those forces.

THOMAS: The theory explains the results that Charlie Billings showed in his photographs. Where particles are shown attaching to each other, there is an electrical effect.

FISH: Yes, that is what is suggested.

FIRST: This is suggested also from the fact that Dr. Billings used polystyrene spheres, which we would all agree have a potentiality for generating large charges. Dr. Billings, did you discharge the charge on the particles which you generated?

BILLINGS: Experimental details are discussed briefly in the paper on accumulation effects on filter life. It was not possible to discharge the aerosol particles and still maintain a reasonable number concentration. As a result, some charge was present and had an effect on the results of the experiments. The apparatus is being modified now to produce uncharged aerosol particles and some of the tests will be repeated, to observe the charge effect.

PROTECTION OF HEPA FILTER SYSTEMS AGAINST HIGH EXPANSION FOAM PLUGGING

C.L. Lindeken and R.D. Taylor

Abstract

When high expansion foam is used as a fire control agent in gloved box enclosures exhausted through HEPA filter systems, the foam volume should be controlled to avoid enclosure flooding and foam-plugged filters. Without such control, provisions for foam condensation must be provided between the enclosure and the filter system. Of the techniques we have investigated, centrifugal separation appears to be the most efficient. Up to five box volumes (~ 60 CF) of foam can be condensed with a cyclone separator operated at 35 cfm and an entry velocity of 10,000 fpm. However, the high pressure drop (~ 30 inches of water) exceeds the capacity of most fans used to ventilate gloved boxes. This problem has been overcome by passing the foam through a squirrel cage fan which is operated at 5,000 rpm and is mounted coaxially in the vertical duct from the box. Foam enters the fan and is impacted against the chamber wall. Coalesced liquid drains back into the box through outer slots in the rotor support. Although this separator has less capacity (about 20 CF of foam), the energy for foam condensation is supplied by the fan and no demands are made on the gloved box ventilation system.

CLL:i

6/23/66

PROTECTION OF HEPA FILTER SYSTEMS AGAINST HIGH EXPANSION FOAM PLUGGING

C.L. Lindeken and R.D. Taylor

Introduction

High expansion foams are made by spraying an aqueous solution of a foaming agent against a fine-mesh, cloth net while forcing air or inert gas through the net. The term "high expansion" is used because the ratio of the volume of foam produced to the volume of foaming solution is about 1000 to 1, compared to an expansion ratio of 10-20 for conventional foams.

These foams are effective fire control agents. Because of their low water content, there has been considerable interest in using high-expansion foams for controlling fires in gloved boxes. However, as air exhaust from these enclosures is normally filtered through high efficiency filters, enclosure flooding must be avoided; if foam is allowed to enter the filter system the filters will become foam plugged, and the air flow is cut off.

In the Hi-X unit we designed for gloved boxes[1] the volume of foaming agent is limited to that which will generate just sufficient foam to fill the enclosure. The intent here was to furnish an automatic system for off-hour protection with a one-shot foam application and a fire alarm signal initiated concurrently.

If foam is to be continuously applied, provisions for foam condensation must be provided between the enclosure and the filter system. This report describes our efforts to develop such a technique.

(1) C.L. Lindeken and R.D. Taylor, "High Expansion Foam Fire Control System for Gloves Boxes," UCRL 7922

Description of Test Equipment and Procedures

Foam Generator

Test foams were produced by the foam generator shown in cut-a-way form in Figure 1*. In normal operation when the temperature within the box exceeds the set point of a thermal switch (about 140° C) the switch opens the solenoid valve, which allows argon gas at a pressure of about 30 psi to flow through the Venturi nozzle. Simultaneously, through a parallel line, the argon pressure energizes a pneumatic operator, which opens the foam port inside the box. Argon flowing through the Venturi Nozzle pulls foaming agent into it, and the argon-foaming agent mixture is forced as a fine spray against the conical cotton net. Once this net is wet, a foam of fairly uniform bubble size (1/8 - 3/8-inch diameter) is produced. Foam is forced through the chamber plenum and enters the gloved box through the opened port.

Figure 2* shows the foam generator attached to the back of one of our standard metal chemistry gloved boxes. These enclosures have a volume of about 13 cubic feet.

Units to be evaluated for their ability to condense or arrest the flow of high expansion foam were installed between the gloved box and the filter. The filter used was our standard 50 cfm combination filter, having a pre-filter and a HEPA filter mounted in an 8 x 8 x 16 inch wooden box. A reservoir holding 1/2-gallon of foaming solution (1% ammonium lauryl sulfate) was connected to the generator. A flow rate of 35-50 cfm of air was established and the initial pressure drop across the filter and the test device was recorded. The generator was started, the enclosure was flooded, and the foam introduction was continued until the increase in pressure drop and decrease in air flow indicated filter plugging.

*Not available

Results

1. Sonic Generators

Although sonic generators (horns) were not evaluated in the present investigation, this approach was among the first suggested to us. From the beginning we were concerned that, when the horn was mounted in the ductwork, coalescence might not be applicable across a large enough radius to be effective. Also, we were apprehensive that the need for protection against the sound levels might be a detriment to acceptance. While we were considering these factors a Hi-X foam breaking demonstration was performed by a sonic generator vendor. Since their (the vendor) observation was that a frequency of 12,000 cycles per second "had no apparent effect," we concluded that we would not investigate this approach at LRL.

2. Demisters

In a separate study to determine the effect of Hi-X foam on electronic components, it was observed that foam did not penetrate perforated metal screens covering the units. This suggested the possibility that demister-used to remove liquid mist droplets from air streams - might retain the foam without disrupting the air flow.

Three different dimister packings were tested: stainless steel, Teflon-coated stainless steel and Teflon fibers. The first two were supplied by the Otto H. York Company; the Teflon fiber unit was fabricated at LRL, Livermore. All demisters were 8 x 8 x 2 inches and were framed in 304 stainless steel Pads were supported in the frame by 1/4-inch stainless steel screens. Demister units were mounted in an adaptor in the exhaust ductwork outside the box as shown in Figure 3*.

*Not available

Using the procedure as already outlined, the foam generator was started and the gloved box was flooded. After the foam entered the exhaust duct from the box there was an immediate increase in pressure drop across both the demister and the HEPA filter.

Upon removing the demister from the holder, it was seen that foam had penetrated the unit and that the texture of the foam coming through was much finer than that entering it. Figure 4* shows this difference for the stainless steel unit. Figure 5* shows the same effect using the Teflon fiber demister.

It is obvious from these tests that demisters will not arrest the flow of Hi-X foam. Accordingly, they offer no protection to the HEPA filter. In fact, the finely textured foam produced when Hi-X foam flows through the demister does more damage to the filter than the original, coarser foam. After exposure to normal foam, filters partially regain their air flow capacity, as the foam covering the filter medium gradually breaks down. This recovery capacity may last through several successive foam applications. When the filters are exposed to foam that has passed through the demister, there is little evidence of recovery.

3. Cyclone Separator

We next attempted to condense the Hi-X foam by impaction using cyclone separators. We had built a small version of a Pease-Anthony wet cyclone for another project so we tried passing the Hi-X foam through it. About all we learned from this test was that the spray tower itself was a good Hi-X generator, and that any addition of water was to be avoided. We took out the water spray tower and installed treated perforated plates through

*Not available

which the foam had to pass. Foam was arrested momentarily, but when the surfaces became coated with foaming agent, foam soon formed on the downstream side of the plate. Likewise, metal chip packings were ineffective. Finally, we removed everything from the cyclone and depended only on the tangential entry velocity of the foam to produce condensation by impaction on the bare, dry wall. This worked best of all.

We then built a cyclone separator, shown schematically in Figure 6.* This cyclone is 8-inches in diameter and 24-inches long. The large volume is required because the unit must serve both as a separator and condensed foam collector. The distance between the guard ring and the cyclone wall must be kept small so as to maintain a high velocity. The guard ring serves as an additional impacting surface for foam coalescence and should be long enough to cover about one spiral length of the foam path. As foam gathers on this ring it will be swept to the cyclone wall, then run down this wall to the bottom of the separator. Without the guard, foam will collect on the center discharge tube and will ultimately be drawn into this tube and enter the filter. In the unit shown, the bottom of the ring is about 2-inches below the center line of the entry. The tangential entry area is about 0.5 in^2;when the separator is operated at 35 cfm the entrance velocity is about 10,000 fpm.

This unit has been by far our most efficient separator. Operating at 35 cfm, up to five volumes of foam can be condensed with no appreciable foam carry-over to the filter. During the run the pressure drop across the filter increased by only 25%.

*Not available

The disadvantage to this solution to the problem is the high pressure drop across the cyclone (~ 30-inches of water). Fans normally used to ventilate gloved boxes do not have the capacity to move air against this resistance, and high head fans would have to be installed in those areas where such a cyclone was to be used.

Centrifugal Separator

Recently we have developed a centrifugal separator that breaks the foam without the high pressure drop characteristics of the cyclone. This unit shown in Figure 7* is designed for mounting on the gloved box in series with the exhaust system. A squirrle cage fan operated at 5000 rpm pulls foam bubbles into the cage and impacts them against the container wall. The coalesced liquid drains back into the box through the outer slots in the rotor support.

The advantage of this unit is that condensation is performed by energy supplied by the fan. No demands are made on the gloved box ventilating fan. The disadvantage is limited capacity. After about 20 cubic feet of foam has been condensed, the slots become plugged with partially regenerated foam and the foam column soon rises to the discharge port and subsequently flows into the filter system.

Conclusion

Although initial separation appears to offer the most promise, we do not at present have a really practical solution for preventing filter clogging, if the enclosure is flooded with Hi-X foam. It is possible that improvements in the capacity of the centrifugal separation can be made. However, most of these changes suggest adding to the size and complexity of a system already too cumbersome for acceptance.

*Not available

We believe that the entire problem can be avoided, simply by limiting the volume of foaming solution to that which will generate just sufficient foam to fill the enclosure.

CLL:i

8/17/66

DISCUSSION

KEIGHER: You commented about foam blinding the filters. I think this is only partially true, in the sense that it is true for smaller filter applications, such as a glove box. For large filter banks, I believe it is almost impossible because it means that you would not have adequate water to blind the filters. What I am trying to say is this: don't be afraid of using high expansion foam on large filter banks and large filter installations.

BROWNING: I would like to suggest an idea about how to get greater gas cleaning efficiency from foam systems. The idea of using foam for decontaminating gas in various applications has been discussed at previous air cleaning conferences and at various symposia and the data have indicated that foam can remove various kinds of radioactive impurities, but efficiency is not as high as might be anticipated. I have always been disappointed in the fact that we didn't get 99 plus per cent efficiency. I am referring to the work by Silverman and others, "Foam and Diffusion Board Approaches to Containment of Reactor Releases, TID 7641, pp 169-184 (1962)," to the work that Ackley and I reported a number of years ago, "Characterization of Millimicron Radioactive Aerosols and Their Removal From Gases, TID 7641, pp 130-147 (1962)," and to the work that was done in the NSPP cell at Oak Ridge by the Harvard people, R. E. Yoder and L. Silverman, "Foam Suppression of Radioactive Iodine and Particulates, TID 7677, pp 297-316 (1963)." In all of those cases, the efficiency wasn't as good as I had hoped. I suggest that the activity was trapped in the foam but was carried along by the moving air bubbles, and then at the top of the foam column, where the bubbles broke, the activity was re-entrained into the air, in part, reducing efficiency.

Now, here is an idea, and whoever is interested in promoting the foam idea might try to apply it. If we could set up a counter flow system, with the clean foam solution flowing down and with the air bubbles flowing up, perhaps we can keep the activity down at the foam bottom of the column. If the foam bubbles at the top are not contaminated, then they would not re-contaminate the emerging air.

I tried this idea on a small scale with a red dye simulating the activity, to see what sort of liquid-to-gas flow ratio would be required. I had a glass cylinder about four inches in diameter, and about 18-inches high. I bubbled air through a soap solution containing dye at the bottom at such a flow rate that the foam almost overflowed. A clean soap solution without dye in it was dripped on the top of the foam column. Only about one drop per second was enough to keep the dye at the bottom of the foam column.

Maybe we could do this on the scale of a reactor containment vessel. By operating a foam generator at the bottom, we could fill the whole containment vessel with foam and, in effect, encapsulate

all of the containment vessel air in little foam bubbles so diffusion time would be brief. We would then wash the foam bubbles with clean soap solution previously stored at the top and flush the mixture down into a sump. This is an idea of how to get maximum advantage from foam encapsulation.

LINDEKEN: In the first place, that we were concerned, not with encapsulation techniques, as Dr. First suggested, but with fire prevention we were looking for a fire control system. The last system I suggested was of the run-down type, except that it uses foam that has already been in the system.

THE COMPARATIVE ENVIRONMENTAL HAZARDS FROM A RELEASE OF METHYL IODIDE OR ELEMENTAL IODINE

D F. Bunch
Health and Safety Division
Idaho Operations Office
U. S. Atomic Energy Commission

Abstract

Serious concern has been expressed over the behavior of methyl iodide and the effect of its behavior on possible environmental hazards from a release of radioiodine to the atmosphere. In an attempt to determine the fate of radioiodine in the environment, a series of planned releases is in progress at the National Reactor Testing Station, known as the Controlled Environmental Radioiodine Tests.

On the basis of 15 field releases and more than 40 laboratory experiments we have found there is no significant difference in the metabolism of methyl iodide (CH_3I) or elemental iodine (I_2) in cows or in humans. The only real factor of importance in assessing the consequences of a release is the difference in the deposition velocity of the two forms. The deposition velocity of CH_3I is about 0.05% that of I_2.

Evaluations of test data indicate that it is unlikely that the consequences from a release of mixtures of I_2 and CH_3I to the environment would be appreciably different from predictions based on the behavior of I_2 alone.

THE COMPARATIVE ENVIRONMENTAL HAZARDS FROM A RELEASE OF METHYL IODIDE OR ELEMENTAL IODINE

Much interest has been aroused in recent years over the possibility of methyl iodide being released as a result of a reactor accident. If CH_3I were released to a containment vessel, it seems likely that there would be a greater release of iodine to the environment than would be expected if only I_2 or other easily removed forms of iodine were present. It should be understood however, that a greater release, resulting from the presence of CH_3I, does not necessarily lead to significantly greater environmental hazards.

There are two primary modes of exposure to radioiodine in the environment; inhalation and consumption of contaminated milk In inhalation there are two points of concern in evaluating potential dose: the depletion of material in transport by turbulent deposition and the retention and metabolism of the inhaled material. In considering ingestion dose there are similar factors; again depletion must be considered in estimating the amount that is available for deposition at any downwind location, deposition determines the amount available to dairy cattle, transfer processes from grass to milk, and finally the retention and metabolism of the ingested radioiodine. Each of these factors, in addition to those relevant to iodine behavior in a containment vessel, must be evaluated before the comparative hazards of I_2 and CH_3I can be determined.

The Health and Safety Division of Idaho Operations Office, USAEC, is attempting to relate the environmental hazards from releases of various forms of radioiodine through a series of planned releases known as the CERT program (Controlled Environmental Radioiodine Tests)[1-3]. Since its inception, there have been 15 field tests and approximately 40 laboratory experiments. Of the field releases, three have been made with CH_3I, the rest with I_2. The CH_3I releases have included an 8 curie daytime release on July 21, 1966 and a 1 curie nighttime release on July 26, 1966. Although the program has not been concluded, we have a considerable body of data which, with results from other workers in the field, allow a reasonable comparison of the behavior of CH_3I and I_2.

1. Relative Deposition of CH_3I and I_2

   It appears that the difference in deposition of the two forms is the major factor in assessing environmental hazards. Tests conducted this year show that the deposition of CH_3I is on the order of 0.05%

that of I_2, under similar conditions. For all practical purposes, CH_3I is a nondepositing tracer.

As a consequence, depletion by turbulent deposition becomes insignificant for this form of iodine. A recent study [4] indicated that the depletion factor for I_2 - the amount originally released divided by amount remaining airborne, under conditions normally assumed for major reactor accidents, (stable meteorological conditions, ground level release, total deposition velocity 0.84 cm/sec) was about 2.7 at a distance of 10^4 meters. Thus, for a given release under these conditions, one would expect doses to be a factor of 2.7 greater for CH_3I than for I_2, since there would be no activity loss by depletion. The difference in deposition greatly reduces the net ingestion potential of CH_3I, since pasture contamination from CH_3I will be only 0.05% that from I_2.

2. Transfer of Iodine to Milk

Efforts have been made to measure and/or account for the movement of iodine from its point of consumption by cows to its secretion in milk. This type of study has been an integral part of the CERT program; cows have been grazed on pasture during several of the tests and a number of "spike" studies have been attempted. Thus far, we have observed no significant difference in the uptake and retention between CH_3I and I_2. Normal values of iodine secretion in each liter of milk range from 0.5 to 2.0% of the activity consumed with forage each day.

Inhalation of iodine by the cow is another way for iodine to enter milk. For I_2, this mode of uptake is insignificant compared to that from ingestion. This is not the case with CH_3I; results from the July 21, 1966 test showed that a time integrated air concentration of 1 C_i - sec/m^3 would lead to a peak concentration on the order of 10^{-5} C_i/liter and to an integrated milk activity of about 2×10^{-5} C_i-day/liter from inhalation alone. This is roughly the same milk activity resulting from ingestion of contaminated grass. Unlike the milk activity from ingestion (which reaches a peak within 50 hours), the milk activity from inhalation appears at the next milking or within 4 hours after the exposure.

3. Uptake by Humans

Although there have been a large number of uptake studies of iodine for clinical purposes, there is little information on the uptake of inhaled iodine. Recent CERT inhalation studies have shown interesting differences in the behavior of the two forms of iodine with respect to human uptake. These differences appear to be closely related to the changing characteristics of the material with distance.

Attempts have been made to determine the physical properties of airborne radioiodine as a function of distance from the source. These studies have shown that I_2 undergoes a rapid interaction with naturally occurring aerosols. This is shown by air samples collected at various distances from the source: for I_2, less than 1 per cent of the collected

activity is found on particulate filters within a few meters of the source while about 50% is found on particulate for distances greater than 100 meters from the source. There is, however, no apparent change with distance with CH_3I; essentially all activity passes through the particulate filters.

This corresponds to data on changes in body retention for individuals exposed at various distances from a release. With both I_2 and CH_3I, individuals exposed to radioiodine close to the release point showed no appreciable skin contamination or residual contamination in the nasopharynx or lung. The retention curves as determined by "in vivo" counting are identical to curves derived from clinical studies 2/. The same is true for CH_3I exposures at distances removed from the source. On the other hand, exposure to radioiodine at greater distances, released as I_2, results in considerable surface contamination and/or deposition in the lung and nasopharynx. Our recent studies show skin contamination, (most of which was removed by showering within a few hours after exposure) on the order of 2-4 times that which is internally retained by inhalation. There was, however, no indication, that this results in greater thyroid uptake than would be expected from inhalation alone.

4. Relative Hazards of CH_3I and I_2

From the results of the Controlled Environmental Radioiodine Tests briefly summarized above, it is clear that the differences in the behavior of CH_3I and I_2 may lead to marked differences in dose from inhalation or ingestion. In those areas where there are no dairy cattle, inhalation of both CH_3I and I_2 becomes controlling. In this case, the dose from methyl iodide is at least a factor of three times that from I_2 - this is primarily due to differences in depletion of iodine by deposition to the point of interest.

Where there are dairy cattle near a release point, the dose from ingestion of contaminated milk may be as much as a factor of 1000 times 3/ greater than from inhalation - if I_2 is the major constitutent of the release. For CH_3I, it is exceedingly improbable that the ingestion hazard would ever approach that from inhalation Thus, two points must be considered in evaluating potential dose from CH_3I or I_2. The initial impact of a release (i.e. - inhalation) will most certainly be greater for CH_3I than I_2. The longer term hazards are, on the other hand, much greater for I_2. Using the results from reference 4 and the techniques described in reference 3, I have attempted to show the net hazard from different combinations of I_2 and CH_3I under typical adverse meteorological conditions. As can be seen in Figure 1 the dose from inhalation becomes controlling at about 95% methyl iodide. The inhalation dose is about twice that for I_2 when the release is a combination of about 50% CH_3I - 50% I_2. The ingestion dose has been estimated on the basis of two days exposure, since it is probable that protective actions would be initiated within this time to preclude further ingestion of contaminated milk.

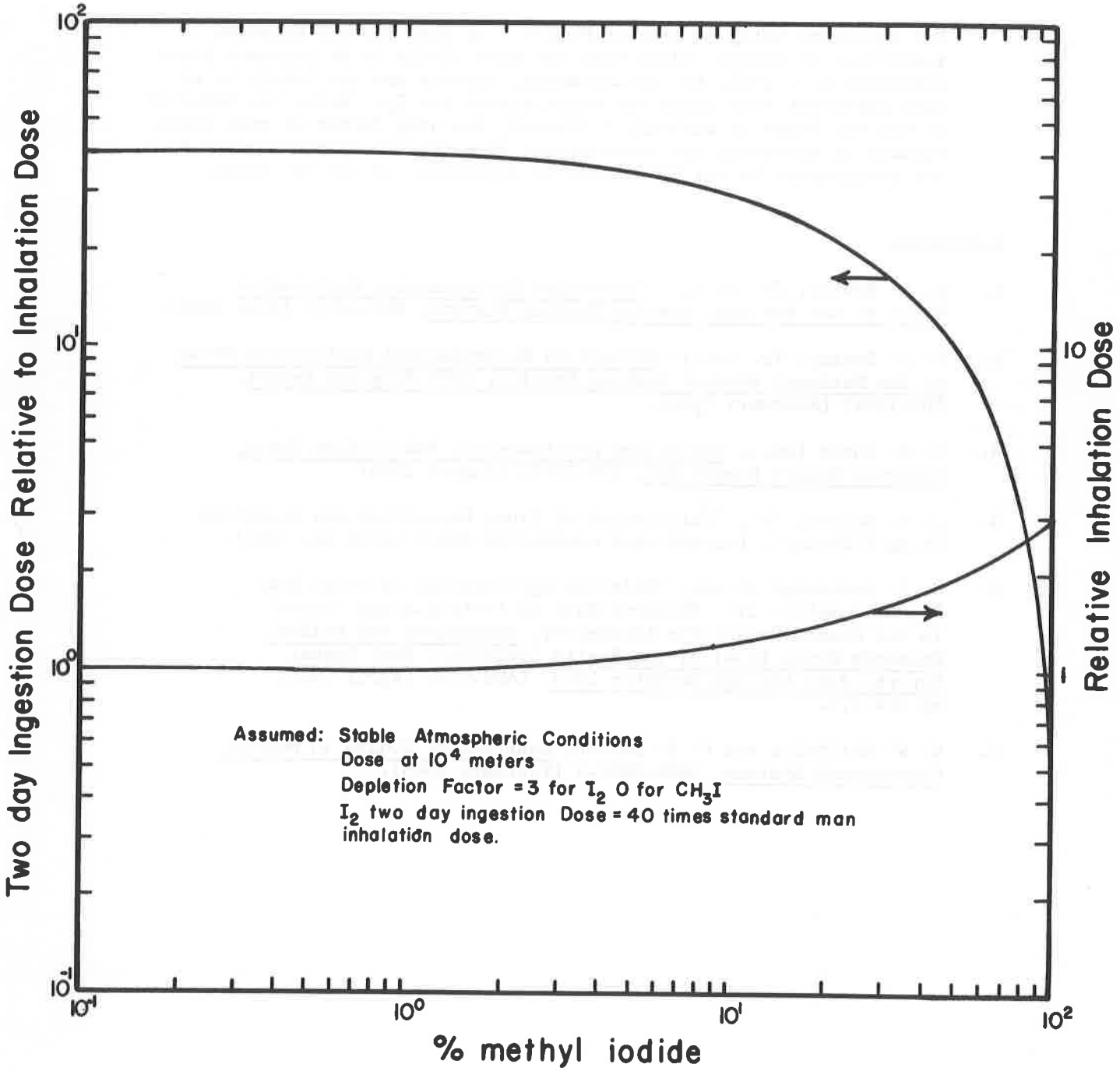

Figure 1 Ingestion and Inhalation Dose for Various Mixtures of $CH_3{}^{131}I$ and $^{131}I_2$

The important thing to note in Figure 1 is that for the relative quantities of methyl iodide that are most likely to be released (from reference 6, < 30%), the environmental hazards are not likely to be much different from those one would expect for I_2. While the behavior of the two forms is markedly different, the only factor of real significance in assessing the consequences of a release of radioiodine to the environment is the difference in deposition of the two forms.

References

1. C. A. Hawley, Jr. et al., Controlled Environmental Radioiodine Tests at the National Reactor Testing Station, IDO-12035 (June 1964).

2. C. A. Hawley, Jr. (ed.), Controlled Environmental Radioiodine Tests at the National Reactor Testing Station, 1965 Progress Report, IDO-12047 (February 1966).

3. D. F. Bunch (ed.), Controlled Environmental Radioiodine Tests, Progress Report Number Two, IDO-12053 (August 1966).

4. E. H. Markee, Jr., "Calculation of Plume Deposition and Depletion Using K-Theory", (unpublished manuscript dated April 12, 1966).

5. C. C. Lushbaugh et al., "Clinical Applications of Whole Body Scintillometry. IV. Turnover Rate of Protein-Bound Iodine", in Los Alamos Scientific Laboratory, Biological and Medical Research Group (H-4) of the Health Division - Semi Annual Report, July through December 1960, LAMS-2526 (April 1961) pp 364-371.

6. G. W. Keilholtz and C. J. Barton, Behavior of Iodine in Reactor Containment Systems, ORNL-NSIC-4 (February 1965).

DISCUSSION

BUNCH: Before I step down, I would like to ask one question. During the Wednesday session, a great many papers discussed filtering. In our last two tests, we used MSA-85851 charcoal and found our collection efficiencies were normally distributed around 70 per cent, with none above 78 per cent collection efficiency. The charcoal was contained in a 4-inch diameter, one-inch deep cartridge. Perhaps Bob Adams would like to comment on this.

ADAMS: Were you using your high volume, May pack sampler in this experiment?

BUNCH: We used both kinds. We used some of the smaller, 3/4-inch diameter samplers, although the bigger one was the primary sampler.

ADAMS: I will suggest that the observed low efficiency for methyl iodide was because the residence time of the gas sample in the 1-inch deep charcoal bed was quite brief; possibly there was not sufficient time for the iodine exchange reaction to achieve completion.

THAXTER: Did you touch upon the metabolism of iodide versus elemental iodine in your written paper?

BUNCH: Unfortunately, we found our release took place over a period of 30 seconds. We were trying to release the material directly from the ampoules by evaporation techniques. However, the evaporating dish was quite hot and we found that because of the short period of release, the retention of the human volunteers was small, in the order of one per cent. Apparently, this was due to the fact that the material did not reach equilibrium in the lungs. As far as we were able to tell, there is no difference in the metabolism of these forms of iodine (CH_3I or I_2) in humans.

BUSCH: You mentioned that the methyl iodide concentration increased relative to the iodine concentration. Is it the consensus of this group that this effect was due mainly to the difference in deposition rate, or was there a conversion of elemental iodine to methyl iodide throughout the accident?

BUNCH: The difference is associated with deposition.

BUSCH: That is right. I would like to ask if anyone has some comments to make on how the production rate of methyl iodide might be varying with time after the release?

PARKER: I will hazard a response to that question. Methyl iodide production is receiving a great deal of careful attention and the

conclusion right now is that there is no coherent explanation for its formation; however, it is only a matter of time, I am sure, until a very reasonable rate constant will be deduced.

I think you have to remember that the subject is a new one and that it has been associated with some difficult problems, such as methods of analysis, that make it pretty hard to analyze the data. We all feel fairly certain that in the course of an accident, both the radiolytic processes which lead to the formation of methane by decomposition of organic materials and the surface reactivity of the containment are going to contribute to methyl iodide production. All such processes are a function of the time over which they are allowed to proceed. Just by intuition, I think that's what we eventually will be able to show.

BROWNING: This is about metabolism of methyl iodide. There was a British report by D. J. Morgan, entitled "Studies on the Retention and Metabolism of Inhaled Methyl Iodide," AERE-R-4821 (1965), telling about experiments in which radioactive methyl iodide was inhaled in small concentrations by human volunteers. As I recall, more than 50 percent and less than 100 percent was retained. That is high enough so that you can't really claim very much credit for the iodine in methyl iodide being in an unavailable form.

FIRST: When you say metabolized, do you mean absorbed?

BROWNING: As I understand it, fifty percent or more of what was in the inhaled air was retained and presumably ended up in the thyroid.

BUNCH: In Morgan's studies, they give no date as to thyroid uptake. Their data gathering was done with a whole body counter at Harwell, and all they have reported in the document you mentioned is whole body retention, which, as indeed, the '65 progress report from Harwell indicates, is a function of the breathing rate. So, it acts very much like a true gas. If you can extrapolate their data, there is some indication that perhaps there is a significant reduction in total thyroid uptake due to the fact it does act like a true gas.

FIRST: When you say it acts like a true gas, I assume you mean a non-absorbable gas or one which is absorbed with difficulty, so that when the exposure ceases, the body tends to exhale the material from the blood. Is this correct?

BUNCH: This is correct.

BROWNING: I accept the idea that Morgan measured whole body retention as opposed to thyroid retention, but I don't recall that there was appreciable exhalation after exposure ceased.

FIRST: This is the sense of the question I asked regarding adsorption versus metabolism, because, obviously, it could be taken up

by the body and then, when the exposure ceases, it could be exhaled or desorbed if it was not metabolized into some other product which became fixed.

BUNCH: I wish to add, at this point, that the material is, indeed, metabolized. There seems to be a hydrolysis reaction in the blood, but the desorption phenomena occurs when there hasn't been active blood transfer. This is what I was referring to.

HILLARY: I have heard indirect comments from our Harwell people. I think the evidence suggests that methyl iodide is fairly well retained. It is probably not wholly a reversible absorption-desorption process.

COMMENT: I think there is a reference to this same work in the Health Physics Journal of January, '66, on page 162.

FIRST: Our next speaker will be Mr. Don Keigher, Atomic Energy Commission, who wishes to talk about fire protection considerations in clean rooms.

KEIGHER: I had expected to hear a little more discussion at this meeting of and about clean rooms because there are many in use within the Atomic Energy Commission and its various contractors, and so many clean room people are present.

Much of the knowledge of ventilation, air cleaning, and containment applicable to clean rooms was learned during the past twenty years in the handling of radioactive materials in the atomic energy program; although there are a couple of basic differences between clean rooms and laboratories handling radioactive materials. These are: (a) clean rooms operate under a positive pressure rather than under a negative pressure, and (b) in the former they recirculate something like 90% or more of the air, whereas atomic energy facilities do not recirculate air, generally using a one-pass ventilation system. The things we have had to learn the hard way in our atomic energy facilities in matters of fire protection should be utilized in white rooms.

Lack of Fire Protection Guidance

The Federal Standard 209, "Federal Specifications for Clean Rooms and Work Station Requirements, Controlled Environment," has just a few words under fire protection. It says, "Clean room fire protection should be consistent with that provided for the surrounding building areas." I understand a revised 209 will be out sometime this month or next month, but this statement was written and agreed upon a year and a half ago. The other authority on the subject, the "bible" for the clean room industry, is "The Design and Operation of Clean Rooms" by Austin and Timmerman out of 400 pages in their book, there are something like 49 words (a paragraph or two) that touch on the subject of fire protection.

Because of this lack of guidance, I felt it would be useful to mention a few points that we know from our own experience. These are points that you, who have influence on clean room designers and operators, should consider.

Filters

Fire resistive high efficiency particulate air filters are most important. I would say that I have seen more clean rooms in operation that have combustible H. E. P. A. filters than have fire resistant filters which are virtually standard for AEC and its contractors. Certainly, I strongly recommend that clean room designers and operators learn of AEC loss experience with combustible filters and then appreciate our long and tortuous development of Underwriters Laboratories Standard 586. Most of the filters now being purchased by AEC contractors are UL listed filters, and these have a level of fire resistance which has some meaning to industry and insurance people.

I would like to point out what fire resistive filters contribute to the fire protection picture. We have had two requirements for at least ten years, (a) a filter must not contribute to a fire that may exist in a facility or ventilation system and (b) a filter should act as a barrier to a fire that may arise in the system.

There is a tendency on the part of many clean room operators to buy high efficiency filters and not be satisfied with their performance. They say the filters leak too much, so they probe and check and wherever they find even the most minute leak point, they plug it; always using a combustible mastic compound. I have seen filters which, by visual appearance, have been 40 percent plugged! The fire loading that has been added to an already combustible filter is amazing.

It seems to me this problem can be handled simply by buying filters which are 99.99% efficient or, if desired, even higher. I am sure all manufacturers can and do make them. You may have to pay a little more because they have to sort them out from the 99.97% filters that atomic energy users find adequate. Plugging with combustible mastic is hazardous and pointless.

Another assist in this direction would be to submit clean room filters to AEC filter testing stations. Hanford has had one shipment from Boeing Aerospace (Seattle) who sent filters for their latest clean room to the station. Hanford Occupational Health Foundation (Frank Adley's group) has a "use permit" to do this work. I am confident that the clean room industry could get high quality filters and not have to spend labor and time and add to the fire hazard by the kind of after-the-fact work noted above.

Other Fire Considerations

One aspect of a fire in a clean room that might be a little different than in an atomic energy situation is the fact that in clean rooms, being under pressure and, in some cases, having a higher movement of air, fire spread

can be accelerated within the space. This is not a serious problem but one that should be considered.

It is of interest that although a clean room starts out to be essentially a sparsely equipped space with very little furniture, equipment, etc., it goes the way of all the rest of our facilities and activities. After a while, quite a combustible load of plastic sheetings, masking tape, coated papers, extra lint-free cloth, and so forth accumulates. Soon, you will find a BTU loading in a clean room that is just as great as in a laboratory; which, generally, we consider as being either ordinary, or extra, hazardous.

If there is any fire extinguishing agent in the room, it is likely to be carbon dioxide, the least effective agent to use in this space because of the high air movement. I think most people consider dry chemical extinguishers, being powders, contaminants when used in a clean room space. However, one must remember that an extinguisher would not be used unless there was a fire and a fire would put the room out of operation in any case. As considerable amounts of the combustible loading already in the space are class A (cellulose), water-type extinguishers are needed most in these spaces. There are many good ones on the market for this use.

Flammable liquids, solvents, and gases are used in clean room operations, particularly acetone and alcohols in miniaturized parts cleaning and drying. As they have high air recirculation rates in these facilities, there can be a rapid buildup of flammable gases and vapors in the space. It is not inconceivable that an explosive atmosphere can occur. I know of no such loss to date, but it cannot be ruled out as a possibility. A related consideration is toxicity to people working in the space; industrial hygienists might look at this problem, too.

Sprinklers - Best Protection

The best fire protection is, or should be, an automatic sprinkler system for virtually every installation. You will hear that people are concerned about water damage, but water will not be used in a clean room unless there is already a fire. If a fire is contaminating the room, the water spray from the sprinkler system will always (97%) extinguish or control the fire and keep the loss to a few hundred dollars. An objection to sprinklers in clean rooms is that they hold and collect dirt particles. This can be overcome by using chrome-plated pendant heads, which reduce exposed surface to catch bits of dirt, etc. One of the manufacturers, Grinnell Company, and possibly other manufacturers as well, are producing heads that recess into the ceiling. Only a smooth surfaced dome is exposed which melts at the same temperature as the fusible link on the sprinkler. The head has a mirror smooth surface that can be wiped and polished easily.

Complaints are heard that a hole through the ceiling of the clean room becomes a source of contamination because dirt and contamination may sift through the hole. This is very easily handled, for sprinkler installers seal holes and openings on every system installation.

Separation of Risk

Another design principle, one which I can remember Dr. Yant and Neis Garden recommending to this group in 1955 at Argonne, is the need for dispersion or division of risk. We shouldn't build larger ventilation systems or larger filter installations than we need for the problem at hand. The same principle applies to clean rooms.

I really question whether clean rooms of 20,000 square feet of undivided space need be built. The original clean room was only about 200 square feet. When these vast rooms are built, it means they have million dollar loss potentials and all the other loss aspects that go with this size.

We must ask, can we reduce the problem of one big room to two, three, or four smaller rooms? Or reduce the problem so that instead of one small room, three or four clean benches will suffice? This, I think, is quite important.

I bring these points of fire concern to your attention. Because of the fire loss potentials, I think measures for a level of fire protection commensurate with the importance of clean rooms are urgently needed. I now know of only one fire, the RCA Color TV Tube Clean Room complex in Lancaster, Pennsylvania, that had a serious fire. I have no details on it but picked it up through a fire loss record when talking about computer losses about a month ago.

FIRST: You have brought up a very important subject. Of course, the point you made about a mention of only 49 words in the "Bible" merely points up the fact that Bibles tend to be an accumulation of ancient lore.

I am sure, if you had more time at your disposal, you would have pointed out that clean room designers have a distressing tendency to put interconnected double locks in a room so people won't disobey clean-room discipline that requires only one door be open at a time. When one door is open, the other cannot be unlocked. These people seem to be mightily astonished when asked how anyone is going to get out if a fire or other disaster occurs. Obviously, one is apt to forget to stop and close a door when trying to rush out of a burning room. With one door open, the second one cannot be opened, a very distressing situation. One solution is to provide kick-out panels in the walls so that there will be a second way of getting out of these rooms should a fire occur.

BILLINGS: The design of large clean room facilities includes a consideration of many of the factors in air cleaning that have been studied extensively by AEC and contractor personnel, and which have been reported at Air Cleaning meetings. When talking with engineers involved in the design of large, specialized clean room facilities, I was surprised to learn that very little, if any, AEC experience was being utilized. Would it be appropriate to suggest that Mr. Keigher consider submitting an article based on his talk to the Journal of the American Association for Contamination Control? Certain of the technology for filter handling and installation, in-place testing, fire hazards, and the like would be of interest.

FIRST: I have had a few experiences in the Guidance System field. Many of these people have the idea that only flammable solvents are satisfactory liquids for their ultrasonic cleaning baths, and fires have occurred from this source. Fortunately, no grave injuries occurred, and this probably prevented these incidents from reaching the fire protection literature.

BURCHSTED: I would like to expand on a couple of the points mentioned by Mr. Keigher. First, clean room designers tend to use filter units that are as large as possible, units that are often as much as two or four feet wide by six feet long but only inches deep. This gives a very large span-to-depth ratio, and the filters are structurally weak. This is borne out by tests made at the Navy Ordnance Lab where a filter unit 2 x 2 x 1 foot withstood a pressure of 3.2 psi, but a unit that was 2 x 2 feet x 6 inches withstood only 2.6 psi. This is a big factor in the leakage experienced in clean room filters because when they are subject to racking and warping during shipment, they get badly damaged and frequently develop cracks in the adhesive between the filter pack and the frame. We have seen quite a bit of evidence of excessive pinholing in clean room filters. The costs must be tremendous because of the plugging required to pass the leak tests. At one manufacturer's plant, we saw filters being plugged with a butyl caulking compound to repair leaks determined by scanning, a very expensive process, in itself, and it sometimes took from three to four days to plug one. Up to ten to fifteen percent of the face area might be plugged and then the process was repeated after they arrived at the installation site.

Another item is that many clean rooms today are using vertical laminar flow. This means that they put in whole ceilings of filter units. If they had a fire, the whole ceiling could fall down.

The common use of CO_2 extinguishers in clean room fire protective systems has been noted. As Murrow mentioned earlier, during fire tests at Livermore last year we found out that CO_2 is quite ineffective for putting out filter fires. Average construction in clean room filters includes kraft paper separators and untreated plywood frames, both of which are flammable. This saves a few dollars in the original installation. A. B. Fuller and I, in our visits to facilities around the country, have seen quite a number of clean rooms and in every case we have observed that combustible construction was used except at Carbide's Y-12 plant at Oak Ridge.

Two years ago, we tested a semi-combustible filter unit and I think we put in about 25 pounds of CO_2. Then we sprinkled it with water from both sides for about 10 minutes and, finally, we took it downstairs and put it in a water batch. It wasn't easy to put this filter fire out.

FIRST: I wish this sort of thing could be documented and photographed so that more people would become aware of it. It is a serious problem, as you have brought out, and I think it deserves careful consideration. It seems to me the white room concept may have overgrown itself. I find that enormous

rooms are being constructed in which to assemble micro circuits about the size of an 1/8" square. I wonder why they don't do this work inside clean benches or gloved boxes and leave the dirty people outside.

KEIGHER: I might mention that Dick Smith, who is the Fire Protection Engineer at AEC office in Washington, has asked us to prepare something for an information release from his office. However, this would receive only limited circulation and I think it would be better to get it into Contamination Control or a similar journal.

ELINSKY: I was going to suggest that the American Association for Contamination Control Journal has a good reputation in the clean-room industry and is read by people who are doing specifying and building of clean rooms.

Secondly, regarding the comments about fire hazards in clean rooms, it might be pointed out that until about two years ago, we, as manufacturers, had been furnishing the larger portion of HEPA filters with kraft paper separators; as they provide equal efficiency at a lower cost.

Since that time, there has been a definite trend away from kraft. By and large, most of the filters being sold today are of aluminum separator construction which is considerably more fire resistant.

This doesn't necessarily apply to the framing, for which a considerable amount of combustible material is still being used.

BURCHSTED: I was going to make one more comment. Many clean rooms are in AEC installations but I have not seen any of the points brought out here put into practice in any AEC clean room.

GILBERT: I think the influence that Mr. Elinsky brought out has been in existence only for the last two years when we have been able to approach the formulation of Federal Standard 209, the so-called Bible, which, I might point out, is by no means perfect. However, it does reflect this fire-resistance influence plus a little more logic in the testing of the filters. The clean room, today, is a little farther removed from the voodoo practices that existed at the beginning of the white room era.

Another point I want to bring out is the impact of the white room era. It is, perhaps, best illustrated by sales figures I have obtained from filter manufacturers relating to the percentage of high efficiency filters going to the white room industry. One company said that 20 percent of their production is going to white room and clean bench use; another said over 40 percent; another, over 50 percent; the fourth was indefinite, but said "a goodly percentage." So you see that white room applications are approaching half the total volume of this segment of the filter industry.

BILLINGS: Perhaps it would be useful to consider an interface committee among people who are concerned with some of the AEC programs, people like Don Keigher, for example, and people from the American Association for Contamination Control, to bridge this gap in technology.

GILBERT: To supplement Dr. Billings' remark, ASTM has a committee which is called a steering committee on contamination control. This subject falls within overlapping jurisdictions of various committees so ASTM established somewhat of an allocation committee to decide where the work must go. This committee makes an excellent focal point for meetings between the filtration industry and the white room business.

KEIGHER: I think this will be of interest to people who aren't yet aware of it: since the fire-resistor filter has been in use almost universally within the AEC program, I do not know of a fire of over $500 loss involving filters anywhere in the program. We have had more serious fires and we have had contamination spread within the laboratories, but they have not gotten out through the filter system. The fire-resistant filters and installation designs that have gone into most of our sites have done a very good job in recent years.

GIESEKE: I might point out that widespread use of clean rooms is a recent development and I think the contamination control people are not really very well organized yet. However, they are represented in the American Association for Contamination Control. The Federal Standard 209, which has been mentioned here a number of times, is not really a specification itself. It is used only as a guide in establishing cleanliness levels for the rooms. In practice the final specifications of the rooms and the operational procedures inside the rooms are often determined by individual manufacturers rather than a governing body.

FIRST: I had a request from a group that wished to talk about methyl iodide carbon test procedures.

Mr. Kovach from Barnebey Cheney Company will start the discussion.

KOVACH: I don't pretend to be an expert on methyl iodide. When we started discussing reports of methyl iodide-charcoal systems there seemed to be differences both in test conditions and in the type of charcoal used. Therefore, we felt it would be desirable to try to find out what these differences are, how significant they are, whether they can be eliminated, whether some uniform test condition can be introduced, and on what basis the different reports can be correlated.

Charcoals react differently with methyl iodide under very high humidity. Near 100% relative humidity, where other factors such as decreasing humidity or superheating to avoid water flooding of the charcoal have to be considered. Rather than say more about my opinions, I would like to invite comments on differences of charcoals and testing procedures.

Apparently British charcoal seems to work much better in England than it does over here.

HILLARY: We are satisfied with the reproducibility of our charcoal testing and I don't think I am really going to say very much more than I said in a comment on this during an earlier session of this conference. We are talking about two separate pieces of work under different experimental conditions, and what I have done is to discuss directly with the experimenters involved (ORNL) where we are different. There may not even be a discrepancy to be accounted for if the poor performance at high R.H. is due to the charcoal being excessively wet. But, I think we are agreed that there is work that needs to be done to sort this out.

In considering the different test conditions, we also identified loading concentration temperature, of course, and whether or not there is an absolute filter immediately before the charcoal, to remove water droplets.

KOVACH: You are aware that shortly before the Conference we exchanged charcoals prepared by us. We sent some to England and some to Oak Ridge. The results came out in a reverse order. Your work shows our coal-base carbon considerably better than our coconut shell charcoal; while in the ORNL tests, our coconut shell charcoal is better. Thus, apparently a reverse order of efficiency for methyl iodide is present in the two test systems

HILLARY: I'm afraid I am not familiar with the results you have mentioned. However, I wouldn't like, at this stage, to have people go away with the impression there are enormous differences, because there are undoubtedly large areas of agreement. I think, to resolve the relatively small area where we disagree, there are a number of things we must do in terms of comparing notes and altering conditions.

So, I think this is too early a stage to discuss the matter in detail in a meeting of this sort. I think the people most likely to benefit are the two or three groups concerned. When we have resolved our differences, then maybe it will be time to report back.

KOVACH: A comment I would like to make here, to add somewhat to this, is the matter of the measurement of the moisture loading of the charcoals. I saw a report showing a direct correlation between the efficiency of the charcoal to remove methyl iodide and the water content of the charcoal. I would like to point out that a much better correlation could have been obtained if the fraction of water loading for the different charcoals was used. This is because a charcoal with a high surface area and large pore structure will pick up considerably more water. Therefore, when you take the fraction of the possible water loading on the particular charcoal and correlate this with methyl iodide removal capacity, rather than the total moisture content, it should work out a little better.

COMMENT: When preparing papers for publication, it's my suggestion that we pay more attention to specifying the temperature at which an experiment was run, the duration, the past history of the charcoal, and other things of this nature.

KOVACH: Should we agree on certain charcoal parameters to be reported with test results, such as raw material, approximate surface area, or some sort of standardized activity measure? There are very large variations in charcoals and, at times, they are designated only by the manufacturers' code number, whereas we would like to know the absolute specification for all charcoals. Everybody who works with charcoals can probably get fairly detailed technical descriptions of the charcoal from the manufacturer. If this was reported, it would help greatly in correlating results.

HILLARY: I will offer a little information that came out recently. A Dutch research group had some studies done on adsorption of methyl iodide on charcoal. The reference is: Nr Ch-D/Int R-29/66, Studies on the Adsorption of Methyl Iodide. I The Texture of a Few Carbons and the Extraction of Methyl Iodide Onto Them. E. G. P. Cornelissens, A. W. M. Derlssen, Th van der Plas, G. J. Zondervan (27/7/66).

FIRST: This discussion suggests that "Standards" is one of the things that might be considered at the next Conference. We do know that ASA and ASTM will accept standards that have been prepared by other organizations provided they receive general agreement. With respect to standards for testing charcoal, methyl iodide, and many other things that have been discussed during the past several days, I don't know of another group that is better prepared to propose and agree upon such standards than this one. They could be submitted to appropriate organization and committees for adoption on a national as well as an international basis.

Wm. Browning will now start a discussion of in-place testing of both particulate filters and iodine adsorbers. What are the requirements for in-place tests? How far towards realism must we go?

BROWNING: An Evaluation of Strategies for Proof Testing of Gas Cleaning Systems Used as Engineering Safeguards for Power Reactors

This morning, we heard described a number of methods of testing filters and gas cleaning systems. Some of these were a little bit more difficult than others. Some of them were designed to make things as easy as possible for the tester, and others were designed to achieve a greater degree of realism. I am interested in the question of how realistic we need to be in tests of gas cleaning systems serving as engineered safeguards for power reactors. The choice of an in-place test has to be a compromise somewhere along the spectrum between the two requirements of simplicity and realism. Or perhaps a strategy can be developed to use a combination of simple and realistic tests.

The ultimate in simplicity is faith in the gas cleaning system. You install it, and you know it will work, because you designed it well.

At the other extreme, a person who is very skeptical about the reliability of engineered safeguards (and there are those whose business it is to be very skeptical) might be satisfied only with the ultimate in realism. He might want to actually vaporize a little high burn-up fuel element in the containment vessel, and run steam and everything else through the gas cleaning system, and see if it works with a real fission product dispersion under real conditions. Well, a test like that would be so horrendously expensive that most people would say it is just impossible, and we would have to find some alternative to that. Somewhere between the two extremes, there is an optimum in-place test. The best choice may differ from one situation to another. It depends upon the consequences of release, on the location, and so forth.

Let me discuss some points along this spectrum. I have already mentioned the extreme one, in which you realistically destroy a fuel element and measure the behavior of the honest-to-goodness fission product activity.

The next most realistic test I can think of is to run a full-scale in-place test on the installed gas-cleaning system under steam conditions using simulants. For the iodine adsorbers, both kinds of iodine would be used at low levels of radioactivity, but at realistic milligram concentrations. For the particulate filters, an aerosol from over-heated, non-radioactive material, such as Bob Adams described yesterday might be used. This method of testing, although it should satisfy almost anybody as far as realism is concerned, would still be pretty expensive. Most reactor operators would be reluctant to let you fill their containment vessels full of steam, with all of the equipment that is necessary in there.

The next thing I can think of, which would still be quite realistic, would be to design the gas cleaning system ahead of time, to handle steam. There would be provided the intake supply of steam, and at the exit a place to dump it. The efficiencies would be measured using simulants. This may be within the realm of possibility. It would be very costly, though, and would no doubt add some mills per kilowatt to our electric costs if we decided to do this in power reactors; but it could be done.

Perhaps we can think of ways to achieve the same result at less cost.

The next easiest thing I can think of, which is still fairly realistic, involves a removable sample of the adsorber or filter. In most designs, the system is modular; you can remove one module, and replace it with a new one. You would take the used one to a testing facility, perhaps at the reactor site or perhaps under contract with somebody who can do the work, and test it under steam conditions with appropriate simulant fission product dispersions to see if the medium and the frame are still capable of doing the job. This would detect any deterioration of the medium, failure of adhesives and things like that. You still have your gasketing and the rest of the system back at the side, but this could be tested with one of

the less expensive tests, one which is not necessarily realistic but proves that the gas is all going through the medium. Tests such as the DOP test, the condensation nuclei detector test, the Freon test, and other tests of this sort are adequate for the purpose.

This particular combination of realistic and simple tests seems to me like a pretty good strategy. I anticipate that when gas cleaning systems are accepted as engineered safeguards for reactors, some such combination of proof tests will be used. Removable modules will be tested under realistic conditions for aging effects, and simultaneously the full-scale system will be tested in the plant with a very simple means for determining whether there is a leak or a by-pass or something like that.

Other combinations of proof tests have been used. One of the simpler ones is to test the new, clean medium under adverse conditions in laboratory tests to prove that the medium is capable of working under adverse conditions. Then you can show by frequent tests, in-place and at full-scale, that the gas is not by-passing the medium. This has been used on certain power reactors which are in operation right now. The most important weakness in this strategy is that with aging a susceptibility to severe damage conditions may develop and may not not show up in tests under severe conditions.

Well, I imagine there will be comments on where we should stop in this spectrum between realism and simplicity.

GILBERT: I agree and disagree with your proposal. I feel that the ventilation system and the reactor have factors that should control the development of tests. By this, I mean that we should have reproducible tests. We should have tests that are economical. Tests should be as rapid as possible, as simply as possible, and the result of the tests should be applied in the field to the installation without resorting to the laboratory.

To take this a step further, I don't know why we should have to test the filter medium to see, for example, whether it was water-proofed. I think that this development should be carried out and applied to the manufacture of the medium so that it would not have to be done by everybody who received the medium in the field. This seems like a more logical and economical procedure than having to resort to a water test of the medium to see if the medium meets the requirements. We should be able to develop a medium as water-proof as possible, recognizing, of course, that there are limitations on technology. We haven't advanced as far as we would like to go, but we will have to be satisfied with what we can get. However, we would like to have the best that we can get, consistent with technology advance. So there are things to do in the testing area, but we should not collect just useful and interesting data from our tests.

BILLINGS: In considering the use of simulants for filter tests, one aspect that has not been satisfactorily resolved is whether a solid or liquid particle is necessary. It appears that the filtration of solid particles (by

diffusion and direct interception) occurs at an efficiency about an order of magnitude higher than for liquid particles, when compared on the basis of experimental findings. It is not certain at this time that the difference is due solely to electrostatic charge effects on the solids. These differences may influence choice of simulants.

BROWNING: I think that is a good point because aerosols are not just aerosols. Solid and liquid aerosols can differ from each other and also there can be differences in behavior between two kinds of solid aerosols. This is an important part of the reactor safety program of the AEC and it requires a large effort to prove that the aerosol or dispersion that is used in experiments or tests really does simulate what you intend it to simulate.

FIRST: I am not sure that we always have to simulate something in these tests. Most tests are actually indices of something, and so long as the particular index that we are measuring has a good relationship to an important parameter of the filter, or whatever is being tested, this is probably all that is necessary.

When someone makes an in-place test, he is not interested in knowing, to four decimal places, whether the DOP particles are one-tenth micron diameter. Rather, he wants to know: Is my installation functional or not? Extreme accuracy is not important as it is pretty much a go, no-go, kind of system. I think that this is an adequate test for in-place testing. I think, however, we will all agree that this kind of a test is completely inadequate for the fundamental studies of filtration and filter performance that we must perform in the laboratory. Similarly, precise tests may be required for specific applications in which we know the exact conditions under which a filter must perform. These are two different situations. Both are valid in their place, but we should not confuse the two.

BROWNING: That is quite right.

BILLINGS: Dr. Brion brought out this morning the need for information about standards in filter plugging. There are none now. It is an interesting field.

It seems to me that he broke the problem down nicely in his paper. There is the medium itself, the element itself, and the in-place situation itself. I was speaking about the first one, the medium, not the other elements.

I quite agree, that if you go into the plant and you want to test the whole system, you don't need refinements.

HILLARY: I would like to make one or two small comments regarding the testing of charcoal and iodine adsorption. I think it has been indicated throughout the sessions of this Conference that probably the most critical iodine compound for retention by charcoal is likely to be methyl iodide, but our feeling is that methyl iodide also serves as a logical, simple, and readily

applicable technique for the in situ testing of charcoal beds.

At the same time, it gives both a test of plant leakage and charcoal performance, because with any charcoal, you are going to get some physical adsorption. Immediately after release, gross penetration will be due to mechanical leakage past the charcoal. Later penetration will depend on the ability of the charcoal itself to retain methyl iodide. This has been shown by our experience of in situ testing with methyl iodide.

FIRST: Are you suggesting, Mr. Hillary, that the methyl iodide used for the tests goes out of the bed and will not constitute a permanent utilization of carbon?

HILLARY: No. I think that point is that you don't need to use very much. If you used a radioactive tracer, only a very small mass is involved and it would do the job in the same way. This will only give you a very small percentage of total loading that it will take.

One of the disadvantages in this, and it is a disadvantage in all testing, is that you don't necessarily test under the most rigorous conditions. This is a point that Bill Browning was making, in line with how far you go towards being realistic. For example, one might wish to test at one hundred per cent relative humidity; but, on most days, the relative humidity will be less than this. On the other hand, the sort of range that we find is critical is around 30 or 40 per cent. There are a lot of days (certainly in England) when humidity is greater than this.

FIRST: But it might be a rare day in Los Alamos.

LINDEKEN: With respect to methyl iodide on charcoal, I believe that it would act as a very limited poison over a length of time. We have been working on respirator cartridges and have been able to desorb up to 80 per cent of the iodide on the cartridge in a period of about two hours at 74 degrees F. and 95 per cent relative humidity. It comes off rapidly.

FIRST: Does this take place immediately after adsorption, or is there some degree of storage?

LINDEKEN: We followed the technique of loading it on, and watching the desorption.

FIRST: Do you have any information on what happens if you store it for a day or two or a week, and then start to desorb? Does the material get into the carbon structure and come out with great difficulty?

LINDEKEN: We don't have any data on that. Now, getting back to the original version of Bill's comment, I would feel that rather than everybody going back home and testing his charcoal beds with methyl iodide again, our collective group ought to be considering sponsoring more fundamental

investigations to get information on the mechanism of just how methyl iodide acts in a charcoal bed.

We are doing too much testing now, and not enough investigation. We don't understand the fundamental physical chemistry of the process.

FIRST: We all realize that it is easier to make tests than it is to figure out why we are doing them.

BROWNING: Carl, is the charcoal you are referring to an iodine impregnated charcoal or ordinary activated charcoal?

LINDEKEN: We have run two series of tests; one with the respirator for mercury, which has the iodine in it, and the other with ordinary coconut charcoal used for organic vapors. We are talking about the desorption rate, conducted on the latter.

BROWNING: We can anticipate there would be less adsorption on ordinary charcoal than on the charcoal impregnated with iodine, because of the isotopic exchange mechanism at work in the latter case.

LINDEKEN: We have been using stable iodine; we weren't using the other. We did find when using methyl iodide with the impregnated charcoal, that is, for mercury and acid gases, that we had a quite rapid breakthrough. We assumed there was some sort of an exchange or saturation. As a matter of fact, we don't know yet about it.

BROWNING: There was a recommendation a few minutes ago that work be done on mechanisms for the formation and trapping of methyl iodide. There is such a program under way, sponsored by the AEC nuclear safety program. Part of this is at Oak Ridge and part of it is at Battelle-Columbus, and of course work is being done in other places. Of the two I have referred to, Battelle is doing work under sub-contract for ORNL on the formation of methyl iodide; on both the equilibrium chemistry and the chemical kinetics. This work has identified a number of avenues by which methyl iodide could be formed, and this will be reported in the not too distant future.

At Oak Ridge, Bob Adams is starting experimental work to check out these results and to explore other possibilities, experimentally, to determine what conditions are necessary for the formation of methyl iodide.

VAN DEN BERGH: I would like to ask if there is information available as to the fraction of iodine released as methyl iodide. You have mentioned that there are investigations on the way. I was wondering whether any results are available.

BROWNING: Do you mean under laboratory conditions or a simulated accident?

VAN DEN BERGH: A simulated accident. From several papers presented at this Conference it may be concluded that the filter efficiencies for various forms of iodine are pretty well known. In order to estimate the consequences of a postulated reactor accident, it is also necessary to know which fraction of the iodine is going to be released in the form of methyl iodide. In other words, in which forms is the iodine going to reach the filters. Knowing this and the filter efficiencies for each form, we then know how much of the iodine is going to get out into the atmosphere.

BROWNING: That is the question we all wish could be answered; how much methyl iodide would be formed in a reactor accident. There have been numerous experiments carried out, giving various results. Unfortunately, the experiments we can refer to are in the past, before we had good ways of distinguishing and of characterizing the gaseous forms of iodine, but there are now ways to distinguish them in our experiments and to determine what we have.

These characterization devices are available, now, but they weren't available in the past, when the experiments were run. So it is not possible to construct a completely convincing calculation of the yield of the methyl iodide in these experiments in the past. We look at the data and can only say that it surely looks like some methyl iodide was there.

There was a survey in the literature on this subject. George Parker conducted the survey and it was included in a report by R. E. Adams, W. E. Browning, Jr., W. B. Cottrell, and G. W. Parker, The Release and Adsorption of Methyl Iodide in the HFIR Maximum Credible Accident, USAEC Report ORNL-TM 1291, October 1965.

VAN DEN BERGH: I have seen the report. I believe the maximum was 5 per cent methyl iodide.

That is the latest, is it? There is nothing more recent than that?

BROWNING: No, there isn't. Things don't work that fast.

GIESEKE: Concerning the work being done at Battelle that Bill mentioned, there is a very short summary of this work included in the first paper presented at this Conference.

BROWNING: You point out that steam is used for stripping adsorbants from charcoal; when you use the term "stripping" that accentuates how difficult the conditions of temperature and moisture content are, under which we must trap methyl iodide. There have been methods devised, and described at this meeting, by which you can indeed trap methyl iodide, even under high temperature steam conditions. But only up to a certain point. In Bob Ackley's paper on Wednesday, we saw that if you get enough water on the charcoal, it begins to interfere with the trapping.

FIRST: Reactivating charcoal by steam stripping may be a good technique when there is a small amount of charcoal. When, however, the system is handling a few hundred thousand cubic feet a minute, there is apt to be tons of charcoal and the problems associated with steaming it out become formidable.

HILLARY: This leads to the point I wanted to make. You should take small representative samples of the charcoal in the bed and do tests on these. I think there are some reasonable things you can do in situ, but, in support of this, you ought then to carry out the more rigorous and extensive tests in the laboratory using small samples. You can also study realistic aging effects by withdrawing a sample from the main bed at various times after installation.

BERNARD: I think that we would like to use as many of the existing methods for testing as we have already developed and for which we have established confidence. The DOP test seems to be working very well; it is relatively simple. A point that has been made concerning a possible drawback is the fact that it is a liquid. We recently initiated work to try to correlate DOP liquid with the established simulants that we are working with now in the nuclear safety program, so we can get the necessary cross linkage in order that we can continue to use the DOP.

Now, as far as destructive charcoal testing is concerned, I, personally, can see nothing wrong with it. However, I wouldn't want to destroy a whole charcoal bank. I don't mind removing periodically a relatively small unit of charcoal that is installed in parallel with the main bank (charcoal that sees exactly the same environmental conditions and flow rates that the parent banks of charcoal sees) and taking this to the laboratory for tests to evaluate the efficiency and capacity of the charcoal in situ. I think that if we are not careful, our thoughts can run away in several areas. For example, putting steam lines in the large ducts, to determine efficiency in situ, periodically, as mentioned several times, may be too far out. Simplicity, reliability, economics, those facets previously mentioned, are the requisites for a realistic in-place testing system.

FIRST: Your thoughts on this and Mr. Hillary's are quite parallel. I am going to call a halt to this topic. I regret the necessity of doing so. We have one individual who has another topic. In all fairness to him, and before the audience completely melts away, I would like to give him an opportunity to speak.

PRODI: I must apologize for my English, but I have a question to give to the floor. There is a kind of a particulate filter, having to do with condensation, developed by a group of Russian scientists in the USSR, who claim a high flux and high efficiency. I am wondering the reason why this is not used generally. By the way, it is a kind of filter that looks good in the case of high humidity. Unfortunately, I do not have the literature here, to give you a citation; I got this information indirectly. It works. I know that

some experiments have been done in Russia on the subject. I was asking the floor if anybody knows if some industrial exploitation has been undertaken of this. I know how it works. I am trying to fix up a small unit, but I don't yet have any data on it.

BILLINGS: I don't believe there is any commercial exploitation of this. I haven't heard of any. And, of course, there is some work in the literature.

PRODI: We have studied this phenomenon. In our experience, as applied to the mechanism of wet removal, which is responsible for 80% of the radioactive material deposition at the surface of the earth. I was wondering if such a factor has been exploited.

FIRST: Let us hope that when the proceedings are published and your questions appear there, someone who has the information will kindly answer you.

BURCHSTED: I was just wondering, is this the German-Pedersey Pressure Jump Separator, which is a wet system. I have seen their literature, but I know nothing about it.

PRODI: The work has been done at the Academy of Sciences of USSR, under the guidance of Professor Derjagin.

FIRST: Mr. Kovach, you had a comment on another topic, I believe.

KOVACH: In our testing system, we found it difficult to scale up the wetting and water flooding characteristics from small charcoal tubes to the full-scale filters.

FIRST: Would you put some numbers on that?

KOVACH: From 1 to 2-inch I.D. tubes to 12" x 12" and 24" x 24" filters. It would be quite interesting to see if the wetting would be as critical in a filter system as it is in small scale tube tests.

I have one other comment. In the so-called full-scale testing or steaming of units to remove different solvents, it would require 3 to 5 pounds of steam to remove a pound of solvent.

That is all I have to say.

FIRST: At this time we will hear from Mr. Walter G. Belter, USAEC, who will make the closing remarks.

CLOSING REMARKS

Mr. W. G. Belter
Division of Reactor Development and Technology
U. S. Atomic Energy Commission

In closing this 9th Air Cleaning Conference, I have a few remarks to make which deal with our planning for future air cleaning symposia. It is desirable to obtain your thoughts and desires on this subject, since we are always striving to plan and develop a program which is responsive to your operational needs and requirements, and at the same time presents an up-to-date status report of new and significant happenings in the research and development program.

In developing my own thoughts on what our future conference program may cover, I took a look at our agenda for this year. We had approximately 54 papers on the program, about 50% more than at Oak Ridge in 1963. We had an opening session on source term characterization. This was followed by several sessions on air clean-up systems, i.e., high-efficiency filters, with papers being presented on their specifications, effects of overpressure, fires, gasket leakage, etc. The removal of iodine, with primary emphasis on methyl iodide removal under reactor accident conditions, occupied a large degree of attention at this meeting. Noble gas removal is receiving greater attention in the AEC R&D program, and also the session on confinement and containment was an important one for this meeting. There were several papers presented on sodium aerosols, and their behavior as this element becomes increasingly important as a reactor coolant. Similarly, plutonium was discussed in a number of papers, as it assumes greater importance in our future reactor programs. From an operational standpoint, the evaluation of filter performance, i.e., the in-place testing of particulate and iodine removal systems was discussed in considerable detail. In order to make room for covering these many areas, we were compelled to de-emphasize the reporting on normal air cleaning operating experience at the various AEC sites, like we have done at past meetings. It was also necessary to eliminate the session on meteorologic aspects of air cleaning.

In summary on this subject then, are we meeting the groups' needs realizing that a program of this type must cover a wide gamut of interest and scientific disciplines. I would appreciate any comments or suggestions on the overall content of this years program and any ideas which you may have for improving it two years from now. Any reactions or comments from our industrial friends would also be most welcomed.

As many of you perhaps know, since 1951 we have held these air cleaning conferences on approximately a two year basis. They have been planned and carried out as part of the Reactor Development Division, research program with the Harvard Air Cleaning Laboratory, with very

close cooperation and assistance from the AEC Division of Operational Safety. Meetings have been held in Los Alamos, Argonne, Idaho, Brookhaven, Oak Ridge, and this is the second conference we have held in the Boston area. We are opened to suggestions for a meeting place approximately two years from now. If you would wish to discuss this back at your installation, I would appreciate hearing from you through the mail on this subject.

I would also like to encourage as many of you to stay for this afternoon's session since it was purposedly planned not to have the normal number of formal papers or presentations. We regret because of the large number of papers which have been presented during the past three days that we have not had as much time for open discussion as many of us would have liked. From this standpoint, I believe this afternoon's session will provide additional time for more questions and open discussion.

For those of you who can't stay, I would like to at this time express my sincere appreciation, on behalf of the Division of Reactor Development and Technology, to Dr. First and Mr. Viles, and all of the other Harvard personnel who have contributed to much in the planning and conduct of this very successful program. I am sure all of us realize the tremendous amount of time and effort which are required in the successful carrying out of a conference of this size. I would also like to extend my personal thanks to Hal Bernard of my own office and Humphrey Gilbert for their many extra efforts in also making this conference a success. I hope that each of you can personally thank Mel and Fred for their efforts at this meeting as I am sure that they would appreciate this. For those who will be leaving after this morning's session, may I wish you all a safe return to your homes and may I thank you for your attendance and participation at this conference. It has been a pleasure seeing many of our foreign colleagues again from the U. K., France, Germany, and Denmark and I hope that you have also found this meeting to be a pleasant and profitable one.

FIRST: Are there additional comments at this time? Hearing none, I now declare this 9th Air Cleaning Conference adjourned and I hope that we will all meet again in two years for the 10th Air Cleaning Conference.

(Whereupon, the 9th Air Cleaning Conference was adjourned at 3:50 o'clock Friday afternoon, September 16, 1966.)

MOISTURE SEPARATOR STUDY FOR IODINE REMOVAL SYSTEMS FOR CONNECTICUT YANKEE REACTOR CONTAINMENT*

This study describes tests carried out on the moisture separator used in the recirculatory iodine removal systems within the Connecticut Yankee Containment. The tests set up were intended to demonstrate the ability of the moisture separator to remove water droplets under actual conditions of the assumed reactor incident. The test facility used was capable of circulating 1000 cfm of saturated air-steam mixture at pressures up to 40 psig and 261° F. Water sprays simulated the droplet cloud expected; up to one gallon per minute of gas borne droplets could be produced.

The moisture separator consisted of a louver section followed by six inch deep pads of phenolic-bonded continuous filament glass fibers. The moisture separator removed essentially all droplets from the air stream under six test conditions with pressures ranging from 10 to 40 psi. High efficiency particulate filters downstream of the separator withstood test periods up to 24 hours at predicted maximum conditions without measurable loss of performance.

During preliminary runs, drainage from the separator was inadequate and the filter system flooded. This was readily corrected, but the experience pointed out the necessity of adequate drainage in the installed system.

A detailed description of the tests and the separator is contained in NYO-3250-6, MOISTURE SEPARATOR STUDY, R. D. Rivers and J. L. Trinkle. (Prepared for Connecticut Yankee Atomic Power Company by American Air Filter Company, Inc.)

* Submitted 27 September 1966 by R. D. Rivers, Manager, G.A.C. Research Laboratory, American Air Filter Company Inc., Louisville, Kentucky

LIST OF ATTENDEES

W.H. Aaroe	N.J. State Dept. of Health, Trenton, New Jersey
F. Ackerman	Univ. of California, Lawrence Radiation Lab., Livermore, California
R.D. Ackley	Oak Ridge National Laboratory, Oak Ridge, Tenn.
T.G. Acierno	Argonne National Laboratory, Argonne, Ill.
R.E. Adams	Oak Ridge National Laboratory, Oak Ridge, Tenn.
F.E. Adley	Hanford Occupational Health Foundation Occupational Hygiene Dept., Richland, Washington
A.R. Allan, Jr.	Flanders Filters Inc., P.O. Box 718 Riverhead, New York
C.G. Amato	N.J. State Dept. of Health, P.O. Box 1540, Trenton 25, New Jersey
C.L. Amos	Dow Chemical Co., Rocky Flats Div., Denver, Colo.
R. Anderson	Idaho Nuclear Corp., 1055 Woodruff, Idaho Falls, Idaho
V.E. Andrews	U.S. Public Health Service, Las Vegas, Nevada
R.E. Baker	U.S. AEC, DSS Washington 25, D.C.
M.W. Barete	Comision Nacional de Energia Nuclear Av. Insurgentes Sur 1079, Apartado, Postal 27-190 Mexico 18, D.F.
L. Baurmash	Atomics International, P.O. Box 309, Canoga Park, California
R.W. Beadle	U.S. AEC, DBM, Washington, D.C.
.C. Belvin	Herty Foundation, Savannah, Ga.
L.E. Benander	Northeastern Radiological Health Laboratory Winchester, Massachusetts
M. Benedict	Dept. of Nuclear Engineering, Mass. Institute of Technology, Boston, Mass.
R.A. Benedict	Fast Inc., 39 Broadway, New York, N.Y.
R.L. Bennett	Oak Ridge National Laboratory, Oak Ridge, Tenn.
A. Benson	A.D. Little Co., 15 Acorn Park, Cambridge, Mass.
H. Bernard	U.S. AEC, Washington, D.C.
D.E. Bernhardt	Public Health Service, Box 684, Las Vegas, Nevada
W.G. Belter	AEC, Reactor Developments, Washington, D.C.
H. Billet	Nuclear Safety Systems, New York, N.Y.
C. Billings	Univ. of Michigan, School of Public Health Ann Arbor, Michigan
E.W. Bloore	U.S. Army Nuclear Defense Lab., Edgewood Arsenal, Edgewood Maryland
S. Blumpkin	Union Carbide Corp., Gaseous Diff. Plant, Oak Ridge, Tenn.
J.C. Boardway	U.S. Army Chem. Research and Dev. Laboratory, Edgewood Arsenal, Edgewood, Maryland
W.J. Bodendorf	Strathmore Paper Co., West Springfield, Mass.
H. Bogardus	Naval Research Lab., Washington, D.C.
R.B. Boies	National Lead Co. of Ohio, Fernald, Ohio
F.C. Boyd	Atomic Energy Control Board, Chalk River, Ontario, Canada
.J. Breslin	U.S. AEC, 376 Hudson St., New York, N.Y. 10014
.D. Briggs	General Electric Co.
J. Brion	Centre d' Etudes Nucleaires, 92-Fontenay-Aux-Roses, France

E.H. Brooks	General Atomic/General Dynamics, San Diego, California
L.R. Busche	C.H. Dexter & Sons, Windsor Locks, Conn.
R.A. Bub	Mine Safety Appliances Co. Callery, Pa.
E. Bulba	Harvard School of Public Health, Boston, Mass.
D.F. Bunch	USAEC, Idaho Operations, Idaho Falls, Idaho
C.A. Burchsted	Oak Ridge National Laboratory, Oak Ridge, Tenn.
F. Burman	R.A. Taft San. Eng. Center, Cincinnati, Ohio
D. Busch	General Atomic, Box 608, San Diego, Calif.
C.D. Cagle	Union Carbide Corp., Oak Ridge National Lab., Oak Ridge, Tenn.
C.L. Cheever	Argonne National Laboratory, Argonne, Ill.
R.H. Cipolla	Johns-Manville Corp., 22 East 40th St., New York, New York
H.A. Clark	Isochem Co., Hanford, Washington
J.A. Cochran	N.E. Rad. Health Laboratory, Winchester, Mass.
R.A. Coerver	E.I. DuPont de Nemours, Wilmington, Delaware
L.F. Coleman	Argonne National Lab., Argonne, Ill.
J. Crawford	Goodyear Atomic Corp., P.O. Box 628, Piketon, Ohio
R.E. Cunningham	U.S. AEC, Washington, D.C.
E.W. Cunnington	Los Alamos Scientific Lab., Los Alamos, New Mexico
J. Dadillon	Sesr. Cen. Cadarache - BP No. 1, 13 Saint Paul Lez- Durance, France
P.R. Davis	AEC, Idaho Falls, Idaho
S.V. Dawson	Harvard School of Public Health, Boston, Mass.
R. Dennis	GCA Corp., Bedford, Mass.
J. Devencentz	Yankee Atomic Electric Co., Boston, Mass.
I.E.H. Dinkelacker	Dev. Dept. Luwa Ltd. 8047 Zurich, Switzerland
P.H. Dobson	Factory Mutual, Norwood, Mass.
W.S. Durant	Savannah River Lab., Aiken, South Carolina
J.F. Ege, Jr.	Argonne National Lab., Argonne, Ill.
P. Engle	Cambridge Filter, Syracuse, N.Y.
D.E. Engleman	American Air Filter Co., 215 Central Ave. Louisville, Kentucky
H.C. Elinsky	Mine Safety Appliances Co., Pittsburgh, Pa.
E.L. Etheridge	Douglas United Nuclear, Richland, Washington
H.J. Ettinger	Los Alamos Scientific Lab., Los Alamos, N.M.
M.W. First	Harvard School of Public Health, Boston, Mass.
H. Flyger	Danish Atomic Energy Commission, Copenhagan, Denmark
B.R. Fish	Oak Ridge National Lab., Oak Ridge, Tenn.
J.F. Fish	American Air Filter Co., Louisville, Kentucky
R. Fisher	Ames Laboratory, I.S.U., Ames, Iowa
C.F. Foelix	Brookhaven National Lab., Upton, New York
M.H. Fontana	Oak Ridge National Lab., Oak Ridge, Tenn.
R. Frohreich	Dow Chemical Co., Golden, Colorado
A.B. Fuller	Oak Ridge National Lab., Oak Ridge, Tenn.
J. Gieseke	Battelle Memorial Institute, Columbus, Ohio
H. Gilbert	U.S. AEC, Washington, D.C.
J. Gleason	C.H. Dexter & Sons Co., Windsor Locks, Conn.
T. Gould	U.S. AEC, Washington, D.C.
R. Goulet	Cambridge Filter, Syracuse, N.Y.
E.E. Grassel	Donaldson Co. Inc., Minneapolis, Minn.
M. Greenfield	Univ. of California, Dept. of Radiology, Berkeley, California

F. Grommers	Harvard School of Public Health, Boston, Mass.
C.A. Gukeisen	Ames Laboratory, Ames, Iowa
R.A. Gussman	Cambridge Technology, 1029 Chestnut St. Newton Upper Falls, Mass.
C.E. Guthrie	Oak Ridge National Lab., Oak Ridge, Tenn.
C.A. Hahs	Union Carbide Corp., Oak Ridge National Lab. P.O. Box X, Oak Ridge, Tenn.
C.A. Haites	Oak Ridge National Lab., Oak Ridge, Tenn.
G. Hake	Atomic Energy of Canada, Chalk River Nuclear Laboratories, Chalk River, Ontario, Canada
H. Hamester	U.S. AEC, Germantown, Maryland
J.B. Harstad	U.S. Army Biological Center, Fort Detrick,Md.
A.F. Hasenbank	Univ. of California, Engineering Department, Berkeley, California
O.M. Hauge	Phillips Petroleum Co., Idaho Falls, Idaho
P.A. Hawkins	Vokes Limited, Guildfork, Surrey, United Kingdom
R.A. Heckman	Lawrence Radiation Lab., Livermore, Calif.
W.T. Heyse	C.H. Dexter & Sons, Windsor Locks, Conn.
J.H. Hillary	United Kingdom Atomic Energy Authority, Windscale Works, Seascale, Cumberland, England
R.K. Hilliard	Battelle Northwest Laboratory, Richland, Washington
P. Himot	Harvard School of Public Health, Boston, Mass.
J. Hooper	AEC, Brookhaven, Upton, New York
F.L. Horn	Brookhaven National Lab., Upton, New York
L.H. Horn	Underwriters' Lab. Inc. P.O. Box 247, Northbrook, Ill.
N.R. Horton	Phillips Petroleum Co., Idaho Falls, Idaho
H.H. Hunter	Battelle Memorial Institute, 505 King Avenue Columbus 1, Ohio
W.P. Ingalls	Isochem Inc., Richland, Washington
S.B. Jacobs	Stone & Webster Engineering Corp. 225 Franklin Street, Boston, Mass.
P.E. Johnson	Factory Mutual Engineering Corp., Norwood, Mass.
S.L. Johnson	Union Carbide, 3250 S. Kedzie, Chicago, Ill.
R.K. Jones	Johns-Manville Products Corp. Celite Div. 22 E. 40th St. New York, N.Y. 10016
R. Joyce	Pittsburgh Activated Carbon Co., Trenton, N.J.
E. Karaian	Mass. Institute of Technology, Boston, Mass.
F. Kaylor	Stone & Webster Engineering Corp. 225 Franklin St., Boston, Mass.
W.G. Keating	Johns-Manville Products Corp. 22 E. 40th St., New York, N.Y. 10016
D.G. Keigher	U.S. AEC, Richland, Washington
G.W. Keilholtz	Oak Ridge National Laboratory, Oak Ridge, Tenn.
R.W. Kessie	Argonne National Lab., Argonne, Ill.
C. Killian	6 Laurel Drive, Needham, Mass.
E. Kimmerly	Union Carbide Corp., Oak Ridge, Tenn.
L.J. Klamerus	Sandia Corp., Albuquerque, New Mexico
F. Kleimola	Combustion Eng., Windsor, Connecticut
H.W. Knudson	Hollingsworth & Vose, East Walpole, Mass.
R.H. Knuth	Health & Safety Laboratory, U.S. AEC New York, N.Y.
R. Koontz	Atomics International, Canoga Park, California

J.L. Kovach	Barnebey Cheney Co., Cassady at 8th St., Columbus, Ohio 43219
B.H. Korneqay	Clemson University, Clemson, S. Carolina
D. Lachapelle	U.S. Army Nuclear Defense Lab., Edgewood, Md.
N. Lauben	Atomics International, Canoga Park, California
H. Lawroski	Argonne National Lab., P.O. Box 2528, Argonne, Ill.
E. Leininger	National Lead Co. of Ohio, P.O. Box 39158, Cincinnati, Ohio.
R. Liberace	U.S. Public Health Service, 1901 Chapman Ave. Rockville, Maryland
A. Liberman	IIT Research Institute, Chicago, Ill.
F. Linck	Dow Chemical Co., Golden, Colorado
W. Lindsey	U.S. AEC, Production Division, Germantown, Md.
C.L. Lindeken	Hazards Control, Lawrence Radiation Laboratory P.O. Box 808, Livermore, California
J.A. List	E.I. DuPont De Nemours, Wilmington, Delaware
B. Liu	Univ. of Minnesota, Minneapolis, Minn.
B. Louros	Pittsburgh Activated Carbon Co., Trenton, N.J.
R. Luken	Babcock & Wilcox, Lynchburg, Va.
J. Manneschmidt	Oak Ridge National Lab., Oak Ridge, Tenn.
R.C. Marsh	Texas Instruments Inc., P.O. Box 5012 Dallas, Texas, 75222
R.W. Matchett	Strathmore Paper Co., W. Springfield, Mass.
G.B. Matheney	Phillips Petroleum Co., Idaho Falls, Idaho
Y.P. Mercier	Schneider Poelman, Paris, France
H.E. Meyer	Mound Laboratory, Miamisburg, Ohio
R.C. Milham	Savannah River Lab., Aiken, S.C.
J. Mishima	Battelle N.W. Lab., Richland, Washington
R.I. Mitchell	Battelle Memorial Institute, 505 King Ave., Columbus, Ohio
R.N. Mitchell	Los Alamos Scientific Lab., Los Alamos, N.M.
D.W. Moeller	Harvard School of Public Health, Boston, Mass.
A. Mogtissi	U.S. Public Health Service, Div. of Radiological Health, Montgomery, Ala.
J.M. Morgan	Johns Hopkins Univ., Baltimore, Md.
D.L. Morrison	Battelle Memorial Institute, 505 King Ave., Columbus, Ohio
D.R. Muhlbaier	Savannah River Lab., Aiken, S. Carolina
J.L. Murrow	Lawrence Radiation Laboratory, Livermore, Calif.
D. Myer	Lawrence Radiation Laboratory, Livermore, Calif.
R.G. McAllister	Liberty Mutual Insurance Co., Hopkinton, Mass.
J.D. McCormack	Battelle N.W. Lab., Richland, Washington
J. McDonough	MSA Research Corp, Callery, Pa.
J. McDougall	White Sands Missile Range, Nuclear Effects Div. New Mexico, 88002
D.R. McFee	Argonne National Lab., Argonne, Ill.
C.T. Nelson	Atomics International, Canoga Park, Calif.
L.J. Nitteberg	Battelle Northwest Lab., Richland, Washington
J.H. Noble	Stone & Webster Engineering Corp., 225 Franklin St., Boston, Mass.
D.P. O'Neil	Argonne National Laboratory, Argonne, Ill.
C.E. Parker	Virginia Military Institute, Lexington, Va.

F. Panchuk	Chalk River Nuclear Laboratories, AEC of Canada Ltd, Chalk River, Ontario, Canada
George Parker	Oak Ridge National Lab., Oak Ridge, Tenn.
Gerald Parker	Mass. Dept. of Public Health, Boston, Mass.
D.L. Parry	Phillips Petroleum Co., P.O. Box 2067, Idaho Falls, Idaho
R.D. Parsons	Hollingsworth & Vose Co., East Walpole, Mass.
A.H. Peters	E.I. DuPont de Nemours, Aiken, South Carolina
H.C. Phelps	Fast Inc., New York, N.Y.
N.J. Pleimann	Monsanto Research Corp., Mound Laboratory Miamisburg, Ohio 45342
V. Prodi	C.N.E.N. Lab. of Nuclear Physics, Bolonga, Italy
W.H. Ray	U.S. AEC, Washington 25, D.C.
J.E. Regnier	U.S. Public Health Service, Div. of Rad. Health, Montgomery, Ala.
D.L. Reid	Battelle Northwest, Richland, Washington
P.C. Reist	Harvard School of Public Health, Boston, Mass.
R. Rivers	American Air Filters Co. Inc., 215 Central Avenue, Louisville, Kentucky
L.C. Rouse	U.S. AEC Materials Licensing, Washington, D.C.
P.E. Ruhter	Phillips Petroleum Co., P.O. Box 2067, Idaho Falls, Idaho
R. Salvatori	Westinghouse Atomic Power Div., Pittsburgh, Pa.
R.E. Schindler	Idaho Nuclear Corp., Box 1845, Idaho Falls, Idaho 83401
M. Schumchyk	U.S. Army Nuclear Defense Lab., Edgewood, Md.
W. Schutze	Univ. of Frankfurt, Inst. for Nuclear Physics 6 Frankfurt Federal Rep of Germany
H.L. Schwalbe	Herty Foundation, P.O. Box 1963, Savannah, Georgia, 31402
G.S. Sethi	Harvard School of Public Health, Boston, Mass.
L.R. Setter	U.S. Public Health Service, Div. of Rad. Health, 1901 Chapman Avenue, Rockville, Md.
J. Shapiro	Harvard School of Public Health, Boston, Mass.
B.O. Shaver	Battelle Northwest, Richland, Washington
B. Shleien	U.S. Public Health Service, N.E. Rad. Health Laboratory, Winchester, Mass.
M. Siegler	General Electric Co.
M. Silberberg	Atomics International, Canoga Park, Calif.
D.G. Smith	Harvard School of Public Health, Boston, Mass.
E.R. Smith	NUS Corp, Washington, D.C.
G. Smith	U.S. Army Edgewood Arsenal, Edgewood, Md.
M.L. Smith	Douglas United Nuclear, Richland, Washington
R. Smith	Reactor Licensing, Washington, D.C.
S.R. Smith	Savannah River Laboratory, Aiken, S. Carolina
W. Smith	A.D. Little Co., Acorn Park, Cambridge, Mass.
P. Spiegler	Atomics International, Canoga Park, Calif.
D. Stanley	Mass. Div. of Eng., Boston State House, Boston, Mass.
S. Steinberg	T.D. Associates Inc., 520 W. Franklin St., Baltimore, Maryland 21201
K. Stewart	Dow Chemical Co., Rocky Flats Div., P.O. Box 888 Golden Colorado, 80402
J.C. Sullivan	Harvard School of Public Health, Boston, Mass.
Y. Sutro-Fourcade	SPR-CEA, Marcoule, France

A.R. Taylor	Spaulding Fibre Co., N. Rochester, N.H.
M.D. Thaxter	Lawrence Radiation Lab., Berkeley, Calif.
J. Thomas	AEC Health & Safety Lab., New York, N.Y.
T. Thompson	Mass. Institute of Technology, Boston, Mass.
W.V. Thompson	Douglas United, Richland, Washington
W.G. Thomson	Todd Shipyards, Galveston, Texas
J. Truitt	Oak Ridge National Lab., Oak Ridge, Tenn.
M. Tscherner	Technischer Uberwachungsverein 5 Koln Lukasstr 90 Hauptabteilung Kernenergie u Strahlenschutz
R.W. Ulm	Union Carbide, Oak Ridge, Tenn.
D. Underhill	Harvard School of Public Health, Boston, Mass.
H.H. Vanden Bergn	General Atomic, Div. of General Dynamics, San Diego, California
Viles, F.J., jr.	Harvard School of Public Health, Boston, Mass.
E. Waibel	GFK Karlsruhe Kernforschungszentrum Karlsruhe 7501 Leopoldshafen b Germany
J. Walkley	Harvard School of Public Health, Boston, Mass.
D. Watson	The Hydro-Electric Power Commission of Ontario NPD Generating Station, Rolphton, Ontario, Canada
G.M. Watson	Oak Ridge National Laboratory, Oak Ridge, Tenn.
C. Weaver	Public Health Service, Washington, D.C.
G.E. Weldon	Factory Mutual Engineering Corp., Norwood, Mass.
C.G. Welty	Div. of Operational Safety, U.S.AEC, Washington, D.C.
D.J. Wenger	Owens Corning Fiberglas Corp., Toledo, Ohio
J. Wengler	Farbwerke Hoechstag 623 Frankfurt Main-Hoechst Germany
E.L. Whittaker	U.S. Public Health Service, S.W. Rad. Health Las Vegas, Nevada
T.K. Wilkinson	National Institute of Health, Bethesda, Md.
G.H. Winsor	General Electric Co., Brokaw Rd., Santa Ciara, California
K. Woodard	U.S. AEC, DRL, Washington, D.C.
J.A. Young	Naval Research Lab., Washington, D.C.
Jensen Young	Lawrence Radiation Lab., Berkeley Calif
W.D. Yuille	Oak Ridge National Lab., Oak Ridge, Tenn.
P. Zilles	Harvard School of Public Health, Boston,Mass.
K. Zuehlke	Kernforschungszentrum Karlsruhe 7501 Leopoldshafen b. Karlsruhe, Germany